

Bo E. Sernelius

# Fundamentals of van der Waals and Casimir Interactions

# **Springer Series on Atomic, Optical, and Plasma Physics**

Volume 102

## **Editor-in-chief**

Gordon W. F. Drake, Department of Physics, University of Windsor, Windsor, ON, Canada

## **Series editors**

James Babb, Harvard-Smithsonian Center for Astrophysics, Cambridge, MA, USA

Andre D. Bandrauk, Faculté des Sciences, Université de Sherbrooke, Sherbrooke, QC, Canada

Klaus Bartschat, Department of Physics and Astronomy, Drake University, Des Moines, IA, USA

Philip George Burke, School of Mathematics and Physics, Queen's University, Belfast, UK

Robert N. Compton, Knoxville, TN, USA

Tom Gallagher, University of Virginia, Charlottesville, VA, USA

Charles J. Joachain, Faculty of Science, Université Libre Bruxelles, Bruxelles, Belgium

Peter Lambropoulos, FORTH, IESL, University of Crete, Iraklion, Crete, Greece

Gerd Leuchs, Institut für Theoretische Physik I, Universität Erlangen-Nürnberg, Erlangen, Germany

Pierre Meystre, Optical Sciences Center, University of Arizona, Tucson, AZ, USA

The Springer Series on Atomic, Optical, and Plasma Physics covers in a comprehensive manner theory and experiment in the entire field of atoms and molecules and their interaction with electromagnetic radiation. Books in the series provide a rich source of new ideas and techniques with wide applications in fields such as chemistry, materials science, astrophysics, surface science, plasma technology, advanced optics, aeronomy, and engineering. Laser physics is a particular connecting theme that has provided much of the continuing impetus for new developments in the field, such as quantum computation and Bose-Einstein condensation. The purpose of the series is to cover the gap between standard undergraduate textbooks and the research literature with emphasis on the fundamental ideas, methods, techniques, and results in the field.

More information about this series at <http://www.springer.com/series/411>

Bo E. Sernelius

# Fundamentals of van der Waals and Casimir Interactions

 Springer

Bo E. Sernelius  
Linköping University  
Linköping, Sweden

ISSN 1615-5653                      ISSN 2197-6791 (electronic)  
Springer Series on Atomic, Optical, and Plasma Physics  
ISBN 978-3-319-99830-5              ISBN 978-3-319-99831-2 (eBook)  
<https://doi.org/10.1007/978-3-319-99831-2>

Library of Congress Control Number: 2018953297

© Springer Nature Switzerland AG 2018

This work is subject to copyright. All rights are reserved by the Publisher, whether the whole or part of the material is concerned, specifically the rights of translation, reprinting, reuse of illustrations, recitation, broadcasting, reproduction on microfilms or in any other physical way, and transmission or information storage and retrieval, electronic adaptation, computer software, or by similar or dissimilar methodology now known or hereafter developed.

The use of general descriptive names, registered names, trademarks, service marks, etc. in this publication does not imply, even in the absence of a specific statement, that such names are exempt from the relevant protective laws and regulations and therefore free for general use.

The publisher, the authors and the editors are safe to assume that the advice and information in this book are believed to be true and accurate at the date of publication. Neither the publisher nor the authors or the editors give a warranty, express or implied, with respect to the material contained herein or for any errors or omissions that may have been made. The publisher remains neutral with regard to jurisdictional claims in published maps and institutional affiliations.

This Springer imprint is published by the registered company Springer Nature Switzerland AG  
The registered company address is: Gewerbestrasse 11, 6330 Cham, Switzerland

# Preface

The material in this monograph has sprung out of my own research and courses I have given on the undergraduate and graduate levels at Linköping University during the last couple of decades.

The book is about dispersion interactions, also known as van der Waals and Casimir interactions. Most scientists know at least a little about van der Waals interactions but not so many have even heard of Casimir interactions. About seven decades ago, the Casimir forces were predicted to exist but the large interest they initially attracted faded away due to lack of reliable experimental verification. They had a renaissance about two decades ago when experimental technique had improved to such an extent that one could make quantitative comparison between theory and experiment. The interest then virtually exploded and Casimir interactions is now a research field of its own, across the globe. Both the van der Waals and Casimir interactions are of electromagnetic origin; they are induced interactions; one can say that they are siblings or two sides of the same coin, or limiting results of the same phenomenon. These interactions are important in physics, chemistry, biology, medicine, colloidal science, food industry, cosmetic industry, paint industry, construction industry (concrete reinforcement), and mining industry (gold enrichment using flotation); they are also important in, e.g., water purification and water desalination, and even in cosmology (dark energy). Since these interactions are active in so many different fields of science and technology, the formalism has developed in many parallel branches. This leads to a confusing diversity in the notation and in whom to give credit for each step in the development.

I derive the interactions beginning with the forces between individual atoms or molecules in gases and ending up with interactions in macroscopic structures. Force between objects is just one manifestation of the interactions; surface tension, surface energy, cohesion, adhesion, capillary forces, and binding of an object are other effects. I have limited the material to planar, spherical, and circular cylindrical structures. The formalism is based on electromagnetic normal modes. In this formalism, the van der Waals and Casimir forces originate in different types of modes: van der Waals forces involve surface modes; Casimir forces involve vacuum modes. The van der Waals interactions are obtained if one neglects retardation

effects, i.e., effects of the finite speed of light. In doing so, the formalism becomes much easier to handle. In the overwhelming majority of situations, one obtains good enough results in this approximate treatment. This has motivated me to devote one part of the book, Part II, to this approximate formalism, producing van der Waals interactions. Another part, Part III, treats the full formalism producing dispersion interactions, where van der Waals and Casimir interactions are found as different limiting cases. The intention is to have a self-contained book. Therefore, I have included a part, Part I, containing material needed from electromagnetism, complex analysis, statistical physics, and a chapter discussing the concept of normal modes in general and of electromagnetic normal modes in particular. This part also contains a chapter, Chap. 6, with a brief description of other approaches, not based on the normal modes.

This book is aimed at M.Sc. and Ph.D. students, last year M.Sc. students, Postdocs, teachers, and professional scientists. The book is suitable as the main text of a course, complimentary to more general courses in electromagnetism, surface physics, and condensed matter. Since the formalism is based on electromagnetic normal modes and I show how these are obtained, the book is also useful for scientists interested in the modes themselves, like those involved in plasmonics and nanoantennas. It may also be useful for physicists wanting to broaden their fields in the direction of biology and chemistry; this is in line with the general trend that the scientific focus shifts away from physics toward these other disciplines and especially toward interdisciplinary work.

Linköping, Sweden  
May 2018

Bo E. Sernelius

# Contents

<b>1</b>	<b>Introduction</b> .....	1
	References .....	5
<b>Part I Background Material</b>		
<b>2</b>	<b>Electromagnetism</b> .....	9
2.1	Maxwell's Equations .....	9
2.2	Unit System .....	11
2.3	Constitutive Relations .....	13
2.4	Potentials .....	16
2.5	Boundary Conditions .....	19
2.6	The Fresnel Equations .....	23
	2.6.1 Reflection and Transmission for Normal Incidence .....	23
	2.6.2 Oblique Incidence .....	25
	2.6.3 Anisotropic Media .....	30
2.7	Special Considerations for 2D Sheets .....	32
	2.7.1 Fourier Transforms of a Special Function .....	32
	2.7.2 Method of Images .....	33
	2.7.3 Screening Functions in a 2D System .....	39
2.8	Fields from a Time-Dependent Electric or Magnetic Dipole .....	42
	References .....	43
<b>3</b>	<b>Complex Analysis</b> .....	45
3.1	Analytic Functions .....	45
3.2	Laurent Expansion and Residues .....	47
3.3	Contour Integration in the Complex Plane .....	47
	3.3.1 Integration Around a Pole .....	48
	3.3.2 Argument Principle and Its Extension .....	50

3.4	Analytic Properties of Response Functions . . . . .	51
3.4.1	Kramers Kronig Dispersion Relations . . . . .	57
	Reference . . . . .	60
<b>4</b>	<b>Statistical Physics</b> . . . . .	61
4.1	Thermodynamic Potentials and Legendre Transformations . . . . .	61
4.2	Distribution Functions . . . . .	65
4.3	Internal Energy and Helmholtz Energy for System of Mass-Less Bosons . . . . .	66
	Reference . . . . .	68
<b>5</b>	<b>Electromagnetic Normal Modes</b> . . . . .	69
5.1	Normal Modes and Their Properties . . . . .	69
5.1.1	The Quantum Mechanical Harmonic Oscillator . . . . .	74
5.1.2	Classical Versus Quantum Systems . . . . .	80
5.2	Interaction from Normal Modes . . . . .	81
5.3	Different Mode Types . . . . .	85
5.3.1	Vacuum Modes . . . . .	86
5.3.2	Bulk Modes . . . . .	87
5.3.3	Surface Modes . . . . .	93
5.4	Modes for a Gap Between Two Half Spaces . . . . .	97
5.4.1	Transverse Magnetic Modes . . . . .	100
5.4.2	Transverse Electric Modes . . . . .	103
5.4.3	Modes in Non-retarded Treatment . . . . .	106
	References . . . . .	107
<b>6</b>	<b>Different Approaches</b> . . . . .	109
6.1	Summation of Pair Interactions . . . . .	109
6.2	Interactions Between Objects at Small Separations: The Proximity Force Approximation . . . . .	115
6.2.1	General Expression for Half Spaces, Cylinders and Spheres . . . . .	117
6.3	Many-Body Approach in Non-Retarded Treatment . . . . .	118
6.4	Many-Body Approach in Fully Retarded Treatment . . . . .	120
6.5	Brief Compilation of Methods or Approaches . . . . .	122
	References . . . . .	123
<b>7</b>	<b>General Method to Find the Normal Modes in Layered Structures</b> . . . . .	125
7.1	The Scheme . . . . .	125
	References . . . . .	131

**Part II Non-Retarded Formalism: van der Waals**

<b>8</b>	<b>Van der Waals Force</b> . . . . .	135
8.1	Equation of State for Ideal Gas . . . . .	135
8.1.1	2D Version . . . . .	137
8.2	Equation of State for Non-ideal Gas . . . . .	138
8.2.1	2D Version . . . . .	140
8.3	Van der Waals Force Between Two Atoms . . . . .	142
8.3.1	Zero Temperature . . . . .	145
8.3.2	Finite Temperature . . . . .	149
	References . . . . .	151
<b>9</b>	<b>Van der Waals Interaction in Planar Structures</b> . . . . .	153
9.1	Adapting the General Method of Chap. 7 to Planar Structures and to the Neglect of Retardation . . . . .	153
9.2	Basic Structure Elements . . . . .	156
9.2.1	Single Planar Interface . . . . .	156
9.2.2	Planar Layer . . . . .	157
9.2.3	2D Planar Film . . . . .	158
9.2.4	Thin Planar Diluted Gas Film . . . . .	159
9.3	Two Half Spaces . . . . .	159
9.3.1	Interaction Between Two Gold Half Spaces . . . . .	160
9.4	Two Slabs . . . . .	163
9.4.1	Interaction Between Two Gold Slabs . . . . .	164
9.5	Two 2D Films . . . . .	164
9.5.1	Interaction Between Two Graphene Sheets . . . . .	165
9.5.2	Interaction Between Two 2D Metal Films . . . . .	166
9.6	Film-Wall . . . . .	168
9.6.1	Interaction Between Graphene and an Au-Wall . . . . .	168
9.6.2	Interaction Between a 2D Metal Film and an Au-Wall . . . . .	169
9.7	Atom-Wall . . . . .	170
9.7.1	Li-Atom–Au-Wall Interaction . . . . .	171
9.8	Atom in Planar Gap . . . . .	172
9.9	Atom-Film . . . . .	174
9.9.1	Li-Atom–Graphene-Sheet Interaction . . . . .	175
9.9.2	Li-Atom–2D-Metal-Film Interaction . . . . .	176
9.10	Atom in Between Two Planar Films . . . . .	176
9.11	Alternative Derivations of the Normal Modes . . . . .	178
9.11.1	Two 2D Films . . . . .	178
9.11.2	A 2D Film Next to a Wall . . . . .	181
9.11.3	Two Half Spaces . . . . .	184
9.12	Interaction Between Two Atoms from Summation of Pair Interactions . . . . .	185

9.13	Spatial Dispersion . . . . .	187
9.13.1	The Formalism . . . . .	188
9.13.2	Electric Modes at a Single Interface . . . . .	192
9.13.3	Magnetic Modes at a Single Interface . . . . .	195
9.13.4	Electric Modes Associated with a Gap Between Two Half Spaces . . . . .	198
9.13.5	Magnetic Modes Associated with a Gap Between Two Half Spaces . . . . .	204
9.13.6	Van der Waals Interactions Between Two Half Spaces . . . . .	206
	References . . . . .	207
<b>10</b>	<b>Van der Waals Interaction in Spherical Structures . . . . .</b>	<b>209</b>
10.1	Adapting the General Method of Chap. 7 to Spherical Structures and to the Neglect of Retardation . . . . .	209
10.2	Basic Structure Elements . . . . .	212
10.2.1	Solid Sphere or Ball . . . . .	212
10.2.2	Spherical Shell . . . . .	213
10.2.3	Thin Spherical Diluted Gas Film . . . . .	214
10.2.4	2D Spherical Film . . . . .	215
10.3	Atom-Ball Interaction . . . . .	216
10.3.1	Li-Atom–Au-Ball Interaction . . . . .	218
10.4	Force on an Atom in a Spherical Cavity . . . . .	219
10.4.1	Force on a Li-Atom in a Spherical Gold Cavity . . . . .	220
10.5	van der Waals Interaction Between Two Atoms . . . . .	221
10.6	Force Between Two Spherical Objects . . . . .	221
10.6.1	Interaction Between Two Gold Balls . . . . .	222
10.6.2	Interaction Between Two Graphene Spheres . . . . .	222
10.7	Force on an Atom in a Spherical Gap . . . . .	223
10.8	Force on an Atom Outside a 2D Spherical Shell . . . . .	224
10.8.1	Interaction Between a Li-Atom and a Graphene Sphere . . . . .	226
10.9	Force on an Atom Inside a 2D Spherical Shell . . . . .	226
10.9.1	Force on a Li-Atom Inside a Graphene Sphere . . . . .	228
10.10	Interaction Between Two 2D Concentric Spherical Shells . . . . .	228
10.10.1	Interaction Between Two Concentric Graphene Spheres . . . . .	229
10.11	Force on an Atom in Between Two 2D Spherical Films . . . . .	230
10.12	Force Between Two Atoms from Summation of Pair Interactions . . . . .	231
	References . . . . .	232

**11 Van der Waals Interaction in Cylindrical Structures** . . . . . 233

11.1 Adapting the General Method of Chap. 7 to Cylindrical Structures and to the Neglect of Retardation . . . . . 233

11.2 Basic Structure Elements . . . . . 236

11.2.1 Solid Cylinder . . . . . 237

11.2.2 Cylindrical Shell . . . . . 237

11.2.3 Thin Cylindrical Diluted Gas Film . . . . . 238

11.2.4 2D Cylindrical Film . . . . . 239

11.3 Force on an Atom Outside a Cylinder . . . . . 241

11.3.1 Force Between a Li-Atom and a Gold Cylinder . . . . . 242

11.4 Force on an Atom in a Cylindrical Cavity . . . . . 243

11.4.1 Force on a Li-Atom in a Cylindrical Gold Cavity . . . . . 245

11.5 Force on an Atom in a Cylindrical Gap . . . . . 245

11.6 Force Between Two Cylindrical Objects . . . . . 247

11.6.1 Interaction Between Two Gold Cylinders . . . . . 247

11.7 Force on an Atom Outside a 2D Cylindrical Shell . . . . . 248

11.7.1 Interaction Between a Li-Atom and a Graphene Cylinder . . . . . 249

11.8 Force on an Atom Inside a 2D Cylindrical Shell . . . . . 250

11.8.1 Force on a Li-Atom Inside a Graphene Cylinder . . . . . 251

11.9 Interaction Between Two 2D Coaxial Cylindrical Shells . . . . . 251

11.9.1 Interaction Between Two Coaxial Cylindrical Graphene Shells . . . . . 252

11.10 Force on an Atom in Between Two 2D Coaxial Cylindrical Films . . . . . 253

References . . . . . 255

**Part III Fully Retarded Formalism: Casimir**

**12 Casimir Interaction** . . . . . 259

12.1 Casimir-Polder Interaction Between Two Atoms . . . . . 259

12.1.1 Zero Temperature Casimir-Polder Potential Between Two Atoms . . . . . 263

12.1.2 Finite Temperature Casimir-Polder Potential Between Two Atoms . . . . . 265

12.2 Equation of State for Casimir-Polder Gas . . . . . 268

References . . . . . 271

**13 Dispersion Interaction in Planar Structures** . . . . . 273

13.1 Adapting the General Method of Chap. 7 to Planar Structures . . . . . 273

13.2 Basic Structure Elements . . . . . 276

13.2.1 Single Planar Interface . . . . . 276

13.2.2 Planar Layer . . . . . 277

13.2.3	2D Planar Film . . . . .	279
13.2.4	Thin Planar Diluted Gas Film . . . . .	280
13.3	Two Half Spaces . . . . .	281
13.3.1	Interaction Between Two Gold Half Spaces . . . . .	281
13.4	Two Slabs . . . . .	282
13.4.1	Interaction Between Two Gold Slabs . . . . .	283
13.5	Two 2D Films . . . . .	284
13.5.1	Interaction Between Two Graphene Sheets . . . . .	285
13.5.2	Interaction Between Two 2D Metal Films . . . . .	287
13.6	Film-Wall . . . . .	288
13.6.1	Interaction Between Graphene and an Au-Wall . . . . .	289
13.6.2	Interaction Between a 2D Metal Film and an Au-Wall . . . . .	289
13.7	Atom-Wall . . . . .	291
13.7.1	Li-Atom–Au-Wall Interaction . . . . .	293
13.8	Atom in Planar Gap . . . . .	294
13.9	Atom-Film . . . . .	296
13.9.1	Li-Atom–Graphene-Sheet Interaction . . . . .	298
13.9.2	Li-Atom–2D-Metal-Film Interaction . . . . .	300
13.10	Atom in Between Two Planar Films . . . . .	301
13.11	Alternative Derivations of the Normal Modes . . . . .	303
13.11.1	Two 2D Films . . . . .	304
13.11.2	A 2D Film Next to a Wall . . . . .	308
13.11.3	Two Half Spaces . . . . .	310
13.12	Casimir Interaction Between Two Atoms from Summation of Pair Interactions . . . . .	311
13.13	Spatial Dispersion . . . . .	313
13.13.1	Modes at a Single Interface . . . . .	321
13.13.2	Modes Associated with a Gap Between Two Half Spaces . . . . .	326
13.13.3	Dispersion Interactions Between Two Gold Plates in Vacuum . . . . .	333
	References . . . . .	336
<b>14</b>	<b>Dispersion Interaction in Spherical Structures . . . . .</b>	<b>339</b>
14.1	Adapting the General Method of Chap. 7 to Spherical Structures . . . . .	339
14.2	Basic Structure Elements . . . . .	344
14.2.1	Solid Sphere or Ball . . . . .	345
14.2.2	Spherical Shell . . . . .	346
14.2.3	Thin Spherical Diluted Gas Film . . . . .	347
14.2.4	2D Spherical Film . . . . .	349

14.3	Coated Sphere in a Medium . . . . .	350
14.4	Atom-Ball Interaction . . . . .	350
14.4.1	Li-Atom–Au-Ball Interaction . . . . .	353
14.5	Force on an Atom in a Spherical Cavity . . . . .	354
14.5.1	Force on a Li-Atom in a Spherical Gold Cavity . . . . .	358
14.6	Casimir-Polder Interaction Between Two Atoms . . . . .	359
14.7	Force on an Atom in a Spherical Gap . . . . .	361
14.8	Force on an Atom Outside a 2D Spherical Shell . . . . .	362
14.8.1	Interaction Between a Li-Atom and a Graphene Sphere . . . . .	363
14.9	Force on an Atom Inside a 2D Spherical Shell . . . . .	364
14.9.1	Force on a Li-Atom Inside a Graphene Sphere . . . . .	365
14.10	Interaction Between Two 2D Spherical Shells . . . . .	365
14.10.1	Interaction Between Two Concentric Graphene Spheres . . . . .	367
14.11	Force on an Atom in Between Two 2D Spherical Films . . . . .	368
14.12	Force Between Two Atoms from Summation of Pair Interactions . . . . .	369
	References . . . . .	371
<b>15</b>	<b>Dispersion Interaction in Cylindrical Structures . . . . .</b>	<b>373</b>
15.1	Adapting the General Method of Chap. 7 to Cylindrical Structures . . . . .	373
15.2	Basic Structure Elements . . . . .	377
15.2.1	Solid Cylinder . . . . .	378
15.2.2	Thin Cylindrical Diluted Gas Film . . . . .	378
15.2.3	2D Cylindrical Film . . . . .	382
15.3	Force on an Atom Outside a Cylinder . . . . .	384
15.3.1	Force Between a Li-Atom and a Gold Cylinder . . . . .	389
15.4	Force on an Atom Outside a 2D Cylindrical Shell . . . . .	389
15.4.1	Interaction Between a Li-Atom and a Graphene Cylinder . . . . .	391
	References . . . . .	391
<b>16</b>	<b>Summary and Outlook . . . . .</b>	<b>393</b>
	<b>Appendix A: Interaction Power Laws Depending on Shape and Orientation. . . . .</b>	<b>397</b>
	<b>Appendix B: Transforming Between Unit Systems. . . . .</b>	<b>401</b>
	<b>Appendix C: The Fourier Transform . . . . .</b>	<b>403</b>
	<b>Appendix D: Dielectric Functions . . . . .</b>	<b>405</b>
	<b>Index . . . . .</b>	<b>411</b>

# Acronyms

2D	Two Dimensional
3D	Three Dimensional
a.u.	atomic units
ABC	Additional Boundary Condition
BC	Boundary Condition
CGS	Centimeter Gram Second
MC	Matching Condition
ME	Maxwell's Equation
MKSA	Meter Kilogram Second Ampère
PFA	Proximity Force Approximation
QED	Quantum Electrodynamics
QFT	Quantum Field Theory
RPA	Random Phase Approximation
SI	Système International (d'unités)
TE	Transverse Electric
TM	Transverse Magnetic
vdW	van der Waals

# Symbols

$\alpha$	Polarizability
$\alpha^{\text{at.}}$	Atomic dielectric polarizability
$\alpha_l^n$	$2^l$ pole polarizability at a spherical interface $n$
$\alpha_l^{n(2)}$	$2^l$ pole polarizability from inside a spherical interface $n$
$\alpha_{k,m}^n$	Multipole polarizability at a cylindrical interface $n$
$\alpha_{k,m}^{n(2)}$	Multipole polarizability from inside a cylindrical interface $n$
$\beta$	$1/k_B T$
$\beta^{\text{at.}}$	Atomic magnetic polarizability
$\gamma_i$	$\gamma_i(\mathbf{k}, \omega) = \sqrt{1 - (\tilde{n}_i \omega / ck)^2}$
$\gamma^{(0)}$	$\gamma^{(0)}(k, \omega) = \sqrt{1 - (\omega / ck)^2}$
$\varepsilon$	Dielectric function
$\tilde{\varepsilon}$	Extended dielectric function
$\zeta_i(z)$	Ricatti-Bessel function of the third kind
$\eta_i$	Wave impedance $\eta_i(\mathbf{k}, \omega) = \sqrt{\mu_i(\mathbf{k}, \omega) / \varepsilon_i(\mathbf{k}, \omega)}$
$\tilde{\eta}_i$	Extended wave impedance $\tilde{\eta}_i(\mathbf{k}, \omega) = \sqrt{\tilde{\mu}_i(\mathbf{k}, \omega) / \tilde{\varepsilon}_i(\mathbf{k}, \omega)}$
$\theta$	Heaviside step function
$\lambda_T$	thermal wave length, $\lambda_T = \sqrt{2\pi\hbar^2 \beta / m}$
$\mu$	Magnetic permeability, chemical potential
$\tilde{\mu}$	Extended magnetic permeability
$i\zeta$	Point along the imaginary axis in complex frequency plane
$\xi_i(z)$	Ricatti-Bessel function of the third kind
$\tilde{\Pi}$	Polarization tensor
$\chi_e$	Electric susceptibility
$\chi_m$	Magnetic susceptibility
$\chi_i(z)$	Ricatti-Bessel function of the second kind
$\psi_i(z)$	Ricatti-Bessel function of the first kind
$\Omega$	Volume of a 3D system

$\omega$	Point along the real axis in complex frequency plane
$A$	Area of a 2D system
$a_0$	Bohr radius
$\mathbf{B}$	Magnetic induction
$c$	Speed of light in vacuum
$\mathbf{D}$	Displacement
$\tilde{\mathbf{D}}$	Displacement in system with $\tilde{\epsilon}$
$\mathbf{E}$	Electric field
$E$	Internal energy
$e$	Electron charge without the minus sign
$e$	Exponential $e$
$\mathcal{E}$	Energy density stored in the electromagnetic fields
$\tilde{\mathcal{E}}$	The Helmholtz (free) energy
$G$	The Gibbs (free) energy
$\mathbf{H}$	Magnetic field
$\tilde{\mathbf{H}}$	Magnetic field in system with $\tilde{\mu}$
$H_v^{(1)}(z)$	Bessel function of the third kind, Hankel function
$H_v^{(2)}(z)$	Bessel function of the third kind, Hankel function
$\hbar$	Plank's constant divided by $2\pi$
$i$	Imaginary $i$
$I_m(z)$	Modified Bessel function
$\mathbf{J}$	Current density
$J_{\pm\nu}(z)$	Bessel function of the first kind
$K_m(z)$	Modified Bessel function
$\mathbf{K}$	Surface current density
$\mathbf{k}$	2D wave vector
$k_B$	Boltzmann constant
$m_e$	Electron mass
$n$	Index of refraction $n(\mathbf{k}, \omega) = \sqrt{\epsilon(\mathbf{k}, \omega)\mu(\mathbf{k}, \omega)}$
$\tilde{n}$	Extended index of refraction $\tilde{n}(k, \omega) = \sqrt{\tilde{\epsilon}(k, \omega)\tilde{\mu}(k, \omega)}$
$\mathfrak{P}$	The partition function
$\mathbf{q}$	3D wave vector
$W$	Wronskian $W[f(x), g(x)] = f(x)g(x)' - f(x)'g(x)$
$Y_\nu(z)$	Bessel function of the second kind
Subscripts	$\perp$ : vector component perpendicular to interface or in-plane component perpendicular to in-plane component $\mathbf{k}$ , $\parallel$ : vector component parallel to interface or in-plane component parallel to in-plane component $\mathbf{k}$ , $L$ : longitudinal version, i.e., parallel to $\mathbf{q}$ , $T$ : transverse version, i.e., perpendicular to $\mathbf{q}$
$z$	General point in complex frequency plane

# Chapter 1

## Introduction

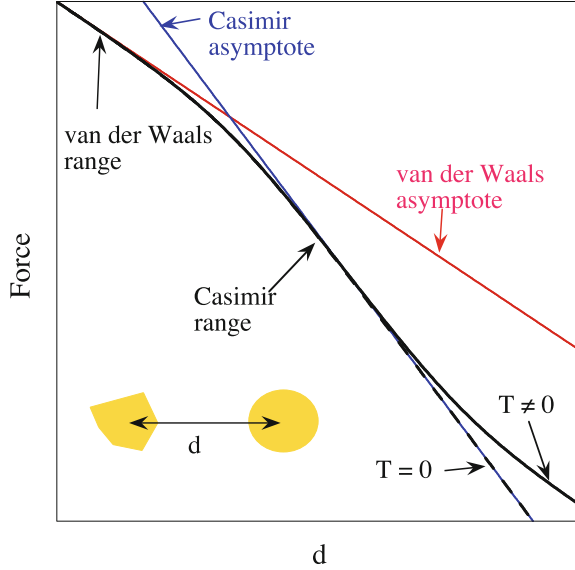


This book is about (electromagnetic) dispersion forces. These forces appear between all objects in the universe. They are weak but may still be the dominating forces on the micrometer and nanometer scales. They were first discovered empirically, for atoms and molecules, by J. D. van der Waals [1] in the 1870s in his research on liquids and gases. The origin of the forces was not understood until much later. F. London [2], gave the explanation in terms of fluctuating dipoles in 1930, an explanation that prevails today. The forces were named after van der Waals. The potential varies with distance,  $r$ , as  $r^{-6}$  and the attractive force as  $r^{-7}$ . The idea of intermolecular forces was not new and the correct distance dependence was predicted already by T. Young [3] in 1805; the correct origin of the interactions was proposed by P. N. Lebedev [4] in a speculative manner in 1894, inspired by the work by H. Hertz [5]. Generalization of these forces are acting between larger objects of mesoscopic and macroscopic size. Here, they are caused by fluctuations in the charge- and current-densities in the objects. The force depends on the shape and material of the objects. If the objects are submerged in a fluid the force can even be repulsive [6–8]. Even with vacuum in between the objects the force can in principle be repulsive for metamaterials of chiral type but the initial suggestions that the sign of the force in vacuum could be altered by metamaterials turned out to be unrealistic [9].

Two decades later than the date of London's explanation one realized that the forces drop off faster with distance beyond some separation value, characteristic of each system. This realization had its origin in the Netherlands in the 1940s where J. T. G. Overbeek performed experiments on suspensions of quartz powder. In order for the theory, that he and E. J. W. Verwey had developed for the stability of colloids, to work the long range forces had to fall off faster than as  $r^{-7}$ . He gave the problem to his students H. B. G. Casimir and D. Polder and they explained [10] it, for a pair of atoms, to be an effect of the finite speed of light.

Casimir was intrigued by the effect and wanted to explore it further by studying the most simple of systems. In 1948 he made a gedanken experiment [11] where he studied two ideal (totally reflecting) metal plates in vacuum. He found there is an attractive force between them. This force is called Casimir force. For real metal plates

**Fig. 1.1** Schematic illustration of the variation of the force between two objects with separation,  $d$ , on a log-log plot. This is the typical behavior for most systems at intermediate and large separations. For very small separations the interaction is modified when contact is approached. We have refrained from adding axis scales since these depend on the shape of the objects and the materials they are made from



this same force is found for large separations, beyond the characteristic separation value where retardation effects are in effect.

For a general system we call the interaction Casimir interaction at separations large enough for retardation effects to be in place; for shorter distances we call it van der Waals interaction.<sup>1</sup> When we refer to the interaction covering both the van der Waals and Casimir regions we refer to dispersion interactions. For atoms the interaction in the whole range with van der Waals and Casimir regions is called Casimir-Polder interaction.

When temperature is increased from zero, effects are noted first at very large separations; the interaction is enhanced. When the temperature is further enhanced the separation above which temperature effects are seen moves toward lower and lower values. The typical variation<sup>2</sup> of the force between two objects with separation,  $d$ , in a log-log plot is shown schematically in Fig. 1.1; in the Casimir gedanken experiment there is no van der Waals range; in the non-retarded treatment there is no Casimir range.

This was a very brief historical background of dispersion interactions. We refer the reader to review articles [12–16] and books [17–26] for a fuller presentation.

The present text is divided into three parts: background material, Part I, the non-retarded formalism, Part II, and the fully retarded formalism, Part III.

<sup>1</sup>This notation is not universal. Some call the Casimir interaction retarded van der Waals interaction and some call the van der Waals interaction non-retarded Casimir interaction.

<sup>2</sup>There are rare exceptions to this behavior. In the case of two pristine graphene sheets the van der Waals and Casimir asymptotes have the same slope.

Part I contains background material, material included to make the book as self-contained as possible. It includes some electromagnetism, some complex analysis, and some statistical physics. It furthermore contains a brief description of alternative methods to find the interactions. It ends with a chapter on normal modes in general and the electromagnetic normal modes in particular. It consists of six chapters, Chaps. 2–7. Chapter 2 treats electromagnetism and defines our electromagnetic notation and unit system; Chap. 3 is devoted to complex analysis and introduces the concept of analytic functions, discusses contour integration in the complex plane, the argument principle and its extensions, and the analytic properties of response functions; Chap. 4 presents a brief discussion of the various thermodynamic potentials that may be defined in a system of equilibrium, and gives the distribution functions for massive and massless particles; Chap. 5 introduces the concept of normal modes in general and of electromagnetic normal modes in particular, demonstrates how the modes lead to interactions, discusses modes of different types, and ends with the example of a system consisting of two half spaces separated by a gap; Chap. 6 is a compilation of alternative methods to attain the dispersion forces, ranging from the summation of pair interactions, especially useful in diluted systems, to the proximity force approximation that comes very handy at small distances between the objects, where other methods run into trouble; Chap. 7 does not really belong to the background material but it had to be placed here since it is the foundation on which the material in both Part II and Part III are built. This very short chapter sets the notation and gives a detailed prescription for how the normal modes can be found in a large number of layered structures. In the following parts this method is applied to three important examples, viz., planar, spherical, and circular-cylindrical layered systems.

Part II is devoted to the non-retarded formalism. This approximate formalism is much easier to use than the fully retarded formalism. In the majority of situations the non-retarded formalism produces good enough results. Part II contains four chapters, Chaps. 8–11. In Chap. 8 the equations of state for ideal and non-ideal gases are derived since this is where the interaction was discovered in the first place, followed by the derivation of the van der Waals interaction between two polarizable atoms. This last derivation is done in line with the general methods of Chap. 5 using both (5.57) and (5.59), with the same result. Numerical results are presented for some alkali-metal dimers. Chapters 9, 10, and 11 are devoted to planar, spherical, and cylindrical structures, respectively. Each chapter begins with an adaptation of Chap. 7 to the specific geometry in neglect of retardation. Then follows the treatment of the basic structure elements: a single interface; a layer; a 2D film; a diluted gas film. A general structure can be formed by stacking these basic elements on top of each other in the planar case; concentrically in the spherical case; coaxially in the cylindrical case. Two of these basic structure elements might need some comment: a 2D film could represent a very thin metallic layer, e.g., a metallic coating or a graphene or graphene like sheet; a diluted gas film is very useful as we will find later. It can be used to find the interaction experienced by an atom somewhere in the structure. At the end of Chap. 9 we have added three extra sections. In the first, Sect. 9.11, we present alternative derivations of the normal modes for some specific planar geometries; in the second, Sect. 9.12, we rederive the expression we found in Sect. 8.3 for the van

der Waals interaction between two atoms by applying the method of summation of pair interactions on the geometry of two half spaces; in the third, Sect. 9.13, we study the effects of spatial dispersion. Appendix A consists of two tables, Table A.1 and Table A.2. In Table A.1 we have compiled the power laws for the van der Waals interaction of objects and compared them to the prediction from the summation of pair interactions.

Part III is devoted to the fully retarded formalism. It contains five chapters, Chaps. 12–16. Chapter 12 begins with the derivation of the Casimir-Polder interaction between two polarizable atoms followed by the equation of state for a Casimir-Polder gas. The interaction is derived in line with the general methods of Chap. 5 using (5.59). Numerical results are presented for some alkali-metal dimers. In this chapter we also take the opportunity to discuss quantum and classical contributions. At zero temperature the dispersion interaction is a purely quantum mechanical effect. At finite temperature there is also a classical contribution. At very high temperatures and/or very large separations between two objects the classical contribution dominates. The interactions at finite temperature are derived in line with the general methods of Chap. 5 using (5.64). Chapters 13, 14, and 15 are devoted to planar, spherical, and cylindrical structures, respectively. Each chapter begins with an adaptation of Chap. 7 to the specific geometry. Then follows the treatment of the basic structure elements: a single interface; a layer; a 2D film; a diluted gas film. A general structure can be formed by stacking these basic elements on top of each other in the planar case; concentrically in the spherical case; coaxially in the cylindrical case. Two of these basic structure elements might need some comment: a 2D film could represent a very thin metallic layer, e.g., a metallic coating or a

graphene or graphene like sheet; a diluted gas film is very useful as we will find later. It can be used to find the interaction experienced by an atom somewhere in the structure. At the end of Chap. 13 we have added three extra sections. In the first, Sect. 13.11, we present alternative derivations of the normal modes for some specific planar geometries; in the second, Sect. 13.12, we rederive the expression we found in Sect. 12.1 for the Casimir interaction between two atoms by applying the method of summation of pair interactions on the atom-wall geometry; in the third, Sect. 13.13, we study the effects of spatial dispersion. At the end of Chap. 14 we have added an extra section, Sect. 14.12, where we rederive the full Casimir-Polder interaction between two atoms by applying the method of summation of pair interactions on the atom-ball geometry. Appendix A consists of two tables, Table A.1 and Table A.2. In Table A.2 we have compiled the power laws for the Casimir interaction between a number of objects and compared them to the prediction from the summation of pair interactions. Before the appendices we have added an extra chapter with a brief summary and some remarks.

Appendix B consists of Table B.1 which shows how expressions in CGS units translate into corresponding expressions in SI units. We have included this table to make life easier for readers that are unfamiliar with the CGS unit system. Appendix C specify our definition of the Fourier transform. There are several different varieties in the literature. They differ in the placement of factors of  $2\pi$  and/or sign conventions; we could have had a factor of  $\sqrt{2\pi}$  in the denominator of both the Fourier transform

and in the inverse Fourier transform to increase the formal symmetry; the convention in optics is to have a minus sign in the exponent inside the integral defining the temporal Fourier transform and a corresponding plus sign in the inverse transform; our opposite sign convention is more convenient for us since then a Fourier component characterized by  $(\mathbf{q}, \omega)$  is for positive  $\omega$  a plane wave moving in the  $\mathbf{q}$  direction; with the other sign convention it would move in the opposite direction. Appendix D lists a number of useful analytical expressions for dielectric functions used in the numerical calculations in the book.

## References

1. J.D. van der Waals, Ph.D. Thesis, University of Leiden (1873)
2. F. London, *Z. Phys., Chem. B* **11**, 222 (1930)
3. T. Young, *Philos. Trans. R. Soc. Lond.* **95**, 65 (1805)
4. P.N. Lebedev, *Wied. Ann.* **52**, 621 (1894); P.N. Lebedev, *Die Druckkräfte des Lichtes* (Engelmann, Leipzig, 1913)
5. H. Hertz, *Ann. Physik* **36**, 1 (1886)
6. I.E. Dzyaloshinskii, E.M. Lifshitz, P.P. Pitaevskii, The general theory of van der Waals forces. *Adv. Phys.* **10**, 165 (1961)
7. J.N. Munday, F. Capasso, V.A. Parsegian, Measured long-range repulsive Casimir-Lifshitz forces. *Nature* **457**, 170–173 (2009)
8. M. Boström, Bo E. Sernelius, I. Brevik, B.W. Ninham, Retardation turns the van der Waals attraction into a Casimir repulsion as close as 3 nm. *Phys. Rev. A* **85**, 010701 (2012)
9. A.P. McCauley et al., Microstructure effects for Casimir forces in chiral metamaterials. *Phys. Rev. B* **82**, 165108 (2010)
10. H.B.G. Casimir, D. Polder, *Phys. Rev.* **73**, 360 (1948)
11. H.B.G. Casimir, On the attraction between two perfectly conducting plates. *Proc. K. Ned. Akad. Wet.* **51**, 793 (1948)
12. K.A. Milton, *J. Phys. A: Math. Gen.* **37**, R209 (2004)
13. M. Bordag, U. Mohideen, V.M. Mostepanenko, *Phys. Rep.* **353**, 1 (2001)
14. G. Plunien, B. Müller, W. Greiner, *Phys. Rep.* **134**(2–3), 87 (1986)
15. S.K. Lamoreaux, *Rep. Prog. Phys.* **68**, 201 (2005)
16. L.M. Woods, D.A.R. Dalvit, A. Tkatchenko, P. Rodriguez-Lopez, A.W. Rodriguez, R. Podgornik, *Rev. Mod. Phys.* **88**, 128 045003 (2016)
17. J.N. Israelachvili, *Intermolecular and Surface Forces*, 3rd edn. (Academic Press, London, 2011)
18. P.W. Milonni, *The Quantum Vacuum* (Academic Press, New York, 1994)
19. D. Langbein, *Van der Waals Attraction* (Springer, Berlin, 1974)
20. J. Mahanty, B.W. Ninham, *Dispersion Forces* (Academic Press, London, 1976)
21. V.M. Mostepanenko, N.N. Trunov, *The Casimir Effect and Its Applications* (Oxford University Press, New York, 1997)
22. V.A. Parsegian, *Van der Waals Forces: A Handbook for Biologists, Chemists, Engineers, and Physicists* (Cambridge University Press, New York, 2005)
23. M.B. Bordag, G.L. Klimchitskaya, U. Mohideen, V.M. Mostepanenko, *Advances in the Casimir Effect* (Oxford University Press, Oxford, 2009)
24. S.Y. Buhmann, *Dispersion forces I: macroscopic quantum electrodynamics and ground-state Casimir, Casimir-Polder and van der Waals forces*, in *Springer Tracts in Modern Physics*, vol. 247 (Springer, Berlin, Heidelberg, 2012)
25. Bo E. Sernelius, *Surface Modes in Physics* (Wiley-VCH, 2001)
26. B.W. Ninham, P. Lo Nostro, *Molecular Forces and Self Assembly*, in *Colloid, Nano Sciences and Biology* (Cambridge University Press, Cambridge 2010)

**Part I**  
**Background Material**

The main material of this book is found in Part II and Part III. In order to have a reasonably self-contained presentation we have included this background part.

The formalism we use throughout is based on electromagnetic normal modes. The interactions we derive are all of electromagnetic origin. This demands that the reader has a solid knowledge in electromagnetism. We have included a chapter, Chap. 2, on electromagnetism to refresh the readers knowledge or to fill in any gaps. In many text books on electromagnetism metals are treated in an idealized way, where the conduction carriers screen out all electric fields. Here we have had to go beyond that simplified view and treat metals on the same footing as all other materials. The response of different materials, not the least metals, when subjected to electromagnetic fields of various frequencies is an important part of the formalism.

In many situations in our derivations we perform contour integrations in the complex frequency plane, e.g., when we use the argument principle to find the interactions. A solid course in complex analysis is not compulsory in the curriculum of every physics education. We have included a chapter, Chap. 3, on this subject and hope that this will add a new very useful tool to the readers toolbox, if it is not already there. It is also needed in the description of the analytical properties of the response functions of different materials.

We have also added a short chapter, Chap. 4, on statistical physics. This is needed to justify the origin of the zero point energy and why it is important for the interactions. It is also important for the motivation for what state functions determine the interaction at zero and at finite temperature.

One chapter, Chap. 5, is devoted to normal modes in general and electromagnetic normal modes in particular. The dispersion interactions at zero temperature is a quantum effect. We show why quantum effects appear in quantum systems and not in classical systems.

A short chapter, Chap. 6, briefly describes competing or complementing techniques used to find the dispersion interactions, not involving electromagnetic normal modes.

The last chapter, Chap. 7, describes our technique to find the normal modes in layered structures. It is valid for both the non-retarded and the fully retarded formalisms. This is the reason for placing the chapter here before the material is divided into those formalisms. Later the material is limited to the three most common geometries, viz., the planar, spherical, and circular cylindrical. Our technique can be applied to many more geometries.

# Chapter 2

## Electromagnetism



**Abstract** Since the interactions treated in this book all are of electromagnetic origin this chapter on electromagnetism takes a central part of the background material. We start, in Sect. 2.1 by discussing Maxwell's equations; we give these on differential form and also on Fourier transformed form. Then we motivate our choice of unit system, in Sect. 2.2. Next, in Sect. 2.3, we treat the constitutive relations relating the auxiliary fields,  $\mathbf{D}$  and  $\mathbf{H}$ , to the true fields,  $\mathbf{E}$  and  $\mathbf{B}$ ; here we also discuss the different versions of the auxiliary fields depending on the book keeping of the sources. In derivations, it is often easier to handle potentials instead of the fields themselves. This motivates the section, Sect. 2.4, on potentials in which we also discuss gauge transformations and in particular the Coulomb and Lorentz gauges. A very important factor for the formation of the normal modes of the system is how the fields behave at the boundary between regions. This is governed by the boundary conditions, Sect. 2.5. These, result in the Fresnel equations, Sect. 2.6. We have added a section, Sect. 2.7, on how to handle 2D sheets in the system. Finally, we end with the fields from time-dependent electric and magnetic dipoles, in Sect. 2.8; these are needed in the derivation of the Casimir-Polder interactions between atoms.

### 2.1 Maxwell's Equations

In principal, all we experience in our every-day life is of electromagnetic origin. At present, we believe that there are four fundamental interactions or forces in nature. These are the weak and strong nuclear forces, the gravitational force and the electromagnetic force. The nuclear forces are of very short range and are negligible outside the atom nucleus. The gravitational force is very weak and the force between two objects is negligible if not at least one of the objects is big as a planet. So here on earth all objects are attracted by earth but the attraction between the objects are negligible. The moon is big enough to cause the tide. Apart from these sparse gravitational effects all other effects are due to electromagnetism. Despite the huge variety

of effects electromagnetism is governed by a handful of fundamental equations, Maxwell's equations.

James Clerk Maxwell summarized the knowledge in electromagnetism in the form of four equations [1] that has come to be known as Maxwell's equations (MEs). They are relations between four fields, the electric field ( $\mathbf{E}$ ), the displacement field ( $\mathbf{D}$ ), the magnetic induction ( $\mathbf{B}$ ), and the magnetic field ( $\mathbf{H}$ ); two are fundamental fields,  $\mathbf{E}$  and  $\mathbf{B}$ , and two are auxiliary fields, or help fields,  $\mathbf{D}$  and  $\mathbf{H}$ . The standard form of MEs is

$$\begin{aligned}\nabla \cdot \mathbf{D} &= 4\pi \rho_f \\ \nabla \cdot \mathbf{B} &= 0 \\ \nabla \times \mathbf{E} + \frac{1}{c} \frac{\partial \mathbf{B}}{\partial t} &= 0 \\ \nabla \times \mathbf{H} - \frac{1}{c} \frac{\partial \mathbf{D}}{\partial t} &= \frac{4\pi}{c} \mathbf{J}_f,\end{aligned}\tag{2.1}$$

where  $c$  is the speed of light in vacuum and the sources  $\rho_f$  and  $\mathbf{J}_f$  are the charge and current density, respectively. The subscript  $f$  denotes free and indicates that the sources include the external ones and the conduction sources if any; bound sources are not included. The total charge and current densities in the system can in general be divided into three groups,

$$\begin{aligned}\rho_t &= \rho_{\text{ext}} + \rho_c + \rho_b, \\ \mathbf{J}_t &= \mathbf{J}_{\text{ext}} + \mathbf{J}_c + \mathbf{J}_b,\end{aligned}\tag{2.2}$$

where the subscripts  $t$ ,  $\text{ext}$ ,  $c$ , and  $b$  stand for total, external, conduction, and bound, respectively. The fields and source densities are all macroscopic averages; they are averaged over a volume as small as possible but still large compared to the volume per charge.

MEs and the  $\mathbf{D}$  and  $\mathbf{H}$  fields depend on how we look upon the different contributions to the charge and current densities; which are sources and which are part of the system itself. In the most extreme choice one considers the system be the vacuum and all charge and current densities be sources. Then the  $\mathbf{D}$  field is identical to the  $\mathbf{E}$  field and the  $\mathbf{H}$  field is identical to the  $\mathbf{B}$  field. The corresponding version of MEs is<sup>1</sup>

$$\begin{aligned}\nabla \cdot \mathbf{E} &= 4\pi \rho_t \\ \nabla \cdot \mathbf{B} &= 0 \\ \nabla \times \mathbf{E} + \frac{1}{c} \frac{\partial \mathbf{B}}{\partial t} &= 0 \\ \nabla \times \mathbf{B} - \frac{1}{c} \frac{\partial \mathbf{E}}{\partial t} &= \frac{4\pi}{c} \mathbf{J}_t.\end{aligned}\tag{2.3}$$

We want to be able to treat metals on the same footing as insulators so we let  $\rho_c$  and  $\mathbf{J}_c$  belong to the system and the only external sources are  $\rho_{\text{ext}}$  and  $\mathbf{J}_{\text{ext}}$ . The  $\mathbf{D}$  and  $\mathbf{H}$  fields are then different from what they are in the standard treatment. We denote this by entering a tilde above these vectors. Of course the true fields,  $\mathbf{E}$  and  $\mathbf{B}$ , are the same whatever version of MEs one chooses. The form we will use throughout is

---

<sup>1</sup>The microscopic version of MEs looks exactly like this but the fields and source densities are then not macroscopic averages.

$$\begin{aligned}
\nabla \cdot \tilde{\mathbf{D}} &= 4\pi \rho_{\text{ext}} \\
\nabla \cdot \mathbf{B} &= 0 \\
\nabla \times \mathbf{E} + \frac{1}{c} \frac{\partial \mathbf{B}}{\partial t} &= 0 \\
\nabla \times \tilde{\mathbf{H}} - \frac{1}{c} \frac{\partial \tilde{\mathbf{D}}}{\partial t} &= \frac{4\pi}{c} \mathbf{J}_{\text{ext}}.
\end{aligned} \tag{2.4}$$

Before we continue we ought to say some words about the unit system. The observant reader has noticed that we are not using the conventional SI unit system.

## 2.2 Unit System

We use Gaussian units, also known as CGS-units. This is not due to retrograde reasons. There is a very strong reason. This unit system is so much better when treating the fundamentals of electromagnetism. The SI unit system is good for electronics. Since SI units are the conventional ones we use them when we present numerical results; sometimes we use other systems more proper for the specific situation at hand, like atomic units or eV for energy and Å for distance.

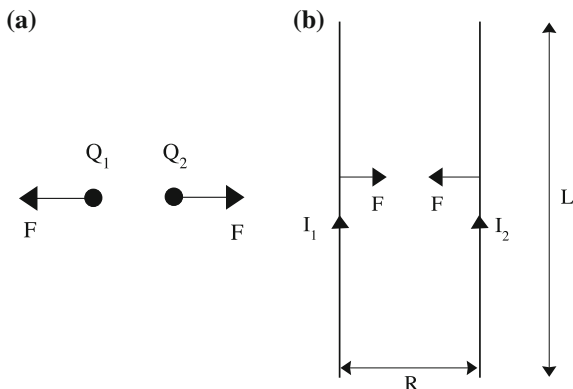
Some readers may be so attached to the SI system that they may feel lost. For those we have included a table in the appendix, Table B.1, with a prescription for how to transform an expression in CGS units into the corresponding expression in SI units.

First we compile a list of benefits from using the CGS units instead of the SI units, also known as rationalized MKSA units. Then we give a brief description of how unit systems are constructed.

### Advantages of CGS Compared to SI:

- Factors of speed of light appear explicitly and appropriately. We are helped by this in our formalism. When neglecting retardation effects we just let  $(\omega/cq)$  go toward zero, with the result that terms drop out from MEs and the formalism gets simplified; if we neglect magnetic effects we just let  $c$  go toward infinity in all expressions.
- $\mathbf{E}$  and  $\mathbf{D}$ , as well as  $\mathbf{H}$  and  $\mathbf{B}$ , become identical in vacuum. There are no “strange”  $\varepsilon_0$  or  $\mu_0$  appearing. This means that the difference between the auxiliary fields and their corresponding true fields is fully due to the medium. In SI units the auxiliary field and its true field are quite different in size and have different units.
- $\mathbf{E}$  and  $\mathbf{B}$  have the same amplitudes for plane waves in vacuum. This is very beneficial for the readers intuition since half of the energy carried by the wave is stored in the electric field and half in the magnetic field.
- It is easy to convert into atomic units: just let  $e$ ,  $m_e$  and  $\hbar$  be unity. Atomic units are very favorable for condensed matter physicists doing actual calculations on a computer; one has not to be afraid that numbers become too large or too small for the computer to handle. In all steps of the calculation the numbers are of the order of unity. When the calculations are done one just puts back the three constants.
- Relativistic electrodynamics is easily formulated.

**Fig. 2.1** Experiments used to determine unit systems: **a** Force between charges  $Q_1$  and  $Q_2$ ; **b** Force between currents  $I_1$  and  $I_2$ . See the text for details



The only advantages of SI as compared to CGS are that SI is chosen as the system of legal metrology and that most people have gotten so used to it.

### How are unit systems constructed?

One starts from two experiments:

1. The force between two charges  $Q_1$  and  $Q_2$ , the distance  $r$  apart, Fig. 2.1a.

$$F = k_e \frac{Q_1 Q_2}{r^2} \quad (2.5)$$

2. The force between two long, parallel, current carrying wires, of length  $L$ , the distance  $R$  apart, Fig. 2.1b.

$$F = k_m \frac{2I_1 I_2 L}{R} \quad (2.6)$$

The parameters  $k_e$  and  $k_m$  are two constants, where  $k_e/k_m = c^2$  and  $c$  is the speed of light in vacuum. One of the constants may be chosen at will.

In the construction of the SI system one chose the value of  $k_m$  by determining the unit of current, Ampère, by stating that the force per meter wire, for wires separated by 1 m is  $2 \times 10^{-7}$  N, when the current of 1 A is running through both wires. This seems like an odd choice to make! With this choice the currents running in our everyday wires are of the order of 1 A. This was the only reason for making that choice. This leads to  $k_m = 10^{-7}$  Vs/Am which in turn leads to  $k_e = 10^{-7} c^2$  Vs/Am.

These are awkward constants to carry around in the equations. Instead one introduced

$$\begin{cases} k_e = 1/4\pi\epsilon_0; \\ k_m = \mu_0/4\pi \end{cases} \rightarrow \mu_0\epsilon_0 = 1/c^2, \quad (2.7)$$

where  $\epsilon_0 = 8.8541878 \times 10^{-12}$  As/Vm, the dielectric constant of vacuum and  $\mu_0 = 4\pi \times 10^{-7}$  Vs/Am, the magnetic permeability of vacuum.

These numbers have nothing to do with some physical properties of vacuum. They are simply the result of the definition of the SI unit system. In CGS one chooses  $k_e = 1$  and no mysterious  $\epsilon_0$  or  $\mu_0$  appears. The basic units in SI are m, kg, s and Ampère. The basic units in CGS are cm, g, s and statcoulomb.

### 2.3 Constitutive Relations

The auxiliary fields are related to the true fields according to the constitutive relations. The  $\mathbf{D}$  and  $\mathbf{H}$  fields are defined as

$$\begin{aligned}\mathbf{D} &\equiv \mathbf{E} + 4\pi\mathbf{P}, \\ \mathbf{H} &\equiv \mathbf{B} - 4\pi\mathbf{M},\end{aligned}\tag{2.8}$$

where  $\mathbf{P}$  and  $\mathbf{M}$  are the polarization and magnetization of the medium, respectively. In most media there is a linear relation between  $\mathbf{P}$  and  $\mathbf{E}$  and between  $\mathbf{M}$  and  $\mathbf{H}$  as long as the fields are not too strong. These relations are in general not local. In a homogenous and isotropic medium the relations are

$$\begin{aligned}\mathbf{P}(\mathbf{r}, t) &= \int \int d^3r' dt' \chi_e(\mathbf{r} - \mathbf{r}', t - t') \mathbf{E}(\mathbf{r}', t'), \\ \mathbf{M}(\mathbf{r}, t) &= \int \int d^3r' dt' \chi_m(\mathbf{r} - \mathbf{r}', t - t') \mathbf{H}(\mathbf{r}', t'),\end{aligned}\tag{2.9}$$

where  $\chi_e$  and  $\chi_m$  are the electric and magnetic susceptibilities, respectively. These relations are so-called convolution integrals. They show that the polarization and magnetization depend on the electric field and the magnetic field, respectively in all points in space and in principle at all times. Now, we believe in causality which means that the polarization and magnetization can not depend on the electric fields at later times, in the future, only on present or past times. This means that  $\chi_e(\mathbf{r}, t) \propto \theta(t)$  and  $\chi_m(\mathbf{r}, t) \propto \theta(t)$ , where  $\theta(t)$  is the Heaviside step function. This is common for all so-called time-correlation functions describing the response of the system to a perturbation. The convolution integrals have the very nice property that

$$\begin{aligned}\mathbf{P}(\mathbf{q}, \omega) &= \chi_e(\mathbf{q}, \omega) \mathbf{E}(\mathbf{q}, \omega), \\ \mathbf{M}(\mathbf{q}, \omega) &= \chi_m(\mathbf{q}, \omega) \mathbf{H}(\mathbf{q}, \omega),\end{aligned}\tag{2.10}$$

i.e., the Fourier transforms (C.1) have this very nice multiplication rule. For this simple relation to hold in “ $\mathbf{r}$  and  $t$ ” space the Fourier transforms of the dielectric function and susceptibility must be constants, i.e., independent of frequency and momentum. This is a good approximation in some limited regions of the  $\omega q$  plane. For dielectrics (semiconductors or insulators) it is valid for small momenta and frequencies.

Now,

$$\begin{aligned}\mathbf{D}(\mathbf{q}, \omega) &= [1 + 4\pi \chi_e(\mathbf{q}, \omega)] \mathbf{E}(\mathbf{q}, \omega) = \varepsilon(\mathbf{q}, \omega) \mathbf{E}(\mathbf{q}, \omega), \\ \mathbf{B}(\mathbf{q}, \omega) &= [1 + 4\pi \chi_m(\mathbf{q}, \omega)] \mathbf{H}(\mathbf{q}, \omega) = \mu(\mathbf{q}, \omega) \mathbf{H}(\mathbf{q}, \omega),\end{aligned}\tag{2.11}$$

where the dielectric function and magnetic permeability are defined by:

$$\begin{aligned}\varepsilon(\mathbf{q}, \omega) &\equiv 1 + 4\pi \chi_e(\mathbf{q}, \omega), \\ \mu(\mathbf{q}, \omega) &\equiv 1 + 4\pi \chi_m(\mathbf{q}, \omega).\end{aligned}\tag{2.12}$$

If the system is anisotropic the susceptibilities are tensors. Then the dielectric function and magnetic permeability are also tensors and the term 1 in their definitions above is replaced by a unit tensor.

All vector fields,  $\mathbf{F}(\mathbf{q}, \omega)$ , can be divided into a longitudinal,  $\mathbf{F} \parallel \mathbf{q}$ , and a transverse,  $\mathbf{F} \perp \mathbf{q}$ , part,

$$\begin{aligned}\mathbf{F} &= \mathbf{F}_T + \mathbf{F}_L, \\ \nabla \cdot \mathbf{F}_T &= 0, \\ \nabla \times \mathbf{F}_L &= 0.\end{aligned}\tag{2.13}$$

The response of the system is in general different for longitudinal and transverse fields. This means that the dielectric function and magnetic permeability both have longitudinal and transverse versions. In the limit of small  $q$  the versions coincide. Most, but not all, electromagnetic problems occur in this limit since the relevant photon momentum is so extremely small. We will in the main part of the text drop the subscript  $L$  or  $T$  on the material functions but we should keep in mind that in relations involving longitudinal and transverse fields the longitudinal and transverse versions, respectively should be used.

It is useful to have the relation between the magnetization and the magnetization-current-density and between the polarization and induced charge density. So far we have only considered bound charges and for these the relations are

$$\begin{aligned}\nabla \times \mathbf{M}_b &= \frac{1}{c} \mathbf{J}_b^m, \\ \nabla \cdot \mathbf{P}_b &= -\rho_b.\end{aligned}\tag{2.14}$$

Note that the magnetization-current-density is a transverse vector field. When we discuss the unbound carriers in conducting media we find the analogous relations for these by just replacing the subscript  $b$  with  $c$ .

We need two more equations. The first is the equation of continuity,

$$\frac{\partial \rho}{\partial t} + \nabla \cdot \mathbf{J} = 0.\tag{2.15}$$

This equation is valid for the total densities, or for the separate parts of the densities. Then in particular

$$\frac{\partial \rho_c}{\partial t} + \nabla \cdot \mathbf{J}_c = 0.\tag{2.16}$$

Let  $\mathbf{J}_c$  from now on denote the polarization current in the unbound carriers. The magnetization current will carry a superscript  $m$ .

The second equation is Ohm's law,

$$\mathbf{J}_c(\mathbf{q}, \omega) = \sigma(\mathbf{q}, \omega) \mathbf{E}(\mathbf{q}, \omega), \quad (2.17)$$

where  $\sigma(\mathbf{q}, \omega)$  is the conductivity.

Because of the non-local character of the response functions it is often favorable to work in Fourier space. MEs and other differential equations will also be more easy to handle. Transformation to Fourier space is done using the transformations given in (C.2).

Let us now start from (2.3) after the MEs have been Fourier transformed,

$$\begin{aligned} \mathbf{iq} \cdot \mathbf{E} &= 4\pi \rho_t = 4\pi (\rho_{\text{ext}} + \rho_b + \rho_c), \\ \mathbf{iq} \cdot \mathbf{B} &= 0, \\ \mathbf{iq} \times \mathbf{E} - \frac{i\omega}{c} \mathbf{B} &= 0, \\ \mathbf{iq} \times \mathbf{B} + \frac{i\omega}{c} \mathbf{E} &= \frac{4\pi}{c} \mathbf{J}_t = \frac{4\pi}{c} (\mathbf{J}_b^m + \mathbf{J}_c^m + \mathbf{J}_{\text{ext}} + \mathbf{J}_b + \mathbf{J}_c). \end{aligned} \quad (2.18)$$

Note that we have included the magnetization currents from bound and unbound carriers. Next we make the substitution  $\rho_b = -\mathbf{iq} \cdot \mathbf{P}_b$  in the first equation and  $\mathbf{J}_b = -i\omega \mathbf{P}_b$  in the fourth and combine with  $\mathbf{E}$  on the left side. We furthermore make the substitution  $\mathbf{J}_b^m = c\mathbf{iq} \times \mathbf{M}_b$  in the fourth line and combine with  $\mathbf{B}$  on the left side

$$\begin{aligned} \mathbf{iq} \cdot \mathbf{D} &= 4\pi \rho_f = 4\pi (\rho_{\text{ext}} + \rho_c), \\ \mathbf{iq} \cdot \mathbf{B} &= 0, \\ \mathbf{iq} \times \mathbf{E} - \frac{i\omega}{c} \mathbf{B} &= 0, \\ \mathbf{iq} \times \mathbf{H} + \frac{i\omega}{c} \mathbf{D} &= \frac{4\pi}{c} \mathbf{J}_f = \frac{4\pi}{c} (\mathbf{J}_c^m + \mathbf{J}_{\text{ext}} + \mathbf{J}_c). \end{aligned} \quad (2.19)$$

Next we make the substitution  $\rho_c = -\mathbf{iq} \cdot \mathbf{P}_c$  in the first equation and  $\mathbf{J}_c = -i\omega \mathbf{P}_c$  in the fourth and combine with  $\mathbf{D}$  on the left side. We furthermore make the substitution  $\mathbf{J}_c^m = c\mathbf{iq} \times \mathbf{M}_c$  in the fourth line and combine with  $\mathbf{H}$  on the left side

$$\begin{aligned} \mathbf{iq} \cdot \tilde{\mathbf{D}} &= 4\pi \rho_{\text{ext}}, \\ \mathbf{iq} \cdot \mathbf{B} &= 0, \\ \mathbf{iq} \times \mathbf{E} - \frac{i\omega}{c} \mathbf{B} &= 0, \\ \mathbf{iq} \times \tilde{\mathbf{D}} + \frac{i\omega}{c} \tilde{\mathbf{D}} &= \frac{4\pi}{c} \mathbf{J}_{\text{ext}}. \end{aligned} \quad (2.20)$$

The constitutive relations for the two formalisms is summarized in the following equation:

$$\begin{aligned} \mathbf{D} &= \mathbf{E} + 4\pi \mathbf{P}_b = \varepsilon \mathbf{E}, \\ \mathbf{H} &= \mathbf{B} - 4\pi \mathbf{M}_b = \mathbf{B}/\mu, \\ \tilde{\mathbf{D}} &= \mathbf{E} + 4\pi \mathbf{P}_b + 4\pi \mathbf{P}_c = \varepsilon \mathbf{E} + 4\pi \mathbf{P}_c = \tilde{\varepsilon} \mathbf{E}, \\ \tilde{\mathbf{H}} &= \mathbf{B} - 4\pi \mathbf{M}_b - 4\pi \mathbf{M}_c = \mathbf{B}/\mu - 4\pi \mathbf{M}_c = \mathbf{B}/\tilde{\mu}. \end{aligned} \quad (2.21)$$

Now we determine the dielectric function  $\tilde{\varepsilon}$  using Ohm's law and the equation of continuity. Ohm's law gives that the substitution we made in the fourth line becomes  $-i\omega\mathbf{P}_c(\mathbf{q}, \omega) = \mathbf{J}_c(\mathbf{q}, \omega) = \sigma(\mathbf{q}, \omega)\mathbf{E}(\mathbf{q}, \omega)$  and  $4\pi\mathbf{P}_c(\mathbf{q}, \omega) = (4\pi i/\omega)\sigma(\mathbf{q}, \omega) \times \mathbf{E}(\mathbf{q}, \omega)$ . The substitution in the first line becomes  $\rho_c(\mathbf{q}, \omega) = \mathbf{q} \cdot \mathbf{J}_c(\mathbf{q}, \omega) / \omega = \sigma(\mathbf{q}, \omega) \mathbf{q} \cdot \mathbf{E}(\mathbf{q}, \omega) / \omega$ . Both demonstrate that the full dielectric function for a conducting medium is

$$\tilde{\varepsilon}(\mathbf{q}, \omega) = \varepsilon(\mathbf{q}, \omega) + \frac{4\pi i}{\omega} \sigma(\mathbf{q}, \omega). \quad (2.22)$$

Let us now distinguish between longitudinal and transverse functions. The first two equations in (2.20) involve longitudinal fields. The third can be separated into two, one transverse and one longitudinal; the longitudinal just gives  $\mathbf{B}_L = 0$ , i.e. redundant with the second equation. The fourth can be separated into two, one transverse and one longitudinal. The longitudinal is  $(i\omega/c)\tilde{\mathbf{D}}_L = (4\pi/c)\mathbf{J}_{\text{ext},L}$ . We operate on both sides with  $(c/\omega)\mathbf{q} \cdot$  and find  $i\mathbf{q} \cdot \tilde{\mathbf{D}}_L = (4\pi/\omega)\mathbf{q} \cdot \mathbf{J}_{\text{ext},L} = 4\pi\rho_{\text{ext}}$ , i.e. identical to the first equation. In the last step we used the equation of continuity in (2.15). Thus we have

$$\begin{aligned} i\mathbf{q}\tilde{\mathbf{D}}_L &= i\mathbf{q}\tilde{\varepsilon}_L E_L = 4\pi\rho_{\text{ext}}, \\ i\mathbf{q}\mathbf{B}_L &= 0, \\ i\mathbf{q} \times \mathbf{E}_T - \frac{i\omega}{c}\mathbf{B}_T &= 0, \\ i\mathbf{q} \times \tilde{\mathbf{H}}_T + \frac{i\omega}{c}\tilde{\mathbf{D}}_T &= i\mathbf{q} \times \mathbf{B}_T / \tilde{\mu}_T + \frac{i\omega}{c}\tilde{\varepsilon}_T \mathbf{E}_T = \frac{4\pi}{c}\mathbf{J}_{\text{ext},T}, \end{aligned} \quad (2.23)$$

where

$$\begin{aligned} \tilde{\varepsilon}_L(\mathbf{q}, \omega) &= \varepsilon_L(\mathbf{q}, \omega) + \frac{4\pi i}{\omega} \sigma_L(\mathbf{q}, \omega), \\ \tilde{\varepsilon}_T(\mathbf{q}, \omega) &= \varepsilon_T(\mathbf{q}, \omega) + \frac{4\pi i}{\omega} \sigma_T(\mathbf{q}, \omega). \end{aligned} \quad (2.24)$$

## 2.4 Potentials

In many cases it is easier to deal with potentials than with the vector fields. So we devote this section to potentials. Let us now start from the two homogeneous MEs. The first equation,

$$\nabla \cdot \mathbf{B} = 0, \quad (2.25)$$

is fulfilled if we let<sup>2</sup>

$$\mathbf{B} = \nabla \times \mathbf{A}. \quad (2.26)$$

Let us now make use of this relation in the second of the homogeneous MEs

$$\nabla \times \left( \mathbf{E} + \frac{1}{c} \frac{\partial \mathbf{A}}{\partial t} \right) = 0. \quad (2.27)$$

---

<sup>2</sup>The divergence of a curl is zero.

This is fulfilled<sup>3</sup> if what is inside the parentheses is the gradient of a scalar,  $\Phi$ . Thus for a choice of potentials the fields are obtained from the relations

$$\begin{aligned}\mathbf{E} &= -\nabla\Phi - \frac{1}{c}\frac{\partial\mathbf{A}}{\partial t}, \\ \mathbf{B} &= \nabla \times \mathbf{A}.\end{aligned}\tag{2.28}$$

From these relations we see that the  $\mathbf{B}$ -field is always purely transverse. Furthermore, the first term of the  $\mathbf{E}$ -field is longitudinal and the second term can have both longitudinal and transverse parts.

We still have a rather large flexibility to choose the potentials to fit our particular problem, but a change in the scalar potential,  $\Phi$ , has to be accompanied by a change in the vector potential,  $\mathbf{A}$ , and vice versa. Let us assume that we have made a choice of  $\mathbf{A}$  and  $\Phi$ . Adding a gradient of a scalar function to  $\mathbf{A}$  will not change  $\mathbf{B}$ . We are allowed to change the potentials in the following way:

$$\begin{aligned}\mathbf{A} &\rightarrow \mathbf{A}' = \mathbf{A} + \nabla\Lambda, \\ \Phi &\rightarrow \Phi' = \Phi - \frac{1}{c}\frac{\partial\Lambda}{\partial t}.\end{aligned}\tag{2.29}$$

These transformations are called gauge transformations. The fields, the real quantities, are not changed with such transformations; only the potentials, the auxiliary functions, are. Let us now turn to the remaining MEs, the inhomogeneous ones. For simplicity we assume vacuum, or use the version in (2.3). We have

$$\begin{aligned}\nabla \cdot \left(\nabla\Phi + \frac{1}{c}\frac{\partial\mathbf{A}}{\partial t}\right) &= -4\pi\rho, \\ \nabla \times (\nabla \times \mathbf{A}) + \frac{1}{c}\frac{\nabla\partial\Phi}{\partial t} + \frac{1}{c^2}\frac{\partial^2\mathbf{A}}{\partial t^2} &= \frac{4\pi}{c}\mathbf{J},\end{aligned}\tag{2.30}$$

which may be rewritten as<sup>4</sup>

$$\begin{aligned}\nabla^2\Phi + \frac{1}{c}\frac{\partial}{\partial t}(\nabla \cdot \mathbf{A}) &= -4\pi\rho, \\ \nabla(\nabla \cdot \mathbf{A}) - \nabla^2\mathbf{A} + \frac{1}{c}\frac{\nabla\partial\Phi}{\partial t} + \frac{1}{c^2}\frac{\partial^2\mathbf{A}}{\partial t^2} &= \frac{4\pi}{c}\mathbf{J},\end{aligned}\tag{2.31}$$

and after rearrangements in the second one we have

$$\begin{aligned}\nabla^2\Phi + \frac{1}{c}\frac{\partial}{\partial t}(\nabla \cdot \mathbf{A}) &= -4\pi\rho, \\ \nabla^2\mathbf{A} - \frac{1}{c^2}\frac{\partial^2\mathbf{A}}{\partial t^2} - \nabla(\nabla \cdot \mathbf{A} + \frac{1}{c}\frac{\partial\Phi}{\partial t}) &= -\frac{4\pi}{c}\mathbf{J}.\end{aligned}\tag{2.32}$$

These are two coupled differential equations; each of them contains both  $\mathbf{A}$  and  $\Phi$ . They can be decoupled by proper gauge transformations. In Coulomb gauge or transverse gauge we choose

$$\nabla \cdot \mathbf{A} = 0.\tag{2.33}$$

<sup>3</sup>The curl of a gradient is zero.

<sup>4</sup>For Cartesian coordinates  $\nabla \times (\nabla \times \mathbf{A}) = \nabla(\nabla \cdot \mathbf{A}) - \nabla^2\mathbf{A}$  is a valid replacement.

With this choice the vector potential is purely transverse. This means that the first equation in (2.28) can be seen as a separation of longitudinal and transverse parts for the  $\mathbf{E}$ -field; the first term is longitudinal and the second transverse. The scalar potential satisfies Poisson's equation:

$$\nabla^2 \Phi = -4\pi\rho. \quad (2.34)$$

This means that the scalar potential is instantaneous. There are no retardation effects for the scalar potential. So if for example someone on the moon were to play around with some charges, the potential would here on earth change immediately, without any time delay as if information could be transferred faster than with the speed of light. We will now get rid of the scalar potential from the equation for the vector potential. Let us take the time derivative of Poisson's equation. We have

$$\nabla \cdot \left( \nabla \frac{\partial \Phi}{\partial t} \right) = -4\pi \frac{\partial \rho}{\partial t}. \quad (2.35)$$

The equation of continuity, is valid for the free charge densities and currents, for the induced quantities, and for the total ones. Thus we have

$$\nabla \cdot \left( \nabla \frac{\partial \Phi}{\partial t} \right) = 4\pi \nabla \cdot \mathbf{J}. \quad (2.36)$$

This means that the longitudinal parts of  $\nabla \partial \Phi / \partial t$  and  $4\pi \mathbf{J}$  are the same. Since the first is purely longitudinal, in the present choice of gauge, we have

$$\nabla \frac{\partial \Phi}{\partial t} = 4\pi \mathbf{J}_L. \quad (2.37)$$

We have divided the current density into transverse and longitudinal parts:

$$\begin{aligned} \mathbf{J} &= \mathbf{J}_T + \mathbf{J}_L, \\ \nabla \cdot \mathbf{J}_T &= 0, \\ \nabla \times \mathbf{J}_L &= 0. \end{aligned} \quad (2.38)$$

Thus the decoupled differential equations for the potentials are in Coulomb gauge:

$$\begin{aligned} \nabla^2 \Phi &= -4\pi\rho, \\ \nabla^2 \mathbf{A} - \frac{1}{c^2} \frac{\partial^2 \mathbf{A}}{\partial t^2} &= -\frac{4\pi}{c} \mathbf{J}_T. \end{aligned} \quad (2.39)$$

From this follows the corresponding Fourier transformed relations,

$$\begin{aligned} \Phi(\mathbf{q}, \omega) &= \frac{4\pi\rho(\mathbf{q}, \omega)}{q^2}; \\ \mathbf{A}(\mathbf{q}, \omega) &= \frac{4\pi\mathbf{J}_T(\mathbf{q}, \omega)}{cq^2} \frac{1}{1 - (\omega/cq)^2}. \end{aligned} \quad (2.40)$$

Another common gauge is the Lorentz gauge. In this case we put

$$\nabla \cdot \mathbf{A} + \frac{1}{c} \frac{\partial \Phi}{\partial t} = 0, \quad (2.41)$$

and get

$$\begin{aligned} \nabla^2 \Phi - \frac{1}{c^2} \frac{\partial^2 \Phi}{\partial t^2} &= -4\pi \rho, \\ \nabla^2 \mathbf{A} - \frac{1}{c^2} \frac{\partial^2 \mathbf{A}}{\partial t^2} &= -\frac{4\pi}{c} \mathbf{J}. \end{aligned} \quad (2.42)$$

On Fourier transformed form the equations are

$$\begin{aligned} \Phi(\mathbf{q}, \omega) &= \frac{4\pi \rho(\mathbf{q}, \omega)}{q^2} \frac{1}{1 - (\omega/cq)^2}; \\ \mathbf{A}(\mathbf{q}, \omega) &= \frac{4\pi \mathbf{J}(\mathbf{q}, \omega)}{cq^2} \frac{1}{1 - (\omega/cq)^2}. \end{aligned} \quad (2.43)$$

We note that in Lorentz gauge the scalar potential and all Cartesian components of the vector potential obey the wave equation and show retardation effects.

We should keep in mind that the potentials are auxiliary functions, help functions. The real functions are the  $\mathbf{E}$ - and  $\mathbf{B}$ -fields. These are the same whatever gauge we choose and show retardation effects. Note that it is the factor  $1/[1 - (\omega/cq)^2]$  in (2.40) and (2.43) that make the potentials retarded. Letting  $(\omega/cq)$  go toward zero removes the retardation effects.

## 2.5 Boundary Conditions

In this section we will derive the very useful boundary conditions at an interface between two media.

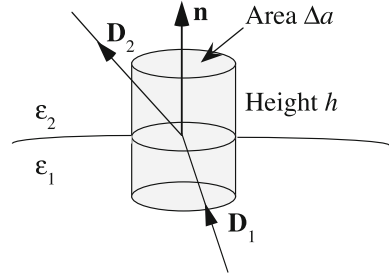
Throughout this book we make the basic approximation that the interfaces are perfectly smooth in the parallel directions and perfectly abrupt in the perpendicular direction. We assume that the material parameters,  $\varepsilon$ ,  $\tilde{\varepsilon}$ ,  $\mu$ , and  $\tilde{\mu}$ , are valid all the way up to the interface so that the constitutive relations for the fields can be used very close to the interface. This is clearly an approximation since the fields and the material parameters are macroscopic quantities.

We will now use the result we have found for Maxwell's macroscopic field equations in the case of charge- and current-distributions to find the boundary conditions for the fields at boundaries between regions of different materials.

We start with the  $\mathbf{D}$ -fields and Maxwell's first equation, Gauss' law, (all three versions),

$$\begin{aligned} \nabla \cdot \tilde{\mathbf{D}} &= 4\pi \rho_{\text{ext}}, \\ \nabla \cdot \mathbf{D} &= 4\pi \rho_f, \\ \nabla \cdot \mathbf{E} &= 4\pi \rho_t, \end{aligned} \quad (2.44)$$

**Fig. 2.2** A Gaussian “pillbox” of volume  $V$ , height  $h$  and bottom-and-top area  $\Delta a$  placed over the interface between regions 1 and 2



and integrate the equations over a small pillbox of volume  $V$  centered on the interface with its two flat surfaces parallel to the interface as illustrated in Fig. 2.2

$$\begin{aligned}
 \oint_S \tilde{\mathbf{D}} \cdot \mathbf{n} dS &= \leftarrow \left[ \int_V \nabla \cdot \tilde{\mathbf{D}} = \int_V 4\pi \rho_{\text{ext}} \right]_{\rightarrow} = 4\pi q_{\text{ext}} \\
 \oint_S \mathbf{D} \cdot \mathbf{n} dS &= \leftarrow \left[ \int_V \nabla \cdot \mathbf{D} = \int_V 4\pi \rho_f \right]_{\rightarrow} = 4\pi q_f \\
 \oint_S \mathbf{E} \cdot \mathbf{n} dS &= \leftarrow \left[ \int_V \nabla \cdot \mathbf{E} = \int_V 4\pi \rho_t \right]_{\rightarrow} = 4\pi q_t
 \end{aligned} \tag{2.45}$$

The notation we use here means the following: we start with the main equation inside the brackets; then in general we perform derivations and simplifications of the right hand side in one or several steps in the right direction; the derivations of the left hand side is performed in the left direction. In this example we only need one derivation in each direction. The one to the right is trivial; in the one to the left we use the Gauss (divergence) theorem.<sup>5</sup>

Let the height  $h$  be very small so that the area of the curved surface of the cylinder is negligible compared to those of the flat surfaces. This gives for a small “pill box”

$$\begin{aligned}
 [\tilde{\mathbf{D}}_2 \cdot \mathbf{n} - \tilde{\mathbf{D}}_1 \cdot \mathbf{n}] \Delta a &= 4\pi (\rho_s)_{\text{ext}} \Delta a, \\
 [\mathbf{D}_2 \cdot \mathbf{n} - \mathbf{D}_1 \cdot \mathbf{n}] \Delta a &= 4\pi (\rho_s)_f \Delta a, \\
 [\mathbf{E}_2 \cdot \mathbf{n} - \mathbf{E}_1 \cdot \mathbf{n}] \Delta a &= 4\pi (\rho_s)_t \Delta a.
 \end{aligned} \tag{2.46}$$

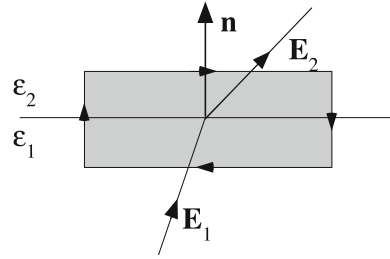
After eliminating  $\Delta a$  we find

$$\begin{aligned}
 [\tilde{\mathbf{D}}_2 - \tilde{\mathbf{D}}_1] \cdot \mathbf{n} &= 4\pi (\rho_s)_{\text{ext}}, \\
 [\mathbf{D}_2 - \mathbf{D}_1] \cdot \mathbf{n} &= 4\pi (\rho_s)_f, \\
 [\mathbf{E}_2 - \mathbf{E}_1] \cdot \mathbf{n} &= 4\pi (\rho_s)_t = 4\pi \rho_s.
 \end{aligned} \tag{2.47}$$

Thus, we find that if there is no external charge density at the interface the normal component of  $\tilde{\mathbf{D}}$  is continuous across the interface. If, on the other hand, there is an

<sup>5</sup>Gauss’ divergence theorem:  $\int_V \nabla \cdot \mathbf{A} dv = \oint_S \mathbf{A} \cdot \mathbf{n} dS$ .

**Fig. 2.3** A Stokesian rectangle at the interface between regions 1 and 2



external charge density at the interface there is a jump in the normal component equal to  $4\pi$  times the external surface-charge density. Similarly, if there is no free surface charge density at the interface, which is most often the case at an interface between two dielectrics, the normal component of  $\mathbf{D}$  is continuous across the interface. For metallic systems there are, with high probability, free surface charge densities at the interface and then the jump in the normal component of the  $\mathbf{D}$ -field is just  $4\pi$  times the free surface-charge density. Finally, if the total surface-charge density, i.e., the contribution from external charges, conduction charges and bound charges, reduce to zero the normal component of  $\mathbf{E}$  is continuous across the interface. Otherwise, the jump is equal to  $4\pi$  times the total surface-charge density.

Next we turn to the  $\mathbf{B}$ -field and Maxwell's second equation,

$$\nabla \cdot \mathbf{B} = 0. \quad (2.48)$$

There are no sources in this case. We may use exactly the same derivations as for the electric fields and find that the normal component of  $\mathbf{B}$  is always continuous across an interface.

Now we are done with the normal components and continue with the tangential components. We begin with the  $\mathbf{E}$ -field and Maxwell's third equation, Faraday's law. We start with static fields,

$$\nabla \times \mathbf{E} = 0. \quad (2.49)$$

We apply the Stokes (curl) theorem<sup>6</sup> on the Stokesian rectangle given in Fig. 2.3.

$$\oint_{\Gamma} \mathbf{E} \cdot d\mathbf{l} = \int_s (\nabla \times \mathbf{E}) \cdot \mathbf{n} da = 0. \quad (2.50)$$

The rectangle is chosen such that the interface normal  $\mathbf{n}$  lies in the plane of the rectangle and is parallel to the short sides. The normal to the rectangle is  $\mathbf{n}_0$  (points into the paper in Fig. 2.3) and  $\Gamma$  denotes the contour around the rectangle. We let the length of the short sides go toward zero and their contributions to the line integral can be neglected. We find that

<sup>6</sup>Stokes' curl theorem:  $\int_S (\nabla \times \mathbf{A}) \cdot \mathbf{n} dS = \oint_{\Gamma} \mathbf{A} \cdot d\mathbf{l}$ .

$$(\mathbf{E}_2 - \mathbf{E}_1) \cdot (\mathbf{n}_0 \times \mathbf{n}) dl = - [(\mathbf{E}_2 - \mathbf{E}_1) \times \mathbf{n}] \cdot \mathbf{n}_0 dl = 0, \quad (2.51)$$

where  $dl$  is the length of the long sides, and

$$(\mathbf{E}_2 - \mathbf{E}_1) \times \mathbf{n} = 0. \quad (2.52)$$

The rectangle can be rotated an arbitrary angle around  $\mathbf{n}$  and at every choice (2.52) is fulfilled. Thus, the tangential component of the  $\mathbf{E}$ -field is continuous.

Now, for time dependent fields there is an extra term in the third Maxwell equation and

$$\oint_{\Gamma} \mathbf{E} \cdot d\mathbf{l} = \int_s (\nabla \times \mathbf{E}) \cdot \mathbf{n}_0 da = - \frac{1}{c} \underbrace{\int_s \left( \frac{\partial \mathbf{B}}{\partial t} \right) \cdot \mathbf{n}_0 da}_{\rightarrow 0}. \quad (2.53)$$

The extra term will not change the results since the area of the rectangle goes to zero when the length of the short sides goes to zero.

Finally we treat the  $\mathbf{H}$ -field for static fields and the derivation is completely analogous to that for the  $\mathbf{E}$ -field but now we have a surface current density linking the Stokesian rectangle at the interface,

$$\begin{aligned} (\tilde{\mathbf{H}}_2 - \tilde{\mathbf{H}}_1) \times \mathbf{n} &= -\frac{4\pi}{c} \mathbf{K}_{\text{ext}} \\ (\mathbf{H}_2 - \mathbf{H}_1) \times \mathbf{n} &= -\frac{4\pi}{c} \mathbf{K}_f \\ (\mathbf{B}_2 - \mathbf{B}_1) \times \mathbf{n} &= -\frac{4\pi}{c} \mathbf{K}_t. \end{aligned} \quad (2.54)$$

The *tangential* component of the  $\tilde{\mathbf{H}}$ -field is *continuous* across the interface only if there is no external surface current at the interface; the *tangential* component of the  $\mathbf{H}$ -field is *continuous* across the interface only if there is no free surface current at the interface; the *tangential* component of the  $\mathbf{B}$ -field is *continuous* across the interface only if there is no surface current at all at the interface.

Now for time dependent fields we have

$$\begin{aligned} \oint_{\Gamma} \tilde{\mathbf{H}} \cdot d\mathbf{l} &= \int_s (\nabla \times \tilde{\mathbf{H}}) \cdot \mathbf{n}_0 da = \frac{1}{c} \underbrace{\int_s \left( \frac{\partial \tilde{\mathbf{D}}}{\partial t} \right) \cdot \mathbf{n}_0 da}_{\rightarrow 0} \\ \oint_{\Gamma} \mathbf{H} \cdot d\mathbf{l} &= \int_s (\nabla \times \mathbf{H}) \cdot \mathbf{n}_0 da = \frac{1}{c} \underbrace{\int_s \left( \frac{\partial \mathbf{D}}{\partial t} \right) \cdot \mathbf{n}_0 da}_{\rightarrow 0} \\ \oint_{\Gamma} \mathbf{B} \cdot d\mathbf{l} &= \int_s (\nabla \times \mathbf{B}) \cdot \mathbf{n}_0 da = \frac{1}{c} \underbrace{\int_s \left( \frac{\partial \mathbf{E}}{\partial t} \right) \cdot \mathbf{n}_0 da}_{\rightarrow 0}, \end{aligned} \quad (2.55)$$

and the extra terms do not change the results.

We can summarize the boundary conditions in the following way:

- Always:  
Tangential component of  $\mathbf{E}$  continuous.  
Normal component of  $\mathbf{B}$  continuous.
- In absence of free surface densities (charge and current):  
Tangential component of  $\mathbf{H}$  continuous.  
Normal component of  $\mathbf{D}$  continuous.
- In absence of external surface densities (charge and current):  
Tangential component of  $\tilde{\mathbf{H}}$  continuous.  
Normal component of  $\tilde{\mathbf{D}}$  continuous.

## 2.6 The Fresnel Equations

In this section we will study how a plane wave behaves when impinging on an interface between two media and derive the “Fresnel Equations” with which we here mean the equations for the amplitude reflection and transmission coefficients<sup>7</sup>; the coefficient  $r$  is the ratio of the reflected wave’s complex electric field amplitude to that of the incident wave; the coefficient  $t$  is the ratio of the transmitted wave’s electric field amplitude to that of the incident wave. We make some basic assumptions. The interface is flat with unlimited extent (to avoid edge effects); there are no external charge- or current-densities at the interface. We make no further restriction on the two media than that they are isotropic and linear (the constitutive relations hold). They may be dielectrics or metals and even magnetic. We start by looking at normal incidence

### 2.6.1 Reflection and Transmission for Normal Incidence

We let the interface lie in the  $xy$ -plane. The incoming wave moves in medium 1 in the  $z$ -direction toward the interface. There will be a reflected wave and a transmitted. This is illustrated in Fig. 2.4. Subscript 0, 1 and 2 represent incident, reflected and transmitted wave, respectively. We have introduced the refractive index,  $\tilde{n}_i = \sqrt{\tilde{\epsilon}_i \tilde{\mu}_i}$ , and the wave impedance,  $\tilde{\eta}_i = \sqrt{\tilde{\mu}_i / \tilde{\epsilon}_i}$ . The tilde above the material functions and  $\mathbf{H}$ -fields indicate that we treat metals on the same footing as dielectrics. We need one electric and one magnetic field to characterize the waves. We have chosen the  $\mathbf{E}$ -

---

<sup>7</sup>The Fresnel Equations can also mean the equations for the power reflection and transmission coefficients.

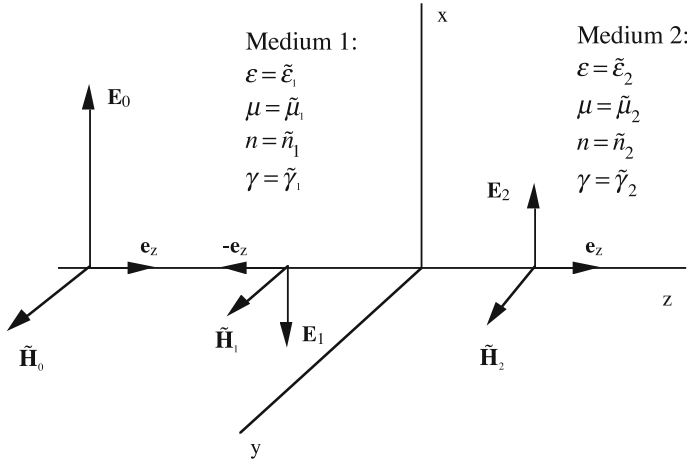


**Fig. 2.4** Normal incidence. An incoming wave in medium 1 is moving perpendicular to the interface separating medium 1 and medium 2. There is one reflected wave and one transmitted

and  $\tilde{\mathbf{H}}$ -fields since these have the same boundary conditions, viz. that the tangential components are continuous across the interface.

We make the ansatz

$$\begin{aligned} \mathbf{E}_0 &= \mathbf{e}_x E_0^0 e^{i(q_1 z - \omega t)} \\ \mathbf{E}_1 &= -\mathbf{e}_x E_1^0 e^{i(-q_1 z - \omega t)} \\ \mathbf{E}_2 &= \mathbf{e}_x E_2^0 e^{i(q_2 z - \omega t)} \end{aligned} \quad (2.56)$$

The scalar amplitudes,  $E_i^0$ , are time-independent and may be complex valued, allowing for a phase difference between the waves.

$$\begin{aligned} q_1 &= \tilde{n}_1 \frac{\omega}{c} = \sqrt{\tilde{\mu}_1 \tilde{\varepsilon}_1} \frac{\omega}{c}, \\ q_2 &= \tilde{n}_2 \frac{\omega}{c} = \sqrt{\tilde{\mu}_2 \tilde{\varepsilon}_2} \frac{\omega}{c}. \end{aligned} \quad (2.57)$$

From the third ME we have  $\tilde{\mathbf{H}} = \tilde{\eta}^{-1} \hat{\mathbf{q}} \times \mathbf{E}$  and

$$\begin{aligned} \tilde{\mathbf{H}}_0 &= \mathbf{e}_y \tilde{\eta}_1^{-1} E_0^0 e^{i(q_1 z - \omega t)}, \\ \tilde{\mathbf{H}}_1 &= \mathbf{e}_y \tilde{\eta}_1^{-1} E_1^0 e^{i(-q_1 z - \omega t)}, \\ \tilde{\mathbf{H}}_2 &= \mathbf{e}_y \tilde{\eta}_2^{-1} E_2^0 e^{i(q_2 z - \omega t)}. \end{aligned} \quad (2.58)$$

The boundary conditions for tangential components give

$$E_0^0 - E_1^0 = E_2^0, \quad (2.59)$$

and

$$\tilde{H}_0^0 + \tilde{H}_1^0 = \tilde{H}_2^0, \quad (2.60)$$

or

$$\tilde{\eta}_1^{-1} (E_0^0 + E_1^0) = \tilde{\eta}_2^{-1} E_2^0. \quad (2.61)$$

This gives

$$\begin{aligned} E_1^0 &= \frac{\tilde{\eta}_2^{-1} - \tilde{\eta}_1^{-1}}{\tilde{\eta}_2^{-1} + \tilde{\eta}_1^{-1}} E_0^0 = \frac{\tilde{\eta}_1 - \tilde{\eta}_2}{\tilde{\eta}_1 + \tilde{\eta}_2} E_0^0, \\ E_2^0 &= \frac{2\tilde{\eta}_1^{-1}}{\tilde{\eta}_2^{-1} + \tilde{\eta}_1^{-1}} E_0^0 = \frac{2\tilde{\eta}_2}{\tilde{\eta}_1 + \tilde{\eta}_2} E_0^0, \end{aligned} \quad (2.62)$$

and hence

$$\begin{aligned} r &= \frac{\tilde{\eta}_1 - \tilde{\eta}_2}{\tilde{\eta}_1 + \tilde{\eta}_2}, \\ t &= \frac{2\tilde{\eta}_2}{\tilde{\eta}_1 + \tilde{\eta}_2}. \end{aligned} \quad (2.63)$$

In the non-magnetic case we have

$$\begin{aligned} r &= \frac{\tilde{n}_2 - \tilde{n}_1}{\tilde{n}_2 + \tilde{n}_1}, \\ t &= \frac{2\tilde{n}_1}{\tilde{n}_2 + \tilde{n}_1}. \end{aligned} \quad (2.64)$$

Now, we continue with oblique incidence.

## 2.6.2 Oblique Incidence

We make the ansatz

$$\begin{aligned} \mathbf{E}_0 &= \mathbf{E}_0^0 e^{i(\mathbf{q}_0 \cdot \mathbf{r} - \omega t)}, \\ \tilde{\mathbf{H}}_0 &= \tilde{\eta}_1^{-1} \hat{\mathbf{q}}_0 \times \mathbf{E}_0, \\ \mathbf{E}_1 &= \mathbf{E}_1^0 e^{i(\mathbf{q}_1 \cdot \mathbf{r} - \omega t)}, \\ \tilde{\mathbf{H}}_1 &= \tilde{\eta}_1^{-1} \hat{\mathbf{q}}_1 \times \mathbf{E}_1, \\ \mathbf{E}_2 &= \mathbf{E}_2^0 e^{i(\mathbf{q}_2 \cdot \mathbf{r} - \omega t)}, \\ \tilde{\mathbf{H}}_2 &= \tilde{\eta}_2^{-1} \hat{\mathbf{q}}_2 \times \mathbf{E}_2. \end{aligned} \quad (2.65)$$

Note that we again use the  $\tilde{\mathbf{H}}$  fields instead of the fundamental  $\mathbf{B}$  fields because the boundary conditions for these fields are the same as for the  $\mathbf{E}$  fields. Now, the tangential components of the fields have to be continuous across the boundary. For this to be possible the periodicities of the field vectors have to be equal at the boundary:

$$\mathbf{q}_0 \cdot \mathbf{e}_x = \mathbf{q}_1 \cdot \mathbf{e}_x = \mathbf{q}_2 \cdot \mathbf{e}_x. \quad (2.66)$$

For symmetry reasons all three propagation vectors are coplanar, i.e. are in the same plane, the *plane of incidence* (the surface normal  $\mathbf{n}$  is also in this plane).

This means that

$$q_0 \sin \theta_0 = q_1 \sin \theta_1 = q_2 \sin \theta_2 = k. \quad (2.67)$$

This can also be viewed as conservation of the momentum parallel to the interface. This conservation holds if the interface is smooth. A rough interface or an intentionally created periodic structure at the interface can relax this condition. Momentum parallel to the interface can then be absorbed from, or provided to, the reflected and refracted waves.<sup>8</sup>

Now,

$$q_0 = q_1 \Rightarrow \theta_0 = \theta_1, \quad (2.68)$$

and

$$\tilde{n}_1 \sin \theta_1 = \tilde{n}_2 \sin \theta_2, \quad \text{Snell's law.} \quad (2.69)$$

Now we have determined the propagation direction of the reflected and refracted waves. The amplitudes of the field components are obtained from using the boundary conditions. It is enough to use the boundary conditions for the tangential components of the  $\mathbf{E}$  and  $\tilde{\mathbf{H}}$  fields. The conditions for the normal components of the  $\mathbf{B}$  and  $\tilde{\mathbf{D}}$  fields give no more information.

The boundary conditions are:

$$\begin{aligned} (\mathbf{E}_0 + \mathbf{E}_1) \times \mathbf{n} &= \mathbf{E}_2 \times \mathbf{n}, \\ (\tilde{\mathbf{H}}_0 + \tilde{\mathbf{H}}_1) \times \mathbf{n} &= \tilde{\mathbf{H}}_2 \times \mathbf{n}. \end{aligned} \quad (2.70)$$

The last can be rewritten in terms of the electric field vectors and we have

$$\begin{aligned} (\mathbf{E}_0 + \mathbf{E}_1) \times \mathbf{n} &= \mathbf{E}_2 \times \mathbf{n}, \\ (\tilde{\eta}_1^{-1} \hat{\mathbf{q}}_0 \times \mathbf{E}_0 + \tilde{\eta}_1^{-1} \hat{\mathbf{q}}_1 \times \mathbf{E}_1) \times \mathbf{n} &= (\tilde{\eta}_2^{-1} \hat{\mathbf{q}}_2 \times \mathbf{E}_2) \times \mathbf{n}. \end{aligned} \quad (2.71)$$

Any plane wave impinging on the interface can be written as a linear combination of two waves, one with the electric vector polarized parallel to the plane of incidence (p-polarized), and one with the electric vector perpendicular to the plane of incidence (s-polarized). We may treat these components separately. We begin with s-polarized waves.

### 2.6.2.1 E Perpendicular to the Plane of Incidence

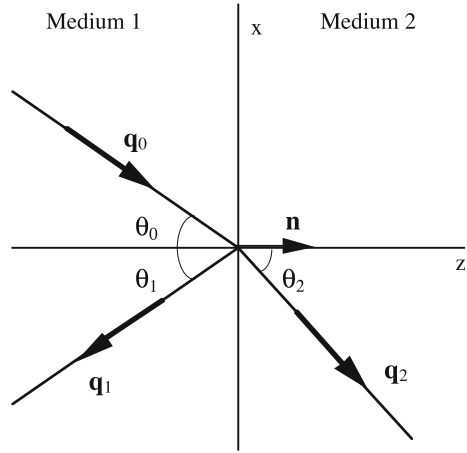
The geometry is illustrated in Fig. 2.6. All  $\mathbf{E}$ -vectors are in the negative  $y$ -direction, i.e., pointing into the paper. This means that the first boundary condition makes:

$$E_0^0 + E_1^0 = E_2^0. \quad (2.72)$$

---

<sup>8</sup>Note that in metallic systems and in regions with dissipation  $q_i$  and  $\sin \theta_i$  may both be complex valued but their product is real valued. The complex valued “angle”  $\theta_i$  in that case does not have the simple geometric meaning of the angle of reflection or angle of refraction.

**Fig. 2.5** Oblique incidence: A plane electromagnetic wave comes in from the left in medium 1 toward the interface between medium 1 and 2, the  $xy$ -plane, at the angle of incidence,  $\theta_0$ . There is a reflected wave at the angle of reflection,  $\theta_1$ , and a refracted wave at the angle of refraction,  $\theta_2$ . The wave vectors of the incident, the reflected, and the refracted waves are  $\mathbf{q}_0$ ,  $\mathbf{q}_1$ , and  $\mathbf{q}_2$ , respectively



The second we expand using the triple curl product<sup>9</sup>

$$\begin{aligned} \mathbf{n} \times (\hat{\mathbf{q}}_0 \times \mathbf{E}_0) + \mathbf{n} \times (\hat{\mathbf{q}}_1 \times \mathbf{E}_1) &= \frac{\tilde{\eta}_1}{\tilde{\eta}_2} \mathbf{n} \times (\hat{\mathbf{q}}_2 \times \mathbf{E}_2) \\ \hat{\mathbf{q}}_0 \underbrace{(\mathbf{n} \cdot \mathbf{E}_0)}_0 - \mathbf{E}_0 \underbrace{(\mathbf{n} \cdot \hat{\mathbf{q}}_0)}_{\cos \theta_0}, & \\ + \hat{\mathbf{q}}_1 \underbrace{(\mathbf{n} \cdot \mathbf{E}_1)}_0 - \mathbf{E}_1 \underbrace{(\mathbf{n} \cdot \hat{\mathbf{q}}_1)}_{-\cos \theta_1} &= \frac{\tilde{\eta}_1}{\tilde{\eta}_2} \hat{\mathbf{q}}_2 \underbrace{(\mathbf{n} \cdot \mathbf{E}_2)}_0 - \frac{\tilde{\eta}_1}{\tilde{\eta}_2} \mathbf{E}_2 \underbrace{(\mathbf{n} \cdot \hat{\mathbf{q}}_2)}_{\cos \theta_2}, \end{aligned} \quad (2.73)$$

or

$$\mathbf{E}_0 \cos \theta_0 - \mathbf{E}_1 \cos \theta_1 = \frac{\tilde{\eta}_1}{\tilde{\eta}_2} \mathbf{E}_2 \cos \theta_2, \quad (2.74)$$

or since  $\theta_1 = \theta_0$  we have

$$(E_0^0 - E_1^0) \cos \theta_0 = \frac{\tilde{\eta}_1}{\tilde{\eta}_2} E_2^0 \cos \theta_2. \quad (2.75)$$

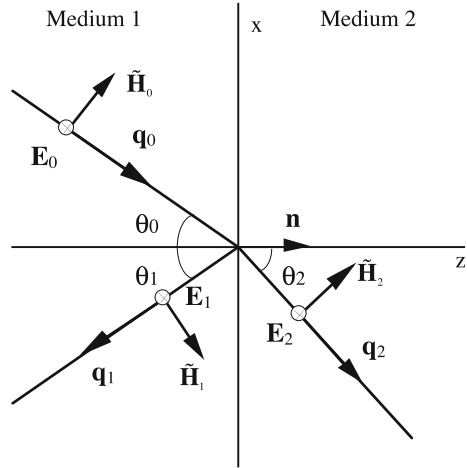
Combining the two relations gives

$$\begin{aligned} E_1^0 &= \frac{\cos \theta_0 - (\tilde{\eta}_1/\tilde{\eta}_2) \cos \theta_2}{\cos \theta_0 + (\tilde{\eta}_1/\tilde{\eta}_2) \cos \theta_2} E_0^0, \\ E_2^0 &= \frac{2 \cos \theta_0}{\cos \theta_0 + (\tilde{\eta}_1/\tilde{\eta}_2) \cos \theta_2} E_0^0. \end{aligned} \quad (2.76)$$

Thus the Fresnel equations for the amplitude- reflection and -transmission coefficients are

<sup>9</sup>The triple curl product:  $\mathbf{A} \times (\mathbf{B} \times \mathbf{C}) = \mathbf{B}(\mathbf{A} \cdot \mathbf{C}) - \mathbf{C}(\mathbf{A} \cdot \mathbf{B})$ .

**Fig. 2.6** The same as Fig. 2.5 but now for a specific polarization, viz. s-polarized waves, where the  $\mathbf{E}$  vectors are perpendicular to the plane of incidence. They are pointing into the page



$$\begin{aligned} r^s &= \frac{\cos \theta_0 - (\tilde{\eta}_1/\tilde{\eta}_2) \cos \theta_2}{\cos \theta_0 + (\tilde{\eta}_1/\tilde{\eta}_2) \cos \theta_2}, \\ t^s &= \frac{2 \cos \theta_0}{\cos \theta_0 + (\tilde{\eta}_1/\tilde{\eta}_2) \cos \theta_2}. \end{aligned} \quad (2.77)$$

For our purpose it is more favorable to express the coefficients in terms of the conserved wave number,  $k$ , in the plane of the interface. We have

$$\begin{aligned} \sin(\theta_i) &= k/q_i = ck/(\tilde{n}_i\omega), \\ \cos(\theta_i) &\equiv \sqrt{1 - \sin^2(\theta_i)} = \sqrt{1 - (ck/\tilde{n}_i\omega)^2} = i(ck/\tilde{n}_i\omega)\gamma_i, \\ \gamma_i &= \sqrt{1 - (\tilde{n}_i\omega/ck)^2}, \end{aligned} \quad (2.78)$$

and the final results are<sup>10</sup>

$$\begin{aligned} r^s(\mathbf{k}, \omega) &= \frac{\tilde{\mu}_2(\omega)\gamma_1(\mathbf{k}, \omega) - \tilde{\mu}_1(\omega)\gamma_2(\mathbf{k}, \omega)}{\tilde{\mu}_2(\omega)\gamma_1(\mathbf{k}, \omega) + \tilde{\mu}_1(\omega)\gamma_2(\mathbf{k}, \omega)}, \\ t^s(\mathbf{k}, \omega) &= \frac{2\tilde{\mu}_2(\omega)\gamma_1(\mathbf{k}, \omega)}{\tilde{\mu}_2(\omega)\gamma_1(\mathbf{k}, \omega) + \tilde{\mu}_1(\omega)\gamma_2(\mathbf{k}, \omega)}. \end{aligned} \quad (2.79)$$

For non-magnetic materials this simplifies into

$$\begin{aligned} r^s(\mathbf{k}, \omega) &= \frac{\gamma_1(\mathbf{k}, \omega) - \gamma_2(\mathbf{k}, \omega)}{\gamma_1(\mathbf{k}, \omega) + \gamma_2(\mathbf{k}, \omega)}, \\ t^s(\mathbf{k}, \omega) &= \frac{2\gamma_1(\mathbf{k}, \omega)}{\gamma_1(\mathbf{k}, \omega) + \gamma_2(\mathbf{k}, \omega)}. \end{aligned} \quad (2.80)$$

<sup>10</sup>Here we neglect spatial dispersion [2], i.e. we neglect the  $\mathbf{q}$ -dependence of the material response functions  $\tilde{\epsilon}$  and  $\tilde{\mu}$ . Taking spatial dispersion into account is possible but the formalism becomes much more complicated [3]. Neglecting spatial dispersion has also the effect that the transverse and longitudinal versions of the response functions are equal (neglecting spatial dispersion means that one takes the small- $q$  limit and in that limit the longitudinal and transverse versions are equal).

Now we continue with p-polarized waves.

### 2.6.2.2 E Parallel to the Plane of Incidence

The geometry is illustrated in Fig. 2.7. Now all  $\tilde{\mathbf{H}}$ -vectors are pointing in the  $y$ -direction, i.e., out of the plane of the figure.

We can make use of our results from the s-polarized case. We just change the electric fields to the electric fields divided by the wave impedance in the condition for the  $\mathbf{E}$ -fields:

$$E_0^0 + E_1^0 = E_2^0 \Rightarrow \frac{1}{\tilde{\eta}_1} (E_0^0 + E_1^0) = \frac{1}{\tilde{\eta}_2} E_2^0, \tag{2.81}$$

and in the condition for the  $\tilde{\mathbf{H}}$ -fields we change the electric fields divided by the wave impedance to the electric fields:

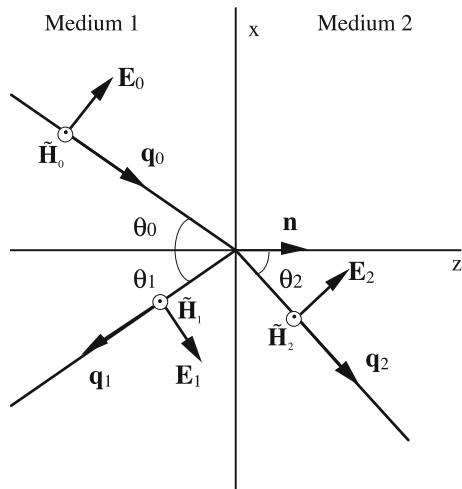
$$(E_0^0 - E_1^0) \cos \theta_0 = \frac{\tilde{\eta}_1}{\tilde{\eta}_2} E_2^0 \cos \theta_2 \Rightarrow (E_0^0 - E_1^0) \cos \theta_0 = E_2^0 \cos \theta_2, \tag{2.82}$$

from which we obtain

$$\begin{aligned} E_1^0 &= \frac{\cos \theta_0 - (\tilde{\eta}_2/\tilde{\eta}_1) \cos \theta_2}{\cos \theta_0 + (\tilde{\eta}_2/\tilde{\eta}_1) \cos \theta_2} E_0^0, \\ E_2^0 &= \frac{2 \cos \theta_0}{\cos \theta_2 + (\tilde{\eta}_1/\tilde{\eta}_2) \cos \theta_0} E_0^0. \end{aligned} \tag{2.83}$$

Thus the Fresnel equations for the amplitude-reflection and -transmission coefficients are

**Fig. 2.7** The same as Fig. 2.5 but now for a specific polarization, viz. p<sub>2</sub>-polarized waves, where the  $\tilde{\mathbf{H}}$  vectors are perpendicular to the plane of incidence. They are pointing out of the page



$$\begin{aligned}
 r^P &= \frac{\cos \theta_0 - (\tilde{\eta}_2 / \tilde{\eta}_1) \cos \theta_2}{\cos \theta_0 + (\tilde{\eta}_2 / \tilde{\eta}_1) \cos \theta_2}, \\
 t^P &= \frac{2 \cos \theta_0}{\cos \theta_2 + (\tilde{\eta}_1 / \tilde{\eta}_2) \cos \theta_0}.
 \end{aligned}
 \tag{2.84}$$

We proceed as for the s-polarized case and express the amplitude reflection coefficient in terms of the conserved wave-number,  $k$ , in the plane of the interface. We find

$$\begin{aligned}
 r^P(\mathbf{k}, \omega) &= \frac{\tilde{\varepsilon}_2(\omega)\gamma_1(\mathbf{k}, \omega) - \tilde{\varepsilon}_1(\omega)\gamma_2(\mathbf{k}, \omega)}{\tilde{\varepsilon}_2(\omega)\gamma_1(\mathbf{k}, \omega) + \tilde{\varepsilon}_1(\omega)\gamma_2(\mathbf{k}, \omega)}, \\
 t^P(\mathbf{k}, \omega) &= \frac{2\sqrt{\tilde{\varepsilon}_1(\omega)\tilde{\varepsilon}_2(\omega)}\sqrt{\tilde{\mu}_2(\omega)/\tilde{\mu}_1(\omega)}\gamma_1(\mathbf{k}, \omega)}{\tilde{\varepsilon}_2(\omega)\gamma_1(\mathbf{k}, \omega) + \tilde{\varepsilon}_1(\omega)\gamma_2(\mathbf{k}, \omega)}.
 \end{aligned}
 \tag{2.85}$$

For non-magnetic materials this simplifies into

$$\begin{aligned}
 r^P(\mathbf{k}, \omega) &= \frac{\tilde{\varepsilon}_2(\omega)\gamma_1(\mathbf{k}, \omega) - \tilde{\varepsilon}_1(\omega)\gamma_2(\mathbf{k}, \omega)}{\tilde{\varepsilon}_2(\omega)\gamma_1(\mathbf{k}, \omega) + \tilde{\varepsilon}_1(\omega)\gamma_2(\mathbf{k}, \omega)}, \\
 t^P(\mathbf{k}, \omega) &= \frac{2\sqrt{\tilde{\varepsilon}_1(\omega)\tilde{\varepsilon}_2(\omega)}\gamma_1(\mathbf{k}, \omega)}{\tilde{\varepsilon}_2(\omega)\gamma_1(\mathbf{k}, \omega) + \tilde{\varepsilon}_1(\omega)\gamma_2(\mathbf{k}, \omega)}.
 \end{aligned}
 \tag{2.86}$$

Thus we have found that for isotropic materials and in neglect of spatial dispersion the Fresnel equations for the amplitude-reflection and -transmission coefficients at an interface between medium 1 and 2 are

$$\begin{aligned}
 r^s(\mathbf{k}, \omega) &= \frac{\tilde{\mu}_2(\omega)\gamma_1(\mathbf{k}, \omega) - \tilde{\mu}_1(\omega)\gamma_2(\mathbf{k}, \omega)}{\tilde{\mu}_2(\omega)\gamma_1(\mathbf{k}, \omega) + \tilde{\mu}_1(\omega)\gamma_2(\mathbf{k}, \omega)}, \\
 t^s(\mathbf{k}, \omega) &= \frac{2\tilde{\mu}_2(\omega)\gamma_1(\mathbf{k}, \omega)}{\tilde{\mu}_2(\omega)\gamma_1(\mathbf{k}, \omega) + \tilde{\mu}_1(\omega)\gamma_2(\mathbf{k}, \omega)}, \\
 r^P(\mathbf{k}, \omega) &= \frac{\tilde{\varepsilon}_2(\omega)\gamma_1(\mathbf{k}, \omega) - \tilde{\varepsilon}_1(\omega)\gamma_2(\mathbf{k}, \omega)}{\tilde{\varepsilon}_2(\omega)\gamma_1(\mathbf{k}, \omega) + \tilde{\varepsilon}_1(\omega)\gamma_2(\mathbf{k}, \omega)}, \\
 t^P(\mathbf{k}, \omega) &= \frac{2[\tilde{n}_2(\omega)/\tilde{n}_1(\omega)]\gamma_1(\mathbf{k}, \omega)}{\tilde{\varepsilon}_2(\omega)\gamma_1(\mathbf{k}, \omega) + \tilde{\varepsilon}_1(\omega)\gamma_2(\mathbf{k}, \omega)}.
 \end{aligned}
 \tag{2.87}$$

### 2.6.3 Anisotropic Media

In an anisotropic medium the dielectric function and refractive index have tensor properties. If a thin film is made from a material that is isotropic in bulk form it still tends to become anisotropic with different properties in the direction perpendicular to its interfaces as compared to in a direction parallel to its interfaces [4]. Then the Fresnel equations are modified. Fresnel amplitude reflection coefficients for a wave impinging at an interface between an isotropic medium  $i$  and an anisotropic medium  $j$ , from the  $i$ -side are [5]

$$\begin{aligned}
 r_{ij}^s &= \frac{\tilde{n}_i \cos \theta_i - \sqrt{\tilde{n}_{xx,j}^2 - \tilde{n}_i^2 \sin^2 \theta_i}}{n_i \cos \theta_i + \sqrt{\tilde{n}_{xx,j}^2 - \tilde{n}_i^2 \sin^2 \theta_i}}, \\
 r_{ij}^p &= \frac{\tilde{n}_{xx,j} \tilde{n}_{zz,j} \cos \theta_i - \tilde{n}_i \sqrt{\tilde{n}_{zz,j}^2 - \tilde{n}_i^2 \sin^2 \theta_i}}{\tilde{n}_{xx,j} \tilde{n}_{zz,j} \cos \theta_i + \tilde{n}_i \sqrt{\tilde{n}_{zz,j}^2 - \tilde{n}_i^2 \sin^2 \theta_i}},
 \end{aligned} \tag{2.88}$$

where the refractive index tensor for the film is

$$\begin{pmatrix} \tilde{n}_{xx,j} & 0 & 0 \\ 0 & \tilde{n}_{xx,j} & 0 \\ 0 & 0 & \tilde{n}_{zz,j} \end{pmatrix}. \tag{2.89}$$

Here  $\tilde{n}_{xx,j}$  and  $\tilde{n}_{zz,j}$  are the refractive indices of medium  $j$  in the plane of the interfaces and perpendicular to the interfaces respectively. From the  $j$ -side we have

$$r_{ji}^s = -r_{ij}^s, \tag{2.90}$$

$$r_{ji}^p = -r_{ij}^p. \tag{2.91}$$

We have let the film be parallel to the  $xy$ -plane. We use the identities (2.78)

$$\begin{aligned}
 \tilde{n}_i \cos \theta_i &= \frac{i\sqrt{1 - (\tilde{n}_i \omega / ck)^2}}{(\omega / ck)}, \\
 \tilde{n}_i \sin \theta_i &= \frac{1}{(\omega / ck)},
 \end{aligned} \tag{2.92}$$

to find the alternative expressions

$$\begin{aligned}
 r_{ij}^s &= \frac{\sqrt{1 - (\tilde{n}_i \omega / ck)^2} - \sqrt{1 - (\tilde{n}_{xx,j} \omega / ck)^2}}{\sqrt{1 - (\tilde{n}_i \omega / ck)^2} + \sqrt{1 - (\tilde{n}_{xx,j} \omega / ck)^2}}, \\
 r_{ij}^p &= \frac{\tilde{n}_{xx,j} \tilde{n}_{zz,j} \sqrt{1 - (\tilde{n}_i \omega / ck)^2} - \tilde{\epsilon}_i \sqrt{[1 - (\tilde{n}_{zz,j} \omega / ck)^2]}}{\tilde{n}_{xx,j} \tilde{n}_{zz,j} \sqrt{1 - (\tilde{n}_i \omega / ck)^2} + \tilde{\epsilon}_i \sqrt{[1 - (\tilde{n}_{zz,j} \omega / ck)^2]}}.
 \end{aligned} \tag{2.93}$$

Now, let us find out what the amplitude reflection coefficients will be at an interface between two isotropic media where one of them now has an anisotropic coating of the type we just discussed. For a system 1|2|3 where media 1 and 3 are isotropic and medium 2 is anisotropic we have:

$$\begin{aligned}
 r_{123}^s &= \frac{r_{12}^s + r_{23}^s e^{i2\beta_2^s}}{1 + r_{12}^s r_{23}^s e^{i2\beta_2^s}}, \\
 r_{123}^p &= \frac{r_{12}^p + r_{23}^p e^{i2\beta_2^p}}{1 + r_{12}^p r_{23}^p e^{i2\beta_2^p}},
 \end{aligned} \tag{2.94}$$

where

$$\begin{aligned}
 \beta_2^s &= \frac{\omega}{c} d \sqrt{\tilde{n}_{xx,2}^2 - \tilde{n}_1^2 \sin^2 \theta_1} = ikd \sqrt{1 - (\tilde{n}_{xx,2} \omega / ck)^2}, \\
 \beta_2^p &= \frac{\omega}{c} d \frac{\tilde{n}_{xx,2}}{\tilde{n}_{zz,2}} \sqrt{\tilde{n}_{zz,2}^2 - \tilde{n}_1^2 \sin^2 \theta_1} = ikd \frac{\tilde{n}_{xx,2}}{\tilde{n}_{zz,2}} \sqrt{1 - (\tilde{n}_{zz,2} \omega / ck)^2},
 \end{aligned} \tag{2.95}$$

and  $d$  is the thickness of medium 2.

## 2.7 Special Considerations for 2D Sheets

In many cases we have to deal with very thin layers or sheets. Sometimes these can be considered to be two-dimensional (2D). They can be thin coatings on an object or free standing thin films like graphene sheets. We have devoted this section to systems containing sheets like this. Here, we need to modify and specify our notation. We let the 2D sheet be parallel to the  $xy$ -plane and the three-dimensional (3D) and 2D spatial vectors be denoted by  $\mathbf{R}$  and  $\mathbf{r}$ , respectively. Thus,  $\mathbf{R} = (\mathbf{r}; z) = x\hat{\mathbf{x}} + y\hat{\mathbf{y}} + z\hat{\mathbf{z}}$ . The corresponding vectors in Fourier space are  $\mathbf{q}$  and  $\mathbf{k}$ , respectively, i.e.,  $\mathbf{q} = (\mathbf{k}; q_z) = k_x\hat{\mathbf{x}} + k_y\hat{\mathbf{y}} + q_z\hat{\mathbf{z}}$ . We follow rather closely an earlier published presentation [6] of this material but have here extended it to include the effects of magnetic permeabilities.

### 2.7.1 Fourier Transforms of a Special Function

The Fourier transform of the function  $F(\mathbf{R}) = 1/R$  appears in different versions in what follows so we compile the results in this subsection. This function is basically the Coulomb potential between two electrons,  $v(\mathbf{R}) = e^2/R$ , but without the charges.

The 3D spatial Fourier transform is

$$F(\mathbf{q}) = \int d^3R e^{-i\mathbf{q}\cdot\mathbf{R}} \frac{1}{R} = \frac{4\pi}{q^2}; \quad (2.96)$$

the 2D Fourier transform performed over a plane the distance  $z$  from the  $xy$ -plane is

$$F(\mathbf{k}; z) = \int d^2r e^{-i\mathbf{k}\cdot\mathbf{r}} F(\mathbf{r}; z) = \int d^2r e^{-i\mathbf{k}\cdot\mathbf{r}} \frac{1}{\sqrt{r^2+z^2}} = \frac{2\pi}{k} e^{-k|z|}; \quad (2.97)$$

the 2D Fourier transform performed over the  $xy$ -plane is

$$F(\mathbf{k}) = \int d^2r e^{-i\mathbf{k}\cdot\mathbf{r}} F(\mathbf{r}) = \int d^2r e^{-i\mathbf{k}\cdot\mathbf{r}} \frac{1}{r} = \frac{2\pi}{k}. \quad (2.98)$$

These versions appear in expressions involving the scalar potential in Coulomb gauge and when retardation effects are negligible. When retardation is important the function has a temporal dependence,  $F(\mathbf{R}, t) = \delta(t - R/c)/R$ . Then the following Fourier transforms are important: The 3D spatial and temporal Fourier transform,

$$F(\mathbf{q}, \omega) = \int d^3R \int_{-\infty}^{\infty} dt e^{-i(\mathbf{q}\cdot\mathbf{R} - \omega t)} \frac{\delta(t - R/c)}{R} = \frac{4\pi}{q^2} \frac{1}{1 - (\omega/cq)^2}; \quad (2.99)$$

the 2D Fourier transform performed over a plane the distance  $z$  from the  $xy$ -plane,

$$\begin{aligned} F(\mathbf{k}; z, \omega) &= \int d^2r e^{-i\mathbf{k}\cdot\mathbf{r}} F(\mathbf{r}; z, t) = \int d^2r \int_{-\infty}^{\infty} dt e^{-i(\mathbf{k}\cdot\mathbf{r}-\omega t)} \frac{\delta(t-\sqrt{r^2+z^2}/c)}{\sqrt{r^2+z^2}} \\ &= \frac{2\pi e^{-k\gamma^{(0)}(k,\omega)|z|}}{k\gamma^{(0)}(k,\omega)}; \end{aligned} \quad (2.100)$$

the 2D Fourier transform performed over the  $xy$ -plane,

$$\begin{aligned} F(\mathbf{k}, \omega) &= \int d^2r e^{-i\mathbf{k}\cdot\mathbf{r}} F(\mathbf{r}, t) = \int d^2r \int_{-\infty}^{\infty} dt e^{-i(\mathbf{k}\cdot\mathbf{r}-\omega t)} \frac{\delta(t-r/c)}{r} \\ &= \frac{2\pi}{k\gamma^{(0)}(k,\omega)}, \end{aligned} \quad (2.101)$$

where in the last two equations

$$\gamma^{(0)}(k, \omega) = \sqrt{1 - (\omega/c k)^2}. \quad (2.102)$$

One further relation is useful to have, viz.

$$\frac{\partial F(\mathbf{k}; z, \omega)}{\partial z} = -k\gamma^{(0)}(k, \omega) \frac{|z|}{z} \frac{2\pi e^{-k\gamma^{(0)}(k,\omega)|z|}}{k\gamma^{(0)}(k,\omega)} = -\frac{|z|}{z} 2\pi e^{-k\gamma^{(0)}(k,\omega)|z|}. \quad (2.103)$$

### 2.7.2 Method of Images

When there is a 2D layer carrying charge- and/or current-densities next to a wall, it is useful to be able to find the image charge- and current-densities produced in the wall. This is what we focus on in this subsection. We start from a given time dependent charge- and current-density in the 2D layer, calculate the potentials and from these the  $\mathbf{E}$ - and  $\mathbf{B}$ -fields. We first make an ansatz for the image densities and then determine these by using the standard boundary conditions. We use the Lorentz gauge in which the scalar and vector potentials are given in (2.43).

$$\begin{aligned} \Phi(\mathbf{q}, \omega) &= \frac{4\pi\rho(\mathbf{q}, \omega)}{q^2} \frac{1}{1-(\omega/cq)^2}, \\ \mathbf{A}(\mathbf{q}, \omega) &= \frac{4\pi\mathbf{J}(\mathbf{q}, \omega)}{cq^2} \frac{1}{1-(\omega/cq)^2}. \end{aligned} \quad (2.104)$$

The electric field in terms of the potentials was given in (2.28). This leads to the following relation between the Fourier transforms

$$\mathbf{E}(\mathbf{q}, \omega) = -i\mathbf{q}\Phi(\mathbf{q}, \omega) + \frac{i\omega}{c}\mathbf{A}(\mathbf{q}, \omega). \quad (2.105)$$

Thus,

$$\mathbf{E}(\mathbf{q}, \omega) = -i\mathbf{q} \frac{4\pi\rho(\mathbf{q}, \omega)}{[q^2 - (\omega/c)^2]} + \frac{i\omega}{c^2} \frac{4\pi\mathbf{J}(\mathbf{q}, \omega)}{[q^2 - (\omega/c)^2]}. \quad (2.106)$$

Now, in our system the charge- and current-densities are surface densities,

$$\begin{aligned} \rho(\mathbf{R}, t) &= \rho_s(\mathbf{r}, t) \delta(z), \\ \mathbf{J}(\mathbf{R}, t) &= \mathbf{K}(\mathbf{r}, t) \delta(z), \end{aligned} \quad (2.107)$$

and

$$\begin{aligned} \rho(\mathbf{k}; z, \omega) &= \rho_s(\mathbf{k}, \omega) \delta(z), \\ \mathbf{J}(\mathbf{k}; z, \omega) &= \mathbf{K}(\mathbf{k}, \omega) \delta(z), \end{aligned} \quad (2.108)$$

which means that

$$\begin{aligned} \rho(\mathbf{q}, \omega) &= \rho_s(\mathbf{k}, \omega), \\ \mathbf{J}(\mathbf{q}, \omega) &= \mathbf{K}(\mathbf{k}, \omega). \end{aligned} \quad (2.109)$$

Thus, we have for the electric field from surface charge- and current-densities, confined to the  $xy$ -plane

$$\mathbf{E}(\mathbf{q}, \omega) = -i\mathbf{q} \frac{4\pi\rho_s(\mathbf{k}, \omega)}{[q^2 - (\omega/c)^2]} + \frac{i\omega}{c^2} \frac{4\pi\mathbf{K}(\mathbf{k}, \omega)}{[q^2 - (\omega/c)^2]}, \quad (2.110)$$

in vacuum. If the source densities are embedded in a medium with dielectric function  $\tilde{\epsilon}_m(\omega)$  and magnetic permeability  $\tilde{\mu}_m(\omega)$  the electric field is

$$\mathbf{E}(\mathbf{q}, \omega) = -i\mathbf{q} \frac{1}{\tilde{\epsilon}_m} \frac{4\pi\rho_s(\mathbf{k}, \omega)}{[q^2 - (\tilde{n}_m\omega/c)^2]} + \frac{i\omega\tilde{\mu}_m}{c^2} \frac{4\pi\mathbf{K}(\mathbf{k}, \omega)}{[q^2 - (\tilde{n}_m\omega/c)^2]}. \quad (2.111)$$

The magnetic induction is

$$\mathbf{B}(\mathbf{q}, \omega) = i\mathbf{q} \times \mathbf{A}(\mathbf{q}, \omega) = i\frac{1}{c}\mathbf{q} \times \frac{4\pi\mathbf{K}(\mathbf{k}, \omega)}{[q^2 - (\omega/c)^2]}, \quad (2.112)$$

in vacuum and

$$\mathbf{B}(\mathbf{q}, \omega) = i\frac{\tilde{\mu}_m}{c}\mathbf{q} \times \frac{4\pi\mathbf{K}(\mathbf{k}, \omega)}{[q^2 - (\tilde{n}_m\omega/c)^2]}, \quad (2.113)$$

in a medium. The electric field is expressed in terms of the charge- and current-densities, while the magnetic induction is expressed in terms of the current density, only. It is possible to express also the electric field in terms of the current density, only.

We may use the equation of continuity to eliminate  $\rho_s(\mathbf{k}, \omega)$  in favor of  $K_{\parallel}(\mathbf{k}, \omega)$ . The equation of continuity reads

$$\nabla \cdot \mathbf{J}(\mathbf{R}, t) + \frac{\partial \rho(\mathbf{R}, t)}{\partial t} = 0. \quad (2.114)$$

The relation for the Fourier transforms becomes

$$i\mathbf{q} \cdot \mathbf{J}(\mathbf{q}, \omega) - i\omega\rho(\mathbf{q}, \omega) = 0. \quad (2.115)$$

In the present system with surface densities we have from (2.109)

$$i\mathbf{q} \cdot \mathbf{K}(\mathbf{k}, \omega) = i\omega\rho_s(\mathbf{k}, \omega). \quad (2.116)$$

Since  $\mathbf{K}$  is in the plane we get

$$i\mathbf{k} \cdot \mathbf{K}(\mathbf{k}, \omega) = i\omega\rho_s(\mathbf{k}, \omega). \quad (2.117)$$

The scalar product picks out the longitudinal part of the surface current density. Thus we have

$$\rho_s(\mathbf{k}, \omega) = (k/\omega) K_{\parallel}(\mathbf{k}, \omega). \quad (2.118)$$

We use this relation to eliminate the charge density from the field relations. To be as general as possible we from now on assume that the 2D layer is embedded in a medium. Without losing generality, we choose the  $x$ -axis to point along  $\mathbf{k}$ . A general vector quantity has a component normal to the planar interfaces. We attach a subscript  $\mathbf{n}$  to this component. The in-plane part of the vector has a longitudinal and a transverse part. The longitudinal is parallel and the transverse perpendicular to  $\mathbf{k}$ . We attach the subscripts  $\parallel$  and  $\perp$ , respectively, to these components. The current density has no normal component. To summarize we have

$$\begin{aligned} \mathbf{K}_{\parallel} &= K_x \hat{x}; & \mathbf{E}_{\parallel} &= E_x \hat{x}; & \mathbf{B}_{\parallel} &= B_x \hat{x}; \\ \mathbf{K}_{\perp} &= K_y \hat{y}; & \mathbf{E}_{\perp} &= E_y \hat{y}; & \mathbf{B}_{\perp} &= B_y \hat{y}; \\ \mathbf{K}_{\mathbf{n}} &= 0 \hat{z}; & \mathbf{E}_{\mathbf{n}} &= E_z \hat{z}; & \mathbf{B}_{\mathbf{n}} &= B_z \hat{z}. \end{aligned} \quad (2.119)$$

In the source plane the field components are

$$\begin{aligned} E_{\parallel}(\mathbf{k}, \omega) &= -i \frac{2\pi}{\epsilon_m(\omega)} (k/\omega) \gamma_m(k, \omega) K_{\parallel}(\mathbf{k}, \omega), \\ E_{\perp}(\mathbf{k}, \omega) &= \frac{i\omega\mu_m(\omega)}{c^2} \frac{2\pi}{k\gamma_m(k, \omega)} K_{\perp}(\mathbf{k}, \omega), \\ E_{\mathbf{n}}(\mathbf{k}, \omega) &= 0, \\ B_{\parallel}(\mathbf{k}, \omega) &= 0, \\ B_{\perp}(\mathbf{k}, \omega) &= 0, \\ B_{\mathbf{n}}(\mathbf{k}, \omega) &= i \frac{\mu_m(\omega)}{c} \frac{2\pi K_{\perp}(\mathbf{k}, \omega)}{\gamma_m(k, \omega)}, \end{aligned} \quad (2.120)$$

where  $\gamma_m(k, \omega) = \sqrt{1 - [\tilde{n}_m(\omega) \omega / ck]^2}$ .

In a plane parallel to the source plane ( $xy$ -plane) and at the distance  $z$  we have

$$\begin{aligned}
E_{\parallel}(\mathbf{k}; z, \omega) &= -i \frac{2\pi}{\tilde{\epsilon}_m(\omega)} (k/\omega) \gamma_m(k, \omega) e^{-\gamma_m(k, \omega)k|z|} K_{\parallel}(\mathbf{k}, \omega), \\
E_{\perp}(\mathbf{k}; z, \omega) &= \frac{i\omega \tilde{\mu}_m}{c^2} \frac{2\pi}{k\gamma_m(k, \omega)} e^{-\gamma_m(k, \omega)k|z|} K_{\perp}(\mathbf{k}, \omega), \\
E_n(\mathbf{k}; z, \omega) &= \frac{2\pi}{\tilde{\epsilon}_m(\omega)} \frac{z}{|z|} e^{-\gamma_m(k, \omega)k|z|} \rho_s(\mathbf{k}, \omega) \\
&= \frac{2\pi}{\tilde{\epsilon}_m(\omega)} \frac{z}{|z|} \frac{k}{\omega} e^{-\gamma_m(k, \omega)k|z|} K_{\parallel}(\mathbf{k}, \omega), \\
B_{\parallel}(\mathbf{k}; z, \omega) &= \gamma_m(k, \omega) k \frac{z}{|z|} \frac{\tilde{\mu}_m}{c} \frac{2\pi K_{\perp}(\mathbf{k}, \omega)}{\gamma_m(k, \omega)k} e^{-\gamma_m(k, \omega)k|z|} \\
&= \frac{z}{|z|} \frac{\tilde{\mu}_m}{c} 2\pi K_{\perp}(\mathbf{k}, \omega) e^{-\gamma_m(k, \omega)k|z|}, \\
B_{\perp}(\mathbf{k}; z, \omega) &= -\gamma_m(k, \omega) k \frac{z}{|z|} \frac{\tilde{\mu}_m}{c} \frac{2\pi K_{\parallel}(\mathbf{k}, \omega)}{\gamma_m(k, \omega)k} e^{-\gamma_m(k, \omega)k|z|} \\
&= -\frac{z}{|z|} \frac{\tilde{\mu}_m}{c} 2\pi K_{\parallel}(\mathbf{k}, \omega) e^{-\gamma_m(k, \omega)k|z|}, \\
B_n(\mathbf{k}; z, \omega) &= i \frac{\tilde{\mu}_m}{c} \frac{2\pi K_{\perp}(\mathbf{k}, \omega)}{\gamma_m(k, \omega)} e^{-\gamma_m(k, \omega)k|z|},
\end{aligned} \tag{2.121}$$

where we have used (2.118) in the third relation.

Now, we turn to the image densities. In the spirit of image theory we assume that the fields outside the substrate can be reproduced by the fields from the actual source densities in the 2D layer (the distance  $d$  from the interface) plus the fields from the mirror densities (the distance  $d$  from the interface on the opposite side), both sources embedded in the medium with dielectric function  $\tilde{\epsilon}_m(\omega)$  and magnetic permeability  $\tilde{\mu}_m(\omega)$ . The field inside the substrate we assume can be reproduced by another mirror density at the position of the 2D layer embedded in the medium with dielectric function  $\tilde{\epsilon}_s(\omega)$  and magnetic permeability  $\tilde{\mu}_s(\omega)$ . The mirror densities of the first kind is indicated by a prime and those of the second kind by a double prime.

We begin with the longitudinal current densities. The boundary condition that the in plane electric field is continuous across the medium-substrate interface gives

$$\frac{\gamma_m(k, \omega)}{\tilde{\epsilon}_m(\omega)} e^{-\gamma_m(k, \omega)kd} [K_{\parallel}(\mathbf{k}, \omega) + K_{\parallel}'(\mathbf{k}, \omega)] = \frac{\gamma_s(k, \omega)}{\tilde{\epsilon}_s(\omega)} e^{-\gamma_s(k, \omega)kd} K_{\parallel}''(\mathbf{k}, \omega). \tag{2.122}$$

The condition that the normal component of the displacement field  $\tilde{\mathbf{D}} = \tilde{\epsilon}\mathbf{E}$  is continuous across the interface gives

$$e^{-\gamma_m(k, \omega)kd} [K_{\parallel}(\mathbf{k}, \omega) - K_{\parallel}'(\mathbf{k}, \omega)] = e^{-\gamma_s(k, \omega)kd} K_{\parallel}''(\mathbf{k}, \omega). \tag{2.123}$$

Combining these two equations results in the two mirror densities

$$\begin{aligned}
K_{\parallel}'(\mathbf{k}, \omega) &= \frac{\tilde{\epsilon}_m \gamma_s - \tilde{\epsilon}_s \gamma_m}{\tilde{\epsilon}_m \gamma_s + \tilde{\epsilon}_s \gamma_m} K_{\parallel}(\mathbf{k}, \omega), \\
K_{\parallel}''(\mathbf{k}, \omega) &= \frac{2\tilde{\epsilon}_s \gamma_m}{\tilde{\epsilon}_m \gamma_s + \tilde{\epsilon}_s \gamma_m} e^{-(\gamma_m - \gamma_s)kd} K_{\parallel}(\mathbf{k}, \omega).
\end{aligned} \tag{2.124}$$

Now, let us continue with the transverse current densities. The boundary condition that the in plane transverse electric field is continuous across the interface gives

$$\frac{\tilde{\mu}_m(\omega)}{\gamma_m(k, \omega)} e^{-\gamma_m(k, \omega)kd} [K_{\perp}(\mathbf{k}, \omega) + K_{\perp}'(\mathbf{k}, \omega)] = \frac{\tilde{\mu}_s(\omega)}{\gamma_s(k, \omega)} e^{-\gamma_s(k, \omega)kd} K_{\perp}''(\mathbf{k}, \omega). \tag{2.125}$$

Then we use the condition that the in plane longitudinal component of the  $\tilde{\mathbf{H}}$ -field is continuous across the interface. Since  $\tilde{\mathbf{H}} = \mathbf{B}/\tilde{\mu}$  this gives

$$e^{-\gamma_m(k,\omega)kd} [K_{\perp}(\mathbf{k}, \omega) - K_{\perp}'(\mathbf{k}, \omega)] = e^{-\gamma_s(k,\omega)kd} K_{\perp}''(\mathbf{k}, \omega). \quad (2.126)$$

These two equations result in the mirror densities

$$\begin{aligned} K_{\perp}'(\mathbf{k}, \omega) &= \frac{\tilde{\mu}_s \gamma_m - \tilde{\mu}_m \gamma_s}{\tilde{\mu}_s \gamma_m + \tilde{\mu}_m \gamma_s} K_{\perp}(\mathbf{k}, \omega), \\ K_{\perp}''(\mathbf{k}, \omega) &= \frac{2\tilde{\mu}_m \gamma_s}{\tilde{\mu}_s \gamma_m + \tilde{\mu}_m \gamma_s} e^{-(\gamma_m - \gamma_s)kd} K_{\perp}(\mathbf{k}, \omega). \end{aligned} \quad (2.127)$$

In later sections we will need the single primed mirror densities in (2.124) and (2.127).

### 2.7.2.1 Non-retarded Treatment

If we want to be general and also include magnetic effects in the non-retarded treatment we cannot just put  $c = \infty$  everywhere. Retardation effects disappear if we put  $\omega/cq = 0$ . Now, (2.111) and (2.113) become

$$\begin{aligned} \mathbf{E}(\mathbf{q}, \omega) &= -i\mathbf{q} \frac{1}{\tilde{\epsilon}_m} \frac{4\pi \rho_s(\mathbf{q}, \omega)}{q^2 [1 - (\tilde{n}_m \omega/cq)^2]} + \frac{i\tilde{\mu}_m(\omega/cq)}{cq} \frac{4\pi \mathbf{K}(\mathbf{q}, \omega)}{[1 - (\tilde{n}_m \omega/cq)^2]} \\ &= -i\mathbf{q} \frac{1}{\tilde{\epsilon}_m} \frac{4\pi \rho_s(\mathbf{q}, \omega)}{q^2}, \end{aligned} \quad (2.128)$$

and

$$\mathbf{B}(\mathbf{q}, \omega) = i \frac{4\pi \tilde{\mu}_m}{cq^2} \mathbf{q} \times \mathbf{K}(\mathbf{q}, \omega), \quad (2.129)$$

respectively. Note that  $c$  still remains in (2.129).

We now proceed just like in the fully retarded treatment and find the field components in the source plane,

$$\begin{aligned} E_{\parallel}(\mathbf{k}, \omega) &= -i \frac{2\pi}{\tilde{\epsilon}_m(\omega)} (k/\omega) K_{\parallel}(\mathbf{k}, \omega), \\ E_{\perp}(\mathbf{k}, \omega) &= 0, \\ E_{\mathbf{n}}(\mathbf{k}, \omega) &= 0, \\ B_{\parallel}(\mathbf{k}, \omega) &= 0, \\ B_{\perp}(\mathbf{k}, \omega) &= 0, \\ B_{\mathbf{n}}(\mathbf{k}, \omega) &= i \frac{2\pi \tilde{\mu}_m(\omega)}{c} K_{\perp}(\mathbf{k}, \omega), \end{aligned} \quad (2.130)$$

and in a plane parallel to the source plane,

$$\begin{aligned}
E_{\parallel}(\mathbf{k}; z, \omega) &= -i \frac{2\pi}{\tilde{\varepsilon}_m(\omega)} (k/\omega) e^{-k|z|} K_{\parallel}(\mathbf{k}, \omega), \\
E_{\perp}(\mathbf{k}; z, \omega) &= 0, \\
E_n(\mathbf{k}; z, \omega) &= \frac{2\pi}{\tilde{\varepsilon}_m(\omega)} \frac{z}{|z|} e^{-k|z|} \rho_s(\mathbf{k}, \omega) \\
&= \frac{2\pi}{\tilde{\varepsilon}_m(\omega)} \frac{z}{|z|} \frac{k}{\omega} e^{-k|z|} K_{\parallel}(\mathbf{k}, \omega), \\
B_{\parallel}(\mathbf{k}; z, \omega) &= k \frac{z}{|z|} \frac{\tilde{\mu}_m(\omega)}{c} \frac{2\pi K_{\perp}(\mathbf{k}, \omega)}{k} e^{-k|z|} \\
&= \frac{z}{|z|} \frac{\tilde{\mu}_m(\omega)}{c} 2\pi K_{\perp}(\mathbf{k}, \omega) e^{-k|z|}, \\
B_{\perp}(\mathbf{k}; z, \omega) &= -k \frac{z}{|z|} \frac{\tilde{\mu}_m(\omega)}{c} \frac{2\pi K_{\parallel}(\mathbf{k}, \omega)}{k} e^{-k|z|} \\
&= -\frac{z}{|z|} \frac{\tilde{\mu}_m(\omega)}{c} 2\pi K_{\parallel}(\mathbf{k}, \omega) e^{-k|z|} \\
&= -\frac{z}{|z|} \tilde{\mu}_m(\omega) (\omega/c k) 2\pi \rho_s(\mathbf{k}, \omega) e^{-k|z|} = 0, \\
B_n(\mathbf{k}; z, \omega) &= i \frac{2\pi \tilde{\mu}_m(\omega)}{c} K_{\perp}(\mathbf{k}, \omega) e^{-k|z|}. \tag{2.131}
\end{aligned}$$

Note that we found that  $B_{\perp}$  vanishes in the non-retarded treatment by substituting  $K_{\parallel}$  in favor of  $\rho_s$  according to (2.118), a substitution producing a factor of  $(\omega/c k)$ .

Now we follow the derivation in the previous section. We first use the boundary condition that the in plane electric field is continuous across the medium-substrate interface. This gives

$$\frac{1}{\tilde{\varepsilon}_m(\omega)} e^{-kd} [K_{\parallel}(\mathbf{k}, \omega) + K_{\parallel}'(\mathbf{k}, \omega)] = \frac{1}{\tilde{\varepsilon}_s(\omega)} e^{-kd} K_{\parallel}''(\mathbf{k}, \omega). \tag{2.132}$$

Then we use the condition that the normal component of the displacement field  $\tilde{\mathbf{D}} = \tilde{\varepsilon}\mathbf{E}$  is continuous across the interface. This gives

$$e^{-kd} [K_{\parallel}(\mathbf{k}, \omega) - K_{\parallel}'(\mathbf{k}, \omega)] = e^{-kd} K_{\parallel}''(\mathbf{k}, \omega). \tag{2.133}$$

Combining these two equations results in the mirror densities

$$\begin{aligned}
K_{\parallel}'(\mathbf{k}, \omega) &= \frac{\tilde{\varepsilon}_m - \tilde{\varepsilon}_s}{\tilde{\varepsilon}_m + \tilde{\varepsilon}_s} K_{\parallel}(\mathbf{k}, \omega), \\
K_{\parallel}''(\mathbf{k}, \omega) &= \frac{2\tilde{\varepsilon}_s}{\tilde{\varepsilon}_m + \tilde{\varepsilon}_s} e^{-kd} K_{\parallel}(\mathbf{k}, \omega). \tag{2.134}
\end{aligned}$$

Now, we turn to the magnetic fields. We first use the boundary condition that the in plane magnetic field is continuous across the medium-substrate interface. This gives

$$\frac{2\pi}{c} e^{-kd} [K_{\perp}(\mathbf{k}, \omega) - K'_{\perp}(\mathbf{k}, \omega)] = \frac{2\pi}{c} e^{-kd} K''_{\perp}(\mathbf{k}, \omega), \quad (2.135)$$

or

$$K_{\perp}(\mathbf{k}, \omega) - K'_{\perp}(\mathbf{k}, \omega) = K''_{\perp}(\mathbf{k}, \omega). \quad (2.136)$$

Then we use that the normal component of the magnetic induction is continuous across the interface,

$$i \frac{2\pi \tilde{\mu}_m(\omega)}{c} e^{-kd} [K_{\perp}(\mathbf{k}, \omega) + K'_{\perp}(\mathbf{k}, \omega)] = i \frac{2\pi \tilde{\mu}_s(\omega)}{c} K''_{\perp}(\mathbf{k}, \omega) e^{-kd} \quad (2.137)$$

or

$$\tilde{\mu}_m(\omega) [K_{\perp}(\mathbf{k}, \omega) + K'_{\perp}(\mathbf{k}, \omega)] = \tilde{\mu}_s(\omega) K''_{\perp}(\mathbf{k}, \omega). \quad (2.138)$$

Combining these two equations results in the mirror densities

$$\begin{aligned} K'_{\perp}(\mathbf{k}, \omega) &= \frac{\tilde{\mu}_s(\omega) - \tilde{\mu}_m(\omega)}{\tilde{\mu}_s(\omega) + \tilde{\mu}_m(\omega)} K_{\perp}(\mathbf{k}, \omega), \\ K''_{\perp}(\mathbf{k}, \omega) &= \frac{2\tilde{\mu}_m(\omega)}{\tilde{\mu}_s(\omega) + \tilde{\mu}_m(\omega)} K_{\perp}(\mathbf{k}, \omega). \end{aligned} \quad (2.139)$$

### 2.7.3 Screening Functions in a 2D System

The expression for the dielectric function,  $\tilde{\epsilon}$ , in terms of the dynamical conductivity,  $\tilde{\sigma}$ , is different in 2D and 3D systems. The relations are

$$\begin{aligned} \tilde{\epsilon}^{3D}(\mathbf{q}, \omega) &= 1 + \tilde{\alpha}^{3D}(\mathbf{q}, \omega) = 1 + 4\pi i \tilde{\sigma}^{3D}(\mathbf{q}, \omega) / \omega, \\ \tilde{\epsilon}^{2D}(\mathbf{k}, \omega) &= 1 + \tilde{\alpha}^{2D}(\mathbf{k}, \omega) = 1 + 2\pi i \tilde{\sigma}^{2D}(\mathbf{k}, \omega) k / \omega, \end{aligned} \quad (2.140)$$

where  $\tilde{\alpha}$  is the polarizability. The relations between the induced current densities and the electric field are

$$\begin{aligned} \mathbf{J}(\mathbf{q}, \omega) &= \tilde{\sigma}^{3D}(\mathbf{q}, \omega) \mathbf{E}(\mathbf{q}, \omega), \\ \mathbf{K}(\mathbf{k}, \omega) &= \tilde{\sigma}^{2D}(\mathbf{k}, \omega) \mathbf{E}(\mathbf{k}, \omega). \end{aligned} \quad (2.141)$$

The *tilde* above the polarizabilities and conductivities indicates that both bound and conduction carriers, if any, contribute to these functions. Sometimes it is convenient to introduce another correlation function,  $\chi$ , the polarization bubble (in the language of Feynman diagrams), or lowest order contribution to the density-density correlation function,

$$\begin{aligned} \tilde{\alpha}^{3D}(\mathbf{q}, \omega) &= -v^{3D}(\mathbf{q}) \chi^{3D}(\mathbf{q}, \omega) = -4\pi e^2 \chi^{3D}(\mathbf{q}, \omega) / q^2, \\ \tilde{\alpha}^{2D}(\mathbf{k}, \omega) &= -v^{2D}(\mathbf{k}) \chi^{2D}(\mathbf{k}, \omega) = -2\pi e^2 \chi^{2D}(\mathbf{k}, \omega) / k. \end{aligned} \quad (2.142)$$

In different places in this book we give numerical results for systems containing graphene or 2D electron gases. Let us first discuss the dielectric function of graphene. We begin with an undoped graphene sheet. In a general point,  $z$ , in the complex frequency plane, away from the real axis the density-density correlation function is [7]

$$\chi^{2D}(\mathbf{k}, z) = -\frac{g}{16\hbar} \frac{k^2}{\sqrt{v^2 k^2 - z^2}}, \quad (2.143)$$

where  $v$  is the carrier velocity which is a constant in graphene ( $E = \pm\hbar vk$ ), and  $g$  represents the degeneracy parameter with the value of 4 (a factor of 2 for spin and a factor of 2 for the cone degeneracy). In our numerical calculations here and in earlier works [8–13] we use the value [14]  $8.73723 \times 10^5$  m/s for  $v$ .

Doping the graphene sheet leads to a much more complicated dielectric function. However it has been derived by several groups [9, 14–16].

The density-density correlation function in a general point in the complex frequency plane,  $z$ , away from the real axis is [9]

$$\begin{aligned} \chi^{2D}(\mathbf{k}, z) &= -D_0 \left\{ 1 + \frac{x^2}{4\sqrt{x^2 - \tilde{z}^2}} [\pi - f(x, \tilde{z})] \right\}, \\ f(x, \tilde{z}) &= \text{asin}\left(\frac{1-\tilde{z}}{x}\right) + \text{asin}\left(\frac{1+\tilde{z}}{x}\right) \\ &\quad - \frac{\tilde{z}-1}{x} \sqrt{1 - \left(\frac{\tilde{z}-1}{x}\right)^2} + \frac{\tilde{z}+1}{x} \sqrt{1 - \left(\frac{\tilde{z}+1}{x}\right)^2}, \end{aligned} \quad (2.144)$$

where  $D_0 = \sqrt{gn/\pi\hbar^2 v^2}$  is the density of states at the Fermi level and  $n$  is the doping concentration. We have used the following dimension-less variables:  $x = k/2k_F$ ;  $y = \hbar\xi/2E_F$ ;  $\tilde{z} = \hbar z/2E_F$ .

The same result holds for excess of electrons and excess of holes. The results have been derived within the so-called conical approximation where the conduction and valence bands consist of two sets of cone-pairs; in each cone-pair (see Fig. 2.8) the valence band is represented by a cone with its point pointing upward and the conduction band is represented by an identical cone but with its point pointing downward; they are vertically aligned with their points coinciding, meaning zero band-gap. In the undoped case this point is where the Fermi-level is; in the  $n$ -doped case the Fermi-level is further up in the conduction band; in the  $p$ -doped case the Fermi-level is further down in the valence band.

In the calculations one often uses the function at the imaginary frequency axis. We have [9, 10] derived a very useful analytical expression valid along the imaginary axis, an expression in terms of real valued functions of real valued variables:

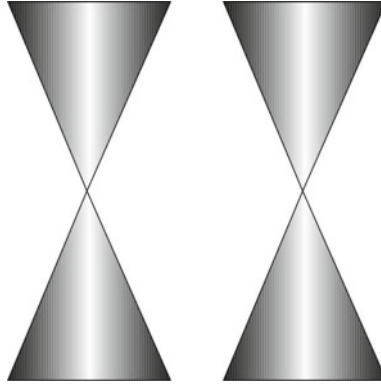


**Fig. 2.8** The two cone-pairs in the interesting part of the graphene band-structure. The lower cones with their points pointing upward are the top of the valence bands; the two upper cones are the bottom of the conduction bands. The band gap has zero value. In pristine (undoped) graphene the Fermi surface consists of two points in the Brillouin zone; in  $n$ -doped graphene it consists of two rings encircling the occupied electron states; in  $p$ -doped graphene it consists of two rings encircling the unoccupied electron states

$$\begin{aligned}
 \chi^{2D}(\mathbf{k}, i\xi) &= -D_0 \left\{ 1 + \frac{x^2}{4\sqrt{y^2+x^2}} [\pi - g(x, y)] \right\}, \\
 g(x, y) &= \text{atan} [h(x, y)k(x, y)] + l(x, y), \\
 h(x, y) &= \frac{2\left\{ [x^2(y^2-1) + (y^2+1)^2]^2 + (2yx^2)^2 \right\}^{1/4}}{\sqrt{(x^2+y^2-1)^2 + (2y)^2 - (y^2+1)}}, \\
 k(x, y) &= \sin \left\{ \frac{1}{2} \text{atan} \left[ \frac{2yx^2}{x^2(y^2-1) + (y^2+1)^2} \right] \right\}, \\
 l(x, y) &= \frac{\sqrt{-2x^2(y^2-1) - 2(y^4 - 6y^2 + 1) + 2(y^2+1)\sqrt{x^4 + 2x^2(y^2-1) + (y^2+1)^2}}}{x^2},
 \end{aligned} \tag{2.145}$$

where the *arcus tangens* function is taken from the branch where  $0 \leq \text{atan} < \pi$ . The density-density correlation function on the imaginary frequency axis has been derived before in a compact and inexplicit form (see [17] and references therein). Here we have chosen to express it in an explicit form in terms of real valued functions of real valued variables.

The 2D polarizability of an electron gas in the Random Phase Approximation (RPA) is given by [18]

$$\alpha^{2D}(Q, i\Xi) = \frac{\gamma}{Q} \left\{ 1 - \frac{1}{Q^2} \left[ \sqrt{(Q^4 - \Xi^2 - Q^2)^2 + (2\Xi Q^2)^2} + (Q^4 - \Xi^2 - Q^2)^2 \right]^{1/2} \right\}, \tag{2.146}$$

where

$$\begin{aligned} y &= \frac{me^2}{\hbar^2 k_F}; \quad \Xi = \frac{\hbar \xi}{4E_F}; \quad Q = \frac{k}{2k_F}; \\ k_F &= \sqrt{2\pi n^{2D}}; \quad E_F = \frac{\hbar^2 k_F^2}{2m}. \end{aligned} \quad (2.147)$$

These analytical expressions will be used in the numerical derivations in later chapters.

## 2.8 Fields from a Time-Dependent Electric or Magnetic Dipole

For the derivation of the Casimir-Polder interaction between two polarizable atoms we need the complete expression for the electric field from a time-varying electric dipole. If one wants to include also magnetic effects one needs the complete expression for the magnetic fields as well and for the electric and magnetic fields from a time-varying magnetic dipole.

It is possible to derive the complete fields [19, 20] from a linear electric dipole in the limit  $d \ll r$ , where  $d$  is the linear extent of the dipole. Heald and Marion [19] based their derivation on the so-called Hertzian-dipole model; Kort-Kamp and Farina [20] used a multipole expansion of an arbitrary but localized charge and current distribution, with an arbitrary time dependence, to find the fields.

The fields for an electric dipole at the origin, pointing in the  $z$ -direction, are

$$\mathbf{E}(\mathbf{r}, t) = \left( \frac{2[p]}{r^3} + \frac{2[\dot{p}]}{cr^2} \right) \cos \theta \mathbf{e}_r + \left( \frac{[p]}{r^3} + \frac{[\dot{p}]}{cr^2} + \frac{[\ddot{p}]}{c^2 r} \right) \sin \theta \mathbf{e}_\theta, \quad (2.148)$$

and

$$\mathbf{B}(\mathbf{r}, t) = \left( \frac{[\dot{p}]}{cr^2} + \frac{[\ddot{p}]}{c^2 r} \right) \sin \theta \mathbf{e}_\varphi. \quad (2.149)$$

The square brackets means that the time argument is the retarded time,  $t - r/c$ .

The terms varying as  $1/r$  are the radiation fields. The effects of the time dependence of the charge and current densities are two fold; one is the time delay of the response; the other is that time derivatives enter the expressions.

For completeness we also give the total fields from a time-dependent magnetic dipole. These can easily be obtained using the duality in electromagnetic theory. With our notation this means that in absence of external sources all relations are valid even after the following replacements:

$$\left\{ \begin{array}{l} \mathbf{E} \rightarrow \tilde{\mathbf{H}}, \tilde{\mathbf{H}} \rightarrow -\mathbf{E} \\ \tilde{\mathbf{D}} \rightarrow \mathbf{B}, \mathbf{B} \rightarrow -\tilde{\mathbf{D}} \\ \mathbf{P} \rightarrow \mathbf{M}, \mathbf{M} \rightarrow -\mathbf{P} \\ \mathbf{p} \rightarrow \mathbf{m}, \mathbf{m} \rightarrow -\mathbf{p} \\ \tilde{\boldsymbol{\varepsilon}} \rightarrow \tilde{\boldsymbol{\mu}}, \tilde{\boldsymbol{\mu}} \rightarrow \tilde{\boldsymbol{\varepsilon}} \\ \chi_e \rightarrow \chi_m, \chi_m \rightarrow \chi_e \\ \boldsymbol{\alpha}^{\text{at.}} \rightarrow \boldsymbol{\beta}^{\text{at.}}, \boldsymbol{\beta}^{\text{at.}} \rightarrow \boldsymbol{\alpha}^{\text{at.}} \end{array} \right. \quad (2.150)$$

The MEs and the constitutive relations are the same after the replacements. They pairwise replace each other. These replacements may be used even in the presence of sources if these are dipoles.

The fields from a time-varying magnetic dipole are

$$\mathbf{E}(\mathbf{r}, t) = -\left( \frac{[\dot{m}]}{cr^2} + \frac{[\ddot{m}]}{c^2 r} \right) \sin \theta \mathbf{e}_\theta, \quad (2.151)$$

and

$$\mathbf{B}(\mathbf{r}, t) = \left( \frac{2[m]}{r^3} + \frac{2[\dot{m}]}{cr^2} \right) \cos \theta \mathbf{e}_r + \left( \frac{[m]}{r^3} + \frac{[\dot{m}]}{cr^2} + \frac{[\ddot{m}]}{c^2 r} \right) \sin \theta \mathbf{e}_\theta. \quad (2.152)$$

## References

1. J.C. Maxwell, *Philos. Trans.* **155**, 459 (1865)
2. P. Halevi, Spatial dispersion in solids and plasmas, in *Electromagnetic Waves: Recent Development in Research*, vol. 1, ed. by P. Halevi (North-Holland, Amsterdam, 1992)
3. Bo E. Sernelius, *Phys. Rev. B* **71**, 235114 (2005)
4. M. Boström, C. Persson, Bo E. Sernelius, *Eur. Phys. J. B* **86**, 43 (2013)
5. H. Fujiwara, in *Spectroscopic Ellipsometry: Principles and Applications* (Wiley, Chichester 2007), (6.19) and (6.20) pp. 223 and 224
6. Bo E. Sernelius, *J. Phys.: Condens. Matter* **27**, 214017 (2015)
7. J. González, F. Guinea, M.A.H. Vozmediano, *Nucl. Phys.* **424**, 595 (1994)
8. Bo E. Sernelius, *Graphene* **1**, 21 (2012)
9. Bo E. Sernelius, *EPL* **95**, 57003 (2011)
10. Bo E. Sernelius, *Phys. Rev. B* **85**, 195427 (2012)
11. Bo E. Sernelius, *FlatChem* **1**, 1 (2016)
12. M. Boström, Bo E. Sernelius, *Phys. Rev. A* **85**, 012508 (2012)
13. Bo E. Sernelius, *Int. J. Mod. Phys. Conf. Ser.* **14**, 531 (2012)
14. B. Wunsch, T. Stauber, F. Sols, F. Guinea, *New J. Phys.* **8**, 318 (2006)
15. E.H. Hwang, D.S. Sarma, *Phys. Rev. B* **75**, 205418 (2007)
16. G.L. Klimchitskaya, V.M. Mostepanenko, Bo E. Sernelius, *Phys. Rev. B* **89**, 125407 (2014)
17. Y. Barlas, T. Pereg-Barnea, M. Polini, R. Asgari, A.H. MacDonald, *Phys. Rev. Lett.* **98**, 236601 (2007)
18. Bo E. Sernelius, *Phys. Rev. B* **90**, 155457 (2014)
19. M.A. Heald, J.B. Marion, *Classical Electromagnetic Radiation*, 3rd edn., chap. 9 (Saunders College Publishing, New York, 1995)
20. W.J.M. Kort-Kamp, C. Farina, *Am. J. Phys.* **79**, 111 (2011)

# Chapter 3

## Complex Analysis



**Abstract** Complex analysis, the theory of functions of a complex variable, is one of the most powerful mathematical instruments of applied mathematicians, engineers, and physicists. We benefit greatly from large segments of this theory. In this chapter we discuss those areas of complex analysis that we need in order to make the presentation as self-contained as possible. We will keep the treatment brief and will not present any proofs of statements or theorems. Instead we demonstrate that the claim holds for specific examples and thereby making the statement at least believable. The interested reader is referred to Churchill (Complex variables and applications, 1960) [1] for further reading. We start by introducing basic concepts like *analytic functions*, *singular points*, *poles*, *residues*, and *contour integration*. Then we continue with response functions. A fundamental property that all physical systems have and that is needed for the interactions treated in this book to occur is that the system responds to an external perturbation. The response of the system to various perturbations are described by response functions, correlation functions. The differential equations all show time-reversal symmetry but the response functions are all retarded time-correlation functions which means that the response comes after the perturbation; they obey the causality principle. This means that they have some characteristic properties in the complex frequency plane. We show how this is handled starting from the simplest of systems, the vacuum.

### 3.1 Analytic Functions

The Fourier transformed functions that we have discussed so far are complex valued functions of two real valued variables, e.g.,  $f(\mathbf{q}, \omega)$ , where the (angular) frequency  $\omega$  is real valued. One can gain much by letting the variable be complex valued. We will find in Sect. 3.4 that by moving up an infinitesimal distance above the real axis will make the response functions casual. One can say that physics occurs on the real axis or just above. However, mathematical calculations can be performed throughout the

hole complex frequency plane where a general point is represented by the coordinate  $z$ . The response functions are much more well-behaved on the imaginary frequency axis than on the real frequency axis. This fact alone makes it worth trying to perform as much of the calculation as possible along that axis. Let us now concentrate on the time- and frequency-dependence of the functions and suppress the spatial and  $\mathbf{q}$ -dependence. First we need to define what we mean by analytic functions.

The complex-valued function,  $f(z)$ , of the complex variable  $z$  is *analytic* at a point  $z_0$  if its derivative  $f'(z)$ <sup>1</sup> exists not only at  $z_0$  but at every point  $z$  in some neighborhood of  $z_0$ . It is analytic in a domain of the  $z$  plane if it is analytic in every point in that domain.

If a function is analytic at some point in every neighborhood of a point  $z_0$  except at the  $z_0$  itself, then  $z_0$  is called a *singular point* or *singularity*, of the function.

If there is some neighborhood of a singular point  $z_0$  throughout which  $f(z)$  is analytic, except at the point itself, then  $z_0$  is called an *isolated singular point*.

Now, the function  $1/z$  is analytic everywhere except at  $z = 0$  where it has an isolated singular point. The function  $|z|^2$  is nowhere analytic and has no singular points.

Let us now discuss some elementary functions that will appear later in the formalism. We begin with the exponential function that is defined by

$$\exp(z) = e^x (\cos y + i \sin y), \quad (3.1)$$

where  $z = x + iy$ . It is analytic in the whole  $z$  plane, which makes it an *entire function*. The exponential function is periodic with the period  $2\pi i$  which means that its inverse, the logarithm, has branches.

The hyperbolic sine and cosine functions are defined as

$$\sinh z = \frac{e^z - e^{-z}}{2}, \quad (3.2)$$

and

$$\cosh z = \frac{e^z + e^{-z}}{2}, \quad (3.3)$$

respectively. They are entire functions since an entire function of an entire function is also entire.

The hyperbolic cotangent is defined by

$$\coth z = \frac{e^z + e^{-z}}{e^z - e^{-z}}, \quad (3.4)$$

and the function has isolated singular points at  $z = in\pi$  where  $n$  is an integer. At those points the denominator vanishes.

---

<sup>1</sup>  $f'(z) = \lim_{\Delta z \rightarrow 0} \frac{f(z+\Delta z) - f(z)}{\Delta z}$ .

The hyperbolic functions will appear when we calculate the interactions at finite temperature. The last elementary function we will treat here is the logarithmic function. It will appear when we use the argument principle both at zero and finite temperature. It is defined as

$$\ln z = \ln r + i\theta, \tag{3.5}$$

where we have expressed  $z$  on polar form,  $z = re^{i\theta}$ , and  $\ln r$  is the ordinary logarithm of a real variable. Unless otherwise stated we stick to the principle branch of the function which means that the angle  $\theta$  is limited to  $-\pi < \theta \leq \pi$ . The function is analytic in the domain  $z \neq 0$ ,  $-\pi < \theta < \pi$  and all points on the negative real axis are singular points; there is a branch cut along the whole negative real axis. The singular point  $z = 0$ , common to all branch cuts for the multivalued logarithm function, is a so-called branch point.

### 3.2 Laurent Expansion and Residues

**Theorem 3.1** *Let  $z_0$  be an isolated singular point of the function  $f(z)$ . There exists a positive number  $r_1$  such that the function is analytic in every point  $z$  for which  $0 < |z - z_0| < r_1$ . In that region the function may be represented by a so-called Laurent series:*

$$f(z) = \sum_{n=0}^{\infty} a_n(z - z_0)^n + \frac{b_1}{z - z_0} + \frac{b_2}{(z - z_0)^2} + \frac{b_3}{(z - z_0)^3} + \dots \tag{3.6}$$

The parameter  $b_1$  is called the *residue* of  $f$  at the isolated singular point  $z_0$ .

The Laurent series consists of two parts, one with positive exponents and one with negative. The part with negative exponents is called the principle part. Suppose that the principle part consists of a finite number of terms. If the highest negative power is  $m$  the singular point is called a *pole* of order  $m$  of the function  $f$ . A pole of order  $m = 1$  is called a *simple pole*. When the principle part of  $f$  about the point  $z_0$  has an infinite number of terms, the point is called an *essential singular point* of  $f$ .

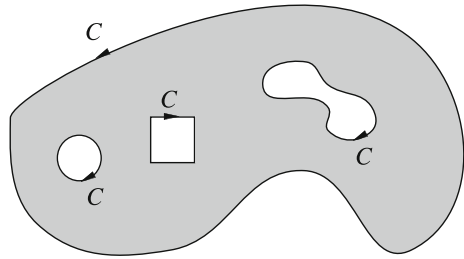
### 3.3 Contour Integration in the Complex Plane

Contour integration is, as we shall see, a very useful tool in many situations. We start by stating the *Cauchy-Goursat theorem*.

**Theorem 3.2** *If a function  $f$  is analytic at all points interior to and on a closed contour  $C$ , then*

$$\int_C f(z) dz = 0. \tag{3.7}$$

**Fig. 3.1** A closed contour in the complex plane. The arrows indicate the direction of integration. The contour encloses the gray region which is the interior of the contour. The interior is always to the left when one follows all parts of the integration path



An example of a contour and its interior is shown in Fig. 3.1. According to the theorem a contour integration around a region where the integrand is analytic produces a zero result. What happens when the integrand is not analytic? This is what we will discuss next and we start by demonstrating what the result is when we integrate around a singular point.

### 3.3.1 Integration Around a Pole

We let the function  $f(z)$  have an isolated singular point, a pole, in  $z_0$  and place a circular contour, Fig. 3.2, of radius  $r$  centered around  $z_0$ . We express the relative coordinate on the contour on polar form,  $z - z_0 = r \exp(i\theta)$  and use the Laurent expansion of  $f(z)$  as given in (3.6). Thus we have

$$f(z) = \sum_{n=0}^{\infty} a_n r^n \exp(in\theta) + \sum_{n=1}^m b_n r^{-n} \exp(-in\theta). \tag{3.8}$$

All terms are of the type  $r^n \exp(in\theta)$  where  $n$  is an integer, positive or negative. The term's contribution to the contour integration is

$$\begin{aligned} & \int_C r^n \exp(in\theta) dz \\ &= \int_0^{2\pi} r^n \exp(in\theta) r \exp(i\theta) i d\theta \\ &= i r^{n+1} \int_0^{2\pi} \exp[i(n+1)\theta] d\theta \\ &= \begin{cases} 0, & n \neq -1 \\ 2\pi i, & n = -1. \end{cases} \end{aligned} \tag{3.9}$$

**Fig. 3.2** Circular integration path around an isolated singular point

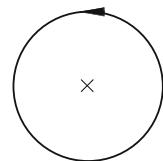
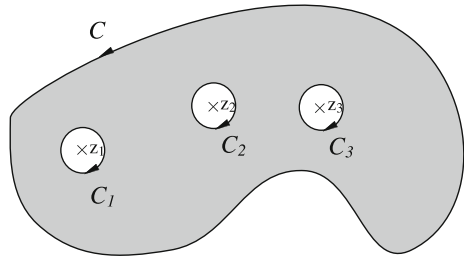


**Fig. 3.3** Contour consisting of  $C$  and small circles,  $C_i$ , around each pole  $i$



Only one term survives the integrations and we find that

$$\int_C f(z)dz = 2\pi i b_1 = 2\pi i Res(z_0). \tag{3.10}$$

Let us now study Fig. 3.3 where the function  $f(z)$  is analytic in all but a few points, denoted by  $\times$ , of the interior of contour  $C$ . We draw small circles around each singular point. The function  $f(z)$  is analytic in the interior of the contour made up from  $C$  and all circular contours in the figure so the contour integration around this contour is zero,

$$\int_C f(z)dz + \int_{C_1} f(z)dz + \int_{C_2} f(z)dz + \dots + \int_{C_n} f(z)dz = 0. \tag{3.11}$$

Thus we find

$$\begin{aligned} \int_C f(z)dz &= \int_{-C_1} f(z)dz + \int_{-C_2} f(z)dz + \dots + \int_{-C_n} f(z)dz \\ &= 2\pi i [Res(z_1) + Res(z_2) + \dots + Res(z_n)], \end{aligned} \tag{3.12}$$

where with  $-C_i$  we mean  $C_i$  taken in the opposite direction. The integration around  $C_i$  is done in the clockwise direction and the one around  $-C_i$  in the counterclockwise direction. Now, we have more or less proven the next theorem, the Residue Theorem.

**Theorem 3.3** *Let  $C$  be a closed contour within and on which the function  $f$  is analytic except for a finite number of singular points  $z_1, z_2, \dots, z_n$  interior to  $C$ . If  $K_1, K_2, \dots, K_n$  denote the residues of  $f$  at those points, then*

$$\int_C f(z)dz = 2\pi i (K_1 + K_2 + \dots + K_n), \tag{3.13}$$

where the integral is taken counterclockwise around  $C$ .

This is a very useful theorem. We end this subsection with another one, establishing the Cauchy's integral formula.

**Theorem 3.4** *Let  $f$  be analytic everywhere within and on a closed contour  $C$ . If  $z_0$  is any point interior to  $C$ , then*

$$f(z_0) = \frac{1}{2\pi i} \int_C \frac{f(z)}{z - z_0} dz, \quad (3.14)$$

where the integral is taken at the positive sense around  $C$ .

### 3.3.2 Argument Principle and Its Extension

The argument principle, or rather its extension, will turn out to be very helpful in the normal-mode formalism. We state this as a theorem here.

**Theorem 3.5** *Let the function  $f$  be analytic in the interior of and on a closed contour  $C$  except for at most a finite number of poles interior to  $C$ . Furthermore, let  $f$  have no zeros on  $C$  and at most a finite number of zeros in the interior of  $C$ . Then*

$$\frac{1}{2\pi i} \int_C \frac{d}{dz} \ln f(z) dz = N_0 - N_\infty, \quad (3.15)$$

where  $N_0$  and  $N_\infty$  is the total number of zeros and total number of poles, respectively, off inside  $C$ . A zero of order  $m_0$  is counted  $m_0$  times and a pole of order  $m_\infty$  is counted  $m_\infty$  times. The contour integral is assumed to be performed in the positive sense, i.e., counterclockwise.

The argument principle has gotten its name from that the integral produces the change, in units of  $2\pi$  radians, in the argument of the function  $f(z)$  as the point  $z$  makes a cycle about  $C$  in the positive sense.

Let us now make this result believable. Let us choose the function  $f(z) = (z - z_0)^{m_0} / (z - z_\infty)^{m_\infty}$ . This function has one zero of order  $m_0$  at  $z_0$  and one pole of order  $m_\infty$  at  $z_\infty$ . We assume that these points are inside  $C$ . Then we have

$$\begin{aligned} & \frac{1}{2\pi i} \int_C \frac{d}{dz} \ln f(z) dz \\ &= \frac{1}{2\pi i} \int_C \frac{d}{dz} [m_0 \ln(z - z_0) - m_\infty \ln(z - z_\infty)] dz \\ &= \frac{1}{2\pi i} \int_C \left( \frac{m_0}{z - z_0} - \frac{m_\infty}{z - z_\infty} \right) dz = \frac{1}{2\pi i} 2\pi i (m_0 - m_\infty), \end{aligned} \quad (3.16)$$

where in the last step we used the residue theorem (3.13). Everything is fine.

The generalized argument principle can be stated in the following way:

**Theorem 3.6** *Let the function  $f$  be analytic and have no zeros on the closed contour  $C$  and have at most a finite number of zeros and poles inside  $C$ . Let another function  $\varphi$  be analytic on and inside  $C$ . Then*

$$\frac{1}{2\pi i} \int_C \varphi(z) \frac{d}{dz} \ln f(z) dz = \sum \varphi(z_0) - \sum \varphi(z_\infty), \quad (3.17)$$

where the sums on the right hand side run over the zeros and poles of  $f$ . A zero of order  $m_0$  is counted  $m_0$  times and a pole of order  $m_\infty$  is counted  $m_\infty$  times. The contour integral is assumed to be performed in the positive sense, i.e., counterclockwise.

Here we use the same function  $f(z)$  as in the previous example and find

$$\begin{aligned} & \frac{1}{2\pi i} \int_C \varphi(z) \frac{d}{dz} \ln f(z) dz \\ &= \frac{1}{2\pi i} \int_C \left( \frac{m_0 \varphi(z)}{z-z_0} - \frac{m_\infty \varphi(z)}{z-z_\infty} \right) dz = m_0 \varphi(z_0) - m_\infty \varphi(z_\infty), \end{aligned} \quad (3.18)$$

where we in the last step used the Cauchy integral (3.14). Everything is fine.

### 3.4 Analytic Properties of Response Functions

In this section we will discuss the analytical properties of the correlation functions that describe the response of the system to various perturbations. From these properties we can derive the very useful Kramers Kronig dispersion relations. We begin with the simplest example, the response to the introduction of a charge density or current density in vacuum. We start with the potentials in static electromagnetism, i.e. we let the charge density be static and the current density stationary. Then we have

$$\begin{aligned} \nabla^2 \Phi(\mathbf{r}) &= -4\pi \rho(\mathbf{r}) \\ \nabla^2 \mathbf{A}(\mathbf{r}) &= -\frac{4\pi}{c} \mathbf{J}(\mathbf{r}). \end{aligned} \quad (3.19)$$

The scalar potential and each component of the vector potential satisfy the same type of differential equation. We can concentrate on one of them, the scalar potential say. Fourier transformation gives

$$(i\mathbf{q})^2 \Phi(\mathbf{q}, \omega) = -4\pi \rho(\mathbf{q}, \omega). \quad (3.20)$$

Thus,

$$\Phi(\mathbf{q}, \omega) = \frac{4\pi}{q^2} \rho(\mathbf{q}, \omega), \quad (3.21)$$

or

$$\Phi(\mathbf{q}, \omega) = v(\mathbf{q}, \omega) \rho(\mathbf{q}, \omega) / e^2; \quad v(\mathbf{q}, \omega) = \frac{4\pi e^2}{q^2}, \quad (3.22)$$

where  $v(\mathbf{q}, \omega)$  is the Fourier transform of the Coulomb potential, the potential energy between two electrons a distance  $r$  apart. Thus, we obtain the following convolution integral relating the potential to the charge distribution:

$$\Phi(\mathbf{r}, t) = \frac{1}{e^2} \int \int d^3 r' dt' v(\mathbf{r} - \mathbf{r}', t - t') \rho(\mathbf{r}', t') \quad (3.23)$$

The function  $v(\mathbf{r}, t)$  is obtained from its Fourier transform,  $v(\mathbf{q}, \omega)$ , above using the inverse Fourier transform. Note that its Fourier transform is independent of  $\omega$ . This means that the function will be a delta function of time. The Coulomb potential is instantaneous. Let us now show that this really is the case. We have

$$\begin{aligned} v(\mathbf{r}, t) &= \int \frac{d^3 q}{(2\pi)^3} \int_{-\infty}^{\infty} \frac{d\omega}{2\pi} v(\mathbf{q}, \omega) e^{i(\mathbf{q}\cdot\mathbf{r} - \omega t)} \\ &= \int \frac{d^3 q}{(2\pi)^3} \int_{-\infty}^{\infty} \frac{d\omega}{2\pi} \frac{4\pi e^2}{q^2} e^{i(\mathbf{q}\cdot\mathbf{r} - \omega t)} \\ &= \int \frac{d^3 q}{(2\pi)^3} \frac{4\pi e^2}{q^2} e^{i(\mathbf{q}\cdot\mathbf{r})} \int_{-\infty}^{\infty} \frac{d\omega}{2\pi} e^{i(-\omega t)} \\ &= \delta(t) \int_0^{\infty} \frac{dq}{(2\pi)^3} 2\pi q^2 \int_{-1}^1 dx \frac{4\pi e^2}{q^2} e^{iqr x} \\ &= \delta(t) \int_0^{\infty} \frac{dq}{(2\pi)^3} 2\pi q^2 \frac{4\pi e^2}{q^2} \frac{1}{iqr} e^{iqr x} \Big|_{-1}^1 \\ &= \delta(t) \frac{2e^2}{\pi r} \int_0^{\infty} dq \frac{\sin(qr)}{q} \\ &= \delta(t) \frac{2e^2}{\pi r} \frac{\pi}{2} = \delta(t) \frac{e^2}{r}. \end{aligned} \quad (3.24)$$

Thus

$$\begin{aligned} \Phi(\mathbf{r}, t) &= \frac{1}{e^2} \int \int d^3 r' dt' \delta(t - t') \frac{e^2}{|\mathbf{r} - \mathbf{r}'|} \rho(\mathbf{r}', t') \\ &= \int d^3 r' \frac{1}{|\mathbf{r} - \mathbf{r}'|} \rho(\mathbf{r}', t) = \int d^3 r' \frac{\rho(\mathbf{r}')}{|\mathbf{r} - \mathbf{r}'|}, \end{aligned} \quad (3.25)$$

since the charge distribution was assumed to be static. If we repeat the same procedure for the vector potential we get

$$\mathbf{A}(\mathbf{r}) = \frac{1}{c} \int d^3r' \frac{\mathbf{J}(\mathbf{r}')}{|\mathbf{r} - \mathbf{r}'|}. \quad (3.26)$$

We now continue with the same examples but in dynamic electromagnetism. We have to specify the gauge. We chose the Lorentz gauge (2.42). We have

$$\begin{aligned} \nabla^2 \Phi - \frac{1}{c^2} \frac{\partial^2 \Phi}{\partial t^2} &= -4\pi\rho, \\ \nabla^2 \mathbf{A} - \frac{1}{c^2} \frac{\partial^2 \mathbf{A}}{\partial t^2} &= -\frac{4\pi}{c} \mathbf{J}. \end{aligned} \quad (3.27)$$

Both potentials satisfy the same type of equation, the wave equation. We concentrate on the equation for the scalar potential

$$(\mathbf{i}\mathbf{q})^2 \Phi(\mathbf{q}, \omega) - \frac{(-i\omega)^2}{c^2} \Phi(\mathbf{q}, \omega) = -4\pi\rho(\mathbf{q}, \omega). \quad (3.28)$$

Rearrangement gives

$$\Phi(\mathbf{q}, \omega) = u(\mathbf{q}, \omega) \rho(\mathbf{q}, \omega) / e^2; \quad u(\mathbf{q}, \omega) = \frac{4\pi e^2}{q^2} \frac{1}{1 - (\omega/cq)^2}. \quad (3.29)$$

Before we continue let us return to the wave equation above. It is quadratic in the time derivative, which means that it describes a system that has time inversion symmetry.

This means that if we are not careful we will find that the potential at a certain time will depend on the charge distribution not only at preceding times but also at future times. This is in conflict with causality. We believe that the response always comes after the perturbation. Note that the response function has poles at  $\omega = \pm cq$ , both on the real axis. The causality is achieved by adding a positive infinitesimal imaginary part to the frequency in the response function,  $u(\mathbf{q}, \omega)$ . This is equivalent to moving the poles down to a position at an infinitesimal distance below the real axis (see Fig. 3.4)a,

$$\begin{aligned} u(\mathbf{q}, \omega) &= \frac{2\pi e^2}{q^2} \left[ \frac{1}{\omega/cq + i\delta + 1} - \frac{1}{\omega/cq + i\delta - 1} \right] \\ &= \frac{2\pi e^2}{q^2} \left[ \frac{1}{\omega/cq + 1} - \frac{1}{\omega/cq - 1} \right] \\ &+ \frac{2\pi^2 e^2 i}{q^2} \left[ -\delta(\omega/cq + 1) + \delta(\omega/cq - 1) \right]. \end{aligned} \quad (3.30)$$

The poles of retarded correlations functions are always below the real frequency axis in the complex frequency plane. If we do not add these imaginary parts half of the response to a perturbation will be in the form of a retarded response and half in the form of an advanced response.

Now, we have

$$u(\mathbf{r}, t) = \int \frac{d^3q}{(2\pi)^3} \int_{-\infty}^{\infty} \frac{d\omega}{2\pi} u(\mathbf{q}, \omega) e^{i(\mathbf{q}\cdot\mathbf{r}-\omega t)}, \quad (3.31)$$

or

$$\begin{aligned} u(\mathbf{r}, t) &= u_1(\mathbf{r}, t) + u_2(\mathbf{r}, t) \\ &= \int \frac{d^3q}{(2\pi)^3} \int_{-\infty}^{\infty} \frac{d\omega}{2\pi} [u_1(\mathbf{q}, \omega) + u_2(\mathbf{q}, \omega)] e^{i(\mathbf{q}\cdot\mathbf{r}-\omega t)}, \end{aligned} \quad (3.32)$$

where

$$\begin{aligned} u_1(\mathbf{q}, \omega) &= \frac{2\pi e^2}{q^2} \left[ \frac{1}{\omega/cq+1} - \frac{1}{\omega/cq-1} \right]; \\ u_2(\mathbf{q}, \omega) &= \frac{2\pi^2 e^2 i}{q^2} [-\delta(\omega/cq+1) + \delta(\omega/cq-1)]. \end{aligned} \quad (3.33)$$

Thus,

$$\begin{aligned} u_1(\mathbf{r}, t) &= \int \frac{d^3q}{(2\pi)^3} \int_{-\infty}^{\infty} \frac{d\omega}{2\pi} \frac{2\pi e^2}{q^2} \left[ \frac{1}{\omega/cq+1} - \frac{1}{\omega/cq-1} \right] e^{i(\mathbf{q}\cdot\mathbf{r}-\omega t)} \\ &= [\omega \rightarrow \omega cq] \\ &= \int \frac{d^3q}{(2\pi)^3} \int_{-\infty}^{\infty} \frac{d\omega}{2\pi} \frac{2\pi e^2 cq}{q^2} \left[ \frac{1}{\omega+1} - \frac{1}{\omega-1} \right] e^{i(\mathbf{q}\cdot\mathbf{r}-cq\omega t)} \\ &= \frac{ce^2}{4\pi^2} \int_0^{\infty} dq q^2 \frac{1}{q} \int_{-1}^1 dx e^{iqr x} \int_{-\infty}^{\infty} d\omega \left[ \frac{1}{\omega+1} - \frac{1}{\omega-1} \right] e^{-icq\omega t} \\ &= \frac{ce^2}{4\pi^2} \int_0^{\infty} dq q 2 \frac{\sin(qr)}{qr} \int_{-\infty}^{\infty} d\omega \frac{1}{\omega} e^{-icq\omega t} [e^{icqt} - e^{-icqt}] \\ &= \frac{ce^2}{2\pi^2 r} \int_0^{\infty} dq \sin(qr) 2i \sin(cqt) \int_0^{\infty} d\omega \frac{1}{\omega} [-2i \sin(cq\omega t)] \\ &= \frac{2ce^2}{\pi^2 r} \int_0^{\infty} dq \left[ \frac{1}{2} \cos(qr - cqt) - \frac{1}{2} \cos(qr + cqt) \right] \frac{\pi}{2} \text{sign}(cqt) \\ &= \frac{ce^2}{4\pi r} \text{sign}(t) \int_{-\infty}^{\infty} dq [\cos(qr - cqt) - \cos(qr + cqt)] \\ &= \frac{ce^2}{4\pi r} \text{sign}(t) [2\pi \delta(r - ct) - 2\pi \delta(r + ct)] \\ &= \frac{ce^2}{2r} [\delta(r - ct) + \delta(r + ct)] \\ &= \frac{e^2}{2r} [\delta(t - r/c) + \delta(t + r/c)], \end{aligned} \quad (3.34)$$

and

$$\begin{aligned}
u_2(\mathbf{r}, t) &= \int \frac{d^3q}{(2\pi)^3} \int_{-\infty}^{\infty} \frac{d\omega}{2\pi} \frac{2\pi^2 e^2 i}{q^2} [-\delta(\omega/cq + 1) + \delta(\omega/cq - 1)] e^{i(\mathbf{q}\cdot\mathbf{r} - \omega t)} \\
&= [\omega \rightarrow \omega cq] \\
&= \int \frac{d^3q}{(2\pi)^3} \int_{-\infty}^{\infty} \frac{d\omega}{2\pi} \frac{2\pi^2 e^2 i cq}{q^2} [-\delta(\omega + 1) + \delta(\omega - 1)] e^{i(\mathbf{q}\cdot\mathbf{r} - cq\omega t)} \\
&= i \frac{ce^2}{4\pi} \int_0^{\infty} dq q^2 \frac{1}{q} \int_{-1}^1 dx e^{iqrx} [-e^{icqt} + e^{-icqt}] \\
&= \frac{ice^2}{4\pi} \int_0^{\infty} dq q 2 \frac{\sin(qr)}{qr} [-2i \sin(cqt)] \\
&= \frac{ce^2}{\pi r} \int_0^{\infty} dq \sin(qr) \sin(cqt) \\
&= \frac{ce^2}{4\pi r} \int_{-\infty}^{\infty} dq [\cos(qr - cqt) - \cos(qr + cqt)] \\
&= \frac{ce^2}{4\pi r} [2\pi \delta(r - ct) - 2\pi \delta(r + ct)] = \\
&= \frac{ce^2}{2r} [\delta(r - ct) - \delta(r + ct)] \\
&= \frac{e^2}{2r} [\delta(t - r/c) - \delta(t + r/c)].
\end{aligned} \tag{3.35}$$

Thus, we end up with

$$\begin{aligned}
u(\mathbf{r}, t) &= u_1(\mathbf{r}, t) + u_2(\mathbf{r}, t) \\
&= \frac{e^2}{2r} [\delta(t - r/c) + \delta(t + r/c)] + \frac{e^2}{2r} [\delta(t - r/c) - \delta(t + r/c)] \\
&= \frac{e^2}{r} \delta(t - r/c),
\end{aligned} \tag{3.36}$$

and

$$\begin{aligned}
\Phi(\mathbf{r}, t) &= \frac{1}{e^2} \int \int d^3r' dt' u(\mathbf{r} - \mathbf{r}', t - t') \rho(\mathbf{r}', t') \\
&= \frac{1}{e^2} \int \int d^3r' dt' \frac{e^2}{|\mathbf{r} - \mathbf{r}'|} \delta(t - t' - |\mathbf{r} - \mathbf{r}'|/c) \rho(\mathbf{r}', t') \\
&= \int \int d^3r' dt' \frac{1}{|\mathbf{r} - \mathbf{r}'|} \delta(t - t' - |\mathbf{r} - \mathbf{r}'|/c) \rho(\mathbf{r}', t') \\
&= \int d^3r' \frac{\rho(\mathbf{r}', t - |\mathbf{r} - \mathbf{r}'|/c)}{|\mathbf{r} - \mathbf{r}'|}.
\end{aligned} \tag{3.37}$$

Treating the vector potential in the same fashion we arrive at

$$\mathbf{A}(\mathbf{r}, t) = \frac{1}{c} \int d^3r' \frac{\mathbf{J}(\mathbf{r}', t - |\mathbf{r} - \mathbf{r}'|/c)}{|\mathbf{r} - \mathbf{r}'|}. \tag{3.38}$$

If we had chosen Coulomb gauge instead of Lorentz gauge we would have obtained

$$\begin{aligned}
\Phi(\mathbf{r}, t) &= \int d^3r' \frac{\rho(\mathbf{r}', t)}{|\mathbf{r} - \mathbf{r}'|}, \\
\mathbf{A}(\mathbf{r}, t) &= \frac{1}{c} \int d^3r' \frac{\mathbf{J}_T(\mathbf{r}', t - |\mathbf{r} - \mathbf{r}'|/c)}{|\mathbf{r} - \mathbf{r}'|}.
\end{aligned} \tag{3.39}$$

So, in Lorentz gauge both potentials are retarded but in Coulomb gauge the scalar potential is instantaneous. Even though the pair of potentials look quite different in

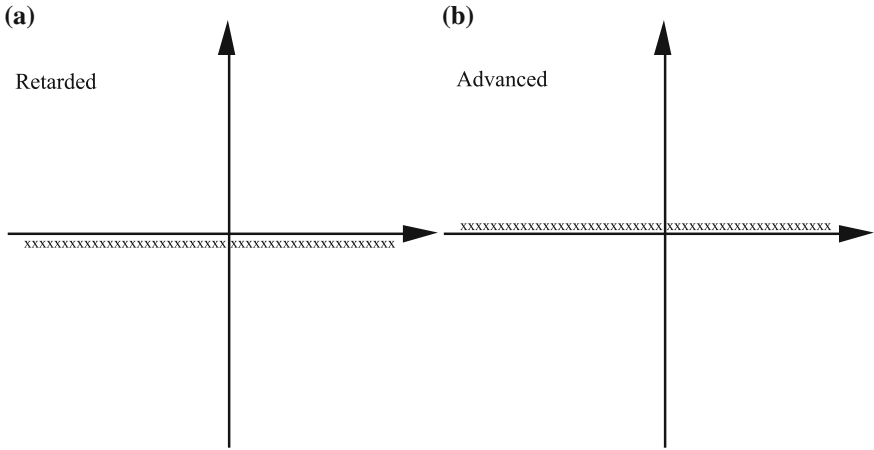


**Fig. 3.4** The position of the poles for a retarded response function (a), and for an advanced function (b)

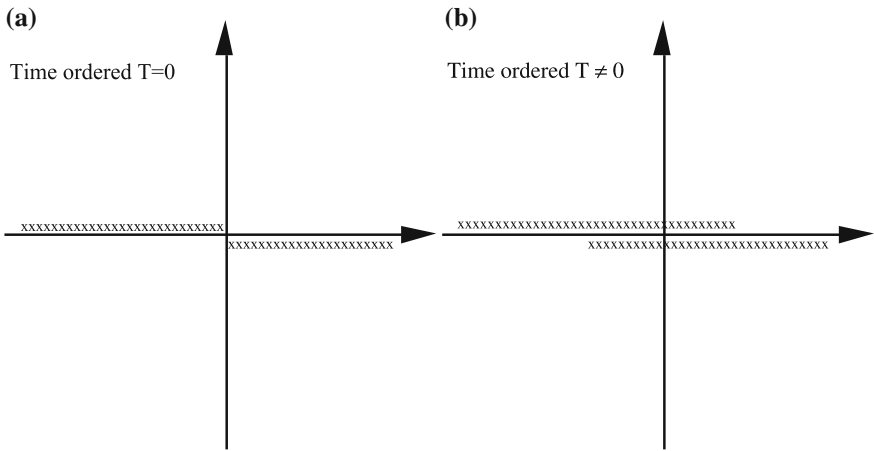


**Fig. 3.5** The position of the poles for a time-ordered response function at  $T = 0$  (a), and for a time-ordered response function at  $T \neq 0$  (b)

the two gauges they produce exactly the same electromagnetic fields and these are retarded.

Now we have discussed a response function of the simplest system, viz. the vacuum. The most important response function for the topic of this text is the dielectric function. For a metallic system we may write

$$\tilde{\epsilon}(\mathbf{q}, \omega) = \epsilon(\mathbf{q}, \omega) + \alpha(\mathbf{q}, \omega), \tag{3.40}$$

where  $\varepsilon(\mathbf{q}, \omega)$  is the contribution from the bound electrons and the polarizability,  $\alpha(\mathbf{q}, \omega)$ , is the contribution from the conduction electrons.

For a metallic system the RPA (Random Phase Approximation) often works very well. The result for the polarizability can be written as

$$\alpha_0(\mathbf{q}, \omega) = \frac{v_q}{\hbar} 2 \int \frac{d^3k}{(2\pi)^3} n(\mathbf{k}) [1 - n(\mathbf{k} + \mathbf{q})] \times \left[ \frac{1}{\omega + \frac{1}{\hbar}(\varepsilon_{\mathbf{k}+\mathbf{q}} - \varepsilon_{\mathbf{k}})} - \frac{1}{\omega - \frac{1}{\hbar}(\varepsilon_{\mathbf{k}+\mathbf{q}} - \varepsilon_{\mathbf{k}})} \right], \quad (3.41)$$

where the integral is the limit of a summation over the electron states characterized by the momentum,  $\mathbf{k}$ , and the spin. The factor of two in front of the integral comes from the summation over spin. The electron energy in state  $\mathbf{k}$  is denoted by  $\varepsilon_{\mathbf{k}}$  and  $n(\mathbf{k})$  is the occupation number of state  $\mathbf{k}$ . All poles of this function are found on the real axis. The retarded version, the one that represents the actual behavior of the real system when it is exposed to a perturbation, is obtained by, as in Fig. 3.4a, shifting the poles down an infinitesimal distance below the real axis. This is done by adding an infinitesimal imaginary part to  $\omega$  in both terms of the integrand. Other versions can be useful mathematically. Adding negative imaginary parts produces the advanced version, as in Fig. 3.4b, which gives a response that always comes before the perturbation. The time-ordered version is very useful in diagrammatic perturbation theory based on Feynman diagrams. This is achieved by adding a negative imaginary part to  $\omega$  in the first term and a positive in the second, which results in the position of the poles shown in Figs. 3.5a and 3.5b.

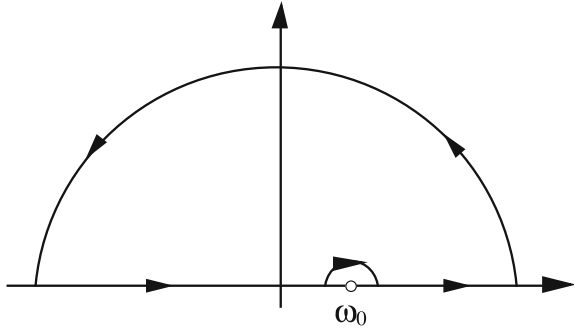
### 3.4.1 Kramers Kronig Dispersion Relations

In this section we will derive the Kramers Kronig dispersion relations. These are very important and useful in physics. Just to give an example: assume that we in an experiment can measure one of the imaginary or real parts of a response function for all frequencies. Then we may with these relations find the other part for all frequencies.

The true response functions, the retarded versions, have all poles in the lower half of the complex frequency plane. We may use the contour shown in Fig. 3.6 and the integrand of (3.14) where now  $z_0 = \omega_0$  and perform the contour integration. The radius of the large semicircle is assumed to go to infinity and the radius of the small semicircle to zero. The integrand is chosen such that the integration along the large semicircle produces zero. Some of the response functions go toward unity for large frequencies. For these we subtract unity. Thus the function  $f(z)$  then may represent, e.g.,  $\tilde{\varepsilon}(z) - 1$ ,  $\tilde{\mu}(z) - 1$ ,  $\tilde{n}(z) - 1$ ,  $\sigma(z)$ ,  $\chi_e(z)$ ,  $\chi_m(z)$ ,  $\alpha(z)$ , and  $\beta(z)$ .

In the present case  $z_0$  is not inside the contour so the result of the integral is zero. The contribution from the straight part is

**Fig. 3.6** The contour used for the Cauchy integral to find  $f(z_0)$  when  $z_0$  is situated on the real axis



$$P \int_{-\infty}^{\infty} d\omega \frac{f(\omega)}{\omega - \omega_0} \equiv \lim_{\varepsilon \rightarrow 0} \left[ \int_{-\infty}^{\omega_0 - \varepsilon} d\omega \frac{f(\omega)}{\omega - \omega_0} + \int_{\omega_0 + \varepsilon}^{\infty} d\omega \frac{f(\omega)}{\omega - \omega_0} \right], \quad (3.42)$$

where the  $P$  denotes the principle value. The contribution from the small semicircle is  $-i\pi f(\omega_0)$ . The integrand has a simple pole at  $\omega_0$ , the center of the small semicircle, and from (3.9) we see that an integration the angle  $\theta$  around the circle in clockwise direction gives  $-i\theta f(\omega_0)$  and here  $\theta = \pi$ . The contribution from the large semicircle is zero. Thus we have

$$P \int_{-\infty}^{\infty} d\omega \frac{f(\omega)}{\omega - \omega_0} - i\pi f(\omega_0) = 0, \quad (3.43)$$

and

$$f(\omega_0) = \frac{1}{i\pi} P \int_{-\infty}^{\infty} d\omega \frac{f(\omega)}{\omega - \omega_0}. \quad (3.44)$$

Separation of real and imaginary parts gives

$$\begin{aligned} \operatorname{Re} f(\omega_0) &= \frac{1}{\pi} P \int_{-\infty}^{\infty} d\omega \frac{\operatorname{Im} f(\omega)}{\omega - \omega_0}, \\ \operatorname{Im} f(\omega_0) &= -\frac{1}{\pi} P \int_{-\infty}^{\infty} d\omega \frac{\operatorname{Re} f(\omega)}{\omega - \omega_0}. \end{aligned} \quad (3.45)$$

We may limit the integration to the positive frequency axis by using the fact that the real part of  $f(\omega)$  is an even function and the imaginary part an odd function. The results are

$$\begin{aligned} \operatorname{Re} f(\omega_0) &= \frac{2}{\pi} P \int_0^{\infty} d\omega \frac{\omega \operatorname{Im} f(\omega)}{\omega^2 - (\omega_0)^2}, \\ \operatorname{Im} f(\omega_0) &= -\frac{2}{\pi} P \int_0^{\infty} d\omega \frac{\omega_0 \operatorname{Re} f(\omega)}{\omega^2 - (\omega_0)^2} \end{aligned} \quad (3.46)$$

Often one performs calculations along the imaginary axis. In the finite temperature formalism one ends up there. Also at zero temperature it can be favorable to stay on the imaginary axis since the response functions are more well-behaved there. To find the value of the function at a point  $i\xi$  at the imaginary axis we can use (3.14) and let the contour be the same as in Fig. 3.6 except that now the small semicircle is not present. The point  $i\xi$  is now inside the contour. We find

$$\begin{aligned}
 f(i\xi) &= \frac{1}{2\pi i} \int_C dz \frac{f(z)}{z - i\xi} \\
 &= \frac{1}{2\pi i} \int_{-\infty}^{\infty} d\omega \frac{f(\omega)}{\omega - i\xi} \\
 &= \frac{1}{2\pi i} \int_{-\infty}^{\infty} d\omega \frac{f(\omega)(\omega + i\xi)}{\omega^2 + \xi^2} \\
 &= \frac{1}{\pi i} \int_0^{\infty} d\omega \frac{\omega \operatorname{Im} f(\omega) + i\xi \operatorname{Re} f(\omega)}{\omega^2 + \xi^2} \\
 &= \frac{1}{\pi} \int_0^{\infty} d\omega \frac{\omega \operatorname{Im} f(\omega) + \xi \operatorname{Re} f(\omega)}{\omega^2 + \xi^2},
 \end{aligned} \tag{3.47}$$

where we again have made use of the fact that the real part of  $f(\omega)$  is an even function and the imaginary part an odd function. Both terms in this integral give the same contribution. Let us now show that the second term gives the same result as the first. We have

$$\begin{aligned}
 &\frac{1}{\pi} \int_0^{\infty} d\omega' \frac{\xi}{(\omega')^2 + \xi^2} \operatorname{Re} f(\omega') \\
 &= \frac{1}{\pi} \int_0^{\infty} d\omega' \frac{\xi}{(\omega')^2 + \xi^2} \frac{2}{\pi} P \int_0^{\infty} d\omega \frac{\omega \operatorname{Im} f(\omega)}{\omega^2 - (\omega')^2} \\
 &= \frac{1}{\pi} \frac{2}{\pi} \int_0^{\infty} d\omega \omega \operatorname{Im} f(\omega) P \underbrace{\int_0^{\infty} d\omega' \frac{\xi}{[(\omega')^2 + \xi^2][\omega^2 - (\omega')^2]}}_{\frac{\pi}{2(\omega^2 + \xi^2)}} \\
 &= \frac{1}{\pi} \int_0^{\infty} d\omega \frac{\omega \operatorname{Im} f(\omega)}{(\omega^2 + \xi^2)}.
 \end{aligned} \tag{3.48}$$

In the first line we changed dummy variables, in the second we used (3.46), and in the third we changed the order of the two integrations. Thus we have shown that

$$\frac{1}{\pi} \int_0^{\infty} d\omega \frac{\xi \operatorname{Re} f(\omega)}{(\omega^2 + \xi^2)} = \frac{1}{\pi} \int_0^{\infty} d\omega \frac{\omega \operatorname{Im} f(\omega)}{(\omega^2 + \xi^2)}, \quad (3.49)$$

and hence we have three different versions for the Kramers Kronig dispersion relation, generalized to the imaginary frequency axis, viz.,

$$f(i\xi) = \frac{1}{\pi} \int_0^{\infty} d\omega \frac{\omega \operatorname{Im} f(\omega) + \xi \operatorname{Re} f(\omega)}{\omega^2 + \xi^2}, \quad (3.50)$$

$$f(i\xi) = \frac{2}{\pi} \int_0^{\infty} d\omega \frac{\xi \operatorname{Re} f(\omega)}{(\omega^2 + \xi^2)}, \quad (3.51)$$

and

$$f(i\xi) = \frac{2}{\pi} \int_0^{\infty} d\omega \frac{\omega \operatorname{Im} f(\omega)}{(\omega^2 + \xi^2)}. \quad (3.52)$$

## Reference

1. R.V. Churchill, *Complex Variables and Applications*, 2nd edn. (McGaw-Hill, New York, 1960)

# Chapter 4

## Statistical Physics



**Abstract** The formalism we use throughout this book in the description of dispersion interactions is limited to systems in thermodynamic equilibrium. In some situations like when we want to find the force between two objects these may be considered to be part of the boundary of the system of electromagnetic normal modes. In other situations like when we want to derive the equation of state for a gas of atoms both the normal modes and the atoms are part of the same system in thermal equilibrium. Equilibrium systems are often described by thermodynamic potentials like the internal energy, the Helmholtz energy, and the Gibbs energy. Which of the potentials are most favorable to use depends on the boundary conditions for the system. To make the reader familiar with thermodynamic potentials we have included a section, Sect. 4.1, where all common potentials are discussed and how one transforms from one to another using Legendre transformations. Another section, Sect. 4.2, contains a compilation of distribution functions for massive fermions and bosons, for massless bosons and for classical particles. The last section, Sect. 4.3, contains a determination of which potential is suitable to use when calculating the force between two objects in a system of massless bosons in thermal equilibrium at finite temperature.

### 4.1 Thermodynamic Potentials and Legendre Transformations

The thermodynamic state of a system is determined by a number of variables. How many variables that are needed depends on the complexity of the system. Let us as an example choose a one-component gas, i.e., a system composed of a large number of atoms of one kind. The system is surrounded by a boundary that divides it from its surroundings. The boundary can have different properties that affects the behavior of the system. For an open system both energy and particles can pass through its boundaries; in a closed system energy (heat and work) but not particles can pass through its boundaries; in an isolated system neither particles nor energy pass through the boundaries. For an open system of a one-component gas one needs three variables to specify the state of the system. These span a 3D space. Each point in this space represents one state of the system.

Just like in electrostatics it is useful to introduce potentials. In electrostatics with a conservative electric field one introduces the scalar potential,  $\Phi$ , which satisfies

$$\oint d\Phi = 0, \quad (4.1)$$

where  $d\Phi$  is the exact differential. We have

$$\begin{aligned} d\Phi &= \left(\frac{\partial\Phi}{\partial x}\right)_{y,z} dx + \left(\frac{\partial\Phi}{\partial y}\right)_{x,z} dy + \left(\frac{\partial\Phi}{\partial z}\right)_{x,y} dz \\ &= \nabla\Phi \cdot d\mathbf{l} = -\mathbf{E} \cdot d\mathbf{l}, \end{aligned} \quad (4.2)$$

and

$$\oint \mathbf{E} \cdot d\mathbf{l} = 0. \quad (4.3)$$

For a thermodynamic system one may introduce several potentials by changing the variables defining the coordinate system. Let us study one of them,  $\Psi$ ,

$$\oint d\Psi = 0. \quad (4.4)$$

The integrand is an exact differential,

$$d\Psi = A(x, y, z) dx + B(x, y, z) dy + C(x, y, z) dz \quad (4.5)$$

where

$$\begin{aligned} A(x, y, z) &= \left(\frac{\partial\Psi}{\partial x}\right)_{y,z}, \\ B(x, y, z) &= \left(\frac{\partial\Psi}{\partial y}\right)_{x,z}, \\ C(x, y, z) &= \left(\frac{\partial\Psi}{\partial z}\right)_{x,y}. \end{aligned} \quad (4.6)$$

For exact differentials follows that

$$\begin{aligned} \left(\frac{\partial A}{\partial y}\right)_{x,z} &= \left(\frac{\partial B}{\partial x}\right)_{y,z}, \\ \left(\frac{\partial A}{\partial z}\right)_{x,y} &= \left(\frac{\partial C}{\partial x}\right)_{y,z}, \\ \left(\frac{\partial B}{\partial z}\right)_{x,y} &= \left(\frac{\partial C}{\partial y}\right)_{x,z}. \end{aligned} \quad (4.7)$$

Now we are ready to discuss the thermodynamic potentials for the open system of a one-component gas. We start with the internal energy,  $E$ . The three natural coordinates for  $E(S, V, N)$  are the entropy,  $S$ , the volume,  $V$ , and the number of particles,  $N$ . The exact differential is

$$dE = TdS - pdV + \mu dN, \quad (4.8)$$

where

$$T = \left( \frac{\partial E}{\partial S} \right)_{VN} ; -p = \left( \frac{\partial E}{\partial V} \right)_{SN} ; \mu = \left( \frac{\partial E}{\partial N} \right)_{SV}. \quad (4.9)$$

$E$  is the energy that is overall conserved; it cannot be destroyed or created; it can be transformed between different forms and it may leave or enter the system through its boundaries. The other potentials have the dimension of energy but need not be conserved.<sup>1</sup> The first term,  $TdS$ , in the differential is the heat flow into the system, the second,  $pdV$ , is the work done by the system, and the third term,  $\mu dN$ , is the energy added to the system from adding particles. For a gas with several components one just adds a term  $\mu_i dN_i$  for each additional component; for each additional component the dimension of the system increases with one unit. (For a closed system the  $\mu dN$  drops out and we would have a 2D system.) Now,  $T$ ,  $S$ ,  $p$ ,  $V$ ,  $\mu$ , and  $N$  are all candidates for variables spanning the 3D space. They come in conjugate pairs where one is extensive and one is intensive;  $S$ ,  $V$ , and  $N$  are extensive, i.e., scales with the size of the system;  $T$ ,  $p$ , and  $\mu$  are intensive, i.e., independent of the system size.

We have the differential for  $E$ . Can we find the expression for  $E$ ? Yes we can! All three variables are extensive and scales with the size of the system, This means that for any positive number  $\alpha$  we have

$$\alpha E(S, V, N) = E(\alpha S, \alpha V, \alpha N). \quad (4.10)$$

Now take the derivative with respect to  $\alpha$  on both sides of the equation. We find

$$\begin{aligned} E(S, V, N) &= S \left( \frac{\partial E}{\partial S} \right)_{VN} + V \left( \frac{\partial E}{\partial V} \right)_{SN} + N \left( \frac{\partial E}{\partial N} \right)_{SV} \\ &= ST(\alpha S, \alpha V, \alpha N) - Vp(\alpha S, \alpha V, \alpha N) + N\mu(\alpha S, \alpha V, \alpha N) \\ &= T(\alpha S, \alpha V, \alpha N)S - p(\alpha S, \alpha V, \alpha N)V + \mu(\alpha S, \alpha V, \alpha N)N. \end{aligned} \quad (4.11)$$

This is valid for any  $\alpha$ . Choose  $\alpha = 1$ . This gives

$$E(S, V, N) = T(S, V, N)S - p(S, V, N)V + \mu(S, V, N)N, \quad (4.12)$$

or more compact

$$E(S, V, N) = TS - pV + \mu N. \quad (4.13)$$

We can now find all other thermodynamic potentials by using a Legendre transformation, just like in classical or analytical mechanics. This means that we subtract one of the terms in the expression of a potential. The effect is that the variable in that term is replaced by its conjugate variable and we have a new potential. We start from

---

<sup>1</sup>Some words about the adjective “free” traditionally attached to Gibbs free energy and Helmholtz free energy: this indicates that it is a part of the energy (internal energy), the part that can be used to produce work with the given boundary conditions. At a 1988 IUPAC meeting, to set unified terminologies for the international scientific community, the adjective “free” was banished. This standard, however, has not yet been universally adopted and it can be quite useful to keep the word free to indicate that these free energies are not energies that are overall conserved.

the **Internal Energy**:

$$\begin{aligned} E(S, V, N) &= TS - pV + \mu N \\ dE &= TdS - pdV + \mu dN \\ T &= \left(\frac{\partial E}{\partial S}\right)_{VN}; \quad -p = \left(\frac{\partial E}{\partial V}\right)_{SN}; \quad \mu = \left(\frac{\partial E}{\partial N}\right)_{SV}. \end{aligned} \quad (4.14)$$

We subtract the  $TS$  term and find  
the **Helmholtz (Free) Energy**:

$$\begin{aligned} \mathfrak{F}(T, V, N) &= E - TS = -pV + \mu N \\ d\mathfrak{F} &= -SdT - pdV + \mu dN \\ -S &= \left(\frac{\partial \mathfrak{F}}{\partial T}\right)_{VN}; \quad -p = \left(\frac{\partial \mathfrak{F}}{\partial V}\right)_{TN}; \quad \mu = \left(\frac{\partial \mathfrak{F}}{\partial N}\right)_{TV}. \end{aligned} \quad (4.15)$$

Next, we subtract the  $-pV$  term from the Helmholtz energy and find  
the **Gibbs (Free) Energy**:

$$\begin{aligned} G(T, p, N) &= \mathfrak{F} + pV = \mu N \\ dG &= -SdT + Vdp + \mu dN \\ -S &= \left(\frac{\partial G}{\partial T}\right)_{pN}; \quad V = \left(\frac{\partial G}{\partial p}\right)_{TN}; \quad \mu = \left(\frac{\partial G}{\partial N}\right)_{Tp}. \end{aligned} \quad (4.16)$$

If instead we subtract the  $\mu N$  term from the Helmholtz energy we find  
the **Thermodynamic Potential**:

$$\begin{aligned} \Omega(T, V, \mu) &= \mathfrak{F} - \mu N = -pV \\ d\Omega &= -SdT - pdV - Nd\mu \\ -S &= \left(\frac{\partial \Omega}{\partial T}\right)_{V\mu}; \quad -p = \left(\frac{\partial \Omega}{\partial V}\right)_{T\mu}; \quad -N = \left(\frac{\partial \Omega}{\partial \mu}\right)_{TV}. \end{aligned} \quad (4.17)$$

Let us now return to the internal energy and subtract the  $-pV$  term to find  
the **Enthalpy**:

$$\begin{aligned} H(S, p, N) &= E + pV = TS + \mu N \\ dH &= TdS + Vdp + \mu dN \\ T &= \left(\frac{\partial H}{\partial S}\right)_{pN}; \quad V = \left(\frac{\partial H}{\partial p}\right)_{SN}; \quad \mu = \left(\frac{\partial H}{\partial N}\right)_{Sp}. \end{aligned} \quad (4.18)$$

Now we have specified the five most common thermodynamic potentials which have been given names. There are two more that have not been given names. The first we find by subtracting the term  $\mu N$  from the internal energy. The result is  
one **Unnamed Potential**

$$\begin{aligned} FF(S, V, \mu) &= E - \mu N = TS - pV \\ dFF &= TdS - pdV - Nd\mu \\ T &= \left(\frac{\partial FF}{\partial S}\right)_{V\mu}; \quad -p = \left(\frac{\partial FF}{\partial V}\right)_{S\mu}; \quad -N = \left(\frac{\partial FF}{\partial \mu}\right)_{SV}. \end{aligned} \quad (4.19)$$

The last potential is obtained by subtracting the term  $\mu N$  from the Enthalpy. We find another **Unnamed Potential**

$$\begin{aligned} GG(S, p, \mu) &= H - \mu N = TS \\ dGG &= TdS + Vdp - Nd\mu \\ T &= \left(\frac{\partial GG}{\partial S}\right)_{p\mu}; \quad V = \left(\frac{\partial GG}{\partial p}\right)_{S\mu}; \quad -N = \left(\frac{\partial GG}{\partial \mu}\right)_{Sp}. \end{aligned} \quad (4.20)$$

We have so far generated seven state functions. The internal energy is a function of only extensive variables. The other six are functions of a mixture of extensive and intensive variables. To find a potential that depends on only intensive variables we can subtract  $\mu N$  from the Gibbs energy, subtract  $-pV$  from the thermodynamic potential or subtract  $TS$  from the last unnamed potential. The result is a trivial potential equal to zero. However its exact differential is the Gibbs-Duham relation:

$$0 = SdT - Vdp + Nd\mu. \quad (4.21)$$

We will make use of  $E$  and  $\mathfrak{F}$  in the calculation of the interactions at zero and finite temperatures. Gibbs energy,  $G$ , will be used in the derivation of the ideal and non-ideal gas laws.

## 4.2 Distribution Functions

Microscopic particles like the electrons are indistinguishable; we can not detect any difference when two electrons are interchanged. Since all measurable quantities are related to the absolute value of quantum-mechanical wave-functions there are two types of indistinguishable particles: one type, fermions, where the wave function changes sign when two particles are interchanged; one, bosons, where the sign does not change. From this difference between fermions and bosons follows the difference in how the particles are distributed over the particle states.

The distribution function for fermions, the Fermi-Dirac distribution function, is

$$n(\varepsilon_i) = 1 / [e^{\beta(\varepsilon_i - \mu)} + 1], \quad (4.22)$$

and for bosons, the Bose-Einstein distribution function, is

$$n(\varepsilon_i) = 1 / [e^{\beta(\varepsilon_i - \mu)} - 1], \quad (4.23)$$

where  $\mu$  is the chemical potential. The value of  $\mu$  is determined from the relation

$$N = \sum_i n(\varepsilon_i), \quad (4.24)$$

where  $N$  is the total number of particles. The number of particles in the system is assumed to stay constant for massive particles, i.e., particles having a rest mass.

There are other particles lacking a rest mass, like photons, phonons and the normal modes we are concerned with in this book. These are so-called massless bosons. They obey the distribution function for massless bosons,

$$n(\varepsilon_i) = 1/[e^{\beta\varepsilon_i} - 1]. \quad (4.25)$$

Here, the chemical potential is zero. The number of this type of particles are not conserved.

For classical, macroscopic, distinguishable particles the distribution is given by the Boltzmann distribution function,

$$n(\varepsilon_i) = n_B(\varepsilon_i) = 1/e^{\beta(\varepsilon_i - \mu)}. \quad (4.26)$$

Even for indistinguishable atoms if the temperature is not extremely low the term  $\pm 1$  in the denominators of the two distribution functions for massive particles is negligible compared to the exponential term. Dropping this  $\pm 1$  term gives for both massive fermions and massive bosons the Boltzmann distribution function.

### 4.3 Internal Energy and Helmholtz Energy for System of Mass-Less Bosons

In this section we will discuss the energies important for our formalism and show what energy governs the interaction in the system. We start with the internal energy,  $E$ . It can be written as

$$\begin{aligned} E &= \sum_i \varepsilon_i \left[ n(\varepsilon_i) + \frac{1}{2} \right] \\ &= \sum_i \varepsilon_i \left[ \frac{1}{e^{\beta\varepsilon_i} - 1} + \frac{1}{2} \right] = \sum_i \varepsilon_i \frac{1}{2} \left[ \frac{e^{\beta\varepsilon_i} + 1}{e^{\beta\varepsilon_i} - 1} \right] = \sum_i \varepsilon_i \frac{1}{2} \coth(\beta\varepsilon_i/2), \end{aligned} \quad (4.27)$$

where  $i$  runs over the particles.

Next we derive the Helmholtz energy,  $\mathfrak{F}$ . To do that we need to introduce the partition function,  $\mathfrak{P}$ ,

$$\mathfrak{P} \equiv \text{tr}(e^{-\beta H}) = \prod_i \sum_{n=0}^{\infty} e^{-\beta\varepsilon_i(n+\frac{1}{2})} = \prod_i \frac{e^{-\beta\frac{1}{2}\varepsilon_i}}{1 - e^{-\beta\varepsilon_i}} = \prod_i \frac{1}{2 \sinh(\beta\varepsilon_i/2)}, \quad (4.28)$$

where now  $n$  is an integer. The eigenvalues of the number operator are integers. The  $n(\varepsilon_i)$  in (4.27) is the expectation value of the number operator of particle  $i$  with energy  $\varepsilon_i$ . The expectation value is not an integer. Now,

$$\mathfrak{F} = -\frac{1}{\beta} \ln \mathfrak{Z} = -\frac{1}{\beta} \sum_i -\ln [2 \sinh (\beta \varepsilon_i / 2)] = \sum_i \frac{1}{\beta} \ln [2 \sinh (\beta \varepsilon_i / 2)]. \quad (4.29)$$

It can be difficult to realize which energy to use for finding the interaction in a system [1]. Let us study two objects the distance  $r$  apart. The system is kept at constant temperature,  $T$ . We want to calculate the interaction potential  $V(r)$ , such that the force between the objects is  $F(r) = -dV(r)/dr$ . We want to determine what energy function  $V(r)$  is. For every  $r$ -value there will be a number of modes with energies that depend on  $r$ . The total energy is

$$E(r) = \sum_i \left\{ n[\varepsilon_i(r)] + \frac{1}{2} \right\} \varepsilon_i(r) = \sum_i \left[ n_i(r) + \frac{1}{2} \right] \varepsilon_i(r). \quad (4.30)$$

Let us now see what happens when we change  $r$  with  $dr$ . It is enough to study one of the modes. Thus we have

$$\begin{aligned} dE(r) &= d\{[n(r) + 1/2] \varepsilon(r)\} \\ &= [n(r) + 1/2] d\varepsilon(r) + \varepsilon(r) \frac{dn(r)}{d\varepsilon(r)} d\varepsilon(r) \\ &= d\Theta + d\Phi. \end{aligned} \quad (4.31)$$

The first term is due to mechanical work, which is the energy we are interested in, and the second to heat exchange with the surroundings. At zero temperature the force is  $F = -dE(r)/dr$ ; at finite temperature the force is  $F = -d\Theta(r)/dr$ , where  $\Theta$  is the free energy.

What free energy is involved? Let us find out. We start by calculating the other energy term,

$$\begin{aligned} \Phi(r) &= \int^{\varepsilon(r)} \varepsilon(r) \frac{dn(\varepsilon(r))}{d\varepsilon(r)} d\varepsilon(r) \\ &= [\varepsilon(r) n[\varepsilon(r)]]^{\varepsilon(r)} - \int^{\varepsilon(r)} n[\varepsilon(r)] d\varepsilon(r) + \text{constant} \\ &= \varepsilon(r) n[\varepsilon(r)] - \frac{1}{\beta} \ln(1 - e^{-\beta \varepsilon(r)}), \end{aligned} \quad (4.32)$$

and

$$\begin{aligned} \Theta &= E - \Phi \\ &= \varepsilon(r) \left\{ n[\varepsilon(r)] + \frac{1}{2} \right\} - \varepsilon(r) n[\varepsilon(r)] + \frac{1}{\beta} \ln(1 - e^{-\beta \varepsilon(r)}) \\ &= \frac{1}{2} \varepsilon(r) + \frac{1}{\beta} \ln(1 - e^{-\beta \varepsilon(r)}) = \frac{1}{\beta} \ln(e^{\beta \varepsilon(r)/2}) + \frac{1}{\beta} \ln(1 - e^{-\beta \varepsilon(r)}) \\ &= \frac{1}{\beta} \ln(e^{\beta \varepsilon(r)/2} - e^{-\beta \varepsilon(r)/2}) = \frac{1}{\beta} \ln[2 \sinh(\beta \varepsilon(r)/2)] \\ &= \mathfrak{F}. \end{aligned} \quad (4.33)$$

Thus, from (4.29) we see that this free energy is the Helmholtz energy.

## Reference

1. Bo E. Sernelius, *Phys. Chem. Chem. Phys.* **6**, 1363 (2004)

# Chapter 5

## Electromagnetic Normal Modes

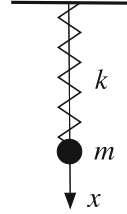


**Abstract** Normal modes appear in all physical systems. In this chapter we explain what is meant with normal modes and what are their properties. Furthermore we discuss the differences in classical and quantum systems. Then we move on to electromagnetic normal modes, the key subject of this book. We show in detail how they lead to interactions in all systems, even in vacuum, and to forces between objects. Given the modes, we demonstrate how the interactions can be derived in a system in thermal equilibrium, at zero as well as at non-zero temperature. In a system of macroscopic objects in vacuum one finds three types of mode: bulk modes, surface modes, and vacuum modes. The bulk modes are responsible for the stability and binding of the objects themselves; we demonstrate that they lead to the well-known exchange and correlation energy of metals; these energies are due to longitudinal modes but we show that there are also a transverse counterpart although much weaker. The surface modes give rise to surface tension for liquid objects and surface energy for solids; they are also responsible for the van der Waals interaction between the objects. The vacuum modes are responsible for the Casimir force.

### 5.1 Normal Modes and Their Properties

We are all surrounded by normal modes in our daily life; sometimes they are a nuisance; sometimes a blessing. If you were to drive in an old car and gradually increase the speed you could experience that when you reach a certain speed the car starts to vibrate and make unwanted noise. Then you have excited a normal mode in the system car. Similar annoying experience you could have from a humming heat pump or refrigerator. On the other side of the spectrum is when you listen to a nice piece of opera or to your favorite music instrument. Here normal modes are also excited. Other examples are: soldiers who are in step across a bridge can hit the right resonance frequency and make the bridge oscillate; for each step they take the amplitude of oscillation increases and the bridge may eventually collapse. According to the legend of the walls of Jericho the attackers were blowing in horns and made the walls collapse. These examples are all from mechanical systems but normal modes

**Fig. 5.1** A mass  $m$  attached to a spring of spring constant  $k$ . The spring is attached to a horizontal wall. The coordinate  $x$  is relative the equilibrium position when the spring has been stretched due to the gravitational force



appear in all types of physical system e.g. in electromagnetic systems, the topic of this book. We keep to mechanical systems for a while and turn to mathematics.

Each physical system is governed by a system of coupled differential equations. The normal modes of a system are solutions to the system of homogeneous equations, i.e., the equations in absence of external sources. The normal modes can be chosen as bases functions. Hence any excitation of the system can be expressed as a linear combination of these functions.

Let us give some simple illustrating examples of mechanical systems. In a simple mechanical system the key equation is Newtons second law, i.e.,  $\mathbf{F} = m\mathbf{a}$ . The force equals the mass times acceleration. The first example, Fig. 5.1, is a mass,  $m$ , attached to a spring of spring constant  $k$ . The spring is attached to a horizontal wall. The mass is pulled downward in the gravitational field. We let the spring stretch until the spring force equals the gravitational force. This is the equilibrium point. If we express  $x$  as the displacement from the equilibrium point we have the equation of motion as

$$m\ddot{x} + kx = 0, \quad (5.1)$$

where a time derivative is indicated by a dot. A double dot means a second order derivative with respect to time. This is just Newton's second law where we have moved the two quantities to the same side of the equal sign.

On Fourier transformed (C.2) form it is

$$(-\omega^2 + k/m)x = 0, \quad (5.2)$$

with a non-trivial solution for

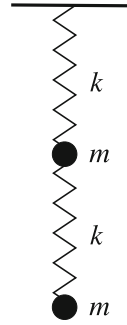
$$\omega = \sqrt{k/m}. \quad (5.3)$$

For two masses, Fig. 5.2, and two springs we have

$$\begin{aligned} \omega_{1,0} &= \sqrt{k/m} = \omega_0, \\ \omega_{2,0} &= \sqrt{2k/m} = \sqrt{2}\omega_0, \end{aligned} \quad (5.4)$$

where the first frequency is the frequency with which the lower mass is oscillating if we keep the upper in fixed position; the second frequency is the frequency with

**Fig. 5.2** Two equal masses,  $m$ , connected by a spring of spring constant  $k$ , attached to an identical spring which in turn is attached to a horizontal wall. The coordinates,  $x_i, i = 1, 2$ , are relative the equilibrium positions when the springs have been stretched due to the gravitational force



which the upper mass is oscillating if we keep the lower in fixed position. When we let them both loose we have the two normal modes from the coupled equations

$$\begin{aligned} m\ddot{x}_1 + 2kx_1 - kx_2 &= 0, \\ m\ddot{x}_2 + kx_2 - kx_1 &= 0, \end{aligned} \tag{5.5}$$

where  $x_1$  and  $x_2$  are the displacements of the upper and lower mass, respectively, from the equilibrium positions. Fourier transforming gives (C.2)

$$\begin{pmatrix} -m\omega^2 + 2k & -k \\ -k & -m\omega^2 + k \end{pmatrix} \begin{pmatrix} x_1 \\ x_2 \end{pmatrix} = 0. \tag{5.6}$$

There are non-trivial solutions if the determinant of the matrix is zero so the condition for modes is

$$\begin{vmatrix} -m\omega^2 + 2k & -k \\ -k & -m\omega^2 + k \end{vmatrix} = 0. \tag{5.7}$$

This gives

$$(-m\omega^2 + 2k)(-m\omega^2 + k) - (-k)^2 = 0, \tag{5.8}$$

and after rearrangement

$$\omega^4 - \omega^2 \left( \frac{3k}{m} \right) + \left( \frac{k}{m} \right)^2 = 0, \tag{5.9}$$

and substitution of  $k/m$  in favor of  $\omega_0^2$ ,

$$\omega^4 - 3\omega^2\omega_0^2 + \omega_0^4 = 0. \tag{5.10}$$

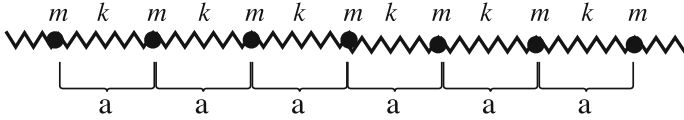


**Fig. 5.3** A general number of  $n$  masses along a line connected to each of their nearest neighbor with a spring of spring constant  $k$ . The equilibrium nearest neighbor distance is  $a$  and the total length of the system is  $L = na$

This equation has two (positive) solutions,

$$\begin{aligned} \omega_1 &= \omega_0 \sqrt{\frac{3-\sqrt{5}}{2}}, \\ \omega_2 &= \omega_0 \sqrt{\frac{3+\sqrt{5}}{2}}. \end{aligned} \tag{5.11}$$

Thus the system has two normal modes. In the first mode the two masses move in the same direction and in the second, with higher frequency, they move in opposite directions.

Next we study a variable number of masses attached to springs as in Fig. 5.3. We find for one mass<sup>1</sup>

$$\omega_0 = \sqrt{2k/m}, \tag{5.12}$$

for three masses,

$$\omega_0 \times \begin{cases} \sqrt{1 - 1/\sqrt{2}} \\ 1 \\ \sqrt{1 + 1/\sqrt{2}} \end{cases}, \tag{5.13}$$

for five masses,

$$\omega_0 \times \begin{cases} \sqrt{1 - \sqrt{3}/\sqrt{2}} \\ \sqrt{1 - 1/2} \\ 1 \\ \sqrt{1 + 1/2} \\ \sqrt{1 + \sqrt{3}/\sqrt{2}} \end{cases}, \tag{5.14}$$

and for seven masses,

---

<sup>1</sup>Note that the  $\omega_0$  is different from in the previous example. Here,  $\omega_0$  is the frequency of oscillation of a mass when the neighboring masses are kept at fixed positions. All masses are attached to two springs.

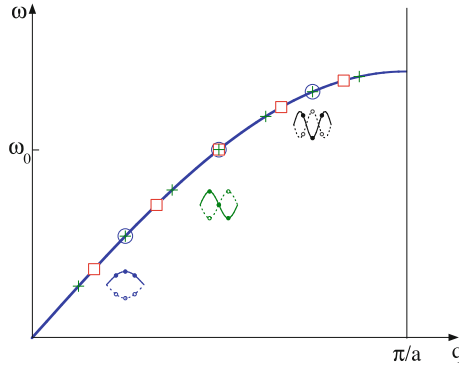


**Fig. 5.4** The dispersion curve for a chain of masses connected with springs. The equilibrium distance between the masses is  $a$ . The results are for 3, circles, 5, squares, and 7, pluses, masses, respectively. The insets show, for each of the three modes in the three-mass chain, how the atoms move. What is shown is the displacements at the two turning points of the oscillations

$$\omega_0 \times \begin{cases} \sqrt{1 - \sqrt{2} + \sqrt{2}/2} \\ \sqrt{1 - \sqrt{2}/2} \\ \sqrt{1 - \sqrt{2} - \sqrt{2}/2} \\ 1 \\ \sqrt{1 + \sqrt{2} - \sqrt{2}/2} \\ \sqrt{1 + \sqrt{2}/2} \\ \sqrt{1 + \sqrt{2} + \sqrt{2}/2} \end{cases} . \tag{5.15}$$

If we were to plot all these modes in a common figure as functions of mode number,  $i = 1, 2 \dots n$ , they would give a rather unorganized impression. If we on the other hand were to plot them as functions of  $q = 2\pi/\lambda = i\pi/L$  all points would fall on one and the same curve,  $\omega_q = 2\sqrt{k/m} \sin(qa/2)$ . Curves like this are named dispersion curves. In Fig. 5.4 we give the results for three masses, circles, five masses, squares, and seven masses, pluses. In the insets are shown how, for the case of three masses, the masses move when these modes are excited. What is shown is the displacements at the two turning points of the oscillations. We see that in the mode with lowest frequency all three masses move back and forth in the same direction. In the second mode the middle mass stands still and the other two move in opposite directions. In the mode with highest frequency the outer masses move in the same direction and the middle one in the opposite. The displacements we discuss here are along the springs, so the excitations are longitudinal. The system also has transverse excitations which we do not consider here.

In general a dispersion curve is a curve that describes the relation between the angular frequency,  $\omega$ , and a variable that characterizes the mode; in this case the wave number,  $q$ , or wave length,  $\lambda$ . If the dispersion curve is a straight line we say that it shows no dispersion; if it is curved it shows dispersion. The light dispersion curve in vacuum is a straight line. In a medium it is curved. The dielectric function and refractive index both increase monotonically with frequency in between all regions of absorption. This is true for all media and means that light of higher frequencies, shorter wavelengths, is refracted more than light of lower frequencies. This is why light is dispersed, spread out, in a glass prism and different colors are separated. This effect made London [1] coin the name dispersion forces for the forces treated in this book. (This effect is also why the sky is blue and the sunset red.)

In a classical treatment, as apposed to quantum mechanical, the amplitude of oscillation is a continuous variable. The energy of the system increases with amplitude. In general one may obtain the normal modes of the system with a classical treatment. This is very fortunate. Let us now treat the system of a single mass attached to a spring quantum mechanically. The system can be viewed as a particle of mass  $m$  in a potential  $V = kx^2/2$ . This is a classical problem in quantum mechanics, the Harmonic Oscillator problem.

### 5.1.1 The Quantum Mechanical Harmonic Oscillator

In solids the vibrational modes of the atoms are quantized because of first quantization. These quantized vibrational modes are called phonons. An electron can scatter and emit a phonon which later is absorbed in a scattering process involving a second electron. This causes an indirect interaction between the electrons. This is an example of second quantization. Phonons in solids can usually be described as harmonic oscillators. The one-dimensional harmonic oscillator has the Hamiltonian

$$H = \frac{p^2}{2m} + \frac{k}{2}x^2 . \quad (5.16)$$

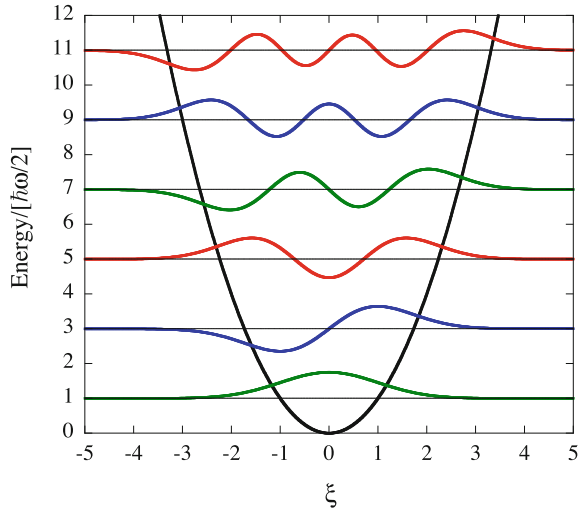
To solve it we introduce the dimensionless coordinate  $\xi$ :

$$\begin{aligned} \omega^2 &= \frac{k}{m}, \\ \xi &= x \left( \frac{m\omega}{\hbar} \right)^{1/2}, \\ \frac{1}{i} \frac{\partial}{\partial \xi} &= p (\hbar m \omega)^{-1/2}, \end{aligned} \quad (5.17)$$

where

$$\omega = \sqrt{k/m}, \quad (5.18)$$

**Fig. 5.5** The harmonic oscillator potential and the quantum mechanical solutions. The wave functions are plotted with their energy eigenvalues as base lines



and

$$H = \frac{\hbar\omega}{2} \left( -\frac{\partial^2}{\partial \xi^2} + \xi^2 \right). \quad (5.19)$$

The harmonic oscillator Hamiltonian has a solution in terms of Hermite polynomials. In Fig. 5.5 we have plotted the first six wave functions. The states are quantized such that

$$H\varphi_n = \hbar\omega \left( n + \frac{1}{2} \right) \varphi_n, \quad (5.20)$$

where  $n$  is an integer.

It is customary to define two dimensionless operators as follows:

$$\begin{aligned} a &= \frac{1}{2^{1/2}} \left( \xi + \frac{\partial}{\partial \xi} \right) = \left( \frac{m\omega}{2\hbar} \right)^{1/2} \left( x + \frac{ip}{m\omega} \right), \\ a^\dagger &= \frac{1}{2^{1/2}} \left( \xi - \frac{\partial}{\partial \xi} \right) = \left( \frac{m\omega}{2\hbar} \right)^{1/2} \left( x - \frac{ip}{m\omega} \right). \end{aligned} \quad (5.21)$$

They are Hermitian conjugates of each other. They are sometimes called *raising* and *lowering operators*, but we shall call them *creation* ( $a^\dagger$ ) and *destruction operators* ( $a$ ). The Hamiltonian may be written in terms of them as

$$\begin{aligned} H &= \frac{\hbar\omega}{2} [aa^\dagger + a^\dagger a] \\ &= \frac{\hbar\omega}{2} \left( -\frac{\partial^2}{\partial \xi^2} + \xi^2 \right). \end{aligned} \quad (5.22)$$

For any function  $f(\xi)$  we have

$$\begin{aligned}
[a, a^\dagger] f(\xi) &\equiv [aa^\dagger - a^\dagger a] f(\xi) = f(\xi) , \\
[a, a] f(\xi) &\equiv [aa - aa] f(\xi) = 0 , \\
[a^\dagger, a^\dagger] f(\xi) &\equiv [a^\dagger a^\dagger - a^\dagger a^\dagger] f(\xi) = 0 ,
\end{aligned} \tag{5.23}$$

which can be written as

$$\begin{aligned}
[a, a^\dagger] &= 1 , \\
[a, a] &= 0 , \\
[a^\dagger, a^\dagger] &= 0 .
\end{aligned} \tag{5.24}$$

These three commutation relations, plus the Hamiltonian

$$H = \frac{\hbar\omega}{2} [aa^\dagger + a^\dagger a] = \frac{\hbar\omega}{2} [aa^\dagger - a^\dagger a + 2a^\dagger a] = \hbar\omega [a^\dagger a + 1/2] , \tag{5.25}$$

completely specify the Harmonic oscillator problem in terms of operators. With these four relationships, one can show that the eigenvalue spectrum is indeed (5.20), where  $n$  is an integer. The eigenstates are

$$|n\rangle = \frac{(a^\dagger)^n}{(n!)^{1/2}} |o\rangle , \tag{5.26}$$

where  $|o\rangle$  is the state which obeys

$$a |o\rangle = 0 , \tag{5.27}$$

and where the  $n!$  is for normalization. If one operates on this state by a creation operator, one gets

$$a^\dagger |n\rangle = \frac{1}{(n!)^{1/2}} (a^\dagger)^{n+1} |o\rangle = \frac{(n+1)^{1/2}}{[(n+1)!]^{1/2}} (a^\dagger)^{n+1} |o\rangle = (n+1)^{1/2} |n+1\rangle , \tag{5.28}$$

the state with the next higher integer. Thus the only matrix element between states is

$$\langle n' | a^\dagger | n \rangle = (n+1)^{1/2} \delta_{n', n+1} . \tag{5.29}$$

If we take the Hermitian conjugate of this matrix element,

$$\langle n | a | n' \rangle = (n+1)^{1/2} \delta_{n', n+1} . \tag{5.30}$$

and exchange dummy variables  $n$  and  $n'$ , we obtain

$$\langle n' | a | n \rangle = (n)^{1/2} \delta_{n', n-1} . \tag{5.31}$$

or

$$a |n\rangle = (n)^{1/2} |n-1\rangle . \tag{5.32}$$

So the destruction operator lowers the quantum number. Thus operating by the sequence

$$a^\dagger a |n\rangle = a^\dagger (n)^{1/2} |n-1\rangle = (n)^{1/2} a^\dagger |n-1\rangle = n |n\rangle, \quad (5.33)$$

gives an eigenvalue  $n$ , which verifies the eigenvalue (5.20). The description of the harmonic oscillator in terms of operators is equivalent to the conventional method of using wave functions  $\varphi_n(\xi)$  of position.

In the Heisenberg representation of quantum mechanics, the time development of operators is given by

$$O(t) = e^{iHt/\hbar} O e^{-iHt/\hbar}, \quad (5.34)$$

so that the operator obeys the equation

$$\frac{\hbar \partial}{\partial t} O(t) = i[H, O(t)]. \quad (5.35)$$

For the destruction operators, this becomes

$$\frac{\partial}{\partial t} a = i/\hbar [H, a] = i\omega [a^\dagger a a - a a^\dagger a] = i\omega [a^\dagger, a] a = -i\omega a, \quad (5.36)$$

which has the simple solution

$$a(t) = e^{-i\omega t} a. \quad (5.37)$$

The reference point of time may be selected arbitrarily, so that the operators have an arbitrary phase factor associated with them. This phase is unimportant, since it cancels out of all final results. The Hermitian conjugate of this expression is

$$a^\dagger(t) = e^{i\omega t} a^\dagger. \quad (5.38)$$

Thus using (5.21) we can represent the time development of the position operator as

$$x(t) = \left( \frac{\hbar}{2m\omega} \right)^{1/2} (a e^{-i\omega t} + a^\dagger e^{i\omega t}). \quad (5.39)$$

This result for  $x(t)$  will be used often in discussing phonon problems.

In a solid there are many atoms that mutually interact. The vibrational modes are collective motions involving many atoms. Some experience can be gained by studying the normal modes of a one-dimensional harmonic chain:

$$H = \sum_i \frac{p_i^2}{2m} + \frac{k}{2} \sum_i (x_i - x_{i+1})^2. \quad (5.40)$$

The quantum mechanical solution begins by defining some normal coordinates, assuming periodic boundary conditions:

$$\begin{aligned} x_l &= \frac{1}{N^{1/2}} \sum_q e^{iqal} x_q, \quad x_q = \frac{1}{N^{1/2}} \sum_l e^{-iqal} x_l, \\ p_l &= \frac{1}{N^{1/2}} \sum_q e^{-iqal} p_q, \quad p_q = \frac{1}{N^{1/2}} \sum_l e^{iqal} p_l. \end{aligned} \quad (5.41)$$

This choice maintains the desired commutation relations in either real space or wave vector space:

$$\begin{aligned} [x_l, p_m] &= i\hbar\delta_{l,m}, \\ [x_q, p_{q'}] &= i\hbar\delta_{q,q'}. \end{aligned} \quad (5.42)$$

The Hamiltonian becomes in wave vector space

$$H = \frac{1}{2m} \sum_q p_q p_{-q} + \frac{m}{2} \sum_q \omega_q^2 x_q x_{-q}, \quad (5.43)$$

where

$$\omega_q^2 = \frac{4k}{m} \sin^2\left(\frac{qa}{2}\right). \quad (5.44)$$

The Hamiltonian has the form of a simple harmonic oscillator for each wave vector. We define

$$\begin{aligned} a_q &= \left(\frac{m\omega_q}{2\hbar}\right)^{1/2} \left(x_q + \frac{i}{m\omega_q} p_{-q}\right), \\ a_q^\dagger &= \left(\frac{m\omega_q}{2\hbar}\right)^{1/2} \left(x_{-q} - \frac{i}{m\omega_q} p_q\right), \end{aligned} \quad (5.45)$$

which obey the commutation relations,

$$\begin{aligned} [a_q, a_{q'}^\dagger] &= \delta_{q,q'}, \\ [a_q, a_{q'}] &= 0, \\ [a_q^\dagger, a_{q'}^\dagger] &= 0, \end{aligned} \quad (5.46)$$

and the Hamiltonian can be written as

$$H = \sum_q \hbar\omega_q [a_q^\dagger a_q + 1/2]. \quad (5.47)$$

These collective modes of vibration are called *phonons*. They are the quantized version of the classical vibrational modes in the solid. These are the same commutator relations and Hamiltonian, as in the simple harmonic oscillator. Each wave vector behaves independently, as a harmonic oscillator, with a possible set of quantum numbers  $n_q = 0, 1, 2, \dots$ . The state of the system at any time is

$$\varphi = |n_{q1}, n_{q2}, \dots, n_{qn}\rangle = \prod_q |n_q\rangle = \prod_q \frac{[a_q^\dagger]^{n_q}}{(n_q!)^{1/2}} |o\rangle, \quad (5.48)$$

so that the expectation value of the Hamiltonian is

$$\langle H \rangle = \sum_q \hbar\omega_q [n_q + 1/2]. \quad (5.49)$$

In thermal equilibrium the states have an average value of  $n_q$  which is given in terms of the temperature  $\beta = 1/k_B T$ ,

$$\langle n_q \rangle \equiv N_q = \frac{1}{e^{\beta \hbar\omega_q} - 1} \equiv n_B(\omega_q). \quad (5.50)$$

The system fluctuates around this average value. The position operator in wave vector space, and real space, is

$$\begin{aligned} x_q(t) &= \left(\frac{\hbar}{2m\omega_q}\right)^{1/2} \left(a_q e^{-i\omega_q t} + a_{-q}^\dagger e^{i\omega_q t}\right), \\ x_l(t) &= \sum_q \left(\frac{\hbar}{2mN\omega_q}\right)^{1/2} e^{iqal} \left(a_q e^{-i\omega_q t} + a_{-q}^\dagger e^{i\omega_q t}\right). \end{aligned} \quad (5.51)$$

In 3D the result is similar in the harmonic approximation and for one atom per unit cell

$$\begin{aligned} \mathbf{Q}_{\mathbf{q},\lambda}(t) &= i \left(\frac{\hbar}{2M\omega_{\mathbf{q},\lambda}}\right)^{1/2} \xi_{\mathbf{q},\lambda} \left(a_{\mathbf{q},\lambda} e^{-i\omega_{\mathbf{q},\lambda} t} + a_{-\mathbf{q},\lambda}^\dagger e^{i\omega_{\mathbf{q},\lambda} t}\right), \\ \mathbf{Q}_i(t) &= i \sum_{\mathbf{q},\lambda} \left(\frac{\hbar}{2MN\omega_{\mathbf{q},\lambda}}\right)^{1/2} \xi_{\mathbf{q},\lambda} \left(a_{\mathbf{q},\lambda} e^{-i\omega_{\mathbf{q},\lambda} t} + a_{-\mathbf{q},\lambda}^\dagger e^{i\omega_{\mathbf{q},\lambda} t}\right) e^{iq \cdot \mathbf{R}_i(0)}, \end{aligned} \quad (5.52)$$

and

$$\begin{aligned} H &= \frac{1}{2M} \sum_{\mathbf{q},\lambda} \left(\mathbf{P}_{\mathbf{q},\lambda} \mathbf{P}_{-\mathbf{q},\lambda} + M^2 \omega_{\mathbf{q},\lambda}^2 \mathbf{Q}_{\mathbf{q},\lambda} \mathbf{Q}_{-\mathbf{q},\lambda}\right), \\ &= \sum_{\mathbf{q},\lambda} \hbar\omega_{\mathbf{q},\lambda} \left(a_{\mathbf{q},\lambda}^\dagger a_{\mathbf{q},\lambda} + 1/2\right). \end{aligned} \quad (5.53)$$

The polarization vector is real valued and  $\xi_{-\mathbf{q},\lambda} = -\xi_{\mathbf{q},\lambda}$ .

To summarize:

The normal modes are massless bosons. The Hamiltonian is

$$H = \sum_i \left(a_i^\dagger a_i + 1/2\right) \hbar\omega_i, \quad (5.54)$$

where  $a_i^\dagger a_i$  and  $\hbar\omega_i$  are the number operator and energy of mode number  $i$ , respectively. The energy can be written as

$$E = \sum_i (n_i + 1/2) \hbar\omega_i . \quad (5.55)$$

The occupation number for mode number  $i$ ,  $n_i$ , can be the result of an external stimuli or it can be due thermal excitations. If the system is in thermal equilibrium the expectation value of the number operator is the distribution function for massless bosons,

$$n_i = 1 / (\exp(\beta\hbar\omega_i) - 1) , \quad (5.56)$$

where  $\beta = 1/k_B T$ .

### 5.1.2 Classical Versus Quantum Systems

We found that for a system of masses connected by springs the number of modes were equal to the number of masses. Each mode oscillates with a specific frequency, the mode frequency. This is true for both the classical and quantum mechanical treatments. In the classical treatment the total energy and the amplitude of oscillation are continuous variables. In the quantum mechanical treatment there is an energy quanta,  $\hbar\omega_i$ , for each mode  $i$  and the total energy and amplitude of oscillation are discrete variables, see Fig. 5.5. Macroscopic systems are usually treated classically. Quantum mechanics is a theory that is superior to classical mechanics and is also valid for macroscopic objects. How come then that we do not see energy quanta in a macroscopic mass-in-a-spring system? We illustrate this in Table 5.1, where we compare various quantities for a macroscopic mass of 15 g in a macroscopic spring of length 50 cm and spring constant 2.94 N/m with the microscopic system consisting of a carbon monoxide molecule attached to a surface, see Fig. 5.6. The carbon atom moves in a potential that is parabolic in a region around the equilibrium position. Thus it behaves as if a spring was connecting the carbon and oxygen atoms. We see that the energy quanta in the macroscopic system is as small as  $10^{-14}$  eV which is much too small to be observed, or resolved. In the quantum system it is 166 meV.

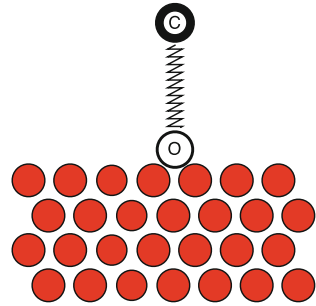
On the third row from the bottom of the table are shown how many quanta on the average are excited at room temperature. In the classical system one trillion<sup>2</sup> of quanta are excited while in the quantum system not even a single quanta is excited. On the last two rows of the table we show result from applying a constant force field so strong that the spring is stretched by 10%. The relaxation energy is then  $2.3 \times 10^{16}$  eV and 504 meV in the classical and quantum case, respectively. The

<sup>2</sup>one trillion in the short scale corresponding to one billion in the long scale.

**Table 5.1** Comparison between a macroscopic (classical) and a microscopic (quantum mechanical) mass-in-a-spring system. See the text for details

Quantity	Classical	Quantum mechanical
Spring length: $l$	50 cm	1.13 Å
Mass: $m$	15 g	$2 \times 10^{-26}$ kg
Spring constant: $k$	2.94 N/m	1264 N/m
Angular frequency: $\omega_0$	$14 \text{ s}^{-1}$	$2.5 \times 10^{14} \text{ s}^{-1}$
Frequency: $\nu$	2.23 Hz	$4 \times 10^{13}$ Hz
Energy quanta: $E = \hbar\omega_0$	$9.218 \times 10^{-15}$ eV	166 meV
Number of quanta excited at 300 K	$2.8 \times 10^{12}$	$1.6 \times 10^{-3}$
Relaxation energy: $E_{\text{relax}} = k(\Delta l)^2/2$	$2.3 \times 10^{16}$ eV	504 meV
Number of quanta: $n_0 = k(\Delta l)^2/2E$	$2.5 \times 10^{30}$	3.0

**Fig. 5.6** A schematic illustration of a carbon monoxide molecule adsorbed on a solid surface. The oxygen atom is stuck to the surface and the carbon atom is sticking out



number of excited quanta is in the classical case as high as one nonillion<sup>3</sup> while it is just three in the quantum system.

Thus the reason quantum effects are not observed in a macroscopic system is that the energy quantum is so extremely small that there is no way to observe the discreteness in the energy and amplitude of oscillation.

## 5.2 Interaction from Normal Modes

At zero temperature the interaction energy, or Casimir energy, of a system can be expressed as the sum of the zero-point energies of all electromagnetic normal modes of the system.<sup>4</sup>

<sup>3</sup>One nonillion in the short scale corresponding to one quintillion in the long scale.

<sup>4</sup>It is rather the shift of the zero-point energies when the interactions, one is concerned with, are “turned on” that should appear in the equation. See Chap. 3 of [2].

$$E = \sum_i \frac{1}{2} \hbar \omega_i . \quad (5.57)$$

In a simple system with a small number of well-defined modes this summation may be performed directly; this method is called the mode-summation method. In most cases it is more complicated. The complications can e.g. be that the modes form continua or that it is difficult to find the zero-point energies explicitly. An extension of the so-called argument principle [2–4] can then be used to find the results (see Sect. 3.3.2).

In what follows we let  $z$  denote a general point in the complex frequency plane,  $\omega$  a point along the real axis, and  $i\xi$  a point along the imaginary axis, respectively.

Let us study a region in the complex frequency plane where two functions are defined; one,  $\varphi(z)$ , is analytic in the whole region and the other,  $f(z)$ , has poles and zeros inside the region. The following relation holds for a counterclockwise integration along a contour around the region:

$$\frac{1}{2\pi i} \oint dz \varphi(z) \frac{d}{dz} \ln f(z) = \sum \varphi(z_0) - \sum \varphi(z_\infty) , \quad (5.58)$$

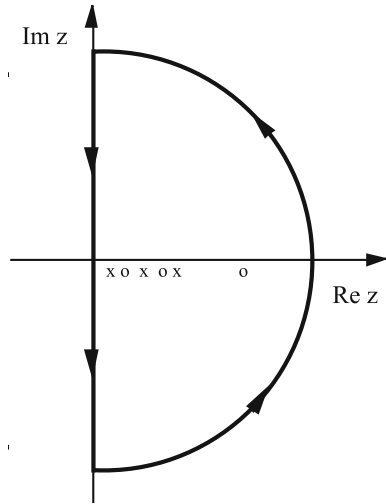
where  $z_0$  and  $z_\infty$  are the zeros and respectively, of function  $f(z)$ . If we choose the function  $f(z)$  to be the function in the defining equation for the normal modes of the system,  $f(\omega_i) = 0$ , the function  $\varphi(z)$  as  $\hbar z/2$ , and let the contour enclose all the zeros and poles of the function  $f(z)$  then (5.58) produces the energy in (5.57). The second term on the right-hand side is just the subtraction of the zero-point energies in absence of the interactions as discussed in the note below (5.57). In the original argument principle the function  $\varphi(z)$  is replaced by unity and the right-hand side then equals to the number of zeros minus the number of poles of the function  $f(z)$  inside the integration path. By using this theorem we end up with integrating along a closed contour in the complex frequency plane. In most cases it is fruitful to choose the contour shown in Fig. 5.7. We have the freedom to multiply the function  $f(z)$  with an arbitrary constant without changing the result on the right-hand side of (5.58). If we choose the constant carefully we can make the contribution from the curved part of the contour vanish and we are only left with an integration along the imaginary frequency axis:

$$E = \frac{\hbar}{4\pi} \int_{-\infty}^{\infty} d\xi \ln f(i\xi) , \quad (5.59)$$

where the result was obtained from an integration by parts. At finite temperatures it is Helmholtz' free energy,

$$\mathfrak{F} = \sum_i \frac{1}{2} \hbar \omega_i(r) + \frac{1}{\beta} \ln(1 - e^{-\beta \hbar \omega_i(r)}) = \sum_i \frac{1}{\beta} \ln \left( 2 \sinh \frac{1}{2} \beta \hbar \omega_i \right) , \quad (5.60)$$

**Fig. 5.7** Integration contour in the complex  $z$  plane suited for zero temperature calculations. Crosses and circles are poles and zeros, respectively, of the function  $f(z)$ . The radius of the circle is let to go to infinity. Adapted from [2]



that is of interest (see Sect. 4.3). Also here we may use the generalized argument principle but now with  $\ln [2 \sinh (\beta \hbar z / 2)] / \beta$  instead of  $\hbar z / 2$  for  $\varphi(z)$  in the integrand [2, 5]. There is one complication. This new function has poles of its own in the complex frequency plane. We have to choose our contour so that it includes all poles and zeros of the function  $f(z)$  but excludes the poles of  $\varphi(z)$ . The poles of function  $\varphi(z)$  all fall on the imaginary frequency axis. The same contour as in Fig. 5.7, is used but now we let the straight part of the contour lie just to the right of, and infinitesimally close to, the imaginary axis. We have

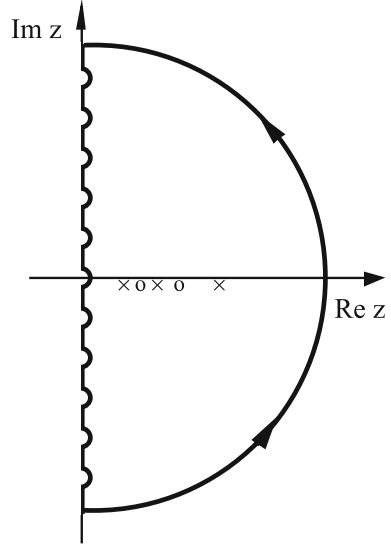
$$\begin{aligned} \mathfrak{F} &= \frac{1}{2\pi i} \int_{-\infty}^{+\infty} d(i\xi) \frac{1}{\beta} \ln \left( 2 \sinh \frac{1}{2} \beta \hbar i \xi \right) \frac{d}{d(i\xi)} \ln f(i\xi) \\ &= \frac{\hbar}{4\pi} \int_{-\infty}^{+\infty} d\xi \coth \left( \frac{1}{2} \beta \hbar i \xi \right) \ln f(i\xi) . \end{aligned} \tag{5.61}$$

The coth function has poles on the imaginary  $z$ -axis and they should not be inside the contour. The poles are at

$$z_n = i\xi_n = i \frac{2\pi n}{\hbar\beta}; \quad n = 0, \pm 1, \pm 2, \dots , \tag{5.62}$$

and all residues are the same, equal to  $2/\hbar\beta$ . The integration is performed along the imaginary axis and the path is deformed along small semicircles around each pole. The integration path is illustrated in Fig. 5.8. The integration along the axis results in zero since the integrand is odd with respect to  $\xi$ . The only surviving contributions are the ones from the small semicircles. The result is

**Fig. 5.8** Integration contour in the complex  $z$  plane suited for finite temperature calculations. Crosses and circles are poles and zeros, respectively, of the function  $f(z)$ . The small semi circles are centered at the poles of the coth function in the integrand. The radius of the large semi circle is let to go to infinity. Adapted from [2]



$$\mathfrak{F} = \frac{\hbar}{4\pi i} \sum_{\xi_n} \frac{2\pi i}{2} \frac{2}{\hbar\beta} \ln f(i\xi_n) = \frac{1}{2\beta} \sum_{\xi_n} \ln f(i\xi_n); \quad \xi_n = \frac{2\pi n}{\hbar\beta}; \quad n = 0, \pm 1, \pm 2, \dots \quad (5.63)$$

Since the summand is even in  $n$  we can write this as

$$\mathfrak{F} = \frac{1}{\beta} \sum'_{\xi_n} \ln f(i\xi_n); \quad \xi_n = \frac{2\pi n}{\hbar\beta}; \quad n = 0, 1, 2, \dots, \quad (5.64)$$

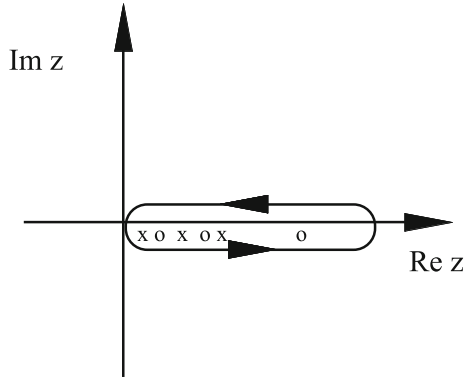
where the prime on the summation sign indicates that the  $n = 0$  term is multiplied by a factor of one half. This factor of one half is because there is only one term with  $|n| = 0$  in the original summation but two for all other integers. When the temperature goes to zero the spacing between the discrete frequencies goes to zero and the summation may be replaced by an integration:

$$\mathfrak{F} = \frac{1}{\beta} \sum'_{\xi_n} \ln f(i\xi_n) \rightarrow \frac{\hbar\beta}{2\pi} \frac{1}{\beta} \int_0^{\infty} d\xi \ln f(i\xi) = \hbar \int_0^{\infty} \frac{d\xi}{2\pi} \ln f(i\xi) = E, \quad (5.65)$$

and we regain the contribution to the internal energy from the interactions, the change in zero-point energy of the modes.

Sometimes the integrand is less well behaved when integrating along the imaginary frequency axis. Then it might be better to use a contour shown in Fig. 5.9. One integrates along the whole real axis, just below the poles and zeros and then back again just above the axis. This contour can be used both for zero and finite temperature.

**Fig. 5.9** Integration contour in the complex  $z$  plane suited for both finite and zero temperature calculations when the integrand is not well behaved along the imaginary axis. Crosses and circles are poles and zeros, respectively, of the function  $f(z)$ . The integration is performed along the whole real axis, just below and just above. Adapted from [2]



To summarize so far, at zero temperature the internal interaction energy is obtained from (5.59) and at finite temperature the Helmholtz free interaction energy is obtained from (5.64). The only input from the system is the mode condition function,  $f(z)$ . Casimir forces, pressures, surface tensions, works of adhesion and cohesion, and so on are obtained from how these energies vary when parameters of the system are changed.

All derivations of the mode conditions are simplified if retardation effects are neglected. The forces obtained if this is done are van der Waals (vdW) forces. If retardation is included in all steps the result span the whole separation region covering both Casimir and van der Waals forces. Since the non-retarded derivations are so much simpler to perform, the results so much simpler to handle and since the distances in the system often are small enough for retardation effects to be negligible we derive the results both without and with retardation effects included. The treatment in this work is limited to objects of a certain class of geometrical shape. One of the coordinates of a proper chosen coordinate system should be constant at the interface between two media. The fully retarded treatment is based on solutions to the Helmholtz equation while in the non-retarded treatment the Laplace equation takes its role. There are 11 coordinate systems in which the Helmholtz equation is separable and 13 for the Laplace equation, so there are quite a few shapes where the treatment is applicable. One should note that the thickness of the layers are not constant in all geometries. They are in the three specific geometries that we apply the theory to here.

### 5.3 Different Mode Types

In this section we will derive the electromagnetic normal modes in three simple geometries: in empty space, vacuum; in the bulk of a medium; at a flat interface between two media. These modes are called Vacuum Modes, Bulk Modes and Surface Modes, respectively. The normal modes are obtained by solving Maxwell's equations

in absence of external sources, i.e., solving the homogeneous equations. To find the surface modes we also need to involve the boundary conditions at the interface.

### 5.3.1 Vacuum Modes

The vacuum modes were found to be responsible for the Casimir force. This force was found by Casimir [6] to act between two ideal (totally reflecting) metal plates in vacuum. They can also be responsible for the Dark Energy in the Universe. When we look for the modes we have a system absent of any external sources. Thus we start from (2.4) without external sources. Now the equations we start from are

$$\begin{aligned}\nabla \cdot \mathbf{E} &= 0, \\ \nabla \cdot \mathbf{B} &= 0, \\ \nabla \times \mathbf{E} + \frac{1}{c} \frac{\partial \mathbf{B}}{\partial t} &= \mathbf{0}, \\ \nabla \times \mathbf{B} - \frac{1}{c} \frac{\partial \mathbf{E}}{\partial t} &= \mathbf{0},\end{aligned}\tag{5.66}$$

since in vacuum  $\tilde{\mathbf{D}} \equiv \mathbf{E}$  and  $\tilde{\mathbf{H}} \equiv \mathbf{B}$ . It is favorable to use the Fourier transformed (C.2) versions,

$$\begin{aligned}\mathbf{q} \cdot \mathbf{E} &= 0, \\ \mathbf{q} \cdot \mathbf{B} &= 0, \\ \mathbf{q} \times \mathbf{E} - \frac{\omega}{c} \mathbf{B} &= \mathbf{0}, \\ \mathbf{q} \times \mathbf{B} + \frac{\omega}{c} \mathbf{E} &= \mathbf{0}.\end{aligned}\tag{5.67}$$

From the first two equations we see that both fields are transverse; there is no longitudinal solution. From the third equation we find that  $\mathbf{B} = (c/\omega) \mathbf{q} \times \mathbf{E}$ . Here we see that  $\mathbf{B}$  is perpendicular to both  $\mathbf{E}$  and  $\mathbf{q}$ . Next we substitute this expression for  $\mathbf{B}$  in the fourth equation and find

$$\underbrace{\mathbf{q} \times (\mathbf{q} \times \mathbf{E})}_{\mathbf{q}(\mathbf{q} \cdot \mathbf{E}) - \mathbf{E}(\mathbf{q} \cdot \mathbf{q}) = -q^2 \mathbf{E}} + (\omega/c)^2 \mathbf{E} = \mathbf{0}.\tag{5.68}$$

Thus

$$[(\omega/c)^2 - q^2] \mathbf{E} = \mathbf{0}.\tag{5.69}$$

Had we instead extracted the  $\mathbf{E}$  field from the fourth equation and made the substitution in the third equation we would have obtained the same results but with  $\mathbf{B}$  replacing  $\mathbf{E}$ . There is a trivial solution to (5.69) viz. that  $\mathbf{E}$  is zero from which follows that also  $\mathbf{B}$  is zero. The nontrivial solution, the normal mode, is found by letting the factor in front of  $\mathbf{E}$  be zero. Thus, the normal mode in vacuum has the dispersion curve  $\omega = cq$  and the fields form a transverse plane wave.

When neglecting retardation one lets the speed of light in vacuum,  $c$ , go to infinity. If we had done that in (5.66) we had found there are neither longitudinal nor transverse solutions. Thus, there are no vacuum modes in the non-retarded treatment.

### 5.3.2 Bulk Modes

Bulk modes are modes in the interior of a macroscopic object where the effect of its boundaries can be neglected. These modes are responsible for the stability and binding of the object. The exchange and correlation energy of a metal, e.g., can be obtained from how these modes change when the object is formed.

We have found that the interaction energy is just the change in the zero-point energy of the normal modes of the system caused by the interaction. Thus if we know the dielectric properties of the system we can determine the normal modes and the interaction energy without involving the complicated many-body theory and even without the use of quantum mechanics. We may get away with using the theory of classical electromagnetic waves, the Maxwell's equations.

If we have a continuum of excitation modes like in a free-electron system there is a normal mode squeezed in between each nearest pair of single-particle excitation modes, and these come infinitely close to each other. Thus it is in practice impossible to keep track of all individual modes and how their energies change with interaction. Then we have to rely on the extension of the argument principle. However, often one may to a good approximation replace the continuum with one or a few discrete modes and the simple approach can be applied. We should note that in the interacting system there are no longer any pure single-particle excitations; in each excitation, characterized by a change in momentum and frequency all electrons are involved; when an electron is promoted from one state to another, all other electrons adjust to this change. Thus all excitations are really collective and in principle not different in this respect from the plasmon excitation. The difference is that all but the plasmon are still bound to the original region of the single-particle continuum; only the uppermost mode is pushed away a finite distance in energy and becomes the plasmon. We should also remember that all objects are finite in size. This means that there are no true continuum of single-particle excitations, all regions are discrete. When we make calculations on a macroscopic object we let the size go to infinity and the distance between the excitation energies goes to zero. In Fig. 5.10 we show the excitation spectrum for a metal (Be) treated within RPA. The single-particle excitations occur within the shaded area. To the left in the figure one may see the plasmon dispersion curve. There are also transverse modes not shown in this figure. Just like in the longitudinal case there is one transverse mode squeezed in between each nearest pair of single-particle excitations. Then there is one mode above the light-dispersion curve in vacuum.<sup>5</sup> We have not shown this in the figure because this upper mode

---

<sup>5</sup>Actually these transverse modes are each a pair of modes, degenerate in isotropic systems, because there are two independent polarization directions for transverse modes.

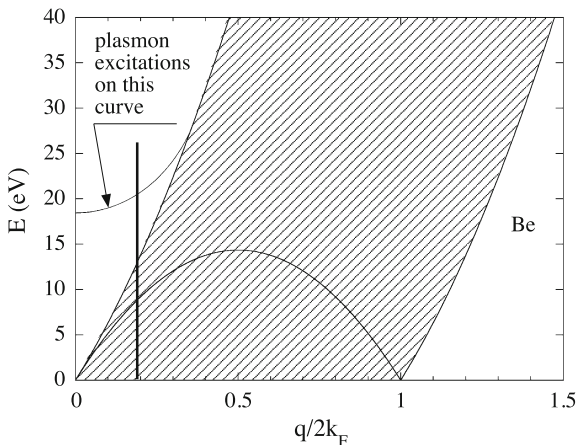


**Fig. 5.10** The longitudinal-excitation spectrum for Be metal in RPA. All single-particle excitations occur within the shaded area. The plasmon dispersion curve is pushed out from the continuum for small momenta but merges with the continuum for larger momenta. If we follow the vertical line to the left from small energies toward higher we move through a very dense region of modes, the continuum. There is one longitudinal mode squeezed in between each neighboring pair of single-particle excitations. Then there is a break followed by a single mode, the plasmon

comes much higher in energy. The light dispersion curve in vacuum is so steep that if plotted in Fig. 5.10 it would not be separated from the vertical axis.

To illustrate what happens with the modes when the interaction turns on we study a simple model dielectric function, which gets its contributions from the four excitation energies, 1, 2, 3 and 4 with weights 1, 2, 3 and 2, respectively

$$\varepsilon^\lambda(\omega) = 1 - \lambda \left[ \frac{1}{\omega - 1} + \frac{2}{\omega - 2} + \frac{3}{\omega - 3} + \frac{2}{\omega - 4} + \frac{1}{-\omega - 1} + \frac{2}{-\omega - 2} + \frac{3}{-\omega - 3} + \frac{2}{-\omega - 4} \right], \quad (5.70)$$

where  $\lambda$  is the coupling constant. When  $\lambda = 1$  we have full interaction and when  $\lambda = 0$  there is no interaction at all. Figure 5.11 illustrates the dielectric function. This can be viewed as modeling of the dielectric function in Fig. 5.10 along the thick vertical line to the left in the figure. The four excitation energies are then single-particle excitation-energies for a given wave number.

To find the modes we start from Maxwell's equations (2.4) in absence of external sources

$$\begin{aligned} \nabla \cdot \tilde{\mathbf{D}} &= 0, \\ \nabla \cdot \mathbf{B} &= 0, \\ \nabla \times \mathbf{E} + \frac{1}{c} \frac{\partial \mathbf{B}}{\partial t} &= \mathbf{0}, \\ \nabla \times \tilde{\mathbf{H}} - \frac{1}{c} \frac{\partial \tilde{\mathbf{D}}}{\partial t} &= \mathbf{0}. \end{aligned} \quad (5.71)$$

It is favorable to use the Fourier transformed (C.2) versions,

$$\begin{aligned}
 \tilde{\varepsilon} \mathbf{q} \cdot \mathbf{E} &= 0, \\
 \mathbf{q} \cdot \mathbf{B} &= 0, \\
 \mathbf{q} \times \mathbf{E} - \frac{\omega}{c} \mathbf{B} &= \mathbf{0}, \\
 \mathbf{q} \times \frac{1}{\mu} \mathbf{B} + \frac{\omega}{c} \tilde{\varepsilon} \mathbf{E} &= \mathbf{0}.
 \end{aligned}
 \tag{5.72}$$

We see that the first two equations concern longitudinal modes and the last two transverse. The dielectric function in the first equation is consequently the longitudinal version and the magnetic permeability and dielectric function in the fourth are the transverse versions. We begin with the longitudinal modes.

### 5.3.2.1 Longitudinal Modes

Now, the second line of (5.72) shows that there is no mode with a longitudinal  $\mathbf{B}$ -field. On the other hand from the first line we find that the condition for a longitudinal  $\mathbf{E}$ -field is

$$\tilde{\varepsilon}(\mathbf{q}, \omega) = 0. \tag{5.73}$$

Thus, the mode-condition function for longitudinal modes is

$$f(\mathbf{q}, \omega) = \tilde{\varepsilon}(\mathbf{q}, \omega). \tag{5.74}$$

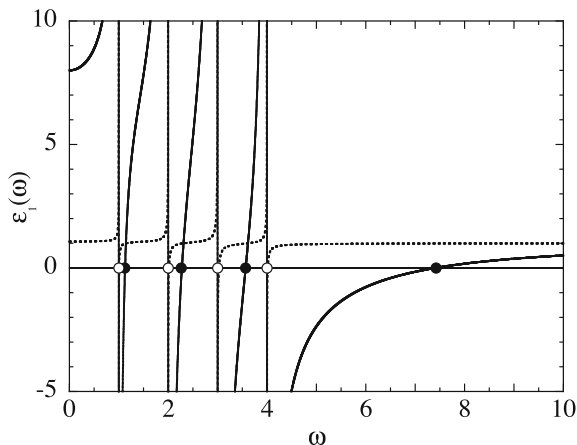
In Fig. 5.11 we notice that in a system represented by the model dielectric function of (5.70) there are four modes. The three left most modes are supposed to represent the continuum and the fourth the split off plasmon mode. The normal modes are shifted from the white to the black positions indicated in the figure by circles. The solid curve is for  $\lambda = 1$  and the dotted one is for  $\lambda = 0.01$ . We note that the zeros when  $\lambda$  goes to zero are at the positions of the poles for  $\lambda = 1$ . The model dielectric function could approximate a real function for a specific  $\mathbf{q}$ , like along the vertical line in Fig. 5.10. The modes are characterized by  $\mathbf{q}$ , but we see that each  $\mathbf{q}$  has several modes, i.e. there are several branches of modes.

The contribution to the interaction energy (per unit volume) from longitudinal modes is then

$$E = \frac{\hbar}{2} \int \frac{d^3 q}{(2\pi)^3} \int_{-\infty}^{\infty} \frac{d\xi}{2\pi} \ln \tilde{\varepsilon}(\mathbf{q}, i\xi). \tag{5.75}$$

This energy contains the self-energy of the electrons. If we treat the electrons as point particles this energy is infinite. We subtract this energy by making a correction to the wave-vector integration,

**Fig. 5.11** The dielectric function with  $\lambda$  equal to unity, *solid curve*, and equal to 0.01, *dotted curve*. The interaction shifts the longitudinal modes toward higher energies, from open circles to filled ones. The modes are obtained from the relation  $\varepsilon(\omega) = 0$



$$E = \frac{1}{2} \int \frac{d^3q}{(2\pi)^3} \left[ \hbar \int_{-\infty}^{\infty} \frac{d\xi}{2\pi} \ln \tilde{\varepsilon}(\mathbf{q}, i\xi) - n v_q \right], \quad (5.76)$$

where  $n$  is the electron density and  $v_q = 4\pi e^2/q^2$ , the Fourier transform of the Coulomb potential.

For a metal the interaction energy in (5.76) is the exchange and correlation energy per unit volume. The exchange and correlation energy is the change in the interaction energy when the solid is formed. So the reference system is a system where all electrons are very far apart so that they do not affect each other. The interaction energy in the reference system is the number of electrons times the interaction energy for a system consisting of a single electron in vacuum. Both the longitudinal and transverse contributions to this energy diverges if one does not introduce a cut off in the wave-vector integration and/or the frequency integral. The longitudinal contribution is just the energy stored in the electric field emerging from the electron. If we assume that the electron is a true point particle this energy diverges; if we assume that the electron has a finite radius the energy is finite; if the radius is chosen to be the classical electron radius the energy equals  $m_e c^2$ , the electron rest-energy (this is how the classical electron radius has been defined). A finite electron radius is equivalent to a wave-vector cutoff.

### 5.3.2.2 Transverse Modes

From the third line of (5.72) we find  $\mathbf{B} = (c/\omega) \mathbf{q} \times \mathbf{E}$ . Substituting for  $\mathbf{B}$  in the fourth line gives

$$\underbrace{\mathbf{q} \times \mathbf{q} \times \mathbf{E}}_{-q^2 \mathbf{E}} + \frac{\omega^2}{c^2} \tilde{\varepsilon} \tilde{\mu} \mathbf{E} = \mathbf{0}, \quad (5.77)$$

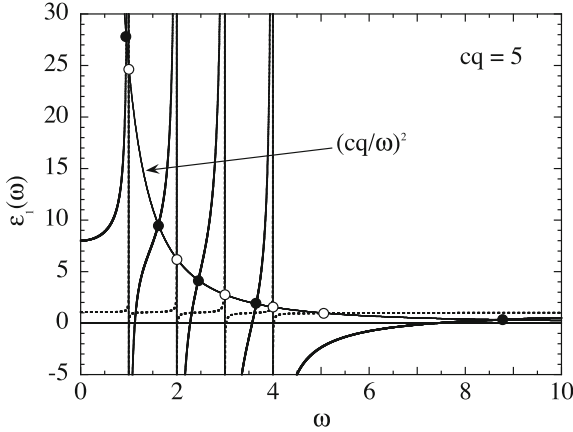


**Fig. 5.12** The dielectric function with  $\lambda$  equal to unity, *solid curve*, and equal to 0.01, *dotted curve*. The interaction shifts the transverse modes toward lower energies, from open circles to filled ones. The highest mode is shifted toward higher energy. The modes are obtained from the relation  $\varepsilon(\omega) = (cq/\omega)^2$ . Note that we have chosen a nonrealistic  $cq$ -value. For a realistic system it would be several orders of magnitude larger; then the shifts of the modes bound to the continuum would be much smaller

and

$$[\tilde{\varepsilon} \tilde{\mu} \omega^2 - (cq)^2] \mathbf{E} = \mathbf{0}. \quad (5.78)$$

Thus the condition for transverse modes is

$$[\tilde{\varepsilon}(\mathbf{q}, \omega) \tilde{\mu}(\mathbf{q}, \omega) \omega^2 - (cq)^2] = 0. \quad (5.79)$$

The dominating majority of materials are non-magnetic. For these materials  $\tilde{\mu}(\mathbf{q}, \omega) \approx 1$ . We will let  $\tilde{\mu}(\mathbf{q}, \omega) \equiv 1$  in most of our examples. We still keep the  $\tilde{\mu}(\mathbf{q}, \omega)$  in the formulas to leave open for the possibility of finding interesting magnetic effects.

In Fig. 5.12 the filled circles indicate the modes for  $\lambda = 1$ . The open circles give the modes when the interaction goes toward zero. We see that four of these modes appear where the mode-condition function for  $\lambda = 1$  has its poles. However, now there is a fifth open circle. It appears at  $\omega = cq$ , i.e. at the light dispersion curve in vacuum. This illustrates the fact that we have to be cautious when applying the calculation scheme based on the generalized argument principle.

The contribution to the interaction energy (per unit volume) from transverse modes is then

$$E = 2 \frac{\hbar}{2} \int \frac{d^3 q}{(2\pi)^3} \int_{-\infty}^{\infty} \frac{d\xi}{2\pi} \ln \left[ \frac{\tilde{\mu}_T(\mathbf{q}, i\xi) \tilde{\varepsilon}_T(\mathbf{q}, i\xi) \xi^2 + (cq)^2}{\xi^2 + (cq)^2} \right], \quad (5.80)$$

where we have taken care of the fifth open circle by introducing the denominator in the argument of the logarithm. The extra factor of two in front of the integral is from a summation over the two independent polarization directions of transverse modes. Note that we have added a subscript  $T$  on the material functions to indicate that they are the transverse versions of the functions.

This result is not yet fully complete. As it stands it is divergent. We want the interaction energy relative the reference system where all electrons are so far apart that they do not affect each other. Let us assume that we have  $N$  electrons in the system of a large volume  $\Omega$ . Thus we subtract the corresponding energy when there is only one electron in the volume. We make this subtraction  $N$  times. The transverse dielectric function for a one-electron system is<sup>6</sup>

$$\tilde{\epsilon}_T(i\xi) = 1 + \frac{4\pi e^2}{m_e \Omega} \frac{1}{\xi^2}. \quad (5.81)$$

The interaction energy in the one-electron system is

$$\begin{aligned} E &= 2 \frac{\hbar}{2} \int \frac{d^3 q}{(2\pi)^3} \int_{-\infty}^{\infty} \frac{d\xi}{2\pi} \ln \left\{ \frac{\left(1 + \frac{4\pi e^2}{m_e \Omega} \frac{1}{\xi^2}\right) \xi^2 + (cq)^2}{\xi^2 + (cq)^2} \right\} \\ &= 2 \frac{\hbar}{2} \int \frac{d^3 q}{(2\pi)^3} \int_{-\infty}^{\infty} \frac{d\xi}{2\pi} \ln \left\{ 1 + \frac{1}{\Omega} \frac{4\pi e^2}{\xi^2 + (cq)^2} \right\}. \end{aligned} \quad (5.82)$$

The total energy for  $N$  such systems is

$$\begin{aligned} E &= 2 \frac{\hbar}{2} \int \frac{d^3 q}{(2\pi)^3} \int_{-\infty}^{\infty} \frac{d\xi}{2\pi} N \ln \left\{ 1 + \frac{1}{\Omega} \frac{4\pi e^2}{\xi^2 + (cq)^2} \right\} \\ &= \hbar \int \frac{d^3 q}{(2\pi)^3} \int_{-\infty}^{\infty} \frac{d\xi}{2\pi} \ln \left\{ \left[ 1 + \frac{1}{\Omega} \frac{4\pi e^2}{\xi^2 + (cq)^2} \right]^N \right\} \\ &= \hbar \int \frac{d^3 q}{(2\pi)^3} \int_{-\infty}^{\infty} \frac{d\xi}{2\pi} \ln \left[ 1 + \frac{N}{\Omega} \frac{4\pi e^2}{\xi^2 + (cq)^2} \right] \\ &= \hbar \int \frac{d^3 q}{(2\pi)^3} \int_{-\infty}^{\infty} \frac{d\xi}{2\pi} \ln \left[ 1 + n \frac{4\pi e^2}{\xi^2 + (cq)^2} \right] \\ &= \hbar \int \frac{d^3 q}{(2\pi)^3} \int_{-\infty}^{\infty} \frac{d\xi}{2\pi} \ln \left[ 1 + \frac{(\omega_{pl})^2}{\xi^2 + (cq)^2} \right], \end{aligned} \quad (5.83)$$

where we have used the fact that  $\Omega$  is very large and have introduced the plasma frequency,  $\omega_{pl} = \sqrt{4\pi n e^2 / m_e}$ . We subtract this energy and obtain

---

<sup>6</sup>This expression resembles the Drude result for the longitudinal dielectric function of a metallic system but it is the exact transverse dielectric function for a system with a single electron in state  $\mathbf{k} = \mathbf{0}$ .

$$\begin{aligned}
E &= 2 \frac{\hbar}{2} \int \frac{d^3 q}{(2\pi)^3} \int_{-\infty}^{\infty} \frac{d\xi}{2\pi} \ln \left[ \frac{\tilde{\epsilon}_T(\mathbf{q}, i\xi) \xi^2 + (cq)^2}{[\xi^2 + (cq)^2] [1 + (\omega_{pl})^2 / (\xi^2 + (cq)^2)]} \right] \\
&= \hbar \int \frac{d^3 q}{(2\pi)^3} \int_{-\infty}^{\infty} \frac{d\xi}{2\pi} \ln \left[ \frac{\tilde{\epsilon}_T(\mathbf{q}, i\xi) \xi^2 + (cq)^2}{\xi^2 + (cq)^2 + (\omega_{pl})^2} \right].
\end{aligned} \tag{5.84}$$

This result is convergent. Note that it is very important to use the transverse dielectric function. The transverse and longitudinal versions are equal for small momenta but differ substantially for large momenta. It is the large-momentum region that makes the original result divergent.

Thus to get a convergent result we have subtracted the transverse contribution to the self-energy of each electron. This contribution to the self-energy is obtained as the interaction energy when there is a single electron in vacuum. The transverse part appears in Feynman's [7] derivation of the Lamb shift for hydrogen. Both Feynman and Bethe [8] subtracted the contribution from the free electron in the treatment of the Lamb shift but in that problem the singularity does not fully go away. Still a logarithmic singularity remains. They both used a cutoff to get finite results.

The appearance of singularities in quantum electrodynamics is quite common. Fortunately most properties of interest involve the difference in value when the system changes state and this difference is finite. The reason this did not work out for the Lamb shift is that one used a non-relativistic treatment of the electron, an approximation that broke down for high frequencies. We were more lucky here. We too have treated the electron non-relativistically but the integrands vanish long before we reach regions where this matters.

For a metal the transverse contribution to the correlation energy is much smaller than that from the longitudinal modes, see Fig. 5.13. The transverse contribution is neglected. The dominating contribution is the exchange energy,

$$E_x = \left( \frac{243}{32\pi^2} \right)^{1/3} \frac{1}{r_s} \text{Ry} \approx 0.916 \frac{1}{r_s} \text{Ry}, \tag{5.85}$$

where the density parameter  $r_s = (3/4\pi n)^{1/3} / a_0$ .

### 5.3.3 Surface Modes

Surface modes are bound to the surface of objects or to interfaces between two media. They are to a large extent<sup>7</sup> responsible for surface tension at liquid surfaces and surface energy at solid surfaces. We find them by solving MEs in the two media

---

<sup>7</sup>There are also other contributions to this energy. In most solids it takes energy (chemical energy) to break up bonds when the solid is split into two pieces. There is also an energy gain from relaxation; the distance between the outermost atomic layers may vary after the splitting and for a metal the conduction electrons may spill out a little into the vacuum, both effects leading to a reduction in energy.

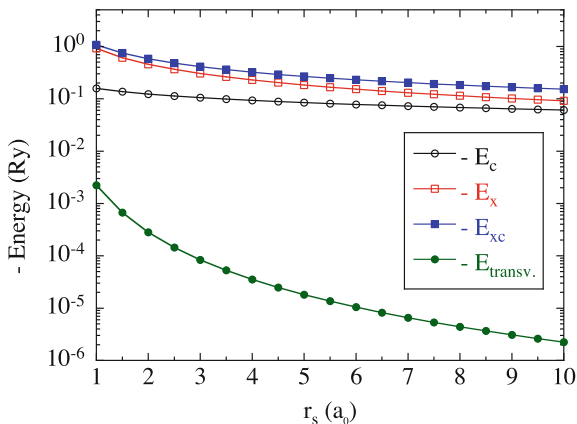


**Fig. 5.13** The different contributions to the dispersion energy in an electron gas, in RPA. The longitudinal exchange-energy contribution,  $E_x$ , dominates; the longitudinal correlation energy,  $E_c$ , comes next in size ( $E_{xc} = E_x + E_c$ ); the transverse interaction energy,  $E_{transv.}$ , is negligible. All energies are negative and per electron. They are plotted as functions of the density parameter  $r_s$  expressed in Bohr radii

on both sides of the surface or interface and then use the standard boundary conditions at the surface. Let us orient the coordinate system so that the surface is in the  $xy$ -plane, the in-plane wave vector  $\mathbf{k}$  points in the  $x$ -direction and the  $z$ -axis is along the surface normal pointing from medium 1 into medium 2. We let a superscript indicate at what side of the surface a quantity is valid.

We use the version of MEs given in (5.72) together with the matching conditions (MCs) at the interface,

$$\begin{aligned}
 \tilde{\mathbf{D}}_{\perp}^1 &= \tilde{\mathbf{D}}_{\perp}^2, \\
 \mathbf{B}_{\perp}^1 &= \mathbf{B}_{\perp}^2, \\
 \mathbf{E}_{\parallel}^1 &= \mathbf{E}_{\parallel}^2, \\
 \tilde{\mathbf{H}}_{\parallel}^1 &= \tilde{\mathbf{H}}_{\parallel}^2,
 \end{aligned} \tag{5.86}$$

and from the orientation of the coordinate system we have  $\mathbf{q}^i = (k, 0, q_z^i)$ .

It is enough to find the relations for one electric and one magnetic field. We choose the  $\mathbf{E}$ - and  $\tilde{\mathbf{H}}$ -fields and make use of the constitutive relations while we make use of the MEs and MCs. We find

$$\text{ME1} : \begin{cases} kE_x^1 + q_z^1 E_z^1 = 0, \\ kE_x^2 + q_z^2 E_z^2 = 0, \end{cases} \tag{5.87}$$

$$\text{ME2} : \begin{cases} k\tilde{H}_x^1 + q_z^1 \tilde{H}_z^1 = 0, \\ k\tilde{H}_x^2 + q_z^2 \tilde{H}_z^2 = 0, \end{cases} \tag{5.88}$$

$$\text{ME3 : } \begin{cases} q_z^1 E_y^1 + (\tilde{\mu}_1 \omega / c) \tilde{H}_x^1 = 0, \\ q_z^2 E_y^2 + (\tilde{\mu}_2 \omega / c) \tilde{H}_x^2 = 0, \\ q_z^1 E_x^1 - k E_z^1 - (\tilde{\mu}_1 \omega / c) \tilde{H}_y^1 = 0, \\ q_z^2 E_x^2 - k E_z^2 - (\tilde{\mu}_2 \omega / c) \tilde{H}_y^2 = 0, \\ k E_y^1 - (\tilde{\mu}_1 \omega / c) \tilde{H}_z^1 = 0, \\ k E_y^2 - (\tilde{\mu}_2 \omega / c) \tilde{H}_z^2 = 0, \end{cases} \quad (5.89)$$

$$\text{ME4 : } \begin{cases} q_z^1 \tilde{H}_y^1 - (\tilde{\epsilon}_1 \omega / c) E_x^1 = 0, \\ q_z^2 \tilde{H}_y^2 - (\tilde{\epsilon}_2 \omega / c) E_x^2 = 0, \\ q_z^1 \tilde{H}_x^1 - k \tilde{H}_z^1 + (\tilde{\epsilon}_1 \omega / c) E_y^1 = 0, \\ q_z^2 \tilde{H}_x^2 - k \tilde{H}_z^2 + (\tilde{\epsilon}_2 \omega / c) E_y^2 = 0, \\ k \tilde{H}_y^1 + (\tilde{\epsilon}_1 \omega / c) E_z^1 = 0, \\ k \tilde{H}_y^2 + (\tilde{\epsilon}_2 \omega / c) E_z^2 = 0, \end{cases} \quad (5.90)$$

and

$$\text{MC : } \begin{cases} \tilde{\epsilon}_1 E_z^1 = \tilde{\epsilon}_2 E_z^2, \\ \tilde{\mu}_1 \tilde{H}_z^1 = \tilde{\mu}_2 \tilde{H}_z^2, \\ E_x^1 = E_x^2, \\ E_y^1 = E_y^2, \\ \tilde{H}_x^1 = \tilde{H}_x^2, \\ \tilde{H}_y^1 = \tilde{H}_y^2. \end{cases} \quad (5.91)$$

We find that  $E_x$ ,  $E_z$ , and  $\tilde{H}_y$  couple to each other. They form TM (transverse magnetic) modes. Furthermore,  $\tilde{H}_x$ ,  $\tilde{H}_z$ , and  $E_y$  couple. They form TE (transverse electric) modes. We start with the TM modes.

### 5.3.3.1 Transverse Magnetic Modes

We have six coupled field components. Let us systematically express all in terms of  $E_x^1$ . We find

$$E_x^1 = E_x^1, \quad (5.92a)$$

$$E_z^1 = -\frac{k}{q_z^1} E_x^1, \quad (5.92b)$$

$$\tilde{H}_y^1 = \frac{(q_z^1)^2 + k^2}{q_z^1 \tilde{\mu}_1 \omega / c} E_x^1, \quad (5.92c)$$

$$E_x^2 = E_x^1, \quad (5.92d)$$

$$E_z^2 = -\frac{k}{q_z^2} E_x^1, \quad (5.92e)$$

$$\tilde{H}_y^2 = \frac{(q_z^2)^2 + k^2}{q_z^2 \tilde{\mu}_2 \omega / c} E_x^1. \quad (5.92f)$$

Equation (5.92a) is trivial; (5.92a) is obtained from the first line of (5.87); (5.92a) from the third line of (5.89); (5.92a) from the third line of (5.91); (5.92a) from the second line of (5.87); (5.92a) from the fourth line of (5.89).

Now, from the first line of (5.90) and the third line of (5.92a) we find  $(q_z^1)^2 + k^2 = \tilde{\mu}_1 \tilde{\epsilon}_1 (\omega/c)^2$ . From the second line of (5.90) and last line of (5.92a) we find  $(q_z^2)^2 + k^2 = \tilde{\mu}_2 \tilde{\epsilon}_2 (\omega/c)^2$ . Finally using these relations and the last line of (5.91) we obtain  $q_z^2 \tilde{\epsilon}_1 = q_z^1 \tilde{\epsilon}_2$ .

Now, in order for the solution to be a surface mode the fields have to decay away from the surface. Thus, we let

$$\begin{aligned} q_z^1 &= ik\gamma_1, \\ q_z^2 &= -ik\gamma_2. \end{aligned} \quad (5.93)$$

Then we have

$$\gamma_i = \sqrt{1 - \tilde{\mu}_i \tilde{\epsilon}_i (\omega/c)^2}, \quad i = 1, 2, \quad (5.94)$$

and

$$\gamma_2 \tilde{\epsilon}_1 = -\gamma_1 \tilde{\epsilon}_2. \quad (5.95)$$

This is the mode condition and the mode condition function is

$$f_{\mathbf{k}}(\omega) = \gamma_2(k, \omega) \tilde{\epsilon}_1(\omega) + \gamma_1(k, \omega) \tilde{\epsilon}_2(\omega), \quad (5.96)$$

and the 2D wave vector  $\mathbf{k}$  in the plane of the surface is the quantum number that characterizes the mode.

### 5.3.3.2 Transverse Electric Modes

Now we repeat the same procedure as in Sect. 5.3.3.1 and express all six fields in  $\tilde{H}_x^1$ .

We find

$$\tilde{H}_x^1 = \tilde{H}_x^1, \quad (5.97a)$$

$$\tilde{H}_z^1 = -\frac{k}{q_z^1} \tilde{H}_x^1, \quad (5.97b)$$

$$E_y^1 = -\frac{1}{q_z^1} (\tilde{\mu}_1 \omega / c) \tilde{H}_x^1, \quad (5.97c)$$

$$\tilde{H}_x^2 = \tilde{H}_x^1, \quad (5.97d)$$

$$\tilde{H}_z^2 = -\frac{k}{q_z^2} \tilde{H}_x^1, \quad (5.97e)$$

$$E_y^2 = -\frac{1}{q_z^2} (\tilde{\mu}_2 \omega / c) \tilde{H}_x^1. \quad (5.97f)$$

Now we use the third and fourth lines of (5.90) and the second line of (5.91). We find

$$\begin{aligned} (q_z^1)^2 + k^2 - \tilde{\epsilon}_1 \tilde{\mu}_1 (\omega/c)^2 &= 0, \\ (q_z^2)^2 + k^2 - \tilde{\epsilon}_2 \tilde{\mu}_2 (\omega/c)^2 &= 0, \\ \tilde{\mu}_1 q_z^2 &= \tilde{\mu}_2 q_z^1. \end{aligned} \quad (5.98)$$

Thus using (5.93) we regain (5.94) and now

$$\gamma_2 \tilde{\mu}_1 = -\gamma_1 \tilde{\mu}_2. \quad (5.99)$$

This is the mode condition and the mode condition function is

$$f_{\mathbf{k}}(\omega) = \gamma_2(k, \omega) \tilde{\mu}_1(\omega) + \gamma_1(k, \omega) \tilde{\mu}_2(\omega), \quad (5.100)$$

and the 2D wave vector  $\mathbf{k}$  in the plane of the surface is the quantum number that characterizes the mode. We note that for a non-magnetic system there are no solution, so we only find surface TM modes at a single interface for non-magnetic systems. However, as we will find later on, if we have more than one interface in the system there will be TE modes also in non-magnetic systems.

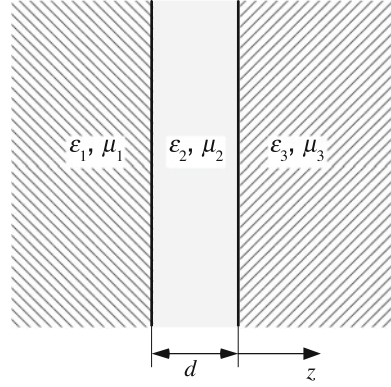
## 5.4 Modes for a Gap Between Two Half Spaces

Now, we study the simplest geometry with more than a single interface, viz., a geometry with two parallel planar interfaces. This geometry can represent a slab or a gap between two half spaces. We use brute force to find the normal modes. We solve the MEs in the three regions defined by the interfaces and use the boundary conditions, in analogy with the preceding sections. We will find that even for this simple geometry the derivations are quite cumbersome. For geometries with a growing number of layers this approach quickly becomes too cumbersome. Then the approach described in Chap. 7 comes very handy. We treat the most general case where the materials in the three regions defined by the interfaces are all different. The geometry is specified in Fig. 5.14.

We make the following ansatz for the fields in the three regions:

$$\mathbf{E} = \begin{cases} (\mathbf{E}^{BR} e^{k\gamma_2 z} + \mathbf{E}^{BL} e^{-k\gamma_2(z+d)}) e^{i(kx-\omega t)}; & -d \leq z \leq 0 \\ \mathbf{E}^R e^{-k\gamma_3 z} e^{i(kx-\omega t)}; & z \geq 0 \\ \mathbf{E}^L e^{+k\gamma_1(z+d)} e^{i(kx-\omega t)}; & z \leq -d \end{cases} \quad (5.101)$$

**Fig. 5.14** Two half spaces separated by a gap of width  $d$



and

$$\tilde{\mathbf{H}} = \begin{cases} \left( \tilde{\mathbf{H}}^{BR} e^{k\gamma_2 z} + \tilde{\mathbf{H}}^{BL} e^{-k\gamma_2(z+d)} \right) e^{i(kx-\omega t)} ; & -d \leq z \leq 0 \\ \tilde{\mathbf{H}}^R e^{-k\gamma_1 z} e^{i(kx-\omega t)} ; & z \geq 0 \\ \tilde{\mathbf{H}}^L e^{+k\gamma_3(z+d)z} e^{i(kx-\omega t)} ; & z \leq -d \end{cases} \quad (5.102)$$

for a mode moving in the  $x$ -direction.

We insert these relations into the Maxwell's equations (5.72) and use the matching conditions at the interfaces:

$$\left\{ \begin{array}{l} \tilde{\mathbf{D}}_{\perp}^{BR} + \tilde{\mathbf{D}}_{\perp}^{BL} e^{-k\gamma_2 d} = \tilde{\mathbf{D}}_{\perp}^R \\ \tilde{\mathbf{D}}_{\perp}^{BL} + \tilde{\mathbf{D}}_{\perp}^{BR} e^{-k\gamma_2 d} = \tilde{\mathbf{D}}_{\perp}^L \\ \mathbf{B}_{\perp}^{BR} + \mathbf{B}_{\perp}^{BL} e^{-k\gamma_2 d} = \mathbf{B}_{\perp}^R \\ \mathbf{B}_{\perp}^{BL} + \mathbf{B}_{\perp}^{BR} e^{-k\gamma_2 d} = \mathbf{B}_{\perp}^L \\ \mathbf{E}_{\parallel}^{BR} + \mathbf{E}_{\parallel}^{BL} e^{-k\gamma_2 d} = \mathbf{E}_{\parallel}^R \\ \mathbf{E}_{\parallel}^{BL} + \mathbf{E}_{\parallel}^{BR} e^{-k\gamma_2 d} = \mathbf{E}_{\parallel}^L \\ \tilde{\mathbf{H}}_{\parallel}^{BR} + \tilde{\mathbf{H}}_{\parallel}^{BL} e^{-k\gamma_2 d} = \tilde{\mathbf{H}}_{\parallel}^R \\ \tilde{\mathbf{H}}_{\parallel}^{BL} + \tilde{\mathbf{H}}_{\parallel}^{BR} e^{-k\gamma_2 d} = \tilde{\mathbf{H}}_{\parallel}^L \end{array} \right. \quad (5.103)$$

From the first ME we get

$$\text{ME1} : \left\{ \begin{array}{l} E_x^{BL}(ik) - E_z^{BL}(k\gamma_2) = 0 \\ E_x^{BR}(ik) + E_z^{BR}(k\gamma_2) = 0 \\ E_x^R(ik) + E_z^R(-k\gamma_3) = 0 \\ E_x^L(ik) + E_z^L(k\gamma_1) = 0, \end{array} \right. \quad (5.104)$$

from the second

$$\text{ME2 : } \begin{cases} \tilde{H}_x^{BL}(\mathbf{i}k) - \tilde{H}_z^{BL}(k\gamma_2) = 0 \\ \tilde{H}_x^{BR}(\mathbf{i}k) + \tilde{H}_z^{BR}(k\gamma_2) = 0 \\ \tilde{H}_x^R(\mathbf{i}k) + \tilde{H}_z^R(-k\gamma_3) = 0 \\ \tilde{H}_x^L(\mathbf{i}k) + \tilde{H}_z^L(k\gamma_1) = 0, \end{cases} \quad (5.105)$$

from the third

$$\text{ME3 : } \begin{cases} -E_y^{BR}(k\gamma_2) = \frac{i\tilde{\mu}_2\omega}{c} \tilde{H}_x^{BR} \\ -E_y^{BL}(-k\gamma_2) = \frac{i\tilde{\mu}_2\omega}{c} \tilde{H}_x^{BL} \\ -E_y^R(-k\gamma_3) = \frac{i\tilde{\mu}_3\omega}{c} \tilde{H}_x^R \\ -E_y^L(k\gamma_1) = \frac{i\tilde{\mu}_1\omega}{c} \tilde{H}_x^L \\ E_x^{BR}(k\gamma_2) - E_z^{BR}(\mathbf{i}k) = \frac{i\tilde{\mu}_2\omega}{c} \tilde{H}_y^{BR} \\ E_x^{BL}(-k\gamma_2) - E_z^{BL}(\mathbf{i}k) = \frac{i\tilde{\mu}_2\omega}{c} \tilde{H}_y^{BL} \\ E_x^R(-k\gamma_3) - E_z^R(\mathbf{i}k) = \frac{i\tilde{\mu}_3\omega}{c} \tilde{H}_y^R \\ E_x^L(k\gamma_1) - E_z^L(\mathbf{i}k) = \frac{i\tilde{\mu}_1\omega}{c} \tilde{H}_y^L \\ E_y^{BR}(\mathbf{i}k) = \frac{i\tilde{\mu}_2\omega}{c} \tilde{H}_z^{BR} \\ E_y^{BL}(\mathbf{i}k) = \frac{i\tilde{\mu}_2\omega}{c} \tilde{H}_z^{BL} \\ E_y^R(\mathbf{i}k) = \frac{i\tilde{\mu}_3\omega}{c} \tilde{H}_z^R \\ E_y^L(\mathbf{i}k) = \frac{i\tilde{\mu}_1\omega}{c} \tilde{H}_z^L, \end{cases} \quad (5.106)$$

and from the forth

$$\text{ME4 : } \begin{cases} -\tilde{H}_y^{BR}(k\gamma_2) = -\frac{i\omega}{c} \tilde{\varepsilon}_2 E_x^{BR} \\ -\tilde{H}_y^{BL}(-k\gamma_2) = -\frac{i\omega}{c} \tilde{\varepsilon}_2 E_x^{BL} \\ -\tilde{H}_y^R(-k\gamma_3) = -\frac{i\omega}{c} \tilde{\varepsilon}_3 E_x^R \\ -\tilde{H}_y^L(k\gamma_1) = -\frac{i\omega}{c} \tilde{\varepsilon}_1 E_x^L \\ \tilde{H}_x^{BR}(k\gamma_2) - \tilde{H}_z^{BR}(\mathbf{i}k) = -\frac{i\omega}{c} \tilde{\varepsilon}_2 E_y^{BR} \\ \tilde{H}_x^{BL}(-k\gamma_2) - \tilde{H}_z^{BL}(\mathbf{i}k) = -\frac{i\omega}{c} \tilde{\varepsilon}_2 E_y^{BL} \\ \tilde{H}_x^R(-k\gamma_3) - \tilde{H}_z^R(\mathbf{i}k) = -\frac{i\omega}{c} \tilde{\varepsilon}_3 E_y^R \\ \tilde{H}_x^L(k\gamma_1) - \tilde{H}_z^L(\mathbf{i}k) = -\frac{i\omega}{c} \tilde{\varepsilon}_1 E_y^L \\ \tilde{H}_y^{BR}(\mathbf{i}k) = -\frac{i\omega}{c} \tilde{\varepsilon}_2 E_z^{BR} \\ \tilde{H}_y^{BL}(\mathbf{i}k) = -\frac{i\omega}{c} \tilde{\varepsilon}_2 E_z^{BL} \\ \tilde{H}_y^R(\mathbf{i}k) = -\frac{i\omega}{c} \tilde{\varepsilon}_3 E_z^R \\ \tilde{H}_y^L(\mathbf{i}k) = -\frac{i\omega}{c} \tilde{\varepsilon}_1 E_z^L. \end{cases} \quad (5.107)$$

From the matching conditions at the interfaces we find

$$\text{MC : } \left\{ \begin{array}{l} \tilde{\varepsilon}_2 (E_z^{BR} + e^{-k\gamma_2 d} E_z^{BL}) = \tilde{\varepsilon}_3 E_z^R \\ \tilde{\varepsilon}_2 (E_z^{BL} + e^{-k\gamma_2 d} E_z^{BR}) = \tilde{\varepsilon}_1 E_z^L \\ (E_x^{BR} + e^{-k\gamma_2 d} E_x^{BL}) = E_x^R \\ (E_x^{BL} + e^{-k\gamma_2 d} E_x^{BR}) = E_x^L \\ (E_y^{BR} + e^{-k\gamma_2 d} E_y^{BL}) = E_y^R \\ (E_y^{BL} + e^{-k\gamma_2 d} E_y^{BR}) = E_y^L \\ \tilde{\mu}_2 (\tilde{H}_z^{BR} + e^{-k\gamma_2 d} \tilde{H}_z^{BL}) = \tilde{\mu}_3 \tilde{H}_z^R \\ \tilde{\mu}_2 (\tilde{H}_z^{BL} + e^{-k\gamma_2 d} \tilde{H}_z^{BR}) = \tilde{\mu}_1 \tilde{H}_z^L \\ (\tilde{H}_x^{BR} + e^{-k\gamma_2 d} \tilde{H}_x^{BL}) = \tilde{H}_x^R \\ (\tilde{H}_x^{BL} + e^{-k\gamma_2 d} \tilde{H}_x^{BR}) = \tilde{H}_x^L \\ (\tilde{H}_y^{BR} + e^{-k\gamma_2 d} \tilde{H}_y^{BL}) = \tilde{H}_y^R \\ (\tilde{H}_y^{BL} + e^{-k\gamma_2 d} \tilde{H}_y^{BR}) = \tilde{H}_y^L. \end{array} \right. \quad (5.108)$$

As before the equations couple into two sets of equation. The so-called TM modes are obtained from the equations that couple  $E_x$ ,  $E_z$ , and  $\tilde{H}_y$  to each other. The equations that couple the three other vectors have the so-called TE modes as solutions. These last modes do not survive in the non-retarded treatment if the materials are non-magnetic; thus they do not contribute to the van der Waals interaction; they are important for the Casimir force, though; they are of a different type not exponential in region 1 but oscillating standing wave type. We need to address them both.

### 5.4.1 Transverse Magnetic Modes

We start with the equations leading to TM modes. We have

$$\text{ME1 : } \left\{ \begin{array}{l} E_x^{BL}(ik) - E_z^{BL}(k\gamma_2) = 0 \\ E_x^{BR}(ik) + E_z^{BR}(k\gamma_2) = 0 \\ E_x^R(ik) + E_z^R(-k\gamma_3) = 0 \\ E_x^L(ik) + E_z^L(k\gamma_1) = 0 \end{array} \right. \quad (5.109)$$

$$\text{ME3 : } \begin{cases} E_x^{BR}(k\gamma_2) - E_z^{BR}(ik) = (i\tilde{\mu}_2\omega/c) \tilde{H}_y^{BR} \\ E_x^{BL}(-k\gamma_2) - E_z^{BL}(ik) = (i\tilde{\mu}_2\omega/c) \tilde{H}_y^{BL} \\ E_x^R(-k\gamma_3) - E_z^R(ik) = (i\tilde{\mu}_3\omega/c) \tilde{H}_y^R \\ E_x^L(k\gamma_1) - E_z^L(ik) = (i\tilde{\mu}_1\omega/c) \tilde{H}_y^L \end{cases} \quad (5.110)$$

$$\text{ME4 : } \begin{cases} -\tilde{H}_y^{BR}(k\gamma_2) = -(\omega/c) \tilde{\epsilon}_2 E_x^{BR} \\ -\tilde{H}_y^{BL}(-k\gamma_2) = -(\omega/c) \tilde{\epsilon}_2 E_x^{BL} \\ -\tilde{H}_y^R(-k\gamma_3) = -(\omega/c) \tilde{\epsilon}_3 E_x^R \\ -\tilde{H}_y^L(k\gamma_1) = -(\omega/c) \tilde{\epsilon}_1 E_x^L \\ \tilde{H}_y^{BR}(ik) = -(\omega/c) \tilde{\epsilon}_2 E_z^{BR} \\ \tilde{H}_y^{BL}(ik) = -(\omega/c) \tilde{\epsilon}_2 E_z^{BL} \\ \tilde{H}_y^R(ik) = -(\omega/c) \tilde{\epsilon}_3 E_z^R \\ \tilde{H}_y^L(ik) = -(\omega/c) \tilde{\epsilon}_1 E_z^L. \end{cases} \quad (5.111)$$

$$\text{MC : } \begin{cases} \tilde{\epsilon}_2 (E_z^{BR} + e^{-k\gamma_2 d} E_z^{BL}) = \tilde{\epsilon}_3 E_z^R \\ \tilde{\epsilon}_2 (E_z^{BL} + e^{-k\gamma_2 d} E_z^{BR}) = \tilde{\epsilon}_1 E_z^L \\ (E_x^{BR} + e^{-k\gamma_2 d} E_x^{BL}) = E_x^R \\ (E_x^{BL} + e^{-k\gamma_2 d} E_x^{BR}) = E_x^L \\ (\tilde{H}_y^{BR} + e^{-k\gamma_2 d} \tilde{H}_y^{BL}) = \tilde{H}_y^R \\ (\tilde{H}_y^{BL} + e^{-k\gamma_2 d} \tilde{H}_y^{BR}) = \tilde{H}_y^L \end{cases} \quad (5.112)$$

Thus we have 22 equations involving 12 field components. We start by expressing all components in the four  $E_z$  components. This we can easily do by using the four *ME1* equations and the last four of the *ME4* equations. We find

$$\begin{aligned} E_x^{BL} &= (k\gamma_2/ik) E_z^{BL} \\ E_x^{BR} &= -(k\gamma_2/ik) E_z^{BR} \\ E_x^R &= (k\gamma_3/ik) E_z^R \\ E_x^L &= -(k\gamma_1/ik) E_z^L \\ \tilde{H}_y^{BR} &= -(\omega/c) \tilde{\epsilon}_2 E_z^{BR} \\ \tilde{H}_y^{BL} &= -(\omega/c) \tilde{\epsilon}_2 E_z^{BL} \\ \tilde{H}_y^R &= -(\omega/c) \tilde{\epsilon}_3 E_z^R \\ \tilde{H}_y^L &= -(\omega/c) \tilde{\epsilon}_1 E_z^L \end{aligned} \quad (5.113)$$

Next we make these replacements in the remaining 14 equations and find

$$\begin{aligned}
& [(\gamma_2)^2 - 1 + \tilde{\mu}_2 \tilde{\epsilon}_2 (\omega/c k)^2] E_z^{BR} = 0 \\
& [(\gamma_2)^2 - 1 + \tilde{\mu}_2 \tilde{\epsilon}_2 (\omega/c k)^2] E_z^{BL} = 0 \\
& [(\gamma_3)^2 - 1 + \tilde{\mu}_3 \tilde{\epsilon}_3 (\omega/c k)^2] E_z^R = 0 \\
& [(\gamma_1)^2 - 1 + \tilde{\mu}_1 \tilde{\epsilon}_1 (\omega/c k)^2] E_z^L = 0 \\
& [0] E_z^{BR} = 0 \\
& [0] E_z^{BL} = 0 \\
& [0] E_z^R = 0 \\
& [0] E_z^L = 0 \\
& E_z^{BR} + e^{-k\gamma_2 d} E_z^{BL} = (\tilde{\epsilon}_3/\tilde{\epsilon}_2) E_z^R \\
& E_z^{BL} + e^{-k\gamma_2 d} E_z^{BR} = (\tilde{\epsilon}_1/\tilde{\epsilon}_2) E_z^L \\
& -E_z^{BR} + e^{-k\gamma_2 d} E_z^{BL} = (\gamma_3/\gamma_2) E_z^R \\
& -E_z^{BL} + e^{-k\gamma_2 d} E_z^{BR} = (\gamma_1/\gamma_2) E_z^L \\
& E_z^{BR} + e^{-k\gamma_2 d} E_z^{BL} = (\tilde{\epsilon}_3/\tilde{\epsilon}_2) E_z^R \\
& E_z^{BL} + e^{-k\gamma_2 d} E_z^{BR} = (\tilde{\epsilon}_1/\tilde{\epsilon}_2) E_z^L
\end{aligned} \tag{5.114}$$

Some of the equations are redundant and some of the trivial form  $0 = 0$ . We are left with

$$\begin{aligned}
& (\gamma_1)^2 = 1 - \tilde{\mu}_1 \tilde{\epsilon}_1 (\omega/c k)^2 \\
& (\gamma_2)^2 = 1 - \tilde{\mu}_2 \tilde{\epsilon}_2 (\omega/c k)^2 \\
& (\gamma_3)^2 = 1 - \tilde{\mu}_3 \tilde{\epsilon}_3 (\omega/c k)^2 \\
& E_z^{BR} + e^{-k\gamma_2 d} E_z^{BL} = (\tilde{\epsilon}_3/\tilde{\epsilon}_2) E_z^R \\
& E_z^{BL} + e^{-k\gamma_2 d} E_z^{BR} = (\tilde{\epsilon}_1/\tilde{\epsilon}_2) E_z^L \\
& -E_z^{BR} + e^{-k\gamma_2 d} E_z^{BL} = (\gamma_3/\gamma_2) E_z^R \\
& -E_z^{BL} + e^{-k\gamma_2 d} E_z^{BR} = (\gamma_1/\gamma_2) E_z^L
\end{aligned} \tag{5.115}$$

The first three equations give the functional form of the  $\gamma_i$ ,  $i = 1, 2, 3$ . The remaining four equations give the condition for modes. We write them on matrix form

$$\begin{pmatrix} 0 & -(\tilde{\epsilon}_3/\tilde{\epsilon}_2) e^{-k\gamma_2 d} & 1 & 1 \\ -(\tilde{\epsilon}_1/\tilde{\epsilon}_2) & 0 & 1 & e^{-k\gamma_2 d} \\ 0 & -(\gamma_3/\gamma_2) e^{-k\gamma_2 d} & -1 & 1 \\ -(\gamma_1/\gamma_2) & 0 & -1 & e^{-k\gamma_2 d} \end{pmatrix} \cdot \begin{pmatrix} E_z^L \\ E_z^R \\ E_z^{\tilde{B}L} \\ E_z^{\tilde{B}R} \end{pmatrix} = 0 \tag{5.116}$$

The non-trivial solution to this matrix equation is found when the determinant of the four-by-four matrix is zero. We find

$$[\tilde{\epsilon}_1/\tilde{\epsilon}_2 + \gamma_1/\gamma_2][\tilde{\epsilon}_3/\tilde{\epsilon}_2 + \gamma_3/\gamma_2] - e^{-2k\gamma_2 d} [\tilde{\epsilon}_1/\tilde{\epsilon}_2 - \gamma_1/\gamma_2][\tilde{\epsilon}_3/\tilde{\epsilon}_2 - \gamma_3/\gamma_2] = 0, \tag{5.117}$$

and the mode condition function is

$$f_{\mathbf{k}}(\omega, d) = [\tilde{\epsilon}_1/\tilde{\epsilon}_2 + \gamma_1/\gamma_2][\tilde{\epsilon}_3/\tilde{\epsilon}_2 + \gamma_3/\gamma_2] - e^{-2k\gamma_2 d} [\tilde{\epsilon}_1/\tilde{\epsilon}_2 - \gamma_1/\gamma_2][\tilde{\epsilon}_3/\tilde{\epsilon}_2 - \gamma_3/\gamma_2]. \tag{5.118}$$

The contribution from TM modes to the interaction energy between the two half spaces is

$$E^{\text{TM}}(d) = \frac{\hbar}{2} \int_{-\infty}^{\infty} \frac{d\xi}{2\pi} \int \frac{d^2k}{(2\pi)^2} \ln \tilde{f}_{\mathbf{k}}(i\xi, d), \quad (5.119)$$

where

$$\tilde{f}_{\mathbf{k}}(\omega, d) = \frac{f_{\mathbf{k}}(\omega, d)}{f_{\mathbf{k}}(\omega, \infty)} = 1 - e^{-2k\gamma_2 d} \frac{[\tilde{\epsilon}_1\gamma_2 - \tilde{\epsilon}_2\gamma_1][\tilde{\epsilon}_3\gamma_2 - \tilde{\epsilon}_2\gamma_3]}{[\tilde{\epsilon}_1\gamma_2 + \tilde{\epsilon}_2\gamma_1][\tilde{\epsilon}_3\gamma_2 + \tilde{\epsilon}_2\gamma_3]} = 1 - e^{-2k\gamma_2 d} r_{21}^p r_{23}^p. \quad (5.120)$$

### 5.4.2 Transverse Electric Modes

Now, we continue with the TE modes. The equations involving  $\tilde{H}_x$ ,  $\tilde{H}_z$ , and  $E_y$  are

$$\text{ME2} : \begin{cases} \tilde{H}_x^{BL}(ik) - \tilde{H}_z^{BL}(k\gamma_2) = 0 \\ \tilde{H}_x^{BR}(ik) + \tilde{H}_z^{BR}(k\gamma_2) = 0 \\ \tilde{H}_x^R(ik) + \tilde{H}_z^R(-k\gamma_3) = 0 \\ \tilde{H}_x^L(ik) + \tilde{H}_z^L(k\gamma_1) = 0, \end{cases} \quad (5.121)$$

$$\text{ME3} : \begin{cases} -E_y^{BR}(k\gamma_2) = (i\tilde{\mu}_2\omega/c) \tilde{H}_x^{BR} \\ -E_y^{BL}(-k\gamma_2) = (i\tilde{\mu}_2\omega/c) \tilde{H}_x^{BL} \\ -E_y^R(-k\gamma_3) = (i\tilde{\mu}_3\omega/c) \tilde{H}_x^R \\ -E_y^L(k\gamma_1) = (i\tilde{\mu}_1\omega/c) \tilde{H}_x^L \\ E_y^{BR}(ik) = (i\tilde{\mu}_2\omega/c) \tilde{H}_z^{BR} \\ E_y^{BL}(ik) = (i\tilde{\mu}_2\omega/c) \tilde{H}_z^{BL} \\ E_y^R(ik) = (i\tilde{\mu}_3\omega/c) \tilde{H}_z^R \\ E_y^L(ik) = (i\tilde{\mu}_1\omega/c) \tilde{H}_z^L \end{cases} \quad (5.122)$$

$$\text{ME4} : \begin{cases} \tilde{H}_x^{BR}(k\gamma_2) - \tilde{H}_z^{BR}(ik) = -(i\omega/c) \tilde{\epsilon}_2 E_y^{BR} \\ \tilde{H}_x^{BL}(-k\gamma_2) - \tilde{H}_z^{BL}(ik) = -(i\omega/c) \tilde{\epsilon}_2 E_y^{BL} \\ \tilde{H}_x^R(-k\gamma_3) - \tilde{H}_z^R(ik) = -(i\omega/c) \tilde{\epsilon}_3 E_y^R \\ \tilde{H}_x^L(k\gamma_1) - \tilde{H}_z^L(ik) = -(i\omega/c) \tilde{\epsilon}_1 E_y^L \end{cases} \quad (5.123)$$

$$\text{M.C. : } \begin{cases} (E_y^{BR} + e^{-k\gamma_2 d} E_y^{BL}) = E_y^R \\ (E_y^{BL} + e^{-k\gamma_2 d} E_y^{BR}) = E_y^L \\ \tilde{\mu}_2 \left( \tilde{H}_z^{BR} + e^{-k\gamma_2 d} \tilde{H}_z^{BL} \right) = \tilde{\mu}_3 \tilde{H}_z^R \\ \tilde{\mu}_2 \left( \tilde{H}_z^{BL} + e^{-k\gamma_2 d} \tilde{H}_z^{BR} \right) = \tilde{\mu}_1 \tilde{H}_z^L \\ \left( \tilde{H}_x^{BR} + e^{-k\gamma_2 d} \tilde{H}_x^{BL} \right) = \tilde{H}_x^R \\ \left( \tilde{H}_x^{BL} + e^{-k\gamma_2 d} \tilde{H}_x^{BR} \right) = \tilde{H}_x^L \end{cases} \quad (5.124)$$

Thus like in derivation of the TM modes we have 22 equations involving 12 field components. We start by expressing all components in the four  $\tilde{H}_z$  components. This we can easily do by using the four *ME2* equations and the last four of the *ME3* equations. We find

$$\begin{aligned} \tilde{H}_x^{BL} &= -(i\gamma_2) \tilde{H}_z^{BL} \\ \tilde{H}_x^{BR} &= (i\gamma_2) \tilde{H}_z^{BR} \\ \tilde{H}_x^R &= -(i\gamma_3) \tilde{H}_z^R \\ \tilde{H}_x^L &= (i\gamma_1) \tilde{H}_z^L \\ E_y^{BR} &= (\tilde{\mu}_2 \omega / ck) \tilde{H}_z^{BR} \\ E_y^{BL} &= (\tilde{\mu}_2 \omega / ck) \tilde{H}_z^{BL} \\ E_y^R &= (\tilde{\mu}_3 \omega / ck) \tilde{H}_z^R \\ E_y^L &= (\tilde{\mu}_1 \omega / ck) \tilde{H}_z^L \end{aligned} \quad (5.125)$$

Next we make these replacements in the remaining 14 equations and find

$$\begin{aligned} (0) \tilde{H}_z^{BR} &= 0 \\ (0) \tilde{H}_z^{BL} &= 0 \\ (0) \tilde{H}_z^R &= 0 \\ (0) \tilde{H}_z^L &= 0 \\ [(\gamma_2)^2 - 1 + \tilde{\mu}_2 \tilde{\epsilon}_2 (\omega / ck)^2] \tilde{H}_z^{BR} &= 0 \\ [(\gamma_2)^2 - 1 + \tilde{\mu}_2 \tilde{\epsilon}_2 (\omega / ck)^2] \tilde{H}_z^{BL} &= 0 \\ [(\gamma_3)^2 - 1 + \tilde{\mu}_3 \tilde{\epsilon}_3 (\omega / ck)^2] \tilde{H}_z^R &= 0 \\ [(\gamma_1)^2 - 1 + \tilde{\mu}_1 \tilde{\epsilon}_1 (\omega / ck)^2] \tilde{H}_z^L &= 0 \\ \tilde{H}_z^{BR} + e^{-k\gamma_2 d} \tilde{H}_z^{BL} &= (\tilde{\mu}_3 / \tilde{\mu}_2) \tilde{H}_z^R \\ \tilde{H}_z^{BL} + e^{-k\gamma_2 d} \tilde{H}_z^{BR} &= (\tilde{\mu}_1 / \tilde{\mu}_2) \tilde{H}_z^L \\ \tilde{H}_z^{BR} + e^{-k\gamma_2 d} \tilde{H}_z^{BL} &= (\tilde{\mu}_3 / \tilde{\mu}_2) \tilde{H}_z^R \\ \tilde{H}_z^{BL} + e^{-k\gamma_2 d} \tilde{H}_z^{BR} &= (\tilde{\mu}_1 / \tilde{\mu}_2) \tilde{H}_z^L \\ \tilde{H}_z^{BR} - e^{-k\gamma_2 d} \tilde{H}_z^{BL} &= -(\gamma_3 / \gamma_2) \tilde{H}_z^R \\ -\tilde{H}_z^{BL} + e^{-k\gamma_2 d} \tilde{H}_z^{BR} &= (\gamma_1 / \gamma_2) \tilde{H}_z^L \end{aligned} \quad (5.126)$$

Some of the equations are redundant and some of the trivial form  $0 = 0$ . We are left with

$$\begin{aligned}
(\gamma_1)^2 &= 1 - \tilde{\mu}_1 \tilde{\epsilon}_1 (\omega / ck)^2 \\
(\gamma_2)^2 &= 1 - \tilde{\mu}_2 \tilde{\epsilon}_2 (\omega / ck)^2 \\
(\gamma_3)^2 &= 1 - \tilde{\mu}_3 \tilde{\epsilon}_3 (\omega / ck)^2 \\
\tilde{H}_z^{BR} + e^{-k\gamma_2 d} \tilde{H}_z^{BL} - (\tilde{\mu}_3 / \tilde{\mu}_2) \tilde{H}_z^R &= 0 \\
\tilde{H}_z^{BL} + e^{-k\gamma_2 d} \tilde{H}_z^{BR} - (\tilde{\mu}_1 / \tilde{\mu}_2) \tilde{H}_z^L &= 0 \\
-\tilde{H}_z^{BR} + e^{-k\gamma_2 d} \tilde{H}_z^{BL} - (\gamma_3 / \gamma_2) \tilde{H}_z^R &= 0 \\
-\tilde{H}_z^{BL} + e^{-k\gamma_2 d} \tilde{H}_z^{BR} - (\gamma_1 / \gamma_2) \tilde{H}_z^L &= 0
\end{aligned} \tag{5.127}$$

The first three equations give the functional form of the  $\gamma_i$ ,  $i = 1, 2, 3$ . The remaining four equations give the condition for modes. We write them on matrix form

$$\begin{pmatrix} 0 & -(\tilde{\mu}_3 / \tilde{\mu}_2) e^{-k\gamma_2 d} & 1 & 0 \\ -(\tilde{\mu}_1 / \tilde{\mu}_2) & 0 & 1 & e^{-k\gamma_2 d} \\ 0 & -(\gamma_3 / \gamma_2) e^{-k\gamma_2 d} & -1 & 0 \\ -(\gamma_1 / \gamma_2) & 0 & -1 & e^{-k\gamma_2 d} \end{pmatrix} \cdot \begin{pmatrix} \tilde{H}_z^L \\ \tilde{H}_z^R \\ \tilde{H}_z^{BL} \\ \tilde{H}_z^{BR} \end{pmatrix} = 0 \tag{5.128}$$

The non-trivial solution to this matrix equation is found when the determinant of the four-by-four matrix is zero. We find

$$[\tilde{\mu}_1 / \tilde{\mu}_2 + \gamma_1 / \gamma_2] [\tilde{\mu}_3 / \tilde{\mu}_2 + \gamma_3 / \gamma_2] - e^{-2k\gamma_2 d} [\tilde{\mu}_1 / \tilde{\mu}_2 - \gamma_1 / \gamma_2] [\tilde{\mu}_3 / \tilde{\mu}_2 - \gamma_3 / \gamma_2] = 0, \tag{5.129}$$

and the mode condition function is

$$\begin{aligned}
f_{\mathbf{k}}(\omega, d) &= [\tilde{\mu}_1 / \tilde{\mu}_2 + \gamma_1 / \gamma_2] [\tilde{\mu}_3 / \tilde{\mu}_2 + \gamma_3 / \gamma_2] \\
&\quad - e^{-2k\gamma_2 d} [\tilde{\mu}_1 / \tilde{\mu}_2 - \gamma_1 / \gamma_2] [\tilde{\mu}_3 / \tilde{\mu}_2 - \gamma_3 / \gamma_2].
\end{aligned} \tag{5.130}$$

The contribution from TE modes to the interaction energy between the two half spaces is

$$E^{\text{TE}}(d) = \frac{\hbar}{2} \int_{-\infty}^{\infty} \frac{d\xi}{2\pi} \int \frac{d^2k}{(2\pi)^2} \ln \tilde{f}_{\mathbf{k}}(i\xi, d), \tag{5.131}$$

where

$$\begin{aligned}
\tilde{f}_{\mathbf{k}}(\omega, d) &= \frac{f_{\mathbf{k}}(\omega, d)}{f_{\mathbf{k}}(\omega, \infty)} = 1 - e^{-2\gamma_2 d} \left[ \frac{\tilde{\mu}_1 \gamma_2 - \tilde{\mu}_2 \gamma_1}{\tilde{\mu}_1 \gamma_2 + \tilde{\mu}_2 \gamma_1} \right] \left[ \frac{\tilde{\mu}_3 \gamma_2 - \tilde{\mu}_2 \gamma_3}{\tilde{\mu}_3 \gamma_2 + \tilde{\mu}_2 \gamma_3} \right] \\
&= 1 - e^{-2\gamma_2 d} r_{21}^s r_{23}^s.
\end{aligned} \tag{5.132}$$

### 5.4.3 Modes in Non-retarded Treatment

When we neglect retardation effects the mode condition functions become simpler and more easy to handle. The TM mode changes into another type of mode, with mode condition function

$$\tilde{f}_{\mathbf{k}}^E(\omega) = 1 - e^{-2kd} \frac{[\tilde{\epsilon}_1(\omega) - \tilde{\epsilon}_2(\omega)] [\tilde{\epsilon}_3(\omega) - \tilde{\epsilon}_2(\omega)]}{[\tilde{\epsilon}_1(\omega) + \tilde{\epsilon}_2(\omega)] [\tilde{\epsilon}_3(\omega) + \tilde{\epsilon}_2(\omega)]}, \quad (5.133)$$

where the electric field vector lies in the  $xz$ -plane like for TM modes but here there are no magnetic component. The field is purely electric which motivates the superscript E. If we neglect magnetic effects, i.e., let  $\tilde{\mu} = 1$  in all regions this is the only mode. If we take the weak magnetic effects into account we find another mode type, with mode condition function

$$\tilde{f}_{\mathbf{k}}^M(\omega) = 1 - e^{-2kd} \frac{[\tilde{\mu}_1(\omega) - \tilde{\mu}_2(\omega)] [\tilde{\mu}_3(\omega) - \tilde{\mu}_2(\omega)]}{[\tilde{\mu}_1(\omega) + \tilde{\mu}_2(\omega)] [\tilde{\mu}_3(\omega) + \tilde{\mu}_2(\omega)]}, \quad (5.134)$$

where the magnetic field vector lies in the  $xz$ -plane like for TE modes but here there are no electric component. The field is purely magnetic which motivates the superscript M.

We now derive an expression for the interaction energy between two planar interfaces (two half spaces) with negligible magnetic effects,  $E_p$ , in the non-retarded case. We need this for the discussion of the proximity force approximation (PFA) in Sect. 6.2. The energy per unit area is

$$\begin{aligned} E_p(d) &= \frac{\hbar}{2} \int_{-\infty}^{\infty} \frac{d\xi}{2\pi} \int \frac{d^2k}{(2\pi)^2} \ln \left[ 1 - e^{-2kd} \frac{[\tilde{\epsilon}_1(i\xi) - \tilde{\epsilon}_2(i\xi)] [\tilde{\epsilon}_3(i\xi) - \tilde{\epsilon}_2(i\xi)]}{[\tilde{\epsilon}_1(i\xi) + \tilde{\epsilon}_2(i\xi)] [\tilde{\epsilon}_3(i\xi) + \tilde{\epsilon}_2(i\xi)]} \right] \\ &= \frac{\hbar}{8\pi^2} \int_{-\infty}^{\infty} d\xi \int_0^{\infty} dk k \ln \left[ 1 - e^{-2kd} \frac{[\tilde{\epsilon}_1(i\xi) - \tilde{\epsilon}_2(i\xi)] [\tilde{\epsilon}_3(i\xi) - \tilde{\epsilon}_2(i\xi)]}{[\tilde{\epsilon}_1(i\xi) + \tilde{\epsilon}_2(i\xi)] [\tilde{\epsilon}_3(i\xi) + \tilde{\epsilon}_2(i\xi)]} \right] \\ &= \frac{\hbar}{8\pi^2(2d)^2} \int_{-\infty}^{\infty} d\xi \int_0^{\infty} dx x \ln \left[ 1 - e^{-x} \frac{[\tilde{\epsilon}_1(i\xi) - \tilde{\epsilon}_2(i\xi)] [\tilde{\epsilon}_3(i\xi) - \tilde{\epsilon}_2(i\xi)]}{[\tilde{\epsilon}_1(i\xi) + \tilde{\epsilon}_2(i\xi)] [\tilde{\epsilon}_3(i\xi) + \tilde{\epsilon}_2(i\xi)]} \right] \\ &\quad - \sum_{n=1}^{\infty} \frac{1}{n^3} \left\{ \frac{[\tilde{\epsilon}_1(i\xi) - \tilde{\epsilon}_2(i\xi)] [\tilde{\epsilon}_3(i\xi) - \tilde{\epsilon}_2(i\xi)]}{[\tilde{\epsilon}_1(i\xi) + \tilde{\epsilon}_2(i\xi)] [\tilde{\epsilon}_3(i\xi) + \tilde{\epsilon}_2(i\xi)]} \right\}^n \\ &= -\frac{\hbar}{32\pi^2 d^2} \sum_{n=1}^{\infty} \frac{\langle \omega_n \rangle}{n^3}, \end{aligned} \quad (5.135)$$

where

$$\langle \omega_n \rangle = \int_{-\infty}^{\infty} d\xi \left\{ \frac{[\tilde{\epsilon}_1(i\xi) - \tilde{\epsilon}_2(i\xi)] [\tilde{\epsilon}_3(i\xi) - \tilde{\epsilon}_2(i\xi)]}{[\tilde{\epsilon}_1(i\xi) + \tilde{\epsilon}_2(i\xi)] [\tilde{\epsilon}_3(i\xi) + \tilde{\epsilon}_2(i\xi)]} \right\}^n. \quad (5.136)$$

## References

1. F. London, *Zeitschrift für Physikalische Chemie B* **11**, 222 (1930); *Zeitschrift für Physik* **63**, 245 (1930)
2. Bo E. Sernelius, *surface Modes in Physics* (Wiley-VCH, Berlin, 2001)
3. G.D. Mahan, *J. Chem. Phys.* **43**, 1569 (1965)
4. N.G. van Kampen, B.R.A. Nijboer, K. Schram, *Phys. Lett.* **26A**, 307 (1968)
5. B.W. Ninham, V.A. Parsegian, G.H. Weiss, *J. Stat. Phys.* **2**, 323 (1970)
6. H.B.G. Casimir, *J. Chim. Phys.* **47**, 407 (1949)
7. R. P. Feynman, The present status of quantum electrodynamics, in *The Quantum Theory of Fields*, ed. by R. Stoops (Wiley Interscience, New York, 1961)
8. H.A. Bethe, The electromagnetic shift of energy levels. *Phys. Rev.* **72**, 241 (1947)

# Chapter 6

## Different Approaches



**Abstract** The underlying theme of this book is the derivation of interactions based on the electromagnetic normal modes. In the present chapter we have compiled a number of competing or complementary methods for deriving the interactions. We start with two methods that we will make use of later in the text. The first is the summation of pair interactions which is an approximate method that can be useful for predicting the results in certain limits. The second, the PFA (Proximity Force Approximation), is a very useful method that is used for calculating the interactions between objects at very small separations; it is often used when experimental results are compared to theoretical. Next we treat a specific system, viz. two parallel 2D sheets, with many-body theory and show that the van der Waals interaction energy we are dealing with in Part II is nothing but what is called the correlation energy in that field; we further extend the treatment by, apart from the Coulomb interaction between the charged particles, including the interaction mediated by photons; then we obtain the fully retarded interaction energy, treated in Part III. We end with a brief compilation of other approaches.

### 6.1 Summation of Pair Interactions

A much faster way to obtain results for the interaction energy is to just sum over pair interactions [1]. One treats the systems as composed of polarizable atoms or molecules and sums the contribution from all pairs; one atom or molecule belongs to one of the objects and the other belongs to the other object. This gives, in general, results that have the right distance dependence<sup>1</sup> but the strength is not quite right. The forces are not strictly additive. The result is asymptotically correct for diluted systems.

---

<sup>1</sup>A note of caution is in order here. There are exceptions where it leads to an incorrect separation dependence.

We will now perform calculations for a number of structures. These approximate results will later be compared to our full results; the van der Waals results in Table A.1; the Casimir results in Table A.2.

Let us begin with such a calculation for two layers of thickness  $\delta_1$ , and  $\delta_2$ , area  $A$ , and separation  $d$ . We perform a general calculation that is valid both in the non-retarded and in the retarded limits. Let the interaction energy between two atoms or molecules be

$$V = -Bd^{-\gamma}, \quad (6.1)$$

where  $d$  is the distance between the atoms and  $B$  a constant. In the van der Waals limit  $\gamma = 6$  and in the Casimir limit  $\gamma = 7$ . First we consider one atom a distance  $d$  from a layer of thickness  $\delta_2$  and atom density  $n_2$ . We place the coordinate system with the origin at the atom and the  $z$ -axis pointing toward the layer. In the integration we let distance to the  $z$ -axis be denoted by  $r$ . The *atom-layer* potential becomes

$$\begin{aligned} V_{al}(d) &= -Bn_2 \int_0^{d+\delta_2} dz \int d^2r (r^2 + z^2)^{-\gamma/2} \\ &= -\frac{Bn_2 2\pi}{(\gamma-2)(\gamma-3)} \left[ d^{-(\gamma-3)} - (d + \delta_2)^{-(\gamma-3)} \right]. \end{aligned} \quad (6.2)$$

From this we can get the result for an atom next to a film, the *atom-film* potential, by letting  $\delta_2$  go toward zero,

$$\begin{aligned} V_{af}(d) &\approx -\frac{Bn_2 2\pi}{(\gamma-2)(\gamma-3)} \left[ d^{-(\gamma-3)} - d^{-(\gamma-3)} (1 - (\gamma-3) \delta_2/d) \right] \\ &= -\frac{Bn_2 2\pi}{(\gamma-2)(\gamma-3)} \left[ d^{-(\gamma-3)} (\gamma-3) \delta_2/d \right] = -\frac{Bn_2 \delta_2 2\pi}{(\gamma-2)d^{(\gamma-2)}} \\ &= -\frac{B2\pi n_f^{2D}}{(\gamma-2)d^{(\gamma-2)}}, \end{aligned} \quad (6.3)$$

where  $n_f^{2D} = n_2 \delta_2$  is the 2D atom density of the film.

We may also get the result for an atom next to a half space from (6.2) by letting  $\delta_2$  go toward infinity. Then the second term in the integral vanishes. We find the *atom-wall* potential is

$$V_{ah}(d) = -\frac{Bn_2 2\pi}{(\gamma-2)(\gamma-3)d^{(\gamma-3)}}. \quad (6.4)$$

The result of (6.2) can further be used to find the results for two layers. We sum the contributions from all atoms in one layer interacting with the other layer. The *layer-layer* potential is

$$\begin{aligned} V_{ll}(d) &= n_1 A \int_0^{\delta_1} dz \left[ -\frac{Bn_2 2\pi}{(\gamma-2)(\gamma-3)} \right] \left[ (d+z)^{-(\gamma-3)} - (d+\delta_2+z)^{-(\gamma-3)} \right] \\ &= -\frac{Bn_2 2\pi n_1 A}{(\gamma-2)(\gamma-3)} \frac{-1}{(\gamma-4)} \left[ (d+z)^{-(\gamma-4)} - (d+\delta_2+z)^{-(\gamma-4)} \right]_0^{\delta_1} \\ &= -\frac{Bn_2 2\pi n_1 A}{(\gamma-2)(\gamma-3)(\gamma-4)} \\ &\quad \times \left[ (d)^{-(\gamma-4)} - (d+\delta_2)^{-(\gamma-4)} - (d+\delta_1)^{-(\gamma-4)} + (d+\delta_1+\delta_2)^{-(\gamma-4)} \right], \end{aligned} \quad (6.5)$$

and the interaction potential per unit area is

$$\frac{V_H(d)}{A} = -\frac{Bn_2n_12\pi}{(\gamma-2)(\gamma-3)(\gamma-4)} \times \left[ (d)^{-(\gamma-4)} - (d+\delta_2)^{-(\gamma-4)} - (d+\delta_1)^{-(\gamma-4)} + (d+\delta_1+\delta_2)^{-(\gamma-4)} \right]. \quad (6.6)$$

From this result we may find the interaction energy between *two half spaces* by letting  $\delta_1$  and  $\delta_2$  go to infinity. Thus,

$$\frac{V_{hh}(d)}{A} = -\frac{Bn_2n_12\pi}{(\gamma-2)(\gamma-3)(\gamma-4)} \frac{1}{d^{\gamma-4}}. \quad (6.7)$$

The result for *two parallel thin films* we get by letting  $\delta_1$  and  $\delta_2$  approach zero. Thus,

$$\begin{aligned} \frac{V_{ff}(d)}{A} &= -\frac{Bn_2n_12\pi(\gamma-3)(\gamma-4)\delta_1\delta_2}{(\gamma-2)(\gamma-3)(\gamma-4)d^{(\gamma-4)}d^2} \\ &= -\frac{B2\pi n_2n_1\delta_1\delta_2}{(\gamma-2)d^{(\gamma-2)}} = -\frac{B2\pi n_1^{2D}n_2^{2D}}{(\gamma-2)d^{(\gamma-2)}}, \end{aligned} \quad (6.8)$$

where  $n_1^{2D}$  and  $n_2^{2D}$  are the two dimensional atom densities in film 1 and 2, respectively. While we are at it we derive the result for a thin film next to (and parallel to) a half space (or wall). This we find by letting one of the  $\delta$ s go to infinity and one approach zero. We find the *film-wall* potential is

$$\frac{V_{fh}(d)}{A} = -\frac{Bn_2n_12\pi\delta_1}{(\gamma-2)(\gamma-3)d^{(\gamma-3)}} = -\frac{2\pi Bn_2n_1^{2D}}{(\gamma-2)(\gamma-3)d^{(\gamma-3)}}, \quad (6.9)$$

where  $n_1^{2D}$  and  $n_2$  are the two dimensional atom density in the film and the three dimensional atom density in the half space, respectively.

Next we calculate the interaction energy for an atom at the distance  $R$  from a spherical shell of radius  $R_2$ . The closest distance between the two objects is  $d = R - R_2$ . The *atom-spherical-shell* potential is

$$\begin{aligned} E(R) &= -\int_d^{d+2R_2} dz \frac{B}{r^\gamma} \frac{4\pi R_2^2 n_2^{2D}}{2R_2} = -\frac{4\pi R_2^2 n_2^{2D} B}{2R_2} \int_d^{d+2R_2} dz \frac{1}{\sqrt{z^2+R_2^2-(R-z)^2}^\gamma} \\ &= -2\pi R_2 n_2^{2D} B \int_d^{d+2R_2} dz \frac{1}{\sqrt{R_2^2-R^2+2Rz}^\gamma} = -2\pi R_2 n_2^{2D} B \int_d^{d+2R_2} dz (R_2^2 - R^2 + 2Rz)^{-\gamma/2} \\ &= -2\pi R_2 n_2^{2D} B \left[ (R_2^2 - R^2 + 2Rz)^{-\gamma/2+1} \frac{1}{2R(-\gamma/2+1)} \right]_d^{d+2R_2} \\ &= -\frac{\pi R_2 n_2^{2D} B}{R(-\gamma/2+1)} \left[ \frac{1}{\sqrt{R_2^2-R^2+2Rd+4RR_2}^{\gamma-2}} - \frac{1}{\sqrt{R_2^2-R^2+2Rd}^{\gamma-2}} \right] \\ &= -\frac{\pi R_2 n_2^{2D} B}{R(-\gamma/2+1)} \left[ \frac{1}{\sqrt{R_2^2-R^2+2R(R-R_2)+4RR_2}^{\gamma-2}} - \frac{1}{\sqrt{R_2^2-R^2+2R(R-R_2)}^{\gamma-2}} \right] \\ &= -\frac{\pi R_2 n_2^{2D} B}{R(-\gamma/2+1)} \left[ \frac{1}{\sqrt{R_2^2+R^2+2RR_2}^{\gamma-2}} - \frac{1}{\sqrt{R_2^2+R^2-2RR_2}^{\gamma-2}} \right] \\ &= -\frac{\pi R_2 n_2^{2D} B}{R(-\gamma/2+1)} \left[ \frac{1}{(R+R_2)^{\gamma-2}} - \frac{1}{(R-R_2)^{\gamma-2}} \right]. \end{aligned} \quad (6.10)$$

In the first line we made use of the fact that if we cut slices, of equal thickness, of a spherical object, each slice has equal part in the area of the spherical surface. This means that in our example a slice of thickness  $dz$  contains  $4\pi R_2^2 n_2^{2D} dz / 2R_2$  number of atoms. Because of the axial symmetry all atoms of the slice are at the same distance from the external atom,  $r = \sqrt{z^2 + R_2^2 - (R - z)^2}$ .

In the limit of large separations,  $R$ , we find

$$\begin{aligned} E(R) &\approx -\frac{\pi R_2 n_2^{2D} B}{R(-\gamma/2+1)} \left[ \frac{1-(\gamma-2)(R_2/R)}{R^{\gamma-2}} - \frac{1+(\gamma-2)(R_2/R)}{R^{\gamma-2}} \right] \\ &= -\frac{\pi n_2^{2D} B 4R_2^2}{R^\gamma} = -\frac{B}{R^\gamma} \frac{4\pi R_2^2 n_2^{2D}}{3} = -\frac{B}{R^\gamma} N_2^{Shell}. \end{aligned} \quad (6.11)$$

where  $N_2^{Shell}$  is the total number of atoms in the spherical shell of radius  $R_2$ .

From (6.10) we find the interaction between an atom and a ball by summing over concentric spherical shells of thickness  $dR_2$  filling a ball of radius  $R_2$ . Then  $n^{2D} \rightarrow n_2^{3D} dR_2$  and we have for the *atom-ball* potential

$$\begin{aligned} E(R) &= -\frac{2\pi n_2^{3D} B}{R(2-\gamma)} \int_0^{R_2} dR_2 R_2 \left[ \frac{1}{(R+R_2)^{\gamma-2}} - \frac{1}{(R-R_2)^{\gamma-2}} \right] \\ &= -\frac{2\pi n_2^{3D} B}{R(2-\gamma)} \left\{ \left[ R_2 \left[ \frac{-1}{(\gamma-3)(R+R_2)^{\gamma-3}} - \frac{1}{(\gamma-3)(R-R_2)^{\gamma-3}} \right] \right]_0^{R_2} \right. \\ &\quad \left. - \int_0^{R_2} dR_2 \frac{1}{(\gamma-3)} \left[ \frac{-1}{(R+R_2)^{\gamma-4}} - \frac{1}{(R-R_2)^{\gamma-4}} \right] \right\} \\ &= -\frac{2\pi n_2^{3D} B}{R(2-\gamma)} \left\{ R_2 \left[ \frac{-1}{(\gamma-3)(R+R_2)^{\gamma-3}} - \frac{1}{(\gamma-3)(R-R_2)^{\gamma-3}} \right] \right. \\ &\quad \left. - \frac{1}{(\gamma-3)(\gamma-4)} \left[ \frac{1}{(R+R_2)^{\gamma-4}} - \frac{1}{(R-R_2)^{\gamma-4}} \right]_0^{R_2} \right\} \\ &= -\frac{2\pi n_2^{3D} B}{R(2-\gamma)} \left\{ R_2 \left[ \frac{-1}{(\gamma-3)(R+R_2)^{\gamma-3}} - \frac{1}{(\gamma-3)(R-R_2)^{\gamma-3}} \right] \right. \\ &\quad \left. - \frac{1}{(\gamma-3)(\gamma-4)} \left[ \frac{1}{(R+R_2)^{\gamma-4}} - \frac{1}{(R-R_2)^{\gamma-4}} \right] \right\} \\ &= -\frac{2\pi n_2^{3D} B}{R(2-\gamma)(\gamma-3)(\gamma-4)} \left\{ \frac{R-R_2(\gamma-3)}{(R-R_2)^{\gamma-3}} - \frac{R+R_2(\gamma-3)}{(R+R_2)^{\gamma-3}} \right\} \\ &= -\frac{2\pi n_2^{3D} B}{(2-\gamma)(\gamma-3)(\gamma-4)R^{\gamma-3}} \left\{ \frac{1-\frac{R_2}{R}(\gamma-3)}{\left(1-\frac{R_2}{R}\right)^{\gamma-3}} - \frac{1+\frac{R_2}{R}(\gamma-3)}{\left(1+\frac{R_2}{R}\right)^{\gamma-3}} \right\} \end{aligned} \quad (6.12)$$

In the limit of large separations we find

$$E(R) \approx -\frac{2\pi n_2^{3D} B R_2^3}{R^\gamma} \frac{2}{3} = -\frac{B}{R^\gamma} \frac{4\pi R_2^3 n_2^{3D}}{3} = -\frac{B}{R^\gamma} N_2, \quad (6.13)$$

where  $N_2$  is the total number of atoms in the ball.

This can be generalized to the interaction between two balls at large separation. It is

$$E(R) = -\frac{B}{R^\gamma} N_1 N_2, \quad (6.14)$$

where  $N_1$  is the total number of atoms in the ball number 1 and  $N_2$  is the total number of atoms in the ball number 2. For general separation it becomes more cumbersome to derive. The non-retarded result was first derived by Hamaker [2]. The result for the non-retarded *ball-ball* potential is

$$E(R) = -\pi^2 n_1^{3D} n_2^{3D} B \frac{1}{6} \times \left[ \frac{2R_1 R_2}{R^2 - (R_1 + R_2)^2} + \frac{2R_1 R_2}{R^2 - (R_1 - R_2)^2} + \ln \frac{R^2 - (R_1 + R_2)^2}{R^2 - (R_1 - R_2)^2} \right]. \quad (6.15)$$

In the large separation limit one finds

$$E(R) \approx -\frac{B}{R^6} \frac{4\pi n_1^{3D} R_1^3}{3} \frac{4\pi n_2^{3D} R_2^3}{3} = -\frac{B N_1 N_2}{R^6}, \quad (6.16)$$

where  $N_1$  is the total number of atoms in the ball number 1 and  $N_2$  is the total number of atoms in the ball number 2. This agrees with (6.14). We also need the limiting result for small separations. The closest distance,  $d$ , is  $d = R - R_1 - R_2$ , and the interaction energy expressed in this variable is

$$E(d) = -\pi^2 n_1^{3D} n_2^{3D} B \frac{1}{6} \left[ \frac{2R_1 R_2}{d^2 + 2d(R_1 + R_2)} + \frac{2R_1 R_2}{d^2 + 2d(R_1 + R_2) + 4R_1 R_2} + \ln \frac{d^2 + 2d(R_1 + R_2)}{d^2 + 2d(R_1 + R_2) + 4R_1 R_2} \right] \quad (6.17)$$

In the small  $d$  limit we find

$$E(d) \approx -\pi^2 n_1^{3D} n_2^{3D} B \frac{R_1 R_2}{(R_1 + R_2)} \frac{1}{6} \frac{1}{d}. \quad (6.18)$$

The interaction energy for a *ball-wall* geometry we find by letting one of the ball radii in (6.17) go toward infinity,  $R_1$  say. Then we find

$$E(d) = -\pi^2 n_1^{3D} n_2^{3D} B \frac{1}{6} \left[ \frac{R_2}{d} + \frac{R_2}{d + 2R_2} + \ln \frac{d}{d + 2R_2} \right]. \quad (6.19)$$

For small separations this is

$$E(d) \approx -\pi^2 n_1^{3D} n_2^{3D} B \frac{1}{6} \frac{R_2}{d}. \quad (6.20)$$

Alternatively we may express (6.19) in terms of the distance,  $r$ , between the center of the ball and the wall, i.e.,  $r = d + R_2$ . Then we have

$$E(r) = -\pi^2 n_1^{3D} n_2^{3D} B \frac{1}{6} \left[ \frac{R_2}{r - R_2} + \frac{R_2}{r + R_2} + \ln \frac{r - R_2}{r + R_2} \right]. \quad (6.21)$$

In the limit of large values of  $r$  we find

$$E(r) \approx -\pi^2 n_1^{3D} n_2^{3D} B \frac{4 R_2^3}{18 r^3} = -\pi n_1^{3D} B \frac{1}{6} \frac{4\pi R_2^3 n_2^{3D}}{3} \frac{1}{r^3} = -\frac{\pi n_1^{3D} N_2 B}{6 r^3}. \quad (6.22)$$

This is just  $N_2$  times the result for one atom the distance  $r$  from a wall, which is exactly what one would expect to find. See (6.4). Next we move on to cylinders. It is difficult to treat a general  $\gamma$ . We start by the van der Waals case, i.e.  $\gamma = 6$ . For an atom at the distance  $d$  from a string of atoms we find the non-retarded *atom-string* potential is

$$E(d) = -n^{1D} B \int_{-\infty}^{\infty} dx \frac{1}{\sqrt{d^2 + x^2}^6} = -n^{1D} \frac{B}{d^5} \int_{-\infty}^{\infty} dx \frac{1}{(1+x^2)^3} = -n^{1D} \frac{3\pi B}{8 d^5}, \quad (6.23)$$

where  $n^{1D}$  is the number of atoms per unit length along the string. For an atom far from a cylinder of radius  $a$  we have non-retarded *atom-cylinder* potential,

$$E(r) = -n_1^{3v} \pi a^2 \frac{3\pi B}{8 r^5}. \quad (6.24)$$

The van der Waals energy per unit length between *two parallel cylinders* of radius  $a$  and  $b$ , respectively, is

$$E(r) = -n_1^{3D} \pi a^2 n_2^{3D} \pi b^2 \frac{3\pi B}{8 r^5} = -\frac{3\pi^3 n_1^{3D} n_2^{3D} a^2 b^2 B}{8 r^5}. \quad (6.25)$$

This result agrees with (6.41) of [3].

We continue with the Casimir case i.e.  $\gamma = 7$ . For an atom at the distance  $d$  from a string of atoms we find the retarded *atom-string* potential is

$$\begin{aligned} E(d) &= -n^{1D} B \int_{-\infty}^{\infty} dx \frac{1}{\sqrt{d^2 + x^2}^7} = -n^{1D} \frac{B}{d^6} \int_{-\infty}^{\infty} dx \frac{1}{(1+x^2)^{3+1/2}} \\ &= -n^{1D} \frac{B}{d^6} \frac{x}{\sqrt{x^2+1}} \sum_{n=0}^2 \frac{2^{6-2n-1} 2! 3! (2n)!}{(6)!(n!)^2 (x^2+1)^n} \Bigg|_{-\infty}^{\infty} \\ &= -n^{1D} 2 \frac{B}{d^6} \frac{2^2 2! 3!}{(6)!} = -n^{1D} \frac{B}{d^6} \frac{16}{15}, \end{aligned} \quad (6.26)$$

where  $n^{1D}$  is the number of atoms per unit length along the string. For an atom far from a cylinder of radius  $a$  we have the retarded *atom-cylinder* potential is

$$E(r) = -n_1^{3D} \pi a^2 \frac{16 B}{15 r^6}. \quad (6.27)$$

The retarded interaction energy per unit length between *two parallel cylinders* of radius  $R_1$  and  $R_2$ , respectively, is then

$$E(d) = -n_1^{1D} n_2^{1D} \frac{B}{d^6} \frac{16}{15} = -\left(n_1^{3D} \pi R_1^2\right) \left(n_2^{3D} \pi R_2^2\right) \frac{B}{d^6} \frac{16}{15} = -\frac{16\pi^2 n_1 n_2 R_1^2 R_2^2}{15} \frac{B}{d^6}, \quad (6.28)$$

where  $n_1$  and  $n_2$  are the 3D atom densities in cylinder 1 and cylinder 2, respectively.

In principle one can use this approximate method for all geometries but we now have all we need so we stop here. Next we study a method that is useful for small separation between objects.

## 6.2 Interactions Between Objects at Small Separations: The Proximity Force Approximation

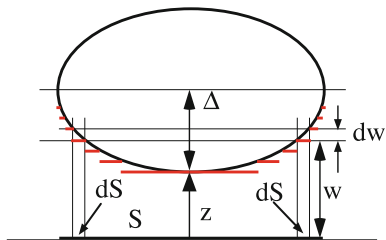
If one wants to calculate the interaction between objects of general shapes there are sophisticated techniques to do this numerically (see Sect. 6.5); the draw back is that these calculations are tedious. For objects of finite size at large distances one may use a simpler technique, viz. multipolar expansions [4]. In the asymptotic limit only dipolar interactions contribute and the two objects can be treated as two spheres. However, for small separations one needs to keep more and more terms in the expansion the smaller the distance; eventually one reaches a limit when the method is no longer feasible to use. In the experimental situation one often ends up in this region of small separations; the force is weak and dies off quickly with separation. Then another method comes handy in this situation, viz. the Proximity Force Approximation (PFA). This approximation relies on the van der Waals and Casimir interactions between two half spaces of the materials the two objects are made of. These interactions are not very difficult to calculate (see Sect. 5.4). PFA was used for the first time already in 1934 [5] in connection with coagulation of aerosols. It is a very powerful and widely used approximation for the interaction at short distances between two objects. It is difficult to say how good the approximation is but it has gained a wide-spread acceptance in recent years. Some attempts have been made to show its validity in some specific cases. However, the lack of a general and rigorous proof still remains, as well as estimates of the level of accuracy at all distances.

The basic idea of the approximation is that the interaction potential between the objects is an average interaction energy between parallel planar interfaces. The surfaces of the objects are discretized and the interaction energy is averaged. When the discretization becomes more and more fine-grained the averaging procedure transcends into an integral,

$$V(z) = \sum_i [S(w_{i+1}) - S(w_i)] E_p(w_i) \rightarrow \int_S dS E_p(w), \quad (6.29)$$

where  $E_p(w)$  is the interaction energy per unit area between planar interfaces a distance  $w$  apart. The variable  $z$  is the closest distance between the two objects. An example with a coarse-grained discretization is shown in Fig. 6.1. It shows an oblate

**Fig. 6.1** Example of coarse-grained discretization of the surface of an oblate spheroid



spheroid above a substrate, or next to a wall. The surface of the spheroid is replaced by the set of rings whose cross sections here appear as horizontal bars. The surface  $S$  coincides with the projection of the spheroid on the substrate.

In the standard PFA of the interaction between two objects one only takes into consideration the surface of each object that is facing the other object. The function  $E_p(w)$ , in (6.29), is the energy per unit area for two half spaces, made up from the materials of the two objects, separated by the distance  $w$ . With this treatment the backsides of the objects have no effects at all. One gets, e.g., the same result for two spheres as for two half spheres. We know that the normal modes contributing to the interaction may extend through the objects and continue on the other side. Thus, the backside may well have important effects on the results. One may extend the treatment by using  $E_p(w)$  from a planar structure with four interfaces instead of two; two for the front-sides and two for the back-sides. Another more severe limitation with the traditional PFA is that coated objects are treated as solid. This could easily be handled by having eight interfaces instead.

Deviations from the PFA results have been observed [6] in experiments on spheres. These deviations might be due to the thin coatings of the objects. However because of limitations in the experimental and theoretical parameters one can not say conclusively that the PFA calculations for coated plates give better predictions than PFA for solid and infinitely thick plates.

Now, let  $E_p(w)$  be the energy per unit area for two half spaces, made up from the materials of the two objects, separated by the distance  $w$ . We may express the potential as

$$V(z) = \int_S dS E_p(w) = \int_z^{z+\Delta} dw \underbrace{\frac{dS}{dw}}_{g(w-z)} E_p(w), \tag{6.30}$$

and find the force as

$$F(z) = -\frac{dV}{dz} = -g(\Delta) E_p(z + \Delta) + g(0) E_p(z) - \int_z^{z+\Delta} dw \frac{dg(w-z)}{dz} E_p(w). \tag{6.31}$$

In many cases  $g(\Delta)$  vanishes, like in the illustrating example in Fig. 6.1. Here we have a spheroid above a substrate. The surface  $S$  is defined through the projection of the object onto the substrate. When  $g(\Delta)$  vanishes we have

$$F(z) = g(0) E_p(z) \left[ 1 + \frac{1}{g(0) E_p(z)} \int_z^{z+\Delta} dw \frac{d^2 S}{dw^2} E_p(w) \right], \quad (6.32)$$

where the first part is what one usually means with PFA. The remaining part, within brackets, is a correction factor depending on the geometry. This factor is often dropped without any motivation at all or with the argument that the resulting error is of the same order of magnitude as the error in PFA itself.

In [7–9] the traditional PFA was extended in two ways; the correction factor in (6.32) was retained; the finite coat thickness of coated objects was taken into account. The effects of these extensions were demonstrated and comparisons were made to numerical results from more accurate calculations.

In next section we give a compact general result for the traditional PFA expression for the most common geometries.

### 6.2.1 General Expression for Half Spaces, Cylinders and Spheres

For solid objects in neglect of the geometrical correction in (6.32) one may find the following general expression for half spaces, cylinders and spheres [1, 10]:

$$E(z) = -\frac{\hbar}{32\pi^2 z^{(1+n/2)}} \Gamma(1+n/2) \left[ \frac{2\pi R_1 R_2}{R_1 + R_2} \right]^{1-n/2} \sum_{l=1}^{\infty} \frac{\langle \omega_l \rangle}{l^3}, \quad (6.33)$$

where  $n = 0$  for spheres,  $n = 1$  for cylinders, and  $n = 2$  for half spaces. The quantity  $\langle \omega_l \rangle$  was given in (5.136). If the objects are in vacuum we have

$$\langle \omega_l \rangle = \int_{-\infty}^{\infty} d\xi \left\{ \frac{[\tilde{\varepsilon}_1(i\xi) - 1][\tilde{\varepsilon}_2(i\xi) - 1]}{[\tilde{\varepsilon}_1(i\xi) + 1][\tilde{\varepsilon}_2(i\xi) + 1]} \right\}^l. \quad (6.34)$$

The result is for the interaction energy in case of spheres, the interaction energy per unit length for cylinders and the interaction energy per unit area for half spaces. The variable  $z$  is the closest distance between the objects. Thus, for two half spaces we have

$$E(z) = -\frac{\hbar}{32\pi^2 z^2} \sum_{l=1}^{\infty} \frac{\langle \omega_l \rangle}{l^3} = E_p(z), \quad (6.35)$$

for two cylinders of radii  $R_1$  and  $R_2$ ,

$$E(z) = -\frac{\hbar}{32\pi^2 z^{3/2}} \Gamma(3/2) \left[ \frac{2\pi R_1 R_2}{R_1 + R_2} \right]^{1/2} \sum_{l=1}^{\infty} \frac{\langle \omega_l \rangle}{l^3} = \Gamma(3/2) \sqrt{\frac{2\pi R_1 R_2 z}{R_1 + R_2}} E_p(z), \quad (6.36)$$

and for two spheres of radii  $R_1$  and  $R_2$  the result is

$$E(z) = -\frac{\hbar}{32\pi^2 z} \left[ \frac{2\pi R_1 R_2}{R_1 + R_2} \right] \sum_{l=1}^{\infty} \frac{\langle \omega_l \rangle}{l^3} = \left[ \frac{2\pi R_1 R_2 z}{R_1 + R_2} \right] E_p(z). \quad (6.37)$$

To get the result for a cylinder of radius  $R$  above a substrate we let  $R_2$  go to infinity and replace  $R_1$  with  $R$  in (6.36). This results in

$$E(z) = -\frac{\hbar}{32\pi^2 z^{3/2}} \Gamma(3/2) \sqrt{2\pi R} \sum_{l=1}^{\infty} \frac{\langle \omega_l \rangle}{l^3} = \Gamma(3/2) \sqrt{2\pi R z} E_p(z). \quad (6.38)$$

To get the result for a sphere of radius  $R$  above a substrate we let  $R_2$  go to infinity and replace  $R_1$  with  $R$  in (6.37). This results in

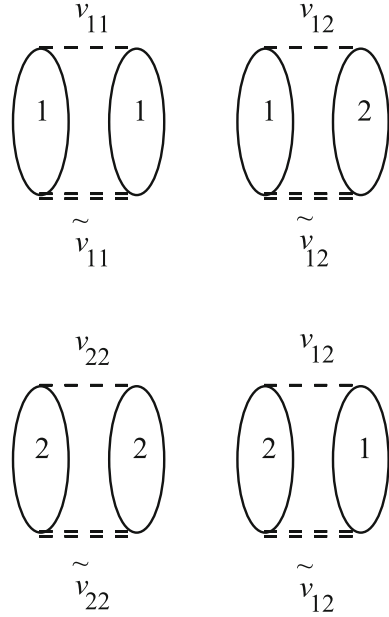
$$E(z) = -\frac{\hbar}{32\pi^2 z} 2\pi R \sum_{l=1}^{\infty} \frac{\langle \omega_l \rangle}{l^3} = 2\pi R z E_p(z). \quad (6.39)$$

Next, we have included two sections where we demonstrate that the dispersion interactions between objects is the correlation energy. The first is a non-retarded treatment of two parallel 2D metallic sheets. Here Coulomb interactions between the carriers give rise to the interaction. In the second fully retarded treatment also photons take part in the processes.

### 6.3 Many-Body Approach in Non-Retarded Treatment

Here we will discuss a specific geometry, viz. two parallel 2D sheets. For this system the derivation in the language of many-body theory becomes very simple, especially when retardation effects can be neglected. In the two-sheet system the interaction energy is nothing but the inter-sheet correlation energy [11]. In diagrammatic perturbation theory the Feynman diagrams representing the correlation energy are given in Fig. 6.2. To get the inter-sheet contribution we can either subtract the intra-sheet part or subtract the total result when the separation between the sheets goes to infinity (at that limit only the intra-sheet contribution remains). For simplicity we let the two sheets be identical. The treatment can easily be extended to different sheets. Each ellipse represents a polarization bubble (2.142),  $\chi(\mathbf{k}, \omega)$ , and the number inside an ellipse indicates in which sheet the process occurs. A dashed line

**Fig. 6.2** Feynman diagrams for the correlation energy in the two 2D sheet system. The ellipses represent polarization bubbles and the dashed lines the interactions; the double lines represent the screened interactions in (6.42). The numbers 1 and 2 refer to which sheet the carrier belongs to. Adapted from [11]. See [11] for details



denotes the Coulomb interaction and a double dashed line the interaction screened by the carriers in both sheets. Each of the four Feynman diagrams,  $FD_i$ ;  $i = 1, 2, 3, 4$ , represents an infinite series of diagrams. For identical sheets the contributions from the diagrams in the second row are equal to those from the diagrams in the first row. We can keep the first row diagrams and multiply the result with a factor of two. The interaction energy per unit area can now be written as [12]

$$E_c(d) = \hbar \int \frac{d^2k}{(2\pi)^2} \int_0^\infty \frac{d\xi}{2\pi} \int_0^1 \frac{d\lambda}{\lambda} 2 [FD_1(k, i\xi; \lambda) + FD_2(k, i\xi; \lambda)], \quad (6.40)$$

where  $d$  is the distance between the sheets,  $\lambda$  is the coupling constant and the factor of two has been inserted. The subscript  $c$  denotes correlation energy. Now, from Sect. 2.7.1 we have that  $v_{11} = v^{2D}(\mathbf{k}, \omega)$  and  $v_{12} = \exp(-kd) v^{2D}(\mathbf{k}, \omega)$ , respectively, where  $v^{2D}$  is the 2D Coulomb interaction,  $v^{2D}(\mathbf{r}) = e^2/r$ . Note that with identical sheets  $v_{22} = v_{11}$  and  $v_{21} = v_{12}$ . The exponential factor in the second potential is the result from taking the 2D Fourier transform of the Coulomb potential in a plane the distance  $d$  from the center of the potential, see (2.97). A double dashed interaction lines represents a series of terms, with zero, one, two ... number of polarization bubbles. This can be expressed as

$$\begin{aligned}
\tilde{v}_{11}(\mathbf{k}, \omega) &= v^{2D}(k) + v^{2D}(k) \chi(\mathbf{k}, \omega) \tilde{v}_{11}(\mathbf{k}, \omega) \\
&\quad + \exp(-kd) v^{2D}(k) \chi(\mathbf{k}, \omega) \tilde{v}_{12}(\mathbf{k}, \omega) \\
\tilde{v}_{12}(\mathbf{k}, \omega) &= \exp(-kd) v^{2D}(k) + v^{2D}(k) \chi(\mathbf{k}, \omega) \tilde{v}_{12}(\mathbf{k}, \omega) \\
&\quad + \exp(-kd) v^{2D}(k) \chi(\mathbf{k}, \omega) \tilde{v}_{11}(\mathbf{k}, \omega),
\end{aligned} \tag{6.41}$$

where we have closed the two infinite series. This system of equations can be solved and the result is

$$\begin{aligned}
\tilde{v}_{11}(\mathbf{k}, \omega) &= \frac{v^{2D}(k) [1 + \tilde{\alpha}(\mathbf{k}, \omega) (1 - \exp(-2kd))]}{[1 + \tilde{\alpha}(\mathbf{k}, \omega)]^2 - \exp(-2kd) \tilde{\alpha}^2(\mathbf{k}, \omega)}, \\
\tilde{v}_{12}(\mathbf{k}, \omega) &= \frac{v^{2D}(k) \exp(-kd)}{[1 + \tilde{\alpha}(\mathbf{k}, \omega)]^2 - \exp(-2kd) \tilde{\alpha}^2(\mathbf{k}, \omega)},
\end{aligned} \tag{6.42}$$

where we have used the relation  $\tilde{\alpha}(\mathbf{k}, \omega) = -v^{2D}(k) \chi(\mathbf{k}, \omega)$  in accordance with (2.142). When we interpret the Feynman diagrams in Fig. 6.2 we find that the square brackets in (6.40) are  $[\tilde{v}_{11}v_{11}\chi^2 + \tilde{v}_{12}v_{12}\chi^2 - (v^{2D}/\varepsilon)v^{2D}\chi^2]$ ; the last term comes from the subtraction of the intra-layer correlation energy. Everywhere there is a factor of  $e^2$  appearing explicitly or implicitly in the expression is multiplied by the coupling constant,  $\lambda$ . Performing the integration over coupling constant gives

$$E_c(d) = \hbar \int \frac{d^2k}{(2\pi)^2} \int_0^\infty \frac{d\xi}{2\pi} \ln \left\{ 1 - e^{-2kd} \left[ \frac{\tilde{\alpha}(k, i\xi)}{1 + \tilde{\alpha}(k, i\xi)} \right]^2 \right\}. \tag{6.43}$$

Here, we assumed that the two 2D sheets were identical. If they are not the result is

$$E_c(d) = \hbar \int \frac{d^2k}{(2\pi)^2} \int_0^\infty \frac{d\omega}{2\pi} \ln \left\{ 1 - e^{-2kd} \left[ \frac{\tilde{\alpha}_1(k, i\omega)}{1 + \tilde{\alpha}_1(k, i\omega)} \right] \left[ \frac{\tilde{\alpha}_2(k, i\omega)}{1 + \tilde{\alpha}_2(k, i\omega)} \right] \right\}. \tag{6.44}$$

This is the result from non-retarded diagrammatic perturbation theory within the random phase approximation (RPA). In next section we extend the derivation to a fully retarded treatment.

## 6.4 Many-Body Approach in Fully Retarded Treatment

We refrain from performing a detailed derivation here, we just scetch how this can be done. We follow the derivation in [11] and refer to that work for more details. We have chosen to work in Coulomb gauge (see Sect. 2.4). In this gauge one part of the interaction between the electrons is in the form of the instantaneous, longitudinal Coulomb interaction (scalar potential) and the other part is via transverse photons (vector potential). The Hamiltonian for the system is

$$H = \sum_i \frac{1}{2m^*} [\mathbf{p}_i - \frac{e_i}{c} \mathbf{A}(\mathbf{R}_i)]^2 + \frac{1}{2} \sum_{ij} \frac{e_i e_j}{R_{ij}} + \sum_{\mathbf{q}, \lambda} \hbar \omega_{\mathbf{q}} \left( a_{\mathbf{q}\lambda}^\dagger a_{\mathbf{q}\lambda} + 1/2 \right), \quad (6.45)$$

where the first term is the kinetic energy that contains the interactions via the vector potential,  $\mathbf{A}$ . The second term represents the scalar potential interaction and the last term is the free photon Hamiltonian. The operators  $a_{\mathbf{q}\lambda}^\dagger$  and  $a_{\mathbf{q}\lambda}$  are creation and annihilation, or destruction, operators, respectively, of photons of wave vector  $\mathbf{q}$  and polarization  $\lambda$  (note that this  $\lambda$  is not the coupling constant). The non-retarded results are obtained by letting the speed of light tend to infinity. From the Hamiltonian we see that this corresponds to neglecting the vector-potential interaction completely. Now, in the specific system we consider here, the electrons are only free to move in a plane (see Sect. 2.7). Only one longitudinal and one transverse electric field can exist in a plane; an electric field normal to the plane cannot lead to a current. It turns out that the longitudinal electric field and the  $p$ -polarized photons combine into one field that is longitudinal in the plane. The induced charge and current densities resulting from such a field will also produce a field that is longitudinal in the plane. The  $s$ -polarized photons produce an electric field that is transverse in the plane. The current induced by such a field results in a field that is transverse in the plane.

The two types of interaction involving longitudinal and transverse electric fields in the planes defined by the two sheets will not mix and the energy is given by a sum of two sets of diagrams of the type given in Fig. 6.2, one set for the longitudinal interaction and one containing only transverse interactions.

Let us first discuss the longitudinal interaction. The coupling to the longitudinal field and  $p$ -polarized photons is given by the scalar potential and the  $\mathbf{p} \cdot \mathbf{A}$  terms in the Hamiltonian. This results in the interaction energy per unit area

$$E_c^{l+p}(d) = \hbar \int \frac{d^2k}{(2\pi)^2} \int_0^\infty \frac{d\xi}{2\pi} \ln \left\{ 1 - e^{-2\gamma^{(0)}(k, i\xi)kd} \left[ \frac{\gamma^{(0)}(k, i\xi) \tilde{\alpha}_\parallel(k, i\xi)}{1 + \gamma^{(0)}(k, i\xi) \tilde{\alpha}_\parallel(k, i\xi)} \right]^2 \right\}, \quad (6.46)$$

where the superscript  $l + p$  indicates the contribution from interactions mediated by longitudinal Coulomb interactions and  $s$ -polarized photons. We see that in comparison with the non-retarded result in (6.43) the polarizability has attained a factor  $\gamma^{(0)}(k, i\omega)$  in front; this is in agreement with the polarizability obtained by Stern [13]. Furthermore, the factor appearing in the interlayer interactions is modified with the same factor in the exponent.

Now, the response to an  $s$ -polarized field is an induced transverse current. The response is determined by the transverse conductivity, which is dominated by the contribution originating from the  $\mathbf{A}^2$ -term in the Hamiltonian. Also the  $\mathbf{p} \cdot \mathbf{A}$  terms in the Hamiltonian give a contribution to the transverse conductivity, in the form of the current-current correlation function. This interaction results in the interaction energy per unit area

$$E_c^s(d) = \hbar \int \frac{d^2k}{(2\pi)^2} \int_0^\infty \frac{d\xi}{2\pi} \ln \left\{ 1 - e^{-2\gamma^{(0)}(k, i\xi)kd} \left[ \frac{-(\xi/c) \tilde{\alpha}_\perp(k, i\xi)}{\gamma^{(0)}(k, i\xi) + (\xi/c) \tilde{\alpha}_\perp(k, i\xi)} \right]^2 \right\}, \quad (6.47)$$

where the superscript  $s$  indicates the contribution from interactions mediated by  $s$ -polarized photons.

We have here shown that the van der Waals and dispersion interactions in the present formalism is, in the field of many-body theory, just the correlation energy and its extension. In next section we give a very brief compilation of other methods to find the interactions.

## 6.5 Brief Compilation of Methods or Approaches

Balian and co-Workers calculate Casimir energies by a *multiple-scattering expansion of the Green's function* [14–17]. Sophisticated *path-integral methods* [18–29] allows one to obtain Casimir forces to arbitrary precision by numerical computation. The *scattering approach* [30–32] is a good tool for describing the Casimir force in realistic experimental configurations taking surface roughness into account and also for calculating the lateral component of the force. All the above approaches are closely related. The relation between them is discussed in [33].

In simpler geometries where the interacting objects are spheres, ellipsoids or spheroids one may use simpler versions of the above [4, 7–9] methods, viz. *multipolar expansions*.

An alternative approach to calculate the Casimir interaction is to use the *Stress Tensor*. This was exploited on the Casimir set-up by Brown and Maclay [34] and later extended by González [35]. To solve problems when the objects are in a medium is more complicated due to the so-called Abraham-Minkowski controversy [36–38].

In the main treatment in this book the electromagnetic fields are classical fields and the quantum effects enter through the quantization of the normal modes. Another approach to dispersion forces is to handle them in *Quantum Electrodynamics (QED)* [11, 39] where the fields themselves are quantized.

The dispersion forces we treat in this book originates from electromagnetic interactions. Similar effects are expected to arise from all other types of basic interactions. These are then handled in *Quantum Field Theory (QFT)*. Sometimes a combination of derivations from different fields can be fruitful [40]. *The World-Line Approach* [41] to the Casimir effect is a string-inspired approach to quantum field theory and its numerical realization with Monte-Carlo techniques.

Interesting *Semiclassical Treatments* have been performed by Schaden and Spruch [42, 43]. The classical term in the thermal Casimir effect has been investigated with the Bohr-van Leeuwen theorem by Bimonte [44] in connection with a controversy regarding dissipation effects in metallic systems.

## References

1. D. Langbein, *Theory of van der Waals Attraction, In the Series Springer Tracts in Modern Physics* (Springer, New York, 1974)
2. H.C. Hamaker, *Physica* **IV**, 1058 (1937)
3. D.J. Mitchel, B.W. Ninham, P. Richmond, *Biophys. J.* **13**, 359 (1973)
4. C. Noguez, C.E. Román-Velázquez, R. Esquivel-Sirvent, C. Villarreal, *Europhys. Lett.* **67**, 191 (2004)
5. B. Derjaguin, *Z. Kolloid* **69**, 155 (1934)
6. A. Rodriguez, M. Ibanescu, D. Iannuzzi, F. Capasso, J.D. Joannopoulos, S.G. Johnson, *Phys. Rev. Lett.* **99**, 080401 (2007)
7. Bo E. Sernelius, C.E. Román-Velázquez, J., *Phys. Conf. Ser.* **161**, 012016 (2009)
8. Bo E. Sernelius, C.E., Román-Velázquez. *Phys. Rev. B* **78**, 032111 (2008)
9. C.E. Román-Velázquez, Bo E. Sernelius, *Phys. A: Math. Theor.* **41**, 164008 (2008)
10. Bo E. Sernelius, *Surface Modes in Physics* (Wiley-VCH, Berlin, 2001)
11. Bo E. Sernelius, P. Björk. *Phys. Rev. B* **57**, 6592 (1998)
12. Bo E. Sernelius, *Int. J. Mod. Phys. Conf. Ser.* **14**, 531 (2012)
13. F. Stern, *Phys. Rev. Lett.* **18**, 546 (1967)
14. R.B. Balian, C. Bloch, *Ann. Phys. (NY)* **60**, 401 (1970)
15. R.B. Balian, C. Bloch, *Ann. Phys. (NY)* **85**, 514 (1974)
16. R. Balian, B. Duplantier, *Ann. Phys.* **104**, 300 (1977)
17. R. Balian, B. Duplantier, *Ann. Phys.* **112**, 165 (1978)
18. C. Schubert, *Phys. Rep.* **355**, 73 (2002)
19. H. Gies, K. Langfeld, *Int. J. Mod. Phys. A* **17**, 966 (2002)
20. H. Gies, K. Klingmüller, *Phys. Rev. Lett.* **96**, 220401 (2006)
21. H. Gies, K. Klingmüller, *Phys. Rev. Lett.* **97**, 220405 (2006)
22. N. Graham, A. Shpunt, T. Emig, S.J. Rahi, R.L. Jaffe, M. Kardar, *Phys. Rev. D* **81**, 061701 (2010)
23. T. Emig, A. Hanke, R. Golestanian, M. Kardar, *Phys. Rev. Lett.* **87**, 260402 (2001)
24. R. Büscher, T. Emig, *Phys. Rev. Lett.* **94**, 133901 (2005)
25. T. Emig, N. Graham, R.L. Jaffe, M. Kardar, *Phys. Rev. Lett.* **99**, 170403 (2007)
26. O. Kenneth, I. Klich, *Phys. Rev. Lett.* **97**, 160401 (2006)
27. O. Kenneth, I. Klich, *Phys. Rev. B* **78**, 014103 (2008)
28. M. Bordag, *Phys. Rev. D* **73**, 125018 (2006)
29. M. Bordag, *Phys. Rev. D* **75**, 065003 (2007)
30. A. Lambrecht, P.A.M. Neto, S. Reynaud, *New J. Phys.* **8**(10), 243 (2006)
31. P.A.M. Neto, A. Lambrecht, S. Reynaud, *Phys. Rev. A* **72**(1), 012115 (2005)
32. G.L. Ingold, A. Lambrecht, *Am. J. Phys.* **83**(2), 156 (2015)
33. K.A. Milton, J. Wagner, *J. Phys. A* **41**, 155402 (2008)
34. L.S. Brown, G.J. Maclay, *Phys. Rev.* **184**, 1272 (1969)
35. A.E. González, *Physica* **131A**, 228 (1985)
36. I. Brevik, *Phys. Rep.* **52**, 133 (1979)
37. I. Brevik, *Phys. Lett.* **88A**, 335 (1982)
38. R.N.C. Pfeifer, T.A. Nieminen, N.R. Heckenberg, *Rev. Mod. Phys.* **79**, 1197 (2007)
39. S.Y. Buhmann, *Dispersion Forces I: Macroscopic Quantum Electrodynamics and Ground-State Casimir, Casimir-Polder and van der Waals forces in Springer Tracts in Modern Physics 247* (Springer-Verlag, Berlin, Heidelberg, 2012)
40. G.L. Klimchitskaya, V.M. Mostepanenko, Bo E. Sernelius, *Phys. Rev. B* **89**, 125407 (2014)
41. L. Moyaerts, K. Langfeld, H. Gies, in *Proceedings of 6th workshop on Quantum Field Theory Under the Influence of External Conditions* held at University of Oklahoma, 15–19 Sept 2003, ed. by K.A. Milton (Rinton Press Princeton, 2004) . [arXiv:hep-th/0311168](https://arxiv.org/abs/hep-th/0311168)
42. M. Schaden, L. Spruch, *Phys. Rev. A* **58**, 935 (1998)
43. M. Schaden, *Phys. Rev. A* **82**, 022113 (2010)
44. G. Bimonte, *Phys. Rev. A* **79**, 042107 (2009)

# Chapter 7

## General Method to Find the Normal Modes in Layered Structures



**Abstract** A general scheme for finding the electromagnetic normal modes in a large class of layered structures is being laid out. In the non-retarded formalism it can be used for 13 geometries and in the fully retarded formalism for 11. This chapter is the foundation on which Part II and III are resting.

### 7.1 The Scheme

In this chapter we introduce our general method to find the electromagnetic normal modes in a layered structure. We first discussed this in [1] and here we follow rather closely that presentation. Later on in Part II and III we adapt the method to planar, spherical and circular cylindrical structures in the non-retarded and fully retarded, respectively, formalisms.

The retarded version of the formalism is based on solutions to the Helmholtz differential equation, or wave equation, which in the non-retarded version coincides with the Laplace equation. The Helmholtz differential equation can be solved by separation of variables in 11 coordinate systems. These are cartesian, confocal ellipsoidal, confocal paraboloidal, conical, cylindrical, elliptic cylindrical, oblate spheroidal, paraboloidal, parabolic cylindrical, prolate spheroidal, and spherical coordinates. Laplace's equation is separable in two additional coordinate systems, viz., the bispherical and toroidal coordinate systems.

For a given layered system the procedure is to choose a coordinate system where the interfaces separating the layers are best represented by the surfaces where one of the variables, defining the coordinate system, has a constant value. Different interfaces correspond to different constant values. Just to give some examples: the parabolic cylindrical coordinates can be used in the case of an edge with rounded off corner or for a wedge; the paraboloidal coordinates are well suited for a needle, a paraboloid of revolution. Let us now turn to the general procedure.

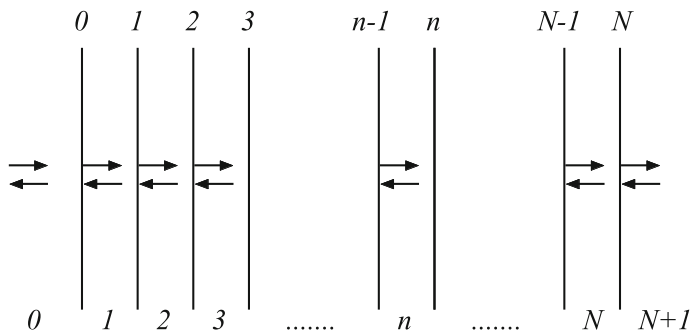


**Fig. 7.1** Schematic illustration of the layered structure. The numbering of the  $N + 2$  media are indicated at the bottom of the figure and the numbering of the  $N + 1$  interfaces at the top. In the general solution of Maxwell's equations there are one wave moving toward the right and one toward the left inside each medium. If a normal mode is excited there is no wave moving to the right in medium 0 which is the ambient medium; if the medium number  $N + 1$  is unlimited there is no wave moving to the left in that medium. See the text for more details. Adapted from [1]

Let the structure we study have  $N$  layers. A layer is a region bounded by two interfaces. In the system there are two more regions, each with just one boundary, a boundary in common with one of the layers. Of these two we choose the ambient to be the neighbor to layer number 1. Thus, there are  $N$  layers,  $N + 1$  interfaces and  $N + 2$  media. This is illustrated in Fig. 7.1. The layers are numbered from 1 to  $N$ , the media from 0 to  $N + 1$  and the interfaces from 0 to  $N$ . This means that layer number  $n$  is filled with medium number  $n$  and interface number  $n$  is the interface to the right of layer number  $n$ . In the general solution of Maxwell's equations there are one wave moving toward the right and one toward the left inside each medium. If a normal mode is excited there is no wave moving to the right in medium 0 which is the ambient medium; if the medium number  $N + 1$  is unlimited there is no wave moving to the left in that medium. We have here somewhat extended the concept of moving. When we say that a wave moves in a direction it either really moves or its amplitude decreases in that direction. In the retarded treatment there are transverse electric (TE) and transverse magnetic (TM) modes. In the planar and spherical geometries these are not mixed when crossing an interface. Then we may solve for these mode types separately. In other geometries like the circular cylindrical they do mix. Then we will have two modes, one TE and one TM, moving toward the right and two moving toward the left in each medium.

Let us start with the general procedure when the TE- and TM-modes do not mix. We denote the variable that is constant on each interface by  $x$ . Then in a general medium  $n$  we have the wave  $a^n R(x) + b^n L(x)$ . The boundary conditions at each interface are the standard ones that the tangential components of  $\mathbf{E}$  and  $\mathbf{H}$  and the normal components of  $\mathbf{D}$  and  $\mathbf{B}$  are continuous across the interface. Only two are needed; the other two lead to redundant results. Making use of the boundary conditions at interface  $n$  gives rise to two equations, one for each boundary condition. The left-hand side of each equation is a linear combination of  $a^n$  and  $b^n$ , where the

coefficients depend on the dielectric function and magnetic permeability of medium  $n$ . The right-hand side of the same equation is a linear combination of  $a^{n+1}$  and  $b^{n+1}$ , where the coefficients are formally the same as on the left-hand side but now depend on the dielectric function and magnetic permeability of medium  $n + 1$ . These two equations can be expressed on matrix form as

$$\tilde{\mathbf{A}}_n(x_n) \cdot \begin{pmatrix} a^n \\ b^n \end{pmatrix} = \tilde{\mathbf{A}}_{n+1}(x_n) \cdot \begin{pmatrix} a^{n+1} \\ b^{n+1} \end{pmatrix}, \quad (7.1)$$

where  $\tilde{\mathbf{A}}_n$  is a  $2 \times 2$  matrix, that depends on the dielectric function and magnetic permeability in medium  $n$ . Operating from the left with the inverse of this matrix gives

$$\begin{pmatrix} a^n \\ b^n \end{pmatrix} = \tilde{\mathbf{M}}_n \cdot \begin{pmatrix} a^{n+1} \\ b^{n+1} \end{pmatrix}, \quad (7.2)$$

where

$$\tilde{\mathbf{M}}_n = \tilde{\mathbf{A}}_n^{-1}(x_n) \cdot \tilde{\mathbf{A}}_{n+1}(x_n). \quad (7.3)$$

We may now find a relation between the coefficients in the left-most and right-most media

$$\begin{pmatrix} a^0 \\ b^0 \end{pmatrix} = \tilde{\mathbf{M}} \cdot \begin{pmatrix} a^{N+1} \\ b^{N+1} \end{pmatrix}, \quad (7.4)$$

where

$$\tilde{\mathbf{M}} = \tilde{\mathbf{M}}_0 \cdot \tilde{\mathbf{M}}_1 \cdots \tilde{\mathbf{M}}_N = \begin{pmatrix} M_{11} & M_{12} \\ M_{21} & M_{22} \end{pmatrix}. \quad (7.5)$$

Now, we want to find the relation between  $a^0$  and  $b^0$ . This relation depends on the boundary conditions at the outermost interfaces in Fig. 7.1. In order to have self-sustained fields or normal modes we must not have any incoming fields from outside the object. In all cases this means that  $a^0 = 0$ . In the planar case also the rightmost interface is the boundary to the outside which means that  $b^{N+1} = 0$ . In the spherical and cylindrical cases the rightmost region is the core and the boundary condition is that the waves are finite. What effect this has on the amplitudes of the waves depends on the choice of functions we make. In our non-retarded treatment it turns out that also for spherical and cylindrical objects  $b^{N+1} = 0$ . This leads to  $a^0 = b^0 (M_{11}/M_{21})$ . In our retarded treatment on the other hand  $b^{N+1} = a^{N+1}$  follows from the condition of finite fields. This leads to  $a^0 = b^0 [(M_{11} + M_{12}) / (M_{21} + M_{22})]$ . The only way we can have a non-zero  $b^0$  at the same time as  $a^0$  vanishes is that the factor multiplying  $b^0$  vanishes. Thus the function  $f(\omega)$  in the mode condition is

$$\begin{aligned} f(\omega) &= M_{11}, \quad b^{N+1} = 0, \\ f(\omega) &= M_{11} + M_{12}, \quad b^{N+1} = a^{N+1}. \end{aligned} \quad (7.6)$$

Let us now continue with the general procedure when the TE- and TM-modes do mix. Then in a general medium  $n$  we have the wave  $a_1^n R_1(x) + b_1^n L_1(x) + a_2^n R_2(x) + b_2^n L_2(x)$ , where the subscript 1 and 2 refers to TM- and TE-waves, respectively. Making use of the boundary conditions at interface  $n$  gives

$$\tilde{\mathbf{A}}_n(x_n) \cdot \begin{pmatrix} a_1^n \\ b_1^n \\ a_2^n \\ b_2^n \end{pmatrix} = \tilde{\mathbf{A}}_{n+1}(x_n) \cdot \begin{pmatrix} a_1^{n+1} \\ b_1^{n+1} \\ a_2^{n+1} \\ b_2^{n+1} \end{pmatrix}, \quad (7.7)$$

where  $\tilde{\mathbf{A}}_n$  is now a  $4 \times 4$  matrix, that depends on the dielectric function and magnetic permeability in medium  $n$ . Operating from the left with the inverse of this matrix gives

$$\begin{pmatrix} a_1^n \\ b_1^n \\ a_2^n \\ b_2^n \end{pmatrix} = \tilde{\mathbf{M}}_n \cdot \begin{pmatrix} a_1^{n+1} \\ b_1^{n+1} \\ a_2^{n+1} \\ b_2^{n+1} \end{pmatrix}, \quad (7.8)$$

where

$$\tilde{\mathbf{M}}_n = \tilde{\mathbf{A}}_n^{-1}(x_n) \cdot \tilde{\mathbf{A}}_{n+1}(x_n). \quad (7.9)$$

We may now find a relation between the coefficients in left-most and right-most media

$$\begin{pmatrix} a_1^0 \\ b_1^0 \\ a_2^0 \\ b_2^0 \end{pmatrix} = \tilde{\mathbf{M}} \cdot \begin{pmatrix} a_1^{N+1} \\ b_1^{N+1} \\ a_2^{N+1} \\ b_2^{N+1} \end{pmatrix}, \quad (7.10)$$

where

$$\tilde{\mathbf{M}} = \tilde{\mathbf{M}}_0 \cdot \tilde{\mathbf{M}}_1 \cdots \tilde{\mathbf{M}}_N = \begin{pmatrix} M_{11} & M_{12} & M_{13} & M_{14} \\ M_{21} & M_{22} & M_{23} & M_{24} \\ M_{31} & M_{32} & M_{33} & M_{34} \\ M_{41} & M_{42} & M_{43} & M_{44} \end{pmatrix}. \quad (7.11)$$

Now we want to find the relation between  $\begin{pmatrix} a_1^0 \\ a_2^0 \end{pmatrix}$  and  $\begin{pmatrix} b_1^0 \\ b_2^0 \end{pmatrix}$ . This relation depends on if  $b_i^{N+1} = 0$  or not. If it is, like in the planar case and in the non-retarded spherical and cylindrical cases, then

$$\begin{pmatrix} a_1^0 \\ a_2^0 \end{pmatrix} = \begin{pmatrix} M_{11} & M_{13} \\ M_{31} & M_{33} \end{pmatrix} \cdot \begin{pmatrix} M_{21} & M_{23} \\ M_{41} & M_{43} \end{pmatrix}^{-1} \cdot \begin{pmatrix} b_1^0 \\ b_2^0 \end{pmatrix}. \quad (7.12)$$

If  $b_i^{N+1} = a_i^{N+1}$ , like in the retarded spherical and cylindrical cases then

$$\begin{pmatrix} a_1^0 \\ a_2^0 \end{pmatrix} = \begin{pmatrix} (M_{11} + M_{12}) (M_{13} + M_{14}) \\ (M_{31} + M_{32}) (M_{33} + M_{34}) \end{pmatrix}^{-1} \cdot \begin{pmatrix} b_1^0 \\ b_2^0 \end{pmatrix}. \quad (7.13)$$

In order to have self-sustained fields or normal modes we must not have any incoming fields from outside the object, i.e.,  $a_1^0$  and  $a_2^0$  must be zero. The only way we can have a non-zero  $b_1^0$  and/or  $b_2^0$  at the same time as  $a_1^0$  and  $a_2^0$  vanish is that the determinant of the matrix in front of  $\begin{pmatrix} b_1^0 \\ b_2^0 \end{pmatrix}$  vanishes. Thus, the condition for modes is

$$\begin{vmatrix} M_{11} & M_{13} \\ M_{31} & M_{33} \end{vmatrix} = 0, \quad (7.14)$$

if  $b_i^{N+1} = 0$  and

$$\begin{vmatrix} (M_{11} + M_{12}) (M_{13} + M_{14}) \\ (M_{31} + M_{32}) (M_{33} + M_{34}) \end{vmatrix} = 0, \quad (7.15)$$

if  $b_i^{N+1} = a_i^{N+1}$ .

Now we will describe how the waves we have discussed are obtained. We treat metals and dielectrics on the same footing, i.e., induced current and charge densities have contributions from both bound electrons and conduction electrons. The dielectric function for a metallic system is (2.22)

$$\tilde{\varepsilon}(\omega) = \varepsilon(\omega) + 4\pi i\sigma(\omega)/\omega, \quad (7.16)$$

where  $\varepsilon(\omega)$  would be the dielectric function if it were not for the conduction carriers. These contribute to the screening through the dynamical conductivity,  $\sigma(\omega)$ . With this choice the Maxwell's equations (ME) read (2.4)

$$\begin{aligned} \nabla \cdot \tilde{\mathbf{D}} &= 4\pi \rho_{ext} \\ \nabla \cdot \mathbf{B} &= 0 \\ \nabla \times \mathbf{E} &= -\frac{1}{c} \frac{\partial \mathbf{B}}{\partial t} \\ \nabla \times \tilde{\mathbf{H}} &= \frac{4\pi}{c} \mathbf{J}_{ext} + \frac{1}{c} \frac{\partial \tilde{\mathbf{D}}}{\partial t}. \end{aligned} \quad (7.17)$$

The external charge and current densities are absent in our system. Furthermore since we are concerned with normal modes the time dependence of each field is given by a factor  $\exp(-i\omega t)$  and we have

$$\begin{aligned} \nabla \cdot \tilde{\mathbf{D}} &= 0 \\ \nabla \cdot \mathbf{B} &= 0 \\ \nabla \times \mathbf{E} &= i(\omega/c) \mathbf{B} \\ \nabla \times \tilde{\mathbf{H}} &= -i(\omega/c) \tilde{\mathbf{D}}. \end{aligned} \quad (7.18)$$

We assume non-magnetic materials but try to be as general as possible and keep  $\tilde{\mu} \neq 1$ , where  $\tilde{\mu}$  is the magnetic permeability; we are not interested in longitudinal bulk modes and assume that  $\tilde{\varepsilon}(\omega) \neq 0$  and  $\tilde{\mu}(\omega) \neq 0$ . We want to keep one electric and one magnetic field. Since the  $\mathbf{E}$ - and  $\tilde{\mathbf{H}}$ -fields have the same boundary conditions at an interface we keep these. Thus we have

$$\begin{aligned}\nabla \cdot \mathbf{E} &= 0 \\ \nabla \cdot \tilde{\mathbf{H}} &= 0 \\ \nabla \times \mathbf{E} &= i\tilde{\mu}(\omega) (\omega/c) \tilde{\mathbf{H}} \\ \nabla \times \tilde{\mathbf{H}} &= -i\tilde{\varepsilon}(\omega) (\omega/c) \mathbf{E}.\end{aligned}\tag{7.19}$$

Neglecting retardation means letting the speed of light go to infinity. Then the MEs reduce to

$$\begin{aligned}\nabla \cdot \mathbf{E} &= 0, \\ \nabla \cdot \tilde{\mathbf{H}} &= 0, \\ \nabla \times \mathbf{E} &= \mathbf{0}, \\ \nabla \times \tilde{\mathbf{H}} &= \mathbf{0}.\end{aligned}\tag{7.20}$$

Equations(7.19) and (7.20) are the basic equations we are starting from in all structures, (7.19) in the fully retarded calculations and (7.20) when retardation is neglected.

In the non-retarded treatment, since  $\nabla \times \mathbf{E} = 0$  the  $\mathbf{E}$ -field is conservative and we may define a scalar potential,  $\Phi$  such that  $\mathbf{E} = -\nabla\Phi$ . Using the first line of (7.20) then leads to Laplace's equation,

$$\nabla^2\Phi = 0.\tag{7.21}$$

So, when we neglect retardation effects we just solve Laplace's equation in each medium and use the proper boundary conditions at each interface to find the normal modes.<sup>1</sup>

In the fully retarded treatment we take the curl of the last two lines of (7.19) and make use of the other relations to find

$$\begin{aligned}\nabla^2\mathbf{E} + [\tilde{n}(\omega) \omega/c]^2\mathbf{E} &= 0 \\ \nabla^2\tilde{\mathbf{H}} + [\tilde{n}(\omega) \omega/c]^2\tilde{\mathbf{H}} &= 0.\end{aligned}\tag{7.22}$$

Thus both the  $\mathbf{E}$ - and  $\tilde{\mathbf{H}}$ -fields obey the vector wave equation, the vector Helmholtz equation. In the planar case it is straight forward to solve these in each region but in other geometries it is not a trivial task. One can solve the problem by introducing Hertz-Debye potentials  $\pi_1$  and  $\pi_2$ . They are solutions to the scalar wave equation,

---

<sup>1</sup>A word of caution is in place here: When using the boundary conditions for potentials, spurious modes may result[2]. One should keep in mind that the potentials are just auxiliary functions introduced to simplify the treatment; the real functions are the electromagnetic fields.

$$\nabla^2 \pi' + q^2 \pi' = 0; \quad \pi = \pi' e^{-i\omega t}; \quad q^2 = [\tilde{n}(\omega) \omega/c]^2. \quad (7.23)$$

We let  $\pi_1$  be the potential that generates TM modes and  $\pi_2$  be the potential that generates TE modes.

Now we are done with the general formalism. We will make use of this when we treat planar, spherical and cylindrical geometries in Part II and Part III.

## References

1. Bo E. Sernelius, *Phys. Rev. B* **90**, 155457 (2014)
2. Bo E. Sernelius, *Surface Modes in Physics* (Wiley, Berlin, 2001)

**Part II**  
**Non-Retarded Formalism:**  
**van der Waals**

Johan Diderik van der Waals (1837–1923) graduated on his thesis: *On the continuity of the gaseous and liquid states*, in 1873. He found deviations for real gases to the ideal gas equation of state. He found empirically  $(p + a/V^2)(V - b) = Nk_B T$  instead of the ideal equation:  $pV = Nk_B T$ . The correction constant  $b$  is due to the fact that the gas atoms take up a finite fraction of the volume, thus reducing the free volume. The factor  $a$ , which is of interest here, is due to the attractive force between the atoms, reducing the pressure exerted on the walls of the container. He was awarded the Nobel Prize in 1910 for this and similar work on the equations of state for gases and fluids. Van der Waals' force was found on empirical grounds.

The most surprising result was that there is an attractive force even between closed-shell atoms, where the charge distribution is spherically symmetric. One would imagine that two spherically symmetric, neutral atoms would not interact as they were so far apart that their electron wave functions were not overlapping. Still, there is a force. This remained a mystery for a long time. In 1930, Fritz Wolfgang London (1900–1954) gave a realistic explanation for this force in terms of fluctuating dipoles.

This interaction can be generalized from the microscopic system of individual atoms to mesoscopic and macroscopic geometries. The force between larger objects is due to fluctuations in the charge and current densities in the objects. The force is still called the van der Waals force.

For very large separations, the force is modified due to retardation effects, effect of the finite speed of light. These effects are treated in Part III. Here, we neglect retardation effects and use a non-retarded formalism. In the non-retarded formalism, one lets  $(\omega/cq)$  go to zero. This corresponds to omitting the terms in MEs containing time derivatives of the fields. Then, Maxwell's equations (2.4) simplify into  $\nabla \cdot \mathbf{D} = 4\pi \rho_{\text{ext}}$ ,  $\nabla \cdot \mathbf{B} = 0$ ,  $\nabla \times \mathbf{E} = \mathbf{0}$ , and  $\nabla \times \mathbf{H} = (4\pi/c) \mathbf{J}_{\text{ext}}$ . The coupling between the electric and magnetic fields is lifted. There are no longer any transverse bulk modes; there are no vacuum modes; there are longitudinal bulk modes and surface modes. The interaction between objects is fully determined by the overlapping surface modes.

Even though this is a very drastic approximation that has profound effects on the electromagnetic normal modes, in an overwhelming majority of situations, the non-retarded formalism produces good enough results for the interactions. We saw in Sect. 5.3.2.2 that the contribution from the transverse modes to the exchange and correlation energy in metals were completely negligible. Retardation effects on the interaction between two objects often appear only for very large separations.

This fact and that the formalism are so much simplified motivated us to devote a separate part to the non-retarded formalism.

# Chapter 8

## Van der Waals Force



**Abstract** We derive the equation of state for an ideal gas in 3D,  $pV = Nk_B T$ , and in 2D,  $\pi A = Nk_B T$ . We then show how these gas laws are modified for a real gas and derive the result found by van der Waals for 3D,  $(p + a/V^2)(V - b) = Nk_B T$ . We also derive the 2D version,  $(\pi + a/A^2)(A - b) = Nk_B T$ . The correction constant  $b$  is due to the fact that the gas atoms take up a finite fraction of the volume, thus reducing the free volume. The factor  $a$ , which is of interest here, is due to the attractive force between the atoms, reducing the pressure exerted on the walls of the container. We derive the result for an attractive potential between the atoms of a general power law form. We end by deriving the van der Waals interaction-potential between two atoms, both at zero temperature and at finite temperature. We give numerical results for alkali-metal dimers.

### 8.1 Equation of State for Ideal Gas

An ideal gas is a system consisting of a low concentration of non-interacting atoms or molecules each of zero spatial extent. These point particles are in thermal equilibrium and the only energy contribution is the kinetic energy of the individual particles. The variables that characterize a gas are three extensive,<sup>1</sup>  $N$ ,  $V$ , and  $S$ , and three intensive,  $p$ ,  $T$ , and  $\mu$ . For an ideal gas we let the temperature,  $T$ , and number of gas molecules,  $N$ , be constant. The volume,  $V$ , can vary. We will derive the equation of state, or ideal gas law,

$$pV = \frac{N}{\beta} = Nk_B T, \tag{8.1}$$

where  $k_B$  is the Boltzmann constant and  $\beta = 1/k_B T$ .

The equation of state is a relation between four state variables out of the possible eight that we discussed in Chap. 4. There are three independent variables and one dependent. The suitable state function to work with is one where its three independent

---

<sup>1</sup>An extensive variable scales with the size of the system, while an intensive does not.

variables are among these four. There are two choices, the Gibbs free energy<sup>2</sup> in (4.16),  $G(p, N, T)$ , and the Helmholtz free energy in (4.15),  $\mathfrak{F}(V, T, N)$ . The best choice is  $G$  since it consists of one term only,  $G = \mu N$ . The fourth variable we get from

$$V = \left( \frac{\partial G}{\partial p} \right)_{T,N} = \left( \frac{\partial \mu N}{\partial p} \right)_{T,N} = N \left( \frac{\partial \mu}{\partial p} \right)_{T,N} \quad (8.2)$$

The chemical potential is set by equating the number of gas molecules,  $N$ , with the summation over all states weighed by the Boltzmann distribution function (4.26),  $n_B(k)$ ,

$$\begin{aligned} N &= \sum_{\mathbf{k}} n_B(k) = V \int \frac{d^3k}{(2\pi)^3} n_B(k) \\ &= V \int_0^\infty dk \frac{4\pi k^2}{(2\pi)^3} \exp \left[ -\beta \left( \frac{\hbar^2 k^2}{2m} - \mu \right) \right] \\ &= \frac{V}{2\pi^2} \exp(\beta\mu) \int_0^\infty dk k^2 \exp \left[ -\beta \left( \frac{\hbar^2 k^2}{2m} \right) \right] \\ &= \frac{V}{2\pi^2} \exp(\beta\mu) \left[ \sqrt{\frac{\hbar^2 \beta}{2m}} \right]^{-3} \underbrace{\int_0^\infty dk k^2 \exp[-k^2]}_{\frac{\sqrt{\pi}}{4}}, \end{aligned} \quad (8.3)$$

with the result

$$\mu = \frac{1}{\beta} \ln(n\lambda_T^3), \quad (8.4)$$

where  $\lambda_T = \sqrt{2\pi\hbar^2\beta/m}$  is the so-called thermal wave length and  $n = N/V$  is the particle density.

Now

$$\begin{aligned} p &= \int_0^n dn \left[ \frac{\partial p}{\partial n} \right]_{NT} = \int_0^n dn \left[ \frac{\partial p}{\partial \mu} \right]_{NT} \left[ \frac{\partial \mu}{\partial n} \right]_{NT} \\ &= \int_0^n dn \underbrace{\left[ \frac{\partial \mu}{\partial n} \right]_{NT}}_{1/(\beta n)} / \underbrace{\left[ \frac{\partial \mu}{\partial p} \right]_{NT}}_{1/n} = \int_0^n dn \frac{1}{\beta} = \frac{n}{\beta} = \frac{N}{V} k_B T, \end{aligned} \quad (8.5)$$

or

$$pV = Nk_B T, \quad (8.6)$$

and the derivation is complete.

<sup>2</sup>IUPAC recommended name: Gibbs energy or Gibbs function.

### 8.1.1 2D Version

We proceed in analogy to Sect. 8.1. We base the derivation on the 2D version of Gibbs free energy,  $G(\pi, N, T)$ , where  $\pi$  is the 2D pressure, the force per unit length. The volume in 3D is here replaced by the area  $A$ . We have

$$A = \left( \frac{\partial G}{\partial \pi} \right)_{T,N} = \left( \frac{\partial \mu N}{\partial \pi} \right)_{T,N} = N \left( \frac{\partial \mu}{\partial \pi} \right)_{T,N}, \quad (8.7)$$

and the chemical potential,  $\mu$ , is obtained from

$$\begin{aligned} N &= \sum_{\mathbf{k}} n_B(\mathbf{k}) = A \int \frac{d^2k}{(2\pi)^2} n_B(\mathbf{k}) \\ &= A \int_0^\infty dk \frac{2\pi k}{(2\pi)^2} \exp \left[ -\beta \left( \frac{\hbar^2 k^2}{2m} - \mu \right) \right] \\ &= \frac{A}{2\pi} \exp(\beta\mu) \int_0^\infty dk k \exp \left[ -\beta \left( \frac{\hbar^2 k^2}{2m} \right) \right] \\ &= \frac{A}{2\pi} \exp(\beta\mu) \underbrace{\int_0^\infty dk k \exp[-k^2]}_{\frac{1}{2}} \\ &= A \exp(\beta\mu) \frac{m}{2\pi \hbar^2 \beta} = \frac{A \exp(\beta\mu)}{\lambda_T^2}. \end{aligned} \quad (8.8)$$

We extract  $\mu$  and find

$$\mu = \frac{1}{\beta} \ln(n^{2D} \lambda_T^2). \quad (8.9)$$

Calculation of the pressure,

$$\begin{aligned} \pi &= \int_0^{n^{2D}} dn^{2D} \left[ \frac{\partial \pi}{\partial n^{2D}} \right]_{NT} = \int_0^{n^{2D}} dn^{2D} \left[ \frac{\partial \pi}{\partial \mu} \right]_{NT} \left[ \frac{\partial \mu}{\partial n^{2D}} \right]_{NT} \\ &= \int_0^{n^{2D}} dn^{2D} \underbrace{\left[ \frac{\partial \mu}{\partial n^{2D}} \right]_{NT}}_{\frac{1}{\beta} \left( \frac{1}{n^{2D}} \right)} / \underbrace{\left[ \frac{\partial \mu}{\partial \pi} \right]_{NT}}_{1/n^{2D}} \\ &= \int_0^{n^{2D}} dn^{2D} \frac{1}{\beta} = \frac{n^{2D}}{\beta}, \end{aligned} \quad (8.10)$$

leads to the equation of state,

$$\pi A = N k_B T. \quad (8.11)$$

## 8.2 Equation of State for Non-ideal Gas

We now treat the gas more realistically. We let the atoms<sup>3</sup> have a finite radius,  $r_0$ , and an attractive interaction. We will see in Sect. 8.3 that the van der Waals interaction potential (energy) between two atoms is of the form,  $V = -Br^{-\gamma}$ , where  $B$  is a constant characteristic of the atoms and  $\gamma = 6$ .

The finite radius leads to a smaller free volume in which the atoms can move,

$$\tilde{V} = V - N4\pi d_0^3/3 = V (1 - n4\pi d_0^3/3) = V (1 - Cn), \quad (8.12)$$

where  $d_0$  is the atomic diameter. We have subtracted the volume taken up by the atoms themselves.<sup>4</sup>

The interaction between the atoms leads to an energy shift for each atom. For a gas one may sum over pair interactions,

$$\begin{aligned} \Delta E &= \int_{d_0}^{\infty} dr 4\pi r^2 n (-Br^{-\gamma}) \\ &= \frac{4\pi Bn}{(\gamma-3)d_0^{\gamma-3}} = -Dn \end{aligned} \quad (8.13)$$

We have introduced the constants  $C$  and  $D$  to make the derivation that follows more transparent. We will now determine the chemical potential for the gas and from this obtain the equation of state. The chemical potential is determined from the relation

$$\begin{aligned} N &= \sum_{\mathbf{k}} n_B(\mathbf{k}) = \tilde{V} \int \frac{d^3k}{(2\pi)^3} n_B(\mathbf{k}) \\ &= \tilde{V} \int_0^{\infty} dk \frac{4\pi k^2}{(2\pi)^3} \exp \left[ -\beta \left( \frac{\hbar^2 k^2}{2m} + \Delta E - \mu \right) \right], \end{aligned} \quad (8.14)$$

where on the right-hand side we have summed over all states weighted by the Boltzmann distribution function (4.26). The above equation can be rewritten as

$$\frac{n}{1 - Cn} = \frac{1}{2\pi^2} \exp[-\beta(\Delta E - \mu)] \int_0^{\infty} dk k^2 \exp \left( -\beta \frac{\hbar^2 k^2}{2m} \right), \quad (8.15)$$

and rearrangement gives

<sup>3</sup>We have here assumed that the gas consists of separate atoms. The treatment is still valid for molecular gases. In that case read molecule instead of atom.

<sup>4</sup>Note that an atom can not come closer to another than the atom diameter. This means that a spherical volume of radius  $d_0$  centered around each atom is excluded from the free volume in which other atoms can move.

$$\begin{aligned} \frac{2\pi^2 n \exp[\beta(\Delta E - \mu)]}{1 - Cn} &= \int_0^\infty dk k^2 \exp\left(-\beta \frac{\hbar^2 k^2}{2m}\right) \\ &= \left(\sqrt{\frac{\hbar^2 \beta}{2m}}\right)^{-3} \int_0^\infty dk k^2 \exp(-k^2) = \left(\sqrt{\frac{\hbar^2 \beta}{2m}}\right)^{-3} \frac{\sqrt{\pi}}{4}. \end{aligned} \quad (8.16)$$

Thus we have

$$\exp[-\beta(\Delta E - \mu)] = \lambda_T^3 \frac{n}{1 - Cn}, \quad (8.17)$$

and the final result is

$$\mu = -Dn + \frac{1}{\beta} \ln\left(\frac{n\lambda_T^3}{1 - Cn}\right). \quad (8.18)$$

We continue along the lines of Sect. 8.1 and find

$$\begin{aligned} p &= \int_0^n dn \left[\frac{\partial p}{\partial n}\right]_{NT} = \int_0^n dn \left[\frac{\partial p}{\partial \mu}\right]_{NT} \left[\frac{\partial \mu}{\partial n}\right]_{NT} \\ &= \int_0^n dn \underbrace{\left[\frac{\partial \mu}{\partial n}\right]_{NT}}_{-D + \frac{1}{\beta} \left(\frac{1}{n} + \frac{C}{1 - Cn}\right)} / \underbrace{\left[\frac{\partial p}{\partial \mu}\right]_{NT}}_{1/n} = \int_0^n dn \left[-Dn + \frac{1}{\beta(1 - Cn)}\right] \\ &= -D \frac{n^2}{2} - \frac{1}{\beta C} \ln(1 - Cn). \end{aligned} \quad (8.19)$$

To get further we have to make use of the fact that  $Cn$  is much smaller than unity, which is fulfilled for a gas. We expand the logarithm and keep the two lowest order terms

$$\begin{aligned} p &= -D \frac{n^2}{2} - \frac{1}{\beta C} \ln(1 - Cn) \approx -D \frac{n^2}{2} + \frac{1}{\beta C} (Cn + \frac{1}{2}(Cn)^2) \\ &\approx -D \frac{n^2}{2} + \frac{n}{\beta} \left(1 + \frac{1}{2}Cn\right) \approx -D \frac{n^2}{2} + \frac{n}{\beta(1 - \frac{1}{2}Cn)}, \end{aligned} \quad (8.20)$$

and rewrite this expression as

$$\left(p + D \frac{n^2}{2}\right) \left(\frac{1}{n} - \frac{1}{2}C\right) = \frac{1}{\beta}, \quad (8.21)$$

or

$$\left(p + D \frac{n^2}{2}\right) \left(\frac{N}{n} - \frac{N}{2}C\right) = \frac{N}{\beta}, \quad (8.22)$$

or

$$\left(p + D \frac{N^2}{2V^2}\right) \left(V - \frac{N}{2}C\right) = Nk_B T. \quad (8.23)$$

Now we may identify the parameters in the van der Waals equation of state [1],  $(p + a/V^2)(V - b) = Nk_B T$ ,

$$a = D \frac{N^2}{2} = \frac{2\pi B N^2}{(\gamma - 3) d_0^{\gamma-3}} = \frac{2\pi B N^2}{3d_0^3}, \quad (8.24)$$

and

$$b = \frac{N}{2} C = \frac{N 2\pi d_0^3}{3}. \quad (8.25)$$

This completes the derivation of the van der Waals equation of state for non-ideal gases.

### 8.2.1 2D Version

We now treat the gas more realistically than in Sect. 8.1.1. We let the atoms<sup>5</sup> have a finite radius,  $r_0$ , and an attractive interaction. We will see in Sect. 8.3 that the van der Waals interaction potential (energy) between two atoms is of the form,  $V = -Br^{-\gamma}$ , where  $B$  is a constant characteristic of the atoms and  $\gamma = 6$ .

The finite radius leads to a smaller free volume in which the atoms can move,

$$\tilde{A} = A - N\pi d_0^2 = A (1 - n^{2D} \pi d_0^2) = A (1 - C^{2D} n^{2D}), \quad (8.26)$$

where  $d_0$  is the atomic diameter. We have subtracted the volume taken up by the atoms themselves.<sup>6</sup>

The interaction between the atoms leads to an energy shift for each atom. For a gas one may sum over pair interactions,

$$\begin{aligned} \Delta E &= \int_{d_0}^{\infty} dr 2\pi r n^{2D} (-Br^{-\gamma}) \\ &= -\frac{2\pi B n^{2D}}{(\gamma-2)d_0^{\gamma-2}} = -D^{2D} n^{2D} \end{aligned} \quad (8.27)$$

We have introduced the constants  $C^{2D}$  and  $D^{2D}$  to make the derivation that follows more transparent. We will now determine the chemical potential for the gas and from this obtain the equation of state. The chemical potential is determined from the relation

$$\begin{aligned} N &= \sum_{\mathbf{k}} n_B(k) = \tilde{A} \int \frac{d^2k}{(2\pi)^2} n_B(k) \\ &= \tilde{A} \int_0^{\infty} dk \frac{2\pi k}{(2\pi)^2} \exp \left[ -\beta \left( \frac{\hbar^2 k^2}{2m} + \Delta E - \mu \right) \right], \end{aligned} \quad (8.28)$$

<sup>5</sup>We have here assumed that the gas consists of separate atoms. The treatment is still valid for molecular gases. In that case read molecule instead of atom.

<sup>6</sup>Note that an atom can not come closer to another than the atom diameter. This means that a spherical volume of radius  $d_0$  centered around each atom is excluded from the free volume in which other atoms can move.

where on the right-hand side we have summed over all states weighted by the Boltzmann distribution function (4.26). The above equation can be rewritten as

$$\frac{n^{2D}}{1 - C^{2D}n^{2D}} = \frac{1}{2\pi} \exp[-\beta(\Delta E - \mu)] \int_0^\infty dk k \exp\left(-\beta \frac{\hbar^2 k^2}{2m}\right), \quad (8.29)$$

and rearrangement gives

$$\begin{aligned} \frac{2\pi n^{2D} \exp[\beta(\Delta E - \mu)]}{1 - C^{2D}n^{2D}} &= \int_0^\infty dk k \exp\left(-\beta \frac{\hbar^2 k^2}{2m}\right) \\ &= \frac{\hbar^2 \beta}{2m} \int_0^\infty dk k \exp(-k^2) = \frac{\hbar^2 \beta}{2m} \frac{1}{2}. \end{aligned} \quad (8.30)$$

Thus we have

$$\exp[-\beta(\Delta E - \mu)] = \frac{2\pi \hbar^2 \beta}{m} \frac{n^{2D}}{1 - C^{2D}n^{2D}} = \lambda_T^2 \frac{n^{2D}}{1 - C^{2D}n^{2D}}, \quad (8.31)$$

and the final result is

$$\mu = -D^{2D}n^{2D} + \frac{1}{\beta} \ln\left(\frac{n^{2D} \lambda_T^2}{1 - C^{2D}n^{2D}}\right). \quad (8.32)$$

We continue along the lines of Sect. 8.1.1 and find

$$\begin{aligned} \pi &= \int_0^{n^{2D}} dn^{2D} \left[ \frac{\partial \pi}{\partial n^{2D}} \right]_{NT} = \int_0^{n^{2D}} dn^{2D} \left[ \frac{\partial \pi}{\partial \mu} \right]_{NT} \left[ \frac{\partial \mu}{\partial n^{2D}} \right]_{NT} \\ &= \int_0^{n^{2D}} dn^{2D} \underbrace{\left[ \frac{\partial \mu}{\partial n^{2D}} \right]_{NT}}_{-D^{2D} + \frac{1}{\beta} \left( \frac{1}{n^{2D}} + \frac{C^{2D}}{1 - C^{2D}n^{2D}} \right)} \underbrace{\left[ \frac{\partial \mu}{\partial \pi} \right]_{NT}}_{1/n^{2D}} \\ &= \int_0^{n^{2D}} dn^{2D} \left[ -D^{2D}n^{2D} + \frac{1}{\beta(1 - C^{2D}n^{2D})} \right] \\ &= -D^{2D} \frac{(n^{2D})^2}{2} - \frac{1}{\beta C^{2D}} \ln(1 - C^{2D}n^{2D}). \end{aligned} \quad (8.33)$$

To get further we have to make use of the fact that  $C^{2D}n^{2D}$  is much smaller than unity, which is fulfilled for a gas. We expand the logarithm and keep the two lowest order terms

$$\begin{aligned}
\pi &= -D^{2D} \frac{(n^{2D})^2}{2} - \frac{1}{\beta C^{2D}} \ln(1 - C^{2D} n^{2D}) \\
&\approx -D^{2D} \frac{(n^{2D})^2}{2} + \frac{1}{\beta C^{2D}} \left( C^{2D} n^{2D} + \frac{1}{2} (C^{2D} n^{2D})^2 \right) \\
&\approx -D^{2D} \frac{(n^{2D})^2}{2} + \frac{n^{2D}}{\beta} \left( 1 + \frac{1}{2} C^{2D} n^{2D} \right) \\
&\approx -D^{2D} \frac{(n^{2D})^2}{2} + \frac{n^{2D}}{\beta(1 - \frac{1}{2} C^{2D} n^{2D})},
\end{aligned} \tag{8.34}$$

and rewrite this expression as

$$\left( \pi + D^{2D} \frac{(n^{2D})^2}{2} \right) \left( \frac{1}{n^{2D}} - \frac{1}{2} C^{2D} \right) = \frac{1}{\beta}, \tag{8.35}$$

or

$$\left( \pi + D^{2D} \frac{(n^{2D})^2}{2} \right) \left( \frac{N}{n^{2D}} - \frac{N}{2} C^{2D} \right) = \frac{N}{\beta}, \tag{8.36}$$

or

$$\left( \pi + D^{2D} \frac{N^2}{2A^2} \right) \left( A - \frac{N}{2} C^{2D} \right) = Nk_B T. \tag{8.37}$$

Now we may identify the parameters in the van der Waals equation of state,  $(\pi + a/A^2)(A - b) = Nk_B T$ ,

$$a = D^{2D} \frac{N^2}{2} = \frac{\pi B N^2}{(\gamma - 2) d_0^{\gamma-2}} = \frac{\pi B N^2}{4d_0^4}, \tag{8.38}$$

and

$$b = \frac{N}{2} C^{2D} = \frac{N\pi d_0^2}{2}. \tag{8.39}$$

This completes the derivation of the van der Waals equation of state for 2D non-ideal gases.

### 8.3 Van der Waals Force Between Two Atoms

The van der Waals attraction between gas atoms was found empirically by van der Waals in his studies of the equation of state of real gases. The cause of this attraction was at that time a mystery. It was not until much later that London [2] resolved this mystery and gave the explanation in terms of fluctuating electric dipoles. He used a model of the atom pair where each atom was represented by three perpendicular dipoles. We will here use a different approach [3] which is more in line with the formalism presented in this book.

For simplicity we choose the coordinate system such that atom 1 is at the origin and atom 2 on the  $z$ -axis at the distance  $r$  from atom 1. A static dipole moment  $\mathbf{p}$  gives rise to an electric field,<sup>7</sup>  $\mathbf{E}$ ,

$$\mathbf{E} = - \left[ \frac{\mathbf{p}}{r^3} - \frac{3(\mathbf{p} \cdot \mathbf{r}) \mathbf{r}}{r^3} \right]. \quad (8.40)$$

When retardation effects are neglected the same relation holds also for a time dependent dipole moment for each instant of time,

$$\mathbf{E}(t) = - \left[ \frac{\mathbf{p}(t)}{r^3} - \frac{3(\mathbf{p}(t) \cdot \mathbf{r}) \mathbf{r}}{r^3} \right]. \quad (8.41)$$

If there is an induced dipole,  $\mathbf{p}_1$ , in atom 1 it gives rise to an electric field

$$\mathbf{E}(t) = - \left[ \frac{\mathbf{p}_1(t)}{r^3} - \frac{3(\mathbf{p}_1(t) \cdot \mathbf{r}) \mathbf{r}}{r^3} \right] \quad (8.42)$$

Alternatively it can be expressed in terms of the dipole-dipole tensor,  $\tilde{\phi}$ ,

$$\mathbf{E} = -\tilde{\phi} \cdot \mathbf{p}_1, \quad (8.43)$$

where the elements of the three by three tensor are

$$\phi_{\mu\nu} = \frac{\delta_{\mu\nu}}{r^3} - \frac{3r_\mu r_\nu}{r^5}. \quad (8.44)$$

Note, that the tensor is symmetric, i.e.  $\phi_{\mu\nu} = \phi_{\nu\mu}$ . The field at the position of atom 2 caused by the dipole of atom 1 is

$$\mathbf{E}^{12} = -\tilde{\phi}^{12} \cdot \mathbf{p}_1, \quad (8.45)$$

where with our choice of coordinate system

$$\tilde{\phi}^{12} = \frac{1}{r^3} \begin{pmatrix} 1 & 0 & 0 \\ 0 & 1 & 0 \\ 0 & 0 & -2 \end{pmatrix}. \quad (8.46)$$

This field will polarize atom 2 and

$$\mathbf{p}_2 = \alpha_2^{at} \mathbf{E}^{12}. \quad (8.47)$$

---

<sup>7</sup>Note that we here use an alternative way to express the field compared to in (2.148).

Here, we should be a little more careful. What was said about convolution integrals in Sect. 2.3 also holds here. Thus,

$$\mathbf{p}_2(t) = \int_{-\infty}^{\infty} dt \alpha_2^{at}(t-t') \mathbf{E}^{12}(t') \quad (8.48)$$

and the simple relation in (8.47) is valid for the Fourier transformed quantities,

$$\mathbf{p}_2(\omega) = \alpha_2^{at}(\omega) \mathbf{E}^{12}(\omega). \quad (8.49)$$

So from now on the dipole moments and electric fields refer to their Fourier transformed (with respect to time) versions.

The field at the position of atom 1 caused by the dipole of atom 2 is

$$\mathbf{E}^{21} = -\tilde{\phi}^{21} \cdot \mathbf{p}_2, \quad (8.50)$$

where

$$\tilde{\phi}^{21} = \tilde{\phi}^{12}. \quad (8.51)$$

Now, this field induces a polarization of atom 1

$$\mathbf{p}_1 = \alpha_1^{at} \mathbf{E}^{21}, \quad (8.52)$$

and if this polarization is what we started from we have found self-sustained fields. A normal mode has been excited. We have

$$\begin{aligned} \mathbf{p}_1 &= \alpha_1^{at} \cdot \mathbf{E}^{21} = \alpha_1^{at} \cdot (-\tilde{\phi}^{21} \cdot \mathbf{p}_2) = \alpha_1^{at} \cdot \left[ -\tilde{\phi}^{21} \cdot (\alpha_2^{at} \cdot \mathbf{E}^{12}) \right] \\ &= -\alpha_1^{at} \cdot \tilde{\phi}^{21} \cdot \left[ \alpha_2^{at} \cdot (-\tilde{\phi}^{12} \cdot \mathbf{p}_1) \right]. \end{aligned} \quad (8.53)$$

From the two end relations we have

$$\left[ \alpha_1^{at}(\omega) \cdot \tilde{\phi}^{21} \cdot \alpha_2^{at}(\omega) \cdot \tilde{\phi}^{12} - \tilde{\mathbf{I}} \right] \cdot \mathbf{p}_1 = \mathbf{0}, \quad (8.54)$$

where  $\tilde{\mathbf{I}}$  is the unit tensor.

This equation has a trivial and a non-trivial solution. The trivial solution is that  $\mathbf{p}_1 = \mathbf{0}$ . For the non-trivial solution which we are interested in we have that the determinant of the matrix operating on  $\mathbf{p}_1$  is zero, i.e.,

$$\text{Det} \left[ \alpha_1^{at}(\omega) \cdot \tilde{\phi}^{21} \cdot \alpha_2^{at}(\omega) \cdot \tilde{\phi}^{12} - \tilde{\mathbf{I}} \right] = 0. \quad (8.55)$$

For anisotropic atoms the polarizabilities are tensors and the expression has to be kept as is. We will now limit ourselves to isotropic atoms where the polarizabilities become scalars. Then the equation simplifies into

$$\text{Det} \left[ \alpha_1^{at}(\omega) \alpha_2^{at}(\omega) \tilde{\phi}^2 - \tilde{1} \right] = 0, \quad (8.56)$$

where, with our choice of coordinate system, we have

$$\tilde{\phi}^2 = \frac{1}{r^6} \begin{pmatrix} 1 & 0 & 0 \\ 0 & 1 & 0 \\ 0 & 0 & 4 \end{pmatrix}. \quad (8.57)$$

The condition for modes in the case of isotropic atoms is

$$\left[ 1 - \alpha_1^{at}(\omega) \alpha_2^{at}(\omega) / r^6 \right]^2 \left[ 1 - 4\alpha_1^{at}(\omega) \alpha_2^{at}(\omega) / r^6 \right] = 0, \quad (8.58)$$

and the mode-condition function is

$$f(z) = \left[ 1 - \alpha_1^{at}(z) \alpha_2^{at}(z) / r^6 \right]^2 \left[ 1 - 4\alpha_1^{at}(z) \alpha_2^{at}(z) / r^6 \right]. \quad (8.59)$$

### 8.3.1 Zero Temperature

If we can find a simple analytical expression for the atomic polarizabilities we might be able to find the normal modes. Then by summing over the zero point energies we may find the interaction energy and force. This approach is called the mode-summation method. London [2] used an approximation which has been named after him. In the London approximation the atomic polarizability for atom  $i$  is

$$\alpha_i^{at}(\omega) = \alpha_i^{at}(0) / \left[ 1 - (\omega/\omega_i)^2 \right] = \frac{\alpha_i^{at}(0) (\omega_i)^2}{(\omega_i)^2 - \omega^2}, \quad (8.60)$$

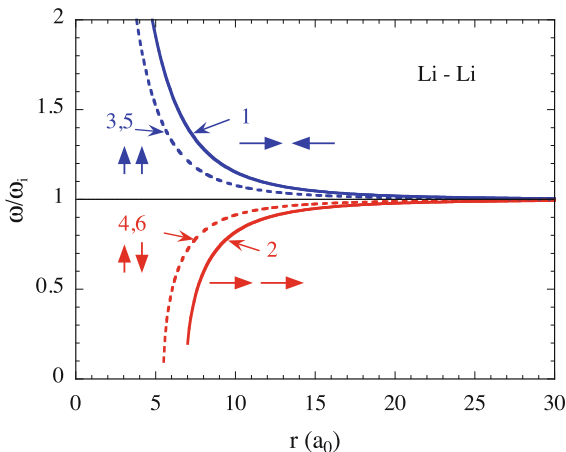
where  $\alpha_i^{at}(0)$  is the static polarizability and  $\omega_i$  is a characteristic frequency of the atom. It need not be the first ionization potential. Thus there are two parameters only and they may be used as fitting parameters.

There are six solutions to (8.58),

$$\begin{aligned} \omega_{1,2} &= \omega_i \sqrt{1 \pm 2\alpha_i^{at}(0) / r^3}, \\ \omega_{3,4} &= \omega_{5,6} = \omega_i \sqrt{1 \pm \alpha_i^{at}(0) / r^3}. \end{aligned} \quad (8.61)$$

It is interesting to note in passing that

**Fig. 8.1** The variation of the frequency of the six modes with atom separation, in Bohr radii ( $a_0$ ), for two Li-atoms. The two arrows placed next to each curve indicate how the two induced dipoles are aligned relative each other. See the text for details



$$\sum_{j=1}^6 (\omega_j)^2 = 6(\omega_i)^2, \tag{8.62}$$

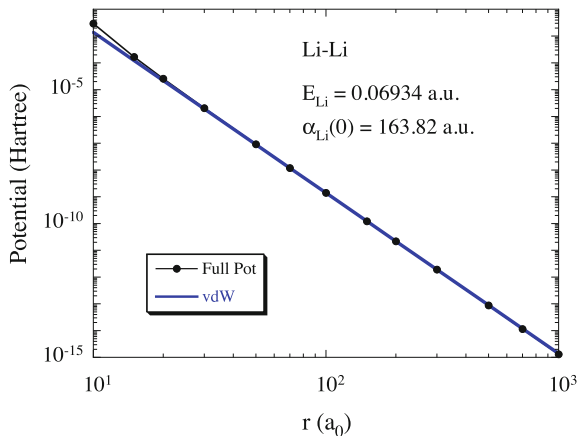
$$\sum_{j=1}^6 \omega_j < 6\omega_i.$$

That the sum of the squares of the frequencies is unaffected by the interaction is typical in the non-retarded treatment. That the sum of the frequencies is reduced causes the net attraction. The modes are shown in Fig. 8.1 for two Li-atoms, where we have indicated with arrows how the oscillating dipoles are oriented. In mode 1 they are along the  $z$ -axis and are pointing in the direction opposite to each other; this is a repelling mode. In mode 2 the dipoles are also aligned along the  $z$ -axis, but now the dipole moments are “moving” in phase; this is an attractive mode. Modes 3 and 5 are repelling modes where both the dipoles are perpendicular to the  $z$ -axis. In one of them they are along the  $x$ -axis and in the other along  $y$ -axis. The dipoles of the two atoms are pointing in the same direction. Modes 4 and 6 are attractive modes where the dipoles of the two atoms are pointing in the opposite direction relative each other. Modes 3 and 5 are degenerate and so are modes 4 and 6. Now, the interaction potential is

$$\begin{aligned} V(r) &= \frac{\hbar}{2} \left( \sum_{j=1}^6 \omega_j - 6\omega_i \right) \\ &\approx \frac{\hbar\omega_i}{2} \left[ 2 - (\alpha_i^{at}(0)/r^3)^2 + 4 - \frac{1}{2}(\alpha_i^{at}(0)/r^3)^2 - 6 \right] \\ &= -\frac{3}{4} \frac{\alpha_i^{at}(0)^2}{r^6} \hbar\omega_i, \end{aligned} \tag{8.63}$$

where we have expanded the square root and kept three terms in the expansion. The expansion is made under the assumption that the separation between the atoms is large enough for the van der Waals attraction to be weak compared to the ionization

**Fig. 8.2** The van der Waals interaction potential for two lithium atoms from (8.63), *solid curve*; the London approximation was used for the atomic polarizability. The *curve with filled circles* is the full result from a quantum-mechanical calculation including both retardation effects and multipole contributions [4]. The deviation for small separations are due to multipole contributions



potential of the atom. The result for two lithium atoms is shown in Fig. 8.2. The London approximation was used for the atomic polarizability and the parameters are given in the figure. Thus we have determined the parameters used to represent the atom interaction in the equation of state for a non-ideal gas in Sect. 8.2 to be  $B = 3\hbar\omega_{Li}\alpha_{Li}(0)^2/4 = 3E_{Li}\alpha_{Li}(0)^2/4$  and  $\gamma = 6$ , respectively. The curve with filled circles is the full result from a quantum-mechanical calculation including both retardation effects and multipole contributions [4]. The deviation for small separations are due to multipole contributions; we are in the van der Waals range so the retardation effects will appear at larger separations.

For a dimer with two different atoms we proceed in the same way and find the modes are

$$\begin{aligned}\omega_{1,2} &= \sqrt{\frac{(\omega_1)^2 + (\omega_2)^2}{2} \pm \frac{(\omega_1)^2 - (\omega_2)^2}{2} \sqrt{1 + \frac{4\alpha_1^{at}(0)\alpha_2^{at}(0)(\omega_1)^2(\omega_2)^2}{r^6[(\omega_1)^2 - (\omega_2)^2]}}}, \\ \omega_{3,5} &= \omega_{4,6} = \sqrt{\frac{(\omega_1)^2 + (\omega_2)^2}{2} \pm \frac{(\omega_1)^2 - (\omega_2)^2}{2} \sqrt{1 + \frac{\alpha_1^{at}(0)\alpha_2^{at}(0)(\omega_1)^2(\omega_2)^2}{r^6[(\omega_1)^2 - (\omega_2)^2]}}}\end{aligned}\quad (8.64)$$

These modes are shown in Fig. 8.3. The notation is the same as in Fig. 8.1. Note that the two repulsive modes approach the highest of the two characteristic frequencies while the attractive modes approach the lowest frequency for large separations. Thus there is an energy gap where there are no modes.

The interaction potential between two non-equal atoms becomes

$$V(r) = -\frac{3}{2} \frac{\alpha_1^{at}(0)\alpha_2^{at}(0)}{r^6} \frac{\hbar\omega_1\hbar\omega_2}{\hbar\omega_1 + \hbar\omega_2}. \quad (8.65)$$

**Fig. 8.3** Same as in Fig. 8.1 but now for a Na-K dimer. The upper modes approach the characteristic frequency for the Na atom in the large separation limit and the lower approach that for the K atom. See the text for details

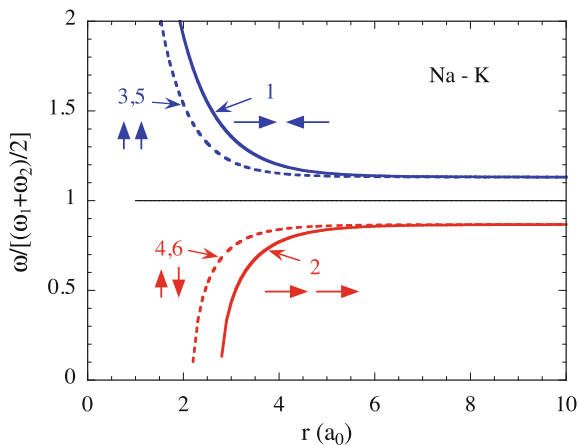
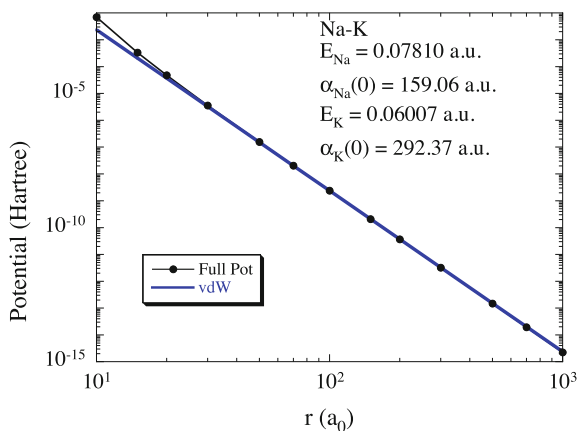


**Fig. 8.4** Same as in Fig. 8.2 but now for a Na-K dimer



These results are identical to the results found by [2]. He used perturbation theory. We think that the present derivation is more straight forward and simple. The result for a Na-K dimer is shown in Fig. 8.4.

If the expression for the atomic polarizability is not simple we put the mode-condition-function in the integral in (5.59) and find

$$\begin{aligned}
 E &= \frac{\hbar}{4\pi} \int_{-\infty}^{\infty} d\xi \ln f(i\xi) \\
 &= \frac{\hbar}{4\pi} \int_{-\infty}^{\infty} d\xi \ln \left\{ \left[ 1 - \alpha_1^{at}(i\xi) \alpha_2^{at}(i\xi) / r^6 \right]^2 \left[ 1 - 4\alpha_1^{at}(i\xi) \alpha_2^{at}(i\xi) / r^6 \right] \right\} \quad (8.66) \\
 &\approx -\frac{6\hbar}{4\pi r^6} \int_{-\infty}^{\infty} d\xi \alpha_1^{at}(i\xi) \alpha_2^{at}(i\xi) = -\frac{3\hbar}{\pi r^6} \int_0^{\infty} d\xi \alpha_1^{at}(i\xi) \alpha_2^{at}(i\xi),
 \end{aligned}$$

**Table 8.1**  $C_6$ -coefficients in atomic units (Hartree  $\cdot a_0^6$ ) for the alkali-metal dimers.  $V_{vdW} = -C_6/r^6$ . The parameters needed for the calculation, i.e. the polarizabilities and characteristic frequencies were obtained from fitting of the retarded result to the full result in [4]

	Li	Na	K	Rb	Cs
Li	1395.6				
Na	1435.6	1482.0			
K	2312.4	2368.6	3851.1		
Rb	2491.4	2550.3	4152.5	4477.9	
Cs	2967.7	3029.0	4964.2	5356.2	6423.1

where we once again have assumed that  $r$  is large enough so that the logarithm can be expanded. If we now use the London approximation for the polarizability we find

$$\begin{aligned}
 E &= -\frac{3\hbar}{\pi r^6} \int_0^\infty d\xi \frac{\alpha_1^{at}(0)}{1+(\xi/\omega_1)^2} \frac{\alpha_2^{at}(0)}{1+(\xi/\omega_2)^2} \\
 &= -\frac{3\hbar\alpha_1^{at}(0)\alpha_2^{at}(0)}{\pi r^6} \underbrace{\int_0^\infty d\xi \frac{1}{1+(\xi/\omega_1)^2} \frac{1}{1+(\xi/\omega_2)^2}}_{\frac{\pi}{2} \frac{\omega_1\omega_2}{\omega_1+\omega_2}} \\
 &= -\frac{3}{2} \frac{\alpha_1^{at}(0)\alpha_2^{at}(0)}{r^6} \frac{\hbar\omega_1\hbar\omega_2}{\hbar\omega_1+\hbar\omega_2}.
 \end{aligned} \tag{8.67}$$

This method was even simpler to use albeit less transparent. The results for the alkali-metal dimers are summarized in Table 8.1.

### 8.3.2 Finite Temperature

We have so far concentrated our treatment to zero temperature. For finite temperatures things are more complicated. When we calculate the force between two objects at finite temperatures, from how the energy changes with separation, it is important to know how the objects are thermodynamically connected to the rest of the world. In most cases the temperature effects are very weak. However, there is an exception: liquids like water with permanent dipole moments have important contributions to their dielectric functions for very small frequencies. This leads to important temperature effects. When we gradually increase the temperature from 0 K the temperature effects first appear at large separations only, and then at smaller and smaller separations.

If the objects are completely isolated with no heat exchange, no particle exchange and if they do not perform any work, except on each other, all work performed by the force between the objects goes to the change of the internal energies of the objects; thus in this case we should calculate the *internal energy* as function of separation and

from this variation obtain the force. It should be noted that in this case the temperature will change with separation.

If the objects are in contact with a heat bath, so that heat is freely exchanged with the surroundings, some of the work that otherwise would go into the change of the internal energy now leaks out (or in) in the form of heat; in this case we should calculate the *Helmholtz free energy* as function of separation and from this obtain the force; this is the most common situation.

If the objects also can exchange particles with the surroundings, energy is leaking out of the objects also via this channel. In this case we should calculate the *thermodynamic potential*. This situation occurs when two particles are in equilibrium with their solution or when two liquid droplets are in equilibrium with their vapor phase.

Often the volume of the objects stays unchanged as well as the surrounding pressure. In this case we can use the internal energy and the *enthalpy* interchangeably; this also holds for the Helmholtz and *Gibbs* free energies. In our problem the interaction is for finite temperature obtained from the Helmholtz free energy  $\mathfrak{F}(T, V, N)$  (see Sect. 4.3),

$$\mathfrak{F} = -\frac{1}{\beta} \ln \mathfrak{P}, \quad (8.68)$$

where  $\mathfrak{P}$  is the partition function,

$$\begin{aligned} \mathfrak{P} &= \text{tr} (e^{-\beta H}) = \prod_i \sum_{n=0}^{\infty} e^{-\beta \hbar \omega_i (n + \frac{1}{2})} \\ &= \prod_i e^{-\beta \frac{1}{2} \hbar \omega_i} \sum_{n=0}^{\infty} e^{-\beta \hbar \omega_i n} = \prod_i e^{-\beta \frac{1}{2} \hbar \omega_i} \frac{1}{1 - e^{-\beta \hbar \omega_i}}. \end{aligned} \quad (8.69)$$

Thus we have

$$\mathfrak{F} = -\frac{1}{\beta} \sum_i \left[ -\beta \frac{1}{2} \hbar \omega_i - \ln (1 - e^{-\beta \hbar \omega_i}) \right] = \sum_i \left[ \frac{1}{2} \hbar \omega_i + \frac{1}{\beta} \ln (1 - e^{-\beta \hbar \omega_i}) \right]. \quad (8.70)$$

Before we derive the result using the method in (5.64), based on generalized argument principle we stay with the mode-summation method for a while. When using the argument principle the physics is somewhat obscured by the mathematics.

The internal energy for our system of two atoms in thermal equilibrium is

$$E(r) = \sum_i \left( n + \frac{1}{2} \right) \varepsilon_i(r) = \sum_i \left( n[\omega_i(r)] + \frac{1}{2} \right) \hbar \omega_i(r), \quad (8.71)$$

where the sum runs over the normal modes, six in our case. Thus we have

$$\begin{aligned} E(r) &= \sum_i \left( n[\omega_i(r)] + \frac{1}{2} \right) \hbar \omega_i(r), \\ \mathfrak{F}(r) &= \sum_i \left[ \frac{1}{2} \hbar \omega_i(r) + \frac{1}{\beta} \ln (1 - e^{-\beta \hbar \omega_i(r)}) \right]. \end{aligned} \quad (8.72)$$

At zero temperature the force is

$$F = -\frac{dE(r)}{dr}, \quad (8.73)$$

and at finite temperature,

$$F = -\frac{d\mathfrak{F}}{dr}. \quad (8.74)$$

The force is obtained by a direct derivation with respect to  $r$ ,

$$F = \begin{cases} -\frac{\hbar}{2} \sum_i \partial\omega_i(r)/\partial r, & T = 0, \\ -\hbar \sum_i \{n[\omega_i(r)] + 1/2\} [\partial\omega_i(r)/\partial r] & T \neq 0. \end{cases} \quad (8.75)$$

We note that a mode with a positive slope in the mode energy as function of  $r$  contributes with an attractive force and one with negative slope gives a repulsive contribution which is fully in line with what we claimed in connection with Figs. 8.1 and 8.3.

Now, if we can find the modes in a simple way like here by using the London approximation for the atomic polarizability we may find the interaction potential directly from (8.70). If not we use (5.64) and arrive at

$$\begin{aligned} \mathfrak{F} &= \frac{1}{\beta} \sum_{\xi_n} f(\xi_n) \\ &= -\frac{6}{\beta} \frac{1}{r^6} \sum_{\xi_n} \alpha_1^{at}(\xi_n) \alpha_2^{at}(\xi_n); \quad \xi_n = \frac{2\pi n}{\hbar\beta}; \quad n = 0, 1, 2, \dots \end{aligned} \quad (8.76)$$

To be noted is that the van der Waals interaction potential follows a simple power law; the same power law for both zero and finite temperature. The potential varies as  $r^{-6}$  and the force as  $r^{-7}$ . The temperature effects start to appear first at very high temperatures in the present problem, viz. when  $\beta$  is of the order of the inverse of the characteristic energy of the atoms. This means that the temperature is thousands of Kelvins.

## References

1. J.D. van der Waals, Ph.D. Thesis, University of Leiden
2. F. London, Z. Phys. Chem. B 11, 222 (1930); Z. Phys. 63, 245 (1930). Trans. Faraday Soc. **33**, 8b-26 (1937)
3. Bo E. Sernelius, *Surface Modes in Physics* (Wiley-VCH, Berlin, 2001)
4. M. Marinescu, L. You, Phys. Rev. A **59**, 1936 (1999)

# Chapter 9

## Van der Waals Interaction in Planar Structures



**Abstract** After a section in which we adapt the general formalism presented in Chap. 7 to planar structures in neglect of retardation we start by introducing the basic structure elements: a single interface, a layer, a 2D film, and a thin diluted gas film. A general planar structure can then be constructed by stacking these elements side by side. The thin gas layer is special; it is used to find the interaction on an atom at a general position in the planar structure. Then we go through some common structures and present illustrating examples; the examples involve gold half spaces, gold slabs, graphene, 2D metal films and lithium atoms. Then we discuss alternative ways to find the normal modes in a planar structure. Next we rederive the van der Waals interaction between two atoms from using the summation over pair interactions. We end with a section on spatial dispersion.

### 9.1 Adapting the General Method of Chap. 7 to Planar Structures and to the Neglect of Retardation

We assume that the spatial extension of the interfaces is very large compared to the thickness of the layers so that we may treat the interfaces as infinite in two directions. If the thickness of the object is finite the rightmost medium,  $n = N + 1$ , in Fig. 7.1 is the ambient as well as the leftmost,  $n = 0$ . If not we have a multiple coated half space. In both situations the modes are solutions with the boundary conditions that there are no incoming waves in the two outer regions, i.e. there is no wave moving toward the right in medium  $n = 0$  and no wave moving toward the left in medium  $n = N + 1$ . The fields are self-sustained; no fields are coming in from outside.

In the non-retarded treatment Maxwell's Equations in (2.4) become

$$\begin{aligned}\nabla \cdot \tilde{\mathbf{D}} &= 0 \\ \nabla \cdot \mathbf{B} &= 0 \\ \nabla \times \mathbf{E} &= \mathbf{0} \\ \nabla \times \tilde{\mathbf{H}} &= \mathbf{0},\end{aligned}\tag{9.1}$$

in absence of external charge densities. We note that the electric and magnetic fields are decoupled. There are both electric modes and magnetic modes but in general the effects from the electric modes are much more important when we limit the treatment to non-magnetic systems, i.e. we let  $\tilde{\mu}(\omega) \equiv 1$ .

Since  $\nabla \times \mathbf{E} = 0$  the  $\mathbf{E}$ -field is conservative and we may define a scalar potential,  $\Phi$  such that  $\mathbf{E} = -\nabla\Phi$ . Now, for  $\nabla \cdot \tilde{\mathbf{D}} = \nabla \cdot \tilde{\varepsilon}(\omega) \mathbf{E} = 0$  there are two possibilities. Either  $\tilde{\varepsilon}(\omega) = 0$  which defines the longitudinal bulk mode of the medium or  $\nabla \cdot \mathbf{E} = 0$ . We are not interested in the bulk modes here. Inserting  $\mathbf{E} = -\nabla\Phi$  into the equation  $\nabla \cdot \mathbf{E} = 0$  then leads to Laplace's equation,

$$\nabla^2 \Phi = 0. \quad (9.2)$$

So, when we neglect retardation effects we just solve Laplace's equation in each medium and use the proper boundary conditions at each interface to find the normal modes.<sup>1</sup>

In the non-retarded treatment of a planar structure we let the waves represent solutions to Laplace's equation, (9.2), in cartesian coordinates, for the scalar potential,  $\Phi$ . The interfaces are parallel to the  $xy$ -plane and the  $z$ -coordinate is the coordinate that is constant on each interface. The solutions are of the form

$$\Phi_{\mathbf{k}}(\mathbf{r}, z) = e^{i\mathbf{k}\cdot\mathbf{r}} e^{\pm kz}, \quad (9.3)$$

where  $\mathbf{k}$  is the two-dimensional wave vector in the plane of the interfaces. We let  $z$  increase toward the right in Fig. 7.1. We want to find the normal modes for a specific wave vector  $\mathbf{k}$ . Then all waves have the common factor  $\exp(i\mathbf{k} \cdot \mathbf{r})$ . We suppress this factor here. Then

$$R(z) = e^{-kz}; \quad L(z) = e^{+kz}. \quad (9.4)$$

Using the boundary conditions that the potential and the normal component of the  $\tilde{\mathbf{D}}$ -field are continuous across interface  $n$  gives

$$\begin{aligned} a^n e^{-kz_n} + b^n e^{kz_n} &= a^{n+1} e^{-kz_n} + b^{n+1} e^{kz_n} \\ a^n \tilde{\varepsilon}_n e^{-kz_n} - b^n \tilde{\varepsilon}_n e^{kz_n} &= a^{n+1} \tilde{\varepsilon}_{n+1} e^{-kz_n} - b^{n+1} \tilde{\varepsilon}_{n+1} e^{kz_n}, \end{aligned} \quad (9.5)$$

and we may identify the matrix  $\tilde{\mathbf{A}}_n(z_n)$  introduced in (7.1) as

$$\tilde{\mathbf{A}}_n(z_n) = \begin{pmatrix} e^{-kz_n} & e^{kz_n} \\ \tilde{\varepsilon}_n e^{-kz_n} & -\tilde{\varepsilon}_n e^{kz_n} \end{pmatrix}, \quad (9.6)$$

---

<sup>1</sup>From the symmetry of (9.1) we can deduce that we may introduce a scalar potential for  $\tilde{\mathbf{H}}$  and obtain an analogous Laplace's equation for the  $\mathbf{B}$ -field. The whole procedure for finding the magnetic modes is identical to the one for finding the electric modes. The only thing one has to do in the final result is to replace  $\tilde{\varepsilon}$  with  $\tilde{\mu}$ .

and the matrix  $\tilde{\mathbf{M}}_n$  in (7.3) as

$$\tilde{\mathbf{M}}_n = \frac{1}{2\tilde{\epsilon}_n} \begin{pmatrix} \tilde{\epsilon}_n + \tilde{\epsilon}_{n+1} & e^{2kz_n} (\tilde{\epsilon}_n - \tilde{\epsilon}_{n+1}) \\ e^{-2kz_n} (\tilde{\epsilon}_n - \tilde{\epsilon}_{n+1}) & \tilde{\epsilon}_n + \tilde{\epsilon}_{n+1} \end{pmatrix}. \quad (9.7)$$

Now we have all we need to determine the non-retarded normal modes in a layered planar structure.

### Summary of key relations for the derivation of van der Waals interactions in planar structures:

In a planar structure the 2D wave vector  $\mathbf{k}$  is the proper quantum number that characterizes a normal mode. The dispersion curve for a mode can have several branches,  $i$ ,  $\omega = \omega_{\mathbf{k}}^i$ . They are solutions to the condition for modes,  $f_{\mathbf{k}}(\omega) = 0$ , where  $f_{\mathbf{k}}(\omega)$  is the mode condition function. When finding the interaction energy of the system one has to sum over both  $\mathbf{k}$  and  $i$ . Since we often let the layers have unlimited extension in the layer plane it is appropriate to calculate the interaction energy per unit area. For zero temperature it is

$$E = \frac{\hbar}{2} \frac{1}{A} \sum_{\mathbf{k}} \int_{-\infty}^{\infty} \frac{d\xi}{2\pi} \ln f_{\mathbf{k}}(i\xi) \rightarrow \frac{\hbar}{2} \int \frac{d^2k}{(2\pi)^2} \int_{-\infty}^{\infty} \frac{d\xi}{2\pi} \ln f_{\mathbf{k}}(i\xi), \quad (9.8)$$

and at finite temperature

$$\tilde{\mathcal{F}} = \frac{1}{A} \sum_{\mathbf{k}} \frac{1}{\beta} \sum_{n=0}^{\infty} ' \ln f_{\mathbf{k}}(i\xi_n) \rightarrow \frac{1}{\beta} \int \frac{d^2k}{(2\pi)^2} \sum_{n=0}^{\infty} ' \ln f_{\mathbf{k}}(i\xi_n) \quad (9.9)$$

where  $A$  is the area of the system and  $\xi_n = 2\pi n/\hbar\beta$ . The arrows indicate what happens when we let  $A$  go toward infinity. In the non-retarded approximation  $f_{\mathbf{k}} \equiv M_{11}$  where  $\tilde{\mathbf{M}}$  is the matrix for the whole structure. The matrix for interface  $n$  is given by

$$\tilde{\mathbf{M}}_n = \frac{1}{2\tilde{\epsilon}_n} \begin{pmatrix} \tilde{\epsilon}_n + \tilde{\epsilon}_{n+1} & e^{2kz_n} (\tilde{\epsilon}_n - \tilde{\epsilon}_{n+1}) \\ e^{-2kz_n} (\tilde{\epsilon}_n - \tilde{\epsilon}_{n+1}) & \tilde{\epsilon}_n + \tilde{\epsilon}_{n+1} \end{pmatrix}. \quad (9.10)$$

Often it is appropriate to give the energy relative a reference system. Then  $f_{\mathbf{k}}$  is replaced by  $\tilde{f}_{\mathbf{k}}$  in (9.8) and (9.9), where  $\tilde{f}_{\mathbf{k}} = f_{\mathbf{k}}/f_{\mathbf{k}}^{\text{ref}}$ . Note that if one is interested in magnetic modes, in a non-magnetic system, and/or the very small effects these have on the interaction the magnetic modes are found by using another matrix where all  $\tilde{\epsilon}$  are replaced by  $\tilde{\mu}$ . The electric and magnetic modes are completely decoupled from each other in the non-retarded formalism.

## 9.2 Basic Structure Elements

A general planar structure can be generated by stacking a number of basic structure elements next to each other. The most basic element is a single planar interface. Sometimes it is convenient to use layers as elements. A special layer is a 2D planar film. Another is a thin diluted gas layer which we will use repeatedly in the derivation of the interaction between atoms and the planar structure. We now discuss these basic elements one by one. We start with the single planar interface.

### 9.2.1 Single Planar Interface

For a single interface, as illustrated in Fig. 9.1, at  $z = a$  between two media having dielectric functions  $\tilde{\epsilon}_0$  and  $\tilde{\epsilon}_1$  we have from (9.10)

$$\tilde{\mathbf{M}} = \tilde{\mathbf{M}}_0 = \frac{1}{2\tilde{\epsilon}_0} \begin{pmatrix} \tilde{\epsilon}_0 + \tilde{\epsilon}_1 & e^{2ka} (\tilde{\epsilon}_0 - \tilde{\epsilon}_1) \\ e^{-2ka} (\tilde{\epsilon}_0 - \tilde{\epsilon}_1) & \tilde{\epsilon}_0 + \tilde{\epsilon}_1 \end{pmatrix}. \quad (9.11)$$

If this is the whole structure the mode condition is

$$\tilde{\epsilon}_0(\omega) + \tilde{\epsilon}_1(\omega) = 0. \quad (9.12)$$

Here, and in several more places we give the condition for modes of a single interface. If we use the corresponding mode condition function to calculate the energy in principle we obtain the surface energy or interface energy. However, to get a realistic result we need to include spatial dispersion [1], i.e., we need a momentum dependence of the dielectric function, otherwise the energy diverges. Furthermore

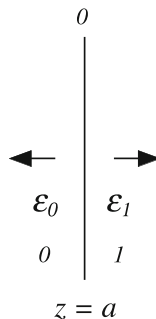


**Fig. 9.1** The geometry of a single planar interface located at  $z = a$ . The material to the left of the interface has the dielectric function  $\tilde{\epsilon}_0(\omega)$  and the material to the right  $\tilde{\epsilon}_1(\omega)$ . If this is the whole structure there are only waves moving away from the interface, as indicated by the arrows. Adapted from [10]

this is not the full story. The surface energy is the energy per unit area of a newly created surface. To be more specific it is half the energy needed to split the solid in two along a plane and to separate the two halves to infinite distance. The “1/2” comes from the fact that we create two new surfaces. When we split the solid we create surface modes at the surface or rather bulk modes are peeled off and form surface modes. This change in collective modes costs energy. This energy constitutes, an important part of the surface energy. Other effects that contribute to, or modify, the energy is possible surface reconstruction, surface relaxation and for metals that the conduction electrons spill out into the vacuum. We refer the reader to an illustrative derivation by Schmit and Lucas [2] which attracted much attention when it was published. A very similar calculation was performed independently by Craig [3]. The derivation is valid for both polar semiconductors or insulators and metals. Here we do not need to bother about these complications. We do not create interfaces. We just move them around.

### 9.2.2 Planar Layer

For a layer, Fig. 9.2, with interfaces at  $z = a$  and  $z = a + d$  made of a medium having dielectric function  $\tilde{\epsilon}_1$  sandwiched in between a medium having dielectric function  $\tilde{\epsilon}_0$  and a medium having dielectric function  $\tilde{\epsilon}_2$  we have from (9.10)

$$\begin{aligned} \tilde{\mathbf{M}} = \tilde{\mathbf{M}}_0 \cdot \tilde{\mathbf{M}}_1 &= \frac{1}{2\tilde{\epsilon}_0} \begin{pmatrix} \tilde{\epsilon}_0 + \tilde{\epsilon}_1 & e^{2ka} (\tilde{\epsilon}_0 - \tilde{\epsilon}_1) \\ e^{-2ka} (\tilde{\epsilon}_0 - \tilde{\epsilon}_1) & \tilde{\epsilon}_0 + \tilde{\epsilon}_1 \end{pmatrix} \\ &\times \frac{1}{2\tilde{\epsilon}_1} \begin{pmatrix} \tilde{\epsilon}_1 + \tilde{\epsilon}_2 & e^{2k(a+d)} (\tilde{\epsilon}_1 - \tilde{\epsilon}_2) \\ e^{-2k(a+d)} (\tilde{\epsilon}_1 - \tilde{\epsilon}_2) & \tilde{\epsilon}_1 + \tilde{\epsilon}_2 \end{pmatrix}. \end{aligned} \tag{9.13}$$

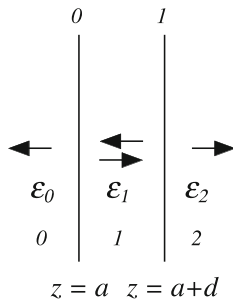


**Fig. 9.2** The geometry of a planar layer of thickness  $d$  and first interface located at  $z = a$ . The material to the left of the layer has the dielectric function  $\tilde{\epsilon}_0(\omega)$  and the material to the right of the layer  $\tilde{\epsilon}_2(\omega)$ . The layer material has the dielectric function  $\tilde{\epsilon}_1(\omega)$ . If this is the whole structure there are only waves moving away from the layer, as indicated by the arrows. In the layer itself there are waves moving in both directions. Adapted from [10]

If this layer constitutes the whole structure the mode condition becomes

$$[\tilde{\epsilon}_0(\omega) + \tilde{\epsilon}_1(\omega)][\tilde{\epsilon}_1(\omega) + \tilde{\epsilon}_2(\omega)] - e^{-2kd} [\tilde{\epsilon}_0(\omega) - \tilde{\epsilon}_1(\omega)][\tilde{\epsilon}_2(\omega) - \tilde{\epsilon}_1(\omega)] = 0. \quad (9.14)$$

This is the geometry of a slab. If we let the medium in the middle be vacuum the geometry represents two half spaces separated by a gap of width  $d$ .

### 9.2.3 2D Planar Film

In many situations one is dealing with very thin films. These may be considered 2D (two dimensional). Important examples are a graphene sheet and a 2D electron gas. In the derivation we let the film have finite thickness  $\delta$  and be characterized by a 3D dielectric function  $\tilde{\epsilon}^{3D}$ . We then let the thickness go toward zero. The 3D dielectric function depends on  $\delta$  as  $\tilde{\epsilon}^{3D} \sim 1/\delta$  for small  $\delta$  and  $\delta\tilde{\epsilon}^{3D} \rightarrow 2\tilde{\alpha}^{2D}/k$  as  $\delta$  goes toward zero [4, 5].  $\tilde{\alpha}^{2D}(\mathbf{k}, \omega)$  is the 2D polarizability of the film. We use the expression for a layer in (9.13) and let  $\tilde{\epsilon}_1$  go toward infinity and the layer thickness  $\delta$  go toward zero. Then we obtain

$$\begin{aligned} \tilde{\mathbf{M}}_{2D} &= \tilde{\mathbf{M}}_0 \cdot \tilde{\mathbf{M}}_1 \\ &= \frac{1}{2\tilde{\epsilon}_0} \begin{pmatrix} \tilde{\epsilon}_0 + \tilde{\epsilon}_2 & e^{2ka}(\tilde{\epsilon}_0 - \tilde{\epsilon}_2) \\ e^{-2ka}(\tilde{\epsilon}_0 - \tilde{\epsilon}_2) & \tilde{\epsilon}_0 + \tilde{\epsilon}_2 \end{pmatrix} + \frac{k(\delta\tilde{\epsilon}_1)}{2\tilde{\epsilon}_0} \begin{pmatrix} 1 & e^{2ka} \\ -e^{-2ka} & -1 \end{pmatrix} \\ &= \frac{1}{2\tilde{\epsilon}_0} \begin{pmatrix} \tilde{\epsilon}_0 + \tilde{\epsilon}_2 & e^{2ka}(\tilde{\epsilon}_0 - \tilde{\epsilon}_2) \\ e^{-2ka}(\tilde{\epsilon}_0 - \tilde{\epsilon}_2) & \tilde{\epsilon}_0 + \tilde{\epsilon}_2 \end{pmatrix} + \frac{\tilde{\alpha}^{2D}}{\tilde{\epsilon}_0} \begin{pmatrix} 1 & e^{2ka} \\ -e^{-2ka} & -1 \end{pmatrix}. \end{aligned} \quad (9.15)$$

If the 2D layer is the whole structure the condition for modes is

$$1 + 2\tilde{\alpha}^{2D}(\mathbf{k}, \omega) / [\tilde{\epsilon}_0(\omega) + \tilde{\epsilon}_2(\omega)] = 0, \quad (9.16)$$

where the modes are the 2D plasmons.

If the 2D film is inside a medium having dielectric function  $\tilde{\epsilon}_0(\omega)$  (9.15) simplifies into

$$\tilde{\mathbf{M}}_{2D} = \tilde{\mathbf{M}}_0 \cdot \tilde{\mathbf{M}}_1 = \begin{pmatrix} 1 & 0 \\ 0 & 1 \end{pmatrix} + \frac{\tilde{\alpha}^{2D}(\mathbf{k}, \omega)}{\tilde{\epsilon}_0(\omega)} \begin{pmatrix} 1 & e^{2ka} \\ -e^{-2ka} & -1 \end{pmatrix}, \quad (9.17)$$

and if the medium is vacuum we find

$$\tilde{\mathbf{M}}_{2D} = \tilde{\mathbf{M}}_0 \cdot \tilde{\mathbf{M}}_1 = \begin{pmatrix} 1 & 0 \\ 0 & 1 \end{pmatrix} + \tilde{\alpha}^{2D}(\mathbf{k}, \omega) \begin{pmatrix} 1 & e^{2ka} \\ -e^{-2ka} & -1 \end{pmatrix}. \quad (9.18)$$

Note that spatial dispersion is taken into account for the film without complications.

### 9.2.4 Thin Planar Diluted Gas Film

It is of interest to find the van der Waals force on an atom in a layered structure. We can obtain this by studying the force on a thin layer of a diluted gas having dielectric function  $\epsilon_g(\omega) = 1 + 4\pi n\alpha^{at}(\omega)$ , where  $\alpha^{at}$  is the polarizability of one atom and  $n$  the density of atoms (we have assumed that the atom is surrounded by vacuum; if not the 1 should be replaced by the dielectric function of the ambient medium and the atomic polarizability should be replaced by the excess polarizability). For a diluted gas layer the atoms do not interact with each other<sup>2</sup> and the force on the layer is just the sum of the forces on the individual atoms. So by dividing with the number of atoms in the film we get the force on one atom. The layer has to be thin in order to have a well defined  $z$ -value of the atom. Since we will derive the force on an atom in different planar geometries it is fruitful to derive the matrix for a thin diluted gas film. This result can be directly used in the derivation of the van der Waals force on an atom in different planar geometries.

We let the film have the thickness  $\delta$  and be placed in the general position  $z$ . We only keep terms up to linear order in  $\delta$  and linear order in  $n$ . We find the result is

$$\begin{aligned}\tilde{\mathbf{M}}_{\text{gaslayer}} &= \tilde{\mathbf{M}}_0 \cdot \tilde{\mathbf{M}}_1 \\ &= \begin{pmatrix} 1 & 0 \\ 0 & 1 \end{pmatrix} + (\delta n) \alpha^{at}(\omega) 4\pi k \begin{pmatrix} 0 & e^{2kz} \\ -e^{-2kz} & 0 \end{pmatrix} \\ &= \begin{pmatrix} 1 & 0 \\ 0 & 1 \end{pmatrix} + n^{2D} \alpha^{at}(\omega) 4\pi k \begin{pmatrix} 0 & e^{2kz} \\ -e^{-2kz} & 0 \end{pmatrix},\end{aligned}\quad (9.19)$$

where  $n^{2D}$  is the 2D atom density. Now we are done with the gas layer. We will use these results later in calculating the van der Waals force on an atom in planar layered structures. We have also gone through all basic structure elements we need. Now we turn to some real structures. We begin with two half spaces.

## 9.3 Two Half Spaces

For a gap, of size  $d$ , filled with a medium having dielectric function  $\tilde{\epsilon}_0$  between two half spaces, one of a material having dielectric function  $\tilde{\epsilon}_1$  and one of a material having dielectric function  $\tilde{\epsilon}_2$  we may reuse the above result in (9.14) with the proper change of dielectric functions. We find

$$[\tilde{\epsilon}_1 + \tilde{\epsilon}_0][\tilde{\epsilon}_2 + \tilde{\epsilon}_0] - e^{-2kd} [\tilde{\epsilon}_1 - \tilde{\epsilon}_0][\tilde{\epsilon}_2 - \tilde{\epsilon}_0] = 0, \quad (9.20)$$

where all dielectric function arguments,  $(\omega)$ , have been suppressed. Equation (9.20) can then be used to find the zero temperature van der Waals energy per unit area as (5.59)

---

<sup>2</sup>It is more correct to say that the effect of the interactions is negligible.

$$\begin{aligned}
E &= \frac{\hbar}{2} \int \frac{d^2k}{(2\pi)^2} \int_{-\infty}^{\infty} \frac{d\xi}{2\pi} [\ln f_{\mathbf{k}}(i\xi) - \ln f_{\mathbf{k}}^{\infty}(i\xi)] \\
&= \frac{\hbar}{2} \int \frac{d^2k}{(2\pi)^2} \int_{-\infty}^{\infty} \frac{d\xi}{2\pi} \ln \tilde{f}_{\mathbf{k}}(i\xi),
\end{aligned} \tag{9.21}$$

and the finite temperature result as (5.64)

$$\begin{aligned}
\mathfrak{F} &= \frac{1}{\beta} \int \frac{d^2k}{(2\pi)^2} \sum_{\xi_n} [\ln f_{\mathbf{k}}(i\xi_n) - \ln f_{\mathbf{k}}^{\infty}(i\xi_n)] \\
&= \frac{1}{\beta} \int \frac{d^2k}{(2\pi)^2} \sum_{\xi_n} \ln \tilde{f}_{\mathbf{k}}(i\xi_n); \xi_n = \frac{2\pi n}{\hbar\beta}; n = 0, 1, 2, \dots,
\end{aligned} \tag{9.22}$$

respectively, where  $f_{\mathbf{k}}^{\infty}(z)$  is the mode condition function at infinite separation and

$$\tilde{f}_{\mathbf{k}}(z) = 1 - e^{-2kd} \frac{[\tilde{\varepsilon}_1(z) - \tilde{\varepsilon}_0(z)][\tilde{\varepsilon}_2(z) - \tilde{\varepsilon}_0(z)]}{[\tilde{\varepsilon}_1(z) + \tilde{\varepsilon}_0(z)][\tilde{\varepsilon}_2(z) + \tilde{\varepsilon}_0(z)]} \tag{9.23}$$

is the mode condition function divided by the function at infinite separation. The expressions in (9.21) and (9.22) mean that we have chosen the reference system to be the system when the gap is infinitely wide. This result agrees with the result in e.g. [6]. In what follows we will indicate when we refer to this modified mode condition function, that produces the energy zero when the objects are at infinite separation, by putting a tilde above the function.

The van der Waals force per unit area is obtained as minus the derivative of these energies with respect to the separation  $d$ .

The mode condition function for this geometry where we have two half spaces with vacuum in between is obtained from (9.23) by letting  $\varepsilon_0 = 1$ . Thus the energy per unit area between two half spaces as function of separation is (9.21) with the mode condition function given by

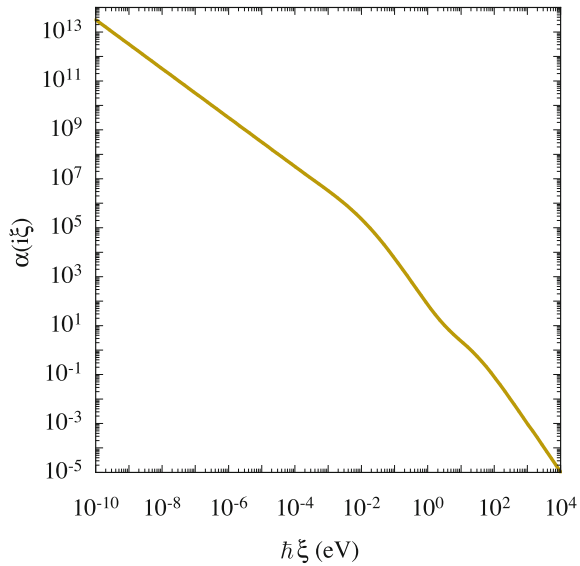
$$\tilde{f}_{\mathbf{k}}(z) = 1 - e^{-2kd} \frac{[\tilde{\varepsilon}_1(z) - 1][\tilde{\varepsilon}_2(z) - 1]}{[\tilde{\varepsilon}_1(z) + 1][\tilde{\varepsilon}_2(z) + 1]} \tag{9.24}$$

### 9.3.1 Interaction Between Two Gold Half Spaces

Now we will present results for a specific system, viz., two gold half spaces. Then the mode condition function is

$$\tilde{f}_{\mathbf{k}}(z) = 1 - e^{-2kd} \frac{[\alpha(z)]^2}{[\alpha(z) + 2]^2}, \tag{9.25}$$

**Fig. 9.3** The polarizability,  $\alpha(i\xi) = \tilde{\epsilon}(i\xi) - 1$ , for gold along the imaginary z-axis, used in our calculations. These results were obtained applying (3.52) to optical data from [7]. See the text for details



where  $\alpha(i\xi)$  is shown in Fig. 9.3 and the energy per unit area is

$$\begin{aligned} \frac{V(d)}{A} &= \hbar \int \frac{d^2k}{(2\pi)^2} \int_0^\infty \frac{d\xi}{2\pi} \ln \left[ 1 - e^{-2kd} \frac{[\alpha(i\xi)]^2}{[\alpha(i\xi)+2]^2} \right] \\ &= \frac{\hbar}{4(2\pi)^2 d^2} \int_0^\infty dx x \int_0^\infty d\xi \ln \left[ 1 - e^{-x} \frac{[\alpha(i\xi)]^2}{[\alpha(i\xi)+2]^2} \right], \end{aligned} \tag{9.26}$$

where we on the last line have made the variable substitution  $x = 2kd$ . The result for two gold half spaces is shown in Fig. 9.5.

The gold polarizability in Fig. 9.3 was obtained in the following way: the experimental data for the imaginary part of the dielectric function as given in [7] was used; these data points are shown in Fig. 9.4 as filled circles. The data were extrapolated on both the small and large frequency sides; these extrapolations are shown as a dotted curve and a thin straight line, respectively; at the large frequency side the extrapolation was a power law,  $\sim \omega^{-3}$ ; at the low frequency side the extrapolation was in the form of a function,

$$\epsilon_2(\omega) = \frac{4\pi}{\omega} \frac{\rho}{\rho^2 + (4\pi\omega/x^2)^2}, \tag{9.27}$$

where  $\rho$  is the experimental static resistivity ( $2.611 \times 10^{-18}$  s) and  $x$  is an adjustable parameter used to get a smooth transition to the experimental points. For  $x = \omega_{pl}$  (9.27) is the Drude expression with dissipation. Then we used one version, (3.52) of the Kramers Kronig dispersion relations,

**Fig. 9.4** The imaginary part of the dielectric function of gold used as input to generate Fig. 9.3. The *filled circles* are the experimental values from [7]. The *dotted curve* is the low frequency extrapolation consistent with the static resistivity. The *solid straight line* is the high frequency extrapolation of  $\sim\omega^{-3}$  type. See the text for details

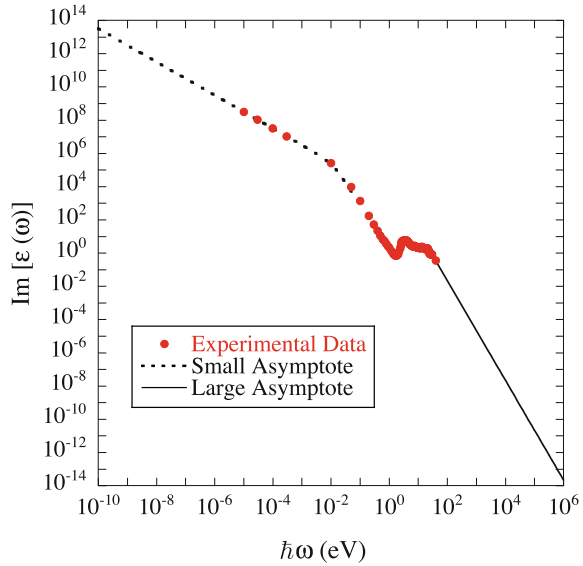
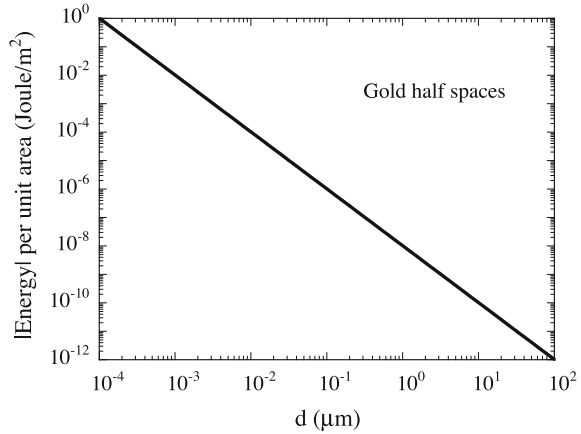


**Fig. 9.5** The van der Waals interaction energy between two gold half spaces as function of separation  $d$ . The result was obtained from using (9.26) with the gold polarizability  $\alpha(i\xi)$  as shown in Fig. 9.3



$$\tilde{\alpha}(i\xi) = \frac{2}{\pi} \int_0^{\infty} d\omega \frac{\omega \tilde{\epsilon}_2(\omega)}{(\omega^2 + \xi^2)}, \quad (9.28)$$

to find the polarizability on the imaginary axis. In performing the calculation we used cubic spline interpolation of the data on a log-log plot and the integration variable was chosen to be  $\ln(\omega)$ .

## 9.4 Two Slabs

We will make this as simple as possible and let the slabs be of the same material having dielectric function  $\tilde{\epsilon}_1$ , be of the same thickness,  $\Delta$ , and be placed in vacuum. The slabs are separated by the closest distance  $d$ . We let the interfaces of the first slab be at  $z = 0$  and  $z = \Delta$ ; then the interfaces of the second are at  $z = d + \Delta$  and at  $z = d + 2\Delta$ .

We can write the matrix for the structure as

$$\begin{aligned} \tilde{\mathbf{M}} &= \tilde{\mathbf{A}} \cdot \tilde{\mathbf{B}}, \\ \tilde{\mathbf{A}} &= \frac{1}{4\tilde{\epsilon}_1} \begin{pmatrix} 1 + \tilde{\epsilon}_1 & 1 - \tilde{\epsilon}_1 \\ 1 - \tilde{\epsilon}_1 & 1 + \tilde{\epsilon}_1 \end{pmatrix} \cdot \begin{pmatrix} \tilde{\epsilon}_1 + 1 & e^{2k\Delta} (\tilde{\epsilon}_1 - 1) \\ e^{-2k\Delta} (\tilde{\epsilon}_1 - 1) & \tilde{\epsilon}_1 + 1 \end{pmatrix}, \\ \tilde{\mathbf{B}} &= \frac{1}{4\tilde{\epsilon}_1} \begin{pmatrix} 1 + \tilde{\epsilon}_1 & e^{2k(d+\Delta)} (1 - \tilde{\epsilon}_1) \\ e^{-2k(d+\Delta)} (1 - \tilde{\epsilon}_1) & 1 + \tilde{\epsilon}_1 \end{pmatrix} \\ &\cdot \begin{pmatrix} \tilde{\epsilon}_1 + 1 & e^{2k(d+2\Delta)} (\tilde{\epsilon}_1 - 1) \\ e^{-2k(d+2\Delta)} (\tilde{\epsilon}_1 - 1) & \tilde{\epsilon}_1 + 1 \end{pmatrix}, \end{aligned} \quad (9.29)$$

where  $\tilde{\mathbf{A}}$  and  $\tilde{\mathbf{B}}$  are matrices for slabs or planar layers according to Fig. 9.2. The matrices are obtained from (9.13) with the proper choice of dielectric functions combinations and positions.

To find the condition for modes and the mode condition function we only need the matrix element  $M_{11}$ . It is

$$M_{11} = \frac{1}{16\tilde{\epsilon}_1^2} \left\{ \left[ (\tilde{\epsilon}_1 + 1)^2 - e^{-2k\Delta} (\tilde{\epsilon}_1 - 1)^2 \right]^2 - (\tilde{\epsilon}_1^2 - 1)^2 e^{-2kd} [e^{-2k\Delta} - 1]^2 \right\}, \quad (9.30)$$

and the condition for modes is

$$\left[ (\tilde{\epsilon}_1 + 1)^2 - e^{-2k\Delta} (\tilde{\epsilon}_1 - 1)^2 \right]^2 - (\tilde{\epsilon}_1^2 - 1)^2 e^{-2kd} [e^{-2k\Delta} - 1]^2 = 0. \quad (9.31)$$

The mode condition function then becomes

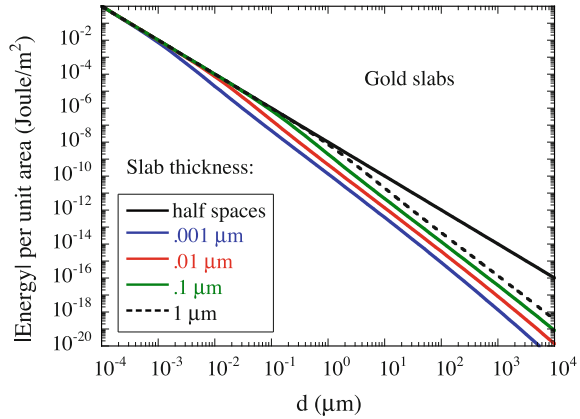
$$\tilde{f}_{\mathbf{k}}(z) = 1 - e^{-2kd} \frac{[\tilde{\epsilon}_1^2(z) - 1]^2 (e^{-2k\Delta} - 1)^2}{\left\{ [\tilde{\epsilon}_1(z) + 1]^2 - e^{-2k\Delta} [\tilde{\epsilon}_1(z) - 1]^2 \right\}^2}, \quad (9.32)$$

or

$$\tilde{f}_{\mathbf{k}}(z) = 1 - e^{-2kd} \frac{\left[ \frac{\tilde{\epsilon}_1(z) - 1}{\tilde{\epsilon}_1(z) + 1} \right]^2 (e^{-2k\Delta} - 1)^2}{\left\{ 1 - e^{-2k\Delta} \left[ \frac{\tilde{\epsilon}_1(z) - 1}{\tilde{\epsilon}_1(z) + 1} \right]^2 \right\}^2}. \quad (9.33)$$

To find this result we have divided the left-hand-side of (9.31) with the corresponding result for  $d = \infty$ . Thus the energy per unit area between two slabs as function of

**Fig. 9.6** The van der Waals interaction energy between two gold slabs of thickness  $\Delta$  as function of separation  $d$ . The result was obtained from using (9.33) with the gold polarizability  $\alpha(i\xi)$  as shown in Fig. 9.3. See the text for details



separation is (9.21) with this mode condition function inserted. The corresponding van der Waals energy at finite temperature is obtained by using this function in (9.22) instead. The force per unit area is in both cases found by taking minus the derivative of the energy with respect to  $d$ .

#### 9.4.1 Interaction Between Two Gold Slabs

The result for two gold slabs is shown in Fig. 9.6 for slab thickness ranging from  $0.001\mu\text{m}$  to infinity; the thinner the slabs the lower the energy. To find the result we have inserted the mode condition function from (9.33) in (9.21). The dielectric function  $\tilde{\epsilon}_1(i\xi) = 1 + \alpha(i\xi)$  with the gold polarizability  $\alpha(i\xi)$  as shown in Fig. 9.3. We notice that when the distance between the slabs is much smaller than the slab thickness the result is that for two half spaces; when the separation is much larger than the slab thickness the result has a steeper slope. If we had used the simple Drude approximation,  $\tilde{\epsilon}_1(i\xi) = 1 + \omega_{pl}^2/\xi^2$ , for the gold dielectric function we would have found the fractional power law [9],  $\sim d^{-5/2}$ , characteristic of two 2D metal films. With the experimental dielectric function of gold the resulting slope is somewhat steeper.

### 9.5 Two 2D Films

The matrix for a system of two parallel 2D films becomes  $\tilde{\mathbf{M}} = \tilde{\mathbf{M}}_0 \cdot \tilde{\mathbf{M}}_1 \cdot \tilde{\mathbf{M}}_2 \cdot \tilde{\mathbf{M}}_3$ , where  $\tilde{\mathbf{M}}_0 \cdot \tilde{\mathbf{M}}_1$  is the matrix for one of the two thin films, and  $\tilde{\mathbf{M}}_2 \cdot \tilde{\mathbf{M}}_3$  is the matrix for the other. These matrices are given in (9.15) the first for  $z = 0$  and the second for  $z = d$ .

The matrices are

$$\begin{aligned}\tilde{\mathbf{M}}_0 \cdot \tilde{\mathbf{M}}_1 &= \begin{pmatrix} 1 & 0 \\ 0 & 1 \end{pmatrix} + \tilde{\alpha}^{2D} \begin{pmatrix} 1 & 1 \\ -1 & -1 \end{pmatrix}; \\ \tilde{\mathbf{M}}_2 \cdot \tilde{\mathbf{M}}_3 &= \begin{pmatrix} 1 & 0 \\ 0 & 1 \end{pmatrix} + \tilde{\alpha}^{2D} \begin{pmatrix} 1 & e^{2kd} \\ -e^{-2kd} & -1 \end{pmatrix},\end{aligned}\quad (9.34)$$

and the element of interest to us is

$$\begin{aligned}M_{11} &= 1 + 2\tilde{\alpha}^{2D} + (1 - e^{-2kd}) (\tilde{\alpha}^{2D})^2 \\ &= (1 + \tilde{\alpha}^{2D})^2 - e^{-2kd} (\tilde{\alpha}^{2D})^2.\end{aligned}\quad (9.35)$$

The first term produces the modes in the two thin films if they are so far apart that they are not affecting each other. We choose as our reference system the system when the two films are at infinite distance from each other. To get the mode condition function we divide  $M_{11}$  with the first term. The mode condition function becomes

$$\tilde{f}_k = 1 - e^{-2kd} \left( \frac{\tilde{\alpha}^{2D}}{1 + \tilde{\alpha}^{2D}} \right)^2. \quad (9.36)$$

From this we find the energy per unit area

$$\begin{aligned}E &= \frac{\hbar}{2} \int \frac{d^2k}{(2\pi)^2} \int_{-\infty}^{\infty} \frac{d\xi}{2\pi} \ln \left[ \tilde{f}_k(i\xi) \right] \\ &= \frac{\hbar}{2} \int \frac{d^2k}{(2\pi)^2} \int_{-\infty}^{\infty} \frac{d\xi}{2\pi} \ln \left[ 1 - e^{-2kd} \left( \frac{\tilde{\alpha}^{2D}(\mathbf{k}, i\xi)}{1 + \tilde{\alpha}^{2D}(\mathbf{k}, i\xi)} \right)^2 \right].\end{aligned}\quad (9.37)$$

This agrees completely with the results of [8].

### 9.5.1 Interaction Between Two Graphene Sheets

The first example where we use the results for two 2D films is two graphene sheets. Graphene is one very promising material in modern nano-technology. We will give results both for pristine (undoped) and for doped graphene. The separation dependence becomes very simple for pristine graphene. We need the 2D polarizability. From (2.143) we get

$$\begin{aligned}\chi(\mathbf{k}, i\xi) &= -\frac{1}{4\hbar} \frac{k^2}{\sqrt{v^2k^2 + \xi^2}}, \\ \alpha(\mathbf{k}, i\xi) &= \frac{\pi e^2}{2\hbar} \frac{k}{\sqrt{v^2k^2 + \xi^2}}.\end{aligned}\quad (9.38)$$

We note the peculiar scaling property  $\alpha(\mathbf{k}/d, i\xi/d) = \alpha(\mathbf{k}, i\xi)$ . Thus if we plot the polarizability on a  $k\xi$  plane and then change units with the same factor on both axes nothing changes. Thus making the substitutions  $\mathbf{k} \rightarrow \mathbf{k}/d$  and  $\xi \rightarrow \xi/d$  in (9.37) gives

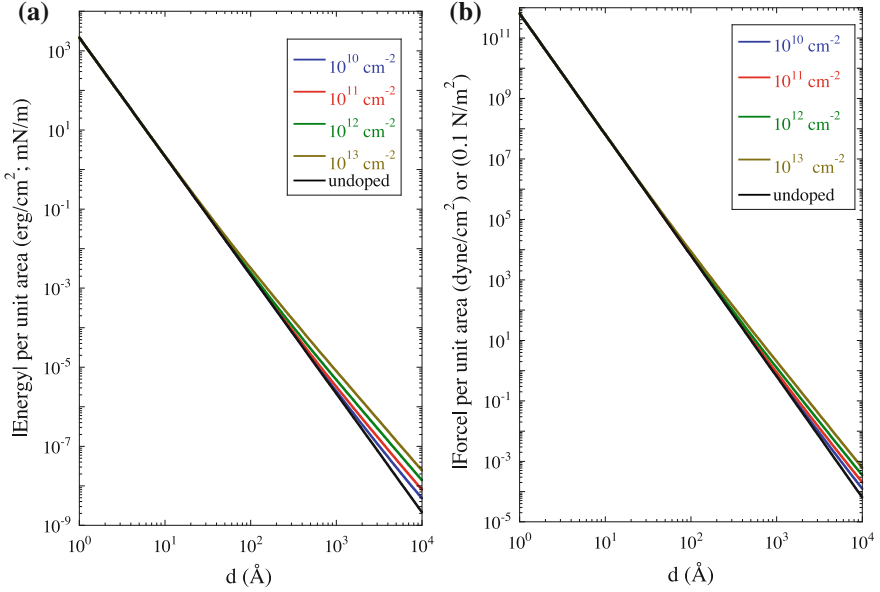


**Fig. 9.7** Interaction energy (a) and force (b) per unit area, respectively, between two graphene sheets a distance  $d$  apart. See the text for details

$$E = \frac{\hbar}{2d^3} \int \frac{d^2k}{(2\pi)^2} \int_{-\infty}^{\infty} \frac{d\xi}{2\pi} \ln \left[ 1 - e^{-2k} \left( \frac{\tilde{\alpha}(k, i\xi)}{1 + \tilde{\alpha}(k, i\xi)} \right)^2 \right], \quad (9.39)$$

and the interaction follows a simple power law  $E \sim d^{-3}$ . The force varies as  $F \sim d^{-4}$ . In the doped case  $\alpha^{2D}(\mathbf{k}, i\xi) = -v_q^{2D} \chi^{2D}(\mathbf{k}, i\xi)$  where  $\chi^{2D}(\mathbf{k}, i\xi)$  is given in (2.145). Here, we do not benefit from the above substitutions and use (9.37) instead. The results are shown in Fig. 9.7 both for pristine graphene and for doped graphene; the deviation from the result for pristine graphene increases with doping concentration. In the doped case the effects of the doping carriers show up gradually for larger separations. The energy approaches asymptotically a fractional power law with  $E \sim d^{-5/2}$  and  $F \sim d^{-7/2}$ . The extra interaction from the free carriers decreases gradually for small separations. This behavior is caused by spatial dispersion. Next, we turn to two thin metal films.

### 9.5.2 Interaction Between Two 2D Metal Films

In calculating the interaction between two 2D metal films we use (9.37) with the polarizability for a 2D electron gas in (2.146). The results are shown in Fig. 9.8. The carrier concentration in each film varies from  $10^{10}$  to  $10^{13}$   $\text{cm}^{-2}$ ; the higher the concentration the higher the interaction energy. The energy approaches asymptotically a fractional power law with  $E \sim d^{-5/2}$  and  $F \sim d^{-7/2}$ .

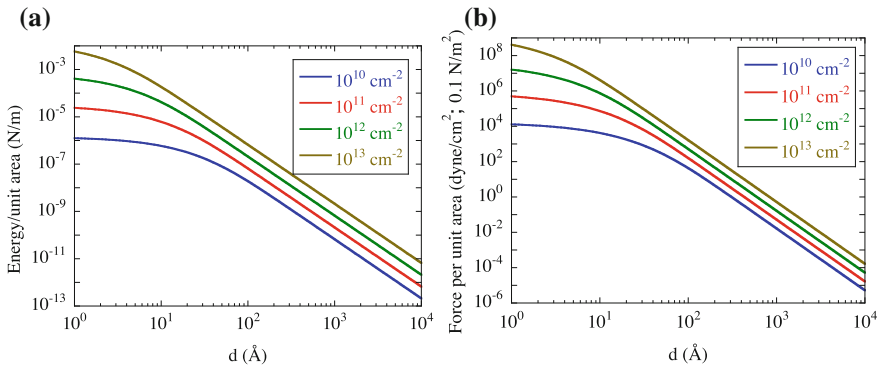


**Fig. 9.8** Interaction energy (a) and force (b) per unit area, respectively, between two 2D metal films a distance  $d$  apart. See the text for details

To see how this power law comes about we note that the exponential factor  $e^{-2kd}$  in the integrand in (9.37) means that for large separations only small  $k$ -values contribute to the momentum integral. The 2D dielectric function (see (2.146)) in the small momentum limit is

$$\tilde{\epsilon}^{2D}(\mathbf{k}, i\xi) \approx 1 + \frac{2\pi n^{2D} e^2 k}{m_e \xi^2}. \quad (9.40)$$

So if we make the substitutions  $k \rightarrow k/d$ , and  $\xi \rightarrow \xi/\sqrt{d}$  in (9.37) we find

$$\tilde{\epsilon}^{2D}(\mathbf{k}/d, i\xi/\sqrt{d}) \approx 1 + \frac{2\pi n^{2D} e^2 k}{m_e \xi^2}, \quad (9.41)$$

i.e. the  $d$ s in the dielectric function cancel out and no  $d$  remains in the integrand. We have

$$E \approx \frac{\hbar}{2d^{5/2}} \int \frac{d^2k}{(2\pi)^2} \int_{-\infty}^{\infty} \frac{d\xi}{2\pi} \ln \left[ 1 - e^{-2k} \left( \frac{\tilde{\alpha}^{2D}(\mathbf{k}, i\xi)}{1 + \tilde{\alpha}^{2D}(\mathbf{k}, i\xi)} \right)^2 \right]. \quad (9.42)$$

The only remaining  $d$ -dependence lies in the factor  $d^{-5/2}$ , which is the result of the substitutions in  $d^2k$  and  $d\xi$ . For smaller separations the energy and force no longer follow simple power laws. For more details of the fractional power dependence see [8, 9]. Now we are done with examples of 2D films and turn to the film-wall geometry.

## 9.6 Film-Wall

We let the film be at  $z = 0$  and the wall interface at  $z = d$ . We assume that the film is surrounded by vacuum. The matrix for the film-wall geometry we find by multiplying the matrix for a 2D film (9.18) for  $a = 0$  with the matrix of a single vacuum-medium interface (9.11), i.e.,

$$\begin{aligned}\tilde{\mathbf{M}} &= \tilde{\mathbf{A}} \cdot \tilde{\mathbf{B}}, \\ \tilde{\mathbf{A}} &= \begin{pmatrix} 1 & 0 \\ 0 & 1 \end{pmatrix} + \tilde{\alpha}^{2D} \begin{pmatrix} 1 & 1 \\ -1 & -1 \end{pmatrix}, \\ \tilde{\mathbf{B}} &= \frac{1}{2} \begin{pmatrix} (1 + \tilde{\varepsilon}_1) & e^{2kd} (1 - \tilde{\varepsilon}_1) \\ e^{-2kd} (1 - \tilde{\varepsilon}_1) & (1 + \tilde{\varepsilon}_1) \end{pmatrix},\end{aligned}\tag{9.43}$$

where  $\tilde{\varepsilon}_1(\omega)$  is the dielectric function of the wall.

We are interested in the matrix element  $M_{11}$ . It is

$$\begin{aligned}M_{11} &= \frac{1}{2} \left\{ (1 + \tilde{\varepsilon}_1) + \tilde{\alpha}^{2D} \left[ (1 + \tilde{\varepsilon}_1) + e^{-2kd} (1 - \tilde{\varepsilon}_1) \right] \right\} \\ &= \frac{1}{2} (1 + \tilde{\varepsilon}_1) (1 + \tilde{\alpha}^{2D}) \left\{ 1 - e^{-2kd} \frac{\tilde{\alpha}^{2D}}{1 + \tilde{\alpha}^{2D}} \frac{\tilde{\varepsilon}_1 - 1}{\tilde{\varepsilon}_1 + 1} \right\}.\end{aligned}\tag{9.44}$$

The condition for modes is  $M_{11} = 0$  and the mode condition function is

$$\tilde{f}_{\mathbf{k}}(z) = \left\{ 1 - e^{-2kd} \frac{\tilde{\alpha}^{2D}(\mathbf{k}, z)}{1 + \tilde{\alpha}^{2D}(\mathbf{k}, z)} \frac{\tilde{\varepsilon}_1(z) - 1}{\tilde{\varepsilon}_1(z) + 1} \right\},\tag{9.45}$$

and the van der Waals interaction energy per unit area between a film and a wall is

$$\begin{aligned}E &= \frac{\hbar}{2} \int \frac{d^2k}{(2\pi)^2} \int_{-\infty}^{\infty} \frac{d\xi}{2\pi} \ln \left[ \tilde{f}_{\mathbf{k}}(i\xi) \right] \\ &= \frac{\hbar}{2} \int \frac{d^2k}{(2\pi)^2} \int_{-\infty}^{\infty} \frac{d\xi}{2\pi} \ln \left[ 1 - e^{-2kd} \frac{\tilde{\alpha}^{2D}(\mathbf{k}, i\xi)}{1 + \tilde{\alpha}^{2D}(\mathbf{k}, i\xi)} \frac{\tilde{\varepsilon}_1(i\xi) - 1}{\tilde{\varepsilon}_1(i\xi) + 1} \right].\end{aligned}\tag{9.46}$$

Again we illustrate the result with two examples where the film is a graphene sheet and a 2D metal film, respectively. We begin with graphene next to a gold wall.

### 9.6.1 Interaction Between Graphene and an Au-Wall

To find the interaction between graphene and a gold wall we insert into (9.46) the polarizability of graphene,  $\tilde{\alpha}^{2D}(\mathbf{k}, i\xi) = -v_{\mathbf{k}}^{2D} \chi^{2D}(\mathbf{k}, i\xi)$  where  $\chi^{2D}(\mathbf{k}, i\xi)$  is taken from (2.145) and the dielectric function of gold,  $\tilde{\varepsilon}_1(i\xi) = 1 + \tilde{\alpha}(i\xi)$ , where  $\tilde{\alpha}(i\xi)$  is shown in Fig. 9.3. The result is shown in Fig. 9.9 for both pristine and doped graphene. The  $d$  dependence does not follow a simple power law. Next example is a 2D metal film next to a gold wall.

**Fig. 9.9** Interaction energy per unit area between a graphene sheet and an Au wall separated by a distance  $d$ ; the results are for pristine graphene and for the doping densities  $10^{10}$ ,  $10^{11}$ ,  $10^{12}$ , and  $10^{13} \text{ cm}^{-2}$ . The bottom curve is for pristine graphene and the deviation from this curve increases with doping concentration

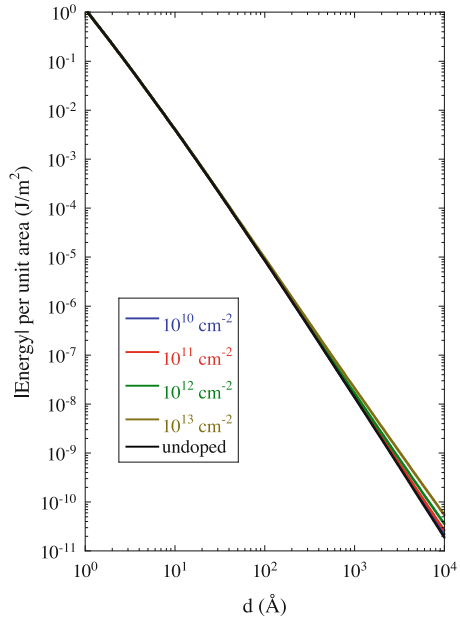
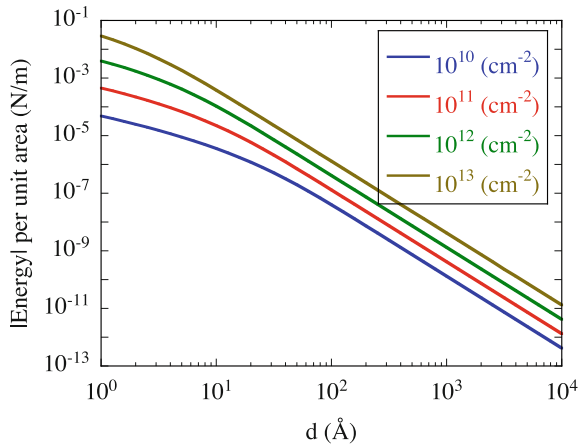


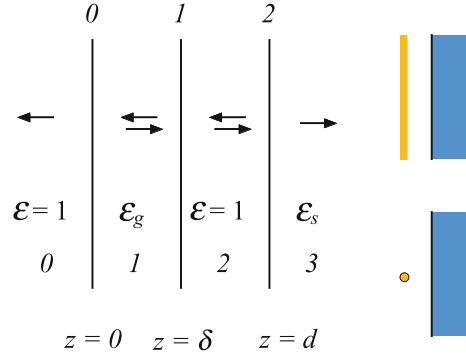
**Fig. 9.10** Interaction energy per unit area between a 2D metal film and an Au wall separated by a distance  $d$ ; the results are for the carrier densities  $10^{10}$ ,  $10^{11}$ ,  $10^{12}$ , and  $10^{13} \text{ cm}^{-2}$ . The interaction energy increases with carrier density



### 9.6.2 Interaction Between a 2D Metal Film and an Au-Wall

To find the interaction between a 2D metal film and a gold wall we insert into (9.46) the polarizability of a 2D electron gas from (2.146) and the dielectric function of gold,  $\tilde{\epsilon}_1(i\xi) = 1 + \tilde{\alpha}(i\xi)$ , where  $\tilde{\alpha}(i\xi)$  is shown in Fig. 9.3. The result is shown in Fig. 9.10 for different doping levels. The  $d$  dependence does not follow a simple power law. We move on to the atom-wall geometry.

**Fig. 9.11** The two planar layer geometry. This geometry is used to find the atom wall interaction as illustrated by the cartoon in the lower right corner. We start from the gas layer wall geometry in the upper right corner. Adapted from [10]



## 9.7 Atom-Wall

The multiple layer results can be used to solve other problems like in this case the atom wall interaction. We start from the two layer structure in Fig. 9.11. We let the ambient be vacuum. The first layer is a thin layer, of thickness  $\delta$ , of a diluted gas of atoms of the kind we consider. Its dielectric function is  $\epsilon_g(\omega) = 1 + 4\pi n\alpha^{at}(\omega)$ , where  $\alpha^{at}$  is the polarizability of one atom. The density of gas atoms,  $n$ , is very low. We let the first interface be at  $z = 0$  and hence the second at  $z = \delta$ . The second layer is a vacuum layer of thickness  $d$ . The remaining medium is the wall which we let be infinitely thick and have the dielectric function  $\tilde{\epsilon}_s(\omega)$ . In what follows we only keep lowest order terms in  $\delta$  and in  $n$ .

The matrix becomes  $\tilde{\mathbf{M}} = \tilde{\mathbf{M}}_0 \cdot \tilde{\mathbf{M}}_1 \cdot \tilde{\mathbf{M}}_2 = \tilde{\mathbf{M}}_{\text{gaslayer}} \cdot \tilde{\mathbf{M}}_2$  where  $\tilde{\mathbf{M}}_{\text{gaslayer}}$  is given in (9.19) with  $z = 0$  and

$$\tilde{\mathbf{M}}_2 = \frac{1}{2} \begin{pmatrix} (\tilde{\epsilon}_s + 1) & -e^{2kd}(\tilde{\epsilon}_s - 1) \\ -e^{-2kd}(\tilde{\epsilon}_s - 1) & (\tilde{\epsilon}_s + 1) \end{pmatrix}. \quad (9.47)$$

Now, the matrix element of interest is

$$M_{11} = \frac{1}{2} [(\tilde{\epsilon}_s + 1) - 4\pi k\alpha^{at}\delta n e^{-2kd}(\tilde{\epsilon}_s - 1)], \quad (9.48)$$

and the condition for modes is

$$(\tilde{\epsilon}_s + 1) - 4\pi k\alpha^{at}\delta n e^{-2kd}(\tilde{\epsilon}_s - 1) = 0. \quad (9.49)$$

The first part of the mode condition function is what one would have in absence of the atom. It gives the surface modes of the wall. We find

$$\tilde{f}_{\mathbf{k}}(z) = 1 - 4\pi k\alpha^{at}(z)\delta n e^{-2kd} \frac{[\tilde{\epsilon}_s(z) - 1]}{[\tilde{\epsilon}_s(z) + 1]}, \quad (9.50)$$

where we have chosen the reference system as the system when the atom is at infinite distance from the wall. The interaction energy per atom is

$$\begin{aligned}
 \frac{E}{n\delta} &= \frac{\hbar}{2n\delta} \int \frac{d^2k}{(2\pi)^2} \int_{-\infty}^{\infty} \frac{d\xi}{2\pi} \\
 &\times \ln \left[ 1 - 4\pi k \alpha^{at} (i\xi) \delta n e^{-2kd} \frac{[\tilde{\varepsilon}_s(i\xi)-1]}{[\tilde{\varepsilon}_s(i\xi)+1]} \right] \\
 &\approx -\frac{\hbar}{2} \int \frac{d^2k}{(2\pi)^2} 4\pi k e^{-2kd} \int_{-\infty}^{\infty} \frac{d\xi}{2\pi} \alpha^{at} (i\xi) \frac{[\tilde{\varepsilon}_s(i\xi)-1]}{[\tilde{\varepsilon}_s(i\xi)+1]} \\
 &= - \underbrace{\int_0^{\infty} dk k^2 2e^{-2kd}}_{\frac{1}{2d^3}} \frac{\hbar}{2} \int_{-\infty}^{\infty} \frac{d\xi}{2\pi} \alpha^{at} (i\xi) \frac{[\tilde{\varepsilon}_s(i\xi)-1]}{[\tilde{\varepsilon}_s(i\xi)+1]} \\
 &= -\frac{\hbar}{4d^3} \int_{-\infty}^{\infty} \frac{d\xi}{2\pi} \alpha^{at} (i\xi) \frac{[\tilde{\varepsilon}_s(i\xi)-1]}{[\tilde{\varepsilon}_s(i\xi)+1]}, \tag{9.51}
 \end{aligned}$$

where we have divided the energy per unit area with the number of gas atoms per unit area resulting in the energy per atom. We have furthermore let the number of atoms per unit area go toward zero and expanded the logarithm  $[\ln(1+x) \rightarrow x]$ .

Thus, the force between an atom a distance  $d$  from a wall is at zero temperature

$$F(d) = -\frac{3\hbar}{2d^4} \int_0^{\infty} \frac{d\xi}{2\pi} \alpha^{at} (i\xi) \frac{[\tilde{\varepsilon}_s(i\xi)-1]}{[\tilde{\varepsilon}_s(i\xi)+1]}, \tag{9.52}$$

and at finite temperature it is

$$F(d) = -\frac{3}{2d^4} \frac{1}{\beta} \sum_{\xi_n} \alpha^{at} (i\xi_n) \frac{[\tilde{\varepsilon}_s(i\xi_n)-1]}{[\tilde{\varepsilon}_s(i\xi_n)+1]}. \tag{9.53}$$

### 9.7.1 Li-Atom–Au-Wall Interaction

As an example of atom-wall interactions we show in Fig. 9.12 the interaction between a Li atom and a gold wall. The polarizability for Li was obtained from the London approximation (8.60) with the parameters given in Fig. 8.2. The  $d$ -dependence follows a simple power law,  $E \sim d^{-3}$ , and  $F \sim d^{-4}$ .

It is of interest to know how atoms interact with the walls when passing through narrow channels. A first step in such an investigation can be to study an atom in a planar gap. This is what we do next.

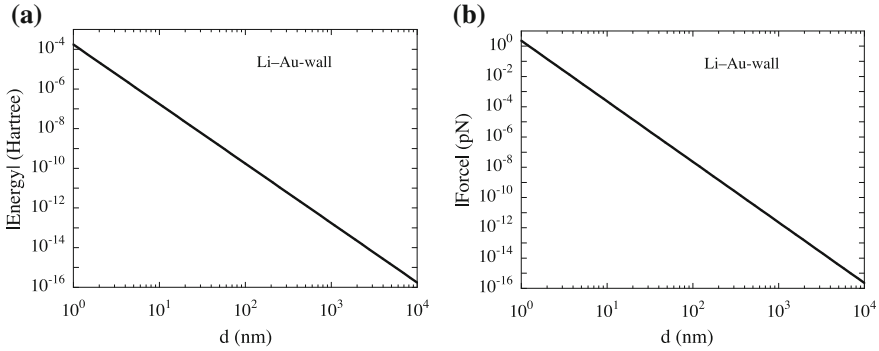
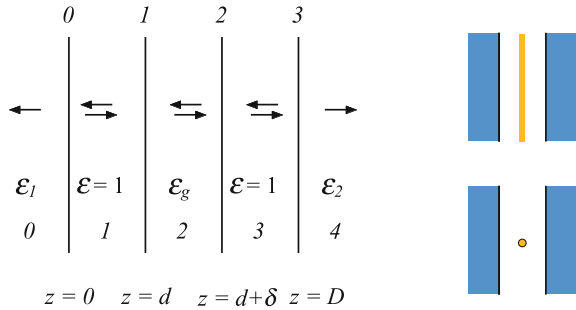


**Fig. 9.12** The van der Waals interaction between a Li atom and a gold wall as function of separation, *d*. **a** The interaction energy; **b** The force

**Fig. 9.13** The three planar layer geometry. Adapted from [10]



### 9.8 Atom in Planar Gap

We study an atom in a gap of width  $D$  between two thick plates (or half spaces). We refer to Fig. 9.13 and let the first interface be located at  $z = 0$  separating one plate having dielectric function  $\tilde{\epsilon}_1$  from the ambient medium which we let be vacuum. Next interface, at  $z = d$ , is the left interface of the gas layer having dielectric function  $\epsilon_g$  and thickness  $\delta$ . Thus the third interface is at  $z = d + \delta$ . The fourth interface is located at  $z = D$  and separates vacuum from the second plate having dielectric function  $\tilde{\epsilon}_2$ . Just as in the previous section we only keep lowest order terms in  $\delta$  and in  $n$ . The matrix becomes  $\tilde{\mathbf{M}} = \tilde{\mathbf{M}}_0 \cdot \tilde{\mathbf{M}}_1 \cdot \tilde{\mathbf{M}}_2 \cdot \tilde{\mathbf{M}}_3 = \tilde{\mathbf{M}}_0 \cdot \tilde{\mathbf{M}}_{\text{gaslayer}} \cdot \tilde{\mathbf{M}}_3$  where  $\tilde{\mathbf{M}}_{\text{gaslayer}}$  is given in (9.19) with  $z = d$  and

$$\begin{aligned} \tilde{\mathbf{M}}_0 &= \frac{1}{2\tilde{\epsilon}_1} \begin{pmatrix} (\tilde{\epsilon}_1 + 1) & (\tilde{\epsilon}_1 - 1) \\ (\tilde{\epsilon}_1 - 1) & (\tilde{\epsilon}_1 + 1) \end{pmatrix}; \\ \tilde{\mathbf{M}}_3 &= \frac{1}{2} \begin{pmatrix} (\tilde{\epsilon}_2 + 1) & -e^{2kD}(\tilde{\epsilon}_2 - 1) \\ -e^{-2kD}(\tilde{\epsilon}_2 - 1) & (\tilde{\epsilon}_2 + 1) \end{pmatrix}. \end{aligned} \tag{9.54}$$

Now,

$$M_{11} = \begin{pmatrix} M_{11}^0 & M_{12}^0 \end{pmatrix} \cdot \tilde{\mathbf{M}}_{\text{gaslayer}} \cdot \begin{pmatrix} M_{11}^3 \\ M_{21}^3 \end{pmatrix}, \quad (9.55)$$

where we have moved the matrix subscript to the superscript position to make room for the element subscripts. The matrix element of interest is

$$M_{11} = \frac{1}{4\tilde{\epsilon}_1} \left\{ [(\tilde{\epsilon}_1 + 1)(\tilde{\epsilon}_2 + 1) - e^{-2kD}(\tilde{\epsilon}_1 - 1)(\tilde{\epsilon}_2 - 1)] \right. \\ \left. - 4\pi k \alpha^{at} \delta n \left[ e^{-2kd}(\tilde{\epsilon}_1 - 1)(\tilde{\epsilon}_2 + 1) \right. \right. \\ \left. \left. + e^{-2k(D-d)}(\tilde{\epsilon}_1 + 1)(\tilde{\epsilon}_2 - 1) \right] \right\}. \quad (9.56)$$

The mode condition function after division with the function in absence of the gas layer is

$$\tilde{f}_{\mathbf{k}} = 1 - 4\pi k \alpha^{at} \delta n \frac{\left[ e^{-2kd} \frac{(\tilde{\epsilon}_1 - 1)}{(\tilde{\epsilon}_1 + 1)} + e^{-2k(D-d)} \frac{(\tilde{\epsilon}_2 - 1)}{(\tilde{\epsilon}_2 + 1)} \right]}{\left[ 1 - e^{-2kD} \frac{(\tilde{\epsilon}_1 - 1)(\tilde{\epsilon}_2 - 1)}{(\tilde{\epsilon}_1 + 1)(\tilde{\epsilon}_2 + 1)} \right]}, \quad (9.57)$$

and the interaction energy per atom becomes

$$\begin{aligned} \frac{E}{n\delta} &= \frac{\hbar}{2n\delta} \int \frac{d^2k}{(2\pi)^2} \int_{-\infty}^{\infty} \frac{d\xi}{2\pi} \ln \left[ \tilde{f}_{\mathbf{k}}(i\xi) \right] \\ &\approx -\frac{\hbar}{2} \int \frac{d^2k}{(2\pi)^2} 4\pi k \int_{-\infty}^{\infty} \frac{d\xi}{2\pi} \alpha^{at} \frac{\left[ e^{-2kd} \frac{(\tilde{\epsilon}_1 - 1)}{(\tilde{\epsilon}_1 + 1)} + e^{-2k(D-d)} \frac{(\tilde{\epsilon}_2 - 1)}{(\tilde{\epsilon}_2 + 1)} \right]}{\left[ 1 - e^{-2kD} \frac{(\tilde{\epsilon}_1 - 1)(\tilde{\epsilon}_2 - 1)}{(\tilde{\epsilon}_1 + 1)(\tilde{\epsilon}_2 + 1)} \right]} \\ &= -\hbar \int_0^{\infty} dk k^2 \int_{-\infty}^{\infty} \frac{d\xi}{2\pi} \alpha^{at} \frac{\left[ e^{-2kd} \frac{(\tilde{\epsilon}_1 - 1)}{(\tilde{\epsilon}_1 + 1)} + e^{-2k(D-d)} \frac{(\tilde{\epsilon}_2 - 1)}{(\tilde{\epsilon}_2 + 1)} \right]}{\left[ 1 - e^{-2kD} \frac{(\tilde{\epsilon}_1 - 1)(\tilde{\epsilon}_2 - 1)}{(\tilde{\epsilon}_1 + 1)(\tilde{\epsilon}_2 + 1)} \right]}. \end{aligned} \quad (9.58)$$

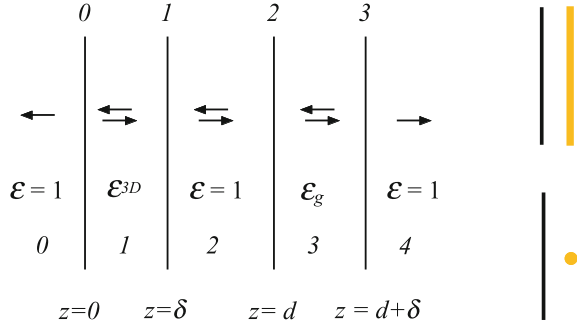
Thus, the force on the atom is

$$\begin{aligned} F(d) &= -4\hbar \int_0^{\infty} dk k^3 \int_{-\infty}^{\infty} \frac{d\xi}{2\pi} \alpha^{at}(i\xi) \\ &\quad \times \frac{\frac{[\tilde{\epsilon}_1(i\xi) - 1]}{[\tilde{\epsilon}_1(i\xi) + 1]} e^{-2kd} - \frac{[\tilde{\epsilon}_2(i\xi) - 1]}{[\tilde{\epsilon}_2(i\xi) + 1]} e^{-2k(D-d)}}{1 - \frac{[\tilde{\epsilon}_1(i\xi) - 1][\tilde{\epsilon}_2(i\xi) - 1]}{[\tilde{\epsilon}_1(i\xi) + 1][\tilde{\epsilon}_2(i\xi) + 1]} e^{-2kD}}, \end{aligned} \quad (9.59)$$

and at finite temperature it is

$$F(d) = -\frac{4}{\beta} \int_0^{\infty} dk k^3 \sum_{\xi_n} \alpha^{at}(i\xi_n) \frac{\frac{[\tilde{\epsilon}_1(i\xi_n) - 1]}{[\tilde{\epsilon}_1(i\xi_n) + 1]} e^{-2kd} - \frac{[\tilde{\epsilon}_2(i\xi_n) - 1]}{[\tilde{\epsilon}_2(i\xi_n) + 1]} e^{-2k(D-d)}}{1 - \frac{[\tilde{\epsilon}_1(i\xi_n) - 1][\tilde{\epsilon}_2(i\xi_n) - 1]}{[\tilde{\epsilon}_1(i\xi_n) + 1][\tilde{\epsilon}_2(i\xi_n) + 1]} e^{-2kD}}. \quad (9.60)$$

**Fig. 9.14** The geometry of a thin gas layer the distance  $d$  from a thin film. This geometry is used to find the interaction between an atom and a thin film. Adapted from [10]



## 9.9 Atom-Film

In this section we derive the van der Waals interaction of an atom near a very thin film. We start from the three layer structure in Fig. 9.14. We take the limit when the thickness of the film goes to zero. The matrix becomes  $\tilde{\mathbf{M}} = \tilde{\mathbf{M}}_0 \cdot \tilde{\mathbf{M}}_1 \cdot \tilde{\mathbf{M}}_2 \cdot \tilde{\mathbf{M}}_3$ , where  $\tilde{\mathbf{M}}_0 \cdot \tilde{\mathbf{M}}_1$  is the matrix for the thin film, and  $\tilde{\mathbf{M}}_2 \cdot \tilde{\mathbf{M}}_3$  is the matrix for the gas film. These matrices are given in (9.15) and (9.19), respectively.

The matrices are

$$\begin{aligned} \tilde{\mathbf{M}}_0 \cdot \tilde{\mathbf{M}}_1 &= \begin{pmatrix} 1 & 0 \\ 0 & 1 \end{pmatrix} + \tilde{\alpha}^{2D} \begin{pmatrix} 1 & 1 \\ -1 & -1 \end{pmatrix}; \\ \tilde{\mathbf{M}}_2 \cdot \tilde{\mathbf{M}}_3 &= \begin{pmatrix} 1 & 0 \\ 0 & 1 \end{pmatrix} + (\delta n) \alpha^{at} 4\pi k \begin{pmatrix} 0 & e^{2kd} \\ -e^{-2kd} & 0 \end{pmatrix}, \end{aligned} \quad (9.61)$$

and the element of interest to us is

$$M_{11} = 1 + \tilde{\alpha}^{2D} - (\delta n) \alpha^{at} 4\pi k \tilde{\alpha}^{2D} e^{-2kd}. \quad (9.62)$$

The first two terms produce the modes in the thin film alone and are not affected by the atom. We choose as our reference system the system when the atom is at infinite distance from the film. To get the mode condition function we divide  $M_{11}$  with the first two terms. The mode condition function becomes

$$\tilde{f}_k = 1 - (\delta n) 4\pi k \alpha^{at} \frac{\tilde{\alpha}^{2D}}{1 + \tilde{\alpha}^{2D}} e^{-2kd}. \quad (9.63)$$

From this we find the energy per atom is

$$\begin{aligned} \frac{E}{n\delta} &= \frac{\hbar}{2n\delta} \int \frac{d^2k}{(2\pi)^2} \int_{-\infty}^{\infty} \frac{d\xi}{2\pi} \ln \left[ \tilde{f}_{\mathbf{k}}(i\xi) \right] \\ &\approx -\hbar \int_0^{\infty} dk k^2 e^{-2kd} \int_{-\infty}^{\infty} \frac{d\xi}{2\pi} \alpha^{at}(i\xi) \frac{\tilde{\alpha}^{2D}(k, i\xi)}{1 + \tilde{\alpha}^{2D}(k, i\xi)}, \end{aligned} \quad (9.64)$$

and the force on the atom is

$$F(d) = -2\hbar \int_0^\infty dk k^3 e^{-2kd} \int_{-\infty}^\infty \frac{d\xi}{2\pi} \alpha^{at}(i\xi) \frac{\tilde{\alpha}^{2D}(k, i\xi)}{1 + \tilde{\alpha}^{2D}(k, i\xi)}. \tag{9.65}$$

Once again we apply this to a graphene sheet and a 2D metal film. We start with the graphene sheet.

### 9.9.1 Li-Atom-Graphene-Sheet Interaction

In Fig. 9.15a we show the results for the interaction between a Li atom and a graphene sheet from using (9.64). The lowest curve is for pristine graphene; the deviation from this curve increases more and more with higher doping concentration. The results do not follow simple power laws. However, for large separations the undoped graphene result approaches the  $d^{-4}$  power law. This can be understood in the following way: the substitutions  $k \rightarrow k/d$  and  $\xi \rightarrow \xi/d$  leave  $\tilde{\alpha}^{2D}(k, i\xi)$  unchanged in (9.64) and we have

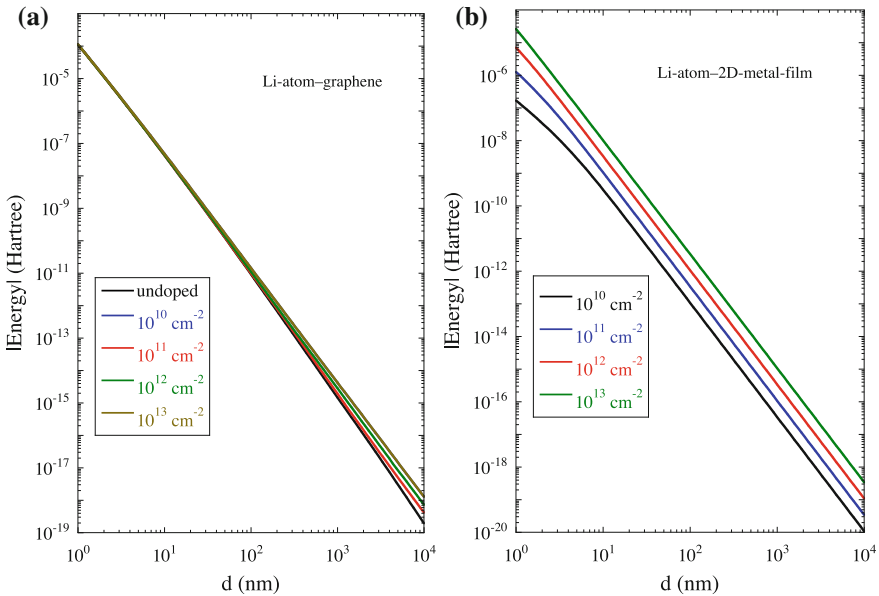


**Fig. 9.15** The van der Waals interaction energy between a Li-atom and a 2D film a distance  $d$  apart. **a** Li atom and a graphene sheet. **b** Li atom and 2D metal film

$$\begin{aligned}
E &= -\frac{\hbar}{d^4} \int_0^\infty dk k^2 e^{-2k} \int_{-\infty}^\infty \frac{d\xi}{2\pi} \alpha^{at} (i\xi/d) \frac{\tilde{\alpha}^{2D}(k, i\xi)}{1 + \tilde{\alpha}^{2D}(k, i\xi)} \\
&\approx -\frac{\hbar}{d^4} \int_0^\infty dk k^2 e^{-2k} \int_{-\infty}^\infty \frac{d\xi}{2\pi} \alpha^{at} (0) \frac{\tilde{\alpha}^{2D}(k, i\xi)}{1 + \tilde{\alpha}^{2D}(k, i\xi)},
\end{aligned} \tag{9.66}$$

for large enough  $d$ -values. Next we continue with the 2D metal film.

### 9.9.2 Li-Atom-2D-Metal-Film Interaction

In Fig. 9.15b we show the results for the interaction between a Li atom and a 2D metal film from using (9.64). The interaction energy increases with carrier concentration so the lowest curve is for the lowest carrier concentration and the uppermost curve for the highest carrier concentration. For large separations the result approaches the  $d^{-7/2}$  power law. This can be understood in the following way: the substitutions  $k \rightarrow k/d$  and  $\xi \rightarrow \xi/\sqrt{d}$  leaves  $\tilde{\alpha}^{2D}(k, i\xi)$  unchanged in (9.64) in the small  $k$ -limit and we have

$$\begin{aligned}
E &= -\frac{\hbar}{d^{7/2}} \int_0^\infty dk k^2 e^{-2k} \int_{-\infty}^\infty \frac{d\xi}{2\pi} \alpha^{at} (i\xi/\sqrt{d}) \frac{\tilde{\alpha}^{2D}(k, i\xi)}{1 + \tilde{\alpha}^{2D}(k, i\xi)} \\
&\approx -\frac{\hbar}{d^{7/2}} \int_0^\infty dk k^2 e^{-2k} \int_{-\infty}^\infty \frac{d\xi}{2\pi} \alpha^{at} (0) \frac{\tilde{\alpha}^{2D}(k, i\xi)}{1 + \tilde{\alpha}^{2D}(k, i\xi)},
\end{aligned} \tag{9.67}$$

for large enough  $d$ -values. This is in agreement with [11].

It is of interest to know how atoms interact with the walls when passing through narrow channels with thin walls. It is furthermore of interest to understand the interactions in intercalation processes [12–14]. A first step in such an investigation can be to study an atom between two films. This is what we do next.

## 9.10 Atom in Between Two Planar Films

Here we let the first 2D film be located at  $z = 0$ , the thin diluted gas film at  $z = d$ , and the second 2D film at  $D$ . There is vacuum between the three films. Thus the matrix becomes  $\tilde{\mathbf{M}} = \tilde{\mathbf{M}}_0 \cdot \tilde{\mathbf{M}}_1 \cdot \tilde{\mathbf{M}}_2$ , where

$$\begin{aligned}
\tilde{\mathbf{M}}_0 &= \begin{pmatrix} 1 & 0 \\ 0 & 1 \end{pmatrix} + \tilde{\alpha}^{2D} \begin{pmatrix} 1 & 1 \\ -1 & -1 \end{pmatrix}; \\
\tilde{\mathbf{M}}_1 &= \begin{pmatrix} 1 & 0 \\ 0 & 1 \end{pmatrix} + \delta n \alpha^{at} 4\pi k \begin{pmatrix} 0 & e^{2kd} \\ -e^{-2kd} & 0 \end{pmatrix}; \\
\tilde{\mathbf{M}}_2 &= \begin{pmatrix} 1 & 0 \\ 0 & 1 \end{pmatrix} + \tilde{\alpha}^{2D} \begin{pmatrix} 1 & e^{2kD} \\ -e^{-2kD} & -1 \end{pmatrix}.
\end{aligned} \tag{9.68}$$

The matrix element of interest is

$$M_{11} = (1 + \tilde{\alpha}^{2D})^2 - e^{-2kD} (\tilde{\alpha}^{2D})^2 - \delta n \alpha^{at} 4\pi k \tilde{\alpha}^{2D} (1 + \tilde{\alpha}^{2D}) (e^{-2kd} + e^{-2k(D-d)}). \quad (9.69)$$

The first term is the mode condition for the two films at infinite separation in absence of the gas layer. The first two terms is the mode condition in absence of the gas layer [see (9.35)]. The mode condition function after division with the function in absence of the gas layer is

$$\tilde{f}_{\mathbf{k}} = 1 - 4\pi k \alpha^{at} \delta n \frac{\tilde{\alpha}^{2D}}{1 + \tilde{\alpha}^{2D}} \frac{[e^{-2kd} + e^{-2k(D-d)}]}{\left[1 - e^{-2kD} \left(\frac{\tilde{\alpha}^{2D}}{1 + \tilde{\alpha}^{2D}}\right)^2\right]}, \quad (9.70)$$

and the interaction energy per atom becomes

$$\begin{aligned} \frac{E}{n\delta} &= \frac{\hbar}{2n\delta} \int \frac{d^2k}{(2\pi)^2} \int_{-\infty}^{\infty} \frac{d\xi}{2\pi} \ln \left[ \tilde{f}_{\mathbf{k}}(i\xi) \right] \\ &\approx -\frac{\hbar}{2} \int \frac{d^2k}{(2\pi)^2} 4\pi k \int_{-\infty}^{\infty} \frac{d\xi}{2\pi} \alpha^{at} \frac{\tilde{\alpha}^{2D}}{1 + \tilde{\alpha}^{2D}} \frac{[e^{-2kd} + e^{-2k(D-d)}]}{\left[1 - e^{-2kD} \left(\frac{\tilde{\alpha}^{2D}}{1 + \tilde{\alpha}^{2D}}\right)^2\right]} \\ &= -\hbar \int_0^{\infty} dk k^2 \int_{-\infty}^{\infty} \frac{d\xi}{2\pi} \alpha^{at}(i\xi) \frac{\tilde{\alpha}^{2D}(k, i\xi)}{1 + \tilde{\alpha}^{2D}(k, i\xi)} \frac{[e^{-2kd} + e^{-2k(D-d)}]}{\left[1 - e^{-2kD} \left(\frac{\tilde{\alpha}^{2D}(k, i\xi)}{1 + \tilde{\alpha}^{2D}(k, i\xi)}\right)^2\right]}. \end{aligned} \quad (9.71)$$

Thus, the force on the atom is

$$F(d) = -4\hbar \int_0^{\infty} dk k^3 \int_0^{\infty} \frac{d\xi}{2\pi} \alpha^{at}(i\xi) \frac{\tilde{\alpha}^{2D}(k, i\xi)}{1 + \tilde{\alpha}^{2D}(k, i\xi)} \frac{[e^{-2kd} - e^{-2k(D-d)}]}{\left[1 - e^{-2kD} \left(\frac{\tilde{\alpha}^{2D}(k, i\xi)}{1 + \tilde{\alpha}^{2D}(k, i\xi)}\right)^2\right]}, \quad (9.72)$$

and at finite temperature it is

$$F(d) = -\frac{4}{\beta} \int_0^{\infty} dk k^3 \sum_{\xi_n}' \alpha^{at}(i\xi_n) \frac{\tilde{\alpha}^{2D}(k, i\xi_n)}{1 + \tilde{\alpha}^{2D}(k, i\xi_n)} \frac{[e^{-2kd} - e^{-2k(D-d)}]}{\left[1 - e^{-2kD} \left(\frac{\tilde{\alpha}^{2D}(k, i\xi_n)}{1 + \tilde{\alpha}^{2D}(k, i\xi_n)}\right)^2\right]}. \quad (9.73)$$

We have now gone through and applied our general method to a number of simple planar geometries. The derivations can easily be extended to more and more complicated planar structures by introducing more and more new interfaces. In next section we present some complementary methods to find the normal modes in some of the planar structures we have already treated. It is always neat to have several alternative

ways to derive things. It furthermore gives a better feeling for and a deeper knowledge of what goes on.

## 9.11 Alternative Derivations of the Normal Modes

In this section we give several complementary ways to derive the normal modes in specific planar geometries. The geometries we consider are two parallel 2D films, a 2D film next to a wall, and two half spaces. The common idea is to generate self-sustained induced sources, fields or potentials. One way to do this is to start from an induced source in one of the objects (film or half space); this source induces a source in the other object which in turn induces a source in the first and so on; with the right frequency the result is self-sustained sources, with the wrong, destructive interference will diminish the sources. A different but equivalent approach is to solve Maxwell's equations in the whole system and use the proper boundary conditions at all interfaces and the condition of no incoming waves from the exterior. A third approach is to introduce a small perturbation in the system; if the response in terms of fields, potentials at the interfaces, or sources diverges the frequency of the perturbation is a mode-frequency. For the geometries containing 2D films we rather closely follow the treatments in [5]. We begin with the modes in a system consisting of two parallel 2D films.

### 9.11.1 Two 2D Films

Here we use three alternative derivations to find the normal modes. In the first approach we let the modes be generated from coupled induced sources; in the second approach we solve Maxwell's equations in the three regions separated by the two films and use the standard boundary conditions at the boundaries defined by the films; in the third approach we find the modes by finding the frequency at which the interaction potential between the carriers diverges. We start with the method involving coupled sources.

#### 9.11.1.1 Coupled Induced Sources

We will now go through one possible way to find the normal modes and their zero-point energies in the geometry of two parallel 2D films. Let film 1 have the induced charge distribution,  $\rho_1(\mathbf{k}, \omega)$ . This charge distribution gives rise to a potential in both films. The resulting potential is<sup>3</sup>  $v(\mathbf{k}, \omega) = v^{2D}(k) \rho_1(\mathbf{k}, \omega)$  and  $\exp(-kd) v^{2D}(k) \rho_1(\mathbf{k}, \omega)$  in films 1 and 2, respectively. There are free and/or bound

---

<sup>3</sup>see Sect. 2.7.

carriers in film 2. These are affected by the potential and are redistributed; expressed in another way they screen the potential. The resulting potential in film 2 after screening by the carriers is  $\exp(-kd) v^{2D}(k) \rho_1(\mathbf{k}, \omega) / [1 + \tilde{\alpha}_2(\mathbf{k}, \omega)]$ , where  $\tilde{\alpha}_2(\mathbf{k}, \omega)$  is the polarizability of film 2. This potential gives rise to an induced charge distribution in film 2,

$$\rho_2(\mathbf{k}, \omega) = \chi_2(\mathbf{k}, \omega) e^{-kd} v^{2D}(k) \frac{\rho_1(\mathbf{k}, \omega)}{[1 + \tilde{\alpha}_2(\mathbf{k}, \omega)]}. \quad (9.74)$$

In complete analogy, this charge distribution in film 2 gives rise to a charge distribution in film 1,

$$\rho_1(\mathbf{k}, \omega) = \chi_1(\mathbf{k}, \omega) e^{-kd} v^{2D}(k) \frac{\rho_2(\mathbf{k}, \omega)}{[1 + \tilde{\alpha}_1(\mathbf{k}, \omega)]}. \quad (9.75)$$

To find the condition for self-sustained fields, normal modes, we let this induced charge density in film 1 be the charge density we started from. This leads to

$$\rho_1(\mathbf{k}, \omega) = \chi_1(\mathbf{k}, \omega) e^{-kd} v^{2D}(k) \frac{\chi_2(\mathbf{k}, \omega) e^{-kd} v^{2D}(k)}{[1 + \tilde{\alpha}_1(\mathbf{k}, \omega)][1 + \tilde{\alpha}_2(\mathbf{k}, \omega)]} \rho_1(\mathbf{k}, \omega), \quad (9.76)$$

and after rearrangements

$$\rho_1(\mathbf{k}, \omega) \left[ 1 - e^{-2kd} \frac{\overbrace{v^{2D}(k) \chi_1(\mathbf{k}, \omega)}^{-\alpha_1(\mathbf{k}, \omega)}}{[1 + \tilde{\alpha}_1(\mathbf{k}, \omega)]} \frac{\overbrace{v^{2D}(k) \chi_2(\mathbf{k}, \omega)}^{-\alpha_2(\mathbf{k}, \omega)}}{[1 + \tilde{\alpha}_2(\mathbf{k}, \omega)]} \right] = 0. \quad (9.77)$$

In order to have a non-zero  $\rho_1(\mathbf{k}, \omega)$  the expression within the brackets has to vanish. Thus,

$$1 - e^{-2kd} \left[ \frac{\tilde{\alpha}_1(\mathbf{k}, \omega)}{1 + \tilde{\alpha}_1(\mathbf{k}, \omega)} \right] \left[ \frac{\tilde{\alpha}_2(\mathbf{k}, \omega)}{1 + \tilde{\alpha}_2(\mathbf{k}, \omega)} \right] = 0, \quad (9.78)$$

and

$$f_{\mathbf{k}}(\omega) = 1 - e^{-2kd} \left[ \frac{\tilde{\alpha}_1(\mathbf{k}, \omega)}{1 + \tilde{\alpha}_1(\mathbf{k}, \omega)} \right] \left[ \frac{\tilde{\alpha}_2(\mathbf{k}, \omega)}{1 + \tilde{\alpha}_2(\mathbf{k}, \omega)} \right]. \quad (9.79)$$

Inserting this function into (9.8) leads to exactly the same energy as in (6.44) and also in (9.37) if we extend that result to two different films. The result in (6.44) was derived using many-body theory and in that derivation there were no talk about zero-point energies at all; the result in (9.37) was derived using our general method.

### 9.11.1.2 Maxwell's Equations and Boundary Conditions

We now solve MEs in the three regions separated by the two 2D films and treat the induced charge and current densities in the 2D films as external to our system. With vacuum in between the films our system is vacuum and the  $\mathbf{D}$  and  $\mathbf{H}$  fields are equal to the  $\mathbf{E}$  and  $\mathbf{B}$  fields, respectively. In the non-retarded treatment it is enough to study the  $\mathbf{E}$ -field. We follow the procedure in [15] and make the following ansatz:

$$\mathbf{E} = \begin{cases} (\mathbf{E}^{\text{BR}} e^{kz} + \mathbf{E}^{\text{BL}} e^{-k(z+d)}) e^{i(kx-\omega t)}, & -d \leq z \leq 0 \\ \mathbf{E}^{\text{R}} e^{-kz} e^{i(kx-\omega t)}, & 0 \leq z \\ \mathbf{E}^{\text{L}} e^{k(z+d)} e^{i(kx-\omega t)}, & z \leq -d. \end{cases} \quad (9.80)$$

Note that the fields die off exponentially away from the region bounded by the two films. Thus, there are no incoming waves from the outside. The two MEs involving the  $\mathbf{E}$ -field,  $\nabla \cdot \mathbf{E} = 0$ , and  $\nabla \times \mathbf{E} = 0$ , both give

$$\begin{aligned} E_z^{\text{BR}} &= -iE_x^{\text{BR}}; \\ E_z^{\text{BL}} &= iE_x^{\text{BL}}; \\ E_z^{\text{R}} &= iE_x^{\text{R}}; \\ E_z^{\text{L}} &= -iE_x^{\text{L}}. \end{aligned} \quad (9.81)$$

The boundary conditions are that the  $x$ -components of the fields are continuous (2.52) across the two interfaces and there is a jump in the  $z$ -component (2.47) equal to  $4\pi\rho_s$ . We find

$$\begin{aligned} E_x^{\text{BR}} + e^{-kd} E_x^{\text{BL}} &= E_x^{\text{R}}; \\ e^{-kd} E_x^{\text{BR}} + E_x^{\text{BL}} &= E_x^{\text{L}}, \end{aligned} \quad (9.82)$$

which on matrix form is

$$\begin{pmatrix} 1 & e^{-kd} \\ e^{-kd} & 1 \end{pmatrix} \cdot \begin{pmatrix} E_x^{\text{BR}} \\ E_x^{\text{BL}} \end{pmatrix} = \begin{pmatrix} E_x^{\text{R}} \\ E_x^{\text{L}} \end{pmatrix}, \quad (9.83)$$

and

$$\begin{aligned} E_z^{\text{BR}} + e^{-kd} E_z^{\text{BL}} + 4\pi\rho_s^{\text{R}} &= E_z^{\text{R}}; \\ e^{-kd} E_z^{\text{BR}} + E_z^{\text{BL}} &= E_z^{\text{L}} + 4\pi\rho_s^{\text{L}}. \end{aligned} \quad (9.84)$$

Now, we eliminate the  $z$ -components in favor of the  $x$ -components using (9.81) and furthermore use that  $\rho_s = kK/\omega = k\tilde{\sigma} E_x/\omega$ . For simplicity we assume that the two films are identical. We find

$$\begin{aligned} E_x^{\text{BR}} - e^{-kd} E_x^{\text{BL}} &= -E_x^{\text{R}} (1 + i4\pi k\tilde{\sigma}/\omega); \\ -e^{-kd} E_x^{\text{BR}} + E_x^{\text{BL}} &= -E_x^{\text{L}} (1 + i4\pi k\tilde{\sigma}/\omega), \end{aligned} \quad (9.85)$$

or on matrix form

$$\begin{pmatrix} 1 & -e^{-kd} \\ -e^{-kd} & 1 \end{pmatrix} \cdot \begin{pmatrix} E_x^{\text{BR}} \\ E_x^{\text{BL}} \end{pmatrix} = -(2\tilde{\varepsilon} - 1) \begin{pmatrix} E_x^{\text{R}} \\ E_x^{\text{L}} \end{pmatrix}. \quad (9.86)$$

Combining (9.83) and (9.86) gives that the condition for having normal modes is that the determinant of the matrix

$$\begin{aligned} & \begin{pmatrix} 1 & -e^{-kd} \\ -e^{-kd} & 1 \end{pmatrix} + (2\tilde{\varepsilon} - 1) \begin{pmatrix} 1 & e^{-kd} \\ e^{-kd} & 1 \end{pmatrix} \\ &= \begin{pmatrix} 2\tilde{\varepsilon} & 2(\tilde{\varepsilon} - 1)e^{-kd} \\ 2(\tilde{\varepsilon} - 1)e^{-kd} & 2\tilde{\varepsilon} \end{pmatrix} \\ &= 2 \begin{pmatrix} 1 + \tilde{\alpha} & \tilde{\alpha}e^{-kd} \\ \tilde{\alpha}e^{-kd} & 1 + \tilde{\alpha} \end{pmatrix} \end{aligned} \quad (9.87)$$

vanishes. Thus, the mode condition function becomes

$$f_{\mathbf{k}}(\omega) = 1 - e^{-2kd} \left[ \frac{\tilde{\alpha}(\mathbf{k}, \omega)}{1 + \tilde{\alpha}(\mathbf{k}, \omega)} \right]^2. \quad (9.88)$$

To arrive at this result we have taken as reference system the system when the two films are at infinite separation. This means that we have divided the mode condition function with the corresponding result when  $d$  is infinite. If the two films are different we instead find

$$f_{\mathbf{k}}(\omega) = 1 - e^{-2kd} \left[ \frac{\tilde{\alpha}_1(\mathbf{k}, \omega)}{1 + \tilde{\alpha}_1(\mathbf{k}, \omega)} \right] \left[ \frac{\tilde{\alpha}_2(\mathbf{k}, \omega)}{1 + \tilde{\alpha}_2(\mathbf{k}, \omega)} \right], \quad (9.89)$$

which agrees with the results we found in the previous section.

### 9.11.1.3 Coupled Potentials

Yet another way to obtain the normal modes is to seek the frequency where the potential between carriers in the same film or in different films diverges. This means that the condition for modes is that the denominators in (6.42) are equal to zero. This leads to the same mode condition function as in (9.79) and (9.89) when we again use as reference system the system when the 2D films are at infinite separation.

## 9.11.2 A 2D Film Next to a Wall

Here we will use two alternative derivations to find the normal modes. In one approach the modes are generated from coupled induced sources; in the other approach we

solve Maxwell's equations in the three regions separated by the film and the wall surface and use the standard boundary conditions at these boundaries. We begin with the method involving coupled sources.

### 9.11.2.1 Coupled Induced Sources

Let us have a 2D film the distance  $d$  from a wall. We proceed in a way very similar to that in Sect. 9.11.1.1. Here we start with an induced mirror charge density,  $\rho_1(\mathbf{k}, \omega)$ , inside the wall at a distance  $d$  from the surface. The induced charge density in the 2D film,  $\rho_2(\mathbf{k}, \omega)$ , is then given by the same expression as in (9.74) except that now the distance between the mirror charge and the 2D film is  $2d$  instead of  $d$ ,

$$\rho_2(\mathbf{k}, \omega) = \chi_2(\mathbf{k}, \omega) e^{-2kd} v^{2D}(k) \frac{\rho_1(\mathbf{k}, \omega)}{[1 + \tilde{\alpha}_2(\mathbf{k}, \omega)]}. \quad (9.90)$$

The mirror charges can be obtained from (2.118) to (2.124) and agree with the traditional results for the mirror charges at a planar vacuum dielectric interface [16]. Equation (9.75) is thus replaced by

$$\rho_1(\mathbf{k}, \omega) = -\rho_2(\mathbf{k}, \omega) \frac{\tilde{\epsilon}_s(\omega) - 1}{\tilde{\epsilon}_s(\omega) + 1}, \quad (9.91)$$

and the condition for normal modes becomes

$$1 - e^{-2kd} \frac{\tilde{\alpha}(\mathbf{k}, \omega)}{1 + \tilde{\alpha}(\mathbf{k}, \omega)} \frac{\tilde{\epsilon}_s(\omega) - 1}{\tilde{\epsilon}_s(\omega) + 1} = 0. \quad (9.92)$$

Hence, the mode condition function is

$$f_{\mathbf{k}}(\omega) = 1 - e^{-2kd} \frac{\tilde{\alpha}(\mathbf{k}, \omega)}{1 + \tilde{\alpha}(\mathbf{k}, \omega)} \frac{\tilde{\epsilon}_s(\omega) - 1}{\tilde{\epsilon}_s(\omega) + 1}, \quad (9.93)$$

where  $\tilde{\alpha}_2(\mathbf{k}, \omega)$  and  $\tilde{\epsilon}_s(\omega)$  are the polarizability of the film and dielectric function of the wall material, respectively. This agrees with (9.45).

### 9.11.2.2 Maxwell's Equations and Boundary Conditions

In Sect. 9.11.1.2 we had a geometry with two interfaces, one at  $z = -d$  and one at  $z = 0$ . There were a 2D film at both interfaces. We use the same geometry here but there is a 2D film only at  $z = -d$ . Again, we treat the induced charge and current densities in the 2D film as external to our system. At  $z = 0$  we place the vacuum-wall interface. Thus we have

$$\mathbf{E} = \begin{cases} (\mathbf{E}^{\text{BR}} e^{kz} + \mathbf{E}^{\text{BL}} e^{-k(z+d)}) e^{i(kx-\omega t)}, & -d \leq z \leq 0 \\ \mathbf{E}^{\text{R}} e^{-kz} e^{i(kx-\omega t)}, & 0 \leq z \\ \mathbf{E}^{\text{L}} e^{k(z+d)} e^{i(kx-\omega t)}, & z \leq -d. \end{cases} \quad (9.94)$$

The two MEs involving the  $\mathbf{E}$ -field,  $\nabla \cdot \mathbf{E} = 0$ , and  $\nabla \times \mathbf{E} = 0$ , both give

$$\begin{aligned} E_z^{\text{BR}} &= -iE_x^{\text{BR}}; \\ E_z^{\text{BL}} &= iE_x^{\text{BL}}; \\ E_z^{\text{R}} &= iE_x^{\text{R}}; \\ E_z^{\text{L}} &= -iE_x^{\text{L}}. \end{aligned} \quad (9.95)$$

The boundary conditions are that the  $E_x$ -components of the fields are continuous (2.52) across the two interfaces, there is a jump in the  $E_z$ -component equal to  $4\pi\rho_s$  (2.47) at the 2D film and the  $D_z$ -component is continuous at the wall surface (2.47). Thus we have

$$\begin{aligned} E_x^{\text{BR}} + e^{-kd} E_x^{\text{BL}} &= E_x^{\text{R}}; \\ e^{-kd} E_x^{\text{BR}} + E_x^{\text{BL}} &= E_x^{\text{L}}, \end{aligned} \quad (9.96)$$

or on matrix form,

$$\begin{pmatrix} 1 & e^{-kd} \\ e^{-kd} & 1 \end{pmatrix} \cdot \begin{pmatrix} E_x^{\text{BR}} \\ E_x^{\text{BL}} \end{pmatrix} = \begin{pmatrix} E_x^{\text{R}} \\ E_x^{\text{L}} \end{pmatrix}, \quad (9.97)$$

and

$$\begin{aligned} E_z^{\text{BR}} + e^{-kd} E_z^{\text{BL}} &= \tilde{\varepsilon}_s(\omega) E_z^{\text{R}}; \\ e^{-kd} E_z^{\text{BR}} + E_z^{\text{BL}} &= E_z^{\text{L}} + 4\pi\rho_s. \end{aligned} \quad (9.98)$$

Next we eliminate the  $z$ -components in favor of the  $x$ -components and use  $\rho_s = kK/\omega = k\tilde{\sigma} E_x/\omega$  leading to

$$\begin{aligned} E_x^{\text{BR}} - e^{-kd} E_x^{\text{BL}} &= -\tilde{\varepsilon}_s E_x^{\text{R}}; \\ -e^{-kd} E_x^{\text{BR}} + E_x^{\text{BL}} &= -E_x^{\text{L}} (1 + i4\pi k\tilde{\sigma}/\omega), \end{aligned} \quad (9.99)$$

or on matrix form

$$\begin{pmatrix} 1 & -e^{-kd} \\ -e^{-kd} & 1 \end{pmatrix} \cdot \begin{pmatrix} E_x^{\text{BR}} \\ E_x^{\text{BL}} \end{pmatrix} = - \begin{pmatrix} \tilde{\varepsilon}_s & 0 \\ 0 & 2\tilde{\varepsilon}_s - 1 \end{pmatrix} \cdot \begin{pmatrix} E_x^{\text{R}} \\ E_x^{\text{L}} \end{pmatrix}. \quad (9.100)$$

Combining (9.97) and (9.100) gives that the condition for having normal modes is that the determinant of the matrix

$$\begin{aligned}
& \begin{pmatrix} 1 & -e^{-kd} \\ -e^{-kd} & 1 \end{pmatrix} + \begin{pmatrix} \tilde{\epsilon}_s & 0 \\ 0 & 2\tilde{\epsilon}_s - 1 \end{pmatrix} \cdot \begin{pmatrix} 1 & e^{-kd} \\ e^{-kd} & 1 \end{pmatrix} \\
&= \begin{pmatrix} \tilde{\epsilon}_s + 1 & (\tilde{\epsilon}_s - 1)e^{-kd} \\ 2(\tilde{\epsilon}_s - 1)e^{-kd} & 2\tilde{\epsilon}_s \end{pmatrix} \\
&= \begin{pmatrix} \tilde{\epsilon}_s + 1 & (\tilde{\epsilon}_s - 1)e^{-kd} \\ 2\tilde{\alpha}e^{-kd} & 2\tilde{\epsilon}_s \end{pmatrix}
\end{aligned} \tag{9.101}$$

is zero. Thus, the mode condition function becomes

$$f_{\mathbf{k}}(\omega) = 1 - e^{-2kd} \left[ \frac{\tilde{\alpha}(\mathbf{k}, \omega)}{1 + \tilde{\alpha}(\mathbf{k}, \omega)} \right] \left[ \frac{\tilde{\epsilon}_s(\omega) - 1}{\tilde{\epsilon}_s(\omega) + 1} \right], \tag{9.102}$$

which agrees with what we found in the previous sections. Our last geometry is that of two half spaces and this is what we treat next.

### 9.11.3 Two Half Spaces

We have already in Sect. 5.4 derived the modes by solving the MEs and using the boundary conditions at the interfaces. We will here use another approach based on coupled induced sources. We use the notation in Fig. 5.14. In Sect. 2.7.2 we derived the mirror current densities caused by current densities in a 2D sheet embedded in a medium next to a wall. The results were given in (2.134) and (2.139). Here the sources are not coming from a 2D sheet. They are from self-induced mirror densities in the two half spaces. We should keep in mind that the actual current densities are at the interfaces and not inside the half spaces. One way to proceed would be to start from an image inside 1 at the distance  $d$  from the surface. It would produce an image in 3, now at the distance  $2d$  from the surface; its image in 1 would be at the distance  $3d$  from the surface and so on.

We will do it in an alternative way. In each step we will replace the mirror image with an effective image at the surface. Let us start with the longitudinal currents and begin with a mirror-image current-density in 3,  $K_{\parallel,3}'(\mathbf{k}, \omega)$  the distance  $d$  from the surface. Remember that this has the effect on 1 as if this current density were at the position  $2d$  from 1 and embedded in the medium 2. The same effect would the current density  $e^{-kd} K_{\parallel,3}'(\mathbf{k}, \omega)$  placed at the distance  $d$  have. Thus we have from (2.134)

$$K_{\parallel,1}'(\mathbf{k}, \omega) = \frac{\tilde{\epsilon}_2 - \tilde{\epsilon}_1}{\tilde{\epsilon}_2 + \tilde{\epsilon}_1} K_{\parallel,3}'(\mathbf{k}, \omega) e^{-kd}. \tag{9.103}$$

In the same way we find

$$K_{\parallel,3}'(\mathbf{k}, \omega) = \frac{\tilde{\epsilon}_2 - \tilde{\epsilon}_3}{\tilde{\epsilon}_2 + \tilde{\epsilon}_3} K_{\parallel,1}'(\mathbf{k}, \omega) e^{-kd}. \tag{9.104}$$

Substituting this result in (9.103) we find

$$K_{\parallel, 1'}(\mathbf{k}, \omega) = \frac{\tilde{\epsilon}_2 - \tilde{\epsilon}_1}{\tilde{\epsilon}_2 + \tilde{\epsilon}_1} \frac{\tilde{\epsilon}_2 - \tilde{\epsilon}_3}{\tilde{\epsilon}_2 + \tilde{\epsilon}_3} K_{\parallel, 1'}(\mathbf{k}, \omega) e^{-2kd}, \quad (9.105)$$

and

$$\left[ 1 - e^{-2kd} \frac{\tilde{\epsilon}_2 - \tilde{\epsilon}_1}{\tilde{\epsilon}_2 + \tilde{\epsilon}_1} \frac{\tilde{\epsilon}_2 - \tilde{\epsilon}_3}{\tilde{\epsilon}_2 + \tilde{\epsilon}_3} \right] K_{\parallel, 1'}(\mathbf{k}, \omega) = 0. \quad (9.106)$$

A non-trivial solution demands that

$$1 - e^{-2kd} \frac{\tilde{\epsilon}_2 - \tilde{\epsilon}_1}{\tilde{\epsilon}_2 + \tilde{\epsilon}_1} \frac{\tilde{\epsilon}_2 - \tilde{\epsilon}_3}{\tilde{\epsilon}_2 + \tilde{\epsilon}_3} = 0, \quad (9.107)$$

which is the mode condition. Thus, the mode condition function is

$$f_{\mathbf{k}}^E(\omega) = 1 - e^{-2kd} \frac{\tilde{\epsilon}_2(\omega) - \tilde{\epsilon}_1(\omega)}{\tilde{\epsilon}_2(\omega) + \tilde{\epsilon}_1(\omega)} \frac{\tilde{\epsilon}_2(\omega) - \tilde{\epsilon}_3(\omega)}{\tilde{\epsilon}_2(\omega) + \tilde{\epsilon}_3(\omega)}. \quad (9.108)$$

This agrees with (9.23) which we obtained with our general method. Only electric fields are associated with these modes. These fields lie in the  $xz$ -plane just as for TM modes but here there are no magnetic fields perpendicular to this plane. Thus we can not call them TM modes. We have attached a superscript E to indicate that the modes are purely electrical. If we neglect any magnetic effects this is all. If we take the small magnetic effects into account we find another set of modes. Proceeding in an analogous way with the transverse current densities we find the mode condition function

$$f_{\mathbf{k}}^M(\omega) = 1 - e^{-2kd} \frac{\tilde{\mu}_2(\omega) - \tilde{\mu}_1(\omega)}{\tilde{\mu}_2(\omega) + \tilde{\mu}_1(\omega)} \frac{\tilde{\mu}_2(\omega) - \tilde{\mu}_3(\omega)}{\tilde{\mu}_2(\omega) + \tilde{\mu}_3(\omega)}. \quad (9.109)$$

Only magnetic fields are associated with these modes. These fields lie in the  $xz$ -plane just as for TE modes but here there are no electric fields perpendicular to this plane. Thus we can not call them TE modes. We have attached a superscript M to indicate that the modes are purely magnetical.

Now, we are done with the alternative derivations of the normal modes in some planar structures. Next, we derive a bonus result from our results for planar structures, viz., the van der Waals interaction between two polarizable atoms.

## 9.12 Interaction Between Two Atoms from Summation of Pair Interactions

We derived the van der Waals interaction between two atoms in Sect. 8.3. It is possible to find this result via a short-cut, viz. by using the result from the summation over pair interactions in Sect. 6.1. The procedure is the following: choose a geometry with

two objects of different material; calculate the result using the summation over pair interactions; calculate the result using the full formalism and take the diluted limit; compare the two results and identify parameters.

We choose to apply this procedure on two half spaces each of one atomic species. We make the ansatz that the interaction between the atoms is given by the potential  $V = -Br^{-6}$  and we intend to identify the coefficient  $B$ . The result from summation over pair interactions (6.7) with this ansatz is

$$\frac{V_{hh}(d)}{A} = -\frac{Bn_2n_1\pi}{12} \frac{1}{d^2}. \quad (9.110)$$

We have assumed that there is vacuum in between the half spaces. The condition for modes in the full formalism (9.20) is

$$[\tilde{\varepsilon}_1 + 1][\tilde{\varepsilon}_2 + 1] - e^{-2kd} [\tilde{\varepsilon}_1 - 1][\tilde{\varepsilon}_2 - 1] = 0, \quad (9.111)$$

and the mode condition function is

$$\begin{aligned} \tilde{f}_{\mathbf{k}}(z) &= 1 - e^{-2kd} \frac{[\tilde{\varepsilon}_1(z)-1][\tilde{\varepsilon}_2(z)-1]}{[\tilde{\varepsilon}_1(z)+1][\tilde{\varepsilon}_2(z)+1]} \\ &\approx 1 - e^{-2kd} [2\pi n_1 \alpha_1(z) 2\pi n_2 \alpha_2(z)], \end{aligned} \quad (9.112)$$

where we on the last line have taken the diluted limit. We have used the expression  $\tilde{\varepsilon}_i(z) = 1 + 4\pi n_i \alpha_i(z)$  for the dielectric function for a gas of atoms of species  $i$ . We have chosen as reference system the geometry when the gap between the half spaces goes to infinity and divided by the corresponding mode condition function. Now the the interaction energy per unit area is

$$\begin{aligned} \frac{V_{hh}(d)}{A} &= \frac{1}{A} \sum_{\mathbf{k}} \int_0^{\infty} \frac{d\xi}{2\pi} \ln [1 - e^{-2kd} (2\pi)^2 n_1 n_2 \alpha_1(\xi) \alpha_2(\xi)] \\ &= \hbar \int \frac{d^2k}{(2\pi)^2} \int_0^{\infty} \frac{d\xi}{2\pi} \ln [1 - e^{-2kd} (2\pi)^2 n_1 n_2 \alpha_1(\xi) \alpha_2(\xi)] \\ &\approx -\hbar \int \frac{d^2k}{(2\pi)^2} \int_0^{\infty} \frac{d\xi}{2\pi} e^{-2kd} (2\pi)^2 n_1 n_2 \alpha_1(\xi) \alpha_2(\xi) \\ &= -\hbar n_1 n_2 \int_0^{\infty} dk k e^{-2kd} \int_0^{\infty} d\xi \alpha_1(\xi) \alpha_2(\xi) = \left| \begin{array}{l} k = x/2d \\ dk = dx/2d \end{array} \right| \\ &= -\frac{\hbar n_1 n_2}{4d^2} \underbrace{\int_0^{\infty} dx x e^{-x}}_1 \int_0^{\infty} d\xi \alpha_1(\xi) \alpha_2(\xi) = -\frac{n_1 n_2}{4d^2} \hbar \int_0^{\infty} d\xi \alpha_1(\xi) \alpha_2(\xi). \end{aligned} \quad (9.113)$$

Equating the results from (9.110) and (9.113) gives

$$B = \frac{3}{\pi} \hbar \int_0^{\infty} d\xi \alpha_1(i\xi) \alpha_2(i\xi) = \frac{3}{2} \alpha_1(0) \alpha_2(0) \frac{\hbar \omega_1 \hbar \omega_2}{\hbar \omega_1 + \hbar \omega_2}, \quad (9.114)$$

where we in the last step have used the London approximation (8.60) for the atomic polarizability. Thus we find

$$E = -\frac{3}{2} \frac{\alpha_1(0) \alpha_2(0)}{r^6} \frac{\hbar\omega_1 \hbar\omega_2}{\hbar\omega_1 + \hbar\omega_2}. \quad (9.115)$$

This result agrees with (8.67). The procedure we have just gone through is a short-cut for finding the van der Waals interaction between two atoms. It furthermore acts as a test of the consistency of our formalism.

### 9.13 Spatial Dispersion

Often the dielectric function is treated as a constant in elementary text books on electromagnetism. Often this crude approximation works well. The Fresnel coefficients describing the reflection and refraction of light in a glass prism can be calculated quite accurately. In other situations it works less well. The group and phase velocities,  $\omega/q$  and  $d\omega/dq$ , respectively, would be equal, there would be no so-called surface modes, [15], and the van der Waals attraction between objects would not be obtained. The frequency dependence of the dielectric function has to be taken into account, i.e. temporal dispersion has to be included in order to incorporate these effects. Now, the dielectric function also depends on the momentum, i.e. there is spatial dispersion. Now, what happens when an electromagnetic wave impinges on an interface between two media? Frequency is conserved but not momentum. This means that the Fresnel coefficients can be used to determine the resulting waves even if the dielectric functions on the two sides of the interface are frequency dependent, but not in systems where the spatial dispersion is important. Spatial dispersion is only important at rare occasions. This is very fortunate for us and our formalism. The planar 2D films that we include in many geometries are handled correctly with respect to spatial dispersion; it enters naturally without any complications. For thicker layers we neglect spatial dispersion.

Spatial dispersion was mentioned in the literature for the first time in 1811 when Arago [17] discovered the rotatory power of quartz. It has since then become a whole research field of its own. The interested reader is referred to a rather recent book: *Spatial Dispersion in Solids and Plasmas* [18], edited by P. Halevi, which is fully devoted to this topic. Two chapters in the book: *Surface Polaritons* [19], edited by V. M. Agronovich and D. L. Mills are of interest here: one by Lagois and Fischer [20] and one by Agronovich [21]. The spatial dispersion problem for metal surfaces has been extensively studied in the past [22, 23] as have the non-local effects on the surface-normal-modes, the surface-plasmon-polaritons [24, 25].

For a metallic system spatial dispersion may be important in some specific frequency regions. These regions are regions where the dielectric function starts to have an important momentum dependence already at small momentum. One region where spatial dispersion may be important is near the plasma frequency. Another region is

near the threshold for interband transitions. A third region is the microwave region where the anomalous skin effect is such a manifestation of spatial dispersion; here the single-particle continuum comes close to the frequency axis in the  $\omega q$ -plane. There are also recent published work [26, 27] about the effects of spatial dispersion on the Casimir force. We have developed a formalism [1] for planar systems that we will outline here within the non-retarded treatment and in Sect. 13.13 within the fully retarded formalism.

### 9.13.1 The Formalism

The sources for electromagnetic fields are charge- and current-densities. One scheme [15] for finding the electromagnetic normal-modes of a system is the following: Start with a reasonable guess for a set of external charge- and current-densities that obey the equation of continuity; find the resulting electromagnetic fields; find the proper combination of  $\omega$  and  $\mathbf{q}$  for which these fields can survive even if the amplitudes of the external densities go toward zero. If one succeeds one has found the dispersion curve,  $\omega(\mathbf{q})$ , of a normal mode.

Here we use another scheme: Start from valid charge- and current-densities at the interface, i.e. densities that obey the equation of continuity, find the resulting fields, use boundary conditions that force the densities to be induced and not external. This leads to two solutions: one is the trivial solution when the densities and fields are all zero; the other solution is one where the densities and fields are in harmony with each other—we have self-sustained fields or equivalently self-sustained, induced charge- and current-densities.

Let us now study the interface between two materials 1 and 2 medium 1 to the left and 2 to the right, see Fig. 9.16a. We use, consistently, the idealization that the interface is perfectly sharp; the dielectric function on each side is represented by the bulk function all the way up to the interface; all potentials on either side of the interface are screened by the corresponding dielectric function. This means that the

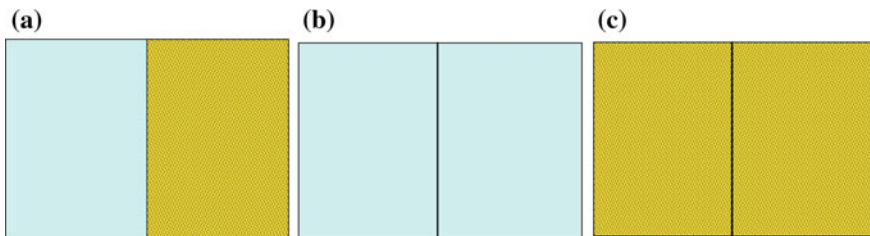


**Fig. 9.16** **a** A single planar interface separating medium 1 to the left from medium 2 to the right; **b** The fields to the left of the interface are generated by effective 2D charge and current densities at the position of the interface calculated as if the whole space were filled with medium 1; **c** The fields to the right of the interface are generated by effective 2D charge and current densities at the position of the interface calculated as if the whole space were filled with medium 2

charge- and current-densities that produce the self-sustained fields, the key element of an electromagnetic normal mode, are two-dimensional charge- and current-densities at the plane of the interface. Keeping strictly to this idealization there is no need to introduce any so-called *ABCs* (*Additional Boundary Conditions*) [28]. The *ABC* problem, i.e. that there are discrepancies between the results obtained from using different *ABCs*, has been eliminated before, then with a proper choice of surface potential [29].

The charge- and current-densities can now be divided into two classes: the strict two-dimensional charge- and current-densities located at the interface,  $\rho_s$  and  $\mathbf{K}$ , respectively; the induced charge- and current-densities in the bulk of the materials on either side of the interface. Each of these separately obeys the equation of continuity. We let the  $xy$ -plane coincide with the interface and let the  $z$ -direction point to the right. To get the fields in material 1, i.e., to the left of the interface we assume that these are generated by charge- and current-densities at the position of the interface, and calculated as if the whole space were filled with medium 1, see Fig. 9.16b. To get the fields in material 2, i.e., to the right of the interface we again assume that these are generated by charge- and current-densities at the position of the interface, and calculated as if the whole space were filled with medium 2, see Fig. 9.16c. These two sets of charge- and current-densities need not be the same. This is in analogy with the mirror-charge formalism. The equation of continuity demands the presence of accompanying surface-current-densities.

The modes at an interface are characterized by the 2D (two-dimensional) wave vector,  $\mathbf{k}$ , in the plane of the interface. We neglect any effects from imperfections of the interface. This means that the in-plane momentum is conserved. Thus  $\mathbf{k}$  is a good quantum number for the modes. For isotropic materials there is no preferred direction in the  $xy$ -plane. We arbitrarily choose the propagation of the mode to be in the  $x$ -direction. We let a general wave vector be denoted by  $\mathbf{q}$ , and  $\mathbf{k}$  is then the in-plane component, i.e.,  $\mathbf{q} = \mathbf{k} + q_z \hat{z} = k\hat{x} + q_z \hat{z}$ . In analogy a general position vector is denoted by  $\mathbf{R}$ , and  $\mathbf{r}$  is then the in-plane component, i.e.,  $\mathbf{R} = \mathbf{r} + z\hat{z} = x\hat{x} + y\hat{y} + z\hat{z}$ . For functions of the spatial coordinates and time the function arguments can be written in the equivalent forms  $(\mathbf{R}, t) = (\mathbf{r}, z; t) = (x, y, z; t)$  and for the Fourier transformed versions they may be written as  $(\mathbf{q}, \omega) = (\mathbf{k}, q_z; \omega)$ . In our treatment of the interfaces the charge- and current-densities are strictly 2D and with our orientation of the coordinate system the Fourier transformed functions are

$$\rho(\mathbf{q}, \omega) = \rho_s(\mathbf{k}, -; \omega) = \rho_s(\mathbf{k}, \omega), \quad (9.116)$$

and

$$\begin{aligned} \mathbf{J}(\mathbf{q}, \omega) &= \mathbf{J}_L(\mathbf{q}, \omega) + \mathbf{J}_T(\mathbf{q}, \omega) = \mathbf{K}(\mathbf{k}, -; \omega) \\ &= \mathbf{K}(\mathbf{k}, \omega) = \mathbf{K}_{\parallel}(\mathbf{k}, \omega) + \mathbf{K}_{\perp}(\mathbf{k}, \omega), \end{aligned} \quad (9.117)$$

respectively. The subscripts  $L$  and  $T$  denote longitudinal and transverse, i.e. parallel and perpendicular to  $\mathbf{q}$ , respectively. The subscripts  $\parallel$  and  $\perp$  denote in plane vectors, parallel and perpendicular to  $\mathbf{k}$ , respectively.

When neglecting retardation the Coulomb and Lorentz gauges coincide and there is only one scalar potential,

$$\Phi^{(i)}(\mathbf{q}, \omega) = \frac{4\pi \rho^{(i)}(\mathbf{q}, \omega)}{q^2 \tilde{\epsilon}_L^{(i)}(\mathbf{q}, \omega)} = \frac{4\pi \rho_s^{(i)}(\mathbf{k}, \omega)}{q^2 \tilde{\epsilon}_L^{(i)}(\mathbf{q}, \omega)}, \quad (9.118)$$

where the index  $i=1, 2$  specifies the medium.

The vector potential is

$$\begin{aligned} \mathbf{A}^{(i)}(\mathbf{q}, \omega) &= \frac{4\pi \tilde{\mu}_T^{(i)}(\mathbf{q}, \omega)}{cq^2} \mathbf{J}^{(i)}(\mathbf{q}, \omega) \\ &= \frac{4\pi \tilde{\mu}_T^{(i)}(\mathbf{q}, \omega)}{cq^2} [\mathbf{K}_{\parallel}(\mathbf{k}, \omega) + \mathbf{K}_{\perp}(\mathbf{k}, \omega)]. \end{aligned} \quad (9.119)$$

From now on we drop the superscript,  $(i)$ , representing the medium on the potentials and fields. The result is valid on each side of the interface, we just add the proper superscript at the end.

We are interested in the electric and magnetic fields associated with the charge- and current-densities. The electric field in neglect of retardation is

$$\mathbf{E} = -\nabla \Phi, \quad (9.120)$$

and its Fourier transform is

$$\begin{aligned} \mathbf{E}(\mathbf{k}, q_z; \omega) &= -i\mathbf{q}\Phi(\mathbf{k}, q_z; \omega) \\ &= -i4\pi \rho_s(\mathbf{k}, \omega) \frac{\hat{x}k + \hat{z}q_z}{q^2 \tilde{\epsilon}_L(\mathbf{q}, \omega)}. \end{aligned} \quad (9.121)$$

The magnetic induction in neglect of retardation is

$$\begin{aligned} \mathbf{B}(\mathbf{k}, q_z; \omega) &= i\mathbf{q} \times \mathbf{A}(\mathbf{k}, q_z; \omega) \\ &= i \frac{4\pi \tilde{\mu}_T^{(i)}(\mathbf{q}, \omega)}{cq^2} (\hat{x}k + \hat{z}q_z) \times [\mathbf{K}_{\parallel}(\mathbf{k}, \omega) + \mathbf{K}_{\perp}(\mathbf{k}, \omega)] \\ &= i \frac{4\pi \tilde{\mu}_T^{(i)}(\mathbf{q}, \omega)}{cq^2} [0 + \hat{z}k K_{\perp}(\mathbf{k}, \omega) + \hat{y}q_z K_{\parallel}(\mathbf{k}, \omega) - \hat{x}q_z K_{\perp}(\mathbf{k}, \omega)] \\ &= i \frac{4\pi \tilde{\mu}_T^{(i)}(\mathbf{q}, \omega)}{cq^2} [\hat{z}k - \hat{x}q_z] K_{\perp}(\mathbf{k}, \omega). \end{aligned} \quad (9.122)$$

The current  $K_{\parallel}(\mathbf{k}, \omega)$  will not contribute to  $\mathbf{B}$  in the non-retarded treatment. See the discussion after (2.131).

To summarize we have the fields

$$\begin{aligned} \tilde{E}_{\parallel}(\mathbf{k}, q_z; \omega) &= -i4\pi k \rho_s(\mathbf{k}, \omega) \frac{1}{q^2 \tilde{\epsilon}_L(\mathbf{q}, \omega)}, \\ \tilde{D}_{\parallel}(\mathbf{k}, q_z; \omega) &= -i4\pi k \rho_s(\mathbf{k}, \omega) \frac{1}{q^2}, \\ \tilde{E}_n(\mathbf{k}, q_z; \omega) &= -i4\pi \rho_s(\mathbf{k}, \omega) \frac{q_z}{q^2 \tilde{\epsilon}_L(\mathbf{q}, \omega)}, \\ \tilde{D}_n(\mathbf{k}, q_z; \omega) &= -i4\pi \rho_s(\mathbf{k}, \omega) \frac{q_z}{q^2}, \\ \tilde{B}_{\parallel}(\mathbf{k}, q_z; \omega) &= -i \frac{4\pi K_{\perp}(\mathbf{k}, \omega)}{c} \frac{q_z \tilde{\mu}_T(\mathbf{q}, \omega)}{q^2}, \\ \tilde{H}_{\parallel}(\mathbf{k}, q_z; \omega) &= -i \frac{4\pi K_{\perp}(\mathbf{k}, \omega)}{c} \frac{q_z}{q^2}, \\ \tilde{B}_n(\mathbf{k}, q_z; \omega) &= i \frac{4\pi k K_{\perp}(\mathbf{k}, \omega)}{c} \frac{\tilde{\mu}_T(\mathbf{q}, \omega)}{q^2}, \\ \tilde{H}_n(\mathbf{k}, q_z; \omega) &= i \frac{4\pi k K_{\perp}(\mathbf{k}, \omega)}{c} \frac{1}{q^2}. \end{aligned} \quad (9.123)$$

Two functions appear repeatedly when we apply the boundary conditions and we give them names to make the expressions simpler. We need the following functions:

$$g_a^{(i)}(k, \omega) = 2k \int_{-\infty}^{\infty} \frac{dq_z}{2\pi} \frac{1}{q^2 \tilde{\varepsilon}_L^{(i)}(q, \omega)}, \quad (9.124)$$

for the electric modes and

$$h_a^{(i)}(k, \omega) = 2k \int_{-\infty}^{\infty} \frac{dq_z}{2\pi} \frac{\tilde{\mu}_T^{(i)}(q, \omega)}{q^2}, \quad (9.125)$$

for the magnetic ones.

The prefactor has been chosen such that the  $g$ - and  $h$ -function are unity in vacuum:

$$\begin{aligned} g_a^0(k, \omega) &= 2k \int_{-\infty}^{\infty} \frac{dq_z}{2\pi} \frac{1}{q^2} = 1, \\ h_a^0(k, \omega) &= 2k \int_{-\infty}^{\infty} \frac{dq_z}{2\pi} \frac{1}{q^2} = 1. \end{aligned} \quad (9.126)$$

This result is easily found from the standard integral:

$$\int_{-\infty}^{\infty} \frac{dr}{2\pi} e^{irs} \frac{1}{r^2 + a^2} = \frac{1}{2a} e^{-a|s|}. \quad (9.127)$$

It can be useful to introduce faster converging integrals,

$$\begin{aligned} \tilde{g}_a^{(i)}(k, \omega) &= 2k \int_{-\infty}^{\infty} \frac{dq_z}{2\pi} \frac{1}{q^2} \left[ \frac{1}{\tilde{\varepsilon}_L^{(i)}(q, \omega)} - 1 \right], \\ \tilde{h}_a^{(i)}(k, \omega) &= 2k \int_{-\infty}^{\infty} \frac{dq_z}{2\pi} \frac{1}{q^2} \left[ \tilde{\mu}_T^{(i)}(q, \omega) - 1 \right]. \end{aligned} \quad (9.128)$$

We also need the functions with neglect of spatial dispersion. If we neglect spatial dispersion, indicated by an extra subscript 1, we have

$$\begin{aligned} g_{a,1}^{(i)}(k, \omega) &= 2k \int_{-\infty}^{\infty} \frac{dq_z}{2\pi} \frac{1}{q^2 \tilde{\varepsilon}^{(i)}(\omega)} = \frac{1}{\tilde{\varepsilon}^{(i)}(\omega)}, \\ h_{a,1}^{(i)}(k, \omega) &= 2k \int_{-\infty}^{\infty} \frac{dq_z}{2\pi} \frac{\tilde{\mu}^{(i)}(\omega)}{q^2} = \tilde{\mu}^{(i)}(\omega). \end{aligned} \quad (9.129)$$

Note that here we have dropped the subscripts on the dielectric function and magnetic permeability since the transverse and longitudinal versions are the same in neglect of spatial dispersion.

We will limit the derivations to two important geometries, viz. a single interface between two media and a gap between two half spaces.

We begin by determining the normal modes at a single interface. If the weak magnetic effects (paramagnetic and diamagnetic) are neglected there are only electric normal modes at a single interface in the non-retarded treatment. We want to be as general as possible and have included a discussion of the magnetic effects. This is done in Sect. 9.13.3. Then also purely magnetic normal modes appear. We start with the electric modes.

### 9.13.2 Electric Modes at a Single Interface

We now derive the condition for having a surface-normal-mode from the standard boundary-conditions for the fields at the interface: the continuity of the in-plane components of the  $\mathbf{E}$ - and  $\tilde{\mathbf{H}}$ -fields and the normal components of the  $\tilde{\mathbf{D}}$ - and  $\mathbf{B}$ -fields; these boundary conditions are valid if there are no external charge- or current-densities at the interface, only induced densities from the self-sustained fields.

We need the  $E_{\parallel}$ -components on the two sides of the interface. We have from (9.123) that

$$E_{\parallel}(\mathbf{k}, z; \omega) = -i4\pi k \rho_s(\mathbf{k}, \omega) \int_{-\infty}^{\infty} \frac{dq_z}{2\pi} e^{iq_z z} \frac{1}{q^2 \tilde{\epsilon}_L(q, \omega)}. \quad (9.130)$$

Just to the left of the interface this becomes

$$E_{\parallel}(\mathbf{k}, 0^-; \omega) = -i2\pi \rho_s^{(1)}(\mathbf{k}, \omega) g_a^{(1)}, \quad (9.131)$$

and just to the right the result is

$$E_{\parallel}(\mathbf{k}, 0^+; \omega) = -i2\pi \rho_s^{(2)}(\mathbf{k}, \omega) g_a^{(2)}. \quad (9.132)$$

We furthermore need the  $\tilde{\mathbf{D}}_n$ -components on the two sides. We have

$$\begin{aligned} \tilde{D}_n(\mathbf{k}, z; \omega) &= -i4\pi \rho_s(\mathbf{k}, \omega) \int_{-\infty}^{\infty} \frac{dq_z}{2\pi} e^{iq_z z} \frac{q_z \tilde{\epsilon}_L(q, \omega)}{q^2 \tilde{\epsilon}_L(q, \omega)} \\ &= -i4\pi k \rho_s(\mathbf{k}, \omega) \underbrace{\int_{-\infty}^{\infty} \frac{dq_z}{2\pi} e^{iq_z z} \frac{q_z}{q^2}}_{\frac{i}{2} \frac{z}{|z|} e^{-k|z|}} \\ &= 2\pi k \rho_s(\mathbf{k}, \omega) \frac{z}{|z|} e^{-k|z|}, \end{aligned} \quad (9.133)$$

where we have used the standard integral:

$$\int_{-\infty}^{\infty} \frac{dr}{2\pi} e^{irs} \frac{r}{r^2 + a^2} = \frac{i}{2} \text{sign}(s) e^{-a|s|}. \quad (9.134)$$

Just to the left of the interface we find

$$\tilde{D}_n(\mathbf{k}, 0^-; \omega) = -2\pi\rho_s^{(1)}(\mathbf{k}, \omega), \quad (9.135)$$

and just to the right we have

$$\tilde{D}_n(\mathbf{k}, 0^+; \omega) = 2\pi\rho_s^{(2)}(\mathbf{k}, \omega). \quad (9.136)$$

To make the expressions for the fields more compact we introduce the common factors  $A$  and  $B$ , not to be confused with the vector potential and magnetic induction,

$$\begin{aligned} A_e &= 2\pi\rho_s^{(1)}(\mathbf{k}, \omega), \\ B_e &= 2\pi\rho_s^{(2)}(\mathbf{k}, \omega). \end{aligned} \quad (9.137)$$

Then the continuity of the  $\mathbf{E}_{\parallel}$ -component gives

$$-ig_a^{(1)}(k, \omega) A_e + ig_a^{(2)}(k, \omega) B_e = 0, \quad (9.138)$$

or

$$g_a^{(1)}(k, \omega) A_e - g_a^{(2)}(k, \omega) B_e = 0. \quad (9.139)$$

The continuity of the  $\tilde{\mathbf{D}}_n$ -component gives

$$A_e + B_e = 0. \quad (9.140)$$

Thus, we have obtained the following system of equations:

$$\begin{pmatrix} 1 & 1 \\ g_a^{(1)}(k, \omega) & -g_a^{(2)}(k, \omega) \end{pmatrix} \begin{pmatrix} A_e \\ B_e \end{pmatrix} = \begin{pmatrix} 0 \\ 0 \end{pmatrix}. \quad (9.141)$$

This system has the trivial solution that  $A_e = B_e = 0$ . It has also non-trivial solutions which are the modes we are looking for. The condition for normal modes is found as

$$\begin{vmatrix} 1 & 1 \\ g_a^{(1)}(k, \omega) & -g_a^{(2)}(k, \omega) \end{vmatrix} = 0, \quad (9.142)$$

or

$$g_a^{(1)}(k, \omega) + g_a^{(2)}(k, \omega) = 0, \quad (9.143)$$

or

$$\int_{-\infty}^{\infty} \frac{dq_z}{2\pi} \frac{1}{q^2} \left[ \frac{1}{\tilde{\varepsilon}_L^{(1)}(q, \omega)} + \frac{1}{\tilde{\varepsilon}_L^{(2)}(q, \omega)} \right] = 0, \quad (9.144)$$

Neglecting spatial dispersion we arrive at

$$\tilde{\varepsilon}^{(1)}(\omega) + \tilde{\varepsilon}^{(2)}(\omega) = 0, \quad (9.145)$$

which is the standard condition for having a normal mode in the neglect of spatial dispersion and retardation [15].

We have now derived the general conditions for having surface-normal-modes at an interface between two media with and without spatial dispersion taken into account. We will here study the effect from spatial dispersion on the surface-plasmon-dispersion, i.e., the over-all effect on the  $k_F$  scale.

Now we determine the normal mode, a surface plasmon, at a metal vacuum interface. We let medium 1 be a metal and medium 2 vacuum. In neglect of retardation effects the condition for modes is

$$g_a^{(1)}(k, \omega) + g_a^0(k, \omega) = 0, \quad (9.146)$$

or

$$g_a^{(1)}(k, \omega) + 1 = 0, \quad (9.147)$$

or

$$\tilde{g}_a^{(1)}(k, \omega) + 2 = 0. \quad (9.148)$$

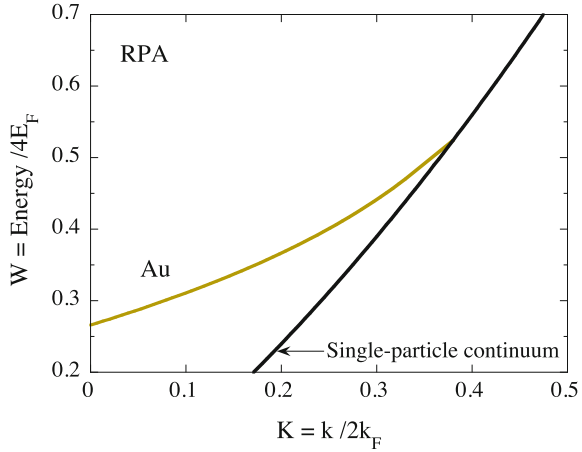
The tilde over a  $g$ -function means the  $g$ -function calculated inside the medium minus the corresponding function calculated in vacuum. The tilde versions of the  $g$ -functions were introduced in (9.128) since they represent faster converging integrals. To benefit from this the two integrals in each tilde version of a  $g$ -function should be combined into one.

Thus, the mode condition function is

$$f_{\mathbf{k}}(\omega) = 2 + 2k \int_{-\infty}^{\infty} \frac{dq_z}{2\pi} \frac{1}{q^2} \left[ \frac{1}{\tilde{\varepsilon}_L^{(i)}(q, \omega)} - 1 \right]. \quad (9.149)$$

In [1] we found the surface-plasmon modes for simple metals for the three different approximations of the dielectric function, the hydrodynamic, the plasmon pole and the RPA. For the two first approximations the  $g_a$ -function can be obtained analytically. The RPA  $g_a$ -function has to be found numerically. Here we present the results for the most accurate function only, the RPA function.

**Fig. 9.17** The surface-plasmon dispersion-curve for gold as a result from taking spatial dispersion into account. The results were obtained using the RPA dielectric functions of Sect. D.1. Neglecting spatial dispersion would produce a dispersion-less horizontal curve at the value where the present curve starts out from the frequency axis



The result for gold is shown in Fig. 9.17. We find the surface-plasmon dispersion-curve start out at the frequency obtained at the neglect of spatial dispersion, and then initially varies linearly with momentum. The thick solid curve is the boundary of the single-particle continuum in the in-plane direction of the surface plasmon. Experimentally it turns out that band-structure effects like those from interband transitions, neglected here, are very important and may actually lead to a negative slope of the dispersion [30–33]. Thus the treatment here is not good enough for obtaining quantitative dispersion curves. However we find that spatial dispersion is one very important component, although not the only one, influencing the dispersion of the surface modes. Now, we turn to the magnetic modes.

### 9.13.3 Magnetic Modes at a Single Interface

If the weak magnetic effects (paramagnetic and diamagnetic) are neglected there are only electric normal modes at a single interface in the non-retarded treatment. These were discussed in Sect. 9.13.2. Here we treat the purely magnetic modes that appear at a single interface when the weak magnetic effects are included. The results for magnetic systems are outside the scope of this book.

We need the  $\tilde{H}_{\parallel}$ -components on the two sides of the interface. We have from (9.123) that

$$\tilde{H}_{\parallel}(\mathbf{k}, z; \omega) = -i \frac{4\pi K_{\perp}(\mathbf{k}, \omega)}{c} \underbrace{\int_{-\infty}^{\infty} \frac{dq_z}{2\pi} e^{iq_z z} \frac{q_z}{q^2}}_{\frac{i}{2} \frac{z}{|z|} e^{-k|z|}} = \frac{2\pi K_{\perp}(\mathbf{k}, \omega)}{c} \frac{z}{|z|} e^{-k|z|}, \tag{9.150}$$

where we have used the standard integral:

$$\int_{-\infty}^{\infty} \frac{dr}{2\pi} e^{irs} \frac{r}{r^2 + a^2} = \frac{i}{2} \text{sign}(s) e^{-a|s|}. \quad (9.151)$$

Just to the left of the interface we have

$$\tilde{H}_{\parallel}(\mathbf{k}, 0^-; \omega) = -\frac{2\pi K_{\perp}^{(1)}(\mathbf{k}, \omega)}{c}, \quad (9.152)$$

and just to the right the corresponding result is

$$\tilde{H}_{\parallel}(\mathbf{k}, 0^+; \omega) = \frac{2\pi K_{\perp}^{(2)}(\mathbf{k}, \omega)}{c}. \quad (9.153)$$

We furthermore need the  $\mathbf{B}_n$ -components on the two sides. We have

$$B_n(\mathbf{k}, z; \omega) = i \frac{4\pi k K_{\perp}(\mathbf{k}, \omega)}{c} \int_{-\infty}^{\infty} \frac{dq_z}{2\pi} e^{iq_z z} \frac{\tilde{\mu}_T(q, \omega)}{q^2}. \quad (9.154)$$

Just to the left of the interface this becomes

$$B_n(\mathbf{k}, 0^-; \omega) = i \frac{2\pi K_{\perp}^{(1)}(\mathbf{k}, \omega)}{c} h_a^{(1)}, \quad (9.155)$$

and just to the right it is

$$B_n(\mathbf{k}, 0^+; \omega) = i \frac{2\pi K_{\perp}^{(2)}(\mathbf{k}, \omega)}{c} h_a^{(2)}. \quad (9.156)$$

To make the expressions for the fields more compact we introduce the common factors  $A_m$  and  $B_m$ , not to be confused with the vector potential and magnetic induction,

$$\begin{aligned} A_m &= 2\pi K_{\perp}^{(1)}(\mathbf{k}, \omega) / c, \\ B_m &= 2\pi K_{\perp}^{(2)}(\mathbf{k}, \omega) / c. \end{aligned} \quad (9.157)$$

Then the continuity of the  $\tilde{H}_{\parallel}$ -component gives

$$A_m + B_m = 0. \quad (9.158)$$

The continuity of the  $\mathbf{B}_n$ -component results in

$$iA_m h_a^{(1)} - iB_m h_a^{(2)} = 0, \quad (9.159)$$

or

$$h_a^{(1)} A_m - h_a^{(2)} B_m = 0. \quad (9.160)$$

Thus, we have obtained the following system of equations

$$\begin{pmatrix} 1 & 1 \\ h_a^{(1)}(k, \omega) & -h_a^{(2)}(k, \omega) \end{pmatrix} \begin{pmatrix} A_m \\ B_m \end{pmatrix} = \begin{pmatrix} 0 \\ 0 \end{pmatrix}. \quad (9.161)$$

This system has the trivial solution that  $A_m = B_m = 0$ . It has also non-trivial solutions which are the modes we are looking for. The condition for normal modes is found as

$$\left| \begin{pmatrix} 1 & 1 \\ h_a^{(1)}(k, \omega) & -h_a^{(2)}(k, \omega) \end{pmatrix} \right| = 0, \quad (9.162)$$

or

$$h_a^{(1)}(k, \omega) + h_a^{(2)}(k, \omega) = 0, \quad (9.163)$$

or

$$\int_{-\infty}^{\infty} \frac{dq_z}{2\pi} \frac{1}{q^2} \left[ \tilde{\mu}_T^{(1)}(q, \omega) + \tilde{\mu}_T^{(2)}(q, \omega) \right] = 0. \quad (9.164)$$

For convergence reasons it is more beneficial to use a modified function,

$$\tilde{h}_a^{(i)}(k, \omega) = \int_{-\infty}^{\infty} \frac{dq_z}{2\pi} \frac{1}{q^2} \left[ \tilde{\mu}_T^{(i)}(q, \omega) - 1 \right], \quad (9.165)$$

in terms of which the condition for modes becomes

$$\tilde{h}_a^{(1)}(k, \omega) + \tilde{h}_a^{(2)}(k, \omega) + 2 = 0. \quad (9.166)$$

Neglecting spatial dispersion we arrive at

$$\tilde{\mu}^{(1)}(\omega) + \tilde{\mu}^{(2)}(\omega) = 0, \quad (9.167)$$

which is the standard condition for having a normal mode in the neglect of spatial dispersion and retardation [15].

We have now derived the general conditions for having surface-normal-modes at an interface between two media with and without spatial dispersion taken into account. We found that one mode type involved electric fields, only, and one only magnetic fields. The “electric” mode was associated with surface charge densities at the interface and the “magnetic” mode with surface current densities at the interface of the type that is perpendicular to  $\mathbf{k}$ , i.e.,  $\mathbf{K}_\perp$ . We could have chosen to say that the “electric” modes were associated with surface current densities of the type that is

parallel to  $\mathbf{k}$ , i.e.,  $\mathbf{K}_{\parallel}$ , since the surface charge density is intimately connected to this type of current density. If one is present then is the other and the relation between them is very simple, see (2.118). The benefit from doing that is that the outline would be more symmetric with the two surface mode types generated from the two surface current types. We make this choice when treating spatial dispersion in the retarded treatment in Sect. 13.13.

Let us now turn to a more complicated geometry, viz. a vacuum gap between two half spaces. We can imagine that we split the system of Fig. 9.16a along the interface and move the pieces apart the distance  $d$ .

### 9.13.4 Electric Modes Associated with a Gap Between Two Half Spaces

Here, we have three regions, the left with medium 1, the gap with vacuum, and the right with medium 2, see Fig. 9.18a. We start with the gap region and assume that there are source densities at the two interfaces. The source at the left interface gives rise to a mirror source in the right region at the distance  $d$  from the right interface. This mirror source itself produces a mirror source in the left region at the distance  $2d$  from the left interface which in turn gives rise to another mirror source in the right region and so on. Thus the source at the left interface generates an infinite number of image sources. In analogy the source density at the right interface also generates an infinite number of mirror sources, see Fig. 9.18b. All these sources and mirror sources produce the fields in the gap region. Each of the mirror sources in the right region can be shifted to and be replaced by a source at the right interface, a source that produces the same fields as the original mirror source. The source density at the interface is the same as the mirror density apart from that it is multiplied by a factor  $\exp(-kd_i)$  where  $d_i$  is the distance the mirror source is shifted to get to the right interface. All mirror sources in the right region can be moved to the right interface and be combined into one. In analogy, all mirror sources in the left region can be moved to the left interface and be combined into one. Thus we end up with two

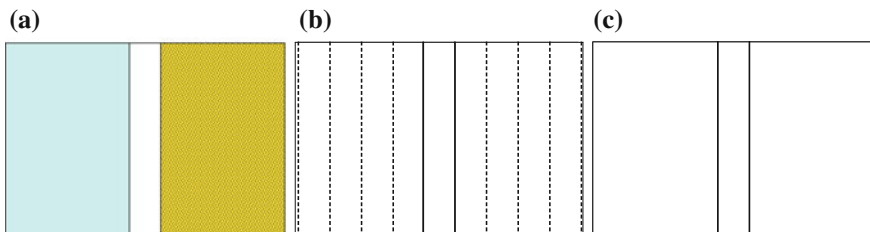


**Fig. 9.18** **a** A gap separating medium 1 to the left from medium 2 to the right; **b** The sources at the two interfaces give rise to mirror sources to the left of the left interface and to the right of the right interface; **c** The fields in the gap are generated by effective 2D charge and current densities at the position of the two interfaces calculated as if the whole space were filled with vacuum

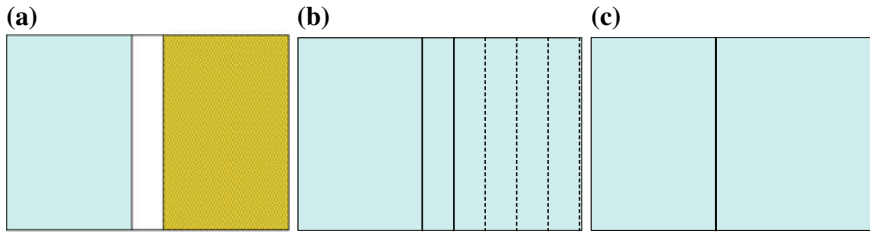


**Fig. 9.19** **a** A gap separating medium 1 to the left from medium 2 to the right; **b** The sources at the two interfaces give rise to mirror sources to the right of the right interface. The fields to the left of the left interface are generated by the sources and mirror sources calculated as if the whole space were filled with medium 1; **c** The sources and all mirror sources can be combined into one source at the left interface. The fields to the left of the left interface are generated by this source and calculated as if the whole space were filled with medium 1

sources, one at each interface, for the fields in the gap region, see Fig. 9.18c. For the problem at hand we do not need to perform these manipulations explicitly. We just postulate that we have effective source densities at the two interfaces. The boundary conditions takes care of the rest.

We study the modes generated by the same type of charge- and accompanying current-densities on the two interfaces. In this more complicated geometry with more than one interface, we need to define two new factors:

$$C_e = 2\pi\rho_s^{(0, left)}(\mathbf{k}, \omega) ; D_e = 2\pi\rho_s^{(0, right)}(\mathbf{k}, \omega) . \quad (9.168)$$

The first superscript represents medium 0, which is vacuum. The second represents which of the two interfaces the charge distribution is located at, the one to the left or the one to the right.

Let us now turn to the sources generating the fields in the left region, see Fig. 9.19a. The fields to the left of the left interface are generated by the sources at the two interfaces and all mirror sources in the right region, see Fig. 9.19b. All these sources and mirror sources can be modified, shifted and combined into one effective source at the left interface, see Fig. 9.19c.

In analogy, the fields in the right region, Fig. 9.20a, are generated by the sources at the two interfaces and all mirror sources in the left region, see Fig. 9.20b. All these sources and mirror sources can be modified, shifted and combined into one effective source at the right interface, see Fig. 9.20c.

The fields inside the left half space are generated by charge- and current-densities at the left interface, and the fields inside the right half space by ones at the right interface. The fields in the middle region, in vacuum, are generated by densities at both interfaces. We have here chosen to express the sources as surface charge densities. One should keep in mind that these surface charge densities are intimately connected to current densities,  $\mathbf{K}_{\parallel}(\mathbf{k}, \omega)$ , through the equation of continuity. Both these sources contribute in general to the fields, but not when retardation is neglected so it feels more natural to choose the charge density to represent the source.

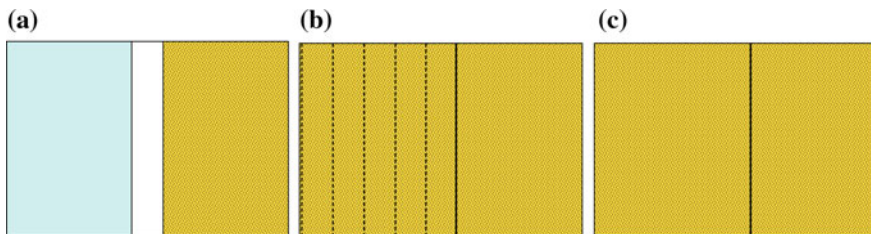


**Fig. 9.20** **a** A gap separating medium 1 to the left from medium 2 to the right; **b** The sources at the two interfaces give rise to mirror sources to the left of the left interface. The fields to the right of the right interface are generated by the sources and mirror sources calculated as if the whole space were filled with medium 2; **c** The sources and all mirror sources can be combined into one source at the right interface. The fields to the right of the right interface are generated by this source and calculated as if the whole space were filled with medium 2

We start by studying the boundary conditions for  $\mathbf{E}$ . The continuity of the  $x$ -component of the  $\mathbf{E}$ -field at the left interface gives

$$A_e g_a^{(1)}(k, \omega) = C_e g_a^{(0)}(k, \omega) + D_e g_a^{(0)}(k, \omega) e^{-kd}, \quad (9.169)$$

or

$$g_a^{(1)}(k, \omega) A_e = C_e + e^{-kd} D_e. \quad (9.170)$$

The corresponding equation from the right interface gives

$$g_a^{(2)}(k, \omega) B_e = e^{-kd} C_e + D_e. \quad (9.171)$$

We will here limit ourselves to having the same material on both sides of the gap. Then we may combine the results into

$$g_a^{(1)}(k, \omega) \begin{pmatrix} A_e \\ B_e \end{pmatrix} = \begin{pmatrix} 1 & e^{-kd} \\ e^{-kd} & 1 \end{pmatrix} \begin{pmatrix} C_e \\ D_e \end{pmatrix}. \quad (9.172)$$

Next we use the boundary condition for the  $\tilde{\mathbf{D}}$ -field at the left and find

$$-A_e = C_e - e^{-kd} D_e. \quad (9.173)$$

The corresponding result to the right gives

$$B_e = e^{-kd} C_e - D_e. \quad (9.174)$$

All the boundary conditions have resulted in the following system of equations:

$$\begin{aligned}
 \begin{pmatrix} A_e \\ B_e \end{pmatrix} &= \begin{pmatrix} -1 & e^{-kd} \\ e^{-kd} & -1 \end{pmatrix} \begin{pmatrix} C_e \\ D_e \end{pmatrix}; \\
 g_a(k, \omega) \begin{pmatrix} A_e \\ B_e \end{pmatrix} &= \begin{pmatrix} 1 & e^{-kd} \\ e^{-kd} & 1 \end{pmatrix} \begin{pmatrix} C_e \\ D_e \end{pmatrix},
 \end{aligned} \tag{9.175}$$

where we have dropped superscripts indicating the medium. We have a system of equations consisting of four equations and four unknowns. We could write this in the form of one matrix equation with a  $4 \times 4$  matrix and end up with the condition for mode being that the determinant of this matrix is zero. However, it is easier to first eliminate the two unknowns  $A_e$  and  $B_e$  in favor of  $C_e$  and  $D_e$  and end up with a  $2 \times 2$  matrix. The elimination leads to

$$\begin{pmatrix} g_a(k, \omega) + 1 & e^{-kd} [1 - g_a(k, \omega)] \\ e^{-kd} [1 - g_a(k, \omega)] & g_a(k, \omega) + 1 \end{pmatrix} \begin{pmatrix} C_e \\ D_e \end{pmatrix} = \begin{pmatrix} 0 \\ 0 \end{pmatrix}. \tag{9.176}$$

The condition for self-sustained fields is that the determinant of the matrix vanishes, i.e.,

$$\begin{vmatrix} g_a(k, \omega) + 1 & e^{-kd} [1 - g_a(k, \omega)] \\ e^{-kd} [1 - g_a(k, \omega)] & g_a(k, \omega) + 1 \end{vmatrix} = 0. \tag{9.177}$$

On the dispersion curves, defined by this equation, fields may appear spontaneously without any external charge- and current-densities at the interfaces. The equation results in the following condition for normal modes

$$[g_a(k, \omega) + 1]^2 - e^{-2kd} [g_a(k, \omega) - 1]^2 = 0. \tag{9.178}$$

This may be generalized to the case of two different materials and results in

$$[g_a^{(1)}(k, \omega) + 1][g_a^{(2)}(k, \omega) + 1] - e^{-2kd} [g_a^{(1)}(k, \omega) - 1][g_a^{(2)}(k, \omega) - 1] = 0, \tag{9.179}$$

or

$$[\tilde{g}_a^{(1)}(k, \omega) + 2][\tilde{g}_a^{(2)}(k, \omega) + 2] - e^{-2kd} \tilde{g}_a^{(1)}(k, \omega) \tilde{g}_a^{(2)}(k, \omega) = 0. \tag{9.180}$$

Let us now find out the corresponding result when spatial dispersion is neglected. Then, since

$$g_a^{(i)}(k, \omega) = \frac{1}{\tilde{\epsilon}^{(i)}(\omega)}, \tag{9.181}$$

our condition is reduced into

$$[\tilde{\epsilon}^{(1)}(\omega) + 1][\tilde{\epsilon}^{(2)}(\omega) + 1] - e^{-2kd} [\tilde{\epsilon}^{(1)}(\omega) - 1][\tilde{\epsilon}^{(2)}(\omega) - 1] = 0. \tag{9.182}$$

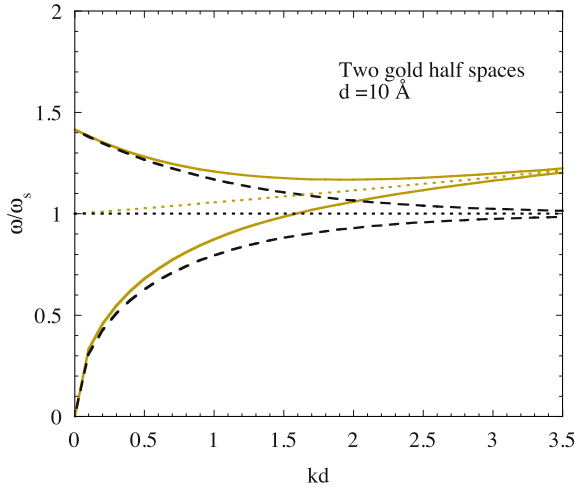


**Fig. 9.21** The dispersion curves for the two normal modes in the gap between two gold half spaces in the non-retarded formalism. The *dashed curves* are the result when spatial dispersion is neglected [15]; the *solid curves* are the result when spatial dispersion is included within RPA. The *upper dotted curve* is the surface-plasmon dispersion-curve of Fig. 9.17 re-plotted with the present choice of axes scaling. The gap between the half spaces is  $10 \text{ \AA}$ . The dashed curves are unaffected by the gap value

This is the well-established condition (9.24) for TM-modes when spatial dispersion is neglected [15].

In Fig. 9.21 we show the two surface-modes for two gold half spaces separated by a gap of  $10 \text{ \AA}$ . When spatial dispersion is neglected, dashed curves, the two dispersion curves approach  $\omega_s$ , the surface plasmon frequency, for large momentum and/or large gap value,  $d$ . With spatial dispersion, solid curves, they instead approach a curve with positive slope. In both treatments one of the modes starts out from zero frequency at zero momentum and the other from the plasma frequency,  $\omega_{pl} = \sqrt{2}\omega_s$ . With this choice of axes the dispersion curves in neglect of spatial dispersion are independent of the  $d$ -value. The curves when spatial dispersion is included depend on the  $d$ -value; the smaller the gap the larger the effect is.

If we were neglecting magnetic effects and retardation effects there would be no more modes so we would now be done. The magnetic effects are very weak for ordinary non-magnetic materials so they are often neglected. Here we want to include them for sake of completeness. We derive these in the next section but let us first present a scheme for finding the actual sources and fields when a mode is excited. We do not need to know these for finding the interactions in the systems but could be of interest to others.

One first determines the sources. One cannot get all four sources directly; one can get three expressed in terms of the fourth. Let us rather arbitrarily choose the fourth to be  $D_e(\mathbf{k}, \omega_{\mathbf{k}})$ . One first finds  $A_e$ ,  $B_e$ , and  $C_e$  expressed in  $D_e$ . Then one may determine all fields in the three regions expressed in terms of  $D_e$ . From the

fields one gets the energy stored in the fields. The energy density of the fields is  $\mathfrak{E} = (\tilde{\mathbf{H}} \cdot \mathbf{B} + \mathbf{E} \cdot \tilde{\mathbf{D}}) / 8\pi$ . Integrating this energy density over all space gives the total energy stored in the fields. Then  $D_e(\mathbf{k}, \omega_k)$  is found by equating this energy with  $\hbar\omega_k$ . The fields are found from (9.123) and an inverse Fourier transform with respect to  $q_z$ . This involves, due to spatial dispersion, calculating  $z$ -depending generalizations of the  $g$ - and  $h$ -functions. This is outside the scope of this book so we are here content to find the relation between the sources.

From (9.178) we find the two modes as solution to

$$[g_a(k, \omega_k) + 1] = \pm e^{-kd} [g_a(k, \omega_k) - 1]. \quad (9.183)$$

Inserting these relations into (9.176) gives

$$C_e = \mp D_e. \quad (9.184)$$

Using (9.175) we find for the first mode that

$$\begin{aligned} A_e &= [1 + e^{-kd}] D_e, \\ B_e &= -[1 + e^{-kd}] D_e, \\ C_e &= -D_e, \end{aligned} \quad (9.185)$$

or

$$\begin{aligned} \rho_s^{(1)}(k, \omega_k) &= [1 + e^{-kd}] \rho_s^{(0, right)}(k, \omega_k), \\ \rho_s^{(2)}(k, \omega_k) &= -[1 + e^{-kd}] \rho_s^{(0, right)}(k, \omega_k), \\ \rho_s^{(0, left)}(k, \omega_k) &= -\rho_s^{(0, right)}(k, \omega_k). \end{aligned} \quad (9.186)$$

For the second mode we find

$$\begin{aligned} A_e &= -[1 - e^{-kd}] D_e, \\ B_e &= -[1 - e^{-kd}] D_e, \\ C_e &= D_e, \end{aligned} \quad (9.187)$$

or

$$\begin{aligned} \rho_s^{(1)}(k, \omega_k) &= -[1 - e^{-kd}] \rho_s^{(0, right)}(k, \omega_k), \\ \rho_s^{(2)}(k, \omega_k) &= -[1 - e^{-kd}] \rho_s^{(0, right)}(k, \omega_k), \\ \rho_s^{(0, left)}(k, \omega_k) &= \rho_s^{(0, right)}(k, \omega_k). \end{aligned} \quad (9.188)$$

Now we have found the relation between the sources for the two “electric” normal modes. Next we derive the “magnetic” normal modes originating from the weak magnetic effects in non-magnetic materials.

### 9.13.5 Magnetic Modes Associated with a Gap Between Two Half Spaces

We study the modes generated by the same type of charge- and accompanying current-densities on the two interfaces. In the more complicated geometry, treated here, we need to define two new factors:

$$C_m = 2\pi K_{\perp}^{(0, left)}(\mathbf{k}, \omega) / c ; D_m = 2\pi K_{\perp}^{(0, right)}(\mathbf{k}, \omega) / c. \quad (9.189)$$

The first superscript represents medium 0, which is vacuum. The second represents which of the two interfaces the current distribution is located at, the one to the left or the one to the right. The fields inside the left half space are generated by the charge- and current-densities at the left interface, and the fields inside the right half space by the ones at the right interface. The fields in the middle region, in vacuum, are generated by both sets of densities. We start by studying the boundary conditions for  $\mathbf{B}$ .

The continuity of the  $z$ -component of the  $\mathbf{B}$ -field at the left interface gives

$$iA_m h_a^{(1)}(k, \omega) = iC_m h_a^{(0)}(k, \omega) + iD_m h_a^{(0)}(k, \omega) e^{-kd}, \quad (9.190)$$

or

$$h_a^{(1)}(k, \omega) A_m = C_m + e^{-kd} D_m. \quad (9.191)$$

The corresponding equation from the right interface gives

$$h_a^{(2)}(k, \omega) B_m = e^{-kd} C_m + D_m. \quad (9.192)$$

We will here limit ourselves to having the same material on both sides of the gap. Then we may combine the results to

$$h_a^{(1)}(k, \omega) \begin{pmatrix} A_m \\ B_m \end{pmatrix} = \begin{pmatrix} 1 & e^{-kd} \\ e^{-kd} & 1 \end{pmatrix} \begin{pmatrix} C_m \\ D_m \end{pmatrix}. \quad (9.193)$$

Next we use the boundary condition for the  $\tilde{\mathbf{H}}$ -field at the left and find

$$-A_m = C_m - e^{-kd} D_m. \quad (9.194)$$

The corresponding result to the right gives

$$B_m = e^{-kd} C_m - D_m. \quad (9.195)$$

All the boundary conditions have resulted in the following system of equations:

$$\begin{aligned}
 \begin{pmatrix} A_m \\ B_m \end{pmatrix} &= \begin{pmatrix} -1 & e^{-kd} \\ e^{-kd} & -1 \end{pmatrix} \begin{pmatrix} C_m \\ D_m \end{pmatrix}; \\
 h_a(k, \omega) \begin{pmatrix} A_m \\ B_m \end{pmatrix} &= \begin{pmatrix} 1 & e^{-kd} \\ e^{-kd} & 1 \end{pmatrix} \begin{pmatrix} C_m \\ D_m \end{pmatrix},
 \end{aligned} \tag{9.196}$$

where we have dropped superscripts indicating the medium. We have a system of equations consisting of four equations and four unknowns. We could write this in the form of one matrix equation with a  $4 \times 4$  matrix and end up with the condition for mode being that the determinant of this matrix is zero. However, it is easier to first eliminate the two unknowns  $A_m$  and  $B_m$  in favor of  $C_m$  and  $D_m$  and end up with a  $2 \times 2$  matrix. The elimination leads to

$$\begin{pmatrix} h_a(k, \omega) + 1 & e^{-kd} [1 - h_a(k, \omega)] \\ e^{-kd} [1 - h_a(k, \omega)] & h_a(k, \omega) + 1 \end{pmatrix} \begin{pmatrix} C_m \\ D_m \end{pmatrix} = \begin{pmatrix} 0 \\ 0 \end{pmatrix}. \tag{9.197}$$

The condition for self-sustained fields is that the determinant of the matrix vanishes, i.e.,

$$\begin{vmatrix} h_a(k, \omega) + 1 & e^{-kd} [1 - h_a(k, \omega)] \\ e^{-kd} [1 - h_a(k, \omega)] & h_a(k, \omega) + 1 \end{vmatrix} = 0. \tag{9.198}$$

On the dispersion curves, defined by this equation, fields may appear spontaneously without any external charge- and current-densities at the interfaces. The equation results in the following condition for normal modes

$$[h_a(k, \omega) + 1]^2 - e^{-2kd} [h_a(k, \omega) - 1]^2 = 0. \tag{9.199}$$

This may be generalized to the case of two different materials and results in

$$[h_a^{(1)}(k, \omega) + 1] [h_a^{(2)}(k, \omega) + 1] - e^{-2kd} [h_a^{(1)}(k, \omega) - 1] [h_a^{(2)}(k, \omega) - 1] = 0, \tag{9.200}$$

or

$$[\tilde{h}_a^{(1)}(k, \omega) + 2] [\tilde{h}_a^{(2)}(k, \omega) + 2] - e^{-2kd} \tilde{h}_a^{(1)}(k, \omega) \tilde{h}_a^{(2)}(k, \omega) = 0. \tag{9.201}$$

Let us now find out the corresponding result when spatial dispersion is neglected. Then, since

$$h_a^{(i)}(k, \omega) = \tilde{\mu}^{(i)}(\omega), \tag{9.202}$$

our condition is reduced into

$$[\tilde{\mu}^{(1)}(\omega) + 1] [\tilde{\mu}^{(2)}(\omega) + 1] - e^{-2kd} [\tilde{\mu}^{(1)}(\omega) - 1] [\tilde{\mu}^{(2)}(\omega) - 1] = 0. \tag{9.203}$$

Now we have completed the derivation of the condition for normal modes associated with a gap between two half spaces. These conditions can be used to find the van der Waals interaction between two half spaces. This we do in the next section.

### 9.13.6 Van der Waals Interactions Between Two Half Spaces

In the previous sections we found that the condition for modes between two half spaces separated by a vacuum gap of thickness  $d$  is

$$\left[\tilde{g}_a(k, \omega) + 2\right]^2 - e^{-2kd} \tilde{g}_a(k, \omega)^2 = 0, \quad (9.204)$$

for electric modes and

$$\left[\tilde{h}_a(k, \omega) + 2\right]^2 - e^{-2kd} \tilde{h}_a(k, \omega)^2 = 0, \quad (9.205)$$

for magnetic. From this the interaction energy is found to be (5.59)

$$E(d) = \hbar \int_0^\infty \frac{d\xi}{2\pi} \int \frac{d^2k}{(2\pi)^2} \left[ \ln \left\{ 1 - e^{-2kd} \frac{\tilde{g}_a(k, i\xi)^2}{[\tilde{g}_a(k, i\xi) + 2]^2} \right\} + \ln \left\{ 1 - e^{-2kd} \frac{\tilde{h}_a(k, i\xi)^2}{[\tilde{h}_a(k, i\xi) + 2]^2} \right\} \right], \quad (9.206)$$

with spatial dispersion and

$$E(d) = \hbar \int_0^\infty \frac{d\xi}{2\pi} \int \frac{d^2k}{(2\pi)^2} \left[ \ln \left\{ 1 - e^{-2kd} \frac{[\tilde{\varepsilon}(i\xi) - 1]^2}{[\tilde{\varepsilon}(i\xi) + 1]^2} \right\} + \ln \left\{ 1 - e^{-2kd} \frac{[\tilde{\mu}(i\xi) - 1]^2}{[\tilde{\mu}(i\xi) + 1]^2} \right\} \right], \quad (9.207)$$

neglecting spatial dispersion. The effects of spatial dispersion on the interaction energy is very small. The exponential factor in the integrands have the effect that only small  $kd$  values contribute. We see in Fig. 9.21 that in the limit of small  $kd$  the effects on the normal modes become increasingly small. To see this in a more clear way we may imagine using the mode-summation method (5.57) and study Fig. 9.21. The contribution from a specific  $\mathbf{k}$  is the average of the values on the two solid curves minus the value on the upper dotted curve. The corresponding contribution in neglect of spatial dispersion is the average of the values on the two dashed curves minus the value on lower dotted curve (horizontal straight line). We see that spatial dispersion has the effect to move the solid curves upward but the upper dotted curve is also moving upward, thus cancelling much of the effect.

## References

1. Bo E. Sernelius, Phys. Rev. B **71**, 235114 (2005)
2. J. Schmit, A.A. Lucas, Solid State Commun. **11**, 415 (1972)
3. R.A. Craig, Phys. Rev. B **6**, 1134 (1972)
4. Bo E. Sernelius, Graphene **1**, 21 (2012)
5. Bo E. Sernelius, Casimir effects in systems containing 2D layers such as graphene and 2D electron gases. J. Phys. Condens. Matter **27**, 214017 (2015)
6. N.G. van Kampen, B.R.A. Nijboer, K. Schram, Phys. Lett. **26A**, 307 (1968)
7. E.D. Palik, *Handbook of Optical Constants of Solids* (Academic Press, New York, 1985)
8. Bo E. Sernelius, P. Björk, Phys. Rev. B )
9. M. Boström, Bo E. Sernelius, Phys. Rev. B **61**, 2204 (2000)
10. Bo E. Sernelius, Phys. Rev. B **90**, 155457 (2014)
11. M. Boström, Bo E. Sernelius, Phys. Rev. A **61**, 052703–052711 (2000)
12. M. Boström, Bo E. Sernelius, Phys. Rev. A **85**, 012508 (2012)
13. U.A. Schröder, M. Petrović, T. Gerber, A.J. Martínez-Galera, E. Grånäs, M.A. Arman, C. Herbig, J. Schnadt, M. Kralj, J. Knudsen, T. Michely, 2D Mater. **4**, 015013 (2017)
14. Bo E. Sernelius, Phys. Rev. B **91**, 045402 (2015)
15. Bo E. Sernelius, *Surface Modes in Physics* (Wiley, Berlin, 2001)
16. J.D. Jackson, *Classical Electrodynamics*, 3rd edn. (Wiley, New York, 1999), p. 156
17. D.F. Arago, Mém. Cl. Sci. Math. Phys. Inst. France **1**, 115 (1811)
18. P. Halevi, *Spatial Dispersion in Solids and Plasmas*, vol. 1, ed. by P. Halevi. Electromagnetic Waves: Recent Developments in Research (North-Holland, Amsterdam, 1992)
19. V.M. Agronovich, D.L. Mills, in *Surface Polaritons: Electromagnetic Waves at Surfaces and Interfaces*, vol. 1, ed. by V.M. Agronovich, D.L. Mills. Modern Problems in Condensed Matter Sciences (Oxford, North-Holland, Amsterdam, New York, 1982)
20. J. Lagois, B. Fischer, *Surface Exciton Polariton from an Experimental Viewpoint*, pp. 69–92
21. V.M. Agranovich, *Effects of the Transition Layer and Spatial Dispersion in the Spectra of Surface Polaritons*, pp. 187–238
22. W.L. Schaich, W. Chen, Phys. Rev. B **39**, 10714 (1984)
23. K.L. Kliewer, Surf. Sci. **101**, 57 (1980)
24. R. Fuchs, K.L. Kliewer, Phys. Rev. B **3**, 2270 (1971)
25. A.F. Alexandrov, L.S. Bogdankevich, A.A. Rukhadze, *Principles of Plasma Electrodynamics* (Springer Series in Electrophysics (Springer, Berlin, New York, 1984))
26. R. Esquivel, C. Villarreal, W.L. Mochan, Phys. Rev. A **68**, 052103 (2003)
27. R. Esquivel, V.B. Svetovoy, Phys. Rev. A **69**, 062102 (2004)
28. S.I. Pekar, J. Phys. Chem. Solids **5**, 11 (1958)
29. R. Ruppin, R. Englman, Phys. Rev. Lett. **53**, 1688 (1989)
30. K.-D. Tsuei, E.W. Plummer, P.J. Feibelman, Phys. Rev. Lett. **63**, 2256 (1989)
31. K.-D. Tsuei, E.W. Plummer, A. Liebsch, K. Kempa, P. Bakshi, Phys. Rev. Lett. **64**, 44 (1990)
32. H. Ishida, A. Liebsch, Phys. Rev. B **54**, 14127 (1996)
33. V.M. Silkin, E.V. Chulkov, P.M. Echenique, Phys. Rev. Lett. **93**, 176801 (2004)

# Chapter 10

## Van der Waals Interaction in Spherical Structures



**Abstract** After a section in which we adapt the general formalism presented in Chap. 7 to spherical structures in neglect of retardation we start by introducing the basic structure elements: a single spherical interface, a spherical shell, a thin diluted spherical gas film, and a 2D spherical film. A general spherical structure can then be constructed by stacking these elements concentrically. The thin gas layer is special; it is used to find the interaction on an atom at a general position in the spherical structure. Then we go through some common structures and present illustrating examples; the examples involve gold spheres, spherical gold cavities, spherical graphene shells, and lithium atoms. We furthermore rederive the van der Waals interaction between two atoms by comparing the full result in the diluted limit with that from the summation of pair interactions.

### 10.1 Adapting the General Method of Chap. 7 to Spherical Structures and to the Neglect of Retardation

For a spherical object the rightmost medium,  $n = N + 1$ , in Fig. 7.1 is the core. The leftmost,  $n = 0$ , is the ambient. The boundary condition is that there are no incoming waves, i.e. there is no wave moving toward the right in medium  $n = 0$ . The fields are self-sustained; no fields are coming in from outside.

In the non-retarded treatment of a spherical structure we let the waves represent solutions to Laplace's equation, (7.21), in spherical coordinates,  $(r, \theta, \varphi)$ , for the scalar potential,  $\Phi$ . The interfaces are spherical surfaces and the  $r$ -coordinate is the coordinate that is constant on each interface. The solutions are of the form

$$\Phi_{l,m}(r, \theta, \varphi) = r^{-l-1} Y_{l,m}(\theta, \varphi), \quad (10.1)$$

where the functions  $Y_{l,m}(\theta, \varphi)$  are the so-called spherical harmonics. We let  $r$  increase toward the left in Fig. 7.1. We want to find the normal modes for a specific set of  $l$  and  $m$  values. Then all waves have the common factor  $Y_{l,m}(\theta, \varphi)$ . We suppress this factor here. Then

$$R(r) = r^l; L(r) = r^{-(l+1)}. \quad (10.2)$$

Using the boundary conditions that the potential and the normal component of the  $\tilde{\mathbf{D}}$ -field are continuous across an interface  $n$  gives

$$\begin{aligned} a^n r_n^l + b^n r_n^{-(l+1)} &= a^{n+1} r_n^l + b^{n+1} r_n^{-(l+1)} \\ a^n \tilde{\varepsilon}_n l r_n^{l-1} - b^n \tilde{\varepsilon}_n (l+1) r_n^{-(l+2)} &= a^{n+1} \tilde{\varepsilon}_{n+1} l r_n^{l-1} - b^{n+1} \tilde{\varepsilon}_{n+1} (l+1) r_n^{-(l+2)}, \end{aligned} \quad (10.3)$$

and we may identify the matrix  $\tilde{\mathbf{A}}_n(r_n)$ , defined in (7.1), as

$$\tilde{\mathbf{A}}_n(r_n) = \begin{pmatrix} r_n^l & r_n^{-(l+1)} \\ \tilde{\varepsilon}_n l r_n^{l-1} & -\tilde{\varepsilon}_n (l+1) r_n^{-(l+2)} \end{pmatrix}. \quad (10.4)$$

The matrix  $\tilde{\mathbf{M}}_n$ , defined in (7.2), is

$$\tilde{\mathbf{M}}_n = \frac{1}{(2l+1)\tilde{\varepsilon}_n} \begin{pmatrix} \tilde{\varepsilon}_n (l+1) + \tilde{\varepsilon}_{n+1} l (l+1) (\tilde{\varepsilon}_n - \tilde{\varepsilon}_{n+1}) r_n^{-(2l+1)} & \\ l (\tilde{\varepsilon}_n - \tilde{\varepsilon}_{n+1}) r_n^{2l+1} & \tilde{\varepsilon}_{n+1} (l+1) + \tilde{\varepsilon}_n l \end{pmatrix}. \quad (10.5)$$

Since the function  $L(r)$  in (10.2) diverges at the origin it is excluded from the core region and hence we have no wave moving toward the left in that region. According to (7.6) this means that

$$f_{l,m}(\omega) = M_{11}. \quad (10.6)$$

Before we end this section we introduce the  $2^l$  pole polarizabilities  $\alpha_l^n$  and  $\alpha_l^{n(2)}$  for the spherical interface since these appear repeatedly in the sections that follow. The first is valid outside the interface and the second inside. The polarizability  $\alpha_l^n = -b^n/a^n$  under the assumption that  $b^{n+1} = 0$ . One obtains  $\alpha_l^n = -M_{21}/M_{11}$  and from (10.5) one finds

$$\alpha_l^n = -\frac{r_n^{2l+1} l (\tilde{\varepsilon}_n - \tilde{\varepsilon}_{n+1})}{\tilde{\varepsilon}_n (l+1) + \tilde{\varepsilon}_{n+1} l}. \quad (10.7)$$

The polarizability  $\alpha_l^{n(2)} = -a^{n+1}/b^{n+1}$  under the assumption that  $a^n = 0$ . One obtains  $\alpha_l^{n(2)} = M_{12}/M_{11}$  and from (10.5) one finds

$$\alpha_l^{n(2)} = \frac{r_n^{-(2l+1)} (l+1) (\tilde{\varepsilon}_n - \tilde{\varepsilon}_{n+1})}{\tilde{\varepsilon}_n (l+1) + \tilde{\varepsilon}_{n+1} l}. \quad (10.8)$$

Sometimes it is convenient to use an alternative form of the matrix  $\tilde{\mathbf{M}}_n$ ,

$$\begin{aligned}
\tilde{\mathbf{M}}_n &= \frac{\tilde{\varepsilon}_n(l+1) + \tilde{\varepsilon}_{n+1}l}{(2l+1)\tilde{\varepsilon}_n} \begin{pmatrix} 1 & \frac{(l+1)(\tilde{\varepsilon}_n - \tilde{\varepsilon}_{n+1})r_n^{-(2l+1)}}{\tilde{\varepsilon}_n(l+1) + \tilde{\varepsilon}_{n+1}l} \\ \frac{l(\tilde{\varepsilon}_n - \tilde{\varepsilon}_{n+1})r_n^{2l+1}}{\tilde{\varepsilon}_n(l+1) + \tilde{\varepsilon}_{n+1}l} & \frac{\tilde{\varepsilon}_{n+1}(l+1) + \tilde{\varepsilon}_n l}{\tilde{\varepsilon}_n(l+1) + \tilde{\varepsilon}_{n+1}l} \end{pmatrix} \\
&= M_{11}^n \begin{pmatrix} 1 & \alpha_l^{n(2)} \\ -\alpha_l^n & \frac{\tilde{\varepsilon}_{n+1}(l+1) + \tilde{\varepsilon}_n l}{\tilde{\varepsilon}_n(l+1) + \tilde{\varepsilon}_{n+1}l} \end{pmatrix}.
\end{aligned} \tag{10.9}$$

Now we have all we need to determine the non-retarded normal modes in a layered spherical structure. We give some examples in the following sections.

### Summary of key relations for the derivation of van der Waals interactions in spherical structures:

In a spherical structure  $l$  and  $m$  are the proper quantum numbers that characterize a normal mode. The dispersion curve for a mode can have several branches,  $i$ ,  $\omega = \omega_{l,m}^i$ . They are solutions to the condition for modes,  $f_{l,m}(\omega) = 0$ , where  $f_{l,m}(\omega)$  is the mode condition function. When finding the interaction energy of the system one has to sum over both  $l$ ,  $m$  and  $i$ . For zero temperature the interaction energy is

$$E = \frac{\hbar}{2} \sum_{l=0}^{\infty} \sum_{m=-l}^l \int_0^{\infty} \frac{d\xi}{2\pi} \ln f_{l,m}(i\xi) = \hbar \sum_{l=0}^{\infty} \sum_{m=-l}^l \int_0^{\infty} \frac{d\xi}{2\pi} \ln f_{l,m}(i\xi), \tag{10.10}$$

and at finite temperature

$$\mathfrak{F} = \sum_{l=0}^{\infty} \sum_{m=-l}^l \frac{1}{\beta} \sum_{n=0}^{\infty} \ln f_{l,m}(i\xi_n); \quad \xi_n = \frac{2\pi n}{\hbar\beta}. \tag{10.11}$$

In the non-retarded approximation  $f_{l,m} \equiv M_{11}$  where  $\tilde{\mathbf{M}}$  is the matrix for the whole structure. The matrix for interface  $n$  is given by

$$\tilde{\mathbf{M}}_n = M_{11}^n \begin{pmatrix} 1 & \alpha_l^{n(2)} \\ -\alpha_l^n & \frac{\tilde{\varepsilon}_{n+1}(l+1) + \tilde{\varepsilon}_n l}{\tilde{\varepsilon}_n(l+1) + \tilde{\varepsilon}_{n+1}l} \end{pmatrix}, \tag{10.12}$$

where

$$M_{11}^n = \frac{\tilde{\varepsilon}_n(l+1) + \tilde{\varepsilon}_{n+1}l}{(2l+1)\tilde{\varepsilon}_n}, \tag{10.13}$$

and the polarizabilities  $\alpha_l^n$  and  $\alpha_l^{n(2)}$  are

$$\alpha_l^n = -\frac{r_n^{2l+1}l(\tilde{\varepsilon}_n - \tilde{\varepsilon}_{n+1})}{\tilde{\varepsilon}_n(l+1) + \tilde{\varepsilon}_{n+1}l}. \tag{10.14}$$

and

$$\alpha_l^{n(2)} = \frac{r_n^{-(2l+1)} (l+1) (\tilde{\epsilon}_n - \tilde{\epsilon}_{n+1})}{\tilde{\epsilon}_n (l+1) + \tilde{\epsilon}_{n+1} l}, \tag{10.15}$$

repectively. Often it is appropriate to give the energy relative a reference system. Then  $f_{l,m}$  is replaced by  $\tilde{f}_{l,m}$  in (10.10) and (10.11), where  $\tilde{f}_{l,m} = f_{l,m}/f_{l,m}^{\text{ref}}$ .

Note that in the non-retarded treatment the matrices do not depend on  $m$  so the summation over  $m$  just renders a factor of  $(2l+1)$ .

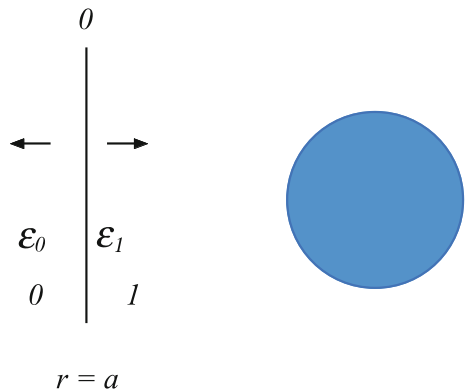
## 10.2 Basic Structure Elements

A general spherical structure can be generated by stacking a number of basic structure elements concentrically around each other. The most basic element is a solid sphere, or ball. Sometimes it is convenient to use layers as elements. A special layer is a 2D spherical film. Another is a thin spherical diluted gas layer which we will use repeatedly in the derivation of the interaction between atoms and the spherical structure. We now discuss these basic elements one by one. We start with the solid sphere.

### 10.2.1 Solid Sphere or Ball

The structure that corresponds to a single interface between two media in the planar case is here a solid sphere. For a solid sphere of radius  $a$  and dielectric function  $\tilde{\epsilon}_1(\omega)$  in an ambient of dielectric function  $\tilde{\epsilon}_0(\omega)$ , as illustrated in Fig. 10.1, we have

**Fig. 10.1** The geometry of a solid sphere, or ball, or a solid cylinder of radius  $a$  in the non-retarded treatment. This is the less complex version of Fig. 7.1 with just a single interface. In the case of a normal mode a single wave is moving away from the interface, on both sides. Adapted from [1]



$$\tilde{\mathbf{M}} = \tilde{\mathbf{M}}_0 = \frac{1}{(2l+1)\tilde{\epsilon}_0} \begin{pmatrix} \tilde{\epsilon}_0(l+1) + \tilde{\epsilon}_1 l & (\tilde{\epsilon}_0 - \tilde{\epsilon}_1)a^{-(2l+1)} \\ l(\tilde{\epsilon}_0 - \tilde{\epsilon}_1)a^{2l+1} & \tilde{\epsilon}_1(l+1) + \tilde{\epsilon}_0 l \end{pmatrix}, \quad (10.16)$$

and the condition for modes is  $\tilde{\epsilon}_1(\omega)/\tilde{\epsilon}_0(\omega) = -(l+1)/l$ . This result covers both solid spheres and spherical cavities. For a solid sphere of dielectric function  $\tilde{\epsilon}(\omega)$  in vacuum and for a spherical cavity in a medium of dielectric function  $\tilde{\epsilon}(\omega)$  the condition for modes is  $\tilde{\epsilon}(\omega) = -(l+1)/l$  and  $\tilde{\epsilon}(\omega) = -l/(l+1)$ , respectively. In passing we give the expression for the  $2^l$  pole polarizability from (10.14),

$$\alpha_l = -\frac{a^{2l+1}l(\tilde{\epsilon}_0 - \tilde{\epsilon}_1)}{\tilde{\epsilon}_0(l+1) + \tilde{\epsilon}_1 l}. \quad (10.17)$$

Next we turn to a spherical shell.

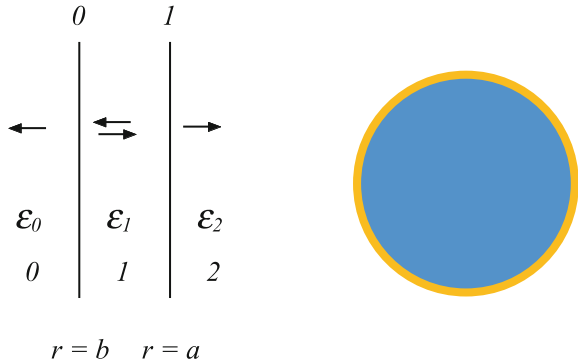
### 10.2.2 Spherical Shell

Here we start from a more general geometry namely that of a coated sphere in a medium and get the spherical shell and gap as special limits. For a solid sphere of dielectric function  $\tilde{\epsilon}_2$  with a coating of inner radius  $a$  and outer radius  $b$ , Fig. 10.2, made of a medium with dielectric function  $\tilde{\epsilon}_1$  in an ambient medium with dielectric function  $\tilde{\epsilon}_0$  we have

$$\begin{aligned} \tilde{\mathbf{M}} &= \tilde{\mathbf{M}}_0 \cdot \tilde{\mathbf{M}}_1 \\ &= \frac{1}{(2l+1)\tilde{\epsilon}_0} \begin{pmatrix} \tilde{\epsilon}_0(l+1) + \tilde{\epsilon}_1 l & \frac{(l+1)(\tilde{\epsilon}_0 - \tilde{\epsilon}_1)}{b^{2l+1}} \\ l(\tilde{\epsilon}_0 - \tilde{\epsilon}_1)b^{2l+1} & \tilde{\epsilon}_1(l+1) + \tilde{\epsilon}_0 l \end{pmatrix} \\ &\times \frac{1}{(2l+1)\tilde{\epsilon}_1} \begin{pmatrix} \tilde{\epsilon}_1(l+1) + \tilde{\epsilon}_2 l & \frac{(l+1)(\tilde{\epsilon}_1 - \tilde{\epsilon}_2)}{a^{2l+1}} \\ l(\tilde{\epsilon}_1 - \tilde{\epsilon}_2)a^{2l+1} & \tilde{\epsilon}_2(l+1) + \tilde{\epsilon}_1 l \end{pmatrix}. \end{aligned} \quad (10.18)$$

From direct derivation of the  $M_{11}$  element the condition for modes becomes

**Fig. 10.2** The geometry of a coated sphere or cylinder in the non-retarded treatment. Adapted from [1]



$$\left(\frac{b}{a}\right)^{2l+1} \left(\frac{\tilde{\varepsilon}_1}{\tilde{\varepsilon}_0} + \frac{(l+1)}{l}\right) \left(\frac{\tilde{\varepsilon}_2}{\tilde{\varepsilon}_1} + \frac{(l+1)}{l}\right) = -\frac{(l+1)}{l} \left(\frac{\tilde{\varepsilon}_1}{\tilde{\varepsilon}_0} - 1\right) \left(\frac{\tilde{\varepsilon}_2}{\tilde{\varepsilon}_1} - 1\right). \quad (10.19)$$

Alternatively we may elaborate using the matrix version in (10.12)

$$\begin{aligned} M_{11} &= M_{11}^0 M_{11}^1 \left(1 - \alpha_l^{0(2)} \alpha_l^1\right) \\ &= M_{11}^0 M_{11}^1 \left[1 - \frac{b^{-(2l+1)}(l+1)(\tilde{\varepsilon}_0 - \tilde{\varepsilon}_1)}{\tilde{\varepsilon}_0(l+1) + \tilde{\varepsilon}_1 l} \frac{a^{2l+1}l(\tilde{\varepsilon}_2 - \tilde{\varepsilon}_1)}{\tilde{\varepsilon}_1(l+1) + \tilde{\varepsilon}_2 l}\right] = 0. \end{aligned} \quad (10.20)$$

Let us now study a spherical shell of inner radius  $a$ , outer radius  $b$  and of a medium with dielectric function  $\tilde{\varepsilon}(\omega)$  in a medium of dielectric function  $\tilde{\varepsilon}_0(\omega)$ . The condition for modes we get from (10.19) by the replacements  $\tilde{\varepsilon}_2(\omega) \rightarrow \tilde{\varepsilon}_0(\omega)$  and  $\tilde{\varepsilon}_1(\omega) \rightarrow \tilde{\varepsilon}(\omega)$ . For a spherical gap of dielectric function  $\tilde{\varepsilon}_0(\omega)$  in a medium of dielectric function  $\tilde{\varepsilon}(\omega)$  we instead make the replacements  $\tilde{\varepsilon}_0(\omega), \tilde{\varepsilon}_2(\omega) \rightarrow \tilde{\varepsilon}(\omega)$  and  $\tilde{\varepsilon}_1(\omega) \rightarrow \tilde{\varepsilon}_0(\omega)$ . For both these geometries we find the same condition for modes, viz.

$$\begin{aligned} \left(\frac{b}{a}\right)^{2l+1} [\tilde{\varepsilon}(\omega)l + \tilde{\varepsilon}_0(\omega)(l+1)] [\tilde{\varepsilon}_0(\omega)l + \tilde{\varepsilon}(\omega)(l+1)] \\ = l(l+1) [\tilde{\varepsilon}(\omega) - \tilde{\varepsilon}_0(\omega)]^2. \end{aligned} \quad (10.21)$$

Next in the pipeline is a diluted gas film.

### 10.2.3 Thin Spherical Diluted Gas Film

It is of interest to find the van der Waals force on an atom in a layered structure. We can obtain this by studying the force on a thin layer of a diluted gas with dielectric function  $\varepsilon_g(\omega) = 1 + 4\pi n\alpha^{at}(\omega)$ , where  $\alpha^{at}$  is the polarizability of one atom and  $n$  the density of atoms (we have assumed that the atom is surrounded by vacuum; if not the 1 should be replaced by the dielectric function of the ambient medium and the atomic polarizability should be replaced by the excess polarizability). For a diluted gas layer the interactions between the gas atoms are negligible compared to all other interactions and the force on the layer is just the sum of the forces on the individual atoms. So by dividing with the number of atoms in the film we get the force on one atom. The layer has to be thin in order to have a well defined  $r$ -value of the atom. Since we will derive the force on an atom in different spherical geometries it is fruitful to derive the matrix for a thin diluted gas shell. This result can be directly used in the derivation of the van der Waals force on an atom in different spherical geometries.

We let the film have the thickness  $\delta$  and be of a general radius  $r$ . We only keep terms up to linear order in  $\delta$  and linear order in  $n$ . We find the result is

$$\begin{aligned}\tilde{\mathbf{M}}_{\text{gaslayer}} &= \tilde{\mathbf{M}}_0 \cdot \tilde{\mathbf{M}}_1 \\ &= \begin{pmatrix} 1 & 0 \\ 0 & 1 \end{pmatrix} + (\delta n) 4\pi \alpha^{at} \begin{pmatrix} 0 & (l+1)r^{-(2l+2)} \\ -lr^{(2l)} & 0 \end{pmatrix}.\end{aligned}\quad (10.22)$$

Now we are done with the gas layer. We will use these results later in calculating the van der Waals force on an atom in spherical layered structures. Next we address 2D films.

### 10.2.4 2D Spherical Film

In many situations one is dealing with very thin films. These may be considered 2D. Important examples are a graphene sheet and a 2D electron gas. In the derivation we let the film have finite thickness  $\delta$  and be characterized by a 3D dielectric function  $\tilde{\epsilon}^{3D}$ . We then let the thickness go toward zero. The 3D dielectric function depends on  $\delta$  as  $\tilde{\epsilon}^{3D} \sim 1/\delta$  for small  $\delta$ . In the planar structure we could in the limit when  $\delta$  goes toward zero obtain a momentum dependent 2D dielectric function. Here we only keep the long wave length limit of the 2D dielectric function [2, 3]. We obtain

$$\tilde{\mathbf{M}}_{2D} = \tilde{\mathbf{M}}_0 \cdot \tilde{\mathbf{M}}_1 = \begin{pmatrix} 1 & 0 \\ 0 & 1 \end{pmatrix} + \frac{(\delta \tilde{\epsilon}^{3D})^{l(l+1)}}{(2l+1)r} \begin{pmatrix} 1 & r^{-(2l+1)} \\ -r^{(2l+1)} & -1 \end{pmatrix}.\quad (10.23)$$

Two examples where these results can be applied are a sphere made of a graphene like film and a thin metal film, respectively. Then [2, 3]

$$\delta \tilde{\epsilon}^{3D}(i\xi) \approx \delta \alpha^{3D}(i\xi) \approx \begin{cases} \frac{\pi e^2}{\hbar |\xi|}, & \text{graphene like film} \\ \frac{4\pi n^{2D} e^2}{m^* m_e \xi^2}, & \text{metal film.} \end{cases}\quad (10.24)$$

The final result is independent of  $\delta$  and is the 2D limit.

We will also need the  $2^l$  pole polarizability of the thin spherical shell in vacuum. It can be obtained from (10.23). The polarizability is  $-b^0/a^0$  under the assumption that  $b^1 = 0$ . One obtains  $\alpha_l^{2D} = -M_{21}/M_{11}$ . We find

$$\alpha_l^{2D}(a; \omega) = \frac{\delta \tilde{\epsilon}^{3D} l(l+1) a^{2l+1}}{(2l+1)a + \delta \tilde{\epsilon}^{3D} l(l+1)},\quad (10.25)$$

where we have reserved the first argument before the semicolon for the radius of the spherical film. Note that for a perfectly reflecting thin spherical shell the  $2^l$  pole polarizability,  $\alpha_l^{2D} = a^{2l+1}$ , coincides with that for a perfectly reflecting sphere of the same radius [compare with (10.17)] and the interaction is the same. This is what one would expect. It is further convenient to define the  $2^l$  pole susceptibility [4] as the polarizability stripped by the factor  $a^{2l+1}$ ,

$$\chi_l^{2D}(a; \omega) = \frac{\delta \tilde{\varepsilon}^{3D} l(l+1)}{(2l+1)a + \delta \tilde{\varepsilon}^{3D} l(l+1)}, \quad (10.26)$$

The  $2^l$  pole polarizability “seen from inside the shell” we get from (10.23). The polarizability is  $-a^1/b^1$  under the assumption that  $a^0 = 0$ . One obtains  $\alpha_l^{2D(2)} = M_{12}/M_{11}$  and

$$\alpha_l^{2D(2)}(a; \omega) = \frac{(\delta \tilde{\varepsilon}^{3D}) l(l+1) a^{-(2l+1)}}{(2l+1)a + (\delta \tilde{\varepsilon}^{3D}) l(l+1)}. \quad (10.27)$$

Note that it is the same as the ordinary  $2^l$  pole polarizability (10.25), for a thin spherical shell except that now the radius of the sphere has been inverted in the numerator. Thus  $\alpha_l^{2D}(a; \omega) = a^{2l+1} \chi_l^{2D}(a; \omega)$  and  $\alpha_l^{2D(2)}(a; \omega) = a^{-(2l+1)} \chi_l^{2D}(a; \omega)$ .

Sometimes it is convenient to use an alternative form of the matrix  $\tilde{\mathbf{M}}_{2D}$ ,

$$\begin{aligned} \tilde{\mathbf{M}}_{2D} &= \frac{(2l+1)r + (\delta \tilde{\varepsilon}^{3D})l(l+1)}{(2l+1)r} \begin{pmatrix} 1 & \frac{(\delta \tilde{\varepsilon}^{3D})l(l+1)r^{-(2l+1)}}{(2l+1)r + (\delta \tilde{\varepsilon}^{3D})l(l+1)} \\ -\frac{(\delta \tilde{\varepsilon}^{3D})l(l+1)r^{(2l+1)}}{(2l+1)r + (\delta \tilde{\varepsilon}^{3D})l(l+1)} & \frac{(2l+1)r - (\delta \tilde{\varepsilon}^{3D})l(l+1)}{(2l+1)r + (\delta \tilde{\varepsilon}^{3D})l(l+1)} \end{pmatrix} \\ &= M_{11}^{2D} \begin{pmatrix} 1 & \alpha_l^{2D(2)} \\ -\alpha_l^{2D} & \frac{(2l+1)r - (\delta \tilde{\varepsilon}^{3D})l(l+1)}{(2l+1)r + (\delta \tilde{\varepsilon}^{3D})l(l+1)} \end{pmatrix}. \end{aligned} \quad (10.28)$$

Now we are done with the list of basic elements and are ready to give examples of different geometrical structures. We start by studying the interaction between an atom and a ball.

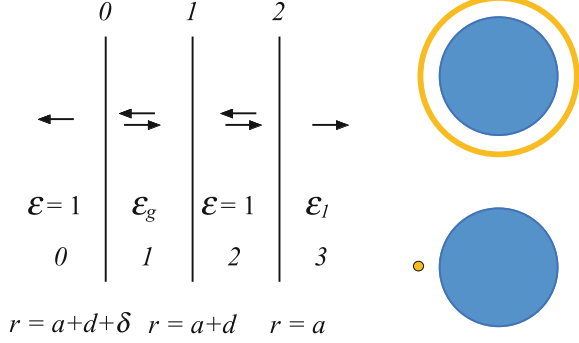
### 10.3 Atom-Ball Interaction

We let the atom be at a distance  $d$  from the ball of radius  $a$  and at a distance  $b$  from the center of the ball. We start from the two layer structure in Fig. 10.3. We let the ambient be vacuum. The first layer is a thin layer, of thickness  $\delta$ , of a diluted gas of atoms of the kind we consider. Its dielectric function is  $\varepsilon_g(\omega) = 1 + 4\pi n \alpha^{at}(\omega)$ , where  $\alpha^{at}$  is the polarizability of one atom. The density of gas atoms,  $n$ , is very low. We let the first interface be at  $r = b + \delta$  and hence the second at  $r = b$ , where  $b = a + d$ . The second layer is a vacuum layer of thickness  $d$ . The remaining medium is the sphere of radius  $a$  with the dielectric function  $\tilde{\varepsilon}_1(\omega)$ . In what follows we only keep lowest order terms in  $\delta$  and in  $n$ .

The matrix becomes  $\tilde{\mathbf{M}} = \tilde{\mathbf{M}}_0 \cdot \tilde{\mathbf{M}}_1 \cdot \tilde{\mathbf{M}}_2 = \tilde{\mathbf{M}}_{\text{gaslayer}} \cdot \tilde{\mathbf{M}}_2$  where  $\tilde{\mathbf{M}}_{\text{gaslayer}}$  is the matrix in (10.22) now for the  $r$  value  $b$  and

$$\mathbf{M}_2 = \frac{1}{(2l+1)} \begin{pmatrix} (l+1) + \tilde{\varepsilon}_1 l & (l+1)(1 - \tilde{\varepsilon}_1) a^{-(2l+1)} \\ l(1 - \tilde{\varepsilon}_1) a^{2l+1} & \tilde{\varepsilon}_1(l+1) + l \end{pmatrix}, \quad (10.29)$$

**Fig. 10.3** The geometry of a thin gas layer the distance  $d$  from a sphere or cylinder of radius  $a$  in the non-retarded treatment. Adapted from [1]



the matrix in (10.16) with the replacement  $\tilde{\epsilon}_0 \rightarrow 1$ . The matrix element of interest is

$$M_{11} \approx \frac{1}{(2l+1)} \left[ (l+1) + \tilde{\epsilon}_1 l - (\delta n) 4\pi \alpha^{at} l (l+1) b^{-(2l+2)} a^{2l+1} (\tilde{\epsilon}_1 - 1) \right]. \quad (10.30)$$

The mode condition function when the reference system is that when the atom is at infinite distance from the sphere then becomes

$$\tilde{f}_{l,m} = 1 - (\delta n) 4\pi \alpha^{at} \left[ \frac{l(l+1) b^{-(2l+2)} a^{2l+1} (\tilde{\epsilon}_1 - 1)}{(l+1) + \tilde{\epsilon}_1 l} \right]. \quad (10.31)$$

The interaction energy per atom we get by dividing the energy with the number of atoms in the gas shell. It is

$$\begin{aligned} \frac{E}{4\pi b^2 \delta n} &= \frac{\hbar}{4\pi b^2 \delta n} \int_0^\infty \frac{d\xi}{2\pi} \sum_{l=0}^\infty \sum_{m=-l}^l \ln \left[ \tilde{f}_{l,m} (i\xi) \right] \\ &\approx -\frac{\hbar}{4\pi b^2 \delta n} \int_0^\infty \frac{d\xi}{2\pi} \sum_{l=0}^\infty \sum_{m=-l}^l 4\pi n \alpha^{at} \delta \left[ \frac{l(l+1) b^{-(2l+2)} a^{2l+1} (\tilde{\epsilon}_1 - 1)}{(l+1) + \tilde{\epsilon}_1 l} \right] \\ &= -\hbar \int_0^\infty \frac{d\xi}{2\pi} \sum_{l=0}^\infty \alpha^{at} (i\xi) \frac{(2l+1)(l+1)}{b^{2(l+2)}} \frac{a^{2l+1} [\tilde{\epsilon}_1 (i\xi) - 1]}{(l+1) + \tilde{\epsilon}_1 (i\xi) l} \\ &= -\hbar \int_0^\infty \frac{d\xi}{2\pi} \sum_{l=0}^\infty \frac{(2l+1)(l+1)}{b^{2(l+2)}} \alpha^{at} (i\xi) \alpha_l (a; i\xi) \\ &= -\hbar \int_0^\infty \frac{d\xi}{2\pi} \sum_{l=0}^\infty \frac{[2l+2]!}{[2l]![2]!} \frac{\alpha^{at} (i\xi) \alpha_l (a; i\xi)}{b^{2(l+2)}}, \end{aligned} \quad (10.32)$$

where  $b = a + d$ , and

$$\alpha_l (a; i\xi) = \frac{a^{2l+1} l [\tilde{\epsilon}_1 (i\xi) - 1]}{(l+1) + \tilde{\epsilon}_1 (i\xi) l} \quad (10.33)$$

is the  $2^l$  pole polarizability, given in (10.17), now for a sphere in vacuum ([5], (5.68)). In the second line of (10.32) we have expanded the logarithm and kept the lowest order term. Note that the  $l = 0$  term does not contribute to the interaction.

The force on the atom is obtained as minus the derivative of the result in (10.32) with respect to  $d$ , i.e.

$$F(b) = -\hbar \int_0^\infty \frac{d\xi}{2\pi} \sum_{l=0}^\infty \frac{[2l+2]!}{[2l]![2]!} 2(l+2) \frac{\alpha^{at}(i\xi) \alpha_l(a; i\xi)}{b^{2l+5}}. \tag{10.34}$$

Now we give a specific example.

### 10.3.1 Li-Atom–Au-Ball Interaction

As an example of atom-ball interactions we show in Fig. 10.4 the interaction between a Li atom and a gold ball. The polarizability for Li was obtained from the London approximation (8.60) with the parameters given in Fig. 8.2. For gold we used the polarizability as shown in Fig. 9.3. The  $b$ -dependence follows a simple power law,  $E \sim d^{-6}$  for large separations. This comes from dipole-dipole interactions. Higher order multipole contributions become important when the objects are in near contact or to be more specific when the distance is of the order of the ball radius. Next we investigate the interactions when the atom is inside a spherical cavity.

**Fig. 10.4** The interaction energy for a Li atom next to a gold sphere of radius  $a = 1$  nm. The distance between their centers is denoted by  $b$ . The results were obtained from (10.32). The result shows that the first term in the summation over  $l$  gives the whole result for large  $b$ -values and that higher order multipole contributions start to be important when the objects are near contact

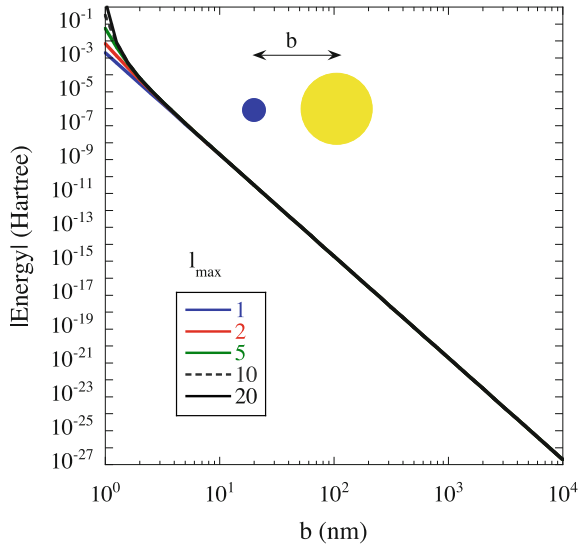
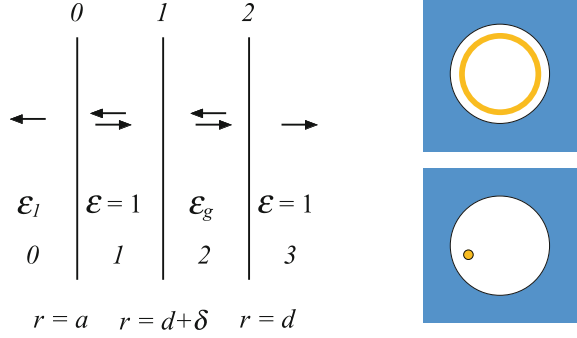


**Fig. 10.5** The geometry of a thin gas layer at radius  $d$  inside a spherical or cylindrical cavity of radius  $a$  in the non-retarded treatment. Adapted from [1]



## 10.4 Force on an Atom in a Spherical Cavity

We let the atom be at a distance  $d$  from the center of the spherical cavity, of radius  $a$ . We start from the two layer structure in Fig. 10.5. We let the medium surrounding the cavity have dielectric function  $\tilde{\epsilon}_1(\omega)$ . The first layer is a vacuum layer. The second is a thin layer, of thickness  $\delta$ , of a diluted gas of atoms of the kind we consider. Its dielectric function is  $\epsilon_g(\omega) = 1 + 4\pi n\alpha^{at}(\omega)$ , where  $\alpha^{at}$  is the polarizability of one atom. The density of gas atoms,  $n$ , is very low. We let the first interface be at  $r = a$  and hence the second at  $r = d + \delta$  and the third at  $r = d$ . In what follows we only keep lowest order terms in  $\delta$  and in  $n$ .

The matrix becomes  $\tilde{\mathbf{M}} = \tilde{\mathbf{M}}_0 \cdot \tilde{\mathbf{M}}_1 \cdot \tilde{\mathbf{M}}_2 = \tilde{\mathbf{M}}_0 \cdot \tilde{\mathbf{M}}_{\text{gaslayer}}$  where  $\tilde{\mathbf{M}}_0$  is obtained from (10.16) with the replacements  $\tilde{\epsilon}_1 \rightarrow 1$  and  $\tilde{\epsilon}_0 \rightarrow \tilde{\epsilon}_1$ .  $\tilde{\mathbf{M}}_{\text{gaslayer}}$  is obtained from (10.22) with  $r = d$ . We find

$$M_{11} \approx \frac{1}{(2l+1)\tilde{\epsilon}_1} \left[ (\tilde{\epsilon}_1(l+1) + l) - \delta n \frac{4\pi\alpha^{at}}{d} (l+1)l(\tilde{\epsilon}_1 - 1)(d/a)^{2l+1} \right]. \quad (10.35)$$

The mode condition function when the reference system is that in absence of the atom is

$$\begin{aligned} \tilde{f}_{l,m} &\approx 1 - (\delta n) 4\pi\alpha^{at} \frac{(l+1)l(\tilde{\epsilon}_1-1)(d/a)^{2l+1}}{d[\tilde{\epsilon}_1(l+1)+l]} \\ &= 1 - (\delta n) 4\pi\alpha^{at} \alpha_l^{(2)}(a; \omega) l d^{2l}, \end{aligned} \quad (10.36)$$

where we have identified the new  $2^l$  pole polarizability that was given in (10.15),

$$\alpha_l^{(2)}(a; \omega) = -\frac{(l+1)(1-\tilde{\epsilon}_1)(1/a)^{2l+1}}{l+\tilde{\epsilon}_1(l+1)}, \quad (10.37)$$

for the spherical cavity of radius  $a$  “as seen from the inside.”

From this we find the interaction energy per atom becomes

$$\begin{aligned}
 \frac{E}{4\pi d^2 \delta n} &= \frac{\hbar}{4\pi d^2 \delta n} \int_0^\infty \frac{d\xi}{2\pi} \sum_{l=0}^\infty \sum_{m=-l}^l \ln \left[ \tilde{f}_{l,m}(\mathrm{i}\xi) \right] \\
 &\approx -\frac{\hbar}{4\pi d^2 \delta n} \int_0^\infty \frac{d\xi}{2\pi} \sum_{l=0}^\infty \sum_{m=-l}^l 4\pi (\delta n) \alpha^{at}(\mathrm{i}\xi) \alpha_l^{(2)}(a; \mathrm{i}\xi) l d^{2l} \\
 &= -\hbar \int_0^\infty \frac{d\xi}{2\pi} \sum_{l=0}^\infty \alpha^{at}(\mathrm{i}\xi) \alpha_l^{(2)}(a; \mathrm{i}\xi) (2l+1) l d^{2(l-1)} \\
 &= -\hbar \int_0^\infty \frac{d\xi}{2\pi} \sum_{l=1}^\infty \frac{[2l+1]!}{[2l-1]![2]!} \alpha^{at}(\mathrm{i}\xi) \alpha_l^{(2)}(a; \mathrm{i}\xi) d^{2(l-1)},
 \end{aligned} \tag{10.38}$$

where we on the second line have expanded the logarithm and kept the lowest order term. The force on the atom is

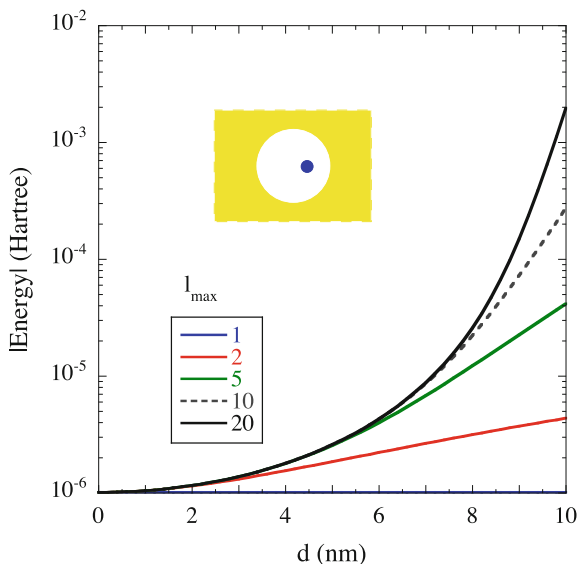
$$F = -\hbar \int_0^\infty \frac{d\xi}{2\pi} \sum_{l=1}^\infty \frac{[2l+1]!}{[2l-1]![2]!} 2(l-1) d^{2l-3} \alpha^{at}(\mathrm{i}\xi) \alpha_l^{(2)}(a; \mathrm{i}\xi). \tag{10.39}$$

Note that the  $l = 0$  and  $l = 1$  terms do not contribute to the force.

### 10.4.1 Force on a Li-Atom in a Spherical Gold Cavity

As an example of interactions on an atom in a cavity we show in Fig. 10.6 the interaction on a Li atom in a gold cavity. The polarizability for Li was obtained from

**Fig. 10.6** The interaction energy for a Li atom in a spherical gold cavity of radius  $a = 10$  nm. The atom is at the distance  $d$  from the centre of the cavity. The results were obtained from (10.38). The closer to the cavity wall the atom is the more terms in the summation over  $l$  is needed



the London approximation (8.60) with the parameters given in Fig. 8.2. For gold we used the polarizability as shown in Fig. 9.3. There is no dipole contribution to the force; the first contribution is a quadrupole term ( $l = 2$ ); the dipole-dipole interaction contributes a constant to the potential. Higher order multipole contributions become important when the atom is close to the cavity wall.

## 10.5 van der Waals Interaction Between Two Atoms

Here we may use the result from the previous section to derive the van der Waals interaction between two atoms. We let the atom outside the sphere be of type 1. We let the spherical core of the structure be made up of a diluted gas of atoms of type 2. Then we let the density of the gas go toward zero and at the same time let the radius of the sphere go to zero ( $b$  goes toward  $d$ ). We furthermore only keep the  $l = 1$  term in the expansion; we are only interested in dipole-dipole interactions. So we divide the energy in (10.32) further with the number of atoms of the other species contained in the sphere and take the limits

$$\begin{aligned} \frac{E}{4\pi b^2 \delta n_1 (n_2 4\pi a^3/3)} &\approx -\frac{\hbar}{b^2 (n_2 4\pi a^3/3)} \int_0^\infty \frac{d\xi}{2\pi} \alpha_1^{at}(\mathbf{i}\xi) \frac{3.2}{b^4} \frac{a^3 [4\pi n_2 \alpha_2^{at}(\mathbf{i}\xi)]}{3} \\ &\approx -\frac{6\hbar}{d^6} \int_0^\infty \frac{d\xi}{2\pi} \alpha_1^{at}(\mathbf{i}\xi) \alpha_2^{at}(\mathbf{i}\xi), \end{aligned} \quad (10.40)$$

which is the van der Waals result (8.67) ([5], (6.39)).

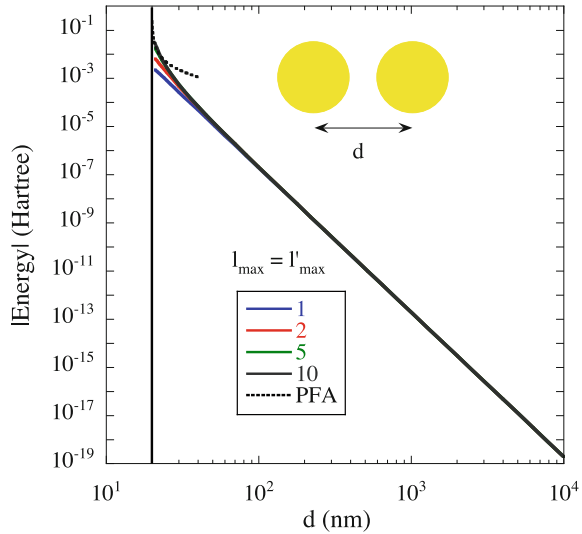
## 10.6 Force Between Two Spherical Objects

In Sect. 10.3 we obtained the force between an atom and a spherical object. We kept contributions from dipolar fluctuations in the atom, only. The dipolar and all higher order fluctuations of the sphere were included. This means that the results are valid for separations large compared to the size of the atom. Equation (10.32) is the first term of the more general expression,

$$E = -\hbar \int_0^\infty \frac{d\xi}{2\pi} \sum_{l'=0}^\infty \sum_{l=0}^\infty \frac{[2l+2l']!}{[2l]! [2l']!} \frac{\alpha_l^1(\mathbf{i}\xi) \alpha_{l'}^2(\mathbf{i}\xi)}{d^{2(l+l'+1)}}, \quad (10.41)$$

which is valid for all spherical objects. Here  $d$  denotes the distance between the centers of the spheres. Note that the superscripts 1 and 2 indicate object number 1 and object number 2, respectively, not an interface number, like in (10.14). The  $2^l$  pole polarizability for a layered spherical object number  $i$  is  $\alpha_i^l = -M_{2l}/M_{1l}$  where the matrix elements are elements of the the full matrix,  $\tilde{\mathbf{M}}$ , for the spherical object.

**Fig. 10.7** The interaction energy for two gold balls of radius  $a = 10$  nm the distance  $d$  apart. The results were obtained from (10.41). When the balls are in near contact more and more terms in the summation are needed. Each curve is for a different truncation of the summations. The dotted piece of curve is the result from PFA as given in (6.33). The vertical line indicates the contact point



### 10.6.1 Interaction Between Two Gold Balls

As an example of ball-ball interactions we show in Fig. 10.7 the interaction between two gold balls. We used (10.41) with the gold polarizability as shown in Fig. 9.3. The  $d$ -dependence follows a simple power law,  $E \sim d^{-6}$  for large separations. This comes from dipole-dipole interactions. Higher order multipole contributions become important when the objects are in near contact. The results are valid for distances larger than the contact value  $2a = 20$  nm indicated by the vertical line in the figure. The closer to contact the more multipole terms one needs to include. Near point of contact it is favorable to use PFA. The dotted curve is the result from (6.33) with  $n = 0$ .

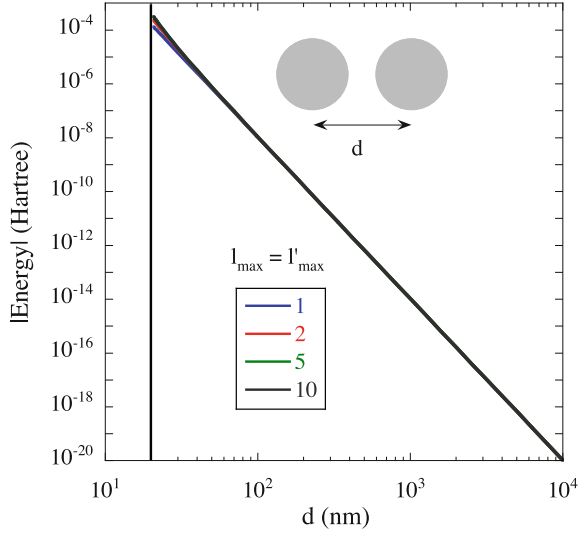
### 10.6.2 Interaction Between Two Graphene Spheres

Another example, Fig. 10.8, of spherical objects is two graphene or rather graphene-like spheres, i.e., two 2D spherical shells. Then (10.41) becomes

$$E = -\hbar \int_0^\infty \frac{d\xi}{2\pi} \sum_{l'=0}^\infty \sum_{l=0}^\infty \frac{[2l+2l']!}{[2l]![2l']!} \frac{\alpha_l^{2D}(a; i\xi) \alpha_{l'}^{2D}(b; i\xi)}{d^{2(l+l'+1)}}, \quad (10.42)$$

where  $\alpha_l^{2D}(a; i\xi)$  is the  $2^l$  pole polarizability of one of the spheres of radius  $a$  and  $\alpha_{l'}^{2D}(b; i\xi)$  is the  $2^{l'}$  pole polarizability of the other of radius  $b$ . The polarizabilities were given in (10.25) and  $\delta\tilde{\epsilon}^{3D}(i\xi)$  entering the polarizabilities was taken from

**Fig. 10.8** The interaction energy two graphene spheres of radius  $a = b = 10$  nm the distance  $d$  apart. The results were obtained from (10.42). When the spheres are in near contact more and more terms in the summation are needed. Each curve is for a different truncation of the summations. The vertical line indicates the contact point



(10.24). The  $d$ -dependence follows a simple power law,  $E \sim d^{-6}$  for large separations. This comes from dipole-dipole interactions. Higher order multipole contributions become important when the objects are in near contact. The results are valid for distances larger than the contact value  $a + b = 20$  nm indicated by the vertical line in the figure. The closer to contact the more multipole terms one needs to include.

## 10.7 Force on an Atom in a Spherical Gap

It is of interest to study the interactions on atoms in narrow channels. Here we study an atom in a spherical vacuum gap with the outer and inner radii  $b$  and  $a$ , respectively. The medium outside the gap has dielectric function  $\tilde{\epsilon}_1(\omega)$  and the medium inside the dielectric function  $\tilde{\epsilon}_2(\omega)$ . The atom is at a distance  $r$  from the center. The matrix for this geometry is  $\tilde{\mathbf{M}} = \tilde{\mathbf{M}}_0 \cdot \tilde{\mathbf{M}}_1 \cdot \tilde{\mathbf{M}}_2$ , where

$$\begin{aligned}
 \tilde{\mathbf{M}}_0 &= \frac{\tilde{\epsilon}_1(l+1)+l}{(2l+1)\tilde{\epsilon}_1} \begin{pmatrix} 1 & \alpha_l^{0(2)} \\ -\alpha_l^0 & \frac{(l+1)+\tilde{\epsilon}_1 l}{\tilde{\epsilon}_1(l+1)+l} \end{pmatrix}; \\
 \tilde{\mathbf{M}}_1 &= \begin{pmatrix} 1 & 0 \\ 0 & 1 \end{pmatrix} + (\delta n) 4\pi \alpha^{at} \begin{pmatrix} 0 & (l+1)r^{-(2l+2)} \\ -lr^{(2l)} & 0 \end{pmatrix}; \\
 \tilde{\mathbf{M}}_2 &= \frac{(l+1)+\tilde{\epsilon}_2 l}{(2l+1)} \begin{pmatrix} 1 & \alpha_l^{2(2)} \\ -\alpha_l^2 & \frac{\tilde{\epsilon}_2(l+1)+l}{(l+1)+\tilde{\epsilon}_2 l} \end{pmatrix}.
 \end{aligned} \tag{10.43}$$

The matrix element of interest is

$$M_{11} = M_{11}^0 M_{11}^2 \left\{ 1 - \alpha_l^2 \alpha_l^{0(2)} - (\delta n) 4\pi \alpha^{at} \left[ (l+1) r^{-(2l+2)} \alpha_l^2 + l r^{(2l)} \alpha_l^{0(2)} \right] \right\}. \quad (10.44)$$

This leads to the following proper mode condition function

$$\tilde{f}_{l,m} = 1 - (\delta n) 4\pi \alpha^{at} \frac{\left[ (l+1) r^{-(2l+2)} \alpha_l^2 + l r^{(2l)} \alpha_l^{0(2)} \right]}{1 - \alpha_l^2 \alpha_l^{0(2)}}, \quad (10.45)$$

where the reference system is the spherical gap in absence of the atom. The two  $2^l$  pole polarizabilities  $\alpha_l^2$  and  $\alpha_l^{0(2)}$  defined in (10.7) and (10.8), respectively, are

$$\begin{aligned} \alpha_l^2 &= \frac{l(\tilde{\epsilon}_2 - 1)a^{2l+1}}{\tilde{\epsilon}_2 l + (l+1)}; \\ \alpha_l^{0(2)} &= -\frac{(l+1)(1-\tilde{\epsilon}_1)(1/b)^{2l+1}}{l + \tilde{\epsilon}_1(l+1)}. \end{aligned} \quad (10.46)$$

The energy per atom is

$$\begin{aligned} \frac{E}{4\pi r^2 \delta n} &= \frac{\hbar}{4\pi r^2 \delta n} \int_0^\infty \frac{d\xi}{2\pi} \sum_{l=0}^\infty \sum_{m=-l}^l \ln \left[ \tilde{f}_{l,m}(\mathbf{i}\xi) \right] \\ &\approx -\frac{\hbar}{4\pi r^2 \delta n} \int_0^\infty \frac{d\xi}{2\pi} \sum_{l=0}^\infty \sum_{m=-l}^l (\delta n) 4\pi \alpha^{at} \frac{(l+1)\alpha_l^2 r^{-(2l+2)} + l\alpha_l^{0(2)} r^{2l}}{1 - \alpha_l^2 \alpha_l^{0(2)}} \\ &= -\hbar \int_0^\infty \frac{d\xi}{2\pi} \sum_{l=0}^\infty \alpha^{at} \frac{[2l+2]!}{[2l]![2]!} \frac{1}{r^3} \frac{\alpha_l^2 r^{-(2l+1)} + \frac{l}{l+1} \alpha_l^{0(2)} r^{2l+1}}{1 - \alpha_l^2 \alpha_l^{0(2)}}, \end{aligned} \quad (10.47)$$

where we on the second line have expanded the logarithm and kept the lowest order term. The force on the atom is

$$F(r) = -\hbar \int_0^\infty \frac{d\xi}{2\pi} \sum_{l=0}^\infty \alpha^{at} \frac{[2l+2]!}{[2l]![2]!} \frac{(2l+4)\alpha_l^2 r^{-(2l+5)} - (2l-2)\frac{l}{l+1}\alpha_l^{0(2)} r^{2l-3}}{1 - \alpha_l^2 \alpha_l^{0(2)}}. \quad (10.48)$$

Next we continue with an atom outside a thin spherical shell.

## 10.8 Force on an Atom Outside a 2D Spherical Shell

In this section we derive the van der Waals interaction experienced by an atom outside a very thin spherical shell. We start from the three layer structure in Fig. 10.9. We take the limit when the thickness,  $\delta$ , goes to zero. The 3D dielectric function of the shell material then goes to infinity. We follow the procedure in Sect. 10.3 but now there is one extra matrix. The matrix becomes  $\tilde{\mathbf{M}} = \tilde{\mathbf{M}}_0 \cdot \tilde{\mathbf{M}}_1 \cdot \tilde{\mathbf{M}}_2 \cdot \tilde{\mathbf{M}}_3$ , where  $\tilde{\mathbf{M}}_0 \cdot \tilde{\mathbf{M}}_1$  is the matrix for a gas layer in (10.22) with  $r = b = a + d$  and  $\tilde{\mathbf{M}}_2 \cdot \tilde{\mathbf{M}}_3$  is the matrix for a thin film in (10.28) with  $r = a$ . The matrix element of interest for us is

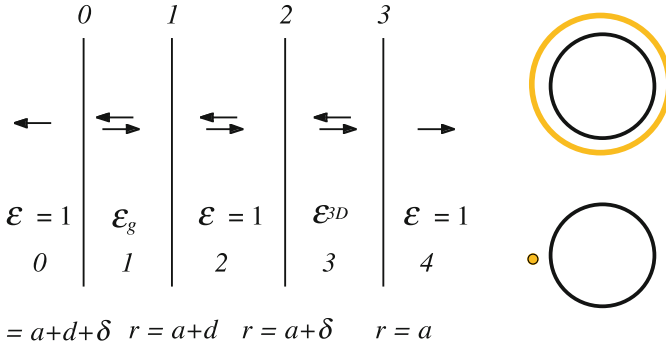


**Fig. 10.9** The geometry of a thin gas layer the distance  $d$  from thin spherical or cylindrical shell of radius  $a$  in the non-retarded treatment. Adapted from [1]

$$M_{11} = \frac{(2l+1)a + (\delta\tilde{\varepsilon}^{3D})l(l+1)}{(2l+1)a} \left[ 1 - (\delta n) 4\pi\alpha^{at}(\omega)\alpha_l^{2D}(a;\omega)(l+1)b^{-(2l+2)} \right]. \quad (10.49)$$

The mode condition function when the reference system is that in absence of the atom is

$$\tilde{f}_{l,m}(i\xi) = 1 - (\delta n) 4\pi\alpha^{at}(i\xi)\alpha_l^{2D}(a;i\xi)(l+1)b^{-(2l+2)}. \quad (10.50)$$

We may identify the  $2^l$  pole polarizability of the thin spherical shell in vacuum given in (10.25). The energy per atom is

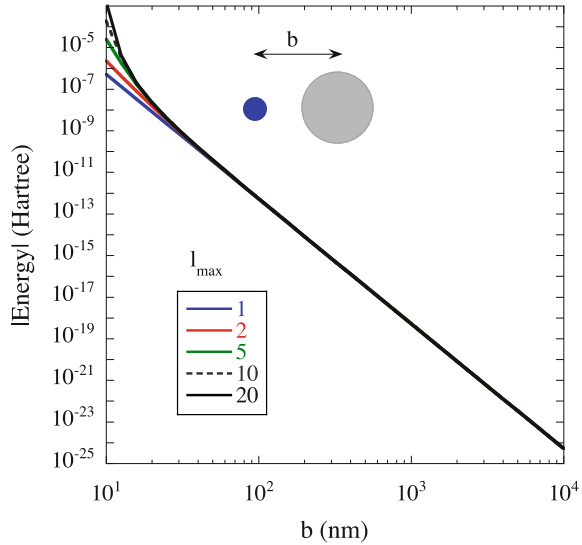
$$\begin{aligned} \frac{E}{4\pi b^2 \delta n} &= \frac{\hbar}{4\pi b^2 \delta n} \int_0^\infty \frac{d\xi}{2\pi} \sum_{l=0}^\infty \sum_{m=-l}^l \ln \left[ \tilde{f}_{l,m}(i\xi) \right] \\ &\approx -\frac{\hbar}{4\pi b^2 \delta n} \int_0^\infty \frac{d\xi}{2\pi} \sum_{l=0}^\infty \sum_{m=-l}^l (\delta n) 4\pi\alpha^{at}(i\xi)\alpha_l^{2D}(a;i\xi)(l+1)b^{-(2l+2)} \\ &= -\hbar \int_0^\infty \frac{d\xi}{2\pi} \sum_{l=0}^\infty \alpha^{at}(i\xi)\alpha_l^{2D}(a;i\xi) \frac{(2l+1)(l+1)}{b^{2(l+2)}} \\ &= -\hbar \int_0^\infty \frac{d\xi}{2\pi} \sum_{l=0}^\infty \frac{[2l+2]!}{[2l]![2]!} \frac{1}{b^{2(l+2)}} \alpha^{at}(i\xi)\alpha_l^{2D}(a;i\xi), \end{aligned} \quad (10.51)$$

where we on the second line have expanded the logarithm and kept the lowest order term. The force on the atom is

$$F(b) = -\hbar \int_0^\infty \frac{d\xi}{2\pi} \sum_{l=0}^\infty \frac{[2l+2]!}{[2l]![2]!} \frac{2(l+2)}{b^{2l+5}} \alpha^{at}(i\xi)\alpha_l^{2D}(a;i\xi). \quad (10.52)$$

Next we treat as an example an atom outside a graphene-like sphere.

**Fig. 10.10** The interaction between a Li atom and a graphene sphere as a function of distance  $b$ . The radius,  $a$ , of the spherical shell is 10 nm. The results are from using (10.51) and each curve is for a different truncation of the summation over  $l$ . See the text for details



### 10.8.1 Interaction Between a Li-Atom and a Graphene Sphere

As an example we give the results for a Li-atom outside a graphene sphere in Fig. 10.10. The results are from using (10.51). The polarizability for Li was obtained from the London approximation (8.60) with the parameters given in Fig. 8.2 and for the spherical shell the  $\delta\tilde{\epsilon}^{3D}(i\xi)$  entering  $\alpha_l^{2D}(a; i\xi)$  was taken from (10.24). The  $b$ -dependence follows a simple power law,  $E \sim d^{-6}$  for large separations. This comes from dipole-dipole interactions. Higher order multipole contributions become important when the objects are in near contact or to be more specific when the distance is of the order of the sphere radius. Next we find out what happens when the atom is inside the thin spherical shell.

## 10.9 Force on an Atom Inside a 2D Spherical Shell

In this section we derive the van der Waals Interaction experienced by an atom inside a very thin spherical shell. We start from the three layer structure in Fig. 10.11. We take the limit when the thickness,  $\delta$ , goes to zero. The derivation is analogous to the one in Sect. 10.8. The matrix becomes  $\tilde{\mathbf{M}} = \tilde{\mathbf{M}}_0 \cdot \tilde{\mathbf{M}}_1 \cdot \tilde{\mathbf{M}}_2 \cdot \tilde{\mathbf{M}}_3$ , where  $\tilde{\mathbf{M}}_0 \cdot \tilde{\mathbf{M}}_1$  is the matrix for the thin film, given in (10.28) for  $r = a$ , and  $\tilde{\mathbf{M}}_2 \cdot \tilde{\mathbf{M}}_3$  is the matrix for the gas film, given in (10.22) for  $r = d$ . The matrix element of interest for us is

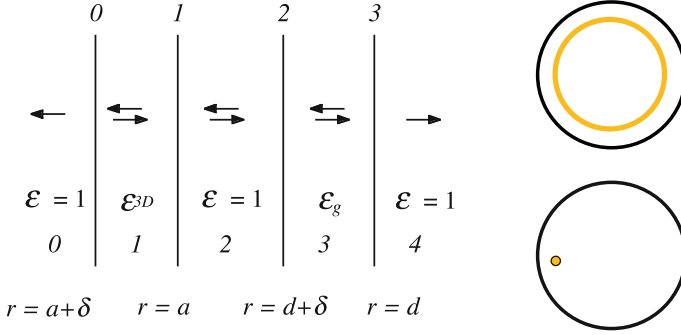


**Fig. 10.11** The geometry of a thin gas layer at radius  $d$  inside a thin spherical or cylindrical shell of radius  $a$  in the non-retarded treatment. Adapted from [1]

$$M_{11} = \frac{(2l+1)a + (\delta\bar{\varepsilon}^{3D})l(l+1)}{(2l+1)a} \left[ 1 - (\delta n) 4\pi\alpha^{at}(\omega) \alpha_l^{2D(2)}(a; \omega) ld^{2l} \right]. \quad (10.53)$$

The mode condition function when the reference system is that in absence of the atom is

$$\tilde{f}_{l,m}(i\xi) = 1 - (\delta n) 4\pi\alpha^{at}(i\xi) \alpha_l^{2D(2)}(a; i\xi) ld^{2l}, \quad (10.54)$$

where we have introduced the  $2^l$  pole polarizability for a thin spherical shell as “seen from the inside,” given in (10.26). The energy per atom is

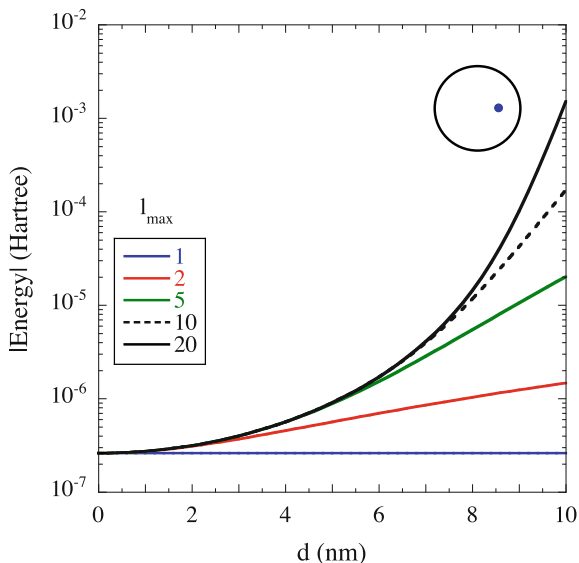
$$\begin{aligned} \frac{E}{4\pi d^2 \delta n} &= \frac{\hbar}{4\pi d^2 \delta n} \int_0^\infty \frac{d\xi}{2\pi} \sum_{l=0}^\infty \sum_{m=-l}^l \ln \left[ \tilde{f}_{l,m}(i\xi) \right] \\ &\approx -\frac{\hbar}{4\pi d^2 \delta n} \int_0^\infty \frac{d\xi}{2\pi} \sum_{l=0}^\infty \sum_{m=-l}^l 4\pi \delta n \alpha^{at}(i\xi) \alpha_l^{2D(2)}(a; i\xi) ld^{2l} \\ &= -\hbar \int_0^\infty \frac{d\xi}{2\pi} \sum_{l=0}^\infty \sum_{m=-l}^l \alpha^{at}(i\xi) \alpha_l^{2D(2)}(a; i\xi) ld^{2(l-1)} \\ &= -\hbar \int_0^\infty \frac{d\xi}{2\pi} \sum_{l=1}^\infty \frac{[2l+1]!}{[2l-1]! [2]!} d^{2(l-1)} \alpha^{at}(i\xi) \alpha_l^{2D(2)}(a; i\xi), \end{aligned} \quad (10.55)$$

where we on the second line have expanded the logarithm and kept the lowest order term. The force on the atom is

$$F = -\hbar \int_0^\infty \frac{d\xi}{2\pi} \sum_{l=1}^\infty \frac{[2l+1]!}{[2l-1]! [2]!} 2(l-1) d^{2l-3} \alpha^{at}(i\xi) \alpha_l^{2D(2)}(a; i\xi). \quad (10.56)$$

Note that the  $l=0$  and  $l=1$  terms do not contribute to the force, just as in the case of an atom in a spherical cavity in Sect. 10.4.

**Fig. 10.12** The interaction on a Li atom inside a graphene sphere as a function of distance  $d$  from the center. The radius,  $a$ , of the spherical shell is 10 nm. The results are from using (10.55) and each curve is for a different truncation of the summation over  $l$ . See the text for details



### 10.9.1 Force on a Li-Atom Inside a Graphene Sphere

As an example we give the results for a Li-atom inside a graphene or rather graphene-like sphere in Fig. 10.12. The results are from using (10.55). The polarizability for Li was obtained from the London approximation (8.60) with the parameters given in Fig. 8.2 and for the spherical shell the  $\delta\tilde{\epsilon}^{3D}(i\xi)$  entering  $\alpha_l^{2D(2)}(a; i\xi)$  was taken from (10.24). We note that the results are very similar to the results for a Li-atom in a gold cavity in Fig. 10.6. The dipole-dipole contribution to the potential is a constant and consequently does not contribute to the force.

Next instead of an atom we place another thin spherical shell inside the shell.

## 10.10 Interaction Between Two 2D Concentric Spherical Shells

We consider two concentric thin spherical shells. The outer shell has radius  $b$  and the inner radius  $a$ . Here the matrix is  $\tilde{\mathbf{M}} = \tilde{\mathbf{M}}_0 \cdot \tilde{\mathbf{M}}_1$  where

$$\begin{aligned} \tilde{\mathbf{M}}_0 &= \begin{pmatrix} 1 & 0 \\ 0 & 1 \end{pmatrix} + \frac{(\delta\tilde{\epsilon}^{3D})_{l(l+1)}}{(2l+1)b} \begin{pmatrix} 1 & b^{-(2l+1)} \\ -b^{(2l+1)} & -1 \end{pmatrix}; \\ \tilde{\mathbf{M}}_1 &= \begin{pmatrix} 1 & 0 \\ 0 & 1 \end{pmatrix} + \frac{(\delta\tilde{\epsilon}^{3D})_{l(l+1)}}{(2l+1)a} \begin{pmatrix} 1 & a^{-(2l+1)} \\ -a^{(2l+1)} & -1 \end{pmatrix}, \end{aligned} \quad (10.57)$$

and the element of interest is

$$M_{11} = 1 + \frac{(\delta\tilde{\varepsilon}^{3D})l(l+1)}{(2l+1)} \left( \frac{1}{a} + \frac{1}{b} \right) + \left[ \frac{(\delta\tilde{\varepsilon}^{3D})l(l+1)}{(2l+1)} \right]^2 \frac{1}{ab} \left[ 1 - \left( \frac{a}{b} \right)^{2l+1} \right]. \quad (10.58)$$

The proper mode condition function becomes

$$\begin{aligned} \tilde{f}_{l,m}(\mathbf{i}\xi) &= 1 - \left[ \frac{\delta\tilde{\varepsilon}^{3D}l(l+1)}{a(2l+1)+\delta\tilde{\varepsilon}^{3D}l(l+1)} \right] \left[ \frac{\delta\tilde{\varepsilon}^{3D}l(l+1)}{b(2l+1)+\delta\tilde{\varepsilon}^{3D}l(l+1)} \right] \left( \frac{a}{b} \right)^{2l+1} \\ &= 1 - \alpha_l^{2D}(a; \mathbf{i}\xi) \alpha_l^{2D(2)}(b; \mathbf{i}\xi), \end{aligned} \quad (10.59)$$

where  $\alpha_l$  is the  $2^l$  pole polarizability of a thin spherical shell of radius  $a$  in vacuum according to (10.25) and  $\alpha_l^{(2)}$  is the  $2^l$  pole polarizability of a thin spherical shell of radius  $b$  in vacuum as seen from inside according to (10.27). We have chosen as reference system a system where the two shells are separated from each other and at infinite distance from each other. The energy obtained by using this mode condition function is the energy change when bringing the two shells at infinite separation together and putting the inner shell inside the outer shell. The energy is

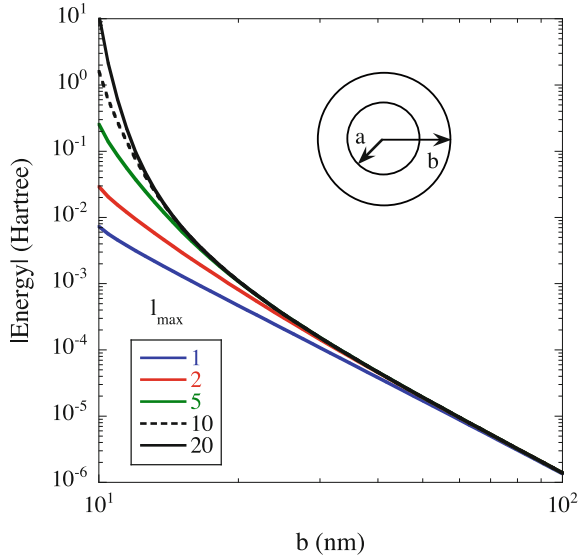
$$\begin{aligned} E &= \hbar \int_0^\infty \frac{d\xi}{2\pi} \sum_{l=0}^\infty \sum_{m=-l}^l \ln \left[ \tilde{f}_{l,m}(\mathbf{i}\xi) \right] \\ &= \hbar \int_0^\infty \frac{d\xi}{2\pi} \sum_{l=0}^\infty (2l+1) \ln \left[ 1 - \alpha_l^{2D}(a; \mathbf{i}\xi) \alpha_l^{2D(2)}(b; \mathbf{i}\xi) \right] \\ &= \hbar \int_0^\infty \frac{d\xi}{2\pi} \sum_{l=0}^\infty (2l+1) \ln \left[ 1 - \frac{\delta\tilde{\varepsilon}^{3D}(\mathbf{i}\xi)l(l+1)a^{2l+1}}{(2l+1)a+\delta\tilde{\varepsilon}^{3D}(\mathbf{i}\xi)l(l+1)} \frac{\delta\tilde{\varepsilon}^{3D}(\mathbf{i}\xi)l(l+1)b^{-(2l+1)}}{(2l+1)b+\delta\tilde{\varepsilon}^{3D}(\mathbf{i}\xi)l(l+1)} \right]. \end{aligned} \quad (10.60)$$

Note that here we cannot safely expand the logarithm and keep the linear term only. The linear term is not necessarily very small. Thus, we keep the logarithm as is. As an example we treat two concentric graphene-like shells in next section.

### 10.10.1 Interaction Between Two Concentric Graphene Spheres

As an example we give in Fig. 10.13 the interaction energy for two concentric graphene spheres. We let the radius,  $a$ , of the inner sphere be 10nm and let the radius,  $b$ , of outer sphere vary between 10nm and 100nm. We have treated the graphene spheres as strictly 2D spherical shells with the effective dielectric function given in (10.24). Each curve is for a different truncation of the summation over  $l$ . The smaller the value of  $b$  the more terms are needed in the summation. The reference system is one where the smaller inner sphere has been taken outside the larger outer sphere and the two are at infinite distance from each other. The energy in Fig. 10.13 is the energy gain when the smaller sphere is brought to and inserted into the larger sphere. The energy in (10.60) is negative.

**Fig. 10.13** The interaction between two concentric graphene spheres as a function of the radius,  $b$ , of the outer sphere. The radius,  $a$  of the inner sphere is 10 nm. The results are from using (10.60) and each curve is for a different truncation of the summation over  $l$ . See the text for details



## 10.11 Force on an Atom in Between Two 2D Spherical Films

Here we study an atom in between two spherical films in vacuum. The outer and inner films are of radii  $b$  and  $a$ , respectively. The atom is at a distance  $r$  from the center. The matrix for this geometry is  $\tilde{\mathbf{M}} = \tilde{\mathbf{M}}_0 \cdot \tilde{\mathbf{M}}_1 \cdot \tilde{\mathbf{M}}_2$ , where

$$\begin{aligned} \tilde{\mathbf{M}}_0 &= \frac{(2l+1)b + (\delta\tilde{\varepsilon}^{3D})l(l+1)}{(2l+1)b} \begin{pmatrix} 1 & \alpha_l^{2D(2)}(b; \omega) \\ -\alpha_l^{2D}(b; \omega) & \frac{(2l+1)b - (\delta\tilde{\varepsilon}^{3D})l(l+1)}{(2l+1)b + (\delta\tilde{\varepsilon}^{3D})l(l+1)} \end{pmatrix}; \\ \tilde{\mathbf{M}}_1 &= \begin{pmatrix} 1 & 0 \\ 0 & 1 \end{pmatrix} + (\delta n) 4\pi\alpha^{at} \begin{pmatrix} 0 & (l+1)r^{-(2l+2)} \\ -lr^{(2l)} & 0 \end{pmatrix}; \\ \tilde{\mathbf{M}}_2 &= \frac{(2l+1)a + (\delta\tilde{\varepsilon}^{3D})l(l+1)}{(2l+1)a} \begin{pmatrix} 1 & \alpha_l^{2D(2)}(a; \omega) \\ -\alpha_l^{2D}(a; \omega) & \frac{(2l+1)a - (\delta\tilde{\varepsilon}^{3D})l(l+1)}{(2l+1)a + (\delta\tilde{\varepsilon}^{3D})l(l+1)} \end{pmatrix}. \end{aligned} \quad (10.61)$$

The matrix element of interest to us is

$$\begin{aligned} M_{11} &= \frac{(2l+1)b + (\delta\tilde{\varepsilon}^{3D})l(l+1)}{(2l+1)b} \frac{(2l+1)a + (\delta\tilde{\varepsilon}^{3D})l(l+1)}{(2l+1)a} \\ &\times \left\{ 1 - \alpha_l^{2D(2)}(b; \omega) \alpha_l^{2D}(a; \omega) - (\delta n) 4\pi\alpha^{at} \right. \\ &\times \left. \left[ \alpha_l^{2D}(a; \omega) (l+1)r^{-(2l+2)} + \alpha_l^{2D(2)}(b; \omega) lr^{(2l)} \right] \right\}, \end{aligned} \quad (10.62)$$

which results in the following, proper mode condition function:

$$\tilde{f}_{l,m}(\mathbf{i}\xi) = 1 - (\delta n) 4\pi\alpha^{at}(\mathbf{i}\xi) \frac{\alpha_l^{2D}(a; \mathbf{i}\xi)(l+1)r^{-(2l+2)} + \alpha_l^{2D(2)}(b; \mathbf{i}\xi)lr^{2l}}{1 - \alpha_l^{2D(2)}(b; \mathbf{i}\xi)\alpha_l^{2D}(a; \mathbf{i}\xi)}. \quad (10.63)$$

From this we obtain the interaction energy of the atom. It is

$$\begin{aligned} \frac{E}{4\pi r^2 \delta n} &= \frac{\hbar}{4\pi r^2 \delta n} \int_0^\infty \frac{d\xi}{2\pi} \sum_{l=0}^\infty \sum_{m=-l}^l \ln \left[ \tilde{f}_{l,m}(\mathbf{i}\xi) \right] \\ &\approx -\frac{\hbar}{4\pi r^2 \delta n} \int_0^\infty \frac{d\xi}{2\pi} \sum_{l=0}^\infty \sum_{m=-l}^l 4\pi \delta n \alpha^{at} \frac{\alpha_l^{2D}(a; \mathbf{i}\xi)(l+1)r^{-(2l+2)} + \alpha_l^{2D(2)}(b; \mathbf{i}\xi)lr^{2l}}{1 - \alpha_l^{2D(2)}(b; \mathbf{i}\xi)\alpha_l^{2D}(a; \mathbf{i}\xi)} \\ &= -\hbar \int_0^\infty \frac{d\xi}{2\pi} \sum_{l=0}^\infty \sum_{m=-l}^l \left[ \frac{\alpha_l^{2D}(a; \mathbf{i}\xi)(l+1)r^{-2(l+2)}}{1 - \alpha_l^{2D(2)}(b; \mathbf{i}\xi)\alpha_l^{2D}(a; \mathbf{i}\xi)} + \frac{\alpha_l^{2D(2)}(b; \mathbf{i}\xi)lr^{2(l-1)}}{1 - \alpha_l^{2D(2)}(b; \mathbf{i}\xi)\alpha_l^{2D}(a; \mathbf{i}\xi)} \right] \\ &= -\hbar \int_0^\infty \frac{d\xi}{2\pi} \sum_{l=1}^\infty \left[ \frac{\frac{[2l+2]!}{[2l]! [2]!} \alpha_l^{2D}(a; \mathbf{i}\xi) r^{-2(l+2)}}{1 - \alpha_l^{2D(2)}(b; \mathbf{i}\xi)\alpha_l^{2D}(a; \mathbf{i}\xi)} + \frac{\frac{[2l+1]!}{[2l-1]! [2]!} \alpha_l^{2D(2)}(b; \mathbf{i}\xi) r^{2(l-1)}}{1 - \alpha_l^{2D(2)}(b; \mathbf{i}\xi)\alpha_l^{2D}(a; \mathbf{i}\xi)} \right], \end{aligned} \quad (10.64)$$

where we on the second line have expanded the logarithm and kept the lowest order term. Note that this expression agrees formally with the results for an atom in a spherical gap, (10.47), but the  $2^l$  pole polarizabilities are of course different. The force on the atom becomes

$$F(r) = -\hbar \int_0^\infty \frac{d\xi}{2\pi} \sum_{l=1}^\infty \left[ \frac{\frac{[2l+2]!}{[2l]! [2]!} 2(l+2)\alpha_l^{2D}(a; \mathbf{i}\xi)r^{-2l-5}}{1 - \alpha_l^{2D(2)}(b; \mathbf{i}\xi)\alpha_l^{2D}(a; \mathbf{i}\xi)} - \frac{\frac{[2l+1]!}{[2l-1]! [2]!} 2(l-1)\alpha_l^{2D(2)}(b; \mathbf{i}\xi)r^{2l-3}}{1 - \alpha_l^{2D(2)}(b; \mathbf{i}\xi)\alpha_l^{2D}(a; \mathbf{i}\xi)} \right]. \quad (10.65)$$

We end this chapter by rederiving the van der Waals interaction of (8.66) between two polarizable atoms in an alternative way.

## 10.12 Force Between Two Atoms from Summation of Pair Interactions

We derived the van der Waals interaction between two atoms in Sect. 8.3. It is possible to find this result via a short-cut, viz. by using the result from the summation over pair interactions in Sect. 6.1. The procedure is the following: choose a geometry with two objects of different material; calculate the result using the summation over pair interactions; calculate the result using the full formalism and take the diluted limit; compare the two results and identify parameters.

We choose to apply this procedure on an atom of species 1 at the distance  $R$  from a ball of atomic species 2. We let the ball have the radius  $R_2$  and the atom density  $n^{3D}$ . We make the ansatz that the interaction between the atoms is given by the potential  $V = -Br^{-6}$  and we intend to identify the coefficient  $B$ . The result from summation over pair interactions (6.13) with this ansatz is

$$E(R) = -\frac{B}{R^6} \frac{4\pi R_2^3 n^{3D}}{3}. \quad (10.66)$$

We have assumed that there is vacuum in between the objects. The condition for modes in the full formalism (10.32) is

$$\begin{aligned}
E(R) &= -\hbar \int_0^\infty \frac{d\xi}{2\pi} \sum_{l=0}^\infty \frac{[2l+2]!}{[2l]![2]!} \frac{\alpha^{at}(\mathbf{i}\xi)\alpha_l(a;\mathbf{i}\xi)}{R^{2(l+2)}} \\
&\approx -\hbar \int_0^\infty \frac{d\xi}{2\pi} \frac{[4]!}{[2]![2]!} \frac{\alpha_1^{at}(\mathbf{i}\xi)\alpha_1(R_2;\mathbf{i}\xi)}{R^{2(l+2)}} = -\frac{1 \cdot 2 \cdot 3 \cdot 4}{1 \cdot 2 \cdot 1 \cdot 2 \cdot 2\pi} \hbar \int_0^\infty d\xi \frac{\alpha_1^{at}(\mathbf{i}\xi)\alpha_1(R_2;\mathbf{i}\xi)}{R^{2(l+2)}} \\
&= -\frac{3}{\pi} \hbar \int_0^\infty d\xi \frac{\alpha_1^{at}(\mathbf{i}\xi)}{R^6} \frac{R^3[\tilde{\varepsilon}_2(\mathbf{i}\xi)-1]}{2+\tilde{\varepsilon}_2(\mathbf{i}\xi)} \approx -\frac{3}{\pi} \hbar \int_0^\infty d\xi \frac{\alpha_1^{at}(\mathbf{i}\xi)}{R^6} \frac{R^3[4\pi n^{3D}\alpha_2^{at}(\mathbf{i}\xi)]}{3} \\
&= -\frac{4\pi R^3 n^{3D}}{3} \frac{1}{R^6} \frac{3}{\pi} \hbar \int_0^\infty d\xi \alpha_1^{at}(\mathbf{i}\xi) \alpha_2^{at}(\mathbf{i}\xi).
\end{aligned} \tag{10.67}$$

For large separations the  $l = 1$  term dominates. We have only kept this term, used that  $\alpha_{l=1}(a; \mathbf{i}\xi) = R^3 [\tilde{\varepsilon}_1(\mathbf{i}\xi) - 1] / [2 + \tilde{\varepsilon}_1(\mathbf{i}\xi)]$  and taken the diluted limit. We have used the expression  $\tilde{\varepsilon}_i(z) = 1 + 4\pi n_i \alpha_i(z)$  for the dielectric function for a gas of atoms of species  $i$ . We have chosen as reference system the geometry when the distance between the atom and the ball goes to infinity and divided by the corresponding mode condition function. Equating the results from (10.66) and (10.67) gives

$$B = \frac{3}{\pi} \hbar \int_0^\infty d\xi \alpha_1(\mathbf{i}\xi) \alpha_2(\mathbf{i}\xi) = \frac{3\hbar}{2} \alpha_1(0) \alpha_2(0) \frac{\omega_1 \omega_2}{\omega_1 + \omega_2}, \tag{10.68}$$

where we in the last step have used the London approximation (8.60) for the atomic polarizability.

The procedure<sup>1</sup> we have just gone through is a short-cut for finding the van der Waals interaction between two atoms. It furthermore acts as a test of the consistency of our formalism.

## References

1. Bo E. Sernelius, Phys. Rev. B **90**, 155457 (2014)
2. Bo E. Sernelius, Graphene **1**, 21 (2012)
3. Bo E. Sernelius, J. Phys.: Condens. Matter **27**, 214017 (2015)
4. D. Langbein, *Theory of van der Waals Attraction* (Springer-Verlag, New York, Heidelberg, 1974)
5. Bo E. Sernelius, *Surface Modes in Physics* (Wiley-VCH, Berlin, 2001)

---

<sup>1</sup>Note that this procedure is different from the one we used in Sect. 10.5 where we did not make any ansatz for the  $r$ -dependence.

# Chapter 11

## Van der Waals Interaction in Cylindrical Structures



**Abstract** After a section in which we adapt the general formalism presented in Chap. 7 to cylindrical structures in neglect of retardation we start by introducing the basic structure elements: a single cylindrical interface, a cylindrical shell, a thin diluted cylindrical gas film, and a 2D cylindrical film. A general cylindrical structure can then be constructed by stacking these elements coaxially. The thin gas layer is special; it is used to find the interaction on an atom at a general position in the cylindrical structure. Then we go through some common structures and present illustrating examples; the examples involve gold cylinders, gold cavities, graphene shells, and lithium atoms. We furthermore rederive the van der Waals interaction between two atoms by comparing the full result in the diluted limit with that from the summation of pair interactions.

### 11.1 Adapting the General Method of Chap. 7 to Cylindrical Structures and to the Neglect of Retardation

The system we consider here is a layered cylinder consisting of  $N$  layers and an inner cylindrical core. We have  $N + 2$  media and  $N + 1$  interfaces. Let the numbering be as follows. Medium 0 is the medium surrounding the cylinder, medium 1 is the outermost layer, medium  $N$  the innermost layer and  $N + 1$  the innermost cylindrical region (the core). Let  $r_n$  be the inner radius of layer  $n$ . The boundary condition is that there are no incoming waves, i.e. there is no wave moving toward the right in medium  $n = 0$  in Fig. 7.1. The fields are self-sustained; no fields are coming in from outside.

In the non-retarded treatment of a cylindrical structure we let the waves represent solutions to Laplace's equation, (7.21), in cylindrical coordinates,  $(r, \theta, z)$ , for the scalar potential,  $\Phi$ . The interfaces are cylindrical surfaces and the  $r$ -coordinate is the coordinate that is constant on each interface. The solutions are of the form

$$\Phi_{k,m}(r, \theta, z) = I_m(kr) e^{im\theta} e^{ikz} \text{ and } K_m(kr) e^{im\theta} e^{ikz}, \quad (11.1)$$

where the functions  $I_m(z)$  and  $K_m(z)$  are so-called modified Bessel functions. The first is bounded for small  $z$  values and the second for large. They are solutions to the modified Bessel equation [1],

$$z^2 \partial^2 \omega / \partial z^2 + z \partial \omega / \partial z - (m^2 + z^2) \omega = 0. \quad (11.2)$$

Note that the variable  $z$  here denotes a general complex variable and should not be mistaken for the spatial  $z$ -variable in (11.1). We let  $r$  increase toward the left in Fig. 7.1. We want to find the normal modes for a specific set of  $k$  and  $m$  values. Then all waves have the common factor  $e^{im\theta} e^{ikz}$ . We suppress this factor here. Then

$$R(r) = I_m(kr); \quad L(r) = K_m(kr). \quad (11.3)$$

Using the boundary conditions that the potential and the normal component of the  $\tilde{\mathbf{D}}$ -field are continuous across an interface  $n$  gives

$$\begin{aligned} a^n I_m(kr_n) + b^n K_m(kr_n) &= a^{n+1} I_m(kr_n) + b^{n+1} K_m(kr_n), \\ a^n \tilde{\varepsilon}_n k I_m'(kr_n) + b^n \tilde{\varepsilon}_n k K_m'(kr_n) &= a^{n+1} \tilde{\varepsilon}_{n+1} k I_m'(kr_n) + b^{n+1} \tilde{\varepsilon}_{n+1} k K_m'(kr_n), \end{aligned} \quad (11.4)$$

and we may identify the matrix  $\tilde{\mathbf{A}}_n(r_n)$  as

$$\tilde{\mathbf{A}}_n(r_n) = \begin{pmatrix} I_m(kr_n) & K_m(kr_n) \\ \tilde{\varepsilon}_n I_m'(kr_n) & \tilde{\varepsilon}_n K_m'(kr_n) \end{pmatrix}. \quad (11.5)$$

The matrix  $\tilde{\mathbf{M}}_n$  is

$$\begin{aligned} \tilde{\mathbf{M}}_n &= \tilde{\mathbf{A}}_n^{-1} \cdot \tilde{\mathbf{A}}_{n+1} \\ &= \frac{1}{W \tilde{\varepsilon}_n} \begin{pmatrix} \tilde{\varepsilon}_{n+1} I_m' K_m - \tilde{\varepsilon}_n I_m K_m' & (\tilde{\varepsilon}_{n+1} - \tilde{\varepsilon}_n) K_m K_m' \\ (\tilde{\varepsilon}_n - \tilde{\varepsilon}_{n+1}) I_m I_m' & \tilde{\varepsilon}_n I_m' K_m - \tilde{\varepsilon}_{n+1} I_m K_m' \end{pmatrix}, \end{aligned} \quad (11.6)$$

where we have suppressed the argument ( $kr_n$ ) of all modified Bessel functions and their derivatives. As before the derivative is with respect to the argument. We have made use of the Wronskian of the two modified Bessel functions:

$$W[K_m(x), I_m(x)] = K_m(x) I_m'(x) - K_m'(x) I_m(x) = 1/x.$$

Since the function  $L(z)$  in (11.3) diverges at the origin it is excluded from the core region and hence we have no wave moving toward the left in that region. According to (7.6) this means that

$$f_{k,m}(\omega) = M_{11}. \quad (11.7)$$

Before we end this section we introduce the two multipole polarizabilities  $\alpha_{k,m}^n$  and  $\alpha_{k,m}^{n(2)}$  for the cylindrical interface since these appear repeatedly in the sections that follow. The first is valid outside the cylindrical interface and the second inside. The polarizability  $\alpha_{k,m}^n = -b^n/a^n$  under the assumption that  $b^{n+1} = 0$ . One obtains  $\alpha_{k,m}^n = -M_{21}/M_{11}$  and from (10.5) one finds

$$\alpha_{k,m}^n(r_n; \omega) = \frac{(\tilde{\epsilon}_{n+1} - \tilde{\epsilon}_n) I_m I_m'}{\tilde{\epsilon}_{n+1} I_m' K_m - \tilde{\epsilon}_n I_m K_m'}. \quad (11.8)$$

The polarizability  $\alpha_{k,m}^{n(2)} = -a^{n+1}/b^{n+1}$  under the assumption that  $a^n = 0$ . One obtains  $\alpha_{k,m}^{n(2)} = M_{12}/M_{11}$  and from (10.5) one finds

$$\alpha_{k,m}^{n(2)}(r_n; \omega) = \frac{(\tilde{\epsilon}_{n+1} - \tilde{\epsilon}_n) K_m K_m'}{\tilde{\epsilon}_{n+1} I_m' K_m - \tilde{\epsilon}_n I_m K_m'}. \quad (11.9)$$

The suppressed argument of the modified Bessel functions in the multipole polarizabilities above is  $(kr_n)$ . Sometimes it is convenient to use an alternative form of the matrix  $\tilde{\mathbf{M}}_n$ ,

$$\tilde{\mathbf{M}}_n = M_{11}^n \begin{pmatrix} 1 & \alpha_{k,m}^{n(2)} \\ -\alpha_{k,m}^n & \frac{\tilde{\epsilon}_n I_m' K_m - \tilde{\epsilon}_{n+1} I_m K_m'}{\tilde{\epsilon}_{n+1} I_m' K_m - \tilde{\epsilon}_n I_m K_m'} \end{pmatrix}. \quad (11.10)$$

Now we have all we need to determine the non-retarded normal modes in a layered cylindrical structure. We give some examples in the following sections.

### Summary of key relations for the derivation of van der Waals interactions in cylindrical structures:

In a cylindrical structure  $k$ , the wave number along the cylinder axis, and  $m$  are the proper quantum numbers that characterize a normal mode. The dispersion curve for a mode can have several branches,  $i$ ,  $\omega = \omega_{k,m}^i$ . They are solutions to the condition for modes,  $f_{k,m}(\omega) = 0$ , where  $f_{k,m}(\omega)$  is the mode condition function. When finding the interaction energy of the system one has to sum over both  $k, m$  and  $i$ . Since we often let the system have unlimited extension along the cylinder axis it is appropriate to calculate the interaction energy per unit length. For zero temperature the interaction energy is

$$E = \frac{\hbar}{2} \frac{1}{L} \sum_k \sum_{m=-\infty}^{\infty} \int_{-\infty}^{\infty} \frac{d\xi}{2\pi} \ln f_{k,m}(i\xi) \rightarrow \frac{\hbar}{2} \int_{-\infty}^{\infty} \frac{dk}{2\pi} \sum_{m=-\infty}^{\infty} \int_{-\infty}^{\infty} \frac{d\xi}{2\pi} \ln f_{k,m}(i\xi), \quad (11.11)$$

and at finite temperature

$$\mathfrak{F} = \frac{1}{L} \sum_k \sum_{m=-\infty}^{\infty} \frac{1}{\beta} \sum_{n=0}^{\infty} \ln f_{k,m}(\mathbf{i}\xi_n) \rightarrow \int_{-\infty}^{\infty} \frac{dk}{2\pi} \sum_{m=-\infty}^{\infty} \frac{1}{\beta} \sum_{n=0}^{\infty} \ln f_{k,m}(\mathbf{i}\xi_n), \quad (11.12)$$

where  $L$  is the length of the system and  $\xi_n = 2\pi n/\hbar\beta$ . The arrows indicate what happens when we let  $L$  go toward infinity. In the non-retarded approximation  $f_{k,m} \equiv M_{11}$  where  $\tilde{\mathbf{M}}$  is the matrix for the whole structure. The matrix for interface  $n$  is given by

$$\begin{aligned} \tilde{\mathbf{M}}_n &= \frac{1}{W\tilde{\varepsilon}_n} \begin{pmatrix} \tilde{\varepsilon}_{n+1}I_m'K_m - \tilde{\varepsilon}_nI_mK_m' & (\tilde{\varepsilon}_{n+1} - \tilde{\varepsilon}_n)K_mK_m' \\ (\tilde{\varepsilon}_n - \tilde{\varepsilon}_{n+1})I_mI_m' & \tilde{\varepsilon}_nI_m'K_m - \tilde{\varepsilon}_{n+1}I_mK_m' \end{pmatrix} \\ &= M_{11}^n \begin{pmatrix} 1 & \alpha_{k,m}^{n(2)} \\ -\alpha_{k,m}^n & \frac{\tilde{\varepsilon}_nI_m'K_m - \tilde{\varepsilon}_{n+1}I_mK_m'}{\tilde{\varepsilon}_{n+1}I_m'K_m - \tilde{\varepsilon}_nI_mK_m'} \end{pmatrix}, \end{aligned} \quad (11.13)$$

where  $W$  is the Wronskian,

$$W[K_m(x), I_m(x)] = K_m(x)I_m'(x) - K_m'(x)I_m(x) = 1/x, \quad (11.14)$$

and the polarizabilities  $\alpha_{k,m}^n$  and  $\alpha_{k,m}^{n(2)}$  are

$$\alpha_{k,m}^n(r_n; \omega) = \frac{(\tilde{\varepsilon}_{n+1} - \tilde{\varepsilon}_n)I_mI_m'}{\tilde{\varepsilon}_{n+1}I_m'K_m - \tilde{\varepsilon}_nI_mK_m'}, \quad (11.15)$$

and

$$\alpha_{k,m}^{n(2)}(r_n; \omega) = \frac{(\tilde{\varepsilon}_{n+1} - \tilde{\varepsilon}_n)K_mK_m'}{\tilde{\varepsilon}_{n+1}I_m'K_m - \tilde{\varepsilon}_nI_mK_m'}, \quad (11.16)$$

respectively. We have suppressed the argument  $(kr_n)$  of all modified Bessel functions and their derivatives. The derivative is with respect to the argument. Often it is appropriate to give the energy relative a reference system. Then  $f_{k,m}$  is replaced by  $\tilde{f}_{k,m}$  in (11.11) and (11.12), where  $\tilde{f}_{k,m} = f_{k,m}/f_{k,m}^{\text{ref}}$ .

## 11.2 Basic Structure Elements

A general cylindrical structure can be generated by stacking a number of basic structure elements coaxially around each other. The most basic element is a solid cylinder. Sometimes it is convenient to use layers as elements. A special layer is a 2D cylindrical film. Another is a thin cylindrical diluted gas layer which we will use repeatedly in the derivation of the interaction between atoms and the cylindrical structure. We now discuss these basic elements one by one. We start with the solid cylinder.

### 11.2.1 Solid Cylinder

For a solid cylinder of radius  $a$  and dielectric function  $\tilde{\epsilon}_1(\omega)$  in an ambient of dielectric function  $\tilde{\epsilon}_0(\omega)$ , as illustrated in Fig. 10.1, we have

$$\tilde{\mathbf{M}} = \tilde{\mathbf{M}}_0 = \frac{ka}{\tilde{\epsilon}_0} \begin{pmatrix} \tilde{\epsilon}_1 I_m' K_m - \tilde{\epsilon}_0 I_m K_m' & (\tilde{\epsilon}_1 - \tilde{\epsilon}_0) K_m K_m' \\ (\tilde{\epsilon}_0 - \tilde{\epsilon}_1) I_m I_m' & \tilde{\epsilon}_0 I_m' K_m - \tilde{\epsilon}_1 I_m K_m' \end{pmatrix}, \quad (11.17)$$

where the suppressed arguments are  $(ka)$  for the modified Bessel functions and  $(\omega)$  for the dielectric functions. The condition for modes is

$$\frac{\tilde{\epsilon}_1(\omega)}{\tilde{\epsilon}_0(\omega)} = \frac{I_m(ka) K_m'(ka)}{I_m'(ka) K_m(ka)}. \quad (11.18)$$

Three important quantities for this structure are

$$\begin{aligned} M_{11} &= \frac{ka}{\tilde{\epsilon}_0(\omega)} [\tilde{\epsilon}_1(\omega) I_m'(ka) K_m(ka) - \tilde{\epsilon}_0(\omega) I_m(ka) K_m'(ka)], \\ \alpha_{k,m}^{\text{cyl.}}(a; \omega) &= \frac{[\tilde{\epsilon}_1(\omega) - \tilde{\epsilon}_0(\omega)] I_m(ka) I_m'(ka)}{\tilde{\epsilon}_1(\omega) I_m'(ka) K_m(ka) - \tilde{\epsilon}_0(\omega) I_m(ka) K_m'(ka)}, \\ \alpha_{k,m}^{\text{cyl.}(2)}(a; \omega) &= \frac{[\tilde{\epsilon}_1(\omega) - \tilde{\epsilon}_0(\omega)] K_m(ka) K_m'(ka)}{\tilde{\epsilon}_1(\omega) I_m'(ka) K_m(ka) - \tilde{\epsilon}_0(\omega) I_m(ka) K_m'(ka)}, \end{aligned} \quad (11.19)$$

where we have placed the superscript *cyl.* on the polarizabilities to indicate cylinder.

### 11.2.2 Cylindrical Shell

Here we start from a more general geometry namely that of a coated cylinder in a medium and get the cylindrical shell and gap as special limits. For a solid cylinder of dielectric function  $\tilde{\epsilon}_2$  with a coating of inner radius  $a$  and outer radius  $b$ , Fig. 10.2, made of a medium with dielectric function  $\tilde{\epsilon}_1$  in an ambient medium with dielectric function  $\tilde{\epsilon}_0$  we have

$$\begin{aligned} \tilde{\mathbf{M}} &= \tilde{\mathbf{M}}_0 \cdot \tilde{\mathbf{M}}_1 \\ &= \frac{kb}{\tilde{\epsilon}_0} [\tilde{\epsilon}_1 I_m'(kb) K_m(kb) - \tilde{\epsilon}_0 I_m(kb) K_m'(kb)] \\ &\quad \times \begin{pmatrix} 1 & \alpha_{k,m}^{0(2)} \\ -\alpha_{k,m}^0 & \frac{\tilde{\epsilon}_0 I_m'(kb) K_m(kb) - \tilde{\epsilon}_1 I_m(kb) K_m'(kb)}{\tilde{\epsilon}_1 I_m'(kb) K_m(kb) - \tilde{\epsilon}_0 I_m(kb) K_m'(kb)} \end{pmatrix} \\ &\times \frac{ka}{\tilde{\epsilon}_1} [\tilde{\epsilon}_2 I_m'(ka) K_m(ka) - \tilde{\epsilon}_1 I_m(ka) K_m'(ka)] \\ &\quad \times \begin{pmatrix} 1 & \alpha_{k,m}^{1(2)} \\ -\alpha_{k,m}^1 & \frac{\tilde{\epsilon}_1 I_m'(ka) K_m(ka) - \tilde{\epsilon}_2 I_m(ka) K_m'(ka)}{\tilde{\epsilon}_2 I_m'(ka) K_m(ka) - \tilde{\epsilon}_1 I_m(ka) K_m'(ka)} \end{pmatrix} \end{aligned} \quad (11.20)$$

and from direct derivation of the  $M_{11}$  element the condition for modes becomes

$$0 = \left(1 - \alpha_{k,m}^{0(2)} \alpha_{k,m}^1\right) \quad (11.21)$$

$$= 1 - \frac{(\tilde{\epsilon}_1 - \tilde{\epsilon}_0) K_m(kb) K_m'(kb)}{\tilde{\epsilon}_1 I_m'(kb) K_m(kb) - \tilde{\epsilon}_0 I_m(kb) K_m'(kb)} \frac{(\tilde{\epsilon}_2 - \tilde{\epsilon}_1) I_m(ka) I_m'(ka)}{\tilde{\epsilon}_2 I_m'(ka) K_m(ka) - \tilde{\epsilon}_1 I_m(ka) K_m'(ka)}$$

Let us now study a cylindrical shell of inner radius  $a$ , outer radius  $b$  and of a medium with dielectric function  $\tilde{\epsilon}(\omega)$  in a medium of dielectric function  $\tilde{\epsilon}_0(\omega)$ . The condition for modes we get from (11.21) by the replacements  $\tilde{\epsilon}_2(\omega) \rightarrow \tilde{\epsilon}_0(\omega)$  and  $\tilde{\epsilon}_1(\omega) \rightarrow \tilde{\epsilon}(\omega)$ . The result is

$$\left[ \tilde{\epsilon} \frac{K_m'(ka)}{I_m'(ka)} - \tilde{\epsilon}_0 \frac{K_m(ka)}{I_m(ka)} \right] \left[ \tilde{\epsilon} \frac{I_m'(kb)}{K_m'(kb)} - \tilde{\epsilon}_0 \frac{I_m(kb)}{K_m(kb)} \right] = (\tilde{\epsilon} - \tilde{\epsilon}_0)^2. \quad (11.22)$$

For a cylindrical gap of dielectric function  $\tilde{\epsilon}_0(\omega)$  in a medium of dielectric function  $\tilde{\epsilon}(\omega)$  we instead make the replacements  $\tilde{\epsilon}_0(\omega)$ ,  $\tilde{\epsilon}_2(\omega) \rightarrow \tilde{\epsilon}(\omega)$  and  $\tilde{\epsilon}_1(\omega) \rightarrow \tilde{\epsilon}_0(\omega)$ . The condition for modes is

$$\left[ \tilde{\epsilon} \frac{K_m(ka)}{I_m(ka)} - \tilde{\epsilon}_0 \frac{K_m'(ka)}{I_m'(ka)} \right] \left[ \tilde{\epsilon} \frac{I_m(kb)}{K_m(kb)} - \tilde{\epsilon}_0 \frac{I_m'(kb)}{K_m'(kb)} \right] = (\tilde{\epsilon} - \tilde{\epsilon}_0)^2. \quad (11.23)$$

### 11.2.3 Thin Cylindrical Diluted Gas Film

It is of interest to find the van der Waals force on an atom in a layered structure. We can obtain this by studying the force on a thin layer of a diluted gas with dielectric function  $\epsilon_g(\omega) = 1 + 4\pi n\alpha^{at}(\omega)$ , where  $\alpha^{at}$  is the polarizability of one atom and  $n$  the density of atoms (we have assumed that the atom is surrounded by vacuum; if not the 1 should be replaced by the dielectric function of the ambient medium and the atomic polarizability should be replaced by the excess polarizability). For a diluted gas layer the interaction between the gas atoms can be neglected and the force on the layer is just the sum of the forces on the individual atoms. So by dividing with the number of atoms in the film we get the force on one atom. The layer has to be thin in order to have a well defined  $r$ -value of the atom. Since we will derive the force on an atom in different cylindrical geometries it is fruitful to derive the matrix for a thin diluted gas shell. This result can be directly used in the derivation of the van der Waals force on an atom in different cylindrical geometries.

We let the film have the thickness  $\delta$  and be of a general radius  $r$ . We only keep terms up to linear order in  $\delta$  and linear order in  $n$ . The matrix for the gas film is  $\tilde{\mathbf{M}}_0 \cdot \tilde{\mathbf{M}}_1$  where

$$\tilde{\mathbf{M}}_0 = \begin{pmatrix} 1 & 0 \\ 0 & 1 \end{pmatrix} + 4\pi n\alpha^{at}kr \begin{pmatrix} I_m'(kr) K_m(kr) & K_m(kr) K_m'(kr) \\ -I_m(kr) I_m'(kr) & -I_m(kr) K_m'(kr) \end{pmatrix}. \quad (11.24)$$

Now,

$$\tilde{\mathbf{M}}_1 = \begin{pmatrix} 1 & 0 \\ 0 & 1 \end{pmatrix} - 4\pi n\alpha^{at}k(r - \delta) \begin{pmatrix} I_m' K_m & K_m K_m' \\ -I_m I_m' & -I_m K_m' \end{pmatrix}, \quad (11.25)$$

where the suppressed arguments of all modified Bessel functions are  $k(r - \delta)$ . Expansion in  $\delta$  and keeping the terms up to linear order gives

$$\begin{aligned} \tilde{\mathbf{M}}^{\text{gas}} = \tilde{\mathbf{M}}_0 \cdot \tilde{\mathbf{M}}_1 &= \begin{pmatrix} 1 & 0 \\ 0 & 1 \end{pmatrix} + 4\pi (\delta n) \alpha^{at} k \\ &\times \begin{pmatrix} \frac{d[(kr)I_m'K_m]}{d(kr)} & \frac{d[(kr)K_m'K_m]}{d(kr)} \\ -\frac{d[(kr)I_m'I_m]}{d(kr)} & -\frac{d[(kr)I_mK_m']}{d(kr)} \end{pmatrix}, \end{aligned} \quad (11.26)$$

where now the arguments of all modified Bessel functions are  $(kr)$ . Performing the derivatives and using the modified Bessel equation, (11.2), we find

$$\begin{aligned} \tilde{\mathbf{M}}_{\text{gaslayer}} &= \begin{pmatrix} 1 & 0 \\ 0 & 1 \end{pmatrix} \\ &+ (\delta n) \frac{4\pi\alpha^{at}[m^2+(kr)^2]}{r} \begin{pmatrix} I_m K_m & K_m K_m' \\ -I_m I_m & -I_m K_m \end{pmatrix} \\ &+ (\delta n) \frac{4\pi\alpha^{at}(kr)^2}{r} \begin{pmatrix} I_m' K_m' & K_m' K_m' \\ -I_m' I_m' & -I_m' K_m' \end{pmatrix}. \end{aligned} \quad (11.27)$$

Three important quantities for this structure is

$$\begin{aligned} M_{11} &= 1 + (\delta n) \frac{4\pi\alpha^{at}}{r} \{ [m^2 + (kr)^2] I_m(kr) K_m(kr) + (kr)^2 I_m'(kr) K_m'(kr) \}, \\ \alpha_{k,m}^{\text{gas}}(r; \omega) &= (\delta n) \frac{4\pi\alpha^{at}(\omega)}{r} \{ [m^2 + (kr)^2] [I_m(kr)]^2 + [(kr) I_m'(kr)]^2 \}, \\ \alpha_{k,m}^{\text{gas}(2)}(r; \omega) &= (\delta n) \frac{4\pi\alpha^{at}(\omega)}{r} \{ [m^2 + (kr)^2] [K_m(kr)]^2 + [(kr) K_m'(kr)]^2 \}, \end{aligned} \quad (11.28)$$

where we have introduced the superscript gas on the polarizabilities to indicate gas film. Note that only terms up to linear order in  $(\delta n)$  are kept. Now we are done with the gas layer. We will use these results later in calculating the van der Waals force on an atom in cylindrical layered structures.

### 11.2.4 2D Cylindrical Film

In many situations one is dealing with very thin films. These may be considered 2D. Important examples are a graphene sheet and a 2D electron gas. In the derivation we let the film have finite thickness  $\delta$  and be characterized by a 3D dielectric function  $\tilde{\epsilon}^{3D}$ . We then let the thickness go toward zero. The 3D dielectric function depends on  $\delta$  as  $\tilde{\epsilon}^{3D} \sim 1/\delta$  for small  $\delta$ . In the planar structure we could, in the limit when  $\delta$  goes toward zero, obtain a momentum dependent 2D dielectric function. Here we only keep the long wave length limit of the 2D dielectric function [2, 3]. The matrix is  $\tilde{\mathbf{M}}^{2D} = \tilde{\mathbf{M}}_0 \cdot \tilde{\mathbf{M}}_1$ . Before we derive these matrices it is convenient to introduce two auxiliary matrices,

$$\begin{aligned}\tilde{\mathbf{B}}(x) &= kx \begin{pmatrix} I_m'(kx) K_m(kx) & K_m(kx) K_m'(kx) \\ -I_m(kx) I_m'(kx) & -I_m(kx) K_m'(kx) \end{pmatrix}; \\ \tilde{\mathbf{C}}(x) &= kx \begin{pmatrix} -I_m(kx) K_m'(kx) & -K_m(kx) K_m'(kx) \\ I_m(kx) I_m'(kx) & I_m'(kx) K_m(kx) \end{pmatrix}.\end{aligned}\quad (11.29)$$

Using the Wronskian for the modified Bessel function we find these matrices have the following properties:

$$\begin{aligned}\tilde{\mathbf{B}}(x) + \tilde{\mathbf{C}}(x) &= \tilde{\mathbf{I}}; \\ \tilde{\mathbf{B}}(x) \cdot \tilde{\mathbf{B}}(x) &= \tilde{\mathbf{B}}(x); \\ \tilde{\mathbf{C}}(x) \cdot \tilde{\mathbf{C}}(x) &= \tilde{\mathbf{C}}(x); \\ \tilde{\mathbf{B}}(x) \cdot \tilde{\mathbf{C}}(x) &= \tilde{\mathbf{0}}.\end{aligned}\quad (11.30)$$

Now, we have

$$\begin{aligned}\tilde{\mathbf{M}}_0 &= \tilde{\varepsilon}^{3D} \tilde{\mathbf{B}}(r) + \tilde{\mathbf{C}}(r); \\ \tilde{\mathbf{M}}_1 &= \frac{1}{\tilde{\varepsilon}^{3D}} \tilde{\mathbf{B}}(r - \delta) + \tilde{\mathbf{C}}(r - \delta),\end{aligned}\quad (11.31)$$

and using (11.30) and the modified Bessel equation, (11.2), we arrive at

$$\begin{aligned}\tilde{\mathbf{M}}^{2D} &= \tilde{\mathbf{M}}_0 \cdot \tilde{\mathbf{M}}_1 \\ &= \tilde{\mathbf{I}} - \delta \tilde{\varepsilon}^{3D} \frac{m^2 + (kr)^2}{r} \begin{pmatrix} -I_m K_m & -K_m K_m \\ I_m I_m & I_m K_m \end{pmatrix},\end{aligned}\quad (11.32)$$

where the suppressed arguments of the modified Bessel functions are  $(kr)$ .

We will also need the multipole polarizability of the thin cylindrical shell in vacuum. It can be obtained from (11.32). The polarizability is  $-b^0/a^0$  under the assumption that  $b^1 = 0$ . One obtains  $\alpha_{k,m}^{2D} = -M_{21}/M_{11}$ . We find

$$\alpha_{k,m}^{2D}(r; \omega) = \frac{\delta \tilde{\varepsilon}^{3D} [m^2 + (kr)^2] [I_m(kr)]^2}{r + \delta \tilde{\varepsilon}^{3D} [m^2 + (kr)^2] I_m(kr) K_m(kr)},\quad (11.33)$$

where we have reserved the first argument before the semicolon for the radius of the cylindrical film.

The multipole polarizability “seen from inside the shell” we get from (11.32). The polarizability is  $-a^1/b^1$  under the assumption that  $a^0 = 0$ . One obtains  $\alpha_{k,m}^{2D(2)} = M_{12}/M_{11}$ , and

$$\alpha_{k,m}^{2D(2)}(r; \omega) = \frac{\delta \tilde{\varepsilon}^{3D} [m^2 + (kr)^2] [K_m(kr)]^2}{r + \delta \tilde{\varepsilon}^{3D} [m^2 + (kr)^2] I_m(kr) K_m(kr)}.\quad (11.34)$$

Sometimes it is convenient to use an alternative form of the matrix  $\tilde{\mathbf{M}}^{2D}$ ,

$$\tilde{\mathbf{M}}^{2D} = M_{11}^{2D} \begin{pmatrix} 1 & \alpha_{k,m}^{2D(2)} \\ -\alpha_{k,m}^{2D} & \frac{r - \delta \tilde{\varepsilon}^{3D} [m^2 + (kr)^2] I_m(kr) K_m(kr)}{r + \delta \tilde{\varepsilon}^{3D} [m^2 + (kr)^2] I_m(kr) K_m(kr)} \end{pmatrix}.\quad (11.35)$$

Now we are done with the basic structure elements and turn to some geometries of common interest. We begin with an atom outside a cylinder.

### 11.3 Force on an Atom Outside a Cylinder

In this section we derive the van der Waals interaction between a polarizable atom and an infinitely long solid cylinder of dielectric function  $\tilde{\epsilon}_1(\omega)$ . We assume, for simplicity, that the atom and cylinder are in vacuum. The geometry of the problem is shown in Fig. 10.3. The radius of the cylinder is  $a$  and the atom is at a distance  $b = a + d$  from the cylinder axis. To obtain the results we proceed as follows. We introduce a thin shell defined by the radii  $b$  and  $b + \delta$ . We let the medium of the shell have the dielectric function  $\epsilon_g = 1 + \alpha = 1 + 4\pi n\alpha^{\text{at}}$  where  $\alpha^{\text{at}}$  is the polarizability of the atom. Furthermore,  $L$  is the length of the cylinder which we let go to infinity at the end. We assume that the medium of the shell is very diluted. We let  $\alpha$  go toward zero and keep only terms up to linear order before we let  $\delta$  go toward zero.

The matrix of the problem is just the matrix of the thin gas shell, (11.27), multiplying that for the cylindrical core, given in (11.17),  $\tilde{\mathbf{M}} = \tilde{\mathbf{M}}^{\text{gas}} \cdot \tilde{\mathbf{M}}^{\text{cyl}}$ . The element of interest is

$$M_{11} = M_{11}^{\text{gas}} M_{11}^{\text{cyl}} + M_{12}^{\text{gas}} M_{21}^{\text{cyl}}. \quad (11.36)$$

The mode condition function becomes

$$\begin{aligned} \tilde{f}_{k,m} &= 1 + \frac{M_{12}^{\text{gas}} M_{21}^{\text{cyl}}}{M_{11}^{\text{gas}} M_{11}^{\text{cyl}}} \\ &= 1 - \alpha_{k,m}^{\text{gas}(2)}(b; \omega) \alpha_{k,m}^{\text{cyl}}(a; \omega) \\ &= 1 - (\delta n) \frac{4\pi\alpha^{\text{at}}(\omega)}{b} \left\{ [m^2 + (kb)^2] [K_m(kb)]^2 + [(kb) K_m'(kb)]^2 \right\} \\ &\quad \times \frac{[\tilde{\epsilon}(\omega) - 1] I_m(ka) I_m'(ka)}{[\tilde{\epsilon}(\omega) I_m'(ka) K_m(ka) - I_m(ka) K_m'(ka)]}, \end{aligned} \quad (11.37)$$

where we have taken as reference system a system where the gas shell and the core are well separated from each other.

Now, the non-retarded (van der Waals) interaction energy between the gas shell and the cylindrical core of length  $L$  is given by

$$\begin{aligned} E &= \hbar \int_0^\infty \frac{d\xi}{2\pi} \sum_{m=-\infty}^\infty L \int_{-\infty}^\infty \frac{dk}{2\pi} \ln \left[ \tilde{f}_{k,m}(i\xi) \right] \\ &= \hbar \int_0^\infty \frac{d\xi}{2\pi} \sum_{m=-\infty}^\infty L \int_{-\infty}^\infty \frac{dk}{2\pi} \ln \left[ 1 - \alpha_{k,m}^{\text{gas}(2)}(b; i\xi) \alpha_{k,m}^{\text{cyl}}(a; i\xi) \right] \\ &\approx -2\hbar \int_0^\infty \frac{d\xi}{2\pi} \sum_{m=-\infty}^\infty L \int_0^\infty \frac{dk}{2\pi} \alpha_{k,m}^{\text{gas}(2)}(b; i\xi) \alpha_{k,m}^{\text{cyl}}(a; i\xi), \end{aligned} \quad (11.38)$$

where we on the third line have expanded the logarithm and kept the lowest order term. The energy per atom we get by dividing by the number of atoms in the gas film. We find

$$\begin{aligned}
\frac{E}{2\pi bL(\delta n)} &= -\frac{2\hbar L}{2\pi bL(\delta n)} \int_0^\infty \frac{d\xi}{2\pi} \sum_{m=-\infty}^\infty \int_0^\infty \frac{dk}{2\pi} \alpha_{k,m}^{\text{gas}(2)}(b; i\xi) \alpha_{k,m}^{\text{cyl.}}(a; i\xi) \\
&= -\frac{2\hbar L}{2\pi bL(\delta n)} \int_0^\infty \frac{d\xi}{2\pi} \sum_{m=-\infty}^\infty \int_0^\infty \frac{dk}{2\pi} (\delta n) \frac{4\pi\alpha^{at}(i\xi)}{b} \\
&\times \left\{ [m^2 + (kb)^2] [K_m(kb)]^2 + [(kb) K_m'(kb)]^2 \right\} \alpha_{k,m}^{\text{cyl.}}(a; i\xi) \quad (11.39) \\
&= -\frac{4\hbar}{b^2} \sum_{m=-\infty}^\infty \int_0^\infty \frac{dk}{2\pi} \left\{ [m^2 + (kb)^2] [K_m(kb)]^2 \right. \\
&\quad \left. + [(kb) K_m'(kb)]^2 \right\} \int_0^\infty \frac{d\xi}{2\pi} \alpha^{at}(i\xi) \alpha_{k,m}^{\text{cyl.}}(a; i\xi),
\end{aligned}$$

where

$$\alpha_{k,m}^{\text{cyl.}}(a; i\xi) = \frac{[\tilde{\varepsilon}(i\xi) - 1] I_m(ka) I_m'(ka)}{\tilde{\varepsilon}(i\xi) I_m'(ka) K_m(ka) - I_m(ka) K_m'(ka)}, \quad (11.40)$$

or expressed in a different way

$$\alpha_{k,m}^{\text{cyl.}}(a; i\xi) = \frac{(ka) [\tilde{\varepsilon}(i\xi) - 1] I_m(ka) I_m'(ka)}{(ka) [\tilde{\varepsilon}(i\xi) - 1] I_m'(ka) K_m(ka) + 1}, \quad (11.41)$$

is the multipole polarizability for a cylinder in vacuum, (11.8). See [4], (5.77). The force on the atom is  $\mathbf{F}(b) = -\hat{\mathbf{r}}dE(b)/db$ .

### 11.3.1 Force Between a Li-Atom and a Gold Cylinder

As an example of atom-cylinder interactions we show in Fig. 11.1a the interaction between a Li atom and a gold cylinder. The polarizability for Li was obtained from the London approximation (8.60) with the parameters given in Fig. 8.2. For gold we used the polarizability as shown in Fig. 9.3. The  $b$ -dependence does not follow a simple power law,  $E \sim b^{-5}$ , predicted by the summation over pair method (6.24). In Fig. 11.1b we give the result for a non-metallic cylinder and here the result complies with the prediction. We made a rough model of a cylinder of densely packed lithium atoms of density  $n = 10^{23} \text{ cm}^{-3}$  and represented the dielectric function by the expression  $\tilde{\varepsilon}(\omega) = 1 + 4\pi n\alpha_{\text{Li}}$ . The figure contains two sets of curves. The lower set is the result when using (11.40) or (11.41) for the cylinder polarizability. From (11.41) we see that the result is not directly proportional to the density of polarizable atoms in the cylinder material. The denominator in (11.41) represents the screening of the interaction. Thus, the three lower curves are the results when screening is in effect. The upper set of curves is the result when we remove the screening by replacing the denominator with unity. The solid black curve (straight line) is the result from the pair-summation method in (6.24). Comparing the screened  $m = 0$  contribution, solid blue curve, with the unscreened, dashed blue curve we find that the screening is effective at small separations but not at large. The screening has large effect on the

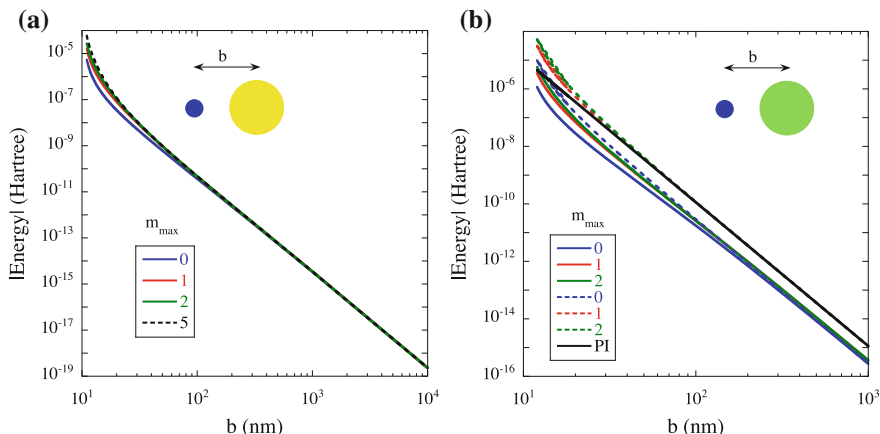


**Fig. 11.1** **a** The interaction energy for a Li atom next to a gold cylinder of radius  $a = 10$  nm. The distance between the atom and the cylinder axis is denoted by  $b$ . The results were obtained from (11.38). The result shows that the first term in the summation over  $m$  gives the whole result for large  $b$ -values and that higher order multipole contributions start to be important when the objects are near contact. **b** The same result but for a non-metallic cylinder. The black solid straight line denoted by PI is the result from the summation of pair interactions (6.24). See the text for details

$m = \pm 1$  contribution also for large separations. When screening is included these contributions are negligible for large separations while in the screening free case they contribute together with three times as much as the  $m = 0$  term. For large separations with the neglect of screening only the  $m = 0$  and  $m = \pm 1$  give appreciable contributions and the relative strength is one quarter for  $m = 0$  and three eighths each for  $m = -1$  and for  $m = +1$ .

### 11.4 Force on an Atom in a Cylindrical Cavity

In this section we derive the van der Waals interaction between a polarizable atom inside an infinitely long cylindrical vacuum cavity in a medium of dielectric function  $\tilde{\epsilon}_1(\omega)$ . The geometry of the problem is shown in Fig. 10.5. The radius of the cavity is  $a$  and the atom is at a distance  $d$  from the cylinder axis. To obtain the results we proceed as follows. We introduce a thin shell defined by the radii  $d$  and  $d + \delta$ . We let the medium of the shell have the dielectric function  $\epsilon_g = 1 + \alpha = 1 + 4\pi n\alpha^{at}$  where  $\alpha^{at}$  is the polarizability of the atom and  $L$  is the length of the cylinder which we let go to infinity at the end. We assume that the medium of the shell is very diluted. We let  $\alpha$  go toward zero and keep only terms up to linear order before we let  $\delta$  go toward zero.

The matrix of the problem is just the matrix of the cavity, (11.17), multiplying that for the diluted gas film, given in (11.27),  $\tilde{\mathbf{M}} = \tilde{\mathbf{M}}^{cav} \cdot \tilde{\mathbf{M}}^{gas}$ . The element of interest is

$$M_{11} = M_{11}^{\text{cav.}} M_{11}^{\text{gas}} + M_{12}^{\text{cav.}} M_{21}^{\text{gas}}. \quad (11.42)$$

The mode condition function becomes

$$\begin{aligned} \tilde{f}_{k,m} &= 1 + \frac{M_{12}^{\text{cav.}} M_{21}^{\text{gas}}}{M_{11}^{\text{cav.}} M_{11}^{\text{gas}}} \\ &= 1 - \alpha_{k,m}^{\text{cav.}(2)}(a; \omega) \alpha_{k,m}^{\text{gas}}(d; \omega) \\ &= 1 - \frac{[1 - \tilde{\epsilon}_1(\omega)] K_m(ka) K_m'(ka)}{I_m'(ka) K_m(ka) - \tilde{\epsilon}_1(\omega) I_m(ka) K_m'(ka)} \\ &\times (\delta n) \frac{4\pi \alpha^{at}(\omega)}{d} \left\{ [m^2 + (kd)^2] [I_m(kd)]^2 + (kd)^2 [I_m'(kd)]^2 \right\}, \end{aligned} \quad (11.43)$$

where we have taken as reference system a system where the gas shell and the cavity are well separated from each other.

Now, the non-retarded (van der Waals) interaction energy for an atom inside a cylindrical cavity is given by

$$\begin{aligned} \frac{E}{2\pi d L \delta n} &= \hbar \int_0^\infty \frac{d\xi}{2\pi} \sum_{m=-\infty}^\infty L \int_{-\infty}^\infty \frac{dk}{2\pi} \ln \left[ \tilde{f}_{k,m}(k, i\xi) \right] \\ &= \frac{\hbar L}{2\pi d L \delta n} \int_0^\infty \frac{d\xi}{2\pi} \sum_{m=-\infty}^\infty \int_{-\infty}^\infty \frac{dk}{2\pi} \ln \left[ 1 - \alpha_{k,m}^{\text{gas}}(k, i\xi) \alpha_{k,m}^{\text{cav.}(2)}(a; i\xi) \right] \\ &\approx -\frac{\hbar L}{2\pi d L \delta n} \int_0^\infty \frac{d\xi}{2\pi} \sum_{m=-\infty}^\infty 2 \int_0^\infty \frac{dk}{2\pi} \alpha_{k,m}^{\text{gas}}(k, i\xi) \alpha_{k,m}^{\text{cav.}(2)}(a; i\xi) \\ &= -\frac{2\hbar L}{2\pi d L \delta n d} \int_0^\infty \frac{d\xi}{2\pi} \sum_{m=-\infty}^\infty \int_0^\infty \frac{dk}{2\pi} (\delta n) 4\pi \alpha^{at}(i\xi) \alpha_{k,m}^{\text{cav.}(2)}(a; i\xi) \\ &\quad \times \left\{ [m^2 + (kd)^2] [I_m(kd)]^2 + (kd)^2 [I_m'(kd)]^2 \right\} \\ &= -\frac{4\hbar}{d^2} \sum_{m=-\infty}^\infty \int_0^\infty \frac{dk}{2\pi} \left\{ [m^2 + (kd)^2] [I_m(kd)]^2 + (kd)^2 [I_m'(kd)]^2 \right\} \\ &\quad \times \int_0^\infty \frac{d\xi}{2\pi} \alpha^{at}(i\xi) \alpha_{k,m}^{(2)}(a; i\xi), \end{aligned} \quad (11.44)$$

where we on the third line have expanded the logarithm and kept the lowest order term. The multipole polarizability,

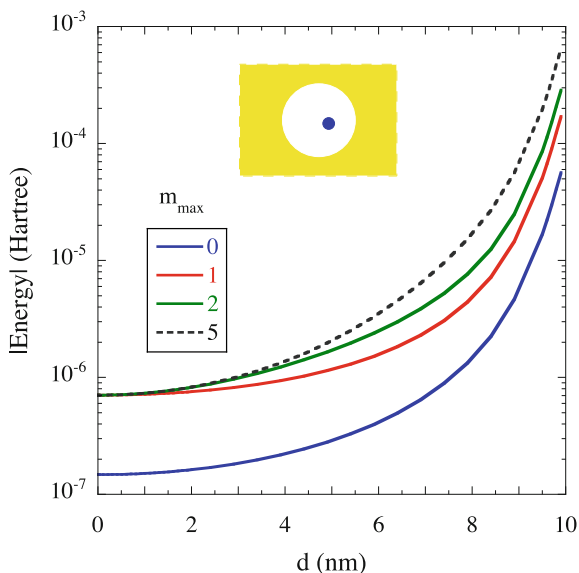
$$\alpha_{k,m}^{\text{cav.}(2)}(a; i\xi) = \frac{(1 - \tilde{\epsilon}_1(i\xi)) K_m(ka) K_m'(ka)}{I_m'(ka) K_m(ka) - \tilde{\epsilon}_1(i\xi) I_m(ka) K_m'(ka)}, \quad (11.45)$$

or expressed in another way

$$\alpha_{k,m}^{\text{cav.}(2)}(a; i\xi) = \frac{-(ka) \tilde{\alpha}_1(i\xi) K_m(ka) K_m'(ka)}{1 - (ka) \tilde{\alpha}_1(i\xi) I_m(ka) K_m'(ka)}, \quad (11.46)$$

is the multipole polarizability for inside a cylindrical vacuum cavity, (11.9). The force on the atom is  $\mathbf{F}(d) = -\hat{\mathbf{r}}dE(d)/dd$ .

**Fig. 11.2** The interaction energy for a Li atom in a cylindrical gold cavity of radius  $a = 10$  nm. The atom is at the distance  $d$  from the axis of the cavity. The results were obtained from (11.44). The closer to the cavity wall the atom is the more terms in the summation over  $m$  is needed



### 11.4.1 Force on a Li-Atom in a Cylindrical Gold Cavity

As an example of interactions on an atom in a cavity we show in Fig. 11.2 the interaction on a Li atom in a gold cavity. The polarizability for Li was obtained from the London approximation (8.60) with the parameters given in Fig. 8.2. For gold we used polarizability as shown in Fig. 9.3. The  $m = 0$  and  $m = \pm 1$  terms are dominating at the center of the cavity. Higher order multipole contributions become important when the atom is close to the cavity wall.

It is of interest to study the interaction on atoms in narrow channels. A first step of such a study could be to find the interactions on an atom in a cylindrical gap. This is our next topic.

## 11.5 Force on an Atom in a Cylindrical Gap

Here we study an atom in a cylindrical vacuum gap with the outer and inner radii  $b$  and  $a$ , respectively. The medium outside the gap has dielectric function  $\tilde{\epsilon}_1(\omega)$  and the medium inside the dielectric function  $\tilde{\epsilon}_2(\omega)$ . The atom is at a distance  $r$  from the center. The matrix for this geometry is  $\tilde{\mathbf{M}} = \tilde{\mathbf{M}}^{\text{cav.}} \cdot \tilde{\mathbf{M}}^{\text{gas}} \cdot \tilde{\mathbf{M}}^{\text{cyl.}}$ , and the matrix element of interest is

$$\begin{aligned}
M_{11} &= (M_{11}^{\text{cav.}}, M_{12}^{\text{cav.}}) \cdot \begin{pmatrix} M_{11}^{\text{gas}} & M_{12}^{\text{gas}} \\ M_{21}^{\text{gas}} & M_{22}^{\text{gas}} \end{pmatrix} \cdot \begin{pmatrix} M_{11}^{\text{cyl.}} \\ M_{21}^{\text{cyl.}} \end{pmatrix} \\
&= M_{11}^{\text{cav.}} M_{11}^{\text{gas}} M_{11}^{\text{cyl.}} \left(1, \alpha_{k,m}^{\text{cav.}(2)}\right) \cdot \begin{pmatrix} 1 & \alpha_{k,m}^{\text{gas}(2)} \\ -\alpha_{k,m}^{\text{gas}} & \frac{M_{22}^{\text{gas}}}{M_{11}^{\text{gas}}} \end{pmatrix} \cdot \begin{pmatrix} 1 \\ -\alpha_{k,m}^{\text{cyl.}} \end{pmatrix} \quad (11.47) \\
&= M_{11}^{\text{cav.}} M_{11}^{\text{gas}} M_{11}^{\text{cyl.}} \left\{ 1 - \alpha_{k,m}^{\text{cyl.}} \alpha_{k,m}^{\text{cav.}(2)} - \alpha_{k,m}^{\text{gas}} \alpha_{k,m}^{\text{cav.}(2)} \right. \\
&\quad \left. - \alpha_{k,m}^{\text{cyl.}} \left[ \alpha_{k,m}^{\text{gas}(2)} + \alpha_{k,m}^{\text{cav.}(2)} \left( \frac{M_{22}^{\text{gas}}}{M_{11}^{\text{gas}}} - 1 \right) \right] \right\}.
\end{aligned}$$

This leads to the following proper mode condition function

$$\begin{aligned}
\tilde{f}_{k,m} &= 1 - \frac{\alpha_{k,m}^{\text{gas}} \alpha_{k,m}^{\text{cav.}(2)} + \alpha_{k,m}^{\text{cyl.}} \left( \alpha_{k,m}^{\text{gas}(2)} + \alpha_{k,m}^{\text{cav.}(2)} \left( \frac{M_{22}^{\text{gas}}}{M_{11}^{\text{gas}}} - 1 \right) \right)}{1 - \alpha_{k,m}^{\text{cyl.}} \alpha_{k,m}^{\text{cav.}(2)}} \quad (11.48) \\
&\approx 1 - \frac{\alpha_{k,m}^{\text{gas}} \alpha_{k,m}^{\text{cav.}(2)} + \alpha_{k,m}^{\text{cyl.}} \left( \alpha_{k,m}^{\text{gas}(2)} + 2\alpha_{k,m}^{\text{cav.}(2)} \left( M_{22}^{\text{gas}} - 1 \right) \right)}{1 - \alpha_{k,m}^{\text{cyl.}} \alpha_{k,m}^{\text{cav.}(2)}},
\end{aligned}$$

where the reference system is the cylindrical gap in absence of the atom. The functions appearing in the expression are

$$\begin{aligned}
\alpha_{k,m}^{\text{gas}} &\approx (\delta n) \frac{4\pi\alpha^{at}(\omega)}{r} \left\{ [m^2 + (kr)^2] [I_m(kr)]^2 + (kr)^2 [I_m'(kr)]^2 \right\}; \\
\alpha_{k,m}^{\text{gas}(2)} &\approx (\delta n) \frac{4\pi\alpha^{at}(\omega)}{r} \left\{ [m^2 + (kr)^2] [K_m(kr)]^2 + (kr)^2 [K_m'(kr)]^2 \right\}; \\
M_{22}^{\text{gas}} - 1 &\approx -(\delta n) \frac{4\pi\alpha^{at}(\omega)}{r} \quad (11.49) \\
&\quad \times \left\{ [m^2 + (kr)^2] I_m(kr) K_m(kr) + (kr)^2 I_m'(kr) K_m'(kr) \right\}; \\
\alpha_{k,m}^{\text{cav.}(2)} &= \alpha_{k,m}^{(2)}(b; \omega) = \frac{[1 - \tilde{\varepsilon}_1(\omega)] K_m(kb) K_m'(kb)}{I_m'(kb) K_m(kb) - \tilde{\varepsilon}_1(\omega) I_m(kb) K_m'(kb)}; \\
\alpha_{k,m}^{\text{cyl.}} &= \alpha_{k,m}(a; \omega) = \frac{[\tilde{\varepsilon}_2(\omega) - 1] (kb) I_m(kb) I_m'(kb)}{1 + [\tilde{\varepsilon}_2(\omega) - 1] (kb) K_m(kb) I_m'(kb)}.
\end{aligned}$$

Before we write down the expression for the energy per atom we make the factor  $(\delta n) 4\pi\alpha^{at}(\omega)$  explicit, a factor that is common for all terms after 1—in the expression for  $\tilde{f}_{k,m}$ . We have

$$\begin{aligned}
\tilde{f}_{k,m} &\approx 1 - (\delta n) \frac{4\pi\alpha^{at}(\omega)}{r} \frac{1}{[1 - \alpha_{k,m}^{\text{cyl.}} \alpha_{k,m}^{\text{cav.}(2)}]} \left\{ [m^2 + (kr)^2] \right. \\
&\quad \times \left[ \alpha_{k,m}^{\text{cav.}(2)} [I_m(kr)]^2 + \alpha_{k,m}^{\text{cyl.}} [K_m(kr)]^2 \right. \\
&\quad \left. \left. - 2\alpha_{k,m}^{\text{cyl.}} \alpha_{k,m}^{\text{cav.}(2)} I_m(kr) K_m(kr) \right] \right. \quad (11.50) \\
&\quad \left. + (kr)^2 \left[ \alpha_{k,m}^{\text{cav.}(2)} [I_m'(kr)]^2 + \alpha_{k,m}^{\text{cyl.}} [K_m'(kr)]^2 \right. \right. \\
&\quad \left. \left. - 2\alpha_{k,m}^{\text{cyl.}} \alpha_{k,m}^{\text{cav.}(2)} I_m'(kr) K_m'(kr) \right] \right\}.
\end{aligned}$$

Now, the energy per atom is

$$\begin{aligned}
\frac{E}{2\pi(\delta n)L} &= \frac{\hbar}{2\pi(\delta n)L} \int_0^\infty \frac{d\xi}{2\pi} \sum_{m=-\infty}^\infty L \int_{-\infty}^\infty \frac{dk}{2\pi} \ln \left[ \tilde{f}_{k,m}(k, i\xi) \right] \\
&\approx \frac{\hbar}{2\pi(\delta n)} \int_0^\infty \frac{d\xi}{2\pi} \sum_{m=-\infty}^\infty \int_{-\infty}^\infty \frac{dk}{2\pi} \left[ \tilde{f}_{k,m}(k, i\xi) - 1 \right] \\
&= -\frac{2\hbar}{r} \int_0^\infty \frac{d\xi}{2\pi} \sum_{m=-\infty}^\infty \int_{-\infty}^\infty \frac{dk}{2\pi} \frac{\alpha^{at}(i\xi)}{\left[ 1 - \alpha_{k,m}^{\text{cyl.}} \alpha_{k,m}^{\text{cav.}(2)} \right]} \\
&\quad \times \left\{ [m^2 + (kr)^2] \left[ \alpha_{k,m}^{\text{cav.}(2)} [I_m(kr)]^2 \right. \right. \\
&\quad + \alpha_{k,m}^{\text{cyl.}} [K_m(kr)]^2 - 2\alpha_{k,m}^{\text{cyl.}} \alpha_{k,m}^{\text{cav.}(2)} I_m(kr) K_m(kr) \left. \right] \\
&\quad + (kr)^2 \left[ \alpha_{k,m}^{\text{cav.}(2)} [I_m'(kr)]^2 + \alpha_{k,m}^{\text{cyl.}} [K_m'(kr)]^2 \right. \\
&\quad \left. \left. - 2\alpha_{k,m}^{\text{cyl.}} \alpha_{k,m}^{\text{cav.}(2)} I_m'(kr) K_m'(kr) \right] \right\}. \tag{11.51}
\end{aligned}$$

where we on the second line have expanded the logarithm and kept the lowest order term. The force on the atom is  $\mathbf{F}(r) = -\hat{\mathbf{r}}dE(r)/dr$ . Next we address the van der Waals interaction between two parallel cylindrical objects.

## 11.6 Force Between Two Cylindrical Objects

The van der Waals interaction between two parallel cylinders of radius  $R_1$  and  $R_2$  is [5]

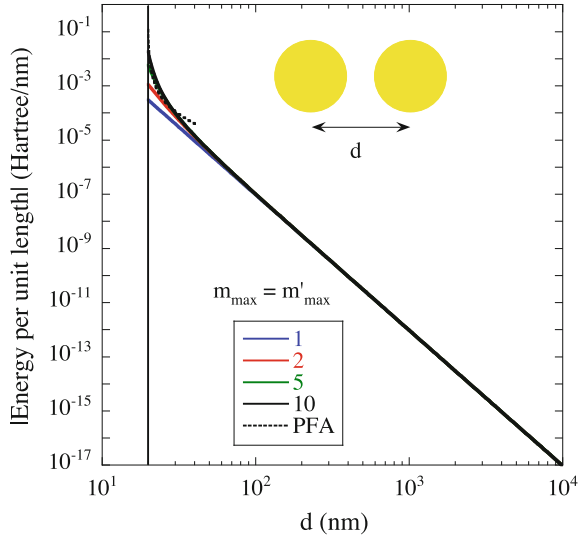
$$\begin{aligned}
E(d) &= -\hbar \frac{L}{d} \int_0^\infty \frac{d\xi}{2\pi} \left[ \frac{\tilde{\epsilon}_1(i\xi) - \tilde{\epsilon}_0(i\xi)}{\tilde{\epsilon}_1(i\xi) - \tilde{\epsilon}_0(i\xi)} \frac{\tilde{\epsilon}_2(i\xi) - \tilde{\epsilon}_0(i\xi)}{\tilde{\epsilon}_2(i\xi) - \tilde{\epsilon}_0(i\xi)} \right] \\
&\quad \times \sum_{m'=1}^\infty \sum_{m=1}^\infty \frac{\Gamma^2(m+m'+1/2)}{m!(m-1)!m'!(m'-1)!} \left( \frac{R_1}{d} \right)^{2m} \left( \frac{R_2}{d} \right)^{2m'}, \tag{11.52}
\end{aligned}$$

where  $d$  denotes the distance between the cylinder axes.

### 11.6.1 Interaction Between Two Gold Cylinders

As an example of cylinder-cylinder interactions we show in Fig. 11.3 the interaction between two gold cylinders in vacuum. We used (11.52) with the gold polarizability as shown in Fig. 9.3. The  $d$ -dependence follows a simple power law,  $E \sim d^{-5}$  for large separations. This comes from the  $m = m' = 1$  term. Higher order multipole contributions become important when the objects are in near contact. The results are valid for distances larger than the contact value  $2a = 20$  nm indicated by the vertical line in the figure. The closer to contact the more multipole terms one needs to include. Near point of contact it is favorable to use PFA. The dotted curve is the result from (6.33) with  $n = 1$ .

**Fig. 11.3** The interaction energy for two parallel gold cylinders of radius  $a = 10$  nm the distance  $d$  apart. The results were obtained from (11.52). When the cylinders are in near contact more and more terms in the summation are needed. Each curve is for a different truncation of the summations. The dotted piece of curve is the PFA result from (6.33). The vertical line indicates the contact point



## 11.7 Force on an Atom Outside a 2D Cylindrical Shell

In this section we derive the interaction between an atom and a very thin cylindrical shell, Fig. 10.9. It could approximate the interaction between an atom and a nano tube. We let the shell have the thickness  $\delta$  and let  $\delta$  be very small so that one keeps only terms linear in  $\delta$ . The 3D dielectric function of the material will then be inversely proportional to  $\delta$  [2, 3]. The derivation proceeds along the lines in Sect. 11.3 and the matrix  $\tilde{\mathbf{M}}^{\text{cyl}}$  is replaced by  $\tilde{\mathbf{M}}^{\text{2D}}$ . The matrix of the problem is just the matrix of the thin gas shell, (11.27), multiplying that for the 2D shell, given in (11.35),  $\tilde{\mathbf{M}} = \tilde{\mathbf{M}}^{\text{gas}} \cdot \tilde{\mathbf{M}}^{\text{2D}}$ . Note that the radius of the 2D cylindrical film is  $a$  and the atom is at a distance  $d$  from the film and distance  $b$  from the cylinder axis. The element of interest is

$$M_{11} = M_{11}^{\text{gas}} M_{11}^{\text{2D}} + M_{12}^{\text{gas}} M_{21}^{\text{2D}}. \quad (11.53)$$

The mode condition function becomes

$$\tilde{f}_{k,m} = 1 + \frac{M_{12}^{\text{gas}} M_{21}^{\text{2D}}}{M_{11}^{\text{gas}} M_{11}^{\text{2D}}} = 1 - \alpha_{k,m}^{\text{gas(2)}} \alpha_{k,m}^{\text{2D}}, \quad (11.54)$$

where

$$\alpha_{k,m}^{\text{gas(2)}} = (\delta n) \frac{4\pi \alpha^{\text{at}}(\omega)}{b} \left\{ [m^2 + (kb)^2] [K_m(kb)]^2 + (kb)^2 [K_m'(kb)]^2 \right\}, \quad (11.55)$$

$$\alpha_{k,m}^{\text{2D}} = \frac{\delta \tilde{\epsilon}^{\text{3D}}(\omega) [m^2 + (ka)^2] [I_m(ka)]^2}{a + \delta \tilde{\epsilon}^{\text{3D}}(\omega) [m^2 + (ka)^2] I_m(ka) K_m(ka)}.$$

Now, the non-retarded (van der Waals) interaction energy between an atom and a 2D cylindrical shell is given by

$$\begin{aligned}
 E &\approx -\frac{2\hbar}{2\pi b\delta Ln} \int_0^\infty \frac{d\xi}{2\pi} \sum_{m=-\infty}^\infty L \int_0^\infty \frac{dk}{2\pi} \alpha_{k,m}^{\text{gas}(2)} \alpha_{k,m}^{2D} \\
 &= -\frac{4\hbar}{b^2} \int_0^\infty \frac{d\xi}{2\pi} \sum_{m=-\infty}^\infty \int_0^\infty \frac{dk}{2\pi} \alpha^{at}(\xi) \\
 &\quad \times \left\{ [m^2 + (kb)^2] [K_m(kb)]^2 + (kb)^2 [K_m'(kb)]^2 \right\} \\
 &\quad \times \frac{\delta\tilde{\epsilon}^{3D}(i\xi) [m^2 + (ka)^2] [I_m(ka)]^2}{a + \delta\tilde{\epsilon}^{3D}(i\xi) [m^2 + (ka)^2] J_m(ka) K_m(ka)}.
 \end{aligned}
 \tag{11.56}$$

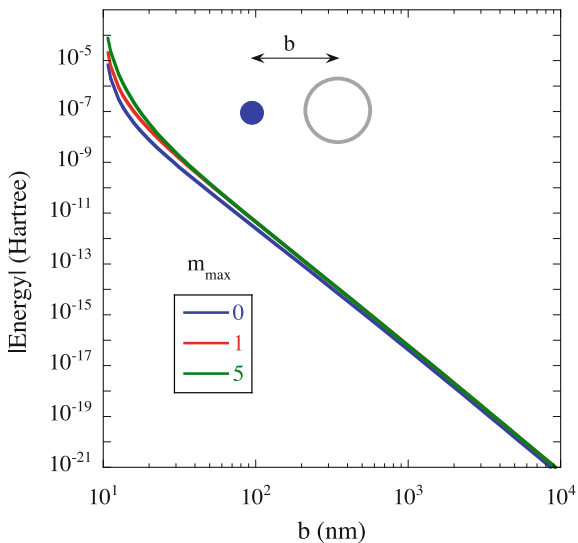
where we from the outset expanded the logarithm and kept the lowest order term. The force on the atom is  $\mathbf{F}(b) = -\hat{\mathbf{r}}dE(b)/db$ .

Two examples where the results apply are a cylinder made of a graphene like film and a thin metal film, respectively. Then the expressions for  $\delta\tilde{\epsilon}(i\xi)$  as given in (10.24) can be used [2, 3]. We treat the graphene example in the next section.

### 11.7.1 Interaction Between a Li-Atom and a Graphene Cylinder

As an example we give the results for a Li-atom outside a graphene like cylinder in Fig. 11.4. The results are from using (11.56). The polarizability for Li was obtained from the London approximation (8.60) with the parameters given in Fig. 8.2 and for

**Fig. 11.4** The interaction between a Li atom and a graphene cylinder as a function of distance  $b$ . The radius,  $a$ , of the cylindrical shell is 10 nm. The results are from using (11.56) and each curve is for a different truncation of the summation over  $m$ . See the text for details



the cylindrical shell the  $\delta\tilde{\epsilon}^{3D}(i\xi)$  entering  $\alpha_i^{2D}(a; i\xi)$  was taken from (10.24). At large distances only the  $m = 0$  and  $m = \pm 1$  terms give important contributions and follow the power law  $\sim b^{-5}$ . Next we move the atom inside the cylindrical shell.

## 11.8 Force on an Atom Inside a 2D Cylindrical Shell

In this section we derive the interaction of an atom inside a very thin cylindrical shell, Fig. 10.11. It could approximate the interaction of an atom inside a nano tube. We let the shell have the thickness  $\delta$  and let  $\delta$  be very small so that one keeps only terms linear in  $\delta$ . The 3D dielectric function of the material will then be inversely proportional to  $\delta$  [2, 3]. The derivation proceeds along the lines in the previous section and the matrix of the problem is just the matrix of the 2D shell, (11.35), multiplying that for the thin gas shell, given in (11.27),  $\tilde{\mathbf{M}} = \tilde{\mathbf{M}}^{2D} \cdot \tilde{\mathbf{M}}^{\text{gas}}$ . Note that the radius of the 2D cylindrical film is  $a$  and the atom is at a distance  $d$  from the cylinder axis. The element of interest is

$$M_{11} = M_{11}^{2D} M_{11}^{\text{gas}} + M_{12}^{2D} M_{21}^{\text{gas}}. \quad (11.57)$$

The mode condition function becomes

$$\tilde{f}_{k,m} = 1 + \frac{M_{12}^{2D} M_{21}^{\text{gas}}}{M_{11}^{2D} M_{11}^{\text{gas}}} = 1 - \alpha_{k,m}^{2D(2)} \alpha_{k,m}^{\text{gas}}, \quad (11.58)$$

where

$$\alpha_{k,m}^{\text{gas}} = (\delta n) \frac{4\pi\alpha^{at}(\omega)}{d} \left\{ [m^2 + (kd)^2] [I_m(kd)]^2 + (kd)^2 [I_m'(kd)]^2 \right\}; \quad (11.59)$$

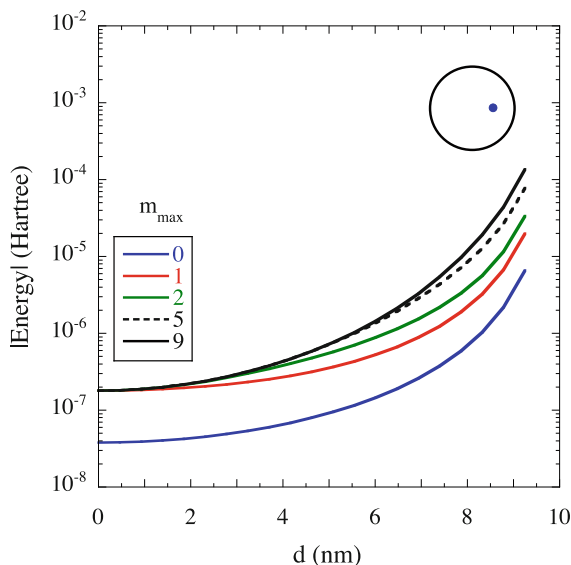
$$\alpha_{k,m}^{2D(2)} = \frac{\delta\tilde{\epsilon}^{3D}(\omega) [m^2 + (ka)^2] [K_m(ka)]^2}{a + \delta\tilde{\epsilon}^{3D}(\omega) [m^2 + (ka)^2] I_m(ka) K_m(ka)}.$$

Now, the non-retarded (van der Waals) interaction energy of an atom inside a thin cylindrical shell is given by

$$\begin{aligned} E &\approx -\frac{2\hbar}{2\pi d \delta L n} \int_0^\infty \frac{d\xi}{2\pi} \sum_{m=-\infty}^\infty L \int_0^\infty \frac{dk}{2\pi} \alpha_{k,m}^{2D(2)} \alpha_{k,m}^{\text{gas}} \\ &= -\frac{4\hbar}{d^2} \int_0^\infty \frac{d\xi}{2\pi} \sum_{m=-\infty}^\infty \int_0^\infty \frac{dk}{2\pi} \alpha^{at}(i\xi) \\ &\quad \times \left\{ [m^2 + (kd)^2] [I_m(kd)]^2 + (kd)^2 [I_m'(kd)]^2 \right\} \\ &\quad \times \frac{\delta\tilde{\epsilon}^{3D}(i\xi) [m^2 + (ka)^2] [K_m(ka)]^2}{a + \delta\tilde{\epsilon}^{3D}(i\xi) [m^2 + (ka)^2] I_m(ka) K_m(ka)}, \end{aligned} \quad (11.60)$$

where we from the outset expanded the logarithm and kept the lowest order term. The force on the atom is  $\mathbf{F}(d) = -\hat{\mathbf{r}}dE(d)/dd$ .

**Fig. 11.5** The interaction on a Li atom inside a graphene cylinder as a function of distance  $d$  from the center. The radius,  $a$ , of the cylindrical shell is 10 nm. The results are from using (11.60) and each curve is for a different truncation of the summation over  $m$ . See the text for details



Two examples where the results apply are a cylinder made of a graphene like film and a thin metal film, respectively. Then the expressions for  $\delta\tilde{\varepsilon}(i\xi)$  as given in (10.24) can be used [2, 3]. We treat the cylinder made of a graphene-like film in the next example.

### 11.8.1 Force on a Li-Atom Inside a Graphene Cylinder

As an example we give the results for a Li-atom inside a graphene cylinder in Fig. 11.5. The results are from using (11.60). The polarizability for Li was obtained from the London approximation (8.60) with the parameters given in Fig. 8.2 and for the cylindrical shell the  $\delta\tilde{\varepsilon}^{3D}(i\xi)$  entering  $\alpha_l^{2D(2)}(a; i\xi)$  was taken from (10.24). We note that only the  $m = 0$  and  $m = \pm 1$  terms give appreciable contributions when the atom is at the center of the cylinder.

## 11.9 Interaction Between Two 2D Coaxial Cylindrical Shells

We consider two coaxial thin cylindrical shells, one outer of radius  $b$  and one inner of radius  $a$ . The matrix for the system is  $\tilde{\mathbf{M}} = \tilde{\mathbf{M}}^{2Do} \cdot \tilde{\mathbf{M}}^{2Di}$  and the matrix of interest is

$$\begin{aligned}
M_{11} &= M_{11}^{2Do} M_{11}^{2Di} + M_{12}^{2Do} M_{21}^{2Di} \\
&= M_{11}^{2Do} M_{11}^{2Di} \left( 1 - \alpha_{k,m}^{2Do(2)} \alpha_{k,m}^{2Di} \right),
\end{aligned} \tag{11.61}$$

where all appearing functions are

$$\begin{aligned}
M_{11}^{2Do} &= 1 + \delta \tilde{\varepsilon}^{3D}(\omega) \frac{[m^2 + (kb)^2] I_m(kb) K_m(kb)}{b}; \\
M_{11}^{2Di} &= 1 + \delta \tilde{\varepsilon}^{3D}(\omega) \frac{[m^2 + (ka)^2] I_m(ka) K_m(ka)}{a}; \\
M_{12}^{2Do} &= \delta \tilde{\varepsilon}^{3D}(\omega) \frac{[m^2 + (kb)^2] [K_m(kb)]^2}{b}; \\
M_{21}^{2Di} &= -\delta \tilde{\varepsilon}^{3D}(\omega) \frac{[m^2 + (ka)^2] [I_m(ka)]^2}{a}; \\
\alpha_{k,m}^{2Do(2)} &= \alpha_{k,m}^{2D(2)}(b; \omega) \\
&= \frac{\delta \tilde{\varepsilon}^{3D}(\omega) [m^2 + (kb)^2] [K_m(kb)]^2}{b + \delta \tilde{\varepsilon}^{3D}(\omega) [m^2 + (kb)^2] I_m(kb) K_m(kb)}; \\
\alpha_{k,m}^{2Di} &= \alpha_{k,m}^{2D}(a; \omega) \\
&= \frac{\delta \tilde{\varepsilon}^{3D}(\omega) [m^2 + (ka)^2] [I_m(ka)]^2}{a + \delta \tilde{\varepsilon}^{3D}(\omega) [m^2 + (ka)^2] I_m(ka) K_m(ka)}.
\end{aligned} \tag{11.62}$$

If one wants to find the electromagnetic normal modes of the system one finds the solutions to  $M_{11} = 0$ . If one wants to find the energy it takes to bring the two thin cylindrical shells from infinite separation together and place the inner inside the outer one uses the proper mode condition function,

$$\tilde{f}_{k,m}(i\xi) = 1 - \alpha_{k,m}^{2D(2)}(b; i\xi) \alpha_{k,m}^{2D}(a; i\xi). \tag{11.63}$$

The energy per unit length is

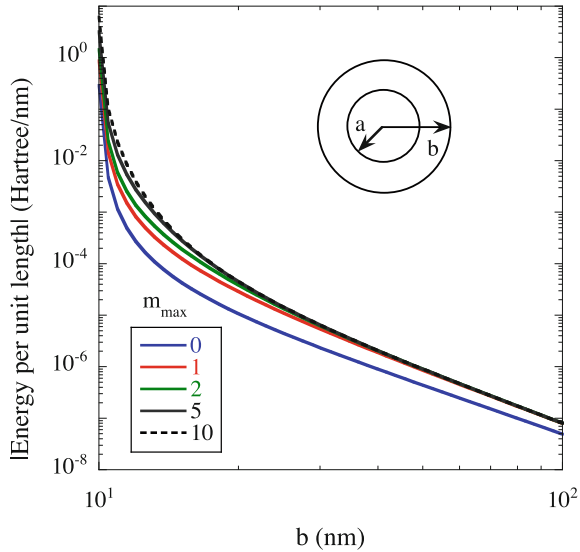
$$\begin{aligned}
E &= 2\hbar \int_0^\infty \frac{d\xi}{2\pi} \sum_{m=-\infty}^\infty \int_0^\infty \frac{dk}{2\pi} \ln \left[ \tilde{f}_{k,m}(i\xi) \right] \\
&= 2\hbar \int_0^\infty \frac{d\xi}{2\pi} \sum_{m=-\infty}^\infty \int_0^\infty \frac{dk}{2\pi} \ln \left[ 1 - \alpha_{k,m}^{2D(2)}(b; i\xi) \alpha_{k,m}^{2D}(a; i\xi) \right] \\
&= 2\hbar \int_0^\infty \frac{d\xi}{2\pi} \sum_{m=-\infty}^\infty \int_0^\infty \frac{dk}{2\pi} \ln \left[ 1 - \frac{\delta \tilde{\varepsilon}^{3D}(i\xi) [m^2 + (kb)^2] [K_m(kb)]^2}{b + \delta \tilde{\varepsilon}^{3D}(i\xi) [m^2 + (kb)^2] I_m(kb) K_m(kb)} \right. \\
&\quad \left. \times \frac{\delta \tilde{\varepsilon}^{3D}(i\xi) [m^2 + (ka)^2] [I_m(ka)]^2}{a + \delta \tilde{\varepsilon}^{3D}(i\xi) [m^2 + (ka)^2] I_m(ka) K_m(ka)} \right].
\end{aligned} \tag{11.64}$$

Note that here we cannot safely expand the logarithm and keep the linear term only. The linear term is not necessarily very small. Thus, we keep the logarithm as is.

### 11.9.1 Interaction Between Two Coaxial Cylindrical Graphene Shells

As an example we give in Fig. 11.6 the interaction energy for two coaxial graphene cylinders. We let the radius,  $a$ , of the inner cylinder be 10 nm and let the radius,  $b$ , of

**Fig. 11.6** The interaction between two coaxial graphene cylinders as a function the radius,  $b$ , of the outer cylinder. The radius,  $a$ , of the inner cylinder is 10 nm. The results are from using (11.64) and each curve is for a different truncation of the summation over  $m$ . See the text for details



outer cylinder vary between 10 and 100 nm. We have treated the graphene cylinders as strictly 2D cylindrical shells with the effective dielectric function given in (10.24). Each curve is for a different truncation of the summation over  $m$ . The smaller the value of  $b$  the more terms are needed in the summation. The reference system is one where the smaller inner cylinder has been taken outside the larger outer cylinder and the two are at infinite distance from each other. The energy in Fig. 11.6 is the energy gain when the smaller cylinder is brought to and inserted into the larger cylinder. The energy in (11.64) is negative. We note that for  $b$  large the  $m = 0$  and  $m = \pm 1$  terms dominate the energy contribution.

Next we address the problem of an atom in between two thin coaxial cylindrical films. The problem could be intercalation of atoms in multi-wall nano tubes.

### 11.10 Force on an Atom in Between Two 2D Coaxial Cylindrical Films

Here we study an atom in a cylindrical vacuum gap between two 2D cylindrical films with the outer and inner radii  $b$  and  $a$ , respectively. The ambient medium in which the films and the atom reside is vacuum. The atom is at a distance  $r$  from the center. Here we may make use of the results in Sect. 11.5. The matrix for this geometry is the product of those for the outer 2D film, the gas shell and the inner 2D film,  $\tilde{\mathbf{M}} = \tilde{\mathbf{M}}^{2Do} \cdot \tilde{\mathbf{M}}^{\text{gas}} \cdot \tilde{\mathbf{M}}^{2Di}$ , and the matrix element of interest is

$$\begin{aligned}
M_{11} &= (M_{11}^{2Do}, M_{12}^{2Do}) \cdot \begin{pmatrix} M_{11}^{\text{gas}} & M_{12}^{\text{gas}} \\ M_{21}^{\text{gas}} & M_{22}^{\text{gas}} \end{pmatrix} \cdot \begin{pmatrix} M_{11}^{2Di} \\ M_{21}^{2Di} \end{pmatrix} \\
&= M_{11}^{2Do} M_{11}^{\text{gas}} M_{11}^{2Di} \begin{pmatrix} 1, \alpha_{k,m}^{2Do(2)} \end{pmatrix} \cdot \begin{pmatrix} 1 & \alpha_{k,m}^{\text{gas}(2)} \\ -\alpha_{k,m}^{\text{gas}} & \frac{M_{22}^{\text{gas}}}{M_{11}^{\text{gas}}} \end{pmatrix} \cdot \begin{pmatrix} 1 \\ -\alpha_{k,m}^{2Di} \end{pmatrix} \\
&= M_{11}^{2Do} M_{11}^{\text{gas}} M_{11}^{2Di} \\
&\times \left\{ 1 - \alpha_{k,m}^{2Di} \alpha_{k,m}^{2Do(2)} - \alpha_{k,m}^{2Di} \alpha_{k,m}^{2Do(2)} - \alpha_{k,m}^{2Di} \left[ \alpha_{k,m}^{\text{gas}(2)} + \alpha_{k,m}^{2Do(2)} \left( \frac{M_{22}^{\text{gas}}}{M_{11}^{\text{gas}}} - 1 \right) \right] \right\}. \tag{11.65}
\end{aligned}$$

This leads to the following proper mode condition function

$$\begin{aligned}
\tilde{f}_{k,m} &= 1 - \frac{\alpha_{k,m}^{\text{gas}} \alpha_{k,m}^{2Do(2)} + \alpha_{k,m}^{2Di} \left[ \alpha_{k,m}^{\text{gas}(2)} + \alpha_{k,m}^{2Do(2)} \left( \frac{M_{22}^{\text{gas}}}{M_{11}^{\text{gas}}} - 1 \right) \right]}{1 - \alpha_{k,m}^{2Di} \alpha_{k,m}^{2Do(2)}} \\
&\approx 1 - \frac{\alpha_{k,m}^{\text{gas}} \alpha_{k,m}^{2Do(2)} + \alpha_{k,m}^{2Di} \left[ \alpha_{k,m}^{\text{gas}(2)} + 2\alpha_{k,m}^{2Do(2)} (M_{22}^{\text{gas}} - 1) \right]}{1 - \alpha_{k,m}^{2Di} \alpha_{k,m}^{2Do(2)}}, \tag{11.66}
\end{aligned}$$

where the reference system is a system where all three shells are well separated from each other. The functions appearing in the expression are

$$\begin{aligned}
\alpha_{k,m}^{\text{gas}} &\approx (\delta n) \frac{4\pi \alpha^{at}(\omega)}{r} \left\{ [m^2 + (kr)^2] [I_m(kr)]^2 + (kr)^2 [I_m'(kr)]^2 \right\}; \\
\alpha_{k,m}^{\text{gas}(2)} &\approx (\delta n) \frac{4\pi \alpha^{at}(\omega)}{r} \left\{ [m^2 + (kr)^2] [K_m(kr)]^2 + (kr)^2 [K_m'(kr)]^2 \right\}; \\
M_{22}^{\text{gas}} - 1 &\approx -(\delta n) \frac{4\pi \alpha^{at}(\omega)}{r} \left\{ [m^2 + (kr)^2] I_m(kr) K_m(kr) \right. \\
&\quad \left. + (kr)^2 I_m'(kr) K_m'(kr) \right\}; \tag{11.67} \\
\alpha_{k,m}^{2Do(2)} &= \alpha_{k,m}^{2D(2)}(b; \omega) = \frac{\delta \tilde{\varepsilon}^{3D}(\omega) [m^2 + (kb)^2] [K_m(kb)]^2}{b + \delta \tilde{\varepsilon}^{3D}(\omega) [m^2 + (kb)^2] I_m(kb) K_m(kb)}; \\
\alpha_{k,m}^{2Di} &= \alpha_{k,m}^{2D}(a; \omega) = \frac{\delta \tilde{\varepsilon}^{3D}(\omega) [m^2 + (ka)^2] [I_m(ka)]^2}{a + \delta \tilde{\varepsilon}^{3D}(\omega) [m^2 + (ka)^2] I_m(ka) K_m(ka)}.
\end{aligned}$$

Before we write down the expression for the energy per atom we make the factor  $(\delta n) 4\pi \alpha^{at}(\omega)$  explicit, a factor that is common for all terms after 1—in the expression for  $\tilde{f}_{k,m}$ . We have

$$\begin{aligned}
\tilde{f}_{k,m} &\approx 1 - (\delta n) \frac{4\pi \alpha^{at}(\omega)}{r \left[ 1 - \alpha_{k,m}^{2Di} \alpha_{k,m}^{2Do(2)} \right]} \left\{ [m^2 + (kr)^2] \right. \\
&\quad \times \left[ \alpha_{k,m}^{2Do(2)} [I_m(kr)]^2 + \alpha_{k,m}^{2Di} [K_m(kr)]^2 \right. \\
&\quad \left. \left. - 2\alpha_{k,m}^{2Di} \alpha_{k,m}^{2Do(2)} I_m(kr) K_m(kr) \right] \right. \\
&\quad \left. + (kr)^2 \left[ \alpha_{k,m}^{2Do(2)} [I_m'(kr)]^2 + \alpha_{k,m}^{2Di} [K_m'(kr)]^2 \right. \right. \\
&\quad \left. \left. - 2\alpha_{k,m}^{2Di} \alpha_{k,m}^{2Do(2)} I_m'(kr) K_m'(kr) \right] \right\}. \tag{11.68}
\end{aligned}$$

Now, the energy per atom is

$$\begin{aligned}
\frac{E}{2\pi(\delta n)L} &= \frac{\hbar}{2\pi(\delta n)L} \int_0^\infty \frac{d\xi}{2\pi} \sum_{m=-\infty}^\infty L \int_{-\infty}^\infty \frac{dk}{2\pi} \ln \left[ \tilde{f}_{k,m}(k, i\xi) \right] \\
&\approx \frac{\hbar}{2\pi(\delta n)} \int_0^\infty \frac{d\xi}{2\pi} \sum_{m=-\infty}^\infty \int_{-\infty}^\infty \frac{dk}{2\pi} \left[ \tilde{f}_{k,m}(k, i\xi) - 1 \right] \\
&= -\frac{2\hbar}{r} \int_0^\infty \frac{d\xi}{2\pi} \sum_{m=-\infty}^\infty \int_{-\infty}^\infty \frac{dk}{2\pi} \frac{\alpha^{ai}(i\xi)}{\left[ 1 - \alpha_{k,m}^{2Di} \alpha_{k,m}^{2Do(2)} \right]} \\
&\quad \times \left\{ [m^2 + (kr)^2] \left[ \alpha_{k,m}^{2Do(2)} [I_m(kr)]^2 \right. \right. \\
&\quad + \alpha_{k,m}^{2Di} [K_m(kr)]^2 - 2\alpha_{k,m}^{2Di} \alpha_{k,m}^{2Do(2)} I_m(kr) K_m(kr) \left. \right] \\
&\quad + (kr)^2 \left[ \alpha_{k,m}^{2Do(2)} [I_m'(kr)]^2 + \alpha_{k,m}^{2Di} [K_m'(kr)]^2 \right. \\
&\quad \left. \left. - 2\alpha_{k,m}^{2Di} \alpha_{k,m}^{2Do(2)} I_m'(kr) K_m(kr) \right] \right\} \tag{11.69}
\end{aligned}$$

where we on the second line have expanded the logarithm and kept the lowest order term. The force on the atom is  $\mathbf{F}(r) = -\hat{\mathbf{r}}dE(r)/dr$ .

## References

1. M. Abramowitz, I.A. Stegun, *Handbook of Mathematical Functions with Formulas, Graphs, and Mathematical Tables* (Wiley, New York, 1972)
2. Bo E. Sernelius, *Graphene* **1**, 21 (2012)
3. Bo E. Sernelius, *J. Phys.: Condens. Matter* **27**, 214017 (2015)
4. Bo E. Sernelius, *Surface Modes in Physics* (Wiley-VCH, Berlin, 2001)
5. D. Langbein, *Theory of Van der Waals Attraction* (Springer, New York, Heidelberg, 1974)

**Part III**  
**Fully Retarded Formalism: Casimir**

It all started in the Netherlands in the 1940s. J. T. G. Overbeek performed experiments on suspensions of quartz powder. He and E. J. W. Verwey had developed a theory for the stability of colloids. The theory relied on the long range interaction between the particles. The experiments suggested that the long range forces did not fall off as  $r^{-7}$ , which is the standard van der Waals interaction, but faster. H. B. G. Casimir and D. Polder were given this problem. They first studied two atoms and found that retardation effects, effects from the finite speed of light, made the force for very large separations vary as  $r^{-8}$  instead of as  $r^{-7}$  (interaction energy as  $r^{-7}$  instead of as  $r^{-6}$ ).

They continued and studied the force between two colloidal particles in a cavity and the force between a particle and the cavity wall. They did this by solving Maxwell's equations and summing the zero-point energy of all modes in the cavity. Both the particles and wall were assumed to totally reflect electromagnetic waves. Here they went from fluctuations in the charge density of the atoms or colloidal particles to fluctuations in the fields. Casimir was intrigued by the simplicity in the actual expression for the force. He thought a lot about these things for a long time. He decided to study the simplest system, the empty cavity. He studied two perfectly reflecting metal plates in vacuum, summed the zero-point energy of all modes, and found that there is a force between the plates. The Casimir force was born.

In the Casimir gedanken experiment the modes are vacuum modes. For real metal plates the force is of van der Waals type for small and intermediate separations. Here the contributing modes are surface modes. For large separations, beyond a separation value characteristic of the metal in question, the force is the Casimir force and the contributing modes are the vacuum modes.

# Chapter 12

## Casimir Interaction



**Abstract** We derive the Casimir-Polder interaction between two polarizable atoms with a method based on electromagnetic normal modes found by generating self-sustained fields. Numerical results are given for the alkali-metal atoms. We give results for both zero temperature and finite temperature. In connection with the finite temperature derivations we discuss classical and quantum contributions. We furthermore derive the equation of state for a Casimir-Polder gas and show that the corrections from going beyond van der Waals interactions are small.

### 12.1 Casimir-Polder Interaction Between Two Atoms

In this section we will derive the dispersion interaction between two polarizable atoms, atom 1 and atom 2, by finding self-sustained fields. We put atom 1 at the origin and atom 2 at  $\mathbf{r}$ . Now, let atom 1 have a time dependent dipole moment  $\mathbf{p}_1$ . This dipole moment gives rise to an electric field.<sup>1</sup> We denote the electric field caused by atom  $i$  at the position of atom  $j$  by  $\mathbf{E}^{ij}$ . Thus,  $\mathbf{p}_1$  produces the field  $\mathbf{E}^{12}(\mathbf{r})$  at the position of atom 2. The field induces a dipole moment in atom 2,

$$\mathbf{p}_2 = \alpha_2^{at} \mathbf{E}^{12}, \tag{12.1}$$

where  $\alpha_2^{at}$  is the atomic polarizability of atom 2. Here, we should be a little more careful. What was said about convolution integrals in Sect. 2.3 also holds here. Thus,

$$\mathbf{p}_2(t) = \int_{-\infty}^{\infty} dt \alpha_2^{at}(t-t') \mathbf{E}^{12}(t') \tag{12.2}$$

and the simple relation in (12.1) is valid for the Fourier transformed quantities,

$$\mathbf{p}_2(\omega) = \alpha_2^{at}(\omega) \mathbf{E}^{12}(\omega). \tag{12.3}$$

<sup>1</sup>Also a magnetic field is produced but we neglect magnetic effects here.

So from now on the dipole moments and electric fields refer to their Fourier transformed (with respect to time) versions.

The dipole moment  $\mathbf{p}_2$  gives rise to a field  $\mathbf{E}^{21}$  at the position of atom 1. This field polarizes atom 1 and

$$\mathbf{p}_1(\omega) = \alpha_1^{at}(\omega) \mathbf{E}^{21}(\omega). \quad (12.4)$$

To find self-sustained fields, normal modes, we close the loop and assume that this induced dipole moment in atom 1 is the dipole moment we started from.

Before we proceed we need the expression for the  $\mathbf{E}$ -field due to a time dependent dipole,  $\mathbf{p}$ , at the origin (2.148)

$$\mathbf{E}(\mathbf{r}, t) = \left( \frac{2[p]}{r^3} + \frac{2[\dot{p}]}{cr^2} \right) \cos \theta \mathbf{e}_r + \left( \frac{[p]}{r^3} + \frac{[\dot{p}]}{cr^2} + \frac{[\ddot{p}]}{c^2 r} \right) \sin \theta \mathbf{e}_\theta. \quad (12.5)$$

Remember that the square bracket means that the time argument of the function inside is the retarded time,  $t - r/c$ .

We want the Fourier transform with respect to  $t$ . The Fourier transform of  $\mathbf{p}(t)$  is  $\mathbf{p}(\omega)$ ; the Fourier transform of  $\mathbf{p}(t - r/c)$  is  $e^{i\omega r/c} \mathbf{p}(\omega)$ ; the Fourier transform of  $\dot{\mathbf{p}}(t)$  is  $(-i\omega) \mathbf{p}(\omega)$ ; the Fourier transform of  $\dot{\mathbf{p}}(t - r/c)$  is  $(-i\omega) e^{i\omega r/c} \mathbf{p}(\omega)$ ; the Fourier transform of  $\ddot{\mathbf{p}}(t - r/c)$  is  $(-i\omega)^2 e^{i\omega r/c} \mathbf{p}(\omega)$ . Thus we have

$$\begin{aligned} \mathbf{E}(\mathbf{r}, \omega) &= 2[1 + (-i\omega r/c)] \frac{e^{i\omega r/c}}{r^3} (\mathbf{p}(\omega) \cdot \mathbf{r}) \mathbf{r} \\ &\quad - [1 + (-i\omega r/c) + (-i\omega r/c)^2] \frac{e^{i\omega r/c}}{r^3} \left[ \mathbf{p}(\omega) - \frac{1}{r^2} (\mathbf{p}(\omega) \cdot \mathbf{r}) \mathbf{r} \right] \\ &= -[1 - (i\omega r/c)] \frac{e^{i\omega r/c}}{r^3} \left[ \mathbf{p} - \frac{3}{r^2} (\mathbf{p} \cdot \mathbf{r}) \mathbf{r} \right] - (i\omega r/c)^2 \frac{e^{i\omega r/c}}{r^3} \left[ \mathbf{p} - \frac{1}{r^2} (\mathbf{p} \cdot \mathbf{r}) \mathbf{r} \right], \end{aligned} \quad (12.6)$$

where we have made the identifications  $\cos \theta \mathbf{e}_r = (\hat{\mathbf{p}} \cdot \hat{\mathbf{r}}) \hat{\mathbf{r}}$ ;  $\sin \theta \mathbf{e}_\theta = -[\hat{\mathbf{p}} - (\hat{\mathbf{p}} \cdot \hat{\mathbf{r}}) \hat{\mathbf{r}}]$ .

We prefer the matrix notation. Then  $\mathbf{E}$  and  $\mathbf{p}$  are column vectors, and

$$\mathbf{E}(\mathbf{r}, \omega) = -[1 - (i\omega r/c)] e^{i\omega r/c} \tilde{\phi}(\mathbf{r}) \cdot \mathbf{p}(\omega) - (i\omega r/c)^2 e^{i\omega r/c} \tilde{\vartheta}(\mathbf{r}) \cdot \mathbf{p}(\omega), \quad (12.7)$$

where  $\tilde{\phi}(\mathbf{r})$  is the dipole-dipole tensor,

$$\phi(\mathbf{r})_{\mu\nu} = \frac{\delta_{\mu\nu}}{r^3} - 3 \frac{r_\mu r_\nu}{r^5}, \quad (12.8)$$

and  $\tilde{\vartheta}(\mathbf{r})$  is the tensor

$$\vartheta(\mathbf{r})_{\mu\nu} = \frac{\delta_{\mu\nu}}{r^3} - \frac{r_\mu r_\nu}{r^5}. \quad (12.9)$$

We note the following properties of these tensors:

$$\tilde{\phi}(-\mathbf{r}) = \tilde{\phi}(\mathbf{r}), \quad (12.10)$$

$$\tilde{\vartheta}(-\mathbf{r}) = \tilde{\vartheta}(\mathbf{r}), \quad (12.11)$$

$$\tilde{\phi}^2(\mathbf{r})_{\mu\nu} = \frac{\delta_{\mu\nu}}{r^6} + 3\frac{r_\mu r_\nu}{r^8}, \quad (12.12)$$

$$\tilde{\vartheta}^2(\mathbf{r}) = \frac{1}{r^3}\tilde{\vartheta}(\mathbf{r}), \quad (12.13)$$

and

$$\tilde{\phi}(\mathbf{r}) \cdot \tilde{\vartheta}(\mathbf{r}) = \frac{1}{r^3}\tilde{\vartheta}(\mathbf{r}). \quad (12.14)$$

We may now find the modes. To be more general we allow the atomic response to be anisotropic. The atomic polarizabilities then are tensors which we indicate by a tilde. Thus we have

$$\begin{aligned} \mathbf{p}_1(\omega) &= \tilde{\alpha}_1^{at}(\omega) \cdot \mathbf{E}^{21}(\omega), \\ \mathbf{E}^{21}(\omega) &= \left\{ -[1 - (i\omega r/c)] e^{i\omega r/c} \tilde{\phi}(-\mathbf{r}) - (i\omega r/c)^2 e^{i\omega r/c} \tilde{\vartheta}(-\mathbf{r}) \right\} \cdot \mathbf{p}_2(\omega), \\ \mathbf{p}_2(\omega) &= \tilde{\alpha}_2^{at}(\omega) \cdot \mathbf{E}^{12}(\omega), \\ \mathbf{E}^{12}(\omega) &= \left\{ -[1 - (i\omega r/c)] e^{i\omega r/c} \tilde{\phi}(\mathbf{r}) - (i\omega r/c)^2 e^{i\omega r/c} \tilde{\vartheta}(\mathbf{r}) \right\} \cdot \mathbf{p}_1(\omega). \end{aligned} \quad (12.15)$$

Now, first we eliminate  $\mathbf{E}^{21}$  by using the first two equations and  $\mathbf{E}^{12}$  by using the remaining two. This results in two new equations. Next, we eliminate  $\mathbf{p}_2$  from these equations and find

$$\begin{aligned} &\left[ \tilde{\mathbf{I}} - \tilde{\alpha}_1^{at}(\omega) \cdot \left\{ -[1 - (i\omega r/c)] e^{i\omega r/c} \tilde{\phi}(\mathbf{r}) - (i\omega r/c)^2 e^{i\omega r/c} \tilde{\vartheta}(\mathbf{r}) \right\} \right. \\ &\quad \left. \cdot \tilde{\alpha}_2^{at}(\omega) \cdot \left\{ -[1 - (i\omega r/c)] e^{i\omega r/c} \tilde{\phi}(\mathbf{r}) - (i\omega r/c)^2 \alpha_1^{at}(\omega) \tilde{\vartheta}(\mathbf{r}) \right\} \right] \cdot \mathbf{p}_1(\omega) = 0. \end{aligned} \quad (12.16)$$

The non-trivial solution is found for

$$\left| \tilde{A} \right| = 0, \quad (12.17)$$

where

$$\begin{aligned} \tilde{A} &= \tilde{\mathbf{I}} - \tilde{\alpha}_1^{at}(\omega) \cdot \left\{ -[1 - (i\omega r/c)] e^{i\omega r/c} \tilde{\phi}(\mathbf{r}) - (i\omega r/c)^2 e^{i\omega r/c} \tilde{\vartheta}(\mathbf{r}) \right\} \\ &\quad \cdot \tilde{\alpha}_2^{at}(\omega) \cdot \left\{ -[1 - (i\omega r/c)] e^{i\omega r/c} \tilde{\phi}(\mathbf{r}) - (i\omega r/c)^2 \alpha_1^{at}(\omega) \tilde{\vartheta}(\mathbf{r}) \right\}. \end{aligned} \quad (12.18)$$

Now, we limit the treatment to isotropic atoms. Then the polarizabilities become scalar and  $\tilde{A}$  is reduced to

$$\begin{aligned} \tilde{A} = \tilde{I} - \alpha_1^{at}(\omega) \alpha_1^{at}(\omega) e^{i2\omega r/c} \left\{ [1 - (i\omega r/c)]^2 \tilde{\phi}^2(\mathbf{r}) + (i\omega r/c)^4 \tilde{\vartheta}^2(\mathbf{r}) \right. \\ \left. + 2[1 - (i\omega r/c)] (i\omega r/c)^2 \tilde{\phi}(\mathbf{r}) \cdot \tilde{\vartheta}(\mathbf{r}) \right\}. \end{aligned} \quad (12.19)$$

We have the freedom to rotate the coordinate system so that atom 2 lies on an axis, the  $z$ -axis say. Then  $\mathbf{r} = r\hat{z}$  and the tensors become as simple as possible. We find

$$\tilde{\phi}(\mathbf{r}) = \frac{1}{r^3} \begin{pmatrix} 1 & 0 & 0 \\ 0 & 1 & 0 \\ 0 & 0 & -2 \end{pmatrix}, \quad (12.20)$$

$$\tilde{\phi}^2(\mathbf{r}) = \frac{1}{r^6} \begin{pmatrix} 1 & 0 & 0 \\ 0 & 1 & 0 \\ 0 & 0 & 4 \end{pmatrix}, \quad (12.21)$$

$$\tilde{\vartheta}(\mathbf{r}) = \frac{1}{r^3} \begin{pmatrix} 1 & 0 & 0 \\ 0 & 1 & 0 \\ 0 & 0 & 0 \end{pmatrix}, \quad (12.22)$$

$$\tilde{\vartheta}^2(\mathbf{r}) = \frac{1}{r^6} \begin{pmatrix} 1 & 0 & 0 \\ 0 & 1 & 0 \\ 0 & 0 & 0 \end{pmatrix}, \quad (12.23)$$

and

$$\tilde{\phi}(\mathbf{r}) \cdot \tilde{\vartheta}(\mathbf{r}) = \frac{1}{r^3} \tilde{\vartheta}(\mathbf{r}) = \frac{1}{r^6} \begin{pmatrix} 1 & 0 & 0 \\ 0 & 1 & 0 \\ 0 & 0 & 0 \end{pmatrix}. \quad (12.24)$$

With these tensor forms the determinant equation becomes

$$\begin{aligned} \left\{ 1 - \alpha_1^{at}(\omega) \alpha_2^{at}(\omega) \frac{e^{i2\omega r/c}}{r^6} [1 - (i\omega r/c) + (i\omega r/c)^2]^2 \right\}^2 \\ \times \left\{ 1 - 4\alpha_1^{at}(\omega) \alpha_2^{at}(\omega) \frac{e^{i2\omega r/c}}{r^6} [1 - (i\omega r/c)]^2 \right\} = 0 \end{aligned} \quad (12.25)$$

where the first factor of the left-hand-side is  $A_{11}$ , the second  $A_{22}$ , and the third  $A_{33}$ . Thus the mode condition function in the upper half of the complex frequency plane is

$$\begin{aligned} f(z) = \left\{ 1 - \alpha_1^{at}(z) \alpha_2^{at}(z) \frac{e^{i2zr/c}}{r^6} [1 - (izr/c) + (izr/c)^2]^2 \right\}^2 \\ \times \left\{ 1 - 4\alpha_1^{at}(z) \alpha_2^{at}(z) \frac{e^{i2zr/c}}{r^6} [1 - (izr/c)]^2 \right\}. \end{aligned} \quad (12.26)$$

We also need the corresponding expression in the lower half. We have to make an analytical continuation. The function we have is a retarded function. We need the time-ordered version. It is even in  $z$ . Now let the  $f_u(z) = f(z)$ . Then  $f_l(z) =$

$f(z^*)^*$ , where the subscripts  $u$  and  $l$  denote upper and lower half plane respectively. This means that on the imaginary frequency axis we have

$$f(i\xi) = \left\{ 1 - \alpha_1^{at}(i\xi) \alpha_2^{at}(i\xi) \frac{e^{-2|\xi|r/c}}{r^6} [1 + (|\xi|r/c) + (|\xi|r/c)^2]^2 \right\}^2 \times \left\{ 1 - 4\alpha_1^{at}(i\xi) \alpha_2^{at}(i\xi) \frac{e^{-2|\xi|r/c}}{r^6} [1 + (|\xi|r/c)]^2 \right\}. \quad (12.27)$$

Now we have all we need to calculate the interaction energy between two atoms.

### 12.1.1 Zero Temperature Casimir-Polder Potential Between Two Atoms

The zero temperature interaction potential (5.59) becomes

$$V(r) = \frac{\hbar}{2} \int_{-\infty}^{\infty} \frac{d\xi}{2\pi} \ln \left[ \left\{ 1 - \alpha_1^{at}(i\xi) \alpha_2^{at}(i\xi) \frac{e^{-2|\xi|r/c}}{r^6} [1 + (|\xi|r/c) + (|\xi|r/c)^2]^2 \right\}^2 \times \left\{ 1 - 4\alpha_1^{at}(i\xi) \alpha_2^{at}(i\xi) \frac{e^{-2|\xi|r/c}}{r^6} [1 + (|\xi|r/c)]^2 \right\} \right]. \quad (12.28)$$

Along the imaginary axis the integrand is even and we can limit the integration to the upper part and multiply by two:

$$V(r) = \hbar \int_0^{\infty} \frac{d\xi}{2\pi} \ln \left[ \left\{ 1 - \alpha_1^{at}(i\xi) \alpha_2^{at}(i\xi) \frac{e^{-2\xi r/c}}{r^6} [1 + (\xi r/c) + (\xi r/c)^2]^2 \right\}^2 \times \left\{ 1 - 4\alpha_1^{at}(i\xi) \alpha_2^{at}(i\xi) \frac{e^{-2\xi r/c}}{r^6} [1 + (\xi r/c)]^2 \right\} \right]. \quad (12.29)$$

For large distances the logarithm may be expanded and only the lowest order term be kept. With large distances we here mean that they are large enough for the interaction to be weak. Then we find:

$$V_{CP}(r) = -\frac{\hbar}{\pi r^6} \int_0^{\infty} d\xi \alpha_1^{at}(i\xi) \alpha_2^{at}(i\xi) e^{-2\xi r/c} \times [3 + 6(\xi r/c) + 5(\xi r/c)^2 + 2(\xi r/c)^3 + (\xi r/c)^4] \quad (12.30)$$

This is the Casimir-Polder interaction and it gives the van der Waals result for intermediate separations and the retarded result for large separations.

In Figs. 12.1 and 12.2 we give some examples of results for alkali-metal dimers; in Fig. 12.1a for two Li atoms; in Fig. 12.1b for two Na atoms; in Fig. 12.2a for two K atoms; in Fig. 12.2b for a Na-K dimer. In all cases the London approximation for the polarizabilities was used,

$$\alpha_i^{at}(i\xi) = \frac{\alpha_i(0)}{1 + (\hbar\xi/E_i)^2}, \quad (12.31)$$

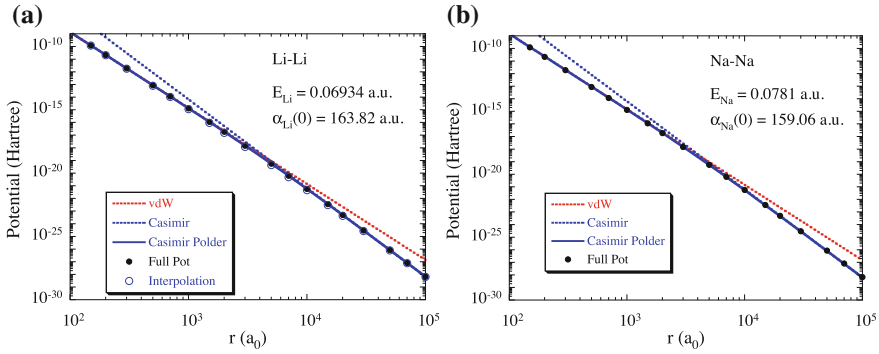


**Fig. 12.1** **a** The Casimir Polder interaction potential for two lithium atoms from (12.30), *solid curve*; the atomic polarizability in the London approximation was used. The *filled circles* show the full result [1] from a quantum-mechanical calculation including both retardation effects and multipole contributions and the full expression for the polarizabilities. **b** The same as in (a) but for the Na dimer

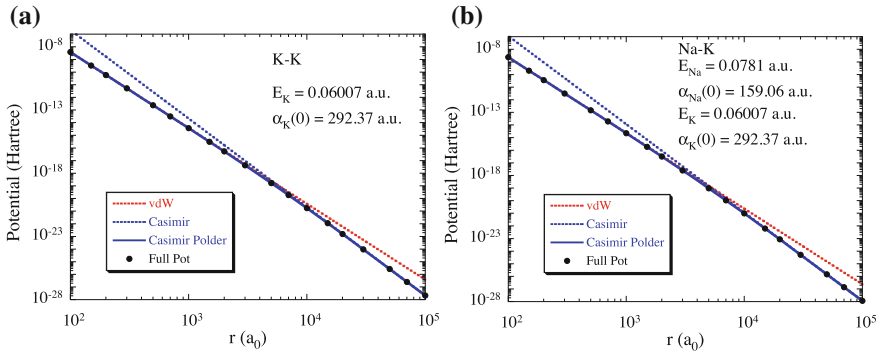


**Fig. 12.2** Same as Fig. 12.1 but now for the K homonuclear dimer in (a) and Na-K heteronuclear dimer in (b)

with the parameters indicated in the figures. These parameters were determined in the following way: The  $\alpha_i(0)$  was obtained first. We assumed that the full result had fully reached the Casimir limit for  $r = 10^5 a_0$ , the highest separation value quoted in [1], and for each homonuclear alkali-metal dimer we equated this result with the Casimir result of (12.34) for homonuclear dimers,  $-23\hbar c\alpha_i(0)^2 / (4\pi r^7)$ . Having determined  $\alpha_i(0)$  we now turn to the parameter  $E_i = \hbar\omega_i$ . At the separation  $r = 10^2 a_0$  all multipole and magnetic contributions have died out. We assume that at this separation the potential is still in the van der Waals region. We equate the full result with the van der Waals result from (8.63),  $-3\alpha_i(0)^2 \hbar\omega_i / (4r^6)$ . The same parameter values were used for all combinations of heteronuclear alkali-metal dimers with the same agreement as in Fig. 12.2b. This demonstrates the robustness of the approximation.

The open circles in Fig. 12.1 is a result from an interpolation approximation,  $V \approx 1/(1/V_{\text{vdW}} + 1/V_{\text{Casimir}})$ , to be used in Sect. 12.2.

We will now demonstrate in a more direct way that the two limiting potentials are obtained. Let us first start with the van der Waals limit. Assume that  $\xi r/c$  is small compared to unity. The expression in the square brackets reduces to 3 and the exponential prefactor to unity:

$$V_{CP}(r) \underset{\xi r/c \rightarrow 0}{\approx} -\frac{3\hbar}{\pi} \frac{1}{r^6} \int_0^\infty d\xi \alpha_1^{at}(i\xi) \alpha_2^{at}(i\xi). \quad (12.32)$$

This is the van der Waals result. To find the other limiting result we make the substitution  $u = \xi r/c$ . Then we have:

$$V_{CP}(r) = -\frac{\hbar c}{\pi r^7} \int_0^\infty du \alpha_1^{at}\left(\frac{uc}{r}\right) \alpha_2^{at}\left(\frac{uc}{r}\right) e^{-2u} (3 + 6u + 5u^2 + 2u^3 + u^4). \quad (12.33)$$

The exponential factor guarantees that only small  $u$  values contribute to the integral. If  $r$  is big enough we can replace the polarizabilities with the static ones and move them outside the integral. Then we have:

$$\begin{aligned} V_{CP}(r) &\underset{r \rightarrow \infty}{\approx} -\frac{\hbar c \alpha_1^{at}(0) \alpha_2^{at}(0)}{\pi r^7} \int_0^\infty du e^{-2u} (3 + 6u + 5u^2 + 2u^3 + u^4) \\ &= -\frac{\hbar c \alpha_1^{at}(0) \alpha_2^{at}(0)}{\pi r^7} \frac{23}{4} = -\frac{23\hbar c}{4\pi} [\alpha_1^{at}(0) \alpha_2^{at}(0)] \frac{1}{r^7}, \end{aligned} \quad (12.34)$$

which is the Casimir result. Thus we see that for intermediate separations, in the van der Waals range, the potential goes as  $r^{-6}$  and for large separations, in the Casimir range, as  $r^{-7}$ .

### 12.1.2 Finite Temperature Casimir-Polder Potential Between Two Atoms

The finite temperature interaction potential (5.64) becomes

$$\begin{aligned} V_{CP}(r) &= -\frac{2}{\beta r^6} \sum_n' \alpha_1^{at}(i\xi_n) \alpha_2^{at}(c) e^{-2\xi_n r/c} \\ &\times [3 + 6(\xi_n r/c) + 5(\xi_n r/c)^2 + 2(\xi_n r/c)^3 + (\xi_n r/c)^4] \\ &= -\frac{3}{\beta r^6} \alpha_1^{at}(0) \alpha_2^{at}(0) - \frac{2}{\beta r^6} \sum_n \alpha_1^{at}(i\xi_n) \alpha_2^{at}(i\xi_n) e^{-2\xi_n r/c} \\ &\times [3 + 6(\xi_n r/c) + 5(\xi_n r/c)^2 + 2(\xi_n r/c)^3 + (\xi_n r/c)^4], \end{aligned} \quad (12.35)$$

where we have separated out the first term in the original summation. This first term is special. It does not depend on  $\hbar$ . All other terms depend implicitly on  $\hbar$  through  $\xi_n$ . A way to find the classical limit of a quantum mechanical result is to let  $\hbar$  go toward zero. If we do that here the first term ( $n = 0$ ) remains unchanged while all other terms go toward zero. Thus we can say that the first term is the classical contribution to the potential while the rest of the terms are the quantum contribution. The classical term is proportional to  $T$ . Thus at zero temperature there are only quantum contributions. If we start from zero K and gradually increase the temperature the classical term increases but at the same time all  $\xi_n$  shift toward higher frequencies and the quantum contribution decreases at the same rate as the increase of the classical term. Thus for very low temperatures there is no temperature dependence. To find an estimate of the temperature at which the transition from quantum to classical results occurs in the Casimir range we equate the  $n = 0$  term with the zero temperature result and find  $T \approx 23\hbar c/12\pi k_B d$ . In the van der Waals range the corresponding result is  $T \approx \hbar\omega_{Li}/4k_B$ . Note that the critical temperature depends on  $d$  in the Casimir range but is independent of  $d$  in the van der Waals range.

In Fig. 12.3a we show the results for two lithium atoms.<sup>2</sup> The temperature effects begin first at large separation, in the Casimir range; the lowest dotted curve is for 4 K; when temperature increases the onset of temperature effects move closer and closer to the van der Waals region; when this region is reached temperature effects appear in the whole region at once. In Fig. 12.3b we see that the potential is temperature independent for low temperatures until the temperature reaches a critical value after which the potential increases linearly with temperature. Then we have moved into the classical region. In the Casimir range the critical temperature is  $d$ -dependent; the larger  $d$ -value the smaller the critical temperature. In the van der Waals range the critical temperature is the same for all separations.

To better understand how this comes about we have included Fig. 12.4. In Fig. 12.4a we give the integrands normalized to unity for a number of  $d$ -values. The first curve, thick solid black, is the van der Waals integrand; it is independent of  $d$ . Then follows two curves in the van der Waals range, for  $d = 10$  nm (blue thin curve) and  $d = 100$  nm (red thin curve); we find that these integrands are virtually identical to the van der Waals integrand. Next follows a  $d$ -value that is in between the van der Waals and Casimir ranges,  $d = 1000$  nm (black thin curve). Then come two curves in the Casimir range, for  $d = 10^4$  nm (blue thin curve) and  $d = 10^5$  nm (red thin curve). At the bottom of the figure we have indicated the energy position of the first quantum term in the summation. This demonstrates that for high enough temperature all summands in the quantum summation vanish and the total result is classical. In Fig. 12.4b we have plotted the integrands on a log-log plot. Here the curves in the van der Waals range separate. We have also indicated the quantum terms at room temperature. To get a better feeling for these contributions we have replotted the curves on a lin-lin plot in Fig. 12.5.

<sup>2</sup>Here we should point out that we have not been strictly stringent. We have neglected the temperature dependence of the polarizabilities. For the very highest temperatures we have included, these are bound to be important. The atoms might even be ionized at these temperatures.

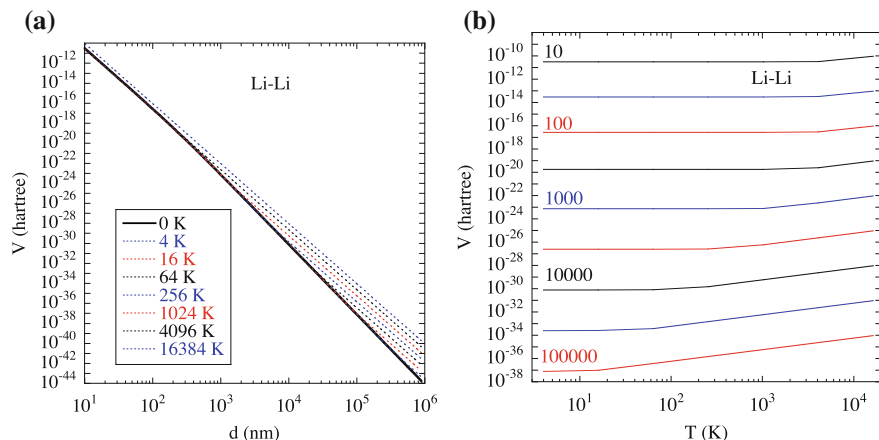


**Fig. 12.3** **a** The interaction potential as function of separation,  $d$ , between two lithium atoms at finite temperature; the temperature effects begin first at large separation, in the Casimir range; the lowest dotted curve is for 4 K; when temperature increases the onset of temperature effects move closer and closer to the van der Waals region; when this region is reached temperature effects appear in the whole region at once. **b** Here each curve is for a fix  $d$ -value; the numbers indicate  $d$  in nm. The four upper curves belong to the van der Waals range; here, we see that the potential is independent of temperature up to a specific temperature common to all four; above that temperature the potential increases linearly with temperature. The rest of the curves belong to the Casimir range; here, the onset of the linear temperature dependence is different for the curves, starting first for the curve with highest  $d$ -value

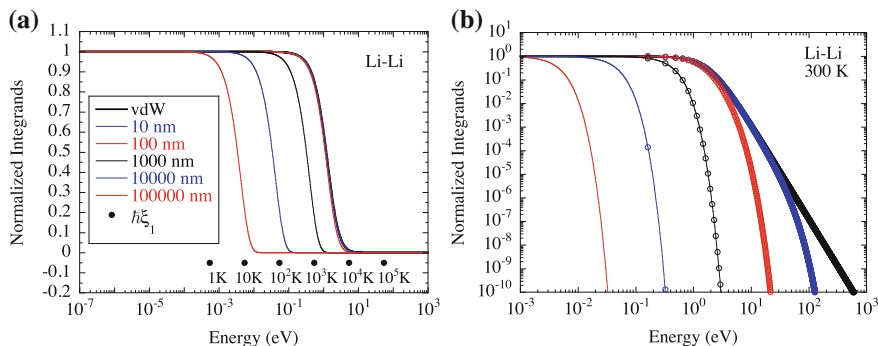
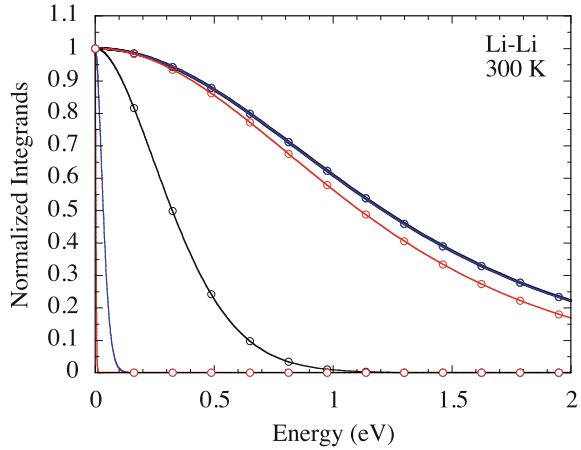


**Fig. 12.4** The normalized integrands for the Casimir Polder interaction between two lithium atoms. **a** Here we use a lin-log plot. The solid thick curve is the van der Waals integrand; it is independent of  $d$ . The next two curves, for 10nm and 100nm, are in the van der Waals range and almost indistinguishable from the vdW curve. The rest of the curves are for  $d$  values in the Casimir range. At the bottom of the figure we have indicated the position of the first ( $n = 1$ ) quantum contribution for different  $d$  values; here we see e.g. that for  $T > 10^4$  K there are no quantum contributions for any  $d$  values; for  $T > 10^3$  K there are no quantum contributions for neither  $d = 10^4$  nm nor  $d = 10^5$  nm. **b** Here we have used a log-log plot. Then we see that the curves for the two lowest  $d$  values, both in the van der Waals range, really deviate from the vdW integrand. We have furthermore indicated with open circles the terms in the summation of quantum contributions in the case of room temperature

**Fig. 12.5** The same as Fig. 12.4b but on a lin-lin plot. Here we get a better feeling for the relative contributions to the interaction at room temperature for the different terms; remember that the  $n = 0$  term should be reduced by a factor of  $1/2$



## 12.2 Equation of State for Casimir-Polder Gas

In this section we derive the non-ideal gas law for a gas of atoms or molecules taking the retarded interaction between the atoms into account. This is done in analogy with the non-retarded derivation in Sect. 8.2. It is interesting to see if retardation effects lead to important corrections.

We let the atoms<sup>3</sup> have a finite radius,  $r_0$ , and an attractive interaction. We have the interaction potential for small separations

$$V_{vdW}(r) = -\frac{3\hbar\omega_0\alpha^{at}(0)^2}{4} \frac{1}{r^6}, \quad (12.36)$$

and for large separations,

$$V_{Casimir}(r) = -\frac{23\hbar c\alpha^{at}(0)^2}{4\pi} \frac{1}{r^7}. \quad (12.37)$$

These are shown as dotted asymptotes in Fig. 12.1. We will use an approximate interpolation formula between these asymptotes,

$$V_{int.} = 1 / (1/V_{vdW} + 1/V_{Casimir}). \quad (12.38)$$

The results using this formula is shown as open circles in Fig. 12.1. The agreement with the full result, solid circles, is good enough for our purpose. The reason we do this approximation is that then we find analytic results for the equation of state constants. Thus, we let

<sup>3</sup>We have here assumed that the gas consists of separate atoms. The treatment is still valid for molecular gases. In that case read molecule instead of atom.

**Table 12.1** The  $B$ -coefficients in the interpolation scheme for the alkali dimers, where  $V(r) = (-B_1 r^{-6}) / (1 + B_2 r)$ . Also the van der Waals radii [2],  $r_0$ , and diameters,  $d_0$ , are given

	$r_0[a_0]$	$d_0[a_0]$	$B_1[\text{Hartree } a_0^6]$	$B_2[a_0^{-1}]$	$B_2 d_0$
Li	4.97	9.94	1396	$0.207 \times 10^{-3}$	$2.06 \times 10^{-3}$
Na	5.23	10.47	1482	$0.234 \times 10^{-3}$	$2.45 \times 10^{-3}$
K	5.71	11.41	3851	$0.180 \times 10^{-3}$	$2.05 \times 10^{-3}$
Rb	5.95	11.91	4478	$0.176 \times 10^{-3}$	$2.10 \times 10^{-3}$
Cs	6.24	12.47	6422	$0.159 \times 10^{-3}$	$1.98 \times 10^{-3}$

$$V = -\frac{3\hbar\omega_0\alpha^{at}(0)^2}{4} \frac{1}{r^6} \frac{1}{1 + \frac{3\pi\omega_0}{23c}r} = (-B_1 r^{-6}) / (1 + B_2 r), \quad (12.39)$$

where

$$\begin{aligned} B_1 &= \frac{3\hbar\omega_0\alpha^{at}(0)^2}{4}, \\ B_2 &= \frac{3\pi\omega_0}{23c}. \end{aligned} \quad (12.40)$$

The values of these constants are given for the alkali dimers in Table 12.1. In the table is also collected the van der Waals radii and diameters. There is some spread in these values in the literature. We have chosen the recommended equilibrium values quoted in Table 9 of [2].

The finite radius leads to a smaller free volume in which the atoms can move,

$$\tilde{V} = V - N4\pi d_0^3/3 = V (1 - n4\pi d_0^3/3) = V (1 - Cn), \quad (12.41)$$

where  $d_0$  is the atomic diameter. We have subtracted the volume taken up by the atoms themselves.<sup>4</sup>

The interaction between the atoms leads to an energy shift for each atom. For a gas one may sum over pair interactions,

$$\begin{aligned} \Delta E &= \int_{d_0}^{\infty} dr 4\pi r^2 n (-B_1 r^{-6}) / (1 + B_2 r) \\ &= -4\pi n B_1 (B_2)^3 \int_{B_2 d_0}^{\infty} dr r^{-4} \frac{2}{1+r} \\ &= -\frac{4\pi n B_1 (B_2)^3}{6(B_2 d_0)^3} \left[ 6x^2 - 3x + 2 - 6x^3 \ln \left( 1 + \frac{1}{x} \right) \right] \\ &= -Dn, \end{aligned} \quad (12.42)$$

where

$$D = \frac{2\pi B_1}{3(d_0)^3} \left[ 6x^2 - 3x + 2 - 6x^3 \ln \left( 1 + \frac{1}{x} \right) \right], \quad (12.43)$$

<sup>4</sup>Note that an atom can not come closer to another than the atom diameter. This means that a spherical volume of radius  $d_0$  centered around each atom is excluded from the free volume in which other atoms can move.

and  $x = B_2 d_0$ . The  $x$ -values for the alkali metals are given in the last column of Table 12.1. We have introduced the constants  $C$  and  $D$  to make the derivation that follows more transparent. We will now determine the chemical potential for the gas and from this obtain the equation of state. The chemical potential is determined from the relation

$$\begin{aligned} N &= \sum_{\mathbf{k}} n_B(\mathbf{k}) = \tilde{V} \int \frac{d^3k}{(2\pi)^3} n_B(\mathbf{k}) \\ &= \tilde{V} \int_0^\infty dk \frac{4\pi k^2}{(2\pi)^3} \exp\left[-\beta\left(\frac{\hbar^2 k^2}{2m} + \Delta E - \mu\right)\right], \end{aligned} \quad (12.44)$$

where on the right-hand side we have summed over all states weighted by the Boltzmann distribution function. The above equation can be rewritten as

$$\frac{n}{1 - Cn} = \frac{1}{2\pi^2} \exp[-\beta(\Delta E - \mu)] \int_0^\infty dk k^2 \exp\left(-\beta \frac{\hbar^2 k^2}{2m}\right), \quad (12.45)$$

and rearrangement gives

$$\begin{aligned} \frac{2\pi^2 n \exp[\beta(\Delta E - \mu)]}{1 - Cn} &= \int_0^\infty dk k^2 \exp\left(-\beta \frac{\hbar^2 k^2}{2m}\right) \\ &= \left(\sqrt{\frac{\hbar^2 \beta}{2m}}\right)^{-3} \int_0^\infty dk k^2 \exp(-k^2) = \left(\sqrt{\frac{\hbar^2 \beta}{2m}}\right)^{-3} \frac{\sqrt{\pi}}{4}. \end{aligned} \quad (12.46)$$

Thus we have

$$\exp[-\beta(\Delta E - \mu)] = \lambda_T^3 \frac{n}{1 - Cn}, \quad (12.47)$$

and the final result is

$$\mu = -Dn + \frac{1}{\beta} \ln\left(\frac{n\lambda_T^3}{1 - Cn}\right). \quad (12.48)$$

We continue along the lines of Sect. 8.1 and find

$$\begin{aligned} p &= \int_0^n dn \left[ \frac{\partial p}{\partial n} \right]_{NT} = \int_0^n dn \left[ \frac{\partial p}{\partial \mu} \right]_{NT} \left[ \frac{\partial \mu}{\partial n} \right]_{NT} \\ &= \int_0^n dn \underbrace{\left[ \frac{\partial \mu}{\partial n} \right]_{NT}}_{-D + \frac{1}{\beta} \left( \frac{1}{n} + \frac{C}{1 - Cn} \right)} / \underbrace{\left[ \frac{\partial p}{\partial \mu} \right]_{NT}}_{1/n} = \int_0^n dn \left[ -Dn + \frac{1}{\beta(1 - Cn)} \right] \\ &= -D \frac{n^2}{2} - \frac{1}{\beta C} \ln(1 - Cn). \end{aligned} \quad (12.49)$$

To get further we have to make use of the fact that  $Cn$  is much smaller than unity, which is fulfilled for a gas. We expand the logarithm and keep the two lowest order terms

$$\begin{aligned}
 p &= -D\frac{n^2}{2} - \frac{1}{\beta C} \ln(1 - Cn) \approx -D\frac{n^2}{2} + \frac{1}{\beta C} (Cn + \frac{1}{2}(Cn)^2) \\
 &\approx -D\frac{n^2}{2} + \frac{n}{\beta} (1 + \frac{1}{2}Cn) \approx -D\frac{n^2}{2} + \frac{n}{\beta(1-\frac{1}{2}Cn)},
 \end{aligned}
 \tag{12.50}$$

and rewrite this expression as

$$\left(p + D\frac{n^2}{2}\right) \left(\frac{1}{n} - \frac{1}{2}C\right) = \frac{1}{\beta},
 \tag{12.51}$$

or

$$\left(p + D\frac{n^2}{2}\right) \left(\frac{N}{n} - \frac{N}{2}C\right) = \frac{N}{\beta},
 \tag{12.52}$$

or

$$\left(p + D\frac{N^2}{2V^2}\right) \left(V - \frac{N}{2}C\right) = Nk_B T.
 \tag{12.53}$$

Now we may identify the parameters in the van der Waals equation of state,  $(p + a/V^2)(V - b) = Nk_B T$ ,

$$a = D\frac{N^2}{2} = \frac{2\pi BN^2}{3d_0^3} \left[1 - \frac{3}{2}x + 3x^2 - 3x^3 \ln\left(1 + \frac{1}{x}\right)\right],
 \tag{12.54}$$

where the bracket is the correction factor due to retardation. Retardation gives a small reduction in  $a$ , of the order of, but smaller than, one percent for the alkali metal atoms. The other parameter,

$$b = \frac{N}{2}C = \frac{N2\pi d_0^3}{3},
 \tag{12.55}$$

is unchanged. This completes the derivation of the equation of state for non-ideal gases when retardation is taken into account. We have learnt that retardation effects have negligible effect on the equation of state for real gases.

## References

1. M. Marinescu, L. You, Phys. Rev. A **59**, 1936 (1999)
2. S.S. Batsanov, Van der Waals Radii of Elements. Inorg. Mater. **37**(9), 871 (2001)

# Chapter 13

## Dispersion Interaction in Planar Structures



**Abstract** After a section in which we adapt the general formalism presented in Chap. 7 to planar structures we start by introducing the basic structure elements: a single interface, a layer, a 2D film, and a thin diluted gas film. A general planar structure can then be constructed by stacking these elements side by side. The thin gas layer is special; it is used to find the interaction on an atom at a general position in the planar structure. Then we go through some common structures and present illustrating examples; the examples involve gold half spaces, gold slabs, graphene, 2D metal films and lithium atoms. Then we discuss alternative ways to find the normal modes in a planar structure. Next we rederive the Casimir interaction between two atoms from using the summation over pair interactions. We end with a section on spatial dispersion.

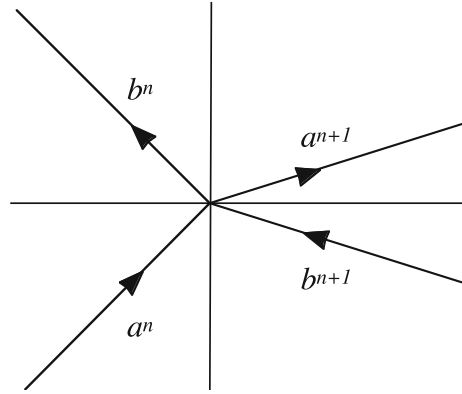
### 13.1 Adapting the General Method of Chap. 7 to Planar Structures

In the planar geometry nothing is gained by introducing the two Hertz-Debye potentials,  $\pi_1$  and  $\pi_2$ . Instead, we study the fields themselves. The solution to the vector Helmholtz equation is a field with the spatial variation  $\exp(\mathbf{i}\mathbf{k} \cdot \mathbf{r}) \exp(\pm\gamma_i kz)$ , where  $\mathbf{k}$  is a two dimensional wave vector in the plane of the interfaces,  $\mathbf{r}$  is the two dimensional component of the position vector in the  $xy$ -plane and

$$\begin{aligned}\gamma_i &= \sqrt{1 - (\tilde{n}_i \omega / ck)^2}; \\ \gamma^{(0)} &= \sqrt{1 - (\omega / ck)^2}.\end{aligned}\tag{13.1}$$

We will make use of the Fresnel coefficients (2.87). The amplitude transmission and reflection coefficients for waves impinging on an interface between medium  $i$  and  $j$  from the  $i$ -side are

**Fig. 13.1** The amplitudes of the waves at the interface number  $n$ . Adapted from [1]



$$\begin{aligned}
 t_{i,j}^s &= \frac{2\tilde{\mu}_j n_i \cos \theta_i}{\tilde{\mu}_j n_i \cos \theta_i + \tilde{\mu}_i n_j \cos \theta_j} = \frac{2\tilde{\mu}_j \gamma_i}{\tilde{\mu}_j \gamma_i + \tilde{\mu}_i \gamma_j}; \\
 r_{i,j}^s &= \frac{\tilde{\mu}_j n_i \cos \theta_i - \tilde{\mu}_i n_j \cos \theta_j}{\tilde{\mu}_j n_i \cos \theta_i + \tilde{\mu}_i n_j \cos \theta_j} = \frac{\tilde{\mu}_j \gamma_i - \tilde{\mu}_i \gamma_j}{\tilde{\mu}_j \gamma_i + \tilde{\mu}_i \gamma_j}; \\
 t_{i,j}^p &= \frac{2n_i \cos \theta_i}{n_j \cos \theta_i + n_i \cos \theta_j} = \frac{2\sqrt{\tilde{\epsilon}_i \tilde{\epsilon}_j} \sqrt{\tilde{\mu}_j / \tilde{\mu}_i} \gamma_i}{\tilde{\epsilon}_j \gamma_i + \tilde{\epsilon}_i \gamma_j}; \\
 r_{i,j}^p &= \frac{n_j \cos \theta_i - n_i \cos \theta_j}{n_j \cos \theta_i + n_i \cos \theta_j} = \frac{\tilde{\epsilon}_j \gamma_i - \tilde{\epsilon}_i \gamma_j}{\tilde{\epsilon}_j \gamma_i + \tilde{\epsilon}_i \gamma_j},
 \end{aligned} \tag{13.2}$$

where  $s$  and  $p$  stands for  $s$ - and  $p$ -polarization, respectively or TE and TM, respectively. Now the wave in Fig. 13.1 with amplitude  $a^{n+1}$  gets contribution from a transmitted part of the wave with amplitude  $a^n$  and a reflected part from the wave with amplitude  $b^{n+1}$ . Similarly the wave with amplitude  $b^n$  gets contribution from a transmitted part of the wave with amplitude  $b^{n+1}$  and a reflected part of the wave with amplitude  $a^n$ . The Fresnel coefficients are valid in our formalism if the interface is at  $z = 0$ . Then we have

$$\begin{aligned}
 a^{n+1} &= a^n t_{n,n+1} + b^{n+1} r_{n+1,n}, \\
 b^n &= a^n r_{n,n+1} + b^{n+1} t_{n+1,n},
 \end{aligned} \tag{13.3}$$

and after rearrangement and making use of the general relations  $t_{n,n+1} t_{n+1,n} - r_{n,n+1} r_{n+1,n} = 1$  and  $r_{n,n+1} = -r_{n+1,n}$  we find

$$\begin{pmatrix} a^n \\ b^n \end{pmatrix} = \frac{1}{t_{n,n+1}} \begin{pmatrix} 1 & r_{n,n+1} \\ r_{n,n+1} & 1 \end{pmatrix} \cdot \begin{pmatrix} a^{n+1} \\ b^{n+1} \end{pmatrix}. \tag{13.4}$$

Now, with the position of the interface at  $z = z_n$  we have

$$\begin{pmatrix} a^n e^{-\gamma_n k z_n} \\ b^n e^{\gamma_n k z_n} \end{pmatrix} = \frac{1}{t_{n,n+1}} \begin{pmatrix} 1 & r_{n,n+1} \\ r_{n,n+1} & 1 \end{pmatrix} \cdot \begin{pmatrix} a^{n+1} e^{-\gamma_{n+1} k z_n} \\ b^{n+1} e^{\gamma_{n+1} k z_n} \end{pmatrix}, \tag{13.5}$$

or

$$\begin{pmatrix} a^n \\ b^n \end{pmatrix} = \tilde{\mathbf{M}}_n \begin{pmatrix} a^{n+1} \\ b^{n+1} \end{pmatrix}, \tag{13.6}$$

where

$$\tilde{\mathbf{M}}_n = \frac{1}{t_{n,n+1}} \begin{pmatrix} e^{-(\gamma_{n+1}-\gamma_n)kz_n} & e^{(\gamma_{n+1}+\gamma_n)kz_n} r_{n,n+1} \\ e^{-(\gamma_{n+1}+\gamma_n)kz_n} r_{n,n+1} & e^{(\gamma_{n+1}-\gamma_n)kz_n} \end{pmatrix}. \quad (13.7)$$

Now we have all we need to determine the fully retarded normal modes in a layered planar structure. We give some examples in the following sections.

### Summary of key relations for the derivation of the dispersion interactions in planar structures:

In a planar structure the 2D wave vector  $\mathbf{k}$  and the two polarization types,  $s$  and  $p$ , are the proper quantum numbers that characterize a normal mode; the  $s$ -polarized mode is called a TE mode and the  $p$ -polarized is called a TM mode. The dispersion curve for a mode can have several branches,  $i$ ,  $\omega = \omega_{\mathbf{k}}^i$ . They are solutions to the condition for modes,  $f_{\mathbf{k}}(\omega) = 0$ , where  $f_{\mathbf{k}}(\omega)$  is the mode condition function. When finding the interaction energy of the system one has to sum over both  $\mathbf{k}$ , the mode type, and  $i$ . Since we often let the layers have unlimited extension in the layer plane it is appropriate to calculate the interaction energy per unit area. For zero temperature it is

$$\begin{aligned} E &= \frac{\hbar}{2} \frac{1}{A} \sum_{\mathbf{k}} \int_{-\infty}^{\infty} \frac{d\xi}{2\pi} [\ln f_{\mathbf{k}}^{\text{TM}}(i\xi) + \ln f_{\mathbf{k}}^{\text{TE}}(i\xi)] \\ &\rightarrow \frac{\hbar}{2} \int \frac{d^2k}{(2\pi)^2} \int_{-\infty}^{\infty} \frac{d\xi}{2\pi} [\ln f_{\mathbf{k}}^{\text{TM}}(i\xi) + \ln f_{\mathbf{k}}^{\text{TE}}(i\xi)], \end{aligned} \quad (13.8)$$

and at finite temperature

$$\begin{aligned} \mathfrak{F} &= \frac{1}{A} \sum_{\mathbf{k}} \frac{1}{\beta} \sum_{n=0}^{\infty} ' [\ln f_{\mathbf{k}}^{\text{TM}}(i\xi_n) + \ln f_{\mathbf{k}}^{\text{TE}}(i\xi_n)] \\ &\rightarrow \frac{1}{\beta} \int \frac{d^2k}{(2\pi)^2} \sum_{n=0}^{\infty} ' [\ln f_{\mathbf{k}}^{\text{TM}}(i\xi_n) + \ln f_{\mathbf{k}}^{\text{TE}}(i\xi_n)], \end{aligned} \quad (13.9)$$

where  $A$  is the area of the system and  $\xi_n = 2\pi n/\hbar\beta$ . The arrows indicate what happens when we let  $A$  go toward infinity. In the planar case  $f_{\mathbf{k}} \equiv M_{11}$  where  $\tilde{\mathbf{M}}$  is the matrix for the whole structure. The matrix for interface  $n$  is given by

$$\tilde{\mathbf{M}}_n = \frac{1}{t_{n,n+1}} \begin{pmatrix} e^{-(\gamma_{n+1}-\gamma_n)kz_n} & e^{(\gamma_{n+1}+\gamma_n)kz_n} r_{n,n+1} \\ e^{-(\gamma_{n+1}+\gamma_n)kz_n} r_{n,n+1} & e^{(\gamma_{n+1}-\gamma_n)kz_n} \end{pmatrix}, \quad (13.10)$$

where the fresnel coefficients for TE modes ( $s$ -polarized) and TM modes ( $p$ -polarized) are

$$\begin{aligned}
t_{i,j}^s &= \frac{2\tilde{\mu}_j\gamma_i}{\tilde{\mu}_j\gamma_i + \tilde{\mu}_i\gamma_j}; \\
r_{i,j}^s &= \frac{\tilde{\mu}_j\gamma_i - \tilde{\mu}_i\gamma_j}{\tilde{\mu}_j\gamma_i + \tilde{\mu}_i\gamma_j}; \\
t_{i,j}^p &= \frac{2\sqrt{\tilde{\varepsilon}_i\tilde{\varepsilon}_j}\sqrt{\tilde{\mu}_j/\tilde{\mu}_i}\gamma_i}{\tilde{\varepsilon}_j\gamma_i + \tilde{\varepsilon}_i\gamma_j}; \\
r_{i,j}^p &= \frac{\tilde{\varepsilon}_j\gamma_i - \tilde{\varepsilon}_i\gamma_j}{\tilde{\varepsilon}_j\gamma_i + \tilde{\varepsilon}_i\gamma_j},
\end{aligned} \tag{13.11}$$

and

$$\gamma_i = \sqrt{1 - (\tilde{n}_i\omega/c\mathbf{k})^2}. \tag{13.12}$$

Often it is appropriate to give the energy relative a reference system. Then  $f_{\mathbf{k}}$  is replaced by  $\tilde{f}_{\mathbf{k}}$  in (13.8) and (13.9), where  $\tilde{f}_{\mathbf{k}} = f_{\mathbf{k}}/f_{\mathbf{k}}^{\text{ref}}$ .

## 13.2 Basic Structure Elements

A general planar structure can be generated by stacking a number of basic structure elements next to each other. The most basic element is a single planar interface. Sometimes it is convenient to use layers as elements. A special layer is a 2D planar film. Another is a thin diluted gas layer which we will use repeatedly in the derivation of the interaction between atoms and the planar structure. We now discuss these basic elements one by one. We start with the single planar interface.

### 13.2.1 Single Planar Interface

For a single interface at  $z = a$  between two media with dielectric functions  $\tilde{\varepsilon}_0$  and  $\tilde{\varepsilon}_1$ , as illustrated in Fig. 9.1, we have

$$\tilde{\mathbf{M}} = \tilde{\mathbf{M}}_0 = \frac{1}{t_{0,1}} \begin{pmatrix} e^{(\gamma_0 - \gamma_1)ka} & e^{(\gamma_0 + \gamma_1)ka} r_{0,1} \\ e^{-(\gamma_0 + \gamma_1)ka} r_{0,1} & e^{-(\gamma_0 - \gamma_1)ka} \end{pmatrix}. \tag{13.13}$$

For TE modes the condition for modes is

$$\tilde{\mu}_1(\omega)\gamma_0(k, \omega) + \tilde{\mu}_0(\omega)\gamma_1(k, \omega) = 0. \tag{13.14}$$

This equation has no solution in absence of magnetic effects so there are no TE modes at a single interface in that case. For the TM modes the condition for modes is

$$\tilde{\varepsilon}_1(\omega)\gamma_0(k, \omega) + \tilde{\varepsilon}_0(\omega)\gamma_1(k, \omega) = 0. \tag{13.15}$$

This equation has solutions, so there are TM modes at a single interface even in neglect of magnetic effects. Let us now continue with next basic element, the planar layer.

### 13.2.2 Planar Layer

For a slab (see Fig. 9.2) with interfaces at  $z = a$  and  $z = a + d$  made of a medium with dielectric function  $\tilde{\epsilon}_1$  and magnetic permeability  $\tilde{\mu}_1$  in an ambient medium with dielectric function  $\tilde{\epsilon}_0$  and magnetic permeability  $\tilde{\mu}_0$  we have

$$\begin{aligned} \tilde{\mathbf{M}} &= \tilde{\mathbf{M}}_0 \cdot \tilde{\mathbf{M}}_1 = \frac{1}{t_{0,1}} \begin{pmatrix} e^{(\gamma_0 - \gamma_1)ka} & e^{(\gamma_0 + \gamma_1)ka} r_{0,1} \\ e^{-(\gamma_0 + \gamma_1)ka} r_{0,1} & e^{-(\gamma_0 - \gamma_1)ka} \end{pmatrix} \\ &\times \frac{1}{t_{1,0}} \begin{pmatrix} e^{-(\gamma_0 - \gamma_1)k(a+d)} & e^{(\gamma_0 + \gamma_1)k(a+d)} r_{1,0} \\ e^{-(\gamma_0 + \gamma_1)k(a+d)} r_{1,0} & e^{(\gamma_0 - \gamma_1)k(a+d)} \end{pmatrix}, \end{aligned} \quad (13.16)$$

and the matrix elements are

$$\begin{aligned} M_{11} &= \frac{1}{t_{0,1}t_{1,0}} \left[ e^{-(\gamma_0 - \gamma_1)kd} + e^{-(\gamma_0 + \gamma_1)kd} r_{0,1} r_{1,0} \right]; \\ M_{12} &= \frac{e^{2\gamma_0 ka}}{t_{0,1}t_{1,0}} \left[ e^{(\gamma_0 + \gamma_1)kd} r_{1,0} + e^{(\gamma_0 - \gamma_1)kd} r_{0,1} \right]; \\ M_{21} &= \frac{e^{-2\gamma_0 ka}}{t_{0,1}t_{1,0}} \left[ e^{-(\gamma_0 - \gamma_1)kd} r_{0,1} + e^{-(\gamma_0 + \gamma_1)kd} r_{1,0} \right]; \\ M_{22} &= \frac{1}{t_{0,1}t_{1,0}} \left[ e^{(\gamma_0 + \gamma_1)kd} r_{0,1} r_{1,0} + e^{(\gamma_0 - \gamma_1)kd} \right]. \end{aligned} \quad (13.17)$$

For TE modes we have

$$(\tilde{\mu}_1 \gamma_0 + \tilde{\mu}_0 \gamma_1)^2 - e^{-2\gamma_1 kd} (\tilde{\mu}_1 \gamma_0 - \tilde{\mu}_0 \gamma_1)^2 = 0, \quad (13.18)$$

and the mode condition function is

$$\begin{aligned} f_{\mathbf{k}}^{\text{TE}}(\omega) &= \left[ \tilde{\mu}_1(\omega) \gamma_0(k, \omega) + \tilde{\mu}_0(\omega) \gamma_1(k, \omega) \right]^2 \\ &\quad - e^{-2\gamma_1(k, \omega)kd} \left[ \tilde{\mu}_0(\omega) \gamma_1(k, \omega) - \tilde{\mu}_1(\omega) \gamma_0(k, \omega) \right]^2. \end{aligned} \quad (13.19)$$

Note that we, as before, have identified the mode condition function as the numerator of the expression in the condition for modes.

For TM modes we have

$$(\tilde{\epsilon}_1 \gamma_0 + \tilde{\epsilon}_0 \gamma_1)^2 - e^{-2\gamma_1 kd} (\tilde{\epsilon}_1 \gamma_0 - \tilde{\epsilon}_0 \gamma_1)^2 = 0, \quad (13.20)$$

and the mode condition function is

$$\begin{aligned} f_{\mathbf{k}}^{\text{TM}}(\omega) &= \left[ \tilde{\epsilon}_1(\omega) \gamma_0(k, \omega) + \tilde{\epsilon}_0(\omega) \gamma_1(k, \omega) \right]^2 \\ &\quad - e^{-2\gamma_1(k, \omega)kd} \left[ \tilde{\epsilon}_0(\omega) \gamma_1(k, \omega) - \tilde{\epsilon}_1(\omega) \gamma_0(k, \omega) \right]^2. \end{aligned} \quad (13.21)$$

For a gap, of size  $d$ , filled with a medium with dielectric function  $\tilde{\epsilon}_0$  and magnetic permeability  $\tilde{\mu}_0$  between two half spaces of material with dielectric function  $\tilde{\epsilon}_1$  and magnetic permeability  $\tilde{\mu}_1$  we may reuse the above result with the interchange of the two dielectric functions. We note that in this case, when retardation is included, the result will change. It did not in the non-retarded treatment. We have

$$\begin{aligned} f_{\mathbf{k}}^{\text{TE}}(\omega) &= [\tilde{\mu}_1(\omega)\gamma_0(k, \omega) + \tilde{\mu}_0(\omega)\gamma_1(k, \omega)]^2 \\ &\quad - e^{-2\gamma_0(k, \omega)kd} [\tilde{\mu}_0(\omega)\gamma_1(k, \omega) - \tilde{\mu}_1(\omega)\gamma_0(k, \omega)]^2; \\ f_{\mathbf{k}}^{\text{TM}}(\omega) &= [\tilde{\epsilon}_1(\omega)\gamma_0(k, \omega) + \tilde{\epsilon}_0(\omega)\gamma_1(k, \omega)]^2 \\ &\quad - e^{-2\gamma_0(k, \omega)kd} [\tilde{\epsilon}_0(\omega)\gamma_1(k, \omega) - \tilde{\epsilon}_1(\omega)\gamma_0(k, \omega)]^2. \end{aligned} \quad (13.22)$$

If the half spaces are made up from two different materials with  $\tilde{\epsilon}_1, \tilde{\mu}_1$  and  $\tilde{\epsilon}_2, \tilde{\mu}_2$  we find

$$\begin{aligned} f_{\mathbf{k}}^{\text{TE}}(\omega) &= [\tilde{\mu}_1(\omega)\gamma_0(k, \omega) + \tilde{\mu}_0(\omega)\gamma_1(k, \omega)] \\ &\quad \times [\tilde{\mu}_2(\omega)\gamma_0(k, \omega) + \tilde{\mu}_0(\omega)\gamma_2(k, \omega)] \\ &\quad - e^{-2\gamma_0(k, \omega)kd} [\tilde{\mu}_0(\omega)\gamma_1(k, \omega) - \tilde{\mu}_1(\omega)\gamma_0(k, \omega)] \\ &\quad \times [\tilde{\mu}_0(\omega)\gamma_2(k, \omega) - \tilde{\mu}_2(\omega)\gamma_0(k, \omega)]; \\ f_{\mathbf{k}}^{\text{TM}}(\omega) &= [\tilde{\epsilon}_1(\omega)\gamma_0(k, \omega) + \tilde{\epsilon}_0(\omega)\gamma_1(k, \omega)] \\ &\quad \times [\tilde{\epsilon}_2(\omega)\gamma_0(k, \omega) + \tilde{\epsilon}_0(\omega)\gamma_2(k, \omega)] \\ &\quad - e^{-2\gamma_0(k, \omega)kd} [\tilde{\epsilon}_0(\omega)\gamma_1(k, \omega) - \tilde{\epsilon}_1(\omega)\gamma_0(k, \omega)] \\ &\quad \times [\tilde{\epsilon}_0(\omega)\gamma_2(k, \omega) - \tilde{\epsilon}_2(\omega)\gamma_0(k, \omega)]. \end{aligned} \quad (13.23)$$

When we want to calculate the Casimir energy between two half spaces we choose the reference system to be the system when the separation is infinite. Then the mode condition functions are

$$\begin{aligned} \tilde{f}_{\mathbf{k}}^{\text{TE}}(\omega) &= 1 - e^{-2\gamma_0 kd} \frac{[\tilde{\mu}_0\gamma_1 - \tilde{\mu}_1\gamma_0][\tilde{\mu}_0\gamma_2 - \tilde{\mu}_2\gamma_0]}{[\tilde{\mu}_1\gamma_0 + \tilde{\mu}_0\gamma_1][\tilde{\mu}_2\gamma_0 + \tilde{\mu}_0\gamma_2]} \\ &= 1 - e^{-2\gamma_0 kd} r_{1,2}^s r_{3,2}^s = 1 - e^{-2\gamma_0 kd} r_{2,1}^s r_{2,3}^s; \\ \tilde{f}_{\mathbf{k}}^{\text{TM}}(\omega) &= 1 - e^{-2\gamma_0 kd} \frac{[\tilde{\epsilon}_0\gamma_1 - \tilde{\epsilon}_1\gamma_0][\tilde{\epsilon}_0\gamma_2 - \tilde{\epsilon}_2\gamma_0]}{[\tilde{\epsilon}_1\gamma_0 + \tilde{\epsilon}_0\gamma_1][\tilde{\epsilon}_2\gamma_0 + \tilde{\epsilon}_0\gamma_2]} \\ &= 1 - e^{-2\gamma_0 kd} r_{1,2}^p r_{3,2}^p = 1 - e^{-2\gamma_0 kd} r_{2,1}^p r_{2,3}^p, \end{aligned} \quad (13.24)$$

where we have used the amplitude reflection coefficients from (13.2). We have suppressed the argument  $\omega$  from all functions. These results agree with the standard Lifshitz formulation [2–4].

Now, let the two half spaces be ideal metals. We let the dielectric functions of the half spaces go to infinity. The amplitude reflection coefficient for a vacuum ideal-metal interface is  $-1$  for  $s$ -polarized waves and  $+1$  for  $p$ -polarized waves, respectively. Then

$$\begin{aligned}
E &= \frac{\hbar}{2} \int \frac{d^2k}{(2\pi)^2} \int_{-\infty}^{\infty} \frac{d\xi}{2\pi} \left[ \ln \tilde{f}_{\mathbf{k}}^{\text{TM}}(i\xi) + \ln \tilde{f}_{\mathbf{k}}^{\text{TE}}(i\xi) \right] \\
&= \frac{\hbar}{2} \int \frac{d^2k}{(2\pi)^2} \int_{-\infty}^{\infty} \frac{d\xi}{2\pi} \left[ \ln(1 - e^{-2\gamma_0 kd}) + \ln(1 - e^{-2\gamma_0 kd}) \right] \\
&= \frac{\hbar}{2\pi^2} \int_0^{\infty} dk k \int_0^{\infty} d\xi \ln \left[ 1 - \exp\left(-2\sqrt{1 + (\xi/c k)^2} kd\right) \right] \\
&= \left| \begin{array}{l} \text{let } k \rightarrow k/2d \\ \text{let } \xi \rightarrow \xi/2d \end{array} \right| = \\
&= \frac{\hbar}{16\pi^2 d^3} \int_0^{\infty} dk k \int_0^{\infty} d\xi \ln \left[ 1 - \exp\left(-\sqrt{k^2 + (\xi/c)^2}\right) \right] \\
&= -\frac{\hbar c \pi^2}{720 d^3},
\end{aligned} \tag{13.25}$$

which is the Casimir classical result for the interaction energy between two ideal metal half spaces [5].

We now move on to next element, which is a 2D film.

### 13.2.3 2D Planar Film

In many situations one is dealing with very thin films. These may be considered 2D (two dimensional). Important examples are a graphene sheet and a 2D electron gas. In the derivation we let the film have finite thickness  $\delta$  and be characterized by a 3D dielectric function  $\varepsilon^{3D}$ . We then let the thickness go toward zero. The 3D dielectric function depends on  $\delta$  as  $\varepsilon^{3D} \sim 1/\delta$  for small  $\delta$  and  $\delta \varepsilon^{3D} \rightarrow 2\alpha^{2D}/k$  as  $\delta$  goes toward zero [6, 7]. We may now start from (13.16) use the proper reflection and transmission coefficients for the mode type under consideration and let  $\delta$  go toward zero.

For the TM modes we obtain

$$\begin{aligned}
\tilde{\mathbf{M}}_{2D}^{\text{TM}} &= \begin{pmatrix} 1 & 0 \\ 0 & 1 \end{pmatrix} + \frac{\gamma^{(0)} k (\delta \varepsilon^{3D})}{2} \begin{pmatrix} 1 & -e^{2\gamma^{(0)} kz} \\ e^{-2\gamma^{(0)} kz} & -1 \end{pmatrix} \\
&= \begin{pmatrix} 1 & 0 \\ 0 & 1 \end{pmatrix} + \tilde{\alpha}^{2D} \gamma^{(0)} \begin{pmatrix} 1 & -e^{2\gamma^{(0)} kz} \\ e^{-2\gamma^{(0)} kz} & -1 \end{pmatrix},
\end{aligned} \tag{13.26}$$

and for the TE modes we find

$$\begin{aligned}
\tilde{\mathbf{M}}_{2D}^{\text{TE}} &= \begin{pmatrix} 1 & 0 \\ 0 & 1 \end{pmatrix} - \frac{(\delta \varepsilon^{3D}) k (\omega/c k)^2}{2\gamma^{(0)}} \begin{pmatrix} 1 & e^{2\gamma^{(0)} kz} \\ -e^{-2\gamma^{(0)} kz} & -1 \end{pmatrix} \\
&= \begin{pmatrix} 1 & 0 \\ 0 & 1 \end{pmatrix} - \tilde{\alpha}^{2D} \frac{(\omega/c k)^2}{\gamma^{(0)}} \begin{pmatrix} 1 & e^{2\gamma^{(0)} kz} \\ -e^{-2\gamma^{(0)} kz} & -1 \end{pmatrix}.
\end{aligned} \tag{13.27}$$

We are now ready to move to our last basic structure element, the thin diluted gas film.

### 13.2.4 Thin Planar Diluted Gas Film

It is of interest to find the force on an atom in a layered structure. We can obtain this by studying the force on a thin layer of a diluted gas with dielectric function  $\varepsilon_g(\omega) = 1 + 4\pi n\alpha^{at}(\omega)$ , where  $\alpha^{at}$  is the polarizability of one atom and  $n$  the density of atoms (we have assumed that the atom is surrounded by vacuum; if not the 1 should be replaced by the dielectric function of the ambient medium and the atomic polarizability should be replaced by the excess polarizability). For a diluted gas layer the interaction amongst the gas atoms is negligible and the force on the layer is just the sum of the forces on the individual atoms. So by dividing with the number of atoms in the film we get the force on one atom. The layer has to be thin in order to have a well defined  $z$ -value of the atom. Since we will derive the force on an atom in different planar geometries it is fruitful to derive the matrix for a thin diluted gas. This result can be directly used in the derivation of the force on an atom in different planar geometries.

We let the film have the thickness  $\delta$  and be placed in the general position  $z$ . We only keep terms up to linear order in  $\delta$  and linear order in  $n$ . We find the result up to linear order in  $\delta$  is

$$\tilde{\mathbf{M}}_0 \cdot \tilde{\mathbf{M}}_1 = \begin{pmatrix} 1 & 0 \\ 0 & 1 \end{pmatrix} + \delta k \begin{pmatrix} -\gamma_0 + \gamma_1 \left[ \frac{1+(r_{0,1})^2}{t_{0,1}t_{1,0}} \right] & -\frac{2\gamma_1 r_{0,1}}{t_{0,1}t_{1,0}} e^{2\gamma_0 k z} \\ \frac{2\gamma_1 r_{0,1}}{t_{0,1}t_{1,0}} e^{-2\gamma_0 k z} & \gamma_0 - \gamma_1 \left[ \frac{1+(r_{0,1})^2}{t_{0,1}t_{1,0}} \right] \end{pmatrix}. \quad (13.28)$$

To go further and find the result to lowest order in  $n$  we have to specify the mode type.

For TM modes we get

$$\tilde{\mathbf{M}}_{\text{gaslayer}}^{\text{TM}} = \begin{pmatrix} 1 & 0 \\ 0 & 1 \end{pmatrix} + \frac{(\delta n)2\pi k\alpha^{at}}{\gamma^{(0)}} \begin{pmatrix} -\left(\frac{\omega}{ck}\right)^2 & -\left[2 - \left(\frac{\omega}{ck}\right)^2\right] e^{2\gamma^{(0)}kz} \\ \left[2 - \left(\frac{\omega}{ck}\right)^2\right] e^{-2\gamma^{(0)}kz} & \left(\frac{\omega}{ck}\right)^2 \end{pmatrix}, \quad (13.29)$$

and for TE modes

$$\tilde{\mathbf{M}}_{\text{gaslayer}}^{\text{TE}} = \begin{pmatrix} 1 & 0 \\ 0 & 1 \end{pmatrix} + \frac{(\delta n)2\pi k\alpha^{at}(\omega/ck)^2}{\gamma^{(0)}} \begin{pmatrix} -1 & -e^{2\gamma^{(0)}kz} \\ e^{-2\gamma^{(0)}kz} & 1 \end{pmatrix}. \quad (13.30)$$

Now we are done with the gas layer. We will use these results later in calculating the force on an atom in planar layered structures. We move on to some general structures and begin with two half spaces.

### 13.3 Two Half Spaces

The interaction between two half spaces with dielectric functions  $\tilde{\epsilon}_1$  and  $\tilde{\epsilon}_2$  is easily obtained from Sect. 13.2.2. The mode condition functions were given in (13.23) and with our choice of dielectric functions they are

$$\begin{aligned} f_{\mathbf{k}}^{\text{TE}}(\omega) &= [\gamma^{(0)}(\omega) + \gamma_1(\omega)] [\gamma^{(0)}(\omega) + \gamma_2(\omega)] \\ &\quad - e^{-2\gamma^{(0)}(\omega)kd} [\gamma_1(\omega) - \gamma^{(0)}(\omega)] [\gamma_2(\omega) - \gamma^{(0)}(\omega)]; \\ f_{\mathbf{k}}^{\text{TM}}(\omega) &= [\tilde{\epsilon}_1(\omega) \gamma^{(0)}(\omega) + \gamma_1(\omega)] [\tilde{\epsilon}_2(\omega) \gamma^{(0)}(\omega) + \gamma_2(\omega)] \\ &\quad - e^{-2\gamma^{(0)}(\omega)kd} [\gamma_1(\omega) - \tilde{\epsilon}_1(\omega) \gamma^{(0)}(\omega)] [\gamma_2(\omega) - \tilde{\epsilon}_2(\omega) \gamma^{(0)}(\omega)], \end{aligned} \quad (13.31)$$

where we have assumed that vacuum occupies the gap between the half spaces. Choosing the reference system to be the system when the half spaces have been brought to infinite separation we find

$$\begin{aligned} \tilde{f}_{\mathbf{k}}^{\text{TE}}(\omega) &= 1 - e^{-2\gamma^{(0)}(\omega)kd} \frac{[\gamma_1(\omega) - \gamma^{(0)}(\omega)] [\gamma_2(\omega) - \gamma^{(0)}(\omega)]}{[\gamma^{(0)}(\omega) + \gamma_1(\omega)] [\gamma^{(0)}(\omega) + \gamma_2(\omega)]}, \\ \tilde{f}_{\mathbf{k}}^{\text{TM}}(\omega) &= 1 - e^{-2\gamma^{(0)}(\omega)kd} \frac{[\gamma_1(\omega) - \tilde{\epsilon}_1(\omega) \gamma^{(0)}(\omega)] [\gamma_2(\omega) - \tilde{\epsilon}_2(\omega) \gamma^{(0)}(\omega)]}{[\tilde{\epsilon}_1(\omega) \gamma^{(0)}(\omega) + \gamma_1(\omega)] [\tilde{\epsilon}_2(\omega) \gamma^{(0)}(\omega) + \gamma_2(\omega)]}. \end{aligned} \quad (13.32)$$

We now apply these results to two gold half spaces.

#### 13.3.1 Interaction Between Two Gold Half Spaces

The interaction energy per unit area between two gold half spaces is obtained as (13.8)

$$E = \frac{\hbar}{2} \int \frac{d^2k}{(2\pi)^2} \int_{-\infty}^{\infty} \frac{d\xi}{2\pi} [\ln f_{\mathbf{k}}^{\text{TM}}(i\xi) + \ln f_{\mathbf{k}}^{\text{TE}}(i\xi)], \quad (13.33)$$

with the mode condition functions,

$$\begin{aligned} \tilde{f}_{\mathbf{k}}^{\text{TE}}(i\xi) &= 1 - e^{-2\gamma^{(0)}(i\xi)kd} \frac{[\gamma_{Au}(i\xi) - \gamma^{(0)}(i\xi)]^2}{[\gamma_{Au}(i\xi) + \gamma^{(0)}(i\xi)]^2}; \\ \tilde{f}_{\mathbf{k}}^{\text{TM}}(i\xi) &= 1 - e^{-2\gamma^{(0)}(i\xi)kd} \frac{[\gamma_{Au}(i\xi) - \tilde{\epsilon}_{Au}(i\xi) \gamma^{(0)}(i\xi)]^2}{[\gamma_{Au}(i\xi) + \tilde{\epsilon}_{Au}(i\xi) \gamma^{(0)}(i\xi)]^2}, \end{aligned} \quad (13.34)$$

inserted. For finite temperature the corresponding results are (13.9)

$$\mathfrak{F} = \frac{1}{\beta} \int \frac{d^2k}{(2\pi)^2} \sum_{n=0}^{\infty} ' [\ln f_{\mathbf{k}}^{\text{TM}}(i\xi_n) + \ln f_{\mathbf{k}}^{\text{TE}}(i\xi_n)]. \quad (13.35)$$

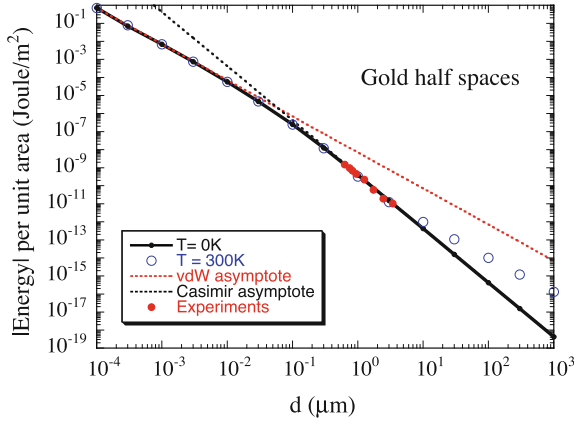


**Fig. 13.2** The dispersion energy between two gold half spaces as function of separation  $d$ ; both the zero temperature, *thick solid curve with filled circles*, and room temperature, *open circles*, results are given; the experimental results by Lamoreaux, *filled circles*, van der Waals asymptote, *dotted line with smallest slope*, and Casimir asymptote, *dotted line with steepest slope*, are also shown

The results are shown in Fig. 13.2 both for zero temperature and room temperature. We see that the thermal effects appear at separations of the order of  $1 \mu\text{m}$  and larger. The experimental points by Lamoreaux [8], cluster of filled circles, are clearly in the Casimir range, i.e. to the right of the bend in the curve. The results were obtained from using (13.34) and (13.35) with the gold polarizability  $\alpha(i\xi)$  as shown in Fig. 9.3.

A half space is an idealization of a very thick plate. Next we will see how the results are modified for plates of finite thickness.

### 13.4 Two Slabs

We will make this as simple as possible and let the slabs be of the same material having dielectric function  $\tilde{\epsilon}_1$ , be of the same thickness,  $\Delta$ , and be placed in vacuum. The slabs are separated by the closest distance  $d$ . We let the interfaces of the first slab be at  $z = 0$  and  $z = \Delta$ ; then the interfaces of the second are at  $z = d + \Delta$  and at  $z = d + 2\Delta$ . We may write the matrix of the whole structure as the products of the matrices of two planar layers,

$$\tilde{\mathbf{M}} = \tilde{\mathbf{M}}_A \cdot \tilde{\mathbf{M}}_B. \quad (13.36)$$

We do not need all eight elements of the matrices, only four, since we have

$$M_{11} = M_{11}^A M_{11}^B + M_{12}^A M_{21}^B. \quad (13.37)$$

From (13.17) we find

$$\begin{aligned}
 M_{11}^A &= \frac{1}{t_{0,1}t_{1,0}} \left[ e^{-(\gamma^{(0)}-\gamma_1)k\Delta} + e^{-(\gamma^{(0)}+\gamma_1)k\Delta} r_{0,1} r_{1,0} \right]; \\
 M_{11}^B &= \frac{1}{t_{0,1}t_{1,0}} \left[ e^{-(\gamma^{(0)}-\gamma_1)k\Delta} + e^{-(\gamma^{(0)}+\gamma_1)k\Delta} r_{0,1} r_{1,0} \right]; \\
 M_{12}^A &= \frac{1}{t_{0,1}t_{1,0}} \left[ e^{(\gamma^{(0)}+\gamma_1)k\Delta} r_{1,0} + e^{(\gamma^{(0)}-\gamma_1)k\Delta} r_{0,1} \right]; \\
 M_{21}^B &= \frac{e^{-2\gamma^{(0)}k(\Delta+d)}}{t_{0,1}t_{1,0}} \left[ e^{-(\gamma^{(0)}-\gamma_1)k\Delta} r_{0,1} + e^{-(\gamma^{(0)}+\gamma_1)k\Delta} r_{1,0} \right],
 \end{aligned} \tag{13.38}$$

and

$$\begin{aligned}
 M_{11} &= \frac{1}{(t_{0,1}t_{1,0})^4} e^{(\gamma_1-\gamma^{(0)})2k\Delta} \\
 &\times \left\{ \left[ 1 - (r_{0,1})^2 e^{-2\gamma_1 k\Delta} \right]^2 - e^{-2\gamma^{(0)}kd} (r_{0,1})^2 \left[ 1 - e^{-2\gamma_1 k\Delta} \right]^2 \right\},
 \end{aligned} \tag{13.39}$$

and

$$\tilde{f}_{\mathbf{k}} = 1 - e^{-2\gamma^{(0)}kd} \frac{(r_{0,1})^2 \left[ 1 - e^{-2\gamma_1 k\Delta} \right]^2}{\left[ 1 - (r_{0,1})^2 e^{-2\gamma_1 k\Delta} \right]^2}. \tag{13.40}$$

Inserting the expressions for the amplitude reflection coefficients we find

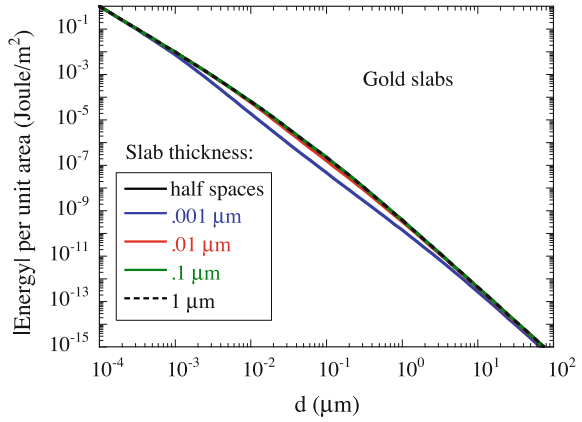
$$\begin{aligned}
 \tilde{f}_{\mathbf{k}}^{\text{TM}} &= 1 - e^{-2\gamma^{(0)}kd} \frac{\left( \frac{\tilde{\epsilon}_1 \gamma^{(0)} - \gamma_1}{\tilde{\epsilon}_1 \gamma^{(0)} + \gamma_1} \right)^2 \left[ 1 - e^{-2\gamma_1 k\Delta} \right]^2}{\left[ 1 - \frac{\left( \frac{\tilde{\epsilon}_1 \gamma^{(0)} - \gamma_1}{\tilde{\epsilon}_1 \gamma^{(0)} + \gamma_1} \right)^2 e^{-2\gamma_1 k\Delta}}{\left( \frac{\tilde{\epsilon}_1 \gamma^{(0)} + \gamma_1}{\tilde{\epsilon}_1 \gamma^{(0)} - \gamma_1} \right)^2} \right]^2}; \\
 \tilde{f}_{\mathbf{k}}^{\text{TE}} &= 1 - e^{-2\gamma^{(0)}kd} \frac{\left( \frac{\gamma^{(0)} - \gamma_1}{\gamma^{(0)} + \gamma_1} \right)^2 \left[ 1 - e^{-2\gamma_1 k\Delta} \right]^2}{\left[ 1 - \frac{\left( \frac{\gamma^{(0)} - \gamma_1}{\gamma^{(0)} + \gamma_1} \right)^2 e^{-2\gamma_1 k\Delta}}{\left( \frac{\gamma^{(0)} + \gamma_1}{\gamma^{(0)} - \gamma_1} \right)^2} \right]^2}.
 \end{aligned} \tag{13.41}$$

Next we apply these results to two gold plates.

### 13.4.1 Interaction Between Two Gold Slabs

The result for two gold slabs is shown in Fig. 13.3. To find this result we have inserted the mode condition functions from (13.41) in (13.8). The dielectric function  $\tilde{\epsilon}_1(i\xi) = 1 + \alpha(i\xi)$  with the gold polarizability  $\alpha(i\xi)$  as shown in Fig. 9.3. We find that in comparison with Fig. 9.6 the curves for the slabs of finite thickness have more difficulties in separating from the result for two half spaces. This is because retardation makes all curves bend down for large separations and merge with the classical Casimir result (13.25) for two ideal metal half spaces. Next we address two parallel 2D films.

**Fig. 13.3** The retarded interaction energy between two gold slabs of thickness  $\Delta$  as function of separation  $d$ . The result is obtained from using (13.33) with the mode condition functions from (13.41) and the gold polarizability  $\alpha(i\xi)$  as shown in Fig. 9.3



### 13.5 Two 2D Films

In this section we derive the Casimir interaction between two thin films. We proceed along the lines of the preceding section. We start from the three layer structure in Fig. 9.14. We take the limit when the thickness of the film goes to zero. The matrix becomes  $\tilde{\mathbf{M}} = \tilde{\mathbf{M}}_0 \cdot \tilde{\mathbf{M}}_1 \cdot \tilde{\mathbf{M}}_2 \cdot \tilde{\mathbf{M}}_3$ , where  $\tilde{\mathbf{M}}_0 \cdot \tilde{\mathbf{M}}_1$  is the matrix for one of the thin films, and  $\tilde{\mathbf{M}}_2 \cdot \tilde{\mathbf{M}}_3$  is the matrix for the other.

We start with the TM modes. The matrices from (13.26), one for  $z = 0$  and one for  $z = d$ , are

$$\begin{aligned} \tilde{\mathbf{M}}_0^{\text{TM}} \cdot \tilde{\mathbf{M}}_1^{\text{TM}} &= \begin{pmatrix} 1 & 0 \\ 0 & 1 \end{pmatrix} + \alpha^{2D} \gamma^{(0)} \begin{pmatrix} 1 & -1 \\ 1 & -1 \end{pmatrix}, \\ \tilde{\mathbf{M}}_2^{\text{TM}} \cdot \tilde{\mathbf{M}}_3^{\text{TM}} &= \begin{pmatrix} 1 & 0 \\ 0 & 1 \end{pmatrix} + \alpha^{2D} \gamma^{(0)} \begin{pmatrix} 1 & -e^{2\gamma^{(0)}kd} \\ e^{-2\gamma^{(0)}kd} & -1 \end{pmatrix}. \end{aligned} \quad (13.42)$$

The matrix element of interest to us is

$$M_{11} = (1 + \alpha^{2D} \gamma^{(0)})^2 - (\alpha^{2D} \gamma^{(0)})^2 e^{-2\gamma^{(0)}kd}, \quad (13.43)$$

and the mode condition function for TM modes is

$$\tilde{f}^{\text{TM}} = 1 - e^{-2\gamma^{(0)}d} \frac{(\alpha^{2D} \gamma^{(0)})^2}{(1 + \alpha^{2D} \gamma^{(0)})^2}. \quad (13.44)$$

Now, we continue with the TE modes. The matrices from (13.27), one for  $z = 0$  and one for  $z = d$ , are

$$\begin{aligned}\tilde{\mathbf{M}}_0^{\text{TE}} \cdot \tilde{\mathbf{M}}_1^{\text{TE}} &= \begin{pmatrix} 1 & 0 \\ 0 & 1 \end{pmatrix} - \alpha^{2D} \frac{(\omega/c k)^2}{\gamma^{(0)}} \begin{pmatrix} 1 & 1 \\ -1 & -1 \end{pmatrix}, \\ \tilde{\mathbf{M}}_2^{\text{TE}} \cdot \tilde{\mathbf{M}}_3^{\text{TE}} &= \begin{pmatrix} 1 & 0 \\ 0 & 1 \end{pmatrix} - \alpha^{2D} \frac{(\omega/c k)^2}{\gamma^{(0)}} \begin{pmatrix} 1 & e^{2\gamma^{(0)} k d} \\ -e^{-2\gamma^{(0)} k d} & -1 \end{pmatrix}.\end{aligned}\quad (13.45)$$

The matrix element of interest to us is

$$M_{11} = \left(1 - \alpha^{2D} \frac{(\omega/c k)^2}{\gamma^{(0)}}\right)^2 - \left(\alpha^{2D} \frac{(\omega/c k)^2}{\gamma^{(0)}}\right)^2 e^{-2\gamma^{(0)} k d}, \quad (13.46)$$

and the mode condition function for TE modes is

$$\tilde{f}^{\text{TE}} = 1 - e^{-2\gamma^{(0)} k d} \frac{\left(\alpha^{2D} \frac{(\omega/c k)^2}{\gamma^{(0)}}\right)^2}{\left(1 - \alpha^{2D} \frac{(\omega/c k)^2}{\gamma^{(0)}}\right)^2}. \quad (13.47)$$

From this we find the energy per unit area. It is

$$\begin{aligned}E &= \frac{\hbar}{2} \int \frac{d^2 k}{(2\pi)^2} \int_{-\infty}^{\infty} \frac{d\xi}{2\pi} \left\{ \ln \left[ \tilde{f}_{\mathbf{k}}^{\text{TM}}(i\xi) \right] + \ln \left[ \tilde{f}_{\mathbf{k}}^{\text{TE}}(i\xi) \right] \right\} \\ &= \frac{\hbar}{2} \int \frac{d^2 k}{(2\pi)^2} \int_{-\infty}^{\infty} \frac{d\xi}{2\pi} \ln \left[ 1 - e^{-2\gamma^{(0)}(i\xi) k d} \left( \frac{\tilde{\alpha}^{2D}(k, i\xi) \gamma^{(0)}(k, i\xi)}{1 + \tilde{\alpha}^{2D}(k, i\xi) \gamma^{(0)}(k, i\xi)} \right)^2 \right] \\ &+ \frac{\hbar}{2} \int \frac{d^2 k}{(2\pi)^2} \int_{-\infty}^{\infty} \frac{d\xi}{2\pi} \ln \left[ 1 - e^{-2\gamma^{(0)}(i\xi) k d} \left( \frac{-\tilde{\alpha}^{2D}(k, i\xi) (\xi/c k)^2}{\gamma^{(0)}(k, i\xi) + \tilde{\alpha}^{2D}(k, i\xi) (\xi/c k)^2} \right)^2 \right].\end{aligned}\quad (13.48)$$

This agrees completely with the results of [9, 10]. Now let us illustrate the results with two numerical examples. We start with two graphene sheets.

### 13.5.1 Interaction Between Two Graphene Sheets

The first example where we use the results for two 2D films is two graphene sheets. The results are shown Figs. 13.4 and 13.5. Figure 13.4 is for pristine graphene where (a) is for zero temperature and (b) for room temperature. We see that the TE modes give very small contributions and at room temperature these contributions is further reduced in the distance range where the temperature effects are important. Comparison between Figs. 13.4a and 9.7 shows that the retardation effects are negligible for pristine graphene. This anomalous behavior can be explained in the following way. The retardation effects can be regarded as the results from that the curves are forced to stay below the curve for two ideal metal half spaces. In a normal system the non-retarded asymptotic power law for large separations has a smaller negative exponent than that for the metal case. This means that the two curves will sooner or

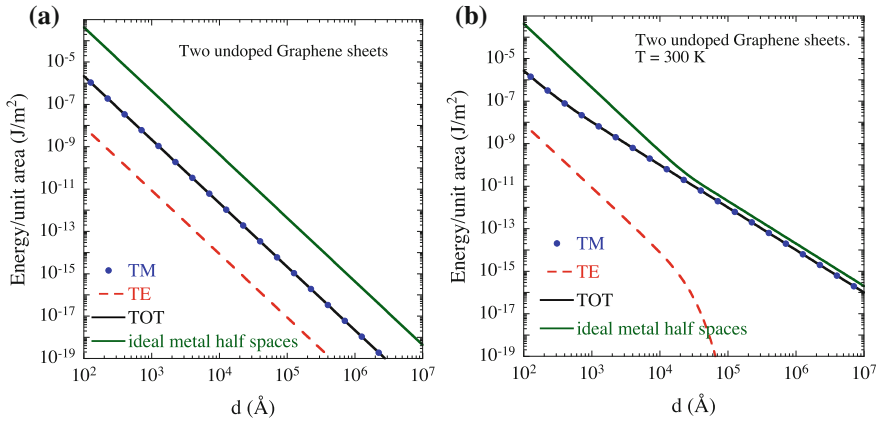


**Fig. 13.4** Interaction energy per unit area between two pristine (undoped) graphene sheets a distance  $d$  apart. The contribution from TE modes, *dashed curve*, TM modes, *filled circles*, and the total result, *solid curve*, are given. For comparison the result for two ideal metal half spaces, *upper solid curve*, is also given. **a** Undoped graphene sheets at zero temperature; **b** Undoped graphene sheets at room temperature. Adapted from [10]

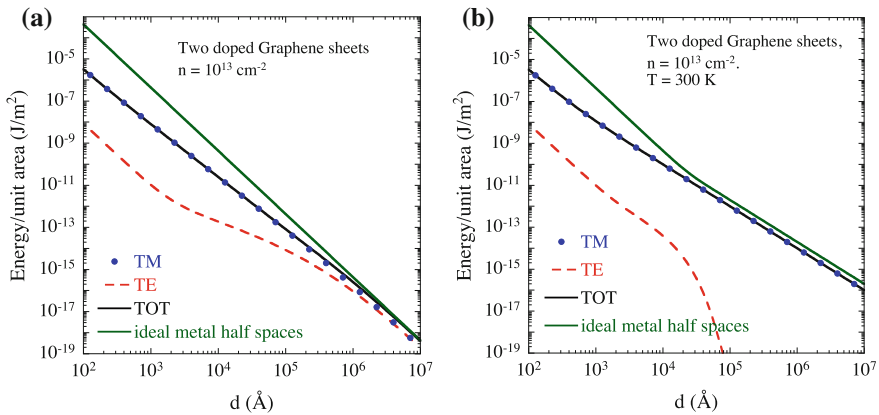


**Fig. 13.5** Interaction energy per unit area between two doped graphene sheets a distance  $d$  apart. The contribution from TE modes, *dashed curve*, TM modes, *filled circles*, and the total result, *solid curve*, are given. For comparison the result for two ideal metal half spaces, *upper solid curve*, is also given. **a** Doped graphene sheets with doping concentration  $n = 10^{13}$  cm<sup>-2</sup> in each sheet at zero temperature; **b** doped graphene sheets with doping concentration  $n = 10^{13}$  cm<sup>-2</sup> in each sheet at room temperature. Adapted from [10]

later cross. In the graphene case the power law is the same as that for the ideal metal case and the curves will never cross.

The situation is somewhat different in the doped case. Figure 13.5 is for doped graphene with doping concentration  $n = 10^{13}$  cm<sup>-2</sup> in each sheet where (a) is for zero temperature and (b) for room temperature. At zero temperature we find that

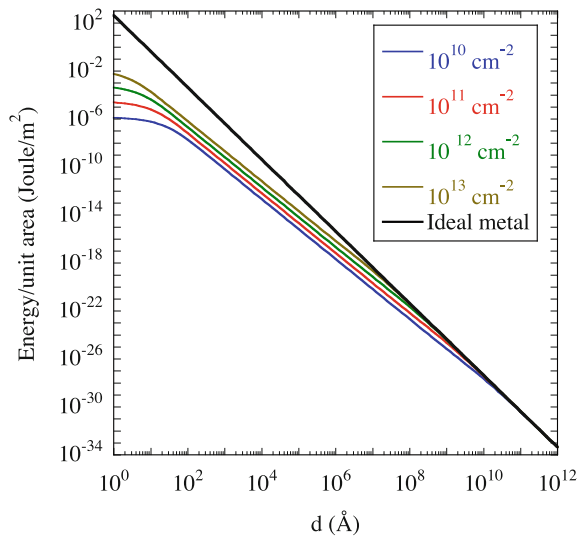
when the doping begins to show effects the TE modes start increase in importance and eventually give the same contribution as the TM modes. We also see that there are retardation effects for large separations. Figure 9.7 shows that for large separation the curves for doped graphene has a non-retarded asymptotic power law with a smaller negative exponent than that for the ideal metal case. This means that the curves would cross at some point and doped graphene has a more normal behavior. At room temperature, Fig. 13.5b, the TE modes again become negligible in the range where the temperature effects are important and the doping has also a very small effect on the results (compare Figs. 13.4b and 13.5b). Next we turn to our second example, two parallel 2D metal films.

### 13.5.2 Interaction Between Two 2D Metal Films

In calculating the interaction between two 2D metal films we use (13.48) with the polarizability for a 2D electron gas in (2.146). The results are shown in Fig. 13.6. There are three characteristic separation regions; for very large separations all curves follow the Casimir result; in the intermediate region the curves separate but follow a common fractional power law; for small separations spatial dispersion effects emerge and the curves flattens out with smaller slopes. The energy approaches asymptotically a fractional power law with  $E \sim d^{-5/2}$ . For very large separations all curves follow asymptotically the classical Casimir result (13.25) for two ideal metal half spaces with the power law  $E \sim d^{-3}$ .

Next we study the interaction between a thin film and a half space or wall.

**Fig. 13.6** Interaction energy per unit area between two 2D metal films a distance  $d$  apart. The curves are for different carrier concentrations; the results are, counted from below, for the carrier densities  $10^{10}$ ,  $10^{11}$ ,  $10^{12}$ , and  $10^{13} \text{ cm}^{-2}$ , respectively. The *thick straight line* is the classical Casimir result (13.25) for two ideal metal half spaces



### 13.6 Film-Wall

We start from the two layer structure in Fig. 9.11. We let the ambient be vacuum. The first layer is the 2D film treated in Sect. 13.2.3. We place it at  $z = 0$ . The second layer is a vacuum layer of thickness  $d$ . The remaining medium is the wall which we let be infinitely thick and have the dielectric function  $\tilde{\epsilon}_s(\omega)$ . The matrix becomes  $\tilde{\mathbf{M}} = \tilde{\mathbf{M}}_0 \cdot \tilde{\mathbf{M}}_1 \cdot \tilde{\mathbf{M}}_2 = \tilde{\mathbf{M}}_{2D} \cdot \tilde{\mathbf{M}}_2$  where we already know the first matrix. It is (13.26) and (13.27) for TM modes and TE modes, respectively with  $z = 0$ . Now, for the TM modes we obtain

$$\begin{aligned} \tilde{\mathbf{M}}_{2D}^{\text{TM}} &= \begin{pmatrix} 1 & 0 \\ 0 & 1 \end{pmatrix} + \tilde{\alpha}^{2D} \gamma^{(0)} \begin{pmatrix} 1 & -1 \\ 1 & -1 \end{pmatrix} \\ &= (1 + \tilde{\alpha}^{2D} \gamma^{(0)}) \begin{pmatrix} 1 & \frac{-\tilde{\alpha}^{2D} \gamma^{(0)}}{1 + \tilde{\alpha}^{2D} \gamma^{(0)}} \\ \frac{\tilde{\alpha}^{2D} \gamma^{(0)}}{1 + \tilde{\alpha}^{2D} \gamma^{(0)}} & \frac{1 - \tilde{\alpha}^{2D} \gamma^{(0)}}{1 + \tilde{\alpha}^{2D} \gamma^{(0)}} \end{pmatrix}, \end{aligned} \quad (13.49)$$

and for the TE modes we find

$$\begin{aligned} \tilde{\mathbf{M}}_{2D}^{\text{TE}} &= \begin{pmatrix} 1 & 0 \\ 0 & 1 \end{pmatrix} - \tilde{\alpha}^{2D} \frac{(\omega/ck)^2}{\gamma^{(0)}} \begin{pmatrix} 1 & 1 \\ -1 & -1 \end{pmatrix} \\ &= (1 - \tilde{\alpha}^{2D} (\omega/ck)^2 / \gamma^{(0)}) \begin{pmatrix} 1 & \frac{-\tilde{\alpha}^{2D} (\omega/ck)^2}{\gamma^{(0)} - \tilde{\alpha}^{2D} (\omega/ck)^2} \\ \frac{\tilde{\alpha}^{2D} (\omega/ck)^2}{\gamma^{(0)} - \tilde{\alpha}^{2D} (\omega/ck)^2} & \frac{\gamma^{(0)} - \tilde{\alpha}^{2D} (\omega/ck)^2}{\gamma^{(0)} + \tilde{\alpha}^{2D} (\omega/ck)^2} \end{pmatrix}. \end{aligned} \quad (13.50)$$

The matrix  $\tilde{\mathbf{M}}_2$  we obtain from (13.13) and with the proper parameters we have

$$\begin{aligned} \tilde{\mathbf{M}}_2 &= \frac{1}{t_{2,3}} \begin{pmatrix} e^{-(\gamma_3 - \gamma_2)kd} & e^{(\gamma_3 + \gamma_2)kd} r_{2,3} \\ e^{-(\gamma_3 + \gamma_2)kd} r_{2,3} & e^{(\gamma_3 - \gamma_2)kd} \end{pmatrix} \\ &= \frac{1}{t_{2,3}} \begin{pmatrix} e^{-(\gamma_s - \gamma^{(0)})kd} & e^{(\gamma_s + \gamma^{(0)})kd} r_{2,3} \\ e^{-(\gamma_s + \gamma^{(0)})kd} r_{2,3} & e^{(\gamma_s - \gamma^{(0)})kd} \end{pmatrix} \\ &= \frac{e^{-(\gamma_s - \gamma^{(0)})kd}}{t_{2,3}} \begin{pmatrix} 1 & e^{2\gamma_s kd} r_{2,3} \\ e^{-2\gamma^{(0)} kd} r_{2,3} & e^{2(\gamma_s - \gamma^{(0)})kd} \end{pmatrix}. \end{aligned} \quad (13.51)$$

For TM modes it becomes

$$\tilde{\mathbf{M}}_2^{\text{TM}} = \frac{\tilde{\epsilon}_s \gamma^{(0)} + \gamma_s}{2\sqrt{\tilde{n}_s} \gamma^{(0)}} e^{-(\gamma_s - \gamma^{(0)})kd} \begin{pmatrix} 1 & e^{2\gamma_s kd} \frac{\tilde{\epsilon}_s \gamma^{(0)} - \gamma_s}{\tilde{\epsilon}_s \gamma^{(0)} + \gamma_s} \\ e^{-2\gamma^{(0)} kd} \frac{\tilde{\epsilon}_s \gamma^{(0)} - \gamma_s}{\tilde{\epsilon}_s \gamma^{(0)} + \gamma_s} & e^{2(\gamma_s - \gamma^{(0)})kd} \end{pmatrix}, \quad (13.52)$$

and for TE modes

$$\tilde{\mathbf{M}}_2^{\text{TE}} = \frac{\gamma^{(0)} + \gamma_s}{2\gamma^{(0)}} e^{-(\gamma_s - \gamma^{(0)})kd} \begin{pmatrix} 1 & e^{2\gamma_s kd} \frac{\gamma^{(0)} - \gamma_s}{\gamma^{(0)} + \gamma_s} \\ e^{-2\gamma^{(0)} kd} \frac{\gamma^{(0)} - \gamma_s}{\gamma^{(0)} + \gamma_s} & e^{2(\gamma_s - \gamma^{(0)})kd} \end{pmatrix}. \quad (13.53)$$

So the condition for TM modes is

$$1 - e^{-2\gamma^{(0)}kd} \frac{\tilde{\alpha}^{2D}\gamma^{(0)}}{1 + \tilde{\alpha}^{2D}\gamma^{(0)}} \left[ \frac{\tilde{\epsilon}_s\gamma^{(0)} - \gamma_s}{\tilde{\epsilon}_s\gamma^{(0)} + \gamma_s} \right] = 0, \quad (13.54)$$

and for TE modes

$$1 - e^{-2\gamma^{(0)}kd} \frac{(\omega/c k)^2 \tilde{\alpha}^{2D}}{\gamma^{(0)} - (\omega/c k)^2 \tilde{\alpha}^{2D}} \left[ \frac{\gamma^{(0)} - \gamma_s}{\gamma^{(0)} + \gamma_s} \right] = 0. \quad (13.55)$$

This agrees with the results in [10].

The mode condition functions become

$$f_k^{\text{TM}}(i\xi) = 1 - e^{-2\gamma^{(0)}(k, i\xi)kd} \frac{\tilde{\alpha}^{2D}(k, i\xi)\gamma^{(0)}(k, i\xi)}{1 + \tilde{\alpha}^{2D}(k, i\xi)\gamma^{(0)}(k, i\xi)} \left[ \frac{\tilde{\epsilon}_s(i\xi)\gamma^{(0)}(k, i\xi) - \gamma_s(k, i\xi)}{\tilde{\epsilon}_s(i\xi)\gamma^{(0)}(k, i\xi) + \gamma_s(k, i\xi)} \right], \quad (13.56)$$

for TM modes and

$$f_k^{\text{TE}}(i\xi) = 1 - e^{-2\gamma^{(0)}(k, i\xi)kd} \frac{-(\xi/c k)^2 \tilde{\alpha}^{2D}(k, i\xi)}{1 - (\xi/c k)^2 \tilde{\alpha}^{2D}(k, i\xi)} \left[ \frac{\gamma^{(0)}(k, i\xi) - \gamma_s(k, i\xi)}{\gamma^{(0)}(k, i\xi) + \gamma_s(k, i\xi)} \right], \quad (13.57)$$

for TE modes, respectively. The interaction energy per unit area is found by inserting these functions in (13.8) at zero temperature and in (13.9) at finite temperature.

### 13.6.1 Interaction Between Graphene and an Au-Wall

In the first numerical example we treat a pristine, or undoped, graphene sheet next to a gold wall. The results are shown in Fig. 13.7a for zero temperature and in Fig. 13.7b for room temperature. The corresponding results for doped graphene, with the doping concentration  $10^{13} \text{ cm}^{-2}$  are shown in Fig. 13.8a, b. The results were found from inserting the mode condition functions from (13.56) and (13.57) in (13.8) at zero temperature and in (13.9) at finite temperature. For  $\tilde{\alpha}^{2D}(k, i\xi)$  we used the polarizability for graphene as given in (2.143) for the pristine case and in (2.145) for the doped case. For  $\tilde{\epsilon}_s(i\xi)$  we used the function for gold. The polarizability  $\alpha(i\xi) = \tilde{\epsilon}_s(i\xi) - 1$  was shown in Fig. 9.3. The discussions in Sect. 13.5.1 concerning the interaction between two graphene sheets can be applied here as well.

### 13.6.2 Interaction Between a 2D Metal Film and an Au-Wall

In the second numerical example we treat a 2D metal film and a gold wall. The results are shown in Fig. 13.9. The results were found from inserting the mode condition functions from (13.56) and (13.57) in (13.8). For  $\tilde{\alpha}^{2D}(k, i\xi)$  we used the polarizability

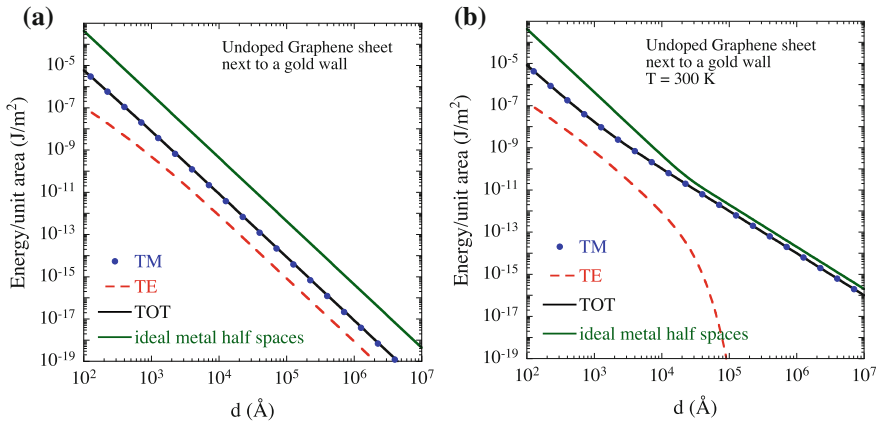


**Fig. 13.7** Interaction energy per unit area between an undoped graphene sheet and a gold wall at the distance  $d$ . The contribution from TE modes, *dashed curve*, TM modes, *filled circles*, and the total result, *solid curve*, are given. For comparison the result for two ideal metal half spaces, *upper solid curve*, is also given. **a** Zero temperature; **b** room temperature. Adapted from [10]

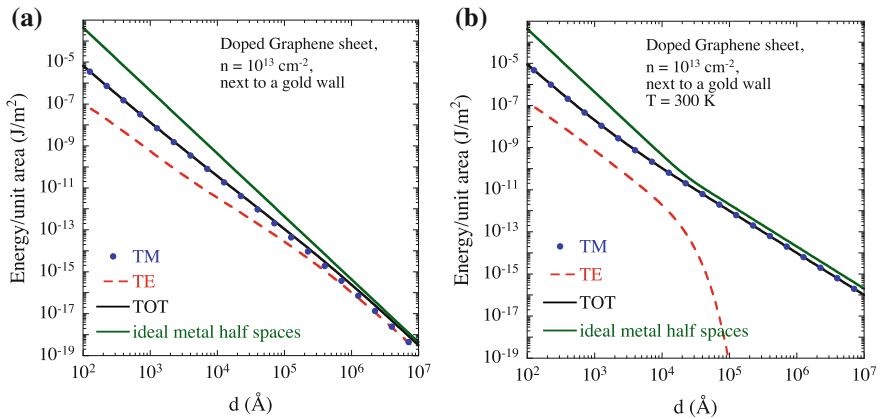
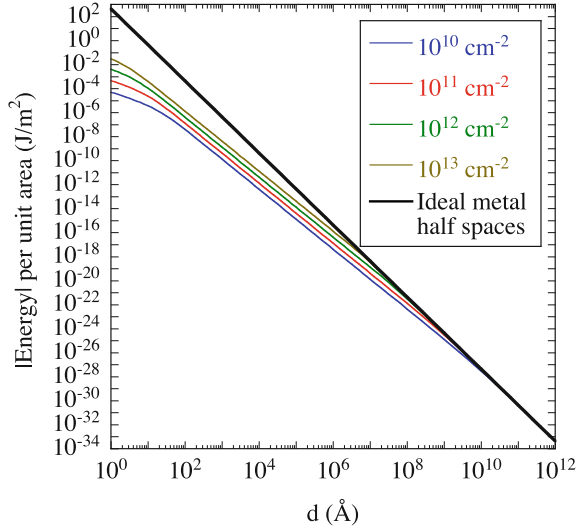


**Fig. 13.8** Interaction energy per unit area between a doped graphene sheet with doping concentration  $n = 10^{13} \text{ cm}^{-2}$  and a gold wall at the distance  $d$ . The contribution from TE modes, *dashed curve*, TM modes, *filled circles*, and the total result, *solid curve*, are given. For comparison the result for two ideal metal half spaces, *upper solid curve*, is also given. **a** Zero temperature; **b** room temperature. Adapted from [10]

**Fig. 13.9** Interaction energy per unit area between a 2D metal film and an Au wall at a distance  $d$ ; the results are, counted from below, for the carrier densities  $10^{10}$ ,  $10^{11}$ ,  $10^{12}$ , and  $10^{13} \text{ cm}^{-2}$ , respectively. The thick straight line, added for comparison, is for two ideal metal half spaces



of a 2D electron gas from (2.146) and the dielectric function of gold,  $\tilde{\epsilon}_1(i\xi) = 1 + \tilde{\alpha}(i\xi)$ , where  $\tilde{\alpha}(i\xi)$  is shown in Fig. 9.3. Next geometry is an atom next to a wall.

### 13.7 Atom-Wall

We start from the two layer structure in Fig. 9.11. We let the ambient be vacuum. The first layer is the thin gas layer treated in Sect. 13.2.4. We place it at  $z = 0$ . The second layer is a vacuum layer of thickness  $d$ . The remaining medium is the wall which we let be infinitely thick and have the dielectric function  $\tilde{\epsilon}_s(\omega)$ . The matrix becomes  $\tilde{\mathbf{M}} = \tilde{\mathbf{M}}_0 \cdot \tilde{\mathbf{M}}_1 \cdot \tilde{\mathbf{M}}_2 = \tilde{\mathbf{M}}_{\text{gaslayer}} \cdot \tilde{\mathbf{M}}_2$  where we already know the first matrix. It was derived in Sect. 13.2.4 for a general position  $z$ . Here  $z = 0$ , and for TM modes we get

$$\tilde{\mathbf{M}}_{\text{gaslayer}}^{\text{TM}} = \begin{pmatrix} 1 & 0 \\ 0 & 1 \end{pmatrix} + \frac{(\delta n)2\pi k\alpha^{at}}{\gamma^{(0)}} \begin{pmatrix} -(\frac{\omega}{ck})^2 & -\left[2 - (\frac{\omega}{ck})^2\right] \\ \left[2 - (\frac{\omega}{ck})^2\right] & (\frac{\omega}{ck})^2 \end{pmatrix}, \quad (13.58)$$

and for TE modes

$$\tilde{\mathbf{M}}_{\text{gaslayer}}^{\text{TE}} = \begin{pmatrix} 1 & 0 \\ 0 & 1 \end{pmatrix} + \frac{(\delta n)2\pi k\alpha^{at}(\omega/ck)^2}{\gamma^{(0)}} \begin{pmatrix} -1 & -1 \\ 1 & 1 \end{pmatrix}. \quad (13.59)$$

Now,  $\tilde{\mathbf{M}}_2$  we find in (13.52) and (13.53) for TM- and TE-modes, respectively.

So, the condition for TM modes is

$$1 - \frac{(\delta n) 2\pi k \alpha^{at}}{\gamma^{(0)}} \left\{ \left( \frac{\omega}{ck} \right)^2 + e^{-2\gamma^{(0)}kd} \left[ 2 - \left( \frac{\omega}{ck} \right)^2 \right] \frac{\tilde{\epsilon}_s \gamma^{(0)} - \gamma_s}{\tilde{\epsilon}_s \gamma^{(0)} + \gamma_s} \right\} = 0, \quad (13.60)$$

and for TE modes

$$1 - \frac{(\delta n) 2\pi k \alpha^{at} (\omega/ck)^2}{\gamma^{(0)}} \left[ 1 + e^{-2\gamma^{(0)}kd} \frac{\gamma^{(0)} - \gamma_s}{\gamma^{(0)} + \gamma_s} \right] = 0. \quad (13.61)$$

The mode condition function for TM modes is

$$f_{\mathbf{k}}^{\text{TM}} = 1 - \frac{(\delta n) 2\pi k \alpha^{at}}{\gamma^{(0)}} \left\{ \left( \frac{\omega}{ck} \right)^2 + e^{-2\gamma^{(0)}kd} \left[ 2 - \left( \frac{\omega}{ck} \right)^2 \right] \frac{\tilde{\epsilon}_s \gamma^{(0)} - \gamma_s}{\tilde{\epsilon}_s \gamma^{(0)} + \gamma_s} \right\}, \quad (13.62)$$

and for TE modes

$$f_{\mathbf{k}}^{\text{TE}} = 1 - \frac{(\delta n) 2\pi k \alpha^{at} (\omega/ck)^2}{\gamma^{(0)}} \left[ 1 + e^{-2\gamma^{(0)}kd} \frac{\gamma^{(0)} - \gamma_s}{\gamma^{(0)} + \gamma_s} \right]. \quad (13.63)$$

Note that the first part in each mode condition function,

$$f_{\mathbf{k}}^0 = 1 - (\delta n) \alpha^{at} \frac{2\pi k (\omega/ck)^2}{\gamma^{(0)}}. \quad (13.64)$$

does not depend on the distance of the atom to the wall. It is the effect of the contribution from the atom to the screening and the resulting change of the dispersion curves for the vacuum modes. This type of interaction was used by Feynman to derive the Lamb shift of the hydrogen atom [11]. We see that it contributes the same in both type of modes. We divide with this function since it leads to a constant energy, independent of the atom distance to the interface. So the relevant mode condition functions relative infinite separation are

$$\begin{aligned} \tilde{f}_{\mathbf{k}}^{\text{TM}} &= 1 - (\delta n) \alpha^{at} \frac{2\pi k [2 - (\omega/ck)^2]}{\gamma^{(0)}} e^{-2\gamma^{(0)}kd} \frac{\tilde{\epsilon}_s \gamma^{(0)} - \gamma_s}{\tilde{\epsilon}_s \gamma^{(0)} + \gamma_s}; \\ \tilde{f}_{\mathbf{k}}^{\text{TE}} &= 1 - (\delta n) \alpha^{at} \frac{2\pi k (\omega/ck)^2}{\gamma^{(0)}} e^{-2\gamma^{(0)}kd} \frac{\gamma^{(0)} - \gamma_s}{\gamma^{(0)} + \gamma_s}. \end{aligned} \quad (13.65)$$

The interaction energy per atom becomes

$$\begin{aligned} \frac{E}{n\delta} &= \frac{\hbar}{n\delta} \int \frac{d^2k}{(2\pi)^2} \int_0^\infty \frac{d\xi}{2\pi} \left\{ \ln \left[ \tilde{f}_{\mathbf{k}}^{\text{TE}}(i\xi) \right] + \ln \left[ \tilde{f}_{\mathbf{k}}^{\text{TM}}(i\xi) \right] \right\} \\ &= 2\pi \hbar \int \frac{d^2k}{(2\pi)^2} k \int_0^\infty \frac{d\xi}{2\pi} \alpha^{at}(i\xi) e^{-2\gamma^{(0)}(i\xi)kd} \\ &\quad \times \left\{ \frac{(\xi/ck)^2 \gamma^{(0)}(i\xi) - \gamma_s(i\xi)}{\gamma^{(0)}(i\xi) \gamma^{(0)}(i\xi) + \gamma_s(i\xi)} + \frac{[2 + (\xi/ck)^2] \gamma_s(i\xi) - \tilde{\epsilon}_s(i\xi) \gamma^{(0)}(i\xi)}{\gamma^{(0)}(i\xi) \gamma_s(i\xi) + \tilde{\epsilon}_s(i\xi) \gamma^{(0)}(i\xi)} \right\} \end{aligned} \quad (13.66)$$

where we have taken the limit when  $(\delta n)$  goes toward zero. The force on the atom is

$$F(d) = 4\pi\hbar \int \frac{d^2k}{(2\pi)^2} k^2 \int_0^\infty \frac{d\xi}{2\pi} \alpha^{at}(\xi) e^{-2\gamma^{(0)}(\xi)kd} \times \left\{ (\xi/c k)^2 \frac{\gamma^{(0)}(\xi) - \gamma_s(\xi)}{\gamma^{(0)}(\xi) + \gamma_s(\xi)} + [2 + (\xi/c k)^2] \frac{\gamma_s(\xi) - \bar{\epsilon}_s(\xi)\gamma^{(0)}(\xi)}{\gamma_s(\xi) + \bar{\epsilon}_s(\xi)\gamma^{(0)}(\xi)} \right\} \tag{13.67}$$

At finite temperature it is

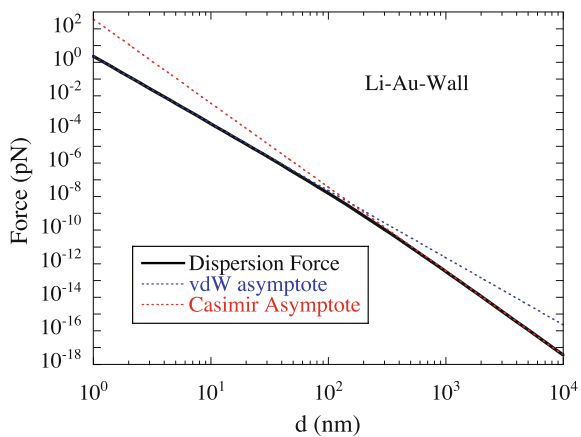
$$F(d) = \frac{4\pi}{\beta} \int \frac{d^2k}{(2\pi)^2} k^2 \sum'_{\xi_n} \alpha^{at}(\xi_n) e^{-2\gamma^{(0)}(\xi_n)d} \times \left\{ (\xi_n/c k)^2 \frac{\gamma^{(0)}(\xi_n) - \gamma_s(\xi_n)}{\gamma^{(0)}(\xi_n) + \gamma_s(\xi_n)} + [2 + (\xi_n/c k)^2] \frac{\gamma_s(\xi_n) - \bar{\epsilon}_s(\xi_n)\gamma^{(0)}(\xi_n)}{\gamma_s(\xi_n) + \bar{\epsilon}_s(\xi_n)\gamma^{(0)}(\xi_n)} \right\}. \tag{13.68}$$

These results are in complete agreement with the results in [12].

### 13.7.1 Li-Atom–Au-Wall Interaction

As an example of atom-wall interactions we show in Fig. 13.10 the force between a Li atom and a gold wall. The polarizability for Li was obtained from the London approximation (8.60) with the parameters given in Fig. 8.2. The  $d$ -dependence follows a simple power law,  $F \sim d^{-4}$ , for small and intermediate separation and  $F \sim d^{-5}$  for large separations. The next geometry we consider is an atom in a planar gap.

**Fig. 13.10** Dispersion force, *solid curve*, between a Li atom and a gold wall as a function of separation  $d$ ; also shown are the van der Waals asymptote, *dotted straight line with smallest slope*, and the Casimir asymptote, *dotted straight line with steepest slope*



### 13.8 Atom in Planar Gap

We refer to Fig. 9.13 and let the first interface be located at  $z = 0$  separating one wall with dielectric function  $\tilde{\epsilon}_1$  from the ambient medium which we let be vacuum. Next interface, at  $z = d$ , is the left interface of the gas layer with dielectric function  $\epsilon_g$  and thickness  $\delta$ . Thus the third interface is at  $z = d + \delta$ . The fourth interface is located at  $z = D$  and separates vacuum from the second wall with dielectric function  $\tilde{\epsilon}_2$ . The matrix becomes  $\tilde{\mathbf{M}} = \tilde{\mathbf{M}}_0 \cdot \tilde{\mathbf{M}}_1 \cdot \tilde{\mathbf{M}}_2 \cdot \tilde{\mathbf{M}}_3 = \tilde{\mathbf{M}}_0 \cdot \tilde{\mathbf{M}}_{\text{gaslayer}} \cdot \tilde{\mathbf{M}}_3$  where  $\tilde{\mathbf{M}}_{\text{gaslayer}}$  is taken from (13.29) or (13.30) for TM modes and TE modes, respectively, and

$$\begin{aligned} \tilde{\mathbf{M}}_0 &= \frac{1}{t_{0,1}} \begin{pmatrix} 1 & r_{0,1} \\ r_{0,1} & 1 \end{pmatrix}; \\ \tilde{\mathbf{M}}_3 &= \frac{1}{t_{3,4}} \begin{pmatrix} e^{-(\gamma_s - \gamma^{(0)})kD} & e^{(\gamma_s + \gamma^{(0)})kD} r_{3,4} \\ e^{-(\gamma_s + \gamma^{(0)})kD} r_{3,4} & e^{(\gamma_s - \gamma^{(0)})kD} \end{pmatrix}. \end{aligned} \quad (13.69)$$

Now,

$$M_{11} = (M_{11}^0 \ M_{12}^0) \cdot \tilde{\mathbf{M}}_{\text{gaslayer}} \cdot \begin{pmatrix} M_{11}^3 \\ M_{21}^3 \end{pmatrix}. \quad (13.70)$$

To find a general expression valid for both mode types we use the expression in (13.28) for  $\tilde{\mathbf{M}}_{\text{gaslayer}}$ . It is the expression to linear order in  $\delta$  but before the lowest order in  $n$  is taken. Then

$$\begin{aligned} M_{11} &= \frac{e^{-(\gamma_s - \gamma^{(0)})kD}}{t_{0,1}t_{3,4}} \left\{ 1 + e^{-2\gamma^{(0)}kD} r_{0,1} r_{3,4} \right. \\ &+ \delta k \left[ (\gamma_g - \gamma^{(0)}) \left( 1 - e^{-2\gamma^{(0)}kD} r_{0,1} r_{3,4} \right) \right. \\ &\left. \left. - 2\gamma^{(0)} r_{2,3} \left( e^{-2\gamma^{(0)}kd} r_{0,1} - e^{2\gamma^{(0)}k(d-D)} r_{3,4} \right) \right] \right\}. \end{aligned} \quad (13.71)$$

The condition for modes is

$$\begin{aligned} &1 + e^{-2\gamma^{(0)}kD} r_{0,1} r_{3,4} \\ &+ \delta k \left[ (\gamma_g - \gamma^{(0)}) \left( 1 - e^{-2\gamma^{(0)}kD} r_{0,1} r_{3,4} \right) \right. \\ &\left. - 2\gamma^{(0)} r_{2,3} \left( e^{-2\gamma^{(0)}kd} r_{0,1} - e^{2\gamma^{(0)}k(d-D)} r_{3,4} \right) \right] = 0. \end{aligned} \quad (13.72)$$

The mode condition function is

$$\begin{aligned}
 \tilde{f}_{\mathbf{k}} &= 1 + \frac{\delta k}{1 + e^{-2\gamma^{(0)}kD} r_{0,1} r_{3,4}} \\
 &\times \left[ (\gamma_g - \gamma^{(0)}) \left( 1 - e^{-2\gamma^{(0)}kD} r_{0,1} r_{3,4} \right) \right. \\
 &\left. - 2\gamma^{(0)} r_{2,3} \left( e^{-2\gamma^{(0)}kd} r_{0,1} - e^{2\gamma^{(0)}k(d-D)} r_{3,4} \right) \right] \\
 &= 1 + \frac{\delta k n \alpha^{at}}{\gamma^{(0)} \left[ 1 + e^{-2\gamma^{(0)}D} r_{0,1} r_{3,4} \right]} \\
 &\times \left[ -2\pi (\omega / ck)^2 \left( 1 - e^{-2\gamma^{(0)}kD} r_{0,1} r_{3,4} \right) \right. \\
 &\left. - 2(\gamma^{(0)})^2 \left( \frac{r_{2,3}}{n \alpha^{at}} \right) \left( e^{-2\gamma^{(0)}kd} r_{0,1} - e^{2\gamma^{(0)}k(d-D)} r_{3,4} \right) \right].
 \end{aligned} \tag{13.73}$$

Just as for the atom next to a wall a part of this function does not depend on the position of the gas layer. The energy change is due to the screening of the vacuum caused by the polarizable atom. It is interesting to note that this effect is modified by the presence of the two planar surfaces. We divide with the function

$$\begin{aligned}
 f_{\mathbf{k}}^0 &= 1 - \frac{\delta k \left( 1 - e^{-2\gamma^{(0)}kD} r_{0,1} r_{3,4} \right)}{1 + e^{-2\gamma^{(0)}kD} r_{0,1} r_{3,4}} (\gamma^{(0)} - \gamma_g) \\
 &= 1 - \delta k n \alpha^{at} \frac{2\pi}{\gamma^{(0)}} \left( \frac{\omega}{ck} \right)^2 \frac{\left( 1 - e^{-2\gamma^{(0)}kD} r_{0,1} r_{3,4} \right)}{\left( 1 + e^{-2\gamma^{(0)}kD} r_{0,1} r_{3,4} \right)}.
 \end{aligned} \tag{13.74}$$

For the energy this means that we subtract a term that is independent of the position of the atom and will not affect the force on the atom. We find

$$\tilde{f}_{\mathbf{k}} = 1 + \delta k n \alpha^{at} \frac{\left[ -2(\gamma^{(0)}) (r_{2,3} / n \alpha^{at}) \left( e^{-2\gamma^{(0)}kd} r_{0,1} - e^{2\gamma^{(0)}k(d-D)} r_{3,4} \right) \right]}{\left[ 1 + e^{-2\gamma^{(0)}kD} r_{0,1} r_{3,4} \right]}, \tag{13.75}$$

and the interaction energy per atom is

$$\frac{E}{n\delta} = \hbar \int \frac{d^2k}{(2\pi)^2} \int_0^\infty \frac{d\xi}{2\pi} \left[ I^{\text{TM}}(k, i\xi) + I^{\text{TE}}(k, i\xi) \right], \tag{13.76}$$

where

$$\begin{aligned}
 I^{\text{TM}}(k, \omega) &= \alpha^{at} \frac{2\pi k \left[ 2 - (\omega / ck)^2 \right] \left[ e^{-2\gamma^{(0)}kd} r_{0,1}^{\text{TM}} - e^{-2\gamma^{(0)}k(d-D)} r_{3,4}^{\text{TM}} \right]}{\gamma^{(0)} \left[ 1 + e^{-2\gamma^{(0)}kD} r_{0,1}^{\text{TM}} r_{3,4}^{\text{TM}} \right]}; \\
 I^{\text{TE}}(k, \omega) &= \alpha^{at} \frac{2\pi k (\omega / ck)^2 \left[ e^{-2\gamma^{(0)}kd} r_{0,1}^{\text{TE}} - e^{-2\gamma^{(0)}k(d-D)} r_{3,4}^{\text{TE}} \right]}{\gamma^{(0)} \left[ 1 + e^{-2\gamma^{(0)}kD} r_{0,1}^{\text{TE}} r_{3,4}^{\text{TE}} \right]}.
 \end{aligned} \tag{13.77}$$

The explicit expressions for the entering reflection coefficients are obtained from (13.2). They are

$$\begin{aligned}
r_{0,1}^{\text{TM}}(k, \omega) &= \frac{\sqrt{1-\tilde{\epsilon}_1(\omega)(\omega/c k)^2}-\tilde{\epsilon}_1(\omega)\sqrt{1-(\omega/c k)^2}}{\sqrt{1-\tilde{\epsilon}_1(\omega)(\omega/c k)^2}+\tilde{\epsilon}_1(\omega)\sqrt{1-(\omega/c k)^2}}; \\
r_{3,4}^{\text{TM}}(k, \omega) &= \frac{\tilde{\epsilon}_2(\omega)\sqrt{1-(\omega/c k)^2}-\sqrt{1-\tilde{\epsilon}_2(\omega/c k)^2}}{\tilde{\epsilon}_2(\omega)\sqrt{1-(\omega/c k)^2}+\sqrt{1-\tilde{\epsilon}_2(\omega/c k)^2}}; \\
r_{0,1}^{\text{TE}}(k, \omega) &= \frac{\sqrt{1-\tilde{\epsilon}_1(\omega)(\omega/c k)^2}-\sqrt{1-(\omega/c k)^2}}{\sqrt{1-\tilde{\epsilon}_1(\omega)(\omega/c k)^2}+\sqrt{1-(\omega/c k)^2}}; \\
r_{3,4}^{\text{TE}}(k, \omega) &= \frac{\sqrt{1-(\omega/c k)^2}-\sqrt{1-\tilde{\epsilon}_2(\omega/c k)^2}}{\sqrt{1-(\omega/c k)^2}+\sqrt{1-\tilde{\epsilon}_2(\omega/c k)^2}}.
\end{aligned} \tag{13.78}$$

Thus the force on the atom is

$$F(d) = \hbar \int \frac{d^2 k}{(2\pi)^2} \int_0^\infty \frac{d\xi}{2\pi} [J^{\text{TM}}(k, i\xi) + J^{\text{TE}}(k, i\xi)], \tag{13.79}$$

where

$$\begin{aligned}
J^{\text{TM}}(k, \omega) &= \alpha^{at} \frac{4\pi k^2 [2-(\omega/c k)^2] [e^{-2\gamma^{(0)} k d} r_{0,1}^{\text{TM}} + e^{-2\gamma^{(0)} k(D-d)} r_{3,4}^{\text{TM}}]}{[1 + e^{-2\gamma^{(0)} k D} r_{0,1}^{\text{TM}} r_{3,4}^{\text{TM}}]}; \\
J^{\text{TE}}(k, \omega) &= \alpha^{at} \frac{4\pi k^2 (\omega/c k)^2 [e^{-2\gamma^{(0)} k d} r_{0,1}^{\text{TE}} + e^{-2\gamma^{(0)} k(D-d)} r_{3,4}^{\text{TE}}]}{[1 + e^{-2\gamma^{(0)} k D} r_{0,1}^{\text{TE}} r_{3,4}^{\text{TE}}]},
\end{aligned} \tag{13.80}$$

and at finite temperature it is

$$F(d) = \frac{1}{\beta} \int \frac{d^2 k}{(2\pi)^2} \sum_{\xi_n} [J^{\text{TM}}(k, i\xi_n) + J^{\text{TE}}(k, i\xi_n)]. \tag{13.81}$$

We do not give any numerical examples here. Instead we continue with the next geometry, which is an atom next to a thin film.

### 13.9 Atom-Film

In this section we derive the Casimir interaction of an atom near a very thin film. We proceed along the lines of Sect. 9.9. We start from the three layer structure in Fig. 9.14. The matrix becomes  $\tilde{\mathbf{M}} = \tilde{\mathbf{M}}_0 \cdot \tilde{\mathbf{M}}_1 \cdot \tilde{\mathbf{M}}_2 \cdot \tilde{\mathbf{M}}_3$ , where  $\tilde{\mathbf{M}}_0 \cdot \tilde{\mathbf{M}}_1$  is the matrix for the thin film, and  $\tilde{\mathbf{M}}_2 \cdot \tilde{\mathbf{M}}_3$  is the matrix for the gas film. These matrices we have derived before. We have two mode types, TM and TE.

We start with the TM modes. The resulting matrices for the two thin layers were given in (13.26) and (13.29), respectively. They are

$$\begin{aligned}
\tilde{\mathbf{M}}_0 \cdot \tilde{\mathbf{M}}_1 &= \begin{pmatrix} 1 & 0 \\ 0 & 1 \end{pmatrix} + \frac{\gamma^{(0)}k(\delta\tilde{\varepsilon}^{3D})}{2} \begin{pmatrix} 1 & -1 \\ 1 & -1 \end{pmatrix}; \\
\tilde{\mathbf{M}}_2 \cdot \tilde{\mathbf{M}}_3 &= \begin{pmatrix} 1 & 0 \\ 0 & 1 \end{pmatrix} + \frac{(\delta n)2\pi k\alpha^{at}}{\gamma^{(0)}} \\
&\times \begin{pmatrix} -\left(\frac{\omega}{ck}\right)^2 & -e^{2\gamma^{(0)}kd} \left[2 - \left(\frac{\omega}{ck}\right)^2\right] \\ e^{-2\gamma^{(0)}kd} \left[2 - \left(\frac{\omega}{ck}\right)^2\right] & \left(\frac{\omega}{ck}\right)^2 \end{pmatrix},
\end{aligned} \tag{13.82}$$

and the resulting matrix element that interests us is

$$\begin{aligned}
M_{11} &= 1 + \frac{\gamma^{(0)}k(\delta\tilde{\varepsilon}^{3D})}{2} - \frac{(\delta n)2\pi k\alpha^{at}}{\gamma^{(0)}} \left(\frac{\omega}{ck}\right)^2 \\
&- (\delta n)\pi k^2\alpha^{at}(\delta\tilde{\varepsilon}^{3D}) \left\{ \left(\frac{\omega}{ck}\right)^2 + e^{-2\gamma^{(0)}kd} \left(2k^2 - \left(\frac{\omega}{ck}\right)^2\right) \right\}.
\end{aligned} \tag{13.83}$$

The TM mode condition function becomes

$$\begin{aligned}
\tilde{f}_{\mathbf{k}}^{\text{TM}}(\omega) &= 1 - \frac{(\delta n)\pi k^2\alpha^{at}(\delta\tilde{\varepsilon}^{3D})\left(2 - \left(\frac{\omega}{ck}\right)^2\right)e^{-2\gamma^{(0)}kd}}{1 + \frac{\gamma^{(0)}k(\delta\tilde{\varepsilon}^{3D})}{2} - \frac{2\pi k(\delta n)\alpha^{at}}{\gamma^{(0)}}\left(\frac{\omega}{ck}\right)^2 - (\delta n)\pi k^2\alpha^{at}(\delta\tilde{\varepsilon}^{3D})\left(\frac{\omega}{ck}\right)^2} \\
&\approx 1 - \frac{(\delta n)\pi k^2\alpha^{at}(\delta\tilde{\varepsilon}^{3D})\left[2 - \left(\frac{\omega}{ck}\right)^2\right]e^{-2\gamma^{(0)}kd}}{1 + \frac{\gamma^{(0)}k(\delta\tilde{\varepsilon}^{3D})}{2}} \\
&= 1 - \frac{(\delta n)2\pi k\alpha^{at}\tilde{\alpha}^{2D}(\mathbf{k},\omega)\left[2 - \left(\frac{\omega}{ck}\right)^2\right]e^{-2\gamma^{(0)}kd}}{1 + \gamma^{(0)}\tilde{\alpha}^{2D}(\mathbf{k},\omega)}.
\end{aligned} \tag{13.84}$$

For the TE modes the matrices for the two films from (13.27) and (13.30), respectively are

$$\begin{aligned}
\tilde{\mathbf{M}}_0 \cdot \tilde{\mathbf{M}}_1 &= \begin{pmatrix} 1 & 0 \\ 0 & 1 \end{pmatrix} - \frac{(\delta\tilde{\varepsilon}^{3D})k(\omega/ck)^2}{2\gamma^{(0)}} \begin{pmatrix} 1 & 1 \\ -1 & -1 \end{pmatrix}; \\
\tilde{\mathbf{M}}_2 \cdot \tilde{\mathbf{M}}_3 &= \begin{pmatrix} 1 & 0 \\ 0 & 1 \end{pmatrix} - \frac{(\delta n)(\omega/ck)^2 2\pi k\alpha^{at}}{\gamma^{(0)}} \begin{pmatrix} 1 & e^{2\gamma^{(0)}kd} \\ -e^{-2\gamma^{(0)}kd} & -1 \end{pmatrix},
\end{aligned} \tag{13.85}$$

and the resulting matrix element that interests us is

$$\begin{aligned}
M_{11} &= 1 - \frac{(\delta\tilde{\varepsilon}^{3D})k(\omega/ck)^2}{2\gamma^{(0)}} - \frac{(\omega/ck)^2 2\pi k(\delta n)\alpha^{at}}{\gamma^{(0)}} \\
&+ \frac{(\omega/ck)^4 \pi k^2 (\delta n)\alpha^{at}(\delta\tilde{\varepsilon}^{3D})}{[\gamma^{(0)}]^2} \left(1 - e^{-2\gamma^{(0)}kd}\right).
\end{aligned} \tag{13.86}$$

The TE mode condition function is

$$\begin{aligned}
 \tilde{f}_{\mathbf{k}}^{\text{TE}}(\omega) &= 1 - \frac{\frac{(\omega/c k)^4 \pi k^2 (\delta n) \alpha^{at} (\delta \tilde{\varepsilon}^{3D})}{[\gamma^{(0)}]^2} e^{-2\gamma^{(0)} k d}}{1 - \frac{(\delta \tilde{\varepsilon}^{3D}) k (\omega/c k)^2}{2\gamma^{(0)}} - \frac{(\delta n) (\omega/c k)^2 2\pi k \alpha^{at}}{\gamma^{(0)}} + \frac{(\delta n) (\omega/c k)^4 \pi k^2 \alpha^{at} (\delta \tilde{\varepsilon}^{3D})}{[\gamma^{(0)}]^2}} \\
 &\approx 1 - \frac{(\delta n) (\omega/c k)^4 \pi k^2 \alpha^{at} (\delta \tilde{\varepsilon}^{3D})}{\gamma^{(0)} \left( \gamma^{(0)} - \frac{(\delta \tilde{\varepsilon}^{3D}) k (\omega/c k)^2}{2} \right)} e^{-2\gamma^{(0)} k d} \\
 &= 1 - \frac{(\delta n) 2\pi k \alpha^{at} \tilde{\alpha}^{2D}(\mathbf{k}, \omega) (\omega/c k)^4}{(\gamma^{(0)}) [(\gamma^{(0)}) - \tilde{\alpha}^{2D}(\mathbf{k}, \omega) (\omega/c k)^2]} e^{-2\gamma^{(0)} k d}.
 \end{aligned} \tag{13.87}$$

The interaction energy per atom is

$$\begin{aligned}
 \frac{E}{n\delta} &= \frac{\hbar}{n\delta} \int \frac{d^2 k}{(2\pi)^2} \int_0^\infty \frac{d\xi}{2\pi} \left\{ \ln \left[ \tilde{f}_{\mathbf{k}}^{\text{TM}}(i\xi) \right] + \ln \left[ \tilde{f}_{\mathbf{k}}^{\text{TE}}(i\xi) \right] \right\} \\
 &\approx \hbar \int \frac{d^2 k}{(2\pi)^2} \int_0^\infty \frac{d\xi}{2\pi} \frac{\left[ \tilde{f}_{\mathbf{k}}^{\text{TM}}(i\xi) - 1 \right] + \left[ \tilde{f}_{\mathbf{k}}^{\text{TE}}(i\xi) - 1 \right]}{n\delta} \\
 &= -\frac{\hbar}{2\pi} \int dk k^2 \int_0^\infty d\xi \alpha^{at}(i\xi) \tilde{\alpha}^{2D}(k, i\xi) e^{-2\sqrt{1+(\xi/c k)^2} k d} \\
 &\quad \times \left\{ \frac{[2+(\xi/c k)^2]}{1+\sqrt{1+(\xi/c k)^2} \tilde{\alpha}^{2D}(k, i\xi)} + \frac{(\xi/c k)^4}{\sqrt{1+(\xi/c k)^2} [\sqrt{1+(\xi/c k)^2} + \tilde{\alpha}^{2D}(k, i\xi) (\xi/c k)^2]} \right\},
 \end{aligned} \tag{13.88}$$

and the force on the atom becomes

$$\begin{aligned}
 F(d) &= -\frac{\hbar}{\pi} \int dk k^3 \int_0^\infty d\xi \alpha^{at}(i\xi) \tilde{\alpha}^{2D}(k, i\xi) e^{-2\sqrt{1+(\xi/c k)^2} k d} \\
 &\quad \times \left[ \frac{[2+(\xi/c k)^2] \sqrt{1+(\xi/c k)^2}}{1+\sqrt{1+(\xi/c k)^2} \tilde{\alpha}^{2D}(k, i\xi)} + \frac{(\xi/c k)^4}{[\sqrt{1+(\xi/c k)^2} + \tilde{\alpha}^{2D}(k, i\xi) (\xi/c k)^2]} \right].
 \end{aligned} \tag{13.89}$$

For this geometrical example we give numerical illustrations. We begin with a lithium atom next to a graphene sheet.

### 13.9.1 Li-Atom–Graphene-Sheet Interaction

The first example of the dispersion interaction between an atom and a 2D planar film we present is the interaction between a Li atom and a graphene sheet. The results are shown in Fig. 13.11a for a number of doping densities. The results do not follow simple power laws. However, for large separations the undoped graphene result approaches the  $d^{-4}$  power law just as it did in the non-retarded treatment in Sect. 9.9.1. This can be understood in the following way: the substitutions  $k \rightarrow k/d$  and  $\xi \rightarrow \xi/d$  leave  $\tilde{\alpha}^{2D}(k, i\xi)$  unchanged in (13.88) and we have

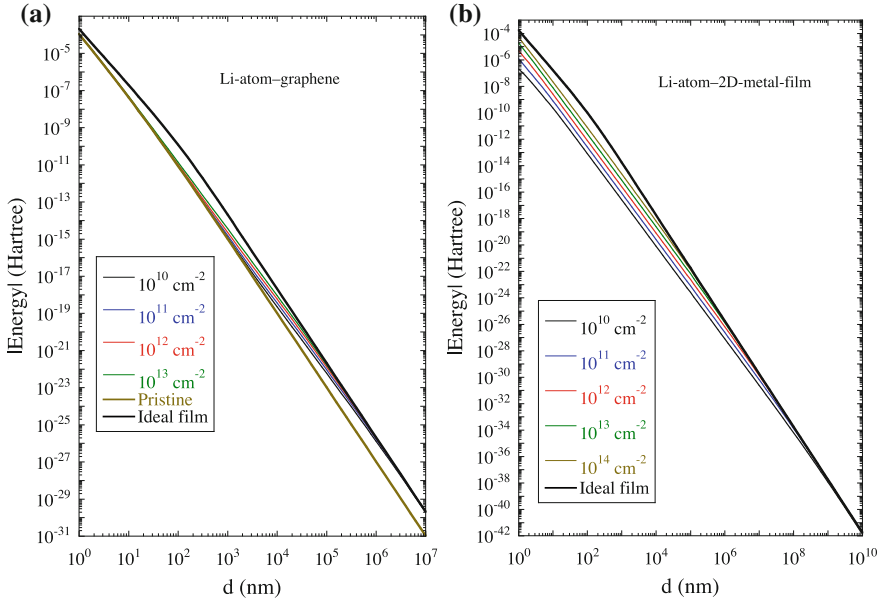


**Fig. 13.11** The dispersion interaction energy between a Li atom and a 2D film a distance  $d$  apart. **a** Li atom and a graphene sheet; the results are, counted from below, for the doping densities 0,  $10^{10}$ ,  $10^{11}$ ,  $10^{12}$ , and  $10^{13}$   $\text{cm}^{-2}$ , respectively. **b** Li atom and 2D metal film; the results are, counted from below, for the carrier densities  $10^{10}$ ,  $10^{11}$ ,  $10^{12}$ ,  $10^{13}$ , and  $10^{14}$   $\text{cm}^{-2}$ , respectively

$$\begin{aligned}
 \frac{E}{n\delta} &= -\frac{\hbar}{2\pi d^4} \int dk k^2 \int_0^\infty d\xi \alpha^{at} (i\xi/d) \tilde{\alpha}^{2D}(k, i\xi) e^{-2\sqrt{1+(\xi/ck)^2}k} \\
 &\quad \times \left[ \frac{[2+(\xi/ck)^2]}{1+\sqrt{1+(\xi/ck)^2}\tilde{\alpha}^{2D}(k, i\xi)} + \frac{(\xi/ck)^4}{\sqrt{1+(\xi/ck)^2}[\sqrt{1+(\xi/ck)^2}+\tilde{\alpha}^{2D}(k, i\xi)(\xi/ck)^2]} \right] \\
 &\approx -\frac{\hbar}{2\pi d^4} \int dk k^2 \int_0^\infty d\xi \alpha^{at} (0) \tilde{\alpha}^{2D}(k, i\xi) e^{-2\sqrt{1+(\xi/ck)^2}k} \\
 &\quad \times \left[ \frac{[2+(\xi/ck)^2]}{1+\sqrt{1+(\xi/ck)^2}\tilde{\alpha}^{2D}(k, i\xi)} + \frac{(\xi/ck)^4}{\sqrt{1+(\xi/ck)^2}[\sqrt{1+(\xi/ck)^2}+\tilde{\alpha}^{2D}(k, i\xi)(\xi/ck)^2]} \right]
 \end{aligned} \tag{13.90}$$

for large enough  $d$ -values. Once again we see that  $d$  only appears in the prefactor.

For doped graphene retardation effects are more important. The effects of the doping appear first at intermediate separations. Then the curves follow  $d^{-7/2}$  asymptotes until they approach the atom–ideal-metal-film-result (thick solid curve in Fig. 13.11). Then they follow this result. The atom–ideal-metal-film-result we find by letting the film polarizability go toward infinity,

$$\begin{aligned}
E^{\text{ideal}} &= - \lim_{\tilde{\alpha}^{2D} \rightarrow \infty} \frac{\hbar}{2\pi} \int dk k^2 \int_0^\infty d\xi \alpha^{at}(i\xi) \tilde{\alpha}^{2D}(k, i\xi) e^{-2\sqrt{1+(\xi/c k)^2}kd} \\
&\times \left[ \frac{[2+(\xi/c k)^2]}{1+\sqrt{1+(\xi/c k)^2}\tilde{\alpha}^{2D}(k, i\xi)} + \frac{(\xi/c k)^4}{\sqrt{1+(\xi/c k)^2}[\sqrt{1+(\xi/c k)^2}+\tilde{\alpha}^{2D}(k, i\xi)(\xi/c k)^2]} \right] \\
&= - \frac{\hbar}{2\pi} \int dk k^2 \int_0^\infty d\xi \alpha^{at}(i\xi) e^{-2\sqrt{1+(\xi/c k)^2}kd} 2\sqrt{1+(\xi/c k)^2}.
\end{aligned} \tag{13.91}$$

The large  $d$  asymptote becomes

$$\begin{aligned}
E^{\text{ideal}} &= - \frac{\hbar}{2\pi} \int dk k^2 \int_0^\infty d\xi \alpha^{at}(i\xi) e^{-2\sqrt{1+(\xi/c k)^2}kd} 2\sqrt{1+(\xi/c k)^2} = \left| \begin{array}{l} k \rightarrow k/d \\ \xi \rightarrow \xi/d \end{array} \right| \\
&= - \frac{\hbar}{2\pi d^4} \int dk k^2 \int_0^\infty d\xi \alpha^{at}(i\xi/d) e^{-2\sqrt{1+(\xi/c k)^2}k} 2\sqrt{1+(\xi/c k)^2} \\
&\approx - \frac{\hbar \alpha^{at}(0)}{2\pi d^4} \int dk k^2 \int_0^\infty d\xi e^{-2\sqrt{1+(\xi/c k)^2}k} 2\sqrt{1+(\xi/c k)^2} = |\xi \rightarrow \xi ck| \\
&= - \frac{\hbar c \alpha^{at}(0)}{2\pi d^4} \int dk k^3 \int_0^\infty d\xi e^{-2\sqrt{1+\xi^2}k} 2\sqrt{1+\xi^2} = \left| k \rightarrow k/2\sqrt{1+\xi^2} \right| \\
&= - \frac{\hbar c \alpha^{at}(0)}{16\pi d^4} \underbrace{\int_0^\infty dk k^3 e^{-k}}_6 \underbrace{\int_0^\infty d\xi \frac{1}{(1+\xi^2)^{3/2}}}_1 = -\frac{3}{8} \frac{\hbar c \alpha^{at}(0)}{\pi d^4}.
\end{aligned} \tag{13.92}$$

The same asymptotic result is obtained for an atom next to an ideal metal wall. This result is in agreement with [13, 14]. Next numerical example is a lithium atom next to a thin metal film.

### 13.9.2 Li-Atom–2D-Metal-Film Interaction

We show the results for the interaction between a Li atom and a 2D metal film for a number of carrier concentrations in Fig. 13.11b. The ideal film result is identical to that in Fig. 13.11a and the large  $d$  asymptote of (13.92) is valid also here. The results are different compared to the doped graphene case in that the carrier concentration affects the results already for the smallest  $d$ -values; spatial dispersion effects show up at the small- $d$  limit and then gradually diminish; then the curves follow  $d^{-7/2}$  asymptotes until they approach the ideal film result.

In next geometry we add another film and study the interaction on an atom in between two films. This is the last geometry we treat in this chapter.

### 13.10 Atom in Between Two Planar Films

Here we let the first 2D film be located at  $z = 0$ , the thin diluted gas film at  $z = d$ , and the second 2D film at  $D$ . There is vacuum between the three films. Thus the matrix becomes  $\tilde{\mathbf{M}} = \tilde{\mathbf{M}}_0 \cdot \tilde{\mathbf{M}}_1 \cdot \tilde{\mathbf{M}}_2$ . These matrices we have derived before. We have two mode types, TM and TE.

We start with the TM modes. The resulting matrices for the two 2D films were given in (13.26) and for the gas film in (13.29), respectively. They are

$$\begin{aligned} \tilde{\mathbf{M}}_0^{\text{TM}} &= \begin{pmatrix} 1 & 0 \\ 0 & 1 \end{pmatrix} + \tilde{\alpha}^{2D} \gamma^{(0)} \begin{pmatrix} 1 & -1 \\ 1 & -1 \end{pmatrix}; \\ \tilde{\mathbf{M}}_1^{\text{TM}} &= \begin{pmatrix} 1 & 0 \\ 0 & 1 \end{pmatrix} + \frac{(\delta n) 2\pi k \alpha^{at}}{\gamma^{(0)}} \\ &\times \begin{pmatrix} -\left(\frac{\omega}{ck}\right)^2 & -\left[2 - \left(\frac{\omega}{ck}\right)^2\right] e^{2\gamma^{(0)} kd} \\ \left[2 - \left(\frac{\omega}{ck}\right)^2\right] e^{-2\gamma^{(0)} kd} & \left(\frac{\omega}{ck}\right)^2 \end{pmatrix}; \\ \tilde{\mathbf{M}}_2^{\text{TM}} &= \begin{pmatrix} 1 & 0 \\ 0 & 1 \end{pmatrix} + \tilde{\alpha}^{2D} \gamma^{(0)} \begin{pmatrix} 1 & -e^{2\gamma^{(0)} kD} \\ e^{-2\gamma^{(0)} kD} & -1 \end{pmatrix}. \end{aligned} \quad (13.93)$$

The matrix element of interest is

$$\begin{aligned} M_{11}^{\text{TM}} &= (1 + \gamma^{(0)} \tilde{\alpha}^{2D})^2 \left[ 1 - \frac{2\pi k \delta n \alpha^{at}}{\gamma^{(0)}} \left(\frac{\omega}{ck}\right)^2 \right] \\ &- e^{-2\gamma^{(0)} kD} (\gamma^{(0)} \tilde{\alpha}^{2D})^2 \left[ 1 + \frac{2\pi k \delta n \alpha^{at}}{\gamma^{(0)}} \left(\frac{\omega}{ck}\right)^2 \right] \\ &+ \frac{2\pi k \delta n \alpha^{at}}{\gamma^{(0)}} \left\{ e^{-2\gamma^{(0)} k(D-d)} (\gamma^{(0)} \tilde{\alpha}^{2D}) [(\gamma^{(0)} \tilde{\alpha}^{2D}) + 1] \left[ \left(\frac{\omega}{ck}\right)^2 - 2 \right] \right. \\ &\left. + e^{-2\gamma^{(0)} kd} (\gamma^{(0)} \tilde{\alpha}^{2D}) [(\gamma^{(0)} \tilde{\alpha}^{2D}) + 1] \left[ \left(\frac{\omega}{ck}\right)^2 - 2 \right] \right\}. \end{aligned} \quad (13.94)$$

The first term is the mode condition when all three films are at infinite distance from each other. The mode condition function after division with the part of the function that is independent of the position of the gas layer is

$$\tilde{f}_{\mathbf{k}}^{\text{TM}} = 1 + \frac{2\pi k \delta n \alpha^{at}(\omega)}{\gamma^{(0)}} \frac{\left[ e^{-2\gamma^{(0)} k(D-d)} + e^{-2\gamma^{(0)} kd} \right] \left[ \left(\frac{\omega}{ck}\right)^2 - 2 \right] \frac{\gamma^{(0)} \tilde{\alpha}^{2D}}{1 + \gamma^{(0)} \tilde{\alpha}^{2D}}}{1 - e^{-2\gamma^{(0)} kD} \left( \frac{\gamma^{(0)} \tilde{\alpha}^{2D}}{1 + \gamma^{(0)} \tilde{\alpha}^{2D}} \right)^2}, \quad (13.95)$$

where the suppressed function arguments are  $(k, \omega)$ . If we instead had divided by the function in absence of the atom we would get one extra energy term that is independent of the position of the atom and does not affect the force. It gives a different contribution to the energy than the result from (13.64) due to the presence of the two 2D sheets. It means a modification of the atom self-energy. The interaction energy per atom from the TM modes becomes

$$\begin{aligned} \frac{E^{\text{TM}}}{n\delta} &= -\hbar \int_0^\infty dk k^2 \int_{-\infty}^\infty \frac{d\xi}{2\pi} \frac{1}{2\gamma^{(0)}} \alpha^{at} (i\xi) \left[ \left( \frac{\xi}{ck} \right)^2 + 2 \right] \\ &\times \frac{\frac{\gamma^{(0)} \tilde{\alpha}^{2D}}{1+\gamma^{(0)} \tilde{\alpha}^{2D}} \left[ e^{-2\gamma^{(0)} kd} + e^{-2\gamma^{(0)} k(D-d)} \right]}{\left[ 1 - e^{-2\gamma^{(0)} kD} \left( \frac{\gamma^{(0)} \tilde{\alpha}^{2D}}{1+\gamma^{(0)} \tilde{\alpha}^{2D}} \right)^2 \right]}, \end{aligned} \quad (13.96)$$

where the suppressed function arguments are  $(k, i\xi)$ . Thus, the force on the atom from the TM modes is

$$\begin{aligned} F^{\text{TM}}(d) &= -\hbar \int_0^\infty dk k^3 \int_{-\infty}^\infty \frac{d\xi}{2\pi} \alpha^{at} (i\xi) \left[ \left( \frac{\xi}{ck} \right)^2 + 2 \right] \\ &\times \frac{\frac{\gamma^{(0)} \tilde{\alpha}^{2D}}{1+\gamma^{(0)} \tilde{\alpha}^{2D}} \left[ e^{-2\gamma^{(0)} kd} - e^{-2\gamma^{(0)} k(D-d)} \right]}{\left[ 1 - e^{-2\gamma^{(0)} kD} \left( \frac{\gamma^{(0)} \tilde{\alpha}^{2D}}{1+\gamma^{(0)} \tilde{\alpha}^{2D}} \right)^2 \right]}, \end{aligned} \quad (13.97)$$

and at finite temperature it is

$$\begin{aligned} F^{\text{TM}}(d) &= -\frac{2}{\beta} \int_0^\infty dk k^3 \sum_{\xi_n} \alpha^{at} (i\xi_n) \left[ \left( \frac{\xi_n}{ck} \right)^2 + 2 \right] \\ &\times \frac{\frac{\gamma^{(0)} \tilde{\alpha}^{2D}}{1+\gamma^{(0)} \tilde{\alpha}^{2D}} \left[ e^{-2\gamma^{(0)} kd} - e^{-2\gamma^{(0)} k(D-d)} \right]}{\left[ 1 - e^{-2\gamma^{(0)} kD} \left( \frac{\gamma^{(0)} \tilde{\alpha}^{2D}}{1+\gamma^{(0)} \tilde{\alpha}^{2D}} \right)^2 \right]}, \end{aligned} \quad (13.98)$$

where the suppressed function arguments are  $(k, i\xi_n)$ .

Now, we continue with the TE modes. The resulting matrices for the two 2D films were given in (13.26) and for the gas film in (13.29), respectively. They are

$$\begin{aligned} \tilde{\mathbf{M}}_0^{\text{TE}} &= \begin{pmatrix} 1 & 0 \\ 0 & 1 \end{pmatrix} + \tilde{\alpha}^{2D} \left( \frac{\omega}{ck} \right)^2 \frac{1}{\gamma^{(0)}} \begin{pmatrix} -1 & -1 \\ 1 & 1 \end{pmatrix}; \\ \tilde{\mathbf{M}}_1^{\text{TE}} &= \begin{pmatrix} 1 & 0 \\ 0 & 1 \end{pmatrix} + \frac{(\delta n) 2\pi k \alpha^{at}}{\gamma^{(0)}} \left( \frac{\omega}{ck} \right)^2 \begin{pmatrix} -1 & -e^{-2\gamma^{(0)} kd} \\ e^{-2\gamma^{(0)} kd} & 1 \end{pmatrix}; \\ \tilde{\mathbf{M}}_2^{\text{TE}} &= \begin{pmatrix} 1 & 0 \\ 0 & 1 \end{pmatrix} + \tilde{\alpha}^{2D} \left( \frac{\omega}{ck} \right)^2 \frac{1}{\gamma^{(0)}} \begin{pmatrix} -1 & -e^{-2\gamma^{(0)} kD} \\ e^{-2\gamma^{(0)} kD} & 1 \end{pmatrix}. \end{aligned} \quad (13.99)$$

The matrix element of interest is

$$\begin{aligned} M_{11}^{\text{TE}} &= \left[ 1 - \tilde{\alpha}^{2D} \left( \frac{\omega}{ck} \right)^2 \frac{1}{\gamma^{(0)}} \right]^2 - \left( \tilde{\alpha}^{2D} \left( \frac{\omega}{ck} \right)^2 \frac{1}{\gamma^{(0)}} \right)^2 e^{-2\gamma^{(0)} kD} \\ &- \frac{(\delta n) 2\pi k \alpha^{at}}{\gamma^{(0)}} \left( \frac{\omega}{ck} \right)^2 \left[ 1 - 2\tilde{\alpha}^{2D} \left( \frac{\omega}{ck} \right)^2 \frac{1}{\gamma^{(0)}} \right]^2 \\ &- \frac{(\delta n) 2\pi k \alpha^{at}}{\gamma^{(0)}} \left( \frac{\omega}{ck} \right)^2 \tilde{\alpha}^{2D} \left( \frac{\omega}{ck} \right)^2 \frac{1}{\gamma^{(0)}} \left( e^{-2\gamma^{(0)} kd} + e^{-2\gamma^{(0)} k(D-d)} \right) \\ &+ \frac{(\delta n) 2\pi k \alpha^{at}}{\gamma^{(0)}} \left( \frac{\omega}{ck} \right)^2 \left[ \tilde{\alpha}^{2D} \left( \frac{\omega}{ck} \right)^2 \right]^2 \left[ e^{-2\gamma^{(0)} kd} - e^{-2\gamma^{(0)} kD} + e^{-2\gamma^{(0)} k(D-d)} \right]. \end{aligned} \quad (13.100)$$

The first term is the mode condition when all three films are at infinite distance from each other. The mode condition function after division with the part of the function that is independent of the position of the gas layer is

$$\tilde{f}_k^{\text{TE}} = 1 - \frac{(\delta n)2\pi k\alpha^{at}}{\gamma^{(0)}} \left(\frac{\omega}{ck}\right)^2 \frac{\left[\frac{\bar{a}^{2D}\left(\frac{\omega}{ck}\right)^2}{\gamma^{(0)} - \bar{a}^{2D}\left(\frac{\omega}{ck}\right)^2}\right] \left(e^{-2\gamma^{(0)}kd} + e^{-2\gamma^{(0)}k(D-d)}\right)}{1 - \left[\frac{\bar{a}^{2D}\left(\frac{\omega}{ck}\right)^2}{\gamma^{(0)} - \bar{a}^{2D}\left(\frac{\omega}{ck}\right)^2}\right]^2 e^{-2\gamma^{(0)}kD}}, \quad (13.101)$$

where the suppressed function arguments are  $(k, \omega)$ .

The interaction energy per atom from the TE modes becomes

$$\frac{E^{\text{TE}}}{n\delta} = -\hbar \int_0^\infty dk k^2 \int_{-\infty}^\infty \frac{d\xi}{2\pi} \frac{\alpha^{at}}{\gamma^{(0)}} \left(\frac{\xi}{ck}\right)^2 \frac{\left[\frac{\bar{a}^{2D}\left(\frac{\xi}{ck}\right)^2}{\gamma^{(0)} + \bar{a}^{2D}\left(\frac{\xi}{ck}\right)^2}\right] \left(e^{-2\gamma^{(0)}kd} + e^{-2\gamma^{(0)}k(D-d)}\right)}{1 - \left[\frac{\bar{a}^{2D}\left(\frac{\xi}{ck}\right)^2}{\gamma^{(0)} + \bar{a}^{2D}\left(\frac{\xi}{ck}\right)^2}\right]^2 e^{-2\gamma^{(0)}kD}}, \quad (13.102)$$

where the suppressed function arguments are  $(k, i\xi)$ . Thus, the force on the atom from the TE modes is

$$F^{\text{TE}}(d) = -2\hbar \int_0^\infty dk k^3 \int_{-\infty}^\infty \frac{d\xi}{2\pi} \alpha^{at} \left(\frac{\xi}{ck}\right)^2 \frac{\left[\frac{\bar{a}^{2D}\left(\frac{\xi}{ck}\right)^2}{\gamma^{(0)} + \bar{a}^{2D}\left(\frac{\xi}{ck}\right)^2}\right] \left(e^{-2\gamma^{(0)}kd} - e^{-2\gamma^{(0)}k(D-d)}\right)}{1 - \left[\frac{\bar{a}^{2D}\left(\frac{\xi}{ck}\right)^2}{\gamma^{(0)} + \bar{a}^{2D}\left(\frac{\xi}{ck}\right)^2}\right]^2 e^{-2\gamma^{(0)}kD}}, \quad (13.103)$$

and at finite temperature it is

$$F^{\text{TE}}(d) = -\frac{1}{\beta} \int_0^\infty dk k^3 \sum_{\xi_n} '4\alpha^{at} \left(\frac{\xi_n}{ck}\right)^2 \frac{\left[\frac{\bar{a}^{2D}\left(\frac{\xi_n}{ck}\right)^2}{\gamma^{(0)} + \bar{a}^{2D}\left(\frac{\xi_n}{ck}\right)^2}\right] \left(e^{-2\gamma^{(0)}kd} - e^{-2\gamma^{(0)}k(D-d)}\right)}{1 - \left[\frac{\bar{a}^{2D}\left(\frac{\xi_n}{ck}\right)^2}{\gamma^{(0)} + \bar{a}^{2D}\left(\frac{\xi_n}{ck}\right)^2}\right]^2 e^{-2\gamma^{(0)}kD}}, \quad (13.104)$$

where the suppressed function arguments are  $(k, i\xi_n)$ . Now we are done with the selection of planar geometries. In next section we present some complementary methods to derive the normal modes in some of the geometries we have discussed above.

## 13.11 Alternative Derivations of the Normal Modes

In this section we give several complementary ways to derive the normal modes in specific planar geometries. A non-retarded version was given in Sect. 9.11. The geometries we consider are two parallel 2D films, a 2D film next to a wall, and two half spaces. For the geometries containing 2D films we rather closely follow the treatments in [7]. We begin with the modes in a system consisting of two parallel 2D films.

### 13.11.1 Two 2D Films

We will use two alternative derivations to find the normal modes. In one approach the modes are generated from coupled induced sources; in the other approach we solve Maxwell's equations in the three regions separated by the two films and use the standard boundary conditions at the boundaries defined by the films. We begin with the method involving coupled sources.

#### 13.11.1.1 Coupled Induced Sources

This approach could be executed in several different ways. One option would be to proceed in a way analogous to how we derived the modes in the non-retarded treatment in Sect. 9.11.1.1. Then we would start with a current density (longitudinal or transverse) in film 1. This current density would give rise to an electric field in film 2; this field would induce a current density in film 2; this current density in film 2 would give rise to an electric field in film 1, which would cause an induced current density in film 1. Letting this current density be the one we had started with would close the loop and produce self-sustained fields, normal modes. When the current densities and electric fields are longitudinal<sup>1</sup> the modes are of TM type and the TE modes are the results when the current densities and fields are transverse (see Sect. 2.7).

To make the presentation more interesting and varied we proceed in a slightly different way. We start with two films, 1 and 2. The electric field in film 1 has contributions from both films and the induced current density in film 1 is the conductivity of film 1 times the electric field in film 1. The corresponding is valid for film 2.

We begin with the TM modes. The longitudinal field in film 1 is according to (2.120) and (2.121) in vacuum given by

$$E_{\parallel}^1(\mathbf{k}, \omega) = -i2\pi (k/\omega) \gamma^{(0)}(k, \omega) \left[ K_{\parallel}^1(\mathbf{k}, \omega) + e^{-\gamma^{(0)}(k, \omega)kd} K_{\parallel}^2(\mathbf{k}, \omega) \right], \quad (13.105)$$

and the induced current density is

$$\begin{aligned} K_{\parallel}^1(\mathbf{k}, \omega) &= \tilde{\sigma}_{\parallel}^1(\mathbf{k}, \omega) E_{\parallel}^1(\mathbf{k}, \omega) \\ &= -i\tilde{\sigma}_{\parallel}^1(\mathbf{k}, \omega) 2\pi (k/\omega) \gamma^{(0)}(k, \omega) \left[ K_{\parallel}^1(\mathbf{k}, \omega) + e^{-\gamma^{(0)}(k, \omega)kd} K_{\parallel}^2(\mathbf{k}, \omega) \right] \\ &= -\tilde{\alpha}_{\parallel}^1(\mathbf{k}, \omega) \gamma^{(0)}(k, \omega) \left[ K_{\parallel}^1(\mathbf{k}, \omega) + e^{-\gamma^{(0)}(k, \omega)kd} K_{\parallel}^2(\mathbf{k}, \omega) \right], \end{aligned} \quad (13.106)$$

where we have made use of the relation between  $\tilde{\sigma}$  and  $\tilde{\alpha}$  obtained from (2.140). The induced current density in film 2 is obtained by interchanging the superscripts. Thus we have

---

<sup>1</sup>With longitudinal and transverse fields we here mean in-plane components that are parallel and perpendicular, respectively, to the in-plane wave vector  $\mathbf{k}$ .

$$\begin{aligned} K_{\parallel}^1(\mathbf{k}, \omega) &= -\tilde{\alpha}_{\parallel}^1(\mathbf{k}, \omega) \gamma^{(0)}(k, \omega) \left[ K_{\parallel}^1(\mathbf{k}, \omega) + e^{-\gamma^{(0)}(k, \omega)kd} K_{\parallel}^2(\mathbf{k}, \omega) \right]; \\ K_{\parallel}^2(\mathbf{k}, \omega) &= -\tilde{\alpha}_{\parallel}^2(\mathbf{k}, \omega) \gamma^{(0)}(k, \omega) \left[ e^{-\gamma^{(0)}(k, \omega)kd} K_{\parallel}^1(\mathbf{k}, \omega) + K_{\parallel}^2(\mathbf{k}, \omega) \right]. \end{aligned} \quad (13.107)$$

On matrix form this becomes

$$\begin{pmatrix} -\tilde{\alpha}_{\parallel}^1 \gamma^{(0)} - 1 & -e^{-\gamma^{(0)}kd} \tilde{\alpha}_{\parallel}^1 \gamma^{(0)} \\ -e^{-\gamma^{(0)}kd} \tilde{\alpha}_{\parallel}^2 \gamma^{(0)} - 1 & -\tilde{\alpha}_{\parallel}^2 \gamma^{(0)} \end{pmatrix} \cdot \begin{pmatrix} K_{\parallel}^1 \\ K_{\parallel}^2 \end{pmatrix} = 0. \quad (13.108)$$

We have omitted all function arguments,  $(\mathbf{k}, \omega)$ . To get the non-trivial solution to this system of equations we let the determinant of the matrix be equal to zero. The mode condition function then becomes

$$f_{\mathbf{k}}^{\text{TM}}(\omega) = 1 - e^{-2\gamma^{(0)}(k, \omega)kd} \frac{\gamma^{(0)}(k, \omega) \tilde{\alpha}_{\parallel}^1(\mathbf{k}, \omega) \gamma^{(0)}(k, \omega) \tilde{\alpha}_{\parallel}^2(\mathbf{k}, \omega)}{\left[1 + \gamma^{(0)}(k, \omega) \tilde{\alpha}_{\parallel}^1(\mathbf{k}, \omega)\right] \left[1 + \gamma^{(0)}(k, \omega) \tilde{\alpha}_{\parallel}^2(\mathbf{k}, \omega)\right]}, \quad (13.109)$$

where we have let the reference system be standard one in which the films are at infinite separation.

For the TE modes we need the transverse fields. They are according to (2.120) and (2.121) found to be

$$\begin{aligned} E_{\perp}^1(\mathbf{k}, \omega) &= \frac{i\omega}{c^2} \frac{2\pi}{k\gamma^{(0)}(k, \omega)} \left[ K_{\perp}^1(\mathbf{k}, \omega) + e^{-\gamma^{(0)}(k, \omega)kd} K_{\perp}^2(\mathbf{k}, \omega) \right]; \\ E_{\perp}^2(\mathbf{k}, \omega) &= \frac{i\omega}{c^2} \frac{2\pi}{k\gamma^{(0)}(k, \omega)} \left[ e^{-\gamma^{(0)}(k, \omega)kd} K_{\perp}^1(\mathbf{k}, \omega) + K_{\perp}^2(\mathbf{k}, \omega) \right], \end{aligned} \quad (13.110)$$

and the induced current densities are in analogy with (13.106) given by

$$\begin{aligned} K_{\perp}^1(\mathbf{k}, \omega) &= \frac{(\omega/c k)^2 \tilde{\alpha}_{\perp}^1}{\gamma^{(0)}(k, \omega)} \left[ K_{\perp}^1(\mathbf{k}, \omega) + e^{-\gamma^{(0)}(k, \omega)kd} K_{\perp}^2(\mathbf{k}, \omega) \right]; \\ K_{\perp}^2(\mathbf{k}, \omega) &= \frac{(\omega/c k)^2 \tilde{\alpha}_{\perp}^2}{\gamma^{(0)}(k, \omega)} \left[ e^{-\gamma^{(0)}(k, \omega)kd} K_{\perp}^1(\mathbf{k}, \omega) + K_{\perp}^2(\mathbf{k}, \omega) \right], \end{aligned} \quad (13.111)$$

or on matrix form

$$\begin{pmatrix} \frac{(\omega/c k)^2 \tilde{\alpha}_{\perp}^1}{\gamma^{(0)}(k, \omega)} - 1 & \frac{e^{-\gamma^{(0)}(k, \omega)kd} (\omega/c k)^2 \tilde{\alpha}_{\perp}^1}{\gamma^{(0)}(k, \omega)} \\ \frac{(\omega/c k)^2 \tilde{\alpha}_{\perp}^2}{\gamma^{(0)}(k, \omega)} e^{-\gamma^{(0)}(k, \omega)kd} & \frac{(\omega/c k)^2 \tilde{\alpha}_{\perp}^2}{\gamma^{(0)}(k, \omega)} - 1 \end{pmatrix} \cdot \begin{pmatrix} K_{\perp}^1(\mathbf{k}, \omega) \\ K_{\perp}^2(\mathbf{k}, \omega) \end{pmatrix} = 0. \quad (13.112)$$

The condition for TE modes is found by letting the determinant of the matrix be zero. This results in the mode condition function,

$$f_{\mathbf{k}}^{\text{TE}}(\omega) = 1 - e^{-2\gamma^{(0)}(k, \omega)kd} \frac{\left[ (\omega/c k)^2 \tilde{\alpha}_{\perp}^1 \right] \left[ (\omega/c k)^2 \tilde{\alpha}_{\perp}^2 \right]}{\left[ \gamma^{(0)}(k, \omega) - (\omega/c k)^2 \tilde{\alpha}_{\perp}^1 \right] \left[ \gamma^{(0)}(k, \omega) - (\omega/c k)^2 \tilde{\alpha}_{\perp}^2 \right]}, \quad (13.113)$$

where we have chosen as reference system the geometry when the films are infinitely apart.<sup>2</sup> Now we continue with the second approach.

### 13.11.1.2 Maxwell's Equations and Boundary Conditions

The normal modes can be found from self-sustained charge- and current-densities, from self-sustained potentials or from self-sustained fields. With the present approach, we find self-sustained fields. To do that we solve the MEs in all regions of the geometry and make use of the standard boundary conditions at all interfaces between the regions. For two 2D parallel films we need a geometry consisting of three regions and two interfaces, 1|2|3. This geometry gives the mode condition function

$$f_{\mathbf{k}} = 1 - e^{-2\gamma_2 kd} r_{21} r_{23}, \quad (13.114)$$

where  $r_{ij}$  is the amplitude reflection coefficient for a wave impinging on the interface between medium  $i$  and  $j$  from the  $i$  side,  $d$  is the thickness of region 2, and  $\gamma_i = \sqrt{1 - \tilde{n}_i(\omega)^2} (\omega/ck)$ . The function  $\tilde{n}_i(\omega)$  is the index of refraction for medium  $i$ . We are interested in two free standing 2D films but we take the opportunity to be more general and allow all three media separated by the films be of different materials. At the end we let them all be vacuum.

At an interface where there is no 2D sheet the TM and TE amplitude reflection coefficients are (2.87) [2]

$$r_{ij}^{\text{TM}} = \frac{\tilde{\epsilon}_j \gamma_i - \tilde{\epsilon}_i \gamma_j}{\tilde{\epsilon}_j \gamma_i + \tilde{\epsilon}_i \gamma_j}, \quad (13.115)$$

and

$$r_{ij}^{\text{TE}} = \frac{\tilde{\mu}_j \gamma_i - \tilde{\mu}_i \gamma_j}{\tilde{\mu}_j \gamma_i + \tilde{\mu}_i \gamma_j}, \quad (13.116)$$

respectively. Note that  $r_{ji} = -r_{ij}$  holds for both mode types.

The presence of a 2D film at the interface modifies the amplitude reflection coefficients. We treat the 2D film at the interface as external to our system which means that fields will induce external surface- charge and current-densities at the interface. Two of the boundary conditions are enough to determine the modified Fresnel coefficients. The other two are redundant. We choose the following two (see Sect. 2.5):

$$\begin{aligned} (\mathbf{E}_2 - \mathbf{E}_1) \times \mathbf{n} &= 0, \\ (\tilde{\mathbf{H}}_2 - \tilde{\mathbf{H}}_1) \times \mathbf{n} &= -\frac{4\pi}{c} \mathbf{K}_{ext} = -\frac{4\pi}{c} \tilde{\sigma} \mathbf{n} \times (\mathbf{E} \times \mathbf{n}), \end{aligned} \quad (13.117)$$

<sup>2</sup>Note that we here have been a little more careful and distinguished between transverse and longitudinal polarizabilities. They become equal in the limit of zero  $k$ , which is the limit taken when spatial dispersion is neglected. However, like in the present case, when spatial dispersion is included the difference could have a minor effect on the results.

where  $\tilde{\sigma}$  is the conductivity of the 2D sheet. The modified amplitude reflection coefficient for a TM mode is [10]

$$r_{ij}^{\text{TM}} = \frac{\tilde{\epsilon}_j \gamma_i - \tilde{\epsilon}_i \gamma_j + 2\gamma_i \gamma_j \tilde{\alpha}_{\parallel}}{\tilde{\epsilon}_j \gamma_i + \tilde{\epsilon}_i \gamma_j + 2\gamma_i \gamma_j \tilde{\alpha}_{\parallel}}, \quad (13.118)$$

where the polarizability of the 2D sheet is obtained from the dynamical conductivity according to (2.140). For TM modes the tangential component of the electric field, which will induce the external current, is parallel to  $\mathbf{k}$ , so the longitudinal 2D dielectric function of the film enters. The bound charges in the 2D sheet also contribute to the dynamical conductivity and the polarizability.

The modified amplitude reflection coefficient for a TE mode is [10]

$$r_{ij}^{\text{TE}} = \frac{\tilde{\mu}_j \gamma_i - \tilde{\mu}_i \gamma_j + 2(\omega/c k)^2 \tilde{\alpha}_{\perp}}{\tilde{\mu}_j \gamma_i + \tilde{\mu}_i \gamma_j - 2(\omega/c k)^2 \tilde{\alpha}_{\perp}}, \quad (13.119)$$

where the polarizability of the 2D sheet is obtained from the dynamical conductivity according to (2.140). For a TE wave the electric field is perpendicular to  $\mathbf{k}$ , so the transverse 2D dielectric function of the film enters. The bound charges in the 2D sheet also contribute to the dynamical conductivity and the polarizability.

These results are very useful. When we have geometrical structures with 2D films at some of the interfaces we just substitute the new reflection coefficients at the proper interfaces. Note that the relation  $r_{ij} = -r_{ji}$  is no longer valid so one has to be careful when making the substitutions. One might have used this relation to arrive at the starting expression. For the three regions system 1|2|3 we find the most general<sup>3</sup> mode condition functions as

$$\begin{aligned} f_{\mathbf{k}} &= 1 - e^{-2\gamma_2 kd} r_{21} r_{23}; \\ f_{\mathbf{k}}^{\text{TM}}(\omega) &= 1 - e^{-2\gamma_2 kd} \left[ \frac{\tilde{\epsilon}_1 \gamma_2 - \tilde{\epsilon}_2 \gamma_1 + 2\gamma_1 \gamma_2 \tilde{\alpha}_{\parallel}^L}{\tilde{\epsilon}_1 \gamma_2 + \tilde{\epsilon}_2 \gamma_1 + 2\gamma_1 \gamma_2 \tilde{\alpha}_{\parallel}^L} \right] \left[ \frac{\tilde{\epsilon}_3 \gamma_2 - \tilde{\epsilon}_2 \gamma_3 + 2\gamma_2 \gamma_3 \tilde{\alpha}_{\parallel}^R}{\tilde{\epsilon}_3 \gamma_2 + \tilde{\epsilon}_2 \gamma_3 + 2\gamma_2 \gamma_3 \tilde{\alpha}_{\parallel}^R} \right]; \\ f_{\mathbf{k}}^{\text{TE}}(\omega) &= 1 - e^{-2\gamma_2 kd} \left[ \frac{\tilde{\mu}_1 \gamma_2 - \tilde{\mu}_2 \gamma_1 + 2(\omega/c k)^2 \tilde{\alpha}_{\perp}^L}{\tilde{\mu}_1 \gamma_2 + \tilde{\mu}_2 \gamma_1 - 2(\omega/c k)^2 \tilde{\alpha}_{\perp}^L} \right] \left[ \frac{\tilde{\mu}_3 \gamma_2 - \tilde{\mu}_2 \gamma_3 + 2(\omega/c k)^2 \tilde{\alpha}_{\perp}^R}{\tilde{\mu}_3 \gamma_2 + \tilde{\mu}_2 \gamma_3 - 2(\omega/c k)^2 \tilde{\alpha}_{\perp}^R} \right], \end{aligned} \quad (13.120)$$

where we assumed that there are 2D sheets at both interfaces. These sheets may be different so we have put the superscripts  $L$  and  $R$  on the polarizability of the left and right sheet, respectively.

It is straight forward to find the results for two freestanding 2D sheets from our geometry by letting all three media be vacuum. Then the mode condition functions in (13.120) reduce to

$$\begin{aligned} f_{\mathbf{k}}^{\text{TM}}(\omega) &= 1 - e^{-2\gamma^{(0)} kd} \left[ \frac{\gamma^{(0)} \tilde{\alpha}_{\parallel}^1(k, \omega)}{1 + \gamma^{(0)} \tilde{\alpha}_{\parallel}^1(k, \omega)} \right] \left[ \frac{\gamma^{(0)} \tilde{\alpha}_{\parallel}^2(k, \omega)}{1 + \gamma^{(0)} \tilde{\alpha}_{\parallel}^2(k, \omega)} \right]; \\ f_{\mathbf{k}}^{\text{TE}}(\omega) &= 1 - e^{-2\gamma^{(0)} kd} \left[ \frac{(\omega/c k)^2 \tilde{\alpha}_{\perp}^1(k, \omega)}{\gamma^{(0)} - (\omega/c k)^2 \tilde{\alpha}_{\perp}^1(k, \omega)} \right] \left[ \frac{(\omega/c k)^2 \tilde{\alpha}_{\perp}^2(k, \omega)}{\gamma^{(0)} - (\omega/c k)^2 \tilde{\alpha}_{\perp}^2(k, \omega)} \right]. \end{aligned} \quad (13.121)$$

<sup>3</sup>Note that we have not excluded possible magnetic effects, i.e., we have allowed  $\tilde{\mu}$  to be different from unity.

These mode condition functions agree with what we found in (13.44) and (13.47), respectively.

Next we treat the geometry of a 2D film parallel to a wall.

### 13.11.2 A 2D Film Next to a Wall

Also here we will use two alternative derivations to find the normal modes. In one approach the modes are generated from coupled induced sources; in the other approach we solve Maxwell's equations in the three regions separated by the film and the wall surface and use the standard boundary conditions at the boundaries defined by these interfaces. We begin with the method involving coupled sources.

#### 13.11.2.1 Coupled Induced Sources

When a 2D film is placed next to a wall there will be induced current densities at the interface. The effect of these densities can be obtained in a much simpler way using mirror images. How these mirror images look like was derived in Sect. 2.7.2 for a more complex system where the 2D film is embedded in a medium. For our system the mirror-image current-densities are

$$\begin{aligned} K_{\parallel}'(\mathbf{k}, \omega) &= \frac{\gamma_s - \tilde{\epsilon}_s(\omega) \gamma^{(0)}}{\gamma_s + \tilde{\epsilon}_s(\omega) \gamma^{(0)}} K_{\parallel}(\mathbf{k}, \omega); \\ K_{\perp}'(\mathbf{k}, \omega) &= \frac{\tilde{\mu}_s(\omega) \gamma^{(0)} - \gamma_s}{\tilde{\mu}_s(\omega) \gamma^{(0)} + \gamma_s} K_{\perp}(\mathbf{k}, \omega), \end{aligned} \quad (13.122)$$

when  $K_{\parallel}(\mathbf{k}, \omega)$  and  $K_{\perp}(\mathbf{k}, \omega)$  are the actual longitudinal and transverse, respectively, current densities in the 2D film. These mirror images are at a distance  $d$  from the wall surface and inside the wall. We have suppressed the argument  $(k, \omega)$  in all  $\gamma$ -functions. The coupled longitudinal current densities give rise to TM modes and the transverse to TE modes.

We start with the TM modes. The resulting longitudinal electric fields from a longitudinal current density was derived in (2.120) and (2.121). The field in the 2D film is

$$E_{\parallel}(\mathbf{k}, \omega) = -i2\pi (k/\omega) \gamma^{(0)}(k, \omega) \left[ K_{\parallel}(\mathbf{k}, \omega) + e^{-2\gamma^{(0)}kd} K_{\parallel}'(\mathbf{k}, \omega) \right]. \quad (13.123)$$

We close the loop by noting that the current density in the 2D film is the conductivity times the electric field. Thus,

$$\begin{aligned} K_{\parallel}(\mathbf{k}, \omega) &= \tilde{\sigma}_{\parallel}(\mathbf{k}, \omega) E_{\parallel}(\mathbf{k}, \omega) \\ &= -\underbrace{2\pi i \tilde{\sigma}_{\parallel}(\mathbf{k}, \omega)}_{\tilde{\alpha}_{\parallel}(\mathbf{k}, \omega)} (k/\omega) \gamma^{(0)} \left[ K_{\parallel}(\mathbf{k}, \omega) + e^{-2\gamma^{(0)}kd} K_{\parallel}'(\mathbf{k}, \omega) \right] \\ &= -\tilde{\alpha}_{\parallel}(\mathbf{k}, \omega) \gamma^{(0)} \left[ 1 + e^{-2\gamma^{(0)}kd} \frac{\gamma_s - \tilde{\epsilon}_s(\omega) \gamma^{(0)}}{\gamma_s + \tilde{\epsilon}_s(\omega) \gamma^{(0)}} \right] K_{\parallel}(\mathbf{k}, \omega), \end{aligned} \quad (13.124)$$

where we have used (13.122) in the last step to eliminate the mirror density. We may now use the first and last parts of this equation to find

$$\left\{ 1 + \tilde{\alpha}_{\parallel}(\mathbf{k}, \omega) \gamma^{(0)} \left[ 1 + e^{-2\gamma^{(0)}kd} \frac{\gamma_s - \tilde{\epsilon}_s(\omega)\gamma^{(0)}}{\gamma_s + \tilde{\epsilon}_s(\omega)\gamma^{(0)}} \right] \right\} K_{\parallel}(\mathbf{k}, \omega) = 0. \quad (13.125)$$

This equation has the trivial solution that the current density is zero. There are non-trivial solutions, the normal modes, if what is inside the curly brackets is zero. This leads to the mode condition function for TM modes,

$$f_{\mathbf{k}}^{\text{TM}}(\omega) = 1 - e^{-2\gamma^{(0)}kd} \left[ \frac{\gamma^{(0)}\tilde{\alpha}_{\parallel}(\mathbf{k}, \omega)}{1 + \gamma^{(0)}\tilde{\alpha}_{\parallel}(\mathbf{k}, \omega)} \right] \left[ \frac{\tilde{\epsilon}_s(\omega)\gamma^{(0)} - \gamma_s}{\tilde{\epsilon}_s(\omega)\gamma^{(0)} + \gamma_s} \right], \quad (13.126)$$

where we have chosen as reference system the system when the 2D film is at infinite distance from the wall. This is in agreement with (13.56).

Now, we proceed with the TE modes. The resulting transverse electric fields from a transverse current density was derived in (2.120) and (2.121). The field in the 2D film is

$$E_{\perp}(\mathbf{k}, \omega) = \frac{i\omega}{c^2} \frac{2\pi}{k\gamma^{(0)}} \left[ K_{\perp}(\mathbf{k}, \omega) + e^{-2\gamma^{(0)}kd} K'_{\perp}(\mathbf{k}, \omega) \right]. \quad (13.127)$$

We close the loop by noting that the current density in the 2D film is the conductivity times the electric field. Thus,

$$\begin{aligned} K_{\perp}(\mathbf{k}, \omega) &= \tilde{\sigma}_{\perp}(\mathbf{k}, \omega) E_{\perp}(\mathbf{k}, \omega) \\ &= \frac{\omega^2}{\gamma^{(0)}(ck)^2} \underbrace{2\pi i \tilde{\sigma}_{\perp}(\mathbf{k}, \omega)}_{\tilde{\alpha}_{\perp}(\mathbf{k}, \omega)} (k/\omega) \left[ K_{\perp}(\mathbf{k}, \omega) + e^{-2\gamma^{(0)}kd} K'_{\perp}(\mathbf{k}, \omega) \right] \\ &= \tilde{\alpha}_{\perp}(\mathbf{k}, \omega) \frac{(\omega/ck)^2}{\gamma^{(0)}} \left[ 1 + e^{-2\gamma^{(0)}kd} \frac{\tilde{\mu}_s(\omega)\gamma^{(0)} - \gamma_s}{\tilde{\mu}_s(\omega)\gamma^{(0)} + \gamma_s} \right] K_{\perp}(\mathbf{k}, \omega), \end{aligned} \quad (13.128)$$

where we have used (13.122) in the last step to eliminate the mirror density. We may now use the first and last parts of this equation to find

$$\left\{ 1 - \tilde{\alpha}_{\perp}(\mathbf{k}, \omega) \frac{(\omega/ck)^2}{\gamma^{(0)}} \left[ 1 + e^{-2\gamma^{(0)}kd} \frac{\tilde{\mu}_s(\omega)\gamma^{(0)} - \gamma_s}{\tilde{\mu}_s(\omega)\gamma^{(0)} + \gamma_s} \right] \right\} K_{\perp}(\mathbf{k}, \omega) = 0. \quad (13.129)$$

This has the trivial solution that the current density is zero. There are non-trivial solutions, the normal modes, if what is inside the curly brackets is zero. This leads to the mode condition function for TE modes,

$$f_{\mathbf{k}}^{\text{TE}}(\omega) = 1 - e^{-2\gamma^{(0)}kd} \frac{(\omega/ck)^2 \tilde{\alpha}_{\perp}(\mathbf{k}, \omega)}{\gamma^{(0)} - (\omega/ck)^2 \tilde{\alpha}_{\perp}(\mathbf{k}, \omega)} \frac{\tilde{\mu}_s(\omega)\gamma^{(0)} - \gamma_s}{\tilde{\mu}_s(\omega)\gamma^{(0)} + \gamma_s}, \quad (13.130)$$

where we have chosen as reference system the system when the 2D film is at infinite distance from the wall. This is in agreement with (13.57) in absence of magnetic effects.

### 13.11.2.2 Maxwell's Equations and Boundary Conditions

We obtain a freestanding 2D film next to a wall from our geometry in Sect. 13.11.1.2 by letting media 1 and 2 be vacuum, medium 3 be the wall and let  $\tilde{\alpha}_R = 0$ . Then the mode condition functions in (13.120) reduce to

$$\begin{aligned} f_{\mathbf{k}}^{\text{TM}}(\omega) &= 1 - e^{-2\gamma^{(0)}kd} \left[ \frac{\gamma^{(0)}\tilde{\alpha}_{\parallel}(\mathbf{k},\omega)}{1+\gamma^{(0)}\tilde{\alpha}_{\parallel}(\mathbf{k},\omega)} \right] \left[ \frac{\tilde{\epsilon}_s(\omega)\gamma^{(0)}-\gamma_s}{\tilde{\epsilon}_s(\omega)\gamma^{(0)}+\gamma_s} \right]; \\ f_{\mathbf{k}}^{\text{TE}}(\omega) &= 1 - e^{-2\gamma^{(0)}kd} \left[ \frac{(\omega/c k)^2\tilde{\alpha}_{\perp}(\mathbf{k},\omega)}{\gamma^{(0)}-(\omega/c k)^2\tilde{\alpha}_{\perp}(\mathbf{k},\omega)} \right] \frac{\tilde{\mu}_s(\omega)\gamma^{(0)}-\gamma_s}{\tilde{\mu}_s(\omega)\gamma^{(0)}+\gamma_s}. \end{aligned} \quad (13.131)$$

If retardation effects are neglected there are no TE modes and the mode condition function for TM modes is reduced further to

$$f_{\mathbf{k}}^{\text{TM}}(\omega) = 1 - e^{-2kd} \left[ \frac{\tilde{\alpha}_{\parallel}(\mathbf{k},\omega)}{1+\tilde{\alpha}_{\parallel}(\mathbf{k},\omega)} \right] \left[ \frac{\tilde{\epsilon}_s(\omega)-1}{\tilde{\epsilon}_s(\omega)+1} \right], \quad (13.132)$$

which is fully in line with what we obtained starting from the non-retarded theory.

Our last geometry is that of two half spaces and this is what we treat next.

### 13.11.3 Two Half Spaces

We have already in Sect. 5.4 derived the modes by solving the MEs and using the boundary conditions at the interfaces. We will here use another approach based on coupled induced sources. We use the notation in Fig. 5.14. In Sect. 2.7.2 we derived the mirror current densities caused by current densities in a 2D film embedded in a medium next to a wall. The results were given in (2.124) and (2.127). Here the sources are not coming from a 2D film. They are from self-induced mirror densities in the two half spaces. We should keep in mind that the actual current densities are at the interfaces and not inside the half spaces. One way to proceed would be to start from an image inside 1 at the distance  $d$  from the surface. It would produce an image in 3, now at the distance  $2d$  from the surface; its image in 1 would be at the distance  $3d$  from the surface and so on.

We will do it in an alternative way. In each step we will replace the mirror image with an effective image at the surface. Let us start with the longitudinal currents and begin with a mirror-image current-density in 3,  $K_{\parallel,3}'(\mathbf{k},\omega)$ , the distance  $d$  from the surface. Remember that this has the effect on 1 as if this current density were at the position  $2d$  from 1 and embedded in the medium 2. The same effect would the current density  $e^{-\gamma_2 kd} K_{\parallel,3}'(\mathbf{k},\omega)$  placed at the distance  $d$  have. Thus we have from (2.124)

$$K_{\parallel,1}'(\mathbf{k},\omega) = \frac{\tilde{\epsilon}_2\gamma_1 - \tilde{\epsilon}_1\gamma_2}{\tilde{\epsilon}_2\gamma_1 + \tilde{\epsilon}_1\gamma_2} K_{\parallel,3}'(\mathbf{k},\omega) e^{-\gamma_2 kd}. \quad (13.133)$$

In the same way we find

$$K_{\parallel,3}'(\mathbf{k}, \omega) = \frac{\tilde{\epsilon}_2\gamma_3 - \tilde{\epsilon}_3\gamma_2}{\tilde{\epsilon}_2\gamma_3 + \tilde{\epsilon}_3\gamma_2} K_{\parallel,1}'(\mathbf{k}, \omega) e^{-\gamma_2 kd}. \quad (13.134)$$

Substituting this result in (13.133) we find

$$K_{\parallel,1}'(\mathbf{k}, \omega) = \frac{\tilde{\epsilon}_2\gamma_1 - \tilde{\epsilon}_1\gamma_2}{\tilde{\epsilon}_2\gamma_1 + \tilde{\epsilon}_1\gamma_2} \frac{\tilde{\epsilon}_2\gamma_3 - \tilde{\epsilon}_3\gamma_2}{\tilde{\epsilon}_2\gamma_3 + \tilde{\epsilon}_3\gamma_2} K_{\parallel,1}'(\mathbf{k}, \omega) e^{-2\gamma_2 kd}, \quad (13.135)$$

and

$$\left[ 1 - e^{-2\gamma_2 kd} \frac{\tilde{\epsilon}_2\gamma_1 - \tilde{\epsilon}_1\gamma_2}{\tilde{\epsilon}_2\gamma_1 + \tilde{\epsilon}_1\gamma_2} \frac{\tilde{\epsilon}_2\gamma_3 - \tilde{\epsilon}_3\gamma_2}{\tilde{\epsilon}_2\gamma_3 + \tilde{\epsilon}_3\gamma_2} \right] K_{\parallel,1}'(\mathbf{k}, \omega) = 0. \quad (13.136)$$

A non-trivial solution demands that

$$1 - e^{-2\gamma_2 kd} \frac{\tilde{\epsilon}_2\gamma_1 - \tilde{\epsilon}_1\gamma_2}{\tilde{\epsilon}_2\gamma_1 + \tilde{\epsilon}_1\gamma_2} \frac{\tilde{\epsilon}_2\gamma_3 - \tilde{\epsilon}_3\gamma_2}{\tilde{\epsilon}_2\gamma_3 + \tilde{\epsilon}_3\gamma_2} = 0, \quad (13.137)$$

which is the mode condition for TM modes. Thus, the mode condition function is

$$f_{\mathbf{k}}^{\text{TM}}(\omega) = 1 - e^{-2\gamma_2(\mathbf{k}, \omega)kd} \frac{\tilde{\epsilon}_2(\omega)\gamma_1(\mathbf{k}, \omega) - \tilde{\epsilon}_1(\omega)\gamma_2(\mathbf{k}, \omega)}{\tilde{\epsilon}_2(\omega)\gamma_1(\mathbf{k}, \omega) + \tilde{\epsilon}_1(\omega)\gamma_2(\mathbf{k}, \omega)} \frac{\tilde{\epsilon}_2(\omega)\gamma_3(\mathbf{k}, \omega) - \tilde{\epsilon}_3(\omega)\gamma_2(\mathbf{k}, \omega)}{\tilde{\epsilon}_2(\omega)\gamma_3(\mathbf{k}, \omega) + \tilde{\epsilon}_3(\omega)\gamma_2(\mathbf{k}, \omega)}. \quad (13.138)$$

Proceeding in an analogous way with the transverse current densities we find

$$f_{\mathbf{k}}^{\text{TE}}(\omega) = 1 - e^{-2\gamma_2(\mathbf{k}, \omega)kd} \frac{\tilde{\mu}_2(\omega)\gamma_1(\mathbf{k}, \omega) - \tilde{\mu}_1(\omega)\gamma_2(\mathbf{k}, \omega)}{\tilde{\mu}_2(\omega)\gamma_1(\mathbf{k}, \omega) + \tilde{\mu}_1(\omega)\gamma_2(\mathbf{k}, \omega)} \frac{\tilde{\mu}_2(\omega)\gamma_3(\mathbf{k}, \omega) - \tilde{\mu}_3(\omega)\gamma_2(\mathbf{k}, \omega)}{\tilde{\mu}_2(\omega)\gamma_3(\mathbf{k}, \omega) + \tilde{\mu}_3(\omega)\gamma_2(\mathbf{k}, \omega)}. \quad (13.139)$$

Now, we are done with the alternative derivations of the normal modes in some planar structures. Next, we derive a bonus result from our results for planar structures, viz., the Casimir interaction between two polarizable atoms.

## 13.12 Casimir Interaction Between Two Atoms from Summation of Pair Interactions

We derived the Casimir interaction between two atoms in (12.34). Rather elaborate derivations were needed to arrive at the result. We can find this result via a short-cut, viz. by using the result from the summation over pair interactions in Sect. 6.1. The general procedure is the following: choose a geometry with two objects of different material; calculate the result using the summation over pair interactions; calculate the result using the full formalism and take the diluted limit; compare the two results and identify parameters.

We could have chosen to apply this procedure on two half spaces each of one atomic species. However, in order to make the derivation simpler we choose to apply it to the atom-wall geometry. We make the ansatz that the interaction between the atoms is given by the potential  $V = -Br^{-7}$  and we intend to identify the coefficient

B. The result from summation over pair interactions (6.4) with this ansatz is

$$E(d) = -\frac{Bn_2\pi}{10d^4}. \quad (13.140)$$

We have assumed that the atom is in vacuum. In the full formalism there are two mode types, TE and TM. The total interaction energy was given in (13.66) and with proper notation we have

$$E(d) = 2\pi\hbar \int \frac{d^2k}{(2\pi)^2} k \int_0^\infty \frac{d\xi}{2\pi} \alpha_1^{at}(\mathbf{i}\xi) e^{-2\gamma^{(0)}(\mathbf{i}\xi)kd} \times \left\{ \frac{(\xi/c k)^2}{\gamma^{(0)}(\mathbf{i}\xi)} \frac{\gamma^{(0)}(\mathbf{i}\xi) - \gamma_s(\mathbf{i}\xi)}{\gamma^{(0)}(\mathbf{i}\xi) + \gamma_s(\mathbf{i}\xi)} + \frac{[2 + (\xi/c k)^2]}{\gamma^{(0)}(\mathbf{i}\xi)} \frac{\gamma_s(\mathbf{i}\xi) - \bar{\varepsilon}_s(\mathbf{i}\xi)\gamma^{(0)}(\mathbf{i}\xi)}{\gamma_s(\mathbf{i}\xi) + \bar{\varepsilon}_s(\mathbf{i}\xi)\gamma^{(0)}(\mathbf{i}\xi)} \right\}. \quad (13.141)$$

Now, we expand the result in  $n_2$  and keep only the lowest order term. We find

$$E(d) = -2\pi\hbar \int \frac{d^2k}{(2\pi)^2} k \int_0^\infty \frac{d\xi}{2\pi} \alpha_1^{at}(\mathbf{i}\xi) e^{-2\gamma^{(0)}(\mathbf{i}\xi)kd} \frac{2\pi n_2 \alpha_2^{at}(\mathbf{i}\xi) [2 + 2(\xi/c k)^2 + (\xi/c k)^4]}{\gamma^{(0)}(\mathbf{i}\xi) [1 + (\xi/c k)^2]}. \quad (13.142)$$

Next we make the substitutions  $k \rightarrow kd$  and  $\xi \rightarrow \xi d$  and obtain

$$E(d) = -2\pi\hbar \frac{1}{d^4} \int \frac{d^2k}{(2\pi)^2} k \int_0^\infty \frac{d\xi}{2\pi} \alpha_1^{at}(\mathbf{i}\xi/d) e^{-2\gamma^{(0)}(\mathbf{i}\xi)k} \frac{2\pi n_2 \alpha_2^{at}(\mathbf{i}\xi/d) [2 + 2(\xi/c k)^2 + (\xi/c k)^4]}{\gamma^{(0)}(\mathbf{i}\xi) [1 + (\xi/c k)^2]}. \quad (13.143)$$

We are interested in the large  $d$  limit,

$$E(d) = -\hbar \frac{n_2 \alpha_1^{at}(0) \alpha_2^{at}(0)}{d^4} \int_0^\infty dk k^2 \int_0^\infty d\xi e^{-2\gamma^{(0)}(\mathbf{i}\xi)k} \frac{[2 + 2(\xi/c k)^2 + (\xi/c k)^4]}{[1 + (\xi/c k)^2]^{3/2}}. \quad (13.144)$$

Now we make a new substitution  $\xi \rightarrow \xi ck$  and find

$$\begin{aligned} E(d) &= -\hbar \frac{n_2 \alpha_1^{at}(0) \alpha_2^{at}(0)}{d^4} \int_0^\infty dk k^2 ck \int_0^\infty d\xi e^{-2\sqrt{1+\xi^2}k} \frac{[2 + 2(\xi)^2 + (\xi)^4]}{[1 + (\xi)^2]^{3/2}} \\ &= -\hbar c \frac{n_2 \alpha_1^{at}(0) \alpha_2^{at}(0)}{d^4} \int_0^\infty d\xi \frac{6}{(2\sqrt{1+\xi^2})^4} \frac{[2 + 2(\xi)^2 + (\xi)^4]}{[1 + (\xi)^2]^{3/2}} \\ &= -\hbar c \frac{n_2 \alpha_1^{at}(0) \alpha_2^{at}(0) 3}{d^4 8} \underbrace{\int_0^\infty d\xi \frac{[2 + 2(\xi)^2 + (\xi)^4]}{[1 + (\xi)^2]^{7/2}}}_{23/15} \\ &= -\hbar c \frac{n_2 \alpha_1^{at}(0) \alpha_2^{at}(0) 23}{d^4 40}, \end{aligned} \quad (13.145)$$

where we first performed the integration with respect to  $k$  and then with respect to  $\xi$ . Now it remains to equate this result with (13.140),

$$\frac{Bn_2\pi}{10d^4} = \hbar c \frac{n_2\alpha_1^{at}(0)\alpha_2^{at}(0)23}{d^440}, \quad (13.146)$$

and we find the correct result for  $B$ :

$$B = \frac{23\hbar c\alpha_1^{at}(0)\alpha_2^{at}(0)}{4\pi}. \quad (13.147)$$

The procedure we have just gone through is a short-cut for finding the Casimir interaction between two atoms. It furthermore acts as a test of the consistency of our formalism.

### 13.13 Spatial Dispersion

In Sect. 9.13 we discussed spatial dispersion in the non-retarded formalism. In order to avoid too much overlapping material we have here refrained from repeating the introductory part and the description of the formalism. We refer the reader to that section. Both here and in Sect. 9.13 we follow rather closely the formalism that we developed in [15]. Effects of spatial dispersion mean effects from the momentum dependence of the dielectric functions and magnetic permeabilities of the media. When an electromagnetic wave impinges on an interface between two media and results in a refracted and a reflected wave the frequency is conserved but not the momentum. The Fresnel coefficients are no longer valid. This may look like an unsurmountable problem to solve. However, it can be solved with the proper assumptions but things become more complicated.

The main reason for including spatial dispersion in this book is to show how it affects the Casimir force between real metal plates. There are two quite different predictions in the literature regarding the room-temperature Casimir-force for large separations. In one version [16] the result is equal to the ideal-metal result; in the other version [3, 17–22] the result is one half of that result. The reason is that in the last version the TE mode does not contribute in this particular limit. The result is very sensitive to the behavior of the transverse dielectric function in the zero-frequency limit [2]; thus, the matching conditions of the fields in the low frequency limit are crucial and this is one of the regions where spatial dispersion can have important effects. We will follow rather closely the presentation of our formalism for spatial dispersion given in [15].

Let us study the interface between two materials 1 and 2; medium 1 to the left and 2 to the right, see Fig. 9.16a. We use, consistently, the idealization that the interface is perfectly sharp; the dielectric function on each side is represented by the bulk function all the way up to the interface; all potentials on either side of the interface are screened by the corresponding dielectric function. This means that the charge- and current-densities that produce the self-sustained fields, the key element of an electromagnetic normal mode, are two-dimensional charge- and current-densities at the plane of the interface. The charge- and current-densities can then be divided into two classes: the strict two-dimensional charge- and current-densities located at the interface,  $\rho$  and  $\mathbf{J}$ , respectively; the induced charge- and current-densities in the bulk of the materials on either side of the interface. Each of these separately obeys the equation of continuity. We let the  $xy$ -plane coincide with the interface and let the  $z$ -direction point to the right. To get the fields in material 1, i.e., to the left of the interface we assume that these are generated by charge- and current-densities at the position of the interface, and as if the whole space were filled with medium 1, see Fig. 9.16b. To get the fields in material 2, i.e., to the right of the interface we again assume that these are generated by charge- and current-densities at the position of the interface, and as if the whole space were filled with medium 2, see Fig. 9.16c. These two sets of charge- and current-densities need not be the same. This is in analogy with the mirror-charge formalism. The equation of continuity demands the presence of accompanying surface-current-densities.

The modes at an interface are characterized by the 2D (two-dimensional) wave vector,  $\mathbf{k}$ , in the plane of the interface. We neglect any effects from imperfections of the interface. This means that the in-plane momentum is conserved. Thus  $\mathbf{k}$  is a good quantum number for the modes. For isotropic materials there is no preferred direction in the  $xy$ -plane. We arbitrarily choose the propagation of the mode to be in the  $x$ -direction. We let a general wave vector be denoted by  $\mathbf{q}$ , and  $\mathbf{k}$  is then the in-plane component, i.e.,  $\mathbf{q} = \mathbf{k} + q_z \hat{z} = k \hat{x} + q_z \hat{z}$ . In analogy a general position vector is denoted by  $\mathbf{R}$ , and  $\mathbf{r}$  is then the in-plane component, i.e.,  $\mathbf{R} = \mathbf{r} + z \hat{z} = x \hat{x} + y \hat{y} + z \hat{z}$ . For functions of the spatial coordinates and time the function arguments can be written in the equivalent forms  $(\mathbf{R}, t) = (\mathbf{r}, z; t) = (x, y, z; t)$  and for the Fourier transformed versions they may be written as  $(\mathbf{q}, \omega) = (\mathbf{k}, q_z; \omega)$ . In our treatment of the interfaces the charge- and current-densities are strictly 2D and with our orientation of the coordinate system the Fourier transformed functions are

$$\rho(\mathbf{q}, \omega) = \rho_s(\mathbf{k}, -; \omega) = \rho_s(\mathbf{k}, \omega), \quad (13.148)$$

and

$$\begin{aligned} \mathbf{J}(\mathbf{q}, \omega) &= \mathbf{J}_L(\mathbf{q}, \omega) + \mathbf{J}_T(\mathbf{q}, \omega) = \mathbf{K}(\mathbf{k}, -; \omega) \\ &= \mathbf{K}(\mathbf{k}, \omega) = \mathbf{K}_{\parallel}(\mathbf{k}, \omega) + \mathbf{K}_{\perp}(\mathbf{k}, \omega), \end{aligned} \quad (13.149)$$

respectively. The subscripts  $L$  and  $T$  denote longitudinal and transverse, i.e. parallel and perpendicular to  $\mathbf{q}$ , respectively. The subscripts  $\parallel$  and  $\perp$  denote in plane vectors, parallel and perpendicular to  $\mathbf{k}$ , respectively.

In Coulomb gauge the surface charge- and current-densities give rise to the following potentials [2]:

$$\begin{aligned}
 \Phi^{(i)}(\mathbf{q}, \omega) &= \frac{4\pi\rho^{(i)}(\mathbf{q}, \omega)}{\varepsilon_L^{(i)}(\mathbf{q}, \omega)q^2} = \frac{4\pi\rho_s^{(i)}(\mathbf{k}, \omega)}{\varepsilon_L^{(i)}(\mathbf{q}, \omega)q^2}, \\
 \mathbf{A}^{(i)}(\mathbf{q}, \omega) &= \frac{4\pi\tilde{\mu}_T^{(i)}(\mathbf{q}, \omega)\mathbf{J}_T^{(i)}(\mathbf{q}, \omega)}{c\left[q^2 - \left(\tilde{n}_T^{(i)}(\mathbf{q}, \omega)/c\right)^2\right]} \\
 &= \frac{4\pi\tilde{\mu}_T^{(i)}(\mathbf{q}, \omega) \left[ \mathbf{K}_\parallel(\mathbf{k}, \omega) + \mathbf{K}_\perp(\mathbf{k}, \omega) - \overbrace{\mathbf{q} \cdot \mathbf{K}_\parallel(\mathbf{k}, \omega)}^{kK_\parallel(\mathbf{k}, \omega)} - \overbrace{\mathbf{q} \cdot \mathbf{K}_\perp(\mathbf{k}, \omega)}^0 \right]}{c\left[q^2 - \left(\tilde{n}_T^{(i)}(\mathbf{q}, \omega)/c\right)^2\right]} \\
 &= \frac{4\pi\tilde{\mu}_T^{(i)}(\mathbf{q}, \omega) \left[ \hat{x}K_\parallel(\mathbf{k}, \omega) + \hat{y}K_\perp(\mathbf{k}, \omega) - \hat{x}\frac{k^2}{q^2}K_\parallel(\mathbf{k}, \omega) - \hat{z}\frac{kq_z}{q^2}K_\parallel(\mathbf{k}, \omega) \right]}{c\left[q^2 - \left(\tilde{n}_T^{(i)}(\mathbf{q}, \omega)/c\right)^2\right]} \\
 &= \frac{4\pi\tilde{\mu}_T^{(i)}(\mathbf{q}, \omega) \left[ \hat{x}\frac{q^2}{q^2}K_\parallel(\mathbf{k}, \omega) + \hat{y}K_\perp(\mathbf{k}, \omega) - \hat{z}\frac{kq_z}{q^2}K_\parallel(\mathbf{k}, \omega) \right]}{c\left[q^2 - \left(\tilde{n}_T^{(i)}(\mathbf{q}, \omega)/c\right)^2\right]},
 \end{aligned} \tag{13.150}$$

where the index  $i = 1, 2$  specifies the medium. In Coulomb gauge the vector potential,  $\mathbf{A}$ , is transverse and depends only on the transverse part of the current density. Note that the transverse part of the current is orthogonal to  $\mathbf{q}$  and not necessarily to  $\mathbf{k}$ .

Let us, in what follows, drop the superscript representing the medium, on the potentials and fields. The result is valid on each side of the interface, we just add the proper superscript at the end. The potentials depend on both the surface charge density and surface current density. These are not entirely independent. They are coupled via the equation of continuity. Let us express the potentials in the surface current densities only. We have the equation of continuity on Fourier transformed form,

$$\omega\rho(\mathbf{q}, \omega) - \mathbf{q} \cdot \mathbf{J}(\mathbf{q}, \omega) = 0, \tag{13.151}$$

and

$$\omega\rho_s(\mathbf{k}, \omega) - \left[ \underbrace{\mathbf{k} \cdot \mathbf{K}(\mathbf{k}, \omega)}_{kK_\parallel(\mathbf{k}, \omega)} + \underbrace{q_z J_z(\mathbf{q}, \omega)}_0 \right] = 0, \tag{13.152}$$

or

$$\rho_s(\mathbf{k}, \omega) = \frac{k}{\omega} K_{\parallel}(\mathbf{k}, \omega). \quad (13.153)$$

We are interested in the electric and magnetic fields associated with the charge- and current-densities. The electric field is

$$\mathbf{E} = -\nabla\Phi - \frac{1}{c} \frac{\partial}{\partial t} \mathbf{A}, \quad (13.154)$$

and its Fourier transform is

$$\begin{aligned} \mathbf{E}(\mathbf{k}, q_z; \omega) &= -i\mathbf{q}\Phi(\mathbf{k}, q_z; \omega) - \left(\frac{-i\omega}{c}\right) \mathbf{A}(\mathbf{k}, q_z; \omega) \\ &= -i(k\hat{x} + q_z\hat{z}) \frac{4\pi k K_{\parallel}(\mathbf{k}, \omega)}{\varepsilon_L^{(i)}(\mathbf{q}, \omega)\omega q^2} \\ &\quad + \frac{i\omega}{c} \frac{4\pi \tilde{\mu}_T^{(i)}(\mathbf{q}, \omega) \left[ \hat{x} \frac{q_z^2}{q^2} K_{\parallel}(\mathbf{k}, \omega) + \hat{y} K_{\perp}(\mathbf{k}, \omega) - \hat{z} \frac{kq_z}{q^2} K_{\parallel}(\mathbf{k}, \omega) \right]}{c \left[ q^2 - \left( \tilde{n}_T^{(i)}(\mathbf{q}, \omega)\omega/c \right)^2 \right]} \\ &= -i\hat{x} 4\pi K_{\parallel}(\mathbf{k}, \omega) \left[ \frac{k^2}{\varepsilon_L^{(i)}(\mathbf{q}, \omega)\omega q^2} - \frac{\omega}{c^2} \frac{q_z^2}{q^2} \frac{\tilde{\mu}_T^{(i)}(\mathbf{q}, \omega)}{\left[ q^2 - \left( \tilde{n}_T^{(i)}(\mathbf{q}, \omega)\omega/c \right)^2 \right]} \right] \\ &\quad - i\hat{z} 4\pi K_{\parallel}(\mathbf{k}, \omega) \frac{kq_z}{\varepsilon_L^{(i)}(\mathbf{q}, \omega)\omega q^2} + i\hat{y} 4\pi K_{\perp}(\mathbf{k}, \omega) \frac{\omega k}{c^2} \frac{q_z \tilde{\mu}_T^{(i)}(\mathbf{q}, \omega)}{q^2 \left[ q^2 - \left( \tilde{n}_T^{(i)}(\mathbf{q}, \omega)\omega/c \right)^2 \right]}. \end{aligned} \quad (13.155)$$

Similarly, the magnetic induction is

$$\mathbf{B} = \nabla \times \mathbf{A}, \quad (13.156)$$

and its Fourier transform is

$$\begin{aligned} \mathbf{B}(\mathbf{k}, q_z; \omega) &= i\mathbf{q} \times \mathbf{A}(\mathbf{k}, q_z; \omega) \\ &= i(k\hat{x} + q_z\hat{z}) \times \frac{4\pi \tilde{\mu}_T^{(i)}(\mathbf{q}, \omega) [\hat{x} K_{\parallel}(\mathbf{k}, \omega) + \hat{y} K_{\perp}(\mathbf{k}, \omega)]}{c \left[ q^2 - \left( \tilde{n}_T^{(i)}(\mathbf{q}, \omega)\omega/c \right)^2 \right]} \\ &= i \frac{4\pi \tilde{\mu}_T^{(i)}(\mathbf{q}, \omega)}{c \left[ q^2 - \left( \tilde{n}_T^{(i)}(\mathbf{q}, \omega)\omega/c \right)^2 \right]} (k\hat{x} + q_z\hat{z}) \times [\hat{x} K_{\parallel}(\mathbf{k}, \omega) + \hat{y} K_{\perp}(\mathbf{k}, \omega)] \\ &= i \frac{4\pi \tilde{\mu}_T^{(i)}(\mathbf{q}, \omega)}{c \left[ q^2 - \left( \tilde{n}_T^{(i)}(\mathbf{q}, \omega)\omega/c \right)^2 \right]} \left[ -q_z K_{\perp}(\mathbf{k}, \omega) \hat{x} + q_z K_{\parallel}(\mathbf{k}, \omega) \hat{y} + k K_{\perp}(\mathbf{k}, \omega) \hat{z} \right]. \end{aligned} \quad (13.157)$$

To summarize we have the fields

$$\begin{aligned}
 E_{\parallel}(\mathbf{k}, q_z; \omega) &= -i4\pi K_{\parallel}(\mathbf{k}, \omega) \frac{k^2}{\omega} \left[ \frac{1}{\tilde{\varepsilon}_L(\mathbf{q}, \omega) q^2} \right. \\
 &\quad \left. - \frac{\omega^2}{(ck)^2} \frac{\tilde{\mu}_T(\mathbf{q}, \omega)}{[q^2 - (\tilde{n}_T(\mathbf{q}, \omega)\omega/c)^2]} + \frac{\omega^2}{c^2} \frac{\tilde{\mu}_T(\mathbf{q}, \omega)}{q^2 [q^2 - (\tilde{n}_T(\mathbf{q}, \omega)\omega/c)^2]} \right], \\
 \tilde{D}_{\parallel}(\mathbf{k}, q_z; \omega) &= -i4\pi K_{\parallel}(\mathbf{k}, \omega) \frac{k^2}{\omega} \left[ \frac{1}{q^2} \right. \\
 &\quad \left. - \frac{\omega^2}{(ck)^2} \frac{\tilde{\varepsilon}_T(\mathbf{q}, \omega)\tilde{\mu}_T(\mathbf{q}, \omega)}{[q^2 - (\tilde{n}_T(\mathbf{q}, \omega)\omega/c)^2]} + \frac{\omega^2}{c^2} \frac{\tilde{\varepsilon}_T(\mathbf{q}, \omega)\tilde{\mu}_T(\mathbf{q}, \omega)}{q^2 [q^2 - (\tilde{n}_T(\mathbf{q}, \omega)\omega/c)^2]} \right], \\
 E_{\perp}(\mathbf{k}, q_z; \omega) &= i4\pi K_{\perp}(\mathbf{k}, \omega) \frac{\omega}{c^2} \frac{\tilde{\mu}_T(\mathbf{q}, \omega)}{[q^2 - (\tilde{n}_T(\mathbf{q}, \omega)\omega/c)^2]}, \\
 \tilde{D}_{\perp}(\mathbf{k}, q_z; \omega) &= i4\pi K_{\perp}(\mathbf{k}, \omega) \frac{\omega}{c^2} \frac{\tilde{\varepsilon}_T(\mathbf{q}, \omega)\tilde{\mu}_T(\mathbf{q}, \omega)}{[q^2 - (\tilde{n}_T(\mathbf{q}, \omega)\omega/c)^2]}, \\
 E_n(\mathbf{k}, q_z; \omega) &= -i4\pi K_{\parallel}(\mathbf{k}, \omega) \frac{kq_z}{\tilde{\varepsilon}_L(\mathbf{q}, \omega)\omega q^2}, \\
 \tilde{D}_n(\mathbf{k}, q_z; \omega) &= -i4\pi K_{\parallel}(\mathbf{k}, \omega) \frac{kq_z}{\omega q^2}, \\
 B_{\parallel}(\mathbf{k}, q_z; \omega) &= -i \frac{4\pi K_{\perp}(\mathbf{k}, \omega)}{c} \frac{q_z \tilde{\mu}_T(\mathbf{q}, \omega)}{[q^2 - (\tilde{n}_T(\mathbf{q}, \omega)\omega/c)^2]}, \\
 \tilde{H}_{\parallel}(\mathbf{k}, q_z; \omega) &= -i \frac{4\pi K_{\perp}(\mathbf{k}, \omega)}{c} \frac{q_z}{[q^2 - (\tilde{n}_T(\mathbf{q}, \omega)\omega/c)^2]}, \\
 B_{\perp}(\mathbf{k}, q_z; \omega) &= i \frac{4\pi K_{\parallel}(\mathbf{k}, \omega)}{c} \frac{q_z \tilde{\mu}_T(\mathbf{q}, \omega)}{[q^2 - (\tilde{n}_T(\mathbf{q}, \omega)\omega/c)^2]}, \\
 \tilde{H}_{\perp}(\mathbf{k}, q_z; \omega) &= i \frac{4\pi K_{\parallel}(\mathbf{k}, \omega)}{c} \frac{q_z}{[q^2 - (\tilde{n}_T(\mathbf{q}, \omega)\omega/c)^2]}, \\
 B_n(\mathbf{k}, q_z; \omega) &= i \frac{4\pi k K_{\perp}(\mathbf{k}, \omega)}{c} \frac{\tilde{\mu}_T(\mathbf{q}, \omega)}{[q^2 - (\tilde{n}_T(\mathbf{q}, \omega)\omega/c)^2]}, \\
 \tilde{H}_n(\mathbf{k}, q_z; \omega) &= i \frac{4\pi k K_{\perp}(\mathbf{k}, \omega)}{c} \frac{1}{[q^2 - (\tilde{n}_T(\mathbf{q}, \omega)\omega/c)^2]}.
 \end{aligned} \tag{13.158}$$

Many functions will appear repeatedly when we apply the boundary conditions and we give them names to make the expressions simpler. We need the following functions:

$$\begin{aligned}
 g_a^{(i)}(k, \omega) &= 2k \int_{-\infty}^{\infty} \frac{dq_z}{2\pi} \frac{1}{q^2 \tilde{\varepsilon}_L^{(i)}(q, \omega)}; \\
 g_b^{(i)}(k, \omega) &= 2\gamma^{(0)} k \int_{-\infty}^{\infty} \frac{dq_z}{2\pi} \frac{\tilde{\mu}_T^{(i)}(q, \omega)}{[q^2 - (\tilde{n}_T^{(i)}(q, \omega)\omega/c)^2]}; \\
 g_c^{(i)}(k, \omega) &= \frac{2(\omega/c)^2 k \gamma^{(0)}}{1 - \gamma^{(0)}} \int_{-\infty}^{\infty} \frac{dq_z}{2\pi} \frac{\tilde{\mu}_T^{(i)}(q, \omega)}{q^2 [q^2 - (\tilde{n}_T^{(i)}(q, \omega)\omega/c)^2]}; \\
 g_d^{(i)}(k, \omega) &= -2i \int_{-\infty}^{\infty} \frac{dq_z}{2\pi} \frac{q_z e^{iq_z 0^+}}{[q^2 - (\tilde{n}_T^{(i)}(q, \omega)\omega/c)^2]}; \\
 h_a^{(i)}(k, \omega) &= 2k \int_{-\infty}^{\infty} \frac{dq_z}{2\pi} \frac{\tilde{\mu}_T^{(i)}(q, \omega)}{q^2}; \\
 h_d^{(i)}(k, \omega) &= -2i \int_{-\infty}^{\infty} \frac{dq_z}{2\pi} \frac{\tilde{\mu}_T^{(i)}(q, \omega) q_z e^{iq_z 0^+}}{[q^2 - (\tilde{n}_T^{(i)}(q, \omega)\omega/c)^2]}.
 \end{aligned} \tag{13.159}$$

where

$$\gamma^{(0)} = \gamma^{(0)}(k, \omega) = \sqrt{1 - (\omega/c k)^2}. \quad (13.160)$$

The prefactors have been chosen such that all  $g$ - and  $h$ -functions are unity in vacuum:

$$\begin{aligned} g_a^0(k, \omega) &= 2k \int_{-\infty}^{\infty} \frac{dq_z}{2\pi} \frac{1}{q^2} = 1; \\ g_b^0(k, \omega) &= 2\gamma^{(0)} k \int_{-\infty}^{\infty} \frac{dq_z}{2\pi} \frac{1}{[q^2 - (\omega/c)^2]} = 1; \\ g_c^0(k, \omega) &= \frac{2(\omega/c)^2 k \gamma^{(0)}}{1 - \gamma^{(0)}} \int_{-\infty}^{\infty} \frac{dq_z}{2\pi} \frac{1}{q^2 [q^2 - (\omega/c)^2]} = 1; \\ g_d^0(k, \omega) &= -2i \int_{-\infty}^{\infty} \frac{dq_z}{2\pi} \frac{q_z e^{iq_z 0^+}}{[q^2 - (\omega/c)^2]} = 1; \\ h_a^0(k, \omega) &= 2k \int_{-\infty}^{\infty} \frac{dq_z}{2\pi} \frac{1}{q^2} = 1; \\ h_d^0(k, \omega) &= -2i \int_{-\infty}^{\infty} \frac{dq_z}{2\pi} \frac{q_z e^{iq_z 0^+}}{[q^2 - (\omega/c)^2]} = 1. \end{aligned} \quad (13.161)$$

These results are easily found from the standard integrals:

$$\begin{aligned} \int_{-\infty}^{\infty} \frac{dr}{2\pi} e^{irs} \frac{1}{r^2 + a^2} &= \frac{1}{2a} e^{-a|s|}; \\ \int_{-\infty}^{\infty} \frac{dr}{2\pi} e^{irs} \frac{r}{r^2 + a^2} &= \frac{i}{2} \text{sign}(s) e^{-a|s|}. \end{aligned} \quad (13.162)$$

We also need the  $g$ - and  $h$ -functions with neglect of spatial dispersion. If we neglect spatial dispersion, indicated by an extra subscript 1, we have

$$\begin{aligned} g_{a,1}^{(i)}(k, \omega) &= 2k \int_{-\infty}^{\infty} \frac{dq_z}{2\pi} \frac{1}{q^2 \tilde{\varepsilon}^{(i)}(\omega)} = \frac{1}{\tilde{\varepsilon}^{(i)}(\omega)}; \\ g_{b,1}^{(i)}(k, \omega) &= 2\gamma^{(0)} k \int_{-\infty}^{\infty} \frac{dq_z}{2\pi} \frac{\tilde{\mu}^{(i)}(\omega)}{[q^2 - (\tilde{n}^{(i)}(\omega)\omega/c)^2]} = \frac{\gamma^{(0)} \tilde{\mu}^{(i)}(\omega)}{\gamma_i}; \\ g_{c,1}^{(i)}(k, \omega) &= \frac{2(\omega/c)^2 k \gamma^{(0)}}{1 - \gamma^{(0)}} \int_{-\infty}^{\infty} \frac{dq_z}{2\pi} \frac{\tilde{\mu}^{(i)}(\omega)}{q^2 [q^2 - (\tilde{n}^{(i)}(\omega)\omega/c)^2]} = \frac{\gamma^{(0)}(\omega/c k)^2 \tilde{\mu}^{(i)}(\omega)}{\gamma_i(1 - \gamma^{(0)})(1 + \gamma_i)}; \\ g_{d,1}^{(i)}(k, \omega) &= -2i \int_{-\infty}^{\infty} \frac{dq_z}{2\pi} \frac{q_z e^{iq_z 0^+}}{[q^2 - (\tilde{n}^{(i)}(\omega)\omega/c)^2]} = 1; \\ h_{a,1}^{(i)}(k, \omega) &= 2k \int_{-\infty}^{\infty} \frac{dq_z}{2\pi} \frac{\tilde{\mu}^{(i)}(\omega)}{q^2} = \tilde{\mu}^{(i)}(\omega); \\ h_{d,1}^{(i)}(k, \omega) &= -2i \int_{-\infty}^{\infty} \frac{dq_z}{2\pi} \frac{\tilde{\mu}^{(i)}(\omega) q_z e^{iq_z 0^+}}{[q^2 - (\tilde{n}^{(i)}(\omega)\omega/c)^2]} = \tilde{\mu}^{(i)}(\omega), \end{aligned} \quad (13.163)$$

where

$$\gamma_i = \gamma_i(k, \omega) = \sqrt{1 + (\tilde{n}^{(i)}(\omega)\omega/c k)^2}. \quad (13.164)$$

The  $g_d$ -functions are calculated just to the right of the interface and have all the value unity. The corresponding value to the left of the interface is minus unity.

We will furthermore need the following combinations of  $g$ -functions:

$$G^{(i),\text{TM}}(k, \omega) = \frac{1}{\gamma^{(0)}} g_a^{(i)}(k, \omega) - \frac{(\omega/ck)^2}{(\gamma^{(0)})^2} g_b^{(i)}(k, \omega) + \frac{(1 - \gamma^{(0)})}{(\gamma^{(0)})^2} g_c^{(i)}(k, \omega), \quad (13.165)$$

and

$$G^{(i),\text{TE}}(k, \omega) = g_b^{(i)}(k, \omega). \quad (13.166)$$

The overall scaling of these functions has been chosen such that the functions are unity in vacuum, i.e.,

$$G^{(0),\text{TM}}(k, \omega) = 1; \quad G^{(0),\text{TE}}(k, \omega) = 1. \quad (13.167)$$

If we neglect spatial dispersion these functions become

$$\begin{aligned} G_1^{(i),\text{TM}}(k, \omega) &= \frac{1}{\gamma^{(0)}} g_{a,1}^{(i)}(k, \omega) + \frac{(1-\gamma^{(0)})}{(\gamma^{(0)})^2} g_{c,1}^{(i)}(k, \omega) - \frac{(\omega/ck)^2}{(\gamma^{(0)})^2} g_{b,1}^{(i)}(k, \omega) \\ &= \frac{1}{\gamma^{(0)}} \frac{1}{\varepsilon^{(i)}(\omega)} + \frac{(\omega/c)^2}{\gamma^{(0)}\gamma(1+\gamma_i)} - \frac{(\omega/ck)^2}{\gamma^{(0)}\gamma_i} = \frac{\gamma_i}{\gamma^{(0)}} \frac{1}{\varepsilon^{(i)}(\omega)}, \end{aligned} \quad (13.168)$$

and

$$G_1^{(i),\text{TE}}(k, \omega) = g_{b,1}^{(i)}(k, \omega) = \frac{\gamma^{(0)}}{\gamma_i}, \quad (13.169)$$

respectively. In the first function we have used the fact that the longitudinal and transverse dielectric functions are equal in the limit of vanishing momentum.

In [15] we used three different model-dielectric-functions. Here we will only use the RPA functions. The RPA dielectric functions, on the real frequency axis, expressed in the dimension-less variables  $Q = q/2k_F$ ,  $K = k/2k_F$ ,  $W = \hbar\omega/4E_F$ ,  $W_{pl} = \hbar\omega_{pl}/4E_F$  and  $y = m_e e^2/\hbar^2 k_F$  are

$$\varepsilon_{L,T}(Q, W) = 1 + \alpha_{L,T}(Q, W), \quad (13.170)$$

where the longitudinal and transverse polarizabilities are [23]

$$\begin{aligned} \alpha_L(Q, W) = \alpha_L^0(Q, W) &= \frac{y}{2\pi} \frac{1}{Q^2} \left\{ 1 + \frac{Q^2 - (W - Q^2)^2}{4Q^3} \ln \left[ \frac{Q - (W - Q^2)}{-Q - (W - Q^2)} \right] \right. \\ &\quad \left. - \frac{Q^2 - (W + Q^2)^2}{4Q^3} \ln \left[ \frac{-Q + (W + Q^2)}{Q + (W + Q^2)} \right] \right\}, \end{aligned} \quad (13.171)$$

and

$$\alpha_T(Q, W) = \alpha_T^0(Q, W) = \frac{y}{2\pi} \frac{1}{Q^2} \frac{1}{4W^2} \times \left\{ - (Q^4 + Q^2 + 3W^2) + \frac{[Q^2 - (W - Q^2)^2]^2}{4Q^3} \ln \left[ \frac{Q - (W - Q^2)}{-Q - (W - Q^2)} \right] - \frac{[Q^2 - (W + Q^2)^2]^2}{4Q^3} \ln \left[ \frac{-Q + (W + Q^2)}{Q + (W + Q^2)} \right] \right\}, \quad (13.172)$$

respectively. The logarithm in these expressions is taken from the branch for which  $|\arg[\ln(z)]| < \pi$ .

These results are in neglect of dissipation. Including dissipation, or damping, in a simple way leads to the following modifications [24]:

$$\alpha_L(Q, W, \Delta) = \frac{(W + i\Delta) \alpha_L^0(Q, W + i\Delta)}{W + i\Delta [\alpha_L^0(Q, W + i\Delta) / \alpha_L^0(Q, 0)]}, \quad (13.173)$$

and [25]

$$\alpha_T(Q, W, \Delta) = \frac{W + i\Delta}{W} \alpha_T^0(Q, W + i\Delta), \quad (13.174)$$

respectively.

For the force calculations we need the polarizabilities on the imaginary frequency axis. There, they are

$$\alpha_L^{0'}(Q, \mathcal{E}) = \alpha_L^0(Q, i\mathcal{E}) = \frac{y}{2\pi Q^2} \left\{ 1 + \frac{(\mathcal{E}^2 + Q^2 - Q^4)}{4Q^3} \ln \left[ \frac{(Q + Q^2)^2 + \mathcal{E}^2}{(Q - Q^2)^2 + \mathcal{E}^2} \right] - \frac{\mathcal{E}}{Q} \left[ \tan^{-1} \left( \frac{Q + Q^2}{\mathcal{E}} \right) + \tan^{-1} \left( \frac{Q - Q^2}{\mathcal{E}} \right) \right] \right\}, \quad (13.175)$$

and

$$\alpha_T^{0'}(Q, \mathcal{E}) = \alpha_T^0(Q, i\mathcal{E}) = \frac{1}{8} \frac{y}{\pi Q^2 \mathcal{E}^2} \left\{ - (3\mathcal{E}^2 - Q^2 - Q^4) + \frac{(2\mathcal{E}Q^2)^2 - (\mathcal{E}^2 + Q^2 - Q^4)^2}{4Q^3} \ln \left[ \frac{(Q + Q^2)^2 + \mathcal{E}^2}{(Q - Q^2)^2 + \mathcal{E}^2} \right] + \frac{2\mathcal{E}(\mathcal{E}^2 + Q^2 - Q^4)}{Q} \left[ \tan^{-1} \left( \frac{Q + Q^2}{\mathcal{E}} \right) + \tan^{-1} \left( \frac{Q - Q^2}{\mathcal{E}} \right) \right] \right\}, \quad (13.176)$$

respectively. The inverse tangent functions are taken from the branch where their absolute values are less than  $\pi/2$ .

Including dissipation we now have

$$\alpha_L'(Q, \mathcal{E}, \Delta) = \alpha_L(Q, i\mathcal{E}, \Delta) = \frac{(\mathcal{E} + \Delta) \alpha_L^{0'}(Q, \mathcal{E} + \Delta)}{\mathcal{E} + \Delta [\alpha_L^{0'}(Q, \mathcal{E} + \Delta) / \alpha_L^{0'}(Q, 0)]}, \quad (13.177)$$

and

$$\alpha_T'(Q, \mathcal{E}, \Delta) = \alpha_T(Q, i\mathcal{E}, \Delta) = \frac{\mathcal{E} + \Delta}{\mathcal{E}} \alpha_T^{0'}(Q, \mathcal{E} + \Delta), \quad (13.178)$$

respectively.

We have now laid out the notation and will in what follows use this material to find the electromagnetic normal modes for a single interface and for a gap between two half spaces. We have two momentum scales in the present problem; one is defined by the Fermi-momentum,  $k_F$ ; one by the surface mode frequency divided by the speed of light,  $\omega_s/c$ . These scales are quite different and  $\omega_s/c \ll k_F$ . Different effects are visible on the two scales and one has to view them separately. The first scale is important if we are interested in the surface energy or the interaction between objects at small separations, the van-der-Waals force. The second scale is important for the interaction at larger separations, in the Casimir range. Retardation effects, effects from the finite speed of light, enter for very small in-plane momenta and should be viewed on the second scale.

### 13.13.1 Modes at a Single Interface

We now derive the condition for having a surface-normal-mode from the standard boundary-conditions for the fields at the interface: the continuity of the in-plane components of the  $\mathbf{E}$ - and  $\tilde{\mathbf{H}}$ -fields and the normal components of the  $\tilde{\mathbf{D}}$ - and  $\mathbf{B}$ -fields; we only need the first two. These boundary conditions are valid if there are no external charge- or current-densities at the interface, only induced densities from the self-sustained fields. We see from (13.158) that  $E_{\parallel}$ ,  $E_n$ , and  $B_{\perp}$  all depend on  $K_{\parallel}$  and will be involved in one of the modes, the TM mode. We also find that  $E_{\perp}$ ,  $B_{\parallel}$ , and  $B_n$  all depend on  $K_{\perp}$  and will be involved in the other mode, the TE mode.

We begin with the TM modes and use the boundary condition that  $E_{\parallel}$  is continuous. We have

$$E_{\parallel}(\mathbf{k}, z; \omega) = -i4\pi K_{\parallel}(\mathbf{k}, \omega) \frac{k^2}{\omega} \int_{-\infty}^{\infty} \frac{dq_z}{2\pi} e^{iq_z z} \left[ \frac{1}{\varepsilon_L^{(i)}(\mathbf{q}, \omega) q^2} - \left(\frac{\omega}{ck}\right)^2 \frac{\tilde{\mu}_T^{(i)}(\mathbf{q}, \omega)}{\left[q^2 - \left(\tilde{n}_T^{(i)}(\mathbf{q}, \omega)\omega/c\right)^2\right]} + \frac{\omega^2}{c^2} \frac{\tilde{\mu}_T^{(i)}(\mathbf{q}, \omega)}{q^2 \left[q^2 - \left(\tilde{n}_T^{(i)}(\mathbf{q}, \omega)\omega/c\right)^2\right]} \right]. \quad (13.179)$$

Just to the left of the interface the field becomes

$$\begin{aligned}
E_{\parallel}(\mathbf{k}, 0^-; \omega) &= -i4\pi K_{\parallel}^{(1)}(\mathbf{k}, \omega) \frac{k^2}{\omega} \int_{-\infty}^{\infty} \frac{dq_z}{2\pi} \left[ \frac{1}{\varepsilon_z^{(1)}(\mathbf{q}, \omega) q^2} \right. \\
&\quad \left. - \left( \frac{\omega}{ck} \right)^2 \frac{\tilde{\mu}_T^{(1)}(\mathbf{q}, \omega)}{\left[ q^2 - (\tilde{n}_T^{(1)}(\mathbf{q}, \omega) \omega/c)^2 \right]} + \frac{\omega^2}{c^2} \frac{\tilde{\mu}_T^{(1)}(\mathbf{q}, \omega)}{q^2 \left[ q^2 - (\tilde{n}_T^{(1)}(\mathbf{q}, \omega) \omega/c)^2 \right]} \right] \\
&= -i4\pi K_{\parallel}^{(1)}(\mathbf{k}, \omega) \frac{k^2}{\omega} \\
&\quad \times \left[ \frac{1}{2k} g_a^{(1)}(k, \omega) - \left( \frac{\omega}{ck} \right)^2 \frac{1}{2\gamma^{(0)} k} g_b^{(1)}(k, \omega) + \frac{\omega^2}{c^2} \frac{1-\gamma^{(0)}}{2(\omega/c)^2 k \gamma^{(0)}} g_c^{(1)}(k, \omega) \right] \\
&= -i4\pi K_{\parallel}^{(1)}(\mathbf{k}, \omega) \frac{k\gamma^{(0)}}{2\omega} \\
&\quad \times \left[ \frac{1}{\gamma^{(0)}} g_a^{(1)}(k, \omega) - \left( \frac{\omega}{ck} \right)^2 \frac{1}{(\gamma^{(0)})^2} g_b^{(1)}(k, \omega) + \frac{1-\gamma^{(0)}}{(\gamma^{(0)})^2} g_c^{(1)}(k, \omega) \right] \\
&= -i4\pi K_{\parallel}^{(1)}(\mathbf{k}, \omega) \frac{k\gamma^{(0)}}{2\omega} G^{(1), \text{TM}}.
\end{aligned} \tag{13.180}$$

In analogy we find for the electric field just to the right of the interface

$$E_{\parallel}(\mathbf{k}, 0^+; \omega) = -i4\pi K_{\parallel}^{(2)}(\mathbf{k}, \omega) \frac{k\gamma^{(0)}}{2\omega} G^{(2), \text{TM}}. \tag{13.181}$$

Now we do the corresponding for the  $\mathbf{H}$ -fields. We have

$$\tilde{H}_{\perp}(\mathbf{k}, q_z; \omega) = i \frac{4\pi K_{\parallel}(\mathbf{k}, \omega)}{c} \frac{q_z}{\left[ q^2 - (\tilde{n}_T^{(i)}(\mathbf{q}, \omega) \omega/c)^2 \right]}, \tag{13.182}$$

and

$$\tilde{H}_{\perp}(\mathbf{k}, z; \omega) = i \frac{4\pi K_{\parallel}(\mathbf{k}, \omega)}{c} \int_{-\infty}^{\infty} \frac{dq_z}{2\pi} e^{iq_z z} \frac{q_z}{\left[ q^2 - (\tilde{n}_T^{(i)}(\mathbf{q}, \omega) \omega/c)^2 \right]}. \tag{13.183}$$

Just to the left of the interface the field becomes

$$\begin{aligned}
\tilde{H}_{\perp}(\mathbf{k}, 0^-; \omega) &= i \frac{4\pi K_{\parallel}^{(1)}(\mathbf{k}, \omega)}{c} \int_{-\infty}^{\infty} \frac{dq_z}{2\pi} e^{iq_z 0^-} \frac{q_z}{\left[ q^2 - (\tilde{n}_T^{(i)}(\mathbf{q}, \omega) \omega/c)^2 \right]} \\
&= i \frac{4\pi K_{\parallel}^{(1)}(\mathbf{k}, \omega)}{c} \left( \frac{1}{-2i} \right) \left( -g_d^{(1)} \right) = \frac{2\pi K_{\parallel}^{(1)}(\mathbf{k}, \omega)}{c} g_d^{(1)}
\end{aligned} \tag{13.184}$$

and just to the right of the interface

$$\tilde{H}_{\perp}(\mathbf{k}, 0^+; \omega) = -\frac{2\pi K_{\parallel}^{(2)}(\mathbf{k}, \omega)}{c} g_d^{(2)}. \tag{13.185}$$

To make the expressions for the fields more compact we introduce the common factors  $A_{\parallel}$  and  $B_{\parallel}$ , not to be confused with the vector potential and magnetic induction,

$$A_{\parallel} = \frac{2\pi K_{\parallel}^{(1)}(\mathbf{k}, \omega)}{c}; \quad B_{\parallel} = \frac{2\pi K_{\parallel}^{(2)}(\mathbf{k}, \omega)}{c}. \quad (13.186)$$

Then the continuity of the  $\tilde{H}_{\perp}$ -component gives

$$g_d^{(1)}(k, \omega) A_{\parallel} = -g_d^{(2)}(k, \omega) B_{\parallel} \rightarrow A_{\parallel} + B_{\parallel} = 0, \quad (13.187)$$

since the  $g_d$  functions are unity. The continuity of the  $E_{\parallel}$ -component gives

$$-i2A_{\parallel}c \frac{k\gamma^{(0)}}{2\omega} G^{(1),\text{TM}} + i2B_{\parallel}c \frac{k\gamma^{(0)}}{2\omega} G^{(2),\text{TM}} = 0, \quad (13.188)$$

or

$$G^{(1),\text{TM}} A_{\parallel} - G^{(2),\text{TM}} B_{\parallel} = 0. \quad (13.189)$$

Thus, we have obtained the following system of equations

$$\begin{pmatrix} 1 \\ G^{(1),\text{TM}}(k, \omega) - G^{(2),\text{TM}}(k, \omega) \end{pmatrix} \begin{pmatrix} A_{\parallel} \\ B_{\parallel} \end{pmatrix} = \begin{pmatrix} 0 \\ 0 \end{pmatrix}. \quad (13.190)$$

This system has the trivial solution that  $A_{\parallel} = B_{\parallel} = 0$ . It has also non-trivial solutions which are the modes we are looking for. The condition for normal modes is found as

$$\left| G^{(1),\text{TM}}(k, \omega) - G^{(2),\text{TM}}(k, \omega) \right| = 0, \quad (13.191)$$

or

$$G^{(1),\text{TM}}(k, \omega) + G^{(2),\text{TM}}(k, \omega) = 0. \quad (13.192)$$

Neglecting spatial dispersion we arrive at

$$\gamma^{(1)}\varepsilon^{(2)}(\omega) + \gamma^{(2)}\varepsilon^{(1)}(\omega) = 0, \quad (13.193)$$

which is the standard condition for having a TM normal mode in the neglect of spatial dispersion [2].

The magnetic effects give rise to another type of mode, the TE mode. These involve surface current densities perpendicular to  $\mathbf{k}$ . We continue with the TE modes and use the boundary condition that  $E_{\perp}$  is continuous. We have

$$E_{\perp}(\mathbf{k}, z; \omega) = i4\pi K_{\perp}(\mathbf{k}, \omega) \frac{\omega}{c^2} \int_{-\infty}^{\infty} \frac{dq_z}{2\pi} e^{iq_z z} \frac{\tilde{\mu}_T^{(i)}(\mathbf{q}, \omega)}{\left[ q^2 - \left( \tilde{n}_T^{(i)}(\mathbf{q}, \omega) \omega/c \right)^2 \right]}. \quad (13.194)$$

Just to the left of the interface the field becomes

$$\begin{aligned}
 E_{\perp}(\mathbf{k}, 0^{-}; \omega) &= i4\pi K_{\perp}^{(1)}(\mathbf{k}, \omega) \frac{\omega}{c^2} \int_{-\infty}^{\infty} \frac{dq_z}{2\pi} \frac{\tilde{\mu}_T^{(1)}(q, \omega)}{\left[ q^2 - (\tilde{n}_T^{(1)}(q, \omega)\omega/c)^2 \right]} \\
 &= i4\pi K_{\perp}^{(1)}(\mathbf{k}, \omega) \frac{\omega}{c^2} \frac{1}{2\gamma^{(0)k}} g_b^{(1)}(k, \omega) \\
 &= i4\pi K_{\perp}^{(1)}(\mathbf{k}, \omega) \frac{\omega}{c^2} \frac{1}{2\gamma^{(0)k}} G^{(1), \text{TE}}(k, \omega).
 \end{aligned} \tag{13.195}$$

In analogy we find for the electric field just to the right of the interface

$$E_{\perp}(\mathbf{k}, 0^{+}; \omega) = i4\pi K_{\perp}^{(2)}(\mathbf{k}, \omega) \frac{\omega}{c^2} \frac{1}{2\gamma^{(0)k}} G^{(2), \text{TE}}(k, \omega). \tag{13.196}$$

Now we do the corresponding for the  $\mathbf{H}$ -fields. We have

$$\tilde{H}_{\parallel}(\mathbf{k}, q_z; \omega) = -i \frac{4\pi K_{\perp}(\mathbf{k}, \omega)}{c} \frac{q_z}{\left[ q^2 - (\tilde{n}_T^{(i)}(\mathbf{q}, \omega)\omega/c)^2 \right]}, \tag{13.197}$$

and

$$\tilde{H}_{\parallel}(\mathbf{k}, z; \omega) = -i \frac{4\pi K_{\perp}(\mathbf{k}, \omega)}{c} \int_{-\infty}^{\infty} \frac{dq_z}{2\pi} e^{iq_z z} \frac{q_z}{\left[ q^2 - (\tilde{n}_T^{(i)}(\mathbf{q}, \omega)\omega/c)^2 \right]}. \tag{13.198}$$

Just to the left of the interface the field becomes

$$\begin{aligned}
 \tilde{H}_{\parallel}(\mathbf{k}, 0^{-}; \omega) &= -i \frac{4\pi K_{\perp}^{(1)}(\mathbf{k}, \omega)}{c} \int_{-\infty}^{\infty} \frac{dq_z}{2\pi} e^{iq_z 0^{-}} \frac{q_z}{\left[ q^2 - (\tilde{n}_T^{(i)}(q, \omega)\omega/c)^2 \right]} \\
 &= -i \frac{4\pi K_{\perp}^{(1)}(\mathbf{k}, \omega)}{c} \left( \frac{1}{-2i} \right) \left( -g_d^{(1)}(k, \omega) \right) = -\frac{2\pi K_{\perp}^{(1)}(\mathbf{k}, \omega)}{c} g_d^{(1)}(k, \omega),
 \end{aligned} \tag{13.199}$$

and just to the right of the interface

$$\tilde{H}_{\parallel}(\mathbf{k}, 0^{+}; \omega) = \frac{2\pi K_{\perp}^{(2)}(\mathbf{k}, \omega)}{c} g_d^{(2)}(k, \omega). \tag{13.200}$$

To make the expressions for the fields more compact we introduce the common factors  $A_{\perp}$  and  $B_{\perp}$ , not to be confused with the vector potential and magnetic induction,

$$A_{\perp} = \frac{2\pi K_{\perp}^{(1)}(\mathbf{k}, \omega)}{c}; \quad B_{\perp} = \frac{2\pi K_{\perp}^{(2)}(\mathbf{k}, \omega)}{c}. \tag{13.201}$$

Then the continuity of the  $\tilde{H}_{\parallel}$ -component gives

$$-g_d^{(1)}(k, \omega) A_{\perp} = g_d^{(2)}(k, \omega) B_{\perp} \rightarrow A_{\perp} + B_{\perp} = 0, \quad (13.202)$$

since the  $g_d$  functions are unity. The continuity of the  $E_{\perp}$ -component gives

$$i4\pi K_{\perp}^{(1)}(\mathbf{k}, \omega) \frac{\omega}{c^2} \frac{1}{2\gamma^{(0)}k} G^{(1),\text{TE}}(k, \omega) - i4\pi K_{\perp}^{(2)}(\mathbf{k}, \omega) \frac{\omega}{c^2} \frac{1}{2\gamma^{(0)}k} G^{(2),\text{TE}}(k, \omega) = 0, \quad (13.203)$$

or

$$G^{(1),\text{TE}}(k, \omega) A_{\perp} - G^{(2),\text{TE}}(k, \omega) B_{\perp} = 0. \quad (13.204)$$

Thus, we have obtained the following system of equations

$$\begin{pmatrix} 1 & 1 \\ G^{(1),\text{TE}}(k, \omega) & -G^{(2),\text{TE}}(k, \omega) \end{pmatrix} \begin{pmatrix} A_{\perp} \\ B_{\perp} \end{pmatrix} = \begin{pmatrix} 0 \\ 0 \end{pmatrix}. \quad (13.205)$$

This system has the trivial solution that  $A_{\perp} = B_{\perp} = 0$ . It has also non-trivial solutions which are the modes we are looking for. The condition for normal modes is found as

$$\begin{vmatrix} 1 & 1 \\ G^{(1),\text{TE}}(k, \omega) & -G^{(2),\text{TE}}(k, \omega) \end{vmatrix} = 0, \quad (13.206)$$

or

$$G^{(1),\text{TE}}(k, \omega) + G^{(2),\text{TE}}(k, \omega) = 0. \quad (13.207)$$

Neglecting spatial dispersion we arrive at

$$\gamma_2 \tilde{\mu}^{(1)}(\omega) + \gamma_1 \tilde{\mu}^{(2)}(\omega) = 0, \quad (13.208)$$

We have now derived the general conditions for having surface-normal-modes at an interface between two media with and without spatial dispersion taken into account. We will here study the effect from spatial dispersion on the surface-plasmon-dispersion, i.e., the over-all effect on the  $k_F$  scale, and the effect on the surface-plasmon-polariton-dispersion, i.e., on the  $\omega_s/c$  scale.

### 13.13.1.1 Retardation Effects at Long Wavelengths

Retardation effects will modify the surface plasmon dispersion at the long wavelength range. The modes are given as solutions to the equation

$$G^{(1),\text{TM}}(k, \omega) + 1 = 0, \quad (13.209)$$

or expressed in modified  $g$ -functions, the ‘‘tilde-functions’’, as

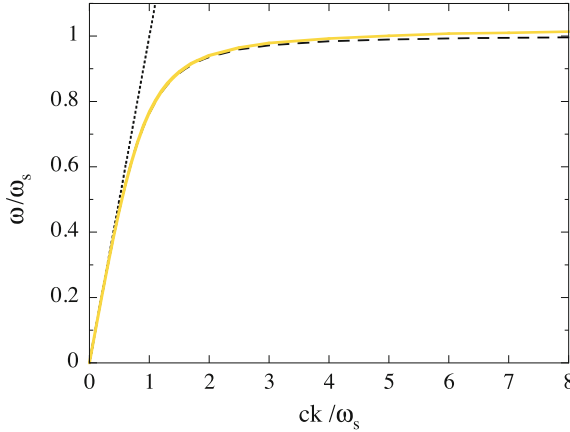


**Fig. 13.12** The surface-plasmon dispersion-curve for gold, *solid curve*, in the range where retardation effects are visible. The *dashed curve* is the universal result when spatial dispersion is neglected. The retardation effects push the surface-plasmon dispersion-curves down below the dispersion curve for light in vacuum, *dotted straight line*

$$\frac{1}{\gamma^{(0)}} \tilde{g}_a^{(1)}(k, \omega) - \frac{(\omega/ck)^2}{\gamma^{(0)}} \tilde{g}_b^{(1)}(k, \omega) + \frac{(1 - \gamma^{(0)})}{(\gamma^{(0)})^2} \tilde{g}_c^{(1)}(k, \omega) + 2 = 0. \quad (13.210)$$

Remember that the tilde over a  $g$ -function means the  $g$ -function calculated inside the medium minus the corresponding function calculated in vacuum. In Fig. 13.12 we show the results in the range where the retardation effects are important. We find that spatial dispersion has very small effect on the results here. The figure gives the result for gold, solid curve, in comparison with the result without spatial dispersion, dashed curve.

Next we study the modes and possible effects of spatial dispersion for the geometry of two half spaces.

### 13.13.2 Modes Associated with a Gap Between Two Half Spaces

Here, we can imagine that we have taken the geometry of a single interface and separated the two half spaces so that a gap of width  $d$  has opened up, see Fig. 9.18a. We have two interfaces; the left interface separates the left half space, of medium 1, from the gap which is assumed to be vacuum; the right interface separates the right half space, of medium 2, from the gap. The fields in the left half space are generated by surface current densities at the left interface; the fields in the right half space are generated by surface current densities at the right interface; the fields in the gap are generated by surface current densities at both interfaces. In this geometry there will be TM and TE modes even in neglect of magnetic effects. We proceed in the

same way as we did for a single interface and express the sources in terms of the two types of surface current density, one parallel to  $\mathbf{k}$ , producing TM modes, and one perpendicular to  $\mathbf{k}$ , producing TE modes. This is a little bit different from the treatment in [15] where we derived the TM modes from surface charge densities.

We need to define four additional factors,

$$\begin{aligned} C_{\parallel} &= \frac{2\pi K_{\parallel}^{(0,\text{left})}(\mathbf{k}, \omega)}{c} ; & D_{\parallel} &= \frac{2\pi K_{\parallel}^{(0,\text{right})}(\mathbf{k}, \omega)}{c}, \\ C_{\perp} &= \frac{2\pi K_{\perp}^{(0,\text{left})}(\mathbf{k}, \omega)}{c} ; & D_{\perp} &= \frac{2\pi K_{\perp}^{(0,\text{right})}(\mathbf{k}, \omega)}{c}. \end{aligned} \quad (13.211)$$

We begin with the TM modes and use the continuity of  $E_{\parallel}$  and  $\tilde{H}_{\perp}$  across the two interfaces. The  $E_{\parallel}$  component at the distance  $z$  from the source was given in (13.179). We may reuse part of the results from the single interface study. Just to the left of the left interface we have

$$E_{\parallel}(\mathbf{k}, 0^-; \omega) = -i4\pi K_{\parallel}^{(1)}(\mathbf{k}, \omega) \frac{k\gamma^{(0)}}{2\omega} G^{(1),\text{TM}} = -i2c \frac{k\gamma^{(0)}}{2\omega} G^{(1),\text{TM}} A_{\parallel}. \quad (13.212)$$

The field just to the right of the left interface has two terms; the first coming from the current density at the left interface; the second coming from the current density at the right interface. The first contribution we can write down directly. It is

$$\begin{aligned} E_{\parallel}(\mathbf{k}, 0^+; \omega)_1 &= -i2\pi K_{\parallel}^{(0,\text{left})}(\mathbf{k}, \omega) \frac{k\gamma^{(0)}}{\omega} G^{(0),\text{TM}} = \\ &= -i2\pi K_{\parallel}^{(0,\text{left})}(\mathbf{k}, \omega) \frac{k\gamma^{(0)}}{\omega} = -ic \frac{k\gamma^{(0)}}{\omega} C_{\parallel}. \end{aligned} \quad (13.213)$$

The second is

$$\begin{aligned} E_{\parallel}(\mathbf{k}, -d; \omega)_2 &= -i4\pi K_{\parallel}^{(0,\text{right})}(\mathbf{k}, \omega) \frac{k^2}{\omega} \int_{-\infty}^{\infty} \frac{dq_z}{2\pi} e^{-iq_z d} \\ &\times \left[ \frac{1}{q^2} - \left(\frac{\omega}{ck}\right)^2 \frac{1}{[q^2 - (\omega/c)^2]} + \frac{\omega^2}{c^2} \frac{1}{q^2 [q^2 - (\omega/c)^2]} \right] \\ &= -i4\pi K_{\parallel}^{(0,\text{right})}(\mathbf{k}, \omega) \frac{k^2}{\omega} \int_{-\infty}^{\infty} \frac{dq_z}{2\pi} e^{-iq_z d} \frac{1 - \left(\frac{\omega}{ck}\right)^2}{[q^2 - (\omega/c)^2]} \\ &= -i4\pi K_{\parallel}^{(0,\text{right})}(\mathbf{k}, \omega) \frac{k^2}{\omega} (\gamma^{(0)})^2 \int_{-\infty}^{\infty} \frac{dq_z}{2\pi} e^{-iq_z d} \frac{1}{[q^2 - (\omega/c)^2]} \\ &= -i8\pi K_{\parallel}^{(0,\text{right})}(\mathbf{k}, \omega) \frac{k^2}{\omega} (\gamma^{(0)})^2 \underbrace{\int_0^{\infty} \frac{dq_z}{2\pi} \frac{\cos(q_z d)}{[(q_z)^2 + (k\gamma^{(0)})^2]}}_{\frac{e^{-k\gamma^{(0)}d}}{4k\gamma^{(0)}}} \\ &= -i2\pi K_{\parallel}^{(0,\text{right})}(\mathbf{k}, \omega) \frac{k\gamma^{(0)}}{\omega} e^{-k\gamma^{(0)}d} = -ic \frac{k\gamma^{(0)}}{\omega} e^{-k\gamma^{(0)}d} D_{\parallel}. \end{aligned} \quad (13.214)$$

The  $E_{\parallel}$  component is continuous across the left interface if

$$G^{(1),\text{TM}} A_{\parallel} - C_{\parallel} - e^{-k\gamma^{(0)}d} D_{\parallel} = 0. \quad (13.215)$$

In analogy we find that the  $E_{\parallel}$  component is continuous across the right interface if

$$G^{(2),\text{TM}} B_{\parallel} - e^{-k\gamma^{(0)}d} C_{\parallel} - D_{\parallel} = 0. \quad (13.216)$$

Next we continue with the  $\tilde{H}_{\perp}$  component. The  $\tilde{H}_{\perp}$  component at the distance  $z$  from the source was given in (13.183). We may again reuse part of the results from the single interface study. Just to the left of the left interface we have

$$\tilde{H}_{\perp}(\mathbf{k}, 0^{-}; \omega) = \frac{2\pi}{c} K_{\parallel}^{(1)}(\mathbf{k}, \omega) g_d^{(1)} = \frac{2\pi}{c} K_{\parallel}^{(1)}(\mathbf{k}, \omega) = A_{\parallel}. \quad (13.217)$$

The field just to the right of the left interface has two terms; the first coming from the current density at the left interface; the second coming from the current density at the right interface. The first contribution we can write down directly. It is

$$\tilde{H}_{\perp}(\mathbf{k}, 0^{+}; \omega)_1 = -\frac{2\pi}{c} K_{\parallel}^{(0,\text{left})}(\mathbf{k}, \omega) g_d^{(0)} = -\frac{2\pi}{c} K_{\parallel}^{(0,\text{left})}(\mathbf{k}, \omega) = -C_{\parallel}. \quad (13.218)$$

The second is

$$\begin{aligned} \tilde{H}_{\perp}(\mathbf{k}, -d; \omega)_2 &= i \frac{4\pi K_{\parallel}^{(0,\text{right})}(\mathbf{k}, \omega)}{c} \int_{-\infty}^{\infty} \frac{dq_z}{2\pi} e^{-iq_z d} \frac{q_z}{[q^2 - (\omega/c)^2]} \\ &= i \frac{4\pi K_{\parallel}^{(0,\text{right})}(\mathbf{k}, \omega)}{c} \underbrace{\int_{-\infty}^{\infty} \frac{dq_z}{2\pi} e^{-iq_z d} \frac{q_z}{[(q_z)^2 + (k\gamma^{(0)})^2]}}_{-\frac{1}{2} e^{-k\gamma^{(0)}d}} \\ &= \frac{2\pi}{c} e^{-k\gamma^{(0)}d} K_{\parallel}^{(0,\text{right})}(\mathbf{k}, \omega) = e^{-k\gamma^{(0)}d} D_{\parallel}. \end{aligned} \quad (13.219)$$

The  $\tilde{H}_{\perp}$  component is continuous across the left interface if

$$A_{\parallel} + C_{\parallel} - e^{-k\gamma^{(0)}d} D_{\parallel} = 0. \quad (13.220)$$

In analogy we find that the  $\tilde{H}_{\perp}$  component is continuous across the right interface if

$$B_{\parallel} - e^{-k\gamma^{(0)}d} C_{\parallel} + D_{\parallel} = 0. \quad (13.221)$$

Thus we have found that the following system of equations should be fulfilled for to have TM modes:

$$\begin{aligned} G^{(1),\text{TM}} A_{\parallel} - C_{\parallel} - e^{-k\gamma^{(0)}d} D_{\parallel} &= 0 \\ G^{(2),\text{TM}} B_{\parallel} - e^{-k\gamma^{(0)}d} C_{\parallel} - D_{\parallel} &= 0 \\ A_{\parallel} + C_{\parallel} - e^{-k\gamma^{(0)}d} D_{\parallel} &= 0 \\ B_{\parallel} - e^{-k\gamma^{(0)}d} C_{\parallel} + D_{\parallel} &= 0. \end{aligned} \quad (13.222)$$

We eliminate  $A_{\parallel}$  and  $B_{\parallel}$  in favor of  $C_{\parallel}$  and  $D_{\parallel}$  and find

$$\begin{aligned} -[G^{(1),\text{TM}} + 1]C_{\parallel} + [G^{(1),\text{TM}} - 1]e^{-k\gamma^{(0)}d}D_{\parallel} &= 0, \\ [G^{(2),\text{TM}} - 1]e^{-k\gamma^{(0)}d}C_{\parallel} - [G^{(2),\text{TM}} + 1]D_{\parallel} &= 0, \end{aligned} \quad (13.223)$$

or on matrix form

$$\begin{pmatrix} -[G^{(1),\text{TM}} + 1] & [G^{(1),\text{TM}} - 1]e^{-k\gamma^{(0)}d} \\ [G^{(2),\text{TM}} - 1]e^{-k\gamma^{(0)}d} & -[G^{(2),\text{TM}} + 1] \end{pmatrix} \begin{pmatrix} C_{\parallel} \\ D_{\parallel} \end{pmatrix} = \begin{pmatrix} 0 \\ 0 \end{pmatrix}. \quad (13.224)$$

The non-trivial solution demands that

$$\begin{vmatrix} -[G^{(1),\text{TM}} + 1] & [G^{(1),\text{TM}} - 1]e^{-k\gamma^{(0)}d} \\ [G^{(2),\text{TM}} - 1]e^{-k\gamma^{(0)}d} & -[G^{(2),\text{TM}} + 1] \end{vmatrix} = 0, \quad (13.225)$$

or

$$[G^{(1),\text{TM}} + 1][G^{(2),\text{TM}} + 1] - e^{-2k\gamma^{(0)}d}[G^{(1),\text{TM}} - 1][G^{(2),\text{TM}} - 1] = 0. \quad (13.226)$$

Let us now find out the corresponding result when spatial dispersion is neglected. Then, since

$$G_1^{(i),\text{TM}}(k, \omega) = \frac{\gamma_i}{\gamma^{(0)}} \frac{1}{\varepsilon^{(i)}(\omega)}, \quad (13.227)$$

our condition is reduced into

$$\begin{aligned} \left[ \frac{\varepsilon^{(1)}(\omega)}{1} + \frac{\gamma_1(k, \omega)}{\gamma^{(0)}(k, \omega)} \right] \left[ \frac{\varepsilon^{(2)}(\omega)}{1} + \frac{\gamma_2(k, \omega)}{\gamma^{(0)}(k, \omega)} \right] \\ - e^{-2\gamma^{(0)}(k, \omega)kd} \left[ \frac{\varepsilon^{(1)}(\omega)}{1} - \frac{\gamma_1(k, \omega)}{\gamma^{(0)}(k, \omega)} \right] \left[ \frac{\varepsilon^{(2)}(\omega)}{1} - \frac{\gamma_2(k, \omega)}{\gamma^{(0)}(k, \omega)} \right] = 0. \end{aligned} \quad (13.228)$$

This is the well-established condition for TM-modes when spatial dispersion is neglected [2].

We are now done with the TM-modes. The TM-modes have both longitudinal and transverse character and both types of dielectric function enter the formalism. The fields involved in the TE modes on the other hand are genuinely transverse in character and only the transverse dielectric function enters the relations. Let us now continue with the TE modes, and use the continuity of  $E_{\perp}$  and  $\vec{H}_{\parallel}$  across the two interfaces. The  $E_{\perp}$  component at the distance  $z$  from the source was given in (13.194). We may reuse part of the results from the single interface study. Just to the left of the left interface we have

$$E_{\perp}(\mathbf{k}, 0^-; \omega) = i4\pi K_{\perp}^{(1)}(\mathbf{k}, \omega) \frac{\omega}{c^2} \frac{1}{2\gamma^{(0)}k} G^{(1),\text{TE}} = i \frac{\omega}{c} \frac{1}{\gamma^{(0)}k} G^{(1),\text{TE}} A_{\perp}. \quad (13.229)$$

The field just to the right of the left interface has two terms; the first coming from the current density at the left interface; the second coming from the current density at the right interface. The first contribution we can write down directly. It is

$$\begin{aligned} E_{\perp}(\mathbf{k}, 0^+; \omega)_1 &= i2\pi K_{\perp}^{(0,\text{left})}(\mathbf{k}, \omega) \frac{\omega}{c^2} \frac{1}{\gamma^{(0)k}} G^{(0),\text{TE}} = \\ &= -i2\pi K_{\perp}^{(0,\text{left})}(\mathbf{k}, \omega) \frac{\omega}{c^2} \frac{1}{\gamma^{(0)k}} = i \frac{\omega}{c} \frac{1}{\gamma^{(0)k}} C_{\perp}. \end{aligned} \quad (13.230)$$

The second is

$$\begin{aligned} E_{\perp}(\mathbf{k}, -d; \omega)_2 &= i4\pi K_{\perp}^{(0,\text{right})}(\mathbf{k}, \omega) \frac{\omega}{c^2} \int_{-\infty}^{\infty} \frac{dq_z}{2\pi} e^{-iq_z d} \frac{1}{[q^2 - (\omega/c)^2]} \\ &= i8\pi K_{\perp}^{(0,\text{right})}(\mathbf{k}, \omega) \frac{\omega}{c^2} \underbrace{\int_0^{\infty} \frac{dq_z}{2\pi} \frac{\cos(q_z d)}{[(q_z)^2 + (\gamma^{(0)k})^2]}_{\frac{e^{-\gamma^{(0)kd}}}{4\gamma^{(0)k}}} \\ &= i2\pi K_{\perp}^{(0,\text{right})}(\mathbf{k}, \omega) \frac{\omega}{c^2 \gamma^{(0)k}} e^{-\gamma^{(0)kd}} = i \frac{\omega}{c \gamma^{(0)k}} e^{-\gamma^{(0)kd}} D_{\perp}. \end{aligned} \quad (13.231)$$

The  $E_{\perp}$  component is continuous across the left interface if

$$G^{(1),\text{TE}} A_{\perp} - C_{\perp} - e^{-\gamma^{(0)kd}} D_{\perp} = 0. \quad (13.232)$$

In analogy we find that the  $E_{\parallel}$  component is continuous across the right interface if

$$G^{(2),\text{TE}} B_{\perp} - e^{-k\gamma^{(0)d}} C_{\perp} - D_{\perp} = 0. \quad (13.233)$$

Next we continue with the  $\tilde{H}_{\parallel}$  component. The  $\tilde{H}_{\parallel}$  component at the distance  $z$  from the source was given in (13.198). We may again reuse part of the results from the single interface study. Just to the left of the left interface we have

$$\tilde{H}_{\parallel}(\mathbf{k}, 0^-; \omega) = -\frac{2\pi}{c} K_{\perp}^{(1)}(\mathbf{k}, \omega) g_d^{(1)} = -\frac{2\pi}{c} K_{\perp}^{(1)}(\mathbf{k}, \omega) = -A_{\perp}. \quad (13.234)$$

The field just to the right of the left interface has two terms; the first coming from the current density at the left interface; the second coming from the current density at the right interface. The first contribution we can write down directly. It is

$$\tilde{H}_{\parallel}(\mathbf{k}, 0^+; \omega)_1 = \frac{2\pi}{c} K_{\perp}^{(0,\text{left})}(\mathbf{k}, \omega) g_d^{(0)} = \frac{2\pi}{c} K_{\perp}^{(0,\text{left})}(\mathbf{k}, \omega) = C_{\perp}. \quad (13.235)$$

The second is

$$\begin{aligned}
 \tilde{H}_{\parallel}(\mathbf{k}, -d; \omega)_2 &= -i \frac{4\pi K_{\perp}^{(0,\text{right})}(\mathbf{k}, \omega)}{c} \int_{-\infty}^{\infty} \frac{dq_z}{2\pi} e^{-iq_z d} \frac{q_z}{[q^2 - (\omega/c)^2]} \\
 &= -i \frac{4\pi K_{\perp}^{(0,\text{right})}(\mathbf{k}, \omega)}{c} \underbrace{\int_{-\infty}^{\infty} \frac{dq_z}{2\pi} e^{-iq_z d} \frac{q_z}{[(q_z)^2 + (k\gamma^{(0)})^2]}}_{-\frac{1}{2} e^{-k\gamma^{(0)}d}} \\
 &= -\frac{2\pi}{c} e^{-k\gamma^{(0)}d} K_{\perp}^{(0,\text{right})}(\mathbf{k}, \omega) = -e^{-k\gamma^{(0)}d} D_{\perp}.
 \end{aligned} \tag{13.236}$$

The  $\tilde{H}_{\parallel}$  component is continuous across the left interface if

$$A_{\perp} + C_{\perp} - e^{-k\gamma^{(0)}d} D_{\perp} = 0. \tag{13.237}$$

In analogy we find that the  $\tilde{H}_{\perp}$  component is continuous across the right interface if

$$B_{\perp} - e^{-k\gamma^{(0)}d} C_{\perp} + D_{\perp} = 0. \tag{13.238}$$

Thus we have found that the following system of equations should be fulfilled for to have TE modes:

$$\begin{aligned}
 G^{(1),\text{TE}} A_{\perp} - C_{\perp} - e^{-\gamma^{(0)}kd} D_{\perp} &= 0, \\
 G^{(2),\text{TE}} B_{\perp} - e^{-k\gamma^{(0)}d} C_{\perp} - D_{\perp} &= 0, \\
 A_{\perp} + C_{\perp} - e^{-k\gamma^{(0)}d} D_{\perp} &= 0, \\
 B_{\perp} - e^{-k\gamma^{(0)}d} C_{\perp} + D_{\perp} &= 0.
 \end{aligned} \tag{13.239}$$

We eliminate  $A_{\perp}$  and  $B_{\perp}$  in favor of  $C_{\perp}$  and  $D_{\perp}$  and find

$$\begin{aligned}
 -[G^{(1),\text{TE}} + 1] C_{\perp} + [G^{(1),\text{TE}} - 1] e^{-k\gamma^{(0)}d} D_{\perp} &= 0, \\
 [G^{(2),\text{TE}} - 1] e^{-k\gamma^{(0)}d} C_{\perp} - [G^{(2),\text{TE}} + 1] D_{\perp} &= 0,
 \end{aligned} \tag{13.240}$$

or on matrix form

$$\begin{pmatrix} -[G^{(1),\text{TE}} + 1] & [G^{(1),\text{TE}} - 1] e^{-k\gamma^{(0)}d} \\ [G^{(2),\text{TE}} - 1] e^{-k\gamma^{(0)}d} & -[G^{(2),\text{TE}} + 1] \end{pmatrix} \begin{pmatrix} C_{\perp} \\ D_{\perp} \end{pmatrix} = \begin{pmatrix} 0 \\ 0 \end{pmatrix}. \tag{13.241}$$

The non-trivial solution demands that

$$\begin{vmatrix} -[G^{(1),\text{TE}} + 1] & [G^{(1),\text{TE}} - 1] e^{-k\gamma^{(0)}d} \\ [G^{(2),\text{TE}} - 1] e^{-k\gamma^{(0)}d} & -[G^{(2),\text{TE}} + 1] \end{vmatrix} = 0, \tag{13.242}$$

or

$$[G^{(1),\text{TE}} + 1][G^{(2),\text{TE}} + 1] - e^{-2k\gamma^{(0)}d} [G^{(1),\text{TE}} - 1][G^{(2),\text{TE}} - 1] = 0. \tag{13.243}$$

Let us now find out the corresponding result when spatial dispersion is neglected. Then, since

$$G_1^{(i),\text{TE}}(k, \omega) = \frac{\gamma^{(0)}}{\gamma_i} \mu^{(i)}(\omega), \quad (13.244)$$

our condition is reduced into

$$[\gamma^{(0)} \mu^{(1)}(\omega) + \gamma_1][\gamma^{(0)} \mu^{(2)}(\omega) + \gamma_2] - e^{-2\gamma^{(0)}(k, \omega)kd} [\gamma^{(0)} \mu^{(1)}(\omega) - \gamma_1][\gamma^{(0)} \mu^{(2)}(\omega) - \gamma_2] = 0. \quad (13.245)$$

This is the well-established condition for TE-modes when spatial dispersion is neglected [2], generalized to take magnetic effects into account. So in summary we have the two mode types from the relations

$$[G^{(1),\text{TM,TE}}(k, \omega) + 1][G^{(2),\text{TM,TE}}(k, \omega) + 1] - e^{-2\gamma^{(0)}(k, \omega)d} [G^{(1),\text{TM,TE}}(k, \omega) - 1][G^{(2),\text{TM,TE}}(k, \omega) - 1] = 0. \quad (13.246)$$

We here just note in passing that the relation between our  $G$ -functions and the so-called surface impedance can be found from the relations above. The surface impedance for  $p$ -polarized and  $s$ -polarized waves are

$$\begin{aligned} Z^p &= E_{\parallel}/H_{\perp} = \left[ -\frac{ick\gamma^{(0)}}{\omega} G^{(i),\text{TM}}(k, \omega) A_{\parallel} \right] / \left[ g_d^{(i)}(k, \omega) A_{\parallel} \right] \\ &= -i \frac{\gamma^{(0)}}{(\omega/ck)} G^{(i),\text{TM}}(k, \omega), \end{aligned} \quad (13.247)$$

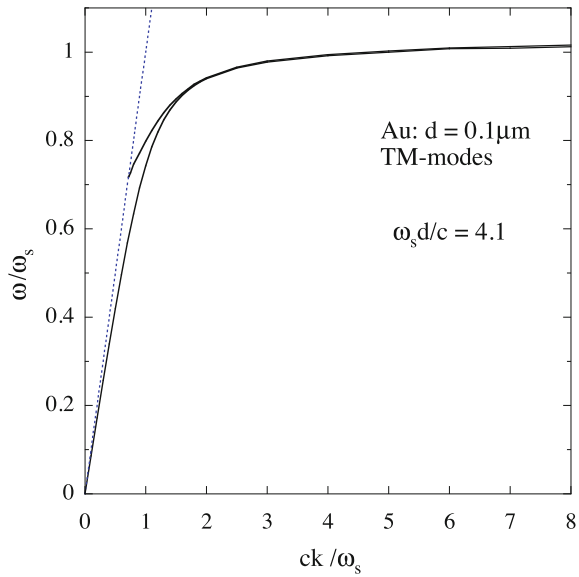
and

$$Z^s = E_{\perp}/H_{\parallel} = i \frac{(\omega/ck)}{\gamma^{(0)}} G^{(i),\text{TE}} A_{\perp} / (-A_{\perp}) = -i \frac{(\omega/ck)}{\gamma^{(0)}} G^{(i),\text{TE}}, \quad (13.248)$$

respectively. One should be a little careful with the sign. It is understood that the  $z$ -direction is into the interface. So to find the relation here we have used the fields at the left interface. If we had used the fields at the interface to the right we would have had to change sign.

In Fig. 13.13 we show the two TM-modes for two gold half spaces separated by a gap of  $0.1 \mu\text{m}$ . In the region where retardation is important the spatial dispersion is once again negligible. This is also the region which is important for the force in the Casimir range. From these findings one would guess that spatial dispersion has negligible effect on the Casimir force. We will show later that this is actually what we find for the contribution from TM-modes, but not from the TE-modes at room temperature. At the high momentum side of the figure we note that the frequency of the mode has increased a little beyond the value unity. This very modest effect is caused by the spatial dispersion. Now, one of the two TM-modes seems to end at the light-dispersion curve in the figure. It actually continues on the other side, but is not a true surface mode there. There the fields do not decay exponentially away from the metal. Instead they form standing waves between the two surfaces. This mode

**Fig. 13.13** The two TM-surface-mode branches for two half spaces of gold separated by a gap of 0.1  $\mu\text{m}$ . The *upper solid curve* is just that part of a branch where the mode is a true surface mode in that the fields decay exponentially away from the two interfaces on both sides. The *dotted straight line* is the light dispersion curve in vacuum. See the text for more details. Adapted from [15]



has one node between the surfaces. There are also modes with 2, 3 ... nodes. All the TE-modes come in the region to the left of and above the light dispersion curve. They have 0, 1, ... number of nodes. There is a larger number of modes present the larger the separation between the surfaces.

In Fig. 13.14 we show the results for a little larger separation and now in neglect of spatial dispersion. In this case there are six TM-modes and four TE-modes. One of the TM-modes is a true surface mode; one is for a part of the dispersion curve a true surface mode and for the rest of the dispersion curve a standing-wave type or wave-guide type. The four remaining TM-modes and the four TE-modes are wave-guide modes. The upper solid curve is the boundary of the continuum of bulk-polariton modes. Above this curve the metals can no longer keep the modes in the gap, they can propagate freely through the geometry and do not contribute to the dispersion forces. The larger the separation between the surfaces the larger the number of modes between the light dispersion curve and the bulk-polariton continuum.

### 13.13.3 Dispersion Interactions Between Two Gold Plates in Vacuum

In the previous section we found that the conditions for the two mode types between two non-magnetic metal half spaces separated by a vacuum gap of thickness  $d$  are

$$[G^{\text{TM,TE}}(k, \omega) + 1]^2 - e^{-2\gamma d} [G^{\text{TM,TE}}(k, \omega) - 1]^2 = 0, \quad (13.249)$$

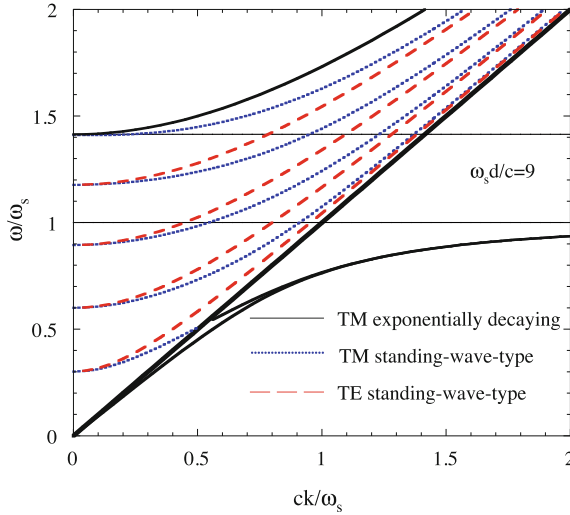


**Fig. 13.14** The complete set of normal modes between gold surfaces (obtained in neglect of spatial dispersion) for roughly twice the separation of the setup in Fig. 13.13. The *upper thick solid curve* is the boundary for bulk-polariton-modes and the *lower thick solid straight line* is the light-dispersion-curve. The *thin solid curves* are the true-surface-mode-type-modes, the *dotted curves* are the standing-wave-type TM-modes and the *dashed curves* the standing-wave-type TE-modes. Note that one of the TM-mode branches changes character when crossing the light-dispersion-curve. Adapted from [15]

where

$$\begin{aligned}
 G^{\text{TM}}(k, \omega) &= \frac{k}{\gamma} \tilde{g}_a(k, \omega) + \frac{k(k-\gamma)}{\gamma^2} \tilde{g}_c(k, \omega) - \frac{(\omega/c)^2}{\gamma^2} \tilde{g}_b(k, \omega) + 1; \\
 G^{\text{TE}}(k, \omega) &= \tilde{g}_b(k, \omega) + 1.
 \end{aligned}
 \tag{13.250}$$

From this the interaction energy (13.9) is found to be [2, 3]

$$\begin{aligned}
 \Delta E(d) &= \frac{1}{2\pi\beta} \sum'_{\xi_n} \int_0^\infty dk k \ln \left\{ 1 - e^{2\gamma(k, i\xi_n)d} \frac{[G^{\text{TM}}(k, i\xi_n) - 1]^2}{[G^{\text{TM}}(k, i\xi_n) + 1]^2} \right\} \\
 &+ \frac{1}{2\pi\beta} \sum'_{\xi_n} \int_0^\infty dk k \ln \left\{ 1 - e^{2\gamma(k, i\xi_n)d} \frac{[G^{\text{TE}}(k, i\xi_n) - 1]^2}{[G^{\text{TE}}(k, i\xi_n) + 1]^2} \right\},
 \end{aligned}
 \tag{13.251}$$

where

$$\xi_n = \frac{2\pi n}{\hbar\beta}; \quad n = 0, 1, 2, \dots
 \tag{13.252}$$

The prime on the summation sign indicates that the  $n = 0$  term is multiplied by the factor 1/2. For zero temperature the summation is replaced by an integration:

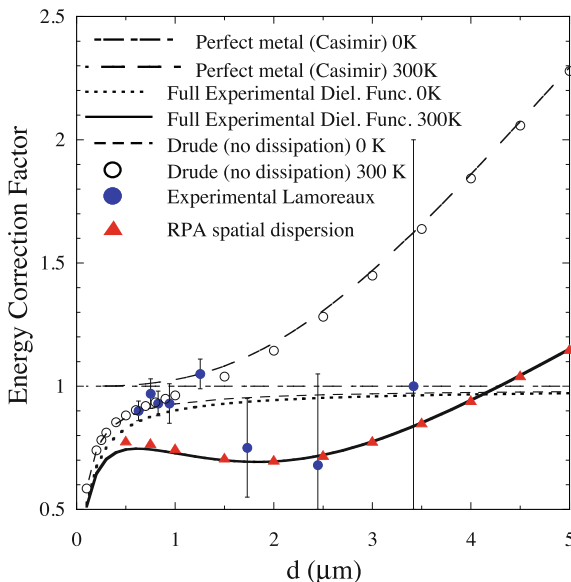


**Fig. 13.15** Energy correction factor as function of separation between two gold plates. The *dash-dotted curve* is the Casimir ideal-metal result at zero temperature; it is by definition constant with value unity. The *long-dashed curve* is the corresponding result at room-temperature. The *solid curve* is the room-temperature result from using the experimental dielectric function and the *dotted curve* is the corresponding zero-temperature result; these results include the effect of dissipation but neglect the spatial dispersion. The *short-dashed curve* is the simple Drude result,  $\tilde{\epsilon}(\omega) = 1 - \omega_{pl}^2/\omega^2$ , at zero temperature and the *open circles* indicate the corresponding room-temperature result; these results neglect both dissipation and spatial dispersion. The *triangles* is the present result including spatial dispersion; dissipation is neglected but inclusion of dissipation leads to an overlapping result. The *solid circles* with error bars is the experimental result by Lamoreaux [8]. Adapted from [15]

$$\frac{1}{\beta} \sum'_{\xi_n} \rightarrow \hbar \int_0^{\infty} \frac{d\xi}{2\pi}. \tag{13.253}$$

The results are presented in Fig. 13.15. All results in the figure are the interaction energy divided by the zero-temperature (Casimir) result  $(\hbar c \pi^2 / 720 d^3)$  for an ideal metal as given in (13.25). The filled circles with error bars is the experimental result by Lamoreaux [8]. The solid curve is the result [3] from using the experimental dielectric properties, given in Fig.9.3. This means that dissipation was included but no spatial dispersion. Very similar results are obtained from using the Drude expression, including dissipation, for the dielectric function [2, 3]. The momentum dependence of the dielectric function can not be obtained experimentally so when taking spatial dispersion into account one is forced to use theoretical expressions for the dielectric functions. The triangles show the result when (13.251) was used. Thus spatial dispersion was taken into account and the RPA dielectric functions were used

with polarizabilities from (13.175) and (13.176). Taking also dissipation into account by using the polarizabilities in (13.177) and (13.178) lead to very small additional corrections. It is very interesting to note that the result with spatial dispersion included is almost identical to the result [3] where the dramatic effect came from dissipation. It is not completely surprising that spatial dispersion has the effect that the TE modes do not contribute to the thermal Casimir effect. We found in the work [9, 26] on the Casimir force between two quantum wells, a problem where the inclusion of spatial dispersion is a necessity, that the contribution from the TE modes dropped out for finite temperature and large separation. Besides we have met this result before in this book at several places. We found it for two graphene sheets, in Fig. 13.4b for pristine graphene and in Fig. 13.5b for doped graphene. We also found it for a graphene sheet next to a gold wall, in Fig. 13.7b for pristine graphene and in Fig. 13.8b for doped graphene.

Furthermore, the failure of the TE-modes to contribute at finite temperature and large separations is not that surprising. For them to contribute the transverse dielectric function has to diverge as  $\xi^{-2}$  when the frequency goes toward zero. When dissipation is included and spatial dispersion neglected it goes as  $\xi^{-1}$  (see Fig. 9.3). It is not equally obvious when spatial dispersion is included instead of dissipation. Here the formalism becomes more involved. The TE-contribution does no longer asymptotically completely vanish but becomes very small as compared to the TM-contribution. It completely vanishes if dissipation is included in the dielectric function, i.e. using the polarizabilities in (13.177) and (13.178). Thus we have seen that dissipation and/or spatial dispersion has very dramatic effects on the thermal Casimir effect.<sup>4</sup> The dramatic effects are absent at zero temperature. The negligible effect of spatial dispersion at zero temperature is in accordance with recent publications [28, 29].

There has been a controversy in the literature as to if the TE modes should contribute or not. The cluster of data points for  $d \approx 1\mu\text{m}$  and experimental results by R. S. Decca et. al [30] support the view that TE modes should contribute. There are however, new [31] experimental data with a more detailed analysis taking patch potentials into account, that support the view that TE modes should not contribute.

## References

1. Bo E. Sernelius, *Phys. Rev. B* **90**, 155457 (2014)
2. Bo E. Sernelius, *Surface Modes in Physics* (Wiley-VCH, Berlin, 2001)
3. M. Boström, Bo E. Sernelius, *Phys. Rev. Lett.* **84**, 4757 (2000)
4. M. Bordag, G.L. Klimchitskaya, U. Mohideen, V.M. Mostepanenko, *Advances in the Casimir Effect* (Oxford University Press, Oxford, 2009)
5. H.B.G. Casimir, *Proc. K. Ned. Akad. Wet.* **51**, 793 (1948)
6. Bo E. Sernelius, *Graphene* **1**, 21 (2012)
7. Bo E. Sernelius, *J. Phys.: Condens. Matter* **27**, 214017 (2015)

<sup>4</sup>Spatial dispersion and/or dissipation has the effects that Nernst heat theorem [27] is obeyed. We had earlier shown [17] that the formalism in this book obeys this theorem in presence of dissipation.

8. S.K. Lamoreaux, Phys. Rev. Lett. **78**, 5 (1997)
9. Bo E. Sernelius, P. Björk. Phys. Rev. B **57**, 6592 (1998)
10. Bo E. Sernelius, Phys. Rev. B **85**, 195427 (2012)
11. E.A. Power, Am. J. Phys. **34**, 516 (1966)
12. Bo E. Sernelius, Phys. Rev. A **80**, 043828 (2009)
13. M. Boström, Bo E. Sernelius, Phys. Rev. A **61**, 052703–1 (2000)
14. H.B.G. Casimir, D. Polder, Phys. Rev. B **73**, 360 (1948)
15. Bo E. Sernelius, Phys. Rev. B **71**, 235114 (2005)
16. B. Geyer, G.L. Klimchitskaya, V.M. Mostepanenko, Phys. Rev. A **67**, 062102 (2003). and references therein
17. Bo E. Sernelius, M. Boström, in *Quantum Field Theory Under the Influence of External Conditions*, ed. by K.A. Milton (Rinton Press, Princeton, 2004)
18. J.S. Høye, I. Brevik, J.B. Aarseth, K.A. Milton, Phys. Rev. E **67**, 056116 (2003)
19. J.S. Høye, I. Brevik, J.B. Aarseth, Phys. Rev. E **63**, 051101 (2001)
20. I. Brevik, J.B. Aarseth, J.S. Høye **66**, 026119 (2002)
21. I. Brevik, J.B. Aarseth, J.S. Høye, K.A. Milton, in *Quantum Field Theory Under the Influence of External Conditions*, ed. by K.A. Milton (Rinton Press, Princeton, 2004)
22. D.A.R. Dalvit, S.K. Lamoreaux, Phys. Rev. Lett. **102**, 189304 (2009)
23. J. Lindhard, Kgl. Danske Videnskab. Selskab, Mat.-Fys. Medd. **28**, No. 8 (1954)
24. N.D. Mermin, Phys. Rev. B **1**, 2362 (1970)
25. K.L. Kliewer, R. Fuchs, Phys. Rev. **181**, 552 (1969)
26. M. Boström, Bo E. Sernelius, Microelectron. Eng. **51–52**, 287–97 (2000)
27. W. Nernst, Nachr. Kgl. Ges. Wiss. Gött., No. **1**, 1 (1906)
28. R. Esquivel, C. Villarreal, W.L. Mochan, Phys. Rev. A **68**, 052103 (2003)
29. R. Esquivel, V.B. Svetovoy, Phys. Rev. A **69**, 062102 (2004)
30. R.S. Decca, D. López, E. Fischbach, G.L. Klimchitskaya, D.E. Krause, V.M. Mostepanenko, Phys. Rev. D **75**, 077101 (2007)
31. A.O. Sushkov, W.J. Kim, D.A.R. Dalvit, S.K. Lamoreaux, Nat. Phys. **7**, 230 (2011)

# Chapter 14

## Dispersion Interaction in Spherical Structures



**Abstract** After a section in which we adapt the general formalism presented in Chap. 7 to spherical structures we start by introducing the basic structure elements: a single spherical interface, a spherical shell, a thin diluted spherical gas film, and a 2D spherical film. A general spherical structure can then be constructed by stacking these elements concentrically. The thin gas layer is special; it is used to find the interaction on an atom at a general position in the spherical structure. Then we go through some common structures and present illustrating examples; the examples involve gold balls, spherical gold cavities, spherical graphene shells, and lithium atoms. We furthermore rederive the Casimir interaction between two atoms by comparing the full result in the diluted limit with that from the summation of pair interactions. We even rederive the full expression for the Casimir-polder interaction between two atoms by studying the atom-ball geometry in the diluted limit.

### 14.1 Adapting the General Method of Chap. 7 to Spherical Structures

To find the normal modes for a layered sphere including retardation effects we need to solve the wave equation for the electric and magnetic fields in all layers and use the proper boundary conditions at the interfaces. To solve the vector wave equation the vector Helmholtz equation, (7.22), is not a trivial task. Instead one may solve the problem by introducing Hertz-Debye potentials  $\pi_1$  and  $\pi_2$ . They are solutions to the scalar wave equation, (7.23). We let  $\pi_1$  be the potential that generates TM modes and  $\pi_2$  be the potential that generates TE modes. In a spherical system the TM mode has its magnetic field perpendicular to the radial direction and the TE mode has its electric field perpendicular to the radial direction. Separation of variables,  $\pi = R(r) \Theta(\theta) \Phi(\phi)$ , leads to one differential equation for each of the variables,

$$\begin{aligned} \frac{d^2[rR(r)]}{dr^2} + \left[ q^2 - \frac{i(i+1)}{r^2} \right] [rR(r)] &= 0; \\ \frac{1}{\sin\theta} \frac{d}{d\theta} \left[ \sin\theta \frac{d\Theta(\theta)}{d\theta} \right] + \left[ i(i+1) - \frac{m^2}{\sin^2\theta} \right] \Theta(\theta) &= 0; \\ \frac{d^2\Phi(\phi)}{d\phi^2} + m^2\Phi(\phi) &= 0, \end{aligned} \quad (14.1)$$

where  $q = [\tilde{n}(\omega)\omega/c]$ .

The angular equations lead to spherical harmonics and for the radial part  $rR(r)$  is a solution to the Ricatti-Bessel equation [1],

$$z^2 \frac{d^2 \omega}{dz^2} + [z^2 - i(i+1)] \omega = 0. \quad (14.2)$$

The Ricatti-Bessel equation has many different solutions:

- Ricatti-Bessel functions of the first kind:

$$S_i(z) = z j_i(z) = \sqrt{\pi z/2} J_{i+1/2}(z) = \psi_i(z); \quad (14.3)$$

- Ricatti-Bessel functions of second kind:

$$C_i(z) = -z y_i(z) = \sqrt{\pi z/2} Y_{i+1/2}(z) = \chi_i(z); \quad (14.4)$$

- Ricatti-Bessel functions of the third kind:

$$\begin{aligned} \xi_i(z) &= z h_i^{(1)}(z) = \sqrt{\pi z/2} H_{i+1/2}^{(1)}(z) \\ &= S_i(z) - i C_i(z) = z j_i(z) + i z y_i(z); \\ \zeta_i(z) &= z h_i^{(2)}(z) = \sqrt{\pi z/2} H_{i+1/2}^{(2)}(z) \\ &= S_i(z) + i C_i(z) = z j_i(z) - i z y_i(z). \end{aligned} \quad (14.5)$$

Let us study a layered sphere of radius  $r_0$  consisting of  $N$  layers and an inner spherical core. We have  $N + 2$  media and  $N + 1$  interfaces. Let the numbering be as follows. Medium 0 is the medium surrounding the sphere, medium 1 is the outermost layer, medium  $N + 1$  the innermost layer, and medium  $N + 2$  the innermost spherical core region. Let  $r_n$  be the inner radius of layer  $n$ . This is completely in line with the system represented by Fig. 7.1.

We will use the two Hankel versions in (14.5) since they represent waves that go in either the positive or negative  $r$ -directions. We assume a time dependence of the form  $e^{-i\omega t}$ . With this choice the first Ricatti-Hankel function,  $\xi_n(qr) e^{-i\omega t} \propto e^{i(qr-\omega t)}$ , represents a wave moving in the positive radial direction (toward the left in Fig. 7.1) while the second,  $\zeta_n(qr) e^{-i\omega t} \propto e^{-i(qr+\omega t)}$ , represents a wave moving in the negative radial direction (toward the right in Fig. 7.1). Thus the general solution for the potentials is

$$r\pi = \sum_{l=1}^{\infty} \sum_{m=-l}^l [a_l \zeta_l(qr) + b_l \xi_l(qr)] Y_{l,m}(\theta, \phi) e^{-i\omega t}. \quad (14.6)$$

From the potentials we get the fields [2–4]

$$\begin{aligned}
E_r &= E_{1r} + E_{2r} = \frac{\partial^2(r\pi_1)}{\partial r^2} + q^2 r \pi_1 + 0; \\
E_\theta &= E_{1\theta} + E_{2\theta} = \frac{1}{r} \frac{\partial^2(r\pi_1)}{\partial r \partial \theta} - \frac{i\omega}{c} \frac{1}{r \sin \theta} \frac{\partial(r\pi_2)}{\partial \phi}; \\
E_\phi &= E_{1\phi} + E_{2\phi} = \frac{1}{r \sin \theta} \frac{\partial^2(r\pi_1)}{\partial r \partial \phi} + \frac{i\omega}{c} \frac{1}{r} \frac{\partial(r\pi_2)}{\partial \theta}; \\
H_r &= H_{1r} + H_{2r} = 0 + \frac{\partial^2(r\pi_2)}{\partial r^2} + q^2 r \pi_2; \\
H_\theta &= H_{1\theta} + H_{2\theta} = \frac{i\omega \tilde{\epsilon}}{c} \frac{1}{r \sin \theta} \frac{\partial(r\pi_1)}{\partial \phi} + \frac{1}{r} \frac{\partial^2(r\pi_2)}{\partial r \partial \theta}; \\
H_\phi &= H_{1\phi} + H_{2\phi} = -\frac{i\omega \tilde{\epsilon}}{c} \frac{1}{r} \frac{\partial(r\pi_1)}{\partial \theta} + \frac{1}{r \sin \theta} \frac{\partial^2(r\pi_2)}{\partial r \partial \phi}.
\end{aligned} \tag{14.7}$$

Let us now use the boundary conditions that the tangential components of  $\mathbf{E}$  and  $\tilde{\mathbf{H}}$  are continuous at the interface between layer  $n$  and  $n + 1$ . We get

$$\begin{aligned}
(\partial/\partial r) [r\pi_1^n]_{r=r_n} &= (\partial/\partial r) [r\pi_1^{n+1}]_{r=r_n}; \\
(\partial/\partial r) [r\pi_2^n]_{r=r_n} &= (\partial/\partial r) [r\pi_2^{n+1}]_{r=r_n}; \\
(\tilde{\epsilon}^n i\omega/c) [r\pi_1^n]_{r=r_n} &= (\tilde{\epsilon}^{n+1} i\omega/c) [r\pi_1^{n+1}]_{r=r_n}; \\
(\omega/c) [r\pi_2^n]_{r=r_n} &= (\omega/c) [r\pi_2^{n+1}]_{r=r_n}.
\end{aligned} \tag{14.8}$$

This gives

$$\begin{aligned}
&q_n [a_{1,l}^n \zeta_l' (q_n r_n) + b_{1,l}^n \xi_l' (q_n r_n)] \\
&= q_{n+1} [a_{1,l}^{n+1} \zeta_l' (q_{n+1} r_n) + b_{1,l}^{n+1} \xi_l' (q_{n+1} r_n)]; \\
&q_n [a_{2,l}^n \zeta_l' (q_n r_n) + b_{2,l}^n \xi_l' (q_n r_n)] \\
&= q_{n+1} [a_{2,l}^{n+1} \zeta_l' (q_{n+1} r_n) + b_{2,l}^{n+1} \xi_l' (q_{n+1} r_n)]; \\
&q_n^2 [a_{1,l}^n \zeta_l (q_n r_n) + b_{1,l}^n \xi_l (q_n r_n)] \\
&= q_{n+1}^2 [a_{1,l}^{n+1} \zeta_l (q_{n+1} r_n) + b_{1,l}^{n+1} \xi_l (q_{n+1} r_n)]; \\
&[a_{2,l}^n \zeta_l (q_n r_n) + b_{2,l}^n \xi_l (q_n r_n)] \\
&= [a_{2,l}^{n+1} \zeta_l (q_{n+1} r_n) + b_{2,l}^{n+1} \xi_l (q_{n+1} r_n)],
\end{aligned} \tag{14.9}$$

where a prime on a function means the derivative with respect to its argument.

Let us first assume pure TM-modes. That means keeping  $\pi_1$  only. Then we have

$$\begin{aligned}
&a_{1,l}^n q_n \zeta_l' (q_n r_n) + b_{1,l}^n q_n \xi_l' (q_n r_n) \\
&= a_{1,l}^{n+1} q_{n+1} \zeta_l' (q_{n+1} r_n) + b_{1,l}^{n+1} q_{n+1} \xi_l' (q_{n+1} r_n); \\
&a_{1,l}^n q_n^2 \zeta_l (q_n r_n) + b_{1,l}^n q_n^2 \xi_l (q_n r_n) \\
&= a_{1,l}^{n+1} q_{n+1}^2 \zeta_l (q_{n+1} r_n) + b_{1,l}^{n+1} q_{n+1}^2 \xi_l (q_{n+1} r_n),
\end{aligned} \tag{14.10}$$

and we may identify the matrix  $\tilde{\mathbf{A}}_n(r_n)$  as

$$\tilde{\mathbf{A}}_n^{\text{TM}}(r_n) = \begin{pmatrix} q_n \zeta_l' (q_n r_n) & q_n \xi_l' (q_n r_n) \\ q_n^2 \zeta_l (q_n r_n) & q_n^2 \xi_l (q_n r_n) \end{pmatrix}, \tag{14.11}$$

and the matrix  $\tilde{\mathbf{M}}_n$  as

$$\tilde{\mathbf{M}}_n^{\text{TM}} = \frac{-q_{n+1}}{q_n^2 (2i)} \begin{pmatrix} q_n \xi_l \zeta_l'^+ - q_{n+1} \xi_l' \zeta_l^+ & q_n \xi_l \xi_l'^+ - q_{n+1} \xi_l' \xi_l^+ \\ -q_n \zeta_l \zeta_l'^+ + q_{n+1} \zeta_l' \zeta_l^+ & -q_n \zeta_l \xi_l'^+ + q_{n+1} \zeta_l' \xi_l^+ \end{pmatrix}, \tag{14.12}$$

where we to save space have omitted the function arguments. All functions with a + added as a superscript have the argument  $(q_{n+1}r_n)$  and the ones without the superscript have the argument  $(q_n r_n)$ . We have also made use of the Wronskian of the two Ricatti-Bessel functions:  $W[\zeta_l(x), \xi_l(x)] = \xi_l'(x)\zeta_l(x) - \zeta_l'(x)\xi_l(x) = 2i$ .

Now we repeat the derivation for TE- modes. That means keeping  $\pi_2$  only. Then we have

$$\begin{aligned} & a_{2,l}^n q_n \zeta_l'(q_n r_n) + b_{2,l}^n q_n \xi_l'(q_n r_n) \\ &= a_{2,l}^{n+1} q_{n+1} \zeta_l'(q_{n+1} r_n) + b_{2,l}^{n+1} q_{n+1} \xi_l'(q_{n+1} r_n); \\ & a_{2,l}^n \zeta_l(q_n r_n) + b_{2,l}^n \xi_l(q_n r_n) \\ &= a_{2,l}^{n+1} \zeta_l(q_{n+1} r_n) + b_{2,l}^{n+1} \xi_l(q_{n+1} r_n), \end{aligned} \quad (14.13)$$

and we may identify the matrix  $\tilde{\mathbf{A}}_n(r_n)$  as

$$\tilde{\mathbf{A}}_n^{\text{TE}}(r_n) = \begin{pmatrix} q_n \zeta_l'(q_n r_n) & q_n \xi_l'(q_n r_n) \\ \zeta_l(q_n r_n) & \xi_l(q_n r_n) \end{pmatrix}, \quad (14.14)$$

and the matrix  $\tilde{\mathbf{M}}_n$  as

$$\tilde{\mathbf{M}}_n^{\text{TE}} = \frac{-1}{q_n(2i)} \begin{pmatrix} -q_n \xi_l' \zeta_l^+ + q_{n+1} \xi_l \zeta_l'^+ & -q_n \xi_l' \xi_l^+ + q_{n+1} \xi_l \xi_l'^+ \\ q_n \zeta_l' \zeta_l^+ - q_{n+1} \zeta_l \zeta_l'^+ & q_n \zeta_l' \xi_l^+ - q_{n+1} \zeta_l \xi_l'^+ \end{pmatrix}. \quad (14.15)$$

Of the solutions to the Ricatti-Bessel equation in (14.2) the Ricatti-Bessel function of the first kind is the function that is regular at the origin. Thus this is the function we should use in the rightmost region of Fig. 7.1. Now, since the function  $\psi_l(z) = [\xi_l(z) + \zeta_l(z)]/2$  we have that  $b_{N+1} = a_{N+1}$ . According to (7.6) this means that

$$f_{l,m}(\omega) = M_{11} + M_{12}. \quad (14.16)$$

Before we end this section we introduce the  $2^l$  pole polarizabilities  $\alpha_l^n$  and  $\alpha_l^{n(2)}$  for the spherical interface since these appear repeatedly in the sections that follow. The first is valid outside and the second inside. The polarizability  $\alpha_l^n = -b^n/a^n$  under the assumption that  $b^{n+1} = a^{n+1}$ . One obtains  $\alpha_l^n = -(M_{21}^n + M_{22}^n)/(M_{11}^n + M_{12}^n)$  and from (14.12) one finds that for TM modes

$$\alpha_l^{\text{TM},n} = \frac{q_n \zeta_l(q_n r_n) \psi_l'(q_{n+1} r_n) - q_{n+1} \zeta_l'(q_n r_n) \psi_l(q_{n+1} r_n)}{q_n \xi_l(q_n r_n) \psi_l'(q_{n+1} r_n) - q_{n+1} \xi_l'(q_n r_n) \psi_l(q_{n+1} r_n)}. \quad (14.17)$$

In the same way one finds from (14.15) that for TE modes

$$\alpha_l^{\text{TE},n} = \frac{q_n \zeta_l'(q_n r_n) \psi_l(q_{n+1} r_n) - q_{n+1} \zeta_l(q_n r_n) \psi_l'(q_{n+1} r_n)}{q_n \xi_l'(q_n r_n) \psi_l(q_{n+1} r_n) - q_{n+1} \xi_l(q_n r_n) \psi_l'(q_{n+1} r_n)}. \quad (14.18)$$

The polarizability  $\alpha_l^{n(2)} = -a^{n+1}/b^{n+1}$  under the assumption that  $a^n = 0$ . One obtains  $\alpha_l^{n(2)} = M_{12}/M_{11}$  and from (14.12) one finds that for the TM modes

$$\alpha_l^{\text{TM},n(2)} = \frac{q_n \xi_l(q_n r_n) \xi_l'(q_{n+1} r_n) - q_{n+1} \xi_l'(q_n r_n) \xi_l(q_{n+1} r_n)}{q_n \xi_l(q_n r_n) \zeta_l'(q_{n+1} r_n) - q_{n+1} \xi_l'(q_n r_n) \zeta_l(q_{n+1} r_n)}. \quad (14.19)$$

From (14.15) one finds that for TE modes

$$\alpha_l^{\text{TE},n(2)} = \frac{q_n \xi_l'(q_n r_n) \xi_l'(q_{n+1} r_n) - q_{n+1} \xi_l(q_n r_n) \xi_l'(q_{n+1} r_n)}{q_n \xi_l'(q_n r_n) \zeta_l(q_{n+1} r_n) - q_{n+1} \xi_l(q_n r_n) \zeta_l'(q_{n+1} r_n)}. \quad (14.20)$$

When we calculate the energy by an integral along the imaginary frequency axis the arguments of the Ricatti-Bessel functions become imaginary. It may be favorable to have real-valued arguments,  $(\xi a/c)$ , and  $(\sqrt{\tilde{\epsilon}}(i\xi)\xi a/c)$  instead of  $(i\xi a/c)$  and  $(\sqrt{\tilde{\epsilon}}(i\xi)i\xi a/c)$ , respectively. To achieve real valued arguments we transform the functions. The transformation rules are: [1]

$$\begin{aligned} \xi_l(ix) &= \frac{1}{i^{l+1}} \frac{1}{\pi} \sqrt{2\pi x} K_{l+1/2}(x); \\ \zeta_l(ix) &= i^{l+1} \sqrt{2\pi x} \left[ I_{l+1/2}(x) + \frac{1}{\pi} (-1)^l K_{l+1/2}(x) \right]; \\ \psi_l(ix) &= i^{l+1} \frac{1}{2} \sqrt{2\pi x} I_{l+1/2}(x); \\ \xi_l'(ix) &= \frac{1}{i^{l+2}} \frac{1}{\pi} \sqrt{2\pi x} \left[ \frac{1}{2x} K_{l+1/2}(x) + K'_{l+1/2}(x) \right]; \\ \zeta_l'(ix) &= i^l \sqrt{2\pi x} \left\{ \frac{1}{2x} \left[ I_{l+1/2}(x) + \frac{1}{\pi} (-1)^l K_{l+1/2}(x) \right] \right. \\ &\quad \left. + \left[ I'_{l+1/2}(x) + \frac{1}{\pi} (-1)^l K'_{l+1/2}(x) \right] \right\}; \\ \psi_l'(ix) &= i^l \frac{1}{2} \sqrt{2\pi x} \left[ \frac{1}{2x} I_{l+1/2}(x) + I'_{l+1/2}(x) \right], \end{aligned} \quad (14.21)$$

where the functions  $I$  and  $K$  are modified Bessel functions.

Now we have all we need to determine the fully retarded normal modes in a layered spherical structure. We give some examples in the following sections.

### Summary of key relations for the derivation of the dispersion interactions in spherical structures:

In a spherical structure the azimuthal quantum number,  $l$ , the magnetic quantum number,  $m$ , and the two polarization types, TM and TE, are the proper quantum numbers that characterize a normal mode. The TM mode has its magnetic field perpendicular to the radial direction and the TE mode has its electric field perpendicular to the radial direction. The dispersion curve for a mode can have several branches,  $i$ ,  $\omega = \omega_{l,m}^i$ . They are solutions to the condition for modes,  $f_{l,m}(\omega) = 0$ , where  $f_{l,m}(\omega)$  is the mode condition function. When finding the interaction energy of the system one has to sum over both  $l$ ,  $m$ , the mode type and  $i$ . For zero temperature it is

$$\begin{aligned} E &= \frac{\hbar}{2} \sum_{l=1}^{\infty} \sum_{m=-l}^l \int_{-\infty}^{\infty} \frac{d\xi}{2\pi} \left[ \ln f_{l,m}^{\text{TM}}(i\xi) + \ln f_{l,m}^{\text{TE}}(i\xi) \right] \\ &= \hbar \sum_{l=1}^{\infty} \sum_{m=-l}^l \int_0^{\infty} \frac{d\xi}{2\pi} \left[ \ln f_{l,m}^{\text{TM}}(i\xi) + \ln f_{l,m}^{\text{TE}}(i\xi) \right], \end{aligned} \quad (14.22)$$

and at finite temperature

$$\mathfrak{F} = \sum_{l=1}^{\infty} \sum_{m=-l}^l \frac{1}{\beta} \sum_{n=0}^{\infty} [\ln f_{l,m}^{\text{TM}}(i\xi_n) + \ln f_{l,m}^{\text{TE}}(i\xi_n)]; \quad \xi_n = \frac{2\pi n}{\hbar\beta}. \quad (14.23)$$

In the fully retarded treatment  $f_{l,m} \equiv M_{11} + M_{12}$  where  $\tilde{\mathbf{M}}$  is the matrix for the whole structure. The matrix for interface  $n$  is given by

$$\tilde{\mathbf{M}}_n^{\text{TM}} = \frac{-q_{n+1}}{q_n^2(2i)} \begin{pmatrix} q_n \xi_l \zeta_l'^+ - q_{n+1} \xi_l' \zeta_l^+ & q_n \xi_l \xi_l'^+ - q_{n+1} \xi_l' \xi_l^+ \\ -q_n \zeta_l \zeta_l'^+ + q_{n+1} \zeta_l' \zeta_l^+ & -q_n \zeta_l \xi_l'^+ + q_{n+1} \zeta_l' \xi_l^+ \end{pmatrix}, \quad (14.24)$$

for TM modes, and

$$\tilde{\mathbf{M}}_n^{\text{TE}} = \frac{-1}{q_n(2i)} \begin{pmatrix} -q_n \xi_l' \zeta_l^+ + q_{n+1} \xi_l \zeta_l'^+ & -q_n \xi_l' \xi_l^+ + q_{n+1} \xi_l \xi_l'^+ \\ -q_n \zeta_l' \zeta_l^+ - q_{n+1} \zeta_l \zeta_l'^+ & q_n \zeta_l' \xi_l^+ - q_{n+1} \zeta_l \xi_l'^+ \end{pmatrix}. \quad (14.25)$$

for TE modes, where we to save space have omitted the function arguments. All functions with a + added as a superscript have the argument  $(q_{n+1}r_n)$  and the ones without the superscript have the argument  $(q_n r_n)$ , where  $q_n = \sqrt{\tilde{\epsilon}_n(\omega)}\omega/c$ . We end with some useful Wronskians:

$$\begin{aligned} W[\xi_l, \zeta_l] &= \xi_l \zeta_l' - \xi_l' \zeta_l = -2i; \\ W[\psi_l, \zeta_l] &= \psi_l \zeta_l' - \psi_l' \zeta_l = -i; \\ W[\psi_l, \xi_l] &= \psi_l \xi_l' - \psi_l' \xi_l = i, \end{aligned} \quad (14.26)$$

where

$$2\psi_l(z) = \zeta_l(z) + \xi_l(z) \quad (14.27)$$

## 14.2 Basic Structure Elements

A general spherical structure can be generated by stacking a number of basic structure elements concentrically around each other. The most basic element is a solid sphere. Sometimes it is convenient to use layers as elements. A special layer is a 2D spherical film. Another is a thin spherical diluted gas layer which we will use repeatedly in the derivation of the interaction between atoms and the spherical structure. We now discuss these basic elements one by one. We start with the solid sphere.

### 14.2.1 Solid Sphere or Ball

For a solid sphere of radius  $a$  and dielectric function  $\tilde{\epsilon}_1(\omega)$  in an ambient of dielectric function  $\tilde{\epsilon}_0(\omega)$ , as illustrated in Fig. 14.1, we have  $\tilde{\mathbf{M}} = \tilde{\mathbf{M}}_0$ , and for the TM modes we find

$$\begin{aligned}
 M_{11} + M_{12} &= \frac{iq_1}{2q_0} \left\{ q_0 \xi_l(q_0 a) [\zeta_l'(q_1 a) + \xi_l'(q_1 a)] \right. \\
 &\quad \left. - q_1 \xi_l'(q_0 a) [\zeta_l(q_1 a) + \xi_l(q_1 a)] \right\} \\
 &= \frac{-iq_1}{2q_0} \left\{ q_0 \xi_l(q_0 a) 2\psi_l'(q_1 a) - q_1 \xi_l'(q_0 a) 2\psi_l(q_1 a) \right\} \\
 &= \frac{-iq_1}{q_0} \left\{ \left[ \tilde{\epsilon}_0(\omega/c)^2 a h_l^{(1)}(q_0 a) \right] [q_1 a j_l(q_1 a)]' \right. \\
 &\quad \left. - \left[ q_0 a h_l^{(1)}(q_0 a) \right]' [\tilde{\epsilon}_1(\omega/c)^2 a j_l(q_1 a)] \right\},
 \end{aligned} \tag{14.28}$$

where we have used the relations between the different solutions to the Ricatti-Bessel equation given in (14.3) and (14.5). We have furthermore used the relations  $q_0^2 = \tilde{\epsilon}_0(\omega/c)^2$  and  $q_1^2 = \tilde{\epsilon}_1(\omega/c)^2$ .

The mode condition function for TM modes is

$$f_{l,m}^{\text{TM}} = \left[ \tilde{\epsilon}_0(\omega) h_l^{(1)}(q_0 a) \right] [(q_1 a) j_l(q_1 a)]' - \left[ (q_0 a) h_l^{(1)}(q_0 a) \right]' [\tilde{\epsilon}_1(\omega) j_l(q_1 a)]. \tag{14.29}$$

This result agrees with the result of Ruppin in (43) on page 353, in [6]. For the TE modes we find

$$\begin{aligned}
 M_{11} + M_{12} &= \frac{i}{2q_0} \left\{ -q_0 \xi_l'(q_0 a) [\zeta_l(q_1 a) + \xi_l(q_1 a)] \right. \\
 &\quad \left. + q_1 \xi_l(q_0 a) [\zeta_l'(q_1 a) + \xi_l'(q_1 a)] \right\} \\
 &= \frac{-i}{2q_0} \left\{ -q_0 \xi_l'(q_0 a) 2\psi_l(q_1 a) + q_1 \xi_l(q_0 a) 2\psi_l'(q_1 a) \right\} \\
 &= -iq_1 a \left\{ - \left[ q_0 a h_l^{(1)}(q_0 a) \right]' [j_l(q_1 a)] \right. \\
 &\quad \left. + \left[ h_l^{(1)}(q_0 a) \right] [q_1 a j_l(q_1 a)]' \right\},
 \end{aligned} \tag{14.30}$$

**Fig. 14.1** The geometry of a solid sphere or cylinder of radius  $a$  in the fully retarded treatment. Adapted from [5]

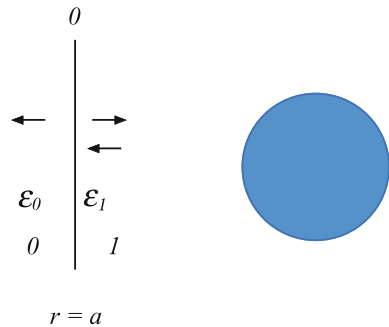
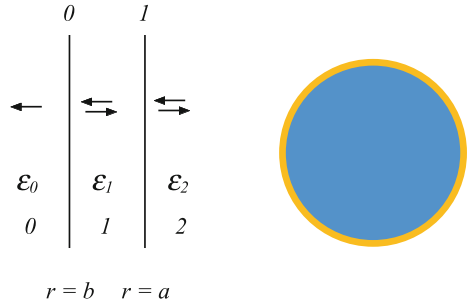


**Fig. 14.2** The geometry of a coated sphere or cylinder of radius  $a$  in the fully retarded treatment. Adapted from [5]



and the mode condition function for TE modes is

$$f_{l,m}^{\text{TE}} = \left[ h_l^{(1)}(q_0 a) \right] \left[ (q_1 a) j_l(q_1 a) \right]' - \left[ (q_0 a) h_l^{(1)}(q_0 a) \right]' \left[ j_l(q_1 a) \right]. \quad (14.31)$$

This result agrees with the result of Ruppin in (34) on page 351, in [6]. The results of (14.29) and (14.31) can also be used for a spherical cavity in a medium if the two dielectric functions are interchanged.

### 14.2.2 Spherical Shell

For a spherical shell of inner radius  $a$  and outer radius  $b$ , Fig. 14.2, made of a medium with dielectric function  $\tilde{\epsilon}_1$  in an ambient medium with dielectric function  $\tilde{\epsilon}_0$  we have  $\tilde{\mathbf{M}} = \tilde{\mathbf{M}}_0 \cdot \tilde{\mathbf{M}}_1$ . This geometry covers the problem of a vacuum gap in the shape of a spherical shell inside an infinite medium, as treated in [7].

We do not need all elements of the two matrices. We have

$$\begin{aligned} & M_{11} + M_{12} \\ &= (M_{11}^0, M_{12}^0) \cdot \begin{pmatrix} M_{11}^1 + M_{12}^1 \\ M_{21}^1 + M_{22}^1 \end{pmatrix} \\ &= M_{11}^0 (M_{11}^1 + M_{12}^1) \begin{pmatrix} 1, \alpha_l^{0(2)} \end{pmatrix} \cdot \begin{pmatrix} 1 \\ -\alpha_l^1 \end{pmatrix} \\ &= M_{11}^0 (M_{11}^1 + M_{12}^1) \left( 1 - \alpha_l^{0(2)} \alpha_l^1 \right). \end{aligned} \quad (14.32)$$

We want to end up with expressions for the mode condition functions that are suitable to use on the imaginary frequency axis. This demands some manipulations. First we note that  $1 - \alpha_l^{0(2)} \alpha_l^1 = 0 \rightarrow 1/\alpha_l^{0(2)} - \alpha_l^1 = 0$  and for TM modes we have

$$\frac{q_0 \xi_l(q_0 b) \zeta_l'(q_1 b) - q_1 \xi_l'(q_0 b) \zeta_l(q_1 b)}{q_0 \xi_l(q_0 b) \xi_l'(q_1 b) - q_1 \xi_l'(q_0 b) \xi_l(q_1 b)} - \frac{q_1 \zeta_l(q_1 a) \psi_l'(q_0 a) - q_0 \zeta_l'(q_1 a) \psi_l(q_0 a)}{q_1 \xi_l(q_1 a) \psi_l'(q_0 a) - q_0 \xi_l'(q_1 a) \psi_l(q_0 a)} = 0. \quad (14.33)$$

We may use the relation  $2\psi_l = \zeta_l + \xi_l$  to find

$$2 \frac{q_0 \xi_l(q_0 b) \psi_l'(q_1 b) - q_1 \xi_l'(q_0 b) \psi_l(q_1 b)}{q_0 \xi_l(q_0 b) \xi_l'(q_1 b) - q_1 \xi_l'(q_0 b) \xi_l(q_1 b)} - 1 - 2 \frac{q_1 \psi_l(q_1 a) \psi_l'(q_0 a) - q_0 \psi_l'(q_1 a) \psi_l(q_0 a)}{q_1 \xi_l(q_1 a) \psi_l'(q_0 a) - q_0 \xi_l'(q_1 a) \psi_l(q_0 a)} + 1 = 0. \quad (14.34)$$

We find the following mode condition function for TM modes

$$\tilde{f}_{l,m}^{\text{TM}}(\omega) = 1 - \frac{q_0 \xi_l(q_0 b) \psi_l'(q_1 b) - q_1 \xi_l'(q_0 b) \psi_l(q_1 b)}{q_0 \xi_l(q_0 b) \xi_l'(q_1 b) - q_1 \xi_l'(q_0 b) \xi_l(q_1 b)} \times \frac{q_1 \xi_l(q_1 a) \psi_l'(q_0 a) - q_0 \xi_l'(q_1 a) \psi_l(q_0 a)}{q_1 \psi_l(q_1 a) \psi_l'(q_0 a) - q_0 \psi_l'(q_1 a) \psi_l(q_0 a)}, \quad (14.35)$$

and analogous manipulations for the TE modes give

$$\tilde{f}_{l,m}^{\text{TE}}(\omega) = 1 - \frac{q_0 \xi_l'(q_0 b) \psi_l(q_1 b) - q_1 \xi_l(q_0 b) \psi_l'(q_1 b)}{q_0 \xi_l'(q_0 b) \xi_l(q_1 b) - q_1 \xi_l(q_0 b) \xi_l'(q_1 b)} \times \frac{q_1 \xi_l'(q_1 a) \psi_l(q_0 a) - q_0 \xi_l(q_1 a) \psi_l'(q_0 a)}{q_1 \psi_l'(q_1 a) \psi_l(q_0 a) - q_0 \psi_l(q_1 a) \psi_l'(q_0 a)}. \quad (14.36)$$

In these equations,  $q_0$  is  $\sqrt{\tilde{\epsilon}_0(\omega)}\omega/c$  and  $q_1$  is  $\sqrt{\tilde{\epsilon}_1(\omega)}\omega/c$ , respectively. We have expressed the mode condition functions in terms of  $\xi_l$  and  $\psi_l$  since these are easier to transform from functions of imaginary arguments into functions of real arguments by following (14.21). For the vacuum gap treated in [7] one should put  $\tilde{\epsilon}_0 = \tilde{\epsilon}$  and  $\tilde{\epsilon}_1 = 1$ . Our results agree with those in [7].

### 14.2.3 Thin Spherical Diluted Gas Film

It is of interest to find the Casimir force on an atom in a layered structure. We can obtain this by studying the force on a thin layer of a diluted gas with dielectric function  $\epsilon_g(\omega) = 1 + 4\pi n \alpha^{at}(\omega)$ , where  $\alpha^{at}$  is the polarizability of one atom and  $n$  the density of atoms (we have assumed that the atom is surrounded by vacuum; if not the 1 should be replaced by the dielectric function of the ambient medium and the atomic polarizability should be replaced by the excess polarizability). For a diluted gas layer the interaction between the gas atoms can be neglected and the force on the layer is just the sum of the forces on the individual atoms. So by dividing with the number of atoms in the film we get the force on one atom. The layer has to be thin in order to have a well defined  $r$ -value of the atom. Since we will derive the force on an atom in different spherical geometries it is fruitful to derive the matrix for a thin diluted gas shell. This result can be directly used in the derivation of the Casimir force on an atom in different spherical geometries.

We let the film have the thickness  $\delta$  and be of general radius  $r$ . We only keep terms up to linear order in  $\delta$  and linear order in  $n$ . We find the result for TM modes is

$$\tilde{\mathbf{M}}_{\text{gaslayer}}^{\text{TM}} = \begin{pmatrix} 1 & 0 \\ 0 & 1 \end{pmatrix} - (\delta n) 2\pi \alpha^{at} q_0 \mathbf{i} \times \begin{pmatrix} \xi_l' \zeta_l' + \xi_l \zeta_l \frac{l(l+1)}{(q_0 r)^2} & [\xi_l']^2 + [\xi_l]^2 \frac{l(l+1)}{(q_0 r)^2} \\ -[\zeta_l']^2 - [\zeta_l]^2 \frac{l(l+1)}{(q_0 r)^2} & -\xi_l' \zeta_l' - \xi_l \zeta_l \frac{l(l+1)}{(q_0 r)^2} \end{pmatrix}, \quad (14.37)$$

where we have suppressed the argument ( $q_0 r$ ) in all Ricatti-Bessel functions. For TE modes we find

$$\tilde{\mathbf{M}}_{\text{gaslayer}}^{\text{TE}} = \begin{pmatrix} 1 & 0 \\ 0 & 1 \end{pmatrix} - (\delta n) 2\pi \alpha^{at} q_0 i \times \begin{pmatrix} \xi_l(q_0 r) \zeta_l(q_0 r) & [\xi_l(q_0 r)]^2 \\ -[\zeta_l(q_0 r)]^2 & -\xi_l(q_0 r) \zeta_l(q_0 r) \end{pmatrix}. \quad (14.38)$$

We may also need the  $2^l$  pole polarizabilities,  $\alpha_l^{\text{gas}}$  and  $\alpha_l^{\text{gas}(2)}$ , for the gas layer. The first is valid outside and the second inside. The polarizability  $\alpha_l^{\text{gas}} = -b^0/a^0$  under the assumption that  $b^1 = a^1$ . One obtains  $\alpha_l^{\text{gas}} = -(M_{21} + M_{22}) / (M_{11} + M_{12})$  and from (14.37) one finds that for TM modes

$$\alpha_l^{\text{gas, TM}} = -\frac{1 - (\delta n) 2\pi \alpha^{at} q_0 i \left[ -[\zeta_l']^2 - [\zeta_l]^2 \frac{l(l+1)}{(q_0 r)^2} - \xi_l' \zeta_l' - \xi_l \zeta_l \frac{l(l+1)}{(q_0 r)^2} \right]}{1 - (\delta n) 2\pi \alpha^{at} q_0 i \left[ \xi_l' \zeta_l' + \xi_l \zeta_l \frac{l(l+1)}{(q_0 r)^2} + [\xi_l']^2 + [\xi_l]^2 \frac{l(l+1)}{(q_0 r)^2} \right]} \approx -1 - (\delta n) 2\pi \alpha^{at} q_0 i \left[ 4[\psi_l']^2 + 4[\psi_l]^2 \frac{l(l+1)}{(q_0 r)^2} \right]. \quad (14.39)$$

In the same way one finds from (14.38) that for TE modes

$$\alpha_l^{\text{gas, TE}} = -\frac{1 - (\delta n) 2\pi \alpha^{at} q_0 i \left[ -[\zeta_l]^2 - \xi_l \zeta_l \right]}{1 - (\delta n) 2\pi \alpha^{at} q_0 i \left[ \xi_l \zeta_l + [\xi_l]^2 \right]} \approx -1 - (\delta n) 2\pi \alpha^{at} q_0 i 4[\psi_l]^2. \quad (14.40)$$

The polarizability  $\alpha_l^{\text{gas}(2)} = -a^1/b^1$  under the assumption that  $a^0 = 0$ . One obtains  $\alpha_l^{\text{gas}(2)} = M_{12}/M_{11}$ , and from (14.37) one finds that for the TM modes

$$\alpha_l^{\text{gas}(2), \text{TM}} = \frac{-(\delta n) 2\pi \alpha^{at} q_0 i \left[ [\xi_l']^2 + [\xi_l]^2 \frac{l(l+1)}{(q_0 r)^2} \right]}{1 - (\delta n) 2\pi \alpha^{at} q_0 i \left[ \xi_l' \zeta_l' + \xi_l \zeta_l \frac{l(l+1)}{(q_0 r)^2} \right]} \approx -(\delta n) 2\pi \alpha^{at} q_0 i \left[ [\xi_l']^2 + [\xi_l]^2 \frac{l(l+1)}{(q_0 r)^2} \right]. \quad (14.41)$$

From (14.38) one finds that for the TE modes

$$\alpha_l^{\text{gas}(2), \text{TE}} = \frac{-(\delta n) 2\pi \alpha^{at} q_0 i [\xi_l]^2}{1 - (\delta n) 2\pi \alpha^{at} q_0 i [\xi_l \zeta_l]} \approx -(\delta n) 2\pi \alpha^{at} q_0 i [\xi_l]^2. \quad (14.42)$$

In (14.39) and (14.40) we have used the relation  $\psi_l(z) = [\xi_l(z) + \zeta_l(z)]/2$ . Now we are done with the gas layer. We will use these results later in calculating the Casimir force on an atom in spherical layered structures. We move on to next structure, a 2D spherical film.

### 14.2.4 2D Spherical Film

In many situations one is dealing with very thin films. These may be considered 2D (two dimensional). Important examples are a graphene sheet and a 2D electron gas. In the derivation we let the film have finite thickness  $\delta$  and be characterized by a 3D dielectric function  $\tilde{\epsilon}^{3D}$ . We then let the thickness go toward zero. The 3D dielectric function depends on  $\delta$  as  $\tilde{\epsilon}^{3D} \sim 1/\delta$  for small  $\delta$ . In the planar structure we could in the limit when  $\delta$  goes toward zero obtain a momentum dependent 2D dielectric function. Here we only obtain the long wave length limit of the 2D dielectric function [8, 9]. We obtain for TM modes

$$\tilde{\mathbf{M}}_{2D}^{TM} = \begin{pmatrix} 1 & 0 \\ 0 & 1 \end{pmatrix} - \frac{\delta \tilde{\epsilon}^{3D} q_0 i}{2} \begin{pmatrix} \xi_l'(q_0 r) \zeta_l'(q_0 r) & [\xi_l'(q_0 r)]^2 \\ -[\zeta_l'(q_0 r)]^2 & -\xi_l'(q_0 r) \zeta_l'(q_0 r) \end{pmatrix}, \quad (14.43)$$

and for TE modes

$$\tilde{\mathbf{M}}_{2D}^{TE} = \begin{pmatrix} 1 & 0 \\ 0 & 1 \end{pmatrix} - \frac{\delta \tilde{\epsilon}^{3D} q_0 i}{2} \begin{pmatrix} \xi_l(q_0 r) \zeta_l(q_0 r) & [\xi_l(q_0 r)]^2 \\ -[\zeta_l(q_0 r)]^2 & -\xi_l(q_0 r) \zeta_l(q_0 r) \end{pmatrix}. \quad (14.44)$$

We will also need the  $2^l$  pole polarizabilities  $\alpha_l^{2D}$  and  $\alpha_l^{2D(2)}$  for the thin spherical film since these appear repeatedly in the sections that follow. The first is valid outside and the second inside. The polarizability  $\alpha_l^{2D} = -b^0/a^0$  under the assumption that  $b^1 = a^1$ . One obtains  $\alpha_l^{2D} = -(M_{21} + M_{22}) / (M_{11} + M_{12})$  and from (14.43) one finds that for TM modes

$$\begin{aligned} \alpha_l^{2D, TM} &= -\frac{2 + \delta \tilde{\epsilon}^{3D} q_0 i [\xi_l'(q_0 r)^2 + \xi_l'(q_0 r) \zeta_l'(q_0 r)]}{2 - \delta \tilde{\epsilon}^{3D} q_0 i [\xi_l'(q_0 r)^2 + \xi_l'(q_0 r) \zeta_l'(q_0 r)]} \\ &= -1 - \frac{4\delta \tilde{\epsilon}^{3D} q_0 i [\psi_l'(q_0 r)^2]}{2 - \delta \tilde{\epsilon}^{3D} q_0 i [\xi_l'(q_0 r)^2 + \xi_l'(q_0 r) \zeta_l'(q_0 r)]} \\ &= -1 - \frac{2\delta \tilde{\epsilon}^{3D} q_0 i [\psi_l'(q_0 r)^2]}{1 - \delta \tilde{\epsilon}^{3D} q_0 i \xi_l'(q_0 r) \psi_l'(q_0 r)}. \end{aligned} \quad (14.45)$$

In the same way one finds from (14.44) that for TE modes

$$\begin{aligned} \alpha_l^{2D, TE} &= -\frac{2 + \delta \tilde{\epsilon}^{3D} q_0 i [\zeta_l(q_0 r)^2 + \xi_l(q_0 r) \zeta_l(q_0 r)]}{2 - \delta \tilde{\epsilon}^{3D} q_0 i [\xi_l(q_0 r)^2 + \xi_l(q_0 r) \zeta_l(q_0 r)]} \\ &= -1 - \frac{4\delta \tilde{\epsilon}^{3D} q_0 i [\psi_l(q_0 r)^2]}{2 - \delta \tilde{\epsilon}^{3D} q_0 i [\xi_l(q_0 r)^2 + \xi_l(q_0 r) \zeta_l(q_0 r)]} \\ &= -1 - \frac{2\delta \tilde{\epsilon}^{3D} q_0 i [\psi_l(q_0 r)^2]}{1 - \delta \tilde{\epsilon}^{3D} q_0 i \xi_l(q_0 r) \psi_l(q_0 r)}. \end{aligned} \quad (14.46)$$

The polarizability  $\alpha_l^{2D(2)} = -a^1/b^1$  under the assumption that  $a^0 = 0$ . One obtains  $\alpha_l^{2D(2)} = M_{12}/M_{11}$  and from (14.43) one finds that for the TM modes

$$\alpha_l^{2D(2), TM} = \frac{-\delta \tilde{\epsilon}^{3D} q_0 i \xi_l'(q_0 r)^2}{2 - \delta \tilde{\epsilon}^{3D} q_0 i \xi_l'(q_0 r) \zeta_l'(q_0 r)}. \quad (14.47)$$

From (14.44) one finds that for TE modes

$$\alpha_l^{2D(2),TE} = \frac{-\delta \tilde{\epsilon}^{3D} q_0 i \xi_l (q_0 r)^2}{2 - \delta \tilde{\epsilon}^{3D} q_0 i \xi_l (q_0 r) \zeta_l (q_0 r)}. \tag{14.48}$$

### 14.3 Coated Sphere in a Medium

The result for a coated sphere in a medium is obtained trivially from Sect. 14.2.2. One just replaces  $q_0$  in the last factor in (14.35) and (14.36) with  $q_2 = \sqrt{\epsilon_2(\omega)}\omega/c$ , where  $\epsilon_2(\omega)$  is the dielectric function of the sphere medium.

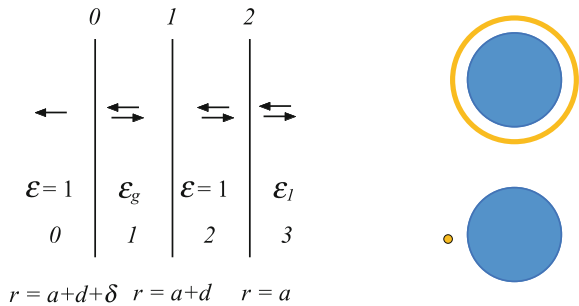
### 14.4 Atom-Ball Interaction

We let the atom be at a distance  $d$  from the sphere of radius  $a$  and at a distance  $b$  from the center of the sphere. For this problem we start with the geometry given in Fig. 14.3, where we let the shell be a very thin gas layer. We have two layers and three interfaces. The matrix  $\tilde{\mathbf{M}} = \tilde{\mathbf{M}}_0 \cdot \tilde{\mathbf{M}}_1 \cdot \tilde{\mathbf{M}}_2$ . Here we could instead of the first two matrices have used the matrix for a thin diluted gas shell as given in (14.37) and (14.38). To vary the derivations to some extent we refrain from doing that. The left-hand side of the condition for modes is

$$M_{11} + M_{12} = (M_{11}^0 \ M_{12}^0) \cdot \tilde{\mathbf{M}}_1 \cdot \begin{pmatrix} M_{11}^2 + M_{12}^2 \\ M_{21}^2 + M_{22}^2 \end{pmatrix}, \tag{14.49}$$

where we have moved the matrix subscripts to superscripts to make room for the element indices. We now list all elements needed in the above equation. We begin with the matrices for TM modes. The elements of the first matrix are

**Fig. 14.3** The geometry of a thin gas layer the distance  $d$  from a sphere or cylinder of radius  $a$  in the fully retarded treatment. Adapted from [5]



$$\begin{aligned}
M_{11}^0 &= \frac{in_g}{2} \left\{ \xi_l [q_0 (b + \delta)] \zeta_l' [q_g (b + \delta)] \right. \\
&\quad \left. - n_g \xi_l' [q_0 (b + \delta)] \zeta_l [q_g (b + \delta)] \right\}; \\
M_{12}^0 &= \frac{in_g}{2} \left\{ \xi_l [q_0 (b + \delta)] \xi_l' [q_g (b + \delta)] \right. \\
&\quad \left. - n_g \xi_l' [q_0 (b + \delta)] \xi_l [q_g (b + \delta)] \right\},
\end{aligned} \tag{14.50}$$

and of the second

$$\begin{aligned}
M_{11}^1 &= \frac{i}{2n_g^2} \left[ n_g \xi_l (q_g b) \zeta_l' (q_0 b) - \xi_l' (q_g b) \zeta_l (q_0 b) \right]; \\
M_{12}^1 &= \frac{i}{2n_g^2} \left[ n_g \xi_l (q_g b) \xi_l' (q_0 b) - \xi_l' (q_g b) \xi_l (q_0 b) \right]; \\
M_{21}^1 &= \frac{i}{2n_g^2} \left[ \zeta_l' (q_g b) \zeta_l (q_0 b) - n_g \zeta_l (q_g b) \zeta_l' (q_0 b) \right]; \\
M_{22}^1 &= \frac{i}{2n_g^2} \left[ \zeta_l' (q_g b) \xi_l (q_0 b) - n_g \zeta_l (q_g b) \xi_l' (q_0 b) \right],
\end{aligned} \tag{14.51}$$

and of the third

$$\begin{aligned}
M_{11}^2 + M_{12}^2 &= \frac{in_1}{2} \left[ \xi_l (q_0 a) \zeta_l' (q_1 a) - n_1 \xi_l' (q_0 a) \zeta_l (q_1 a) \right. \\
&\quad \left. + \xi_l (q_0 a) \xi_l' (q_1 a) - n_1 \xi_l' (q_0 a) \xi_l (q_1 a) \right] \\
&= in_1 \left[ \xi_l (q_0 a) \psi_l' (q_1 a) - n_1 \xi_l' (q_0 a) \psi_l (q_1 a) \right]; \\
M_{21}^2 + M_{22}^2 &= \frac{in_1}{2} \left[ n_1 \zeta_l' (q_0 a) \zeta_l (q_1 a) - \zeta_l (q_0 a) \zeta_l' (q_1 a) \right. \\
&\quad \left. + n_1 \zeta_l' (q_0 a) \xi_l (q_1 a) - \zeta_l (q_0 a) \xi_l' (q_1 a) \right] \\
&= in_1 \left[ n_1 \zeta_l' (q_0 a) \psi_l (q_1 a) - \zeta_l (q_0 a) \psi_l' (q_1 a) \right],
\end{aligned} \tag{14.52}$$

where  $n_g$  and  $n_1$  are the refractive indices of the gas layer and the sphere, respectively.

We now make a series expansion of the first matrix up to linear order in  $\delta$ . The other matrices do not depend on  $\delta$ . The zeroth order term multiplied with the second matrix produces the matrix  $\begin{pmatrix} 1 & 0 \end{pmatrix}$ , so it contributes with  $M_{11}^2 + M_{12}^2$  to the condition for modes. We then expand in  $\alpha_g$ , the polarizability of the gas. There is no zeroth order term in the term linear in  $\delta$ . The lowest order term is linear in  $\alpha_g$ . This means that we do not need to expand  $\tilde{\mathbf{M}}_1$  in  $\alpha_g$ . The zeroth order term is just the unit matrix. Thus if we denote the term of the matrix  $\tilde{\mathbf{M}}_0$  that is linear in both  $\delta$  and  $\alpha_g$  with  $\delta \tilde{\mathbf{M}}_0$  the condition for modes can be written as

$$(M_{11}^2 + M_{12}^2) + \delta M_{11}^0 (M_{11}^2 + M_{12}^2) + \delta M_{12}^0 (M_{21}^2 + M_{22}^2) = 0, \tag{14.53}$$

and the mode condition function is

$$\begin{aligned}
\tilde{f}_l^{\text{TM}}(\omega) &= 1 + \delta M_{12}^0 \frac{(M_{21}^2 + M_{22}^2) - (M_{11}^2 + M_{12}^2)}{(M_{11}^2 + M_{12}^2)} \\
&= 1 - \delta M_{12}^0 2 \frac{n_1 \psi_l' (q_0 a) \psi_l (q_1 a) - \psi_l (q_0 a) \psi_l' (q_1 a)}{n_1 \xi_l' (q_0 a) \psi_l (q_1 a) - \xi_l (q_0 a) \psi_l' (q_1 a)},
\end{aligned} \tag{14.54}$$

where

$$\delta M_{12}^0 = -\delta \alpha_g q_0 \frac{i}{2} \left[ [\xi_l' (q_0 b)]^2 + \frac{i(l+1) [\xi_l (q_0 b)]^2}{(q_0 b)^2} \right]. \tag{14.55}$$

To obtain the mode condition function in (14.54) we have divided the function (the left-hand side of (14.53)) both with the corresponding function for the sphere alone,  $M_{11}^2 + M_{12}^2$ , and for the spherical shell alone,  $1 + \delta M_{11}^0 + \delta M_{12}^0$ . Note that the final expression does not contain any elements of matrix  $\tilde{\mathbf{M}}_1$  and just one of  $\delta\tilde{\mathbf{M}}_0$ .

Now, we proceed with the TE modes. The elements of the first matrix are

$$\begin{aligned} M_{11}^0 &= \frac{i}{2} \left\{ -\xi_l' [q_0 (b + \delta)] \zeta_l [q_g (b + \delta)] \right. \\ &\quad \left. + n_g \xi_l [q_0 (b + \delta)] \zeta_l' [q_g (b + \delta)] \right\}; \\ M_{12}^0 &= \frac{i}{2} \left\{ -\xi_l' [q_0 (b + \delta)] \xi_l [q_g (b + \delta)] \right. \\ &\quad \left. + n_g \xi_l [q_0 (b + \delta)] \xi_l' [q_g (b + \delta)] \right\}, \end{aligned} \quad (14.56)$$

and of the second

$$\begin{aligned} M_{11}^1 &= \frac{i}{2n_g} \left[ -n_g \xi_l' (q_g b) \zeta_l (q_0 b) + \xi_l (q_g b) \zeta_l' (q_0 b) \right]; \\ M_{12}^1 &= \frac{i}{2n_g} \left[ -n_g \xi_l' (q_g b) \xi_l (q_0 b) + \xi_l (q_g b) \xi_l' (q_0 b) \right]; \\ M_{21}^1 &= \frac{i}{2n_g} \left[ n_g \zeta_l' (q_g b) \zeta_l (q_0 b) - \zeta_l (q_g b) \zeta_l' (q_0 b) \right]; \\ M_{22}^1 &= \frac{i}{2n_g} \left[ n_g \zeta_l' (q_g b) \xi_l (q_0 b) - \zeta_l (q_g b) \xi_l' (q_0 b) \right], \end{aligned} \quad (14.57)$$

and of the third

$$\begin{aligned} M_{11}^2 + M_{12}^2 &= \frac{i}{2} \left[ -\xi_l' (q_0 a) \zeta_l (q_1 a) + n_1 \xi_l (q_0 a) \zeta_l' (q_1 a) \right. \\ &\quad \left. - \xi_l' (q_0 a) \xi_l (q_1 a) + n_1 \xi_l (q_0 a) \xi_l' (q_1 a) \right]; \\ &= i \left[ -\xi_l' (q_0 a) \psi_l (q_1 a) + n_1 \xi_l (q_0 a) \psi_l' (q_1 a) \right]; \\ M_{21}^2 + M_{22}^2 &= \frac{i}{2} \left[ \zeta_l' (q_0 a) \zeta_l (q_1 a) - n_1 \zeta_l (q_0 a) \zeta_l' (q_1 a) \right. \\ &\quad \left. + \zeta_l' (q_0 a) \xi_l (q_1 a) - n_1 \zeta_l (q_0 a) \xi_l' (q_1 a) \right]; \\ &= i \left[ \zeta_l' (q_0 a) \psi_l (q_1 a) - n_1 \zeta_l (q_0 a) \psi_l' (q_1 a) \right], \end{aligned} \quad (14.58)$$

where  $n_g$  and  $n_1$  are the refractive indices of the gas layer and the sphere, respectively.

We now make a series expansion of the first matrix up to linear order in  $\delta$ . The other matrices do not depend on  $\delta$ . The zeroth order term multiplied with the second matrix produces the matrix  $\begin{pmatrix} 1 & 0 \end{pmatrix}$ , so it contributes with  $M_{11}^2 + M_{12}^2$  to the condition for modes. We then expand in  $\alpha_g$ , the polarizability of the gas. There is no zeroth order term in the term linear in  $\delta$ . The lowest order term is linear in  $\alpha_g$ . This means that we do not need to expand  $\tilde{\mathbf{M}}_1$  in  $\alpha_g$ . The zeroth order term is just the unit matrix. Thus if we denote the term of the matrix  $\tilde{\mathbf{M}}_0$  that is linear in both  $\delta$  and  $\alpha_g$  by  $\delta\tilde{\mathbf{M}}_0$  the condition for modes can be written as

$$(M_{11}^2 + M_{12}^2) + \delta M_{11}^0 (M_{11}^2 + M_{12}^2) + \delta M_{12}^0 (M_{21}^2 + M_{22}^2) = 0, \quad (14.59)$$

and the mode condition function is

$$\begin{aligned} \tilde{f}_i^{\text{TE}}(\omega) &= 1 + \delta M_{12}^0 \frac{(M_{21}^2 + M_{22}^2) - (M_{11}^2 + M_{12}^2)}{(M_{11}^2 + M_{12}^2)} \\ &= 1 - \delta M_{12}^0 2 \frac{\psi_l'(q_0 a) \psi_l(q_1 a) - n_1 \psi_l(q_0 a) \psi_l'(q_1 a)}{-\xi_l'(q_0 a) \psi_l(q_1 a) + n_1 \xi_l(q_0 a) \psi_l'(q_1 a)}, \end{aligned} \quad (14.60)$$

where

$$\delta M_{12}^0 = -\delta\alpha_g q_0 \frac{i}{2} [\xi_l (q_0 b) \xi_l (q_0 b)]. \quad (14.61)$$

To obtain the mode condition function in (14.60) we have divided the function (the left-hand side of (14.59)) both with the corresponding function for the sphere alone,  $M_{11}^2 + M_{12}^2$ , and for the spherical shell alone,  $1 + \delta M_{11}^0 + \delta M_{12}^0$ .

The interaction energy per atom is

$$\begin{aligned} \frac{E(b)}{4\pi b^2 \delta n_g} &= \frac{\hbar}{4\pi b^2 \delta n_g} \int_0^\infty \frac{d\xi}{2\pi} \sum_{l=1}^\infty (2l+1) \ln \left[ \tilde{f}_l^{\text{TM}}(i\xi) \tilde{f}_l^{\text{TE}}(i\xi) \right] \\ &\approx \frac{\hbar}{4\pi b^2 \delta n_g} \int_0^\infty \frac{d\xi}{2\pi} \sum_{l=1}^\infty (2l+1) \left\{ \left[ \tilde{f}_l^{\text{TM}}(i\xi) - 1 \right] + \left[ \tilde{f}_l^{\text{TE}}(i\xi) - 1 \right] \right\} \\ &= \frac{\hbar}{4\pi b^2 \delta n_g} \int_0^\infty \frac{d\xi}{2\pi} \sum_{l=1}^\infty (2l+1) 4\pi n_g \alpha^{at}(i\xi) \delta \frac{i(i\xi b/c)}{2b} \\ &\quad \times \left\{ - \left[ [\xi_l'(i\xi b/c)]^2 + \frac{l(l+1)[\xi_l(i\xi b/c)]^2}{(i\xi b/c)^2} \right] \right. \\ &\quad \times 2 \frac{n_1 \psi_l'(i\xi a/c) \psi_l(i\xi n_1 a/c) - \psi_l(i\xi a/c) \psi_l'(i\xi n_1 a/c)}{n_1 \xi_l'(i\xi a/c) \psi_l(i\xi n_1 a/c) - \xi_l(i\xi a/c) \psi_l'(i\xi n_1 a/c)} \\ &\quad \left. + 2[\xi_l(i\xi b/c)]^2 \frac{\psi_l'(i\xi a/c) \psi_l(i\xi n_1 a/c) - n_1 \psi_l(i\xi a/c) \psi_l'(i\xi n_1 a/c)}{-\xi_l'(i\xi a/c) \psi_l(i\xi n_1 a/c) + n_1 \xi_l(i\xi a/c) \psi_l'(i\xi n_1 a/c)} \right\} \\ &= \frac{\hbar}{b^2} \int_0^\infty \frac{d\xi}{2\pi} \sum_{l=1}^\infty (2l+1) \alpha^{at}(i\xi) \frac{i(i\xi b/c)}{b} \\ &\quad \times \left\{ - \left[ [\xi_l'(i\xi b/c)]^2 + \frac{l(l+1)[\xi_l(i\xi b/c)]^2}{(i\xi b/c)^2} \right] \right. \\ &\quad \times \frac{n_1 \psi_l'(i\xi a/c) \psi_l(i\xi n_1 a/c) - \psi_l(i\xi a/c) \psi_l'(i\xi n_1 a/c)}{n_1 \xi_l'(i\xi a/c) \psi_l(i\xi n_1 a/c) - \xi_l(i\xi a/c) \psi_l'(i\xi n_1 a/c)} \\ &\quad \left. + [\xi_l(i\xi b/c)]^2 \frac{\psi_l'(i\xi a/c) \psi_l(i\xi n_1 a/c) - n_1 \psi_l(i\xi a/c) \psi_l'(i\xi n_1 a/c)}{-\xi_l'(i\xi a/c) \psi_l(i\xi n_1 a/c) + n_1 \xi_l(i\xi a/c) \psi_l'(i\xi n_1 a/c)} \right\}, \end{aligned} \quad (14.62)$$

where now  $n_g$  is the density of gas atoms in the gas shell. The force on the atom is  $\mathbf{F}(b) = -\hat{\mathbf{r}} dE(b)/db$ . In next section we illustrate the result with the interaction between a lithium atom and a gold ball.

### 14.4.1 Li-Atom–Au-Ball Interaction

As an example of atom-ball interactions we show in Fig. 14.4 the interaction between a Li atom and a gold ball. The polarizability for Li was obtained from the London approximation (8.60) with the parameters given in Fig. 8.2. For gold we used the polarizability as shown in Fig. 9.3. The  $b$ -dependence follows a simple power law,  $E \sim b^{-7}$  for large separations. Retardation effects make the curve fall off faster with separation, from a  $b^{-6}$ - to a  $b^{-7}$ -dependence. This is in line with the typical behavior we discussed in Chap. 1 and sketched in Fig. 1.1. We should also mention that the TM-contributions dominate completely. For large  $b$  values the fully retarded result approaches an asymptote that can be found from using (12.34), where one of the static polarizabilities is that of the lithium atom,  $\alpha_{\text{Li}}(0)$ , and one is the gold ball polarizability,  $\alpha_{\text{Auball}}(0)$ . The polarizability for the gold ball we get from (10.14),

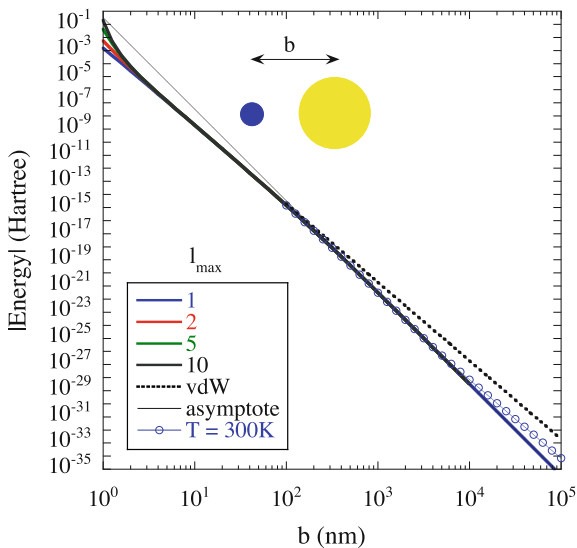


**Fig. 14.4** The interaction energy for a Li atom next to a gold ball of radius  $a = 1\text{nm}$ . The distance between their centers is denoted by  $b$ . The results were obtained from (14.62). The first term in the summation over  $l$  gives the whole result for large  $b$ -values and higher order multipole contributions start to be important when the objects are near contact. The *dotted curve* is the non-retarded van der Waals result from Fig. 10.4. The *thin curve with circles* is the room temperature result

$$\alpha_l^n(\omega) = -\frac{r_n^{2l+1}l[\tilde{\epsilon}_n(\omega) - \tilde{\epsilon}_{n+1}(\omega)]}{\tilde{\epsilon}_n(\omega)(l+1) + \tilde{\epsilon}_{n+1}(\omega)l}, \quad (14.63)$$

with  $\tilde{\epsilon}_{n+1} = \tilde{\epsilon}_{\text{gold}}$ ,  $\tilde{\epsilon}_n = 1$ ,  $l = 1$ ,  $r_n^{2l+1} = a^3$ , and  $\omega = 0$ . Since the static dielectric function for gold diverges  $\alpha_{\text{Auball}}(0) = a^3$ . Thus the large  $b$  asymptote is

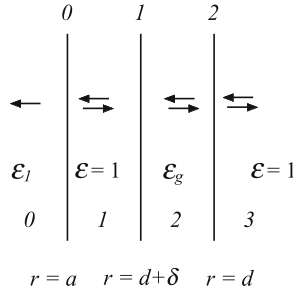
$$E(b) = -\frac{23\hbar c \alpha_{\text{Li}}(0) \alpha_{\text{Auball}}(0)}{4\pi b^7} = -\frac{23\hbar c (163.82a_0^3)(a^3)}{4\pi b^7}. \quad (14.64)$$

This asymptote is given as the thin straight line in Fig. 14.4. We have furthermore added the room temperature result ( $T = 300\text{K}$ ) at the large  $b$  end of the figure, the thin curve with circles. Next we see what happens when we put the atom inside a spherical cavity.

## 14.5 Force on an Atom in a Spherical Cavity

We let the atom be at a distance  $d$  from the center of the spherical cavity, of radius  $a$ . We start from the two layer structure in Fig. 14.5. We let the medium surrounding the cavity have dielectric function  $\tilde{\epsilon}_1(\omega)$ . The first layer is a vacuum layer. The second

**Fig. 14.5** The geometry of a thin gas layer at radius  $d$  inside a spherical or cylindrical cavity of radius  $a$  in the fully retarded treatment. Adapted from [5]



is a thin layer, of thickness  $\delta$ , of a diluted gas of atoms of the kind we consider. Its dielectric function is  $\epsilon_g(\omega) = 1 + 4\pi N\alpha^{at}(\omega)$ , where  $\alpha^{at}$  is the polarizability of one atom. The density of gas atoms,  $N$ , is very low. We use upper case  $N$  for the density here to distinguish the densities from the refractive indices that we denote by lower case  $n$ . We let the first interface be at  $r = a$  and hence the second at  $r = d + \delta$  and the third at  $r = d$ . In what follows we only keep lowest order terms in  $\delta$  and in  $N$ .

Just as in Sect. 14.4 the matrix becomes  $\tilde{\mathbf{M}} = \tilde{\mathbf{M}}_0 \cdot \tilde{\mathbf{M}}_1 \cdot \tilde{\mathbf{M}}_2$  and the left-hand side of the condition for modes is given by (14.49). In this section  $q_0 = \omega/c$ ,  $q_1 = \sqrt{\epsilon_l(\omega)}\omega/c$  and  $q_g = \sqrt{\epsilon_g(\omega)}\omega/c$ .

We now list all elements needed in (14.49). We begin with the matrices for TM modes. The elements of the first matrix are

$$\begin{aligned} M_{11}^0 &= \frac{i}{2\epsilon_1} \{ n_1 \xi_l(q_1 a) \zeta_l'(q_0 a) - \xi_l'(q_1 a) \zeta_l(q_0 a) \}; \\ M_{12}^0 &= \frac{i}{2\epsilon_1} \{ n_1 \xi_l(q_1 a) \xi_l'(q_0 a) - \xi_l'(q_1 a) \xi_l(q_0 a) \}, \end{aligned} \tag{14.65}$$

and of the second

$$\begin{aligned} M_{11}^1 &= \frac{in_g}{2} \{ \xi_l[q_0(d + \delta)] \zeta_l'[q_g(d + \delta)] \\ &\quad - n_g \xi_l'[q_0(d + \delta)] \zeta_l[q_g(d + \delta)] \}; \\ M_{12}^1 &= \frac{in_g}{2} \{ \xi_l[q_0(d + \delta)] \xi_l'[q_g(d + \delta)] \\ &\quad - n_g \xi_l'[q_0(d + \delta)] \xi_l[q_g(d + \delta)] \}; \\ M_{21}^1 &= \frac{in_g}{2} \{ n_g \zeta_l'[q_0(d + \delta)] \zeta_l[q_g(d + \delta)] \\ &\quad - \zeta_l[q_0(d + \delta)] \zeta_l'[q_g(d + \delta)] \}; \\ M_{22}^1 &= \frac{in_g}{2} \{ n_g \zeta_l'[q_0(d + \delta)] \xi_l[q_g(d + \delta)] \\ &\quad - \zeta_l[q_0(d + \delta)] \xi_l'[q_g(d + \delta)] \}, \end{aligned} \tag{14.66}$$

and of the third

$$\begin{aligned}
M_{11}^2 + M_{12}^2 &= \frac{i}{2\varepsilon_g} \left[ n_g \xi_l(q_g d) \zeta_l'(q_0 d) - \xi_l'(q_g d) \zeta_l(q_0 d) \right. \\
&\quad \left. + n_g \xi_l(q_g d) \xi_l'(q_0 d) - \xi_l'(q_g d) \xi_l(q_0 d) \right]; \\
M_{21}^2 + M_{22}^2 &= \frac{i}{2\varepsilon_g} \left[ \zeta_l'(q_g d) \zeta_l(q_0 d) - n_g \zeta_l(q_g d) \zeta_l'(q_0 d) \right. \\
&\quad \left. + \zeta_l'(q_g d) \xi_l(q_0 d) - n_g \zeta_l(q_g d) \xi_l'(q_0 d) \right] \\
&= \frac{i}{\varepsilon_g} \left[ \zeta_l'(q_g d) \psi_l(q_0 d) - n_g \zeta_l(q_g d) \psi_l'(q_0 d) \right],
\end{aligned} \tag{14.67}$$

where  $n_g$  and  $n_1$  are the refractive indices of the gas layer and the surrounding medium, respectively.

We now make a series expansion of the second matrix, (14.66), up to linear order in  $\delta$ . The other matrices do not depend on  $\delta$ . The zeroth order term multiplied with the third matrix produces the matrix  $\begin{pmatrix} 1 \\ 1 \end{pmatrix}$ , so it contributes with  $M_{11}^0 + M_{12}^0$  to the condition for modes. We then expand in  $\alpha_g$ , the polarizability of the gas. There is no zeroth order term in the term linear in  $\delta$ . The lowest order term is linear in  $\alpha_g$ . This means that we do not need to expand the third matrix in  $\alpha_g$ . Thus if we denote the term of the matrix  $\tilde{\mathbf{M}}_1$  that is linear in both  $\delta$  and  $\alpha_g$  by  $\delta\tilde{\mathbf{M}}_1$  the condition for modes can be written as

$$\begin{aligned}
(M_{11}^0 + M_{12}^0) + M_{11}^0 (\delta M_{11}^1 + \delta M_{12}^1) \\
+ M_{12}^0 (\delta M_{21}^1 + \delta M_{22}^1) = 0.
\end{aligned} \tag{14.68}$$

To get mode condition function we first rewrite this as

$$\begin{aligned}
(M_{11}^0 + M_{12}^0) + (M_{11}^0 + M_{12}^0) (\delta M_{11}^1 + \delta M_{12}^1) \\
+ M_{12}^0 [(\delta M_{21}^1 + \delta M_{22}^1) - (\delta M_{11}^1 + \delta M_{12}^1)] = 0,
\end{aligned} \tag{14.69}$$

and the proper mode condition function becomes

$$\begin{aligned}
\tilde{f}_l^{\text{TM}}(\omega) &= 1 + M_{12}^0 \frac{(\delta M_{21}^1 + \delta M_{22}^1) - (\delta M_{11}^1 + \delta M_{12}^1)}{(M_{11}^0 + M_{12}^0)} \\
&= 1 + 4\pi N \alpha^{ar} i \delta q_0 \left\{ [\psi_l'(q_0 d)]^2 + \frac{l(l+1)}{(q_0 d)^2} [\psi_l(q_0 d)]^2 \right\} \\
&\quad \times \frac{n_1 \xi_l(q_1 a) \xi_l'(q_0 a) - \xi_l'(q_1 a) \xi_l(q_0 a)}{n_1 \xi_l(q_1 a) \psi_l'(q_0 a) - \xi_l'(q_1 a) \psi_l(q_0 a)}.
\end{aligned} \tag{14.70}$$

To obtain the mode condition function in (14.70) we have divided the function (the left-hand side of (14.69)) both with the corresponding function for the cavity alone,  $M_{11}^0 + M_{12}^0$ , and for the spherical shell alone,  $1 + \delta M_{11}^1 + \delta M_{12}^1$ .

Now, we proceed with the TE modes. The elements of the first matrix are

$$\begin{aligned}
M_{11}^0 &= \frac{i}{2n_1} \left\{ -n_1 \xi_l'(q_1 a) \zeta_l(q_0 a) + \xi_l(q_1 a) \zeta_l'(q_0 a) \right\}; \\
M_{12}^0 &= \frac{i}{2n_1} \left\{ -n_1 \xi_l'(q_1 a) \xi_l(q_0 a) + \xi_l(q_1 a) \xi_l'(q_0 a) \right\},
\end{aligned} \tag{14.71}$$

and of the second

$$\begin{aligned}
M_{11}^1 &= \frac{i}{2} \left\{ -\xi_l' [q_0 (d + \delta)] \zeta_l [q_g (d + \delta)] \right. \\
&\quad \left. + n_g \xi_l [q_0 (d + \delta)] \zeta_l' [q_g (d + \delta)] \right\}; \\
M_{12}^1 &= \frac{i}{2} \left\{ -\xi_l' [q_0 (d + \delta)] \xi_l [q_g (d + \delta)] \right. \\
&\quad \left. + n_g \xi_l [q_0 (d + \delta)] \xi_l' [q_g (d + \delta)] \right\}; \\
M_{21}^1 &= \frac{i}{2} \left\{ -n_g \zeta_l [q_0 (d + \delta)] \zeta_l' [q_g (d + \delta)] \right. \\
&\quad \left. + \zeta_l' [q_0 (d + \delta)] \zeta_l [q_g (d + \delta)] \right\}; \\
M_{22}^1 &= \frac{i}{2} \left\{ -n_g \zeta_l [q_0 (d + \delta)] \xi_l' [q_g (d + \delta)] \right. \\
&\quad \left. + \zeta_l' [q_0 (d + \delta)] \xi_l [q_g (d + \delta)] \right\},
\end{aligned} \tag{14.72}$$

and of the third

$$\begin{aligned}
M_{11}^2 + M_{12}^2 &= \frac{i}{2n_g} \left[ -n_g \xi_l' (q_g d) \zeta_l (q_0 d) + \xi_l (q_g d) \zeta_l' (q_0 d) \right. \\
&\quad \left. - n_g \xi_l' (q_g d) \xi_l (q_0 d) + \xi_l (q_g d) \xi_l' (q_0 d) \right]; \\
M_{21}^2 + M_{22}^2 &= \frac{i}{2n_g} \left[ -\zeta_l (q_g d) \zeta_l' (q_0 d) + n_g \zeta_l' (q_g d) \zeta_l (q_0 d) \right. \\
&\quad \left. - \zeta_l (q_g d) \xi_l' (q_0 d) + n_g \zeta_l' (q_g d) \xi_l (q_0 d) \right] \\
&= \frac{i}{n_g} \left[ -\zeta_l (q_g d) \psi_l' (q_0 d) + n_g \zeta_l' (q_g d) \psi_l (q_0 d) \right],
\end{aligned} \tag{14.73}$$

where  $n_g$  and  $n_1$  are the refractive indices of the gas layer and the surrounding medium, respectively.

We now make a series expansion of the second matrix, (14.72), up to linear order in  $\delta$ . The other matrices do not depend on  $\delta$ . The zeroth order term multiplied with the third matrix produces the matrix  $\begin{pmatrix} 1 \\ 1 \end{pmatrix}$ , so it contributes with  $M_{11}^0 + M_{12}^0$  to the condition for modes. We then expand in  $\alpha_g$ , the polarizability of the gas. There is no zeroth order term in the term linear in  $\delta$ . The lowest order term is linear in  $\alpha_g$ . This means that we do not need to expand the third matrix in  $\alpha_g$ . Thus if we denote the term of the matrix  $\tilde{\mathbf{M}}_1$  that is linear in both  $\delta$  and  $\alpha_g$  by  $\delta\tilde{\mathbf{M}}_1$  the condition for modes can be written as

$$(M_{11}^0 + M_{12}^0) + M_{11}^0 (\delta M_{11}^1 + \delta M_{12}^1) + M_{12}^0 (\delta M_{21}^1 + \delta M_{22}^1) = 0. \tag{14.74}$$

To get the mode condition function we first rewrite this as

$$(M_{11}^0 + M_{12}^0) + (M_{11}^0 + M_{12}^0) (\delta M_{11}^1 + \delta M_{12}^1) + M_{12}^0 [(\delta M_{21}^1 + \delta M_{22}^1) - (\delta M_{11}^1 + \delta M_{12}^1)] = 0, \tag{14.75}$$

and the proper mode condition function becomes

$$\begin{aligned}
\tilde{f}_l^{\text{TE}}(\omega) &= 1 + M_{12}^0 \frac{(\delta M_{21}^1 + \delta M_{22}^1) - (\delta M_{11}^1 + \delta M_{12}^1)}{(M_{11}^0 + M_{12}^0)} \\
&= 1 + 4\pi N \alpha^{at} i \delta q_0 [\psi_l [q_0 d]]^2 \frac{[-n_1 \xi_l' (q_1 a) \xi_l (q_0 a) + \xi_l (q_1 a) \xi_l' (q_0 a)]}{[-n_1 \xi_l' (q_1 a) \psi_l (q_0 a) + \xi_l (q_1 a) \psi_l' (q_0 a)]}.
\end{aligned} \tag{14.76}$$

To obtain the mode condition function in (14.76) we have divided the function (the left-hand side of (14.75)) both with the corresponding function for the cavity alone,  $M_{11}^0 + M_{12}^0$ , and for the spherical shell alone,  $1 + \delta M_{11}^1 + \delta M_{12}^1$ .

The interaction energy per atom is

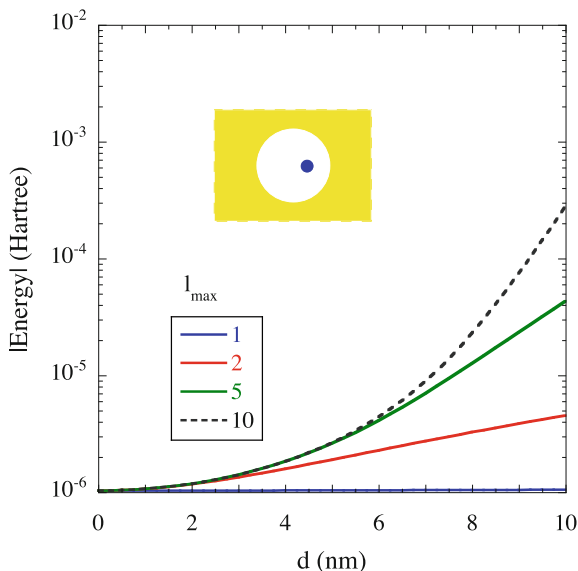
$$\begin{aligned} \frac{E(d)}{4\pi N d^2 \delta} &= \frac{\hbar}{4\pi N d^2 \delta} \int_0^\infty \frac{d\xi}{2\pi} \sum_{l=1}^\infty (2l+1) \ln \left[ \tilde{f}_l^{\text{TM}}(i\xi) \tilde{f}_l^{\text{TE}}(i\xi) \right] \\ &= -\frac{\hbar}{d^2} \int_0^\infty \frac{d\xi}{2\pi} \sum_{l=1}^\infty (2l+1) \alpha^{at} \frac{\xi}{c} \left\{ \left[ \psi_l' \left( \frac{i\xi d}{c} \right) \right]^2 + \frac{l(l+1)}{\left( \frac{i\xi d}{c} \right)^2} \left[ \psi_l \left( \frac{i\xi d}{c} \right) \right]^2 \right\} \\ &\quad \times \frac{n_1 \xi_l \left( \frac{i n_1 \xi a}{c} \right) \xi_l' \left( \frac{i \xi a}{c} \right) - \xi_l' \left( \frac{i n_1 \xi a}{c} \right) \xi_l \left( \frac{i \xi a}{c} \right)}{n_1 \xi_l \left( \frac{i n_1 \xi a}{c} \right) \psi_l' \left( \frac{i \xi a}{c} \right) - \xi_l' \left( \frac{i n_1 \xi a}{c} \right) \psi_l \left( \frac{i \xi a}{c} \right)} \\ &\quad + \left[ \psi_l \left( \frac{i \xi d}{c} \right) \right]^2 \frac{n_1 \xi_l' \left( \frac{i n_1 \xi a}{c} \right) \xi_l \left( \frac{i \xi a}{c} \right) - \xi_l \left( \frac{i n_1 \xi a}{c} \right) \xi_l' \left( \frac{i \xi a}{c} \right)}{n_1 \xi_l' \left( \frac{i n_1 \xi a}{c} \right) \psi_l \left( \frac{i \xi a}{c} \right) - \xi_l \left( \frac{i n_1 \xi a}{c} \right) \psi_l' \left( \frac{i \xi a}{c} \right)}, \end{aligned} \quad (14.77)$$

where we have let  $\delta$ , the thickness of the gas layer, go to zero when passing from the first to the second line. The force on the atom is  $\mathbf{F}(d) = -\hat{\mathbf{r}} dE(d)/dd$ . To illustrate the results we show in next section the interaction on a lithium atom in a gold cavity.

### 14.5.1 Force on a Li-Atom in a Spherical Gold Cavity

As an example of interactions on an atom in a cavity we show in Fig. 14.6 the interaction on a Li atom in a gold cavity. The polarizability for Li was obtained from

**Fig. 14.6** The interaction energy for a Li atom in a spherical gold cavity of radius  $a = 10$  nm. The atom is at the distance  $d$  from the centre of the cavity. The results were obtained from (14.77). The closer to the cavity wall the atom is the more terms in the summation over  $l$  is needed



the London approximation (8.60) with the parameters given in Fig. 8.2. For gold we used polarizability as shown in Fig. 9.3. There is no dipole contribution to the force. The  $l = 1$  contribution to the energy is a constant. The first contribution to the force is a quadrupole term ( $l = 2$ ). Higher order multipole contributions become important when the atom is close to the cavity wall. We note by comparing with the corresponding result in the non-retarded derivation that retardation effects are completely negligible in this example. In order to find retardation effects one would have to study a much larger cavity. The agreement between Figs. 14.6 and 10.6 can be looked upon as a verification of the correctness of the two derivations and their final results.

Next we take the opportunity to rederive the Casimir-Polder interaction between two polarizable atoms using the spherical geometry.

## 14.6 Casimir-Polder Interaction Between Two Atoms

Here, we start with the geometry in Fig. 14.3. We let the thin shell consist of a diluted gas of atoms of type 2 with density  $N_2$  and the sphere consist of a diluted gas of atoms of type 1 with density  $N_1$ . We use upper case  $N$  for the density here to distinguish the densities from the refractive indices that we denote by lower case  $n$ . The thickness of the shell,  $\delta$ , and the radius of the sphere,  $a$ , we let go toward zero at the end. This means that the interaction energy becomes the sum of the interaction energy between all pairs of atoms of type 1 and 2, all with the separation  $b = a + d$ . To get the energy for one atom pair we divide the result by the number of atoms of type 1 and by the number of atoms of type 2. Since we let the thickness of the layer,  $\delta$ , go toward zero we may expand the logarithm in the integrand and keep the lowest order term,  $\ln(1 + x) \approx x$ . We are furthermore only interested in the dipole-dipole interactions which means that only the  $l = 1$  term is kept in the integrand.

Both the TE and TM contributions have the same structure,

$$E = \hbar \int_0^\infty \frac{d\xi}{2\pi} (2l + 1) A(b) N_1 \left. \frac{\partial B(a)}{\partial N_1} \right|_{N_1=0}, \quad (14.78)$$

where

$$A(b) = \delta M_{12}^0(b), \quad (14.79)$$

and

$$B(a) = \frac{(M_{21}^2 + M_{22}^2) - (M_{11}^2 + M_{12}^2)}{(M_{11}^2 + M_{12}^2)}, \quad (14.80)$$

respectively. Now,

$$N_1 \left. \frac{\partial B(a)}{\partial N_1} \right|_{N_1=0} = N_1 \frac{1}{2} 4\pi \alpha_1^{at} \left. \frac{\partial B(a)}{\partial n_1} \right|_{n_1=1}. \quad (14.81)$$

In the contribution for TE modes we have

$$A^{\text{TE}}(b) = -\delta\alpha_g(i\xi) \frac{i\xi}{c} \frac{1}{2} \left[ \xi_1 \left( \frac{i\xi b}{c} \right) \right]^2 = \delta\alpha_g(i\xi) \frac{\xi}{c} \frac{1}{2} e^{-2\xi b/c} \left[ \frac{1+\xi b/c}{\xi b/c} \right]^2, \quad (14.82)$$

and

$$B^{\text{TE}}(a) = 2 \frac{\psi_1'(i\xi a/c) \psi_1(in_1 \xi a/c) - n_1 \psi_1(i\xi a/c) \psi_1'(in_1 \xi a/c)}{\xi_1'(i\xi a/c) \psi_1(in_1 \xi a/c) - n_1 \xi_1(i\xi a/c) \psi_1'(in_1 \xi a/c)}. \quad (14.83)$$

Now,

$$\left. \frac{\partial B^{\text{TE}}(a)}{\partial n_1} \right|_{n_1=1} = 0, \quad (14.84)$$

so there is no TE contribution to the dipole dipole interaction between two polarizable atoms. In the contribution for TM modes we have

$$\begin{aligned} A^{\text{TM}}(b) &= -\delta 4\pi N_2 \alpha_2^{at} (i\xi) \frac{i\xi}{c} \frac{1}{2} \left[ \left[ \xi_1'(i\xi b/c) \right]^2 + \frac{1(1+1)[\xi_1(i\xi b/c)]^2}{(i\xi b/c)^2} \right] \\ &= -\delta 4\pi N_2 \alpha_2^{at} (i\xi) \frac{\xi}{c} \frac{1}{2} \frac{1}{(\xi b/c)^4} e^{-2\xi b/c} \\ &\quad \times \left[ 3 + 6(\xi b/c) + 5(\xi b/c)^2 + 2(\xi b/c)^3 + (\xi b/c)^4 \right], \end{aligned} \quad (14.85)$$

and

$$B^{\text{TM}}(a) = -2 \frac{n_1 \psi_1'(i\xi a/c) \psi_1(in_1 \xi a/c) - \psi_1(i\xi a/c) \psi_1'(in_1 \xi a/c)}{n_1 \xi_1'(i\xi a/c) \psi_1(in_1 \xi a/c) - \xi_1(i\xi a/c) \psi_1'(in_1 \xi a/c)}. \quad (14.86)$$

Now,

$$\left. \frac{\partial B^{\text{TM}}(a)}{\partial n_1} \right|_{n_1=1} = \frac{8}{9} (\xi a/c)^3, \quad (14.87)$$

so the energy per atom pair is

$$\begin{aligned} \frac{E}{(N_1 4\pi a^3/3)(N_2 4\pi b^2 \delta)} &= \frac{\hbar}{(N_1 4\pi a^3/3)(N_2 4\pi b^2 \delta)} \int_0^\infty \frac{d\xi}{2\pi} 3A^{\text{TM}}(b) N_1 \left. \frac{\partial B^{\text{TM}}(a)}{\partial N_1} \right|_{N_1=0} \\ &= -\frac{9\hbar}{(N_1 4\pi a^3)(N_2 4\pi b^2 \delta) 2\pi} \int_0^\infty d\xi \delta 4\pi N_2 \alpha_2^{at} (i\xi) \frac{\xi}{c} \frac{1}{2} \frac{1}{(\xi b/c)^4} \\ &\quad \times N_1 \frac{1}{2} 4\pi \alpha_1^{at} (i\xi) \frac{8}{9} (\xi a/c)^3 e^{-2\xi b/c} \\ &\quad \times \left[ 3 + 6(\xi b/c) + 5(\xi b/c)^2 + 2(\xi b/c)^3 + (\xi b/c)^4 \right] \\ &= -\frac{\hbar}{b^6 \pi} \int_0^\infty d\xi \alpha_2^{at} (i\xi) \alpha_1^{at} (i\xi) e^{-2\xi b/c} \\ &\quad \times \left[ 3 + 6(\xi b/c) + 5(\xi b/c)^2 + 2(\xi b/c)^3 + (\xi b/c)^4 \right]. \end{aligned} \quad (14.88)$$

It is interesting to note that we reproduce the Casimir-Polder interaction (12.30) between two polarizable atoms [10, 11]. Thus we have three quite different methods

to derive the Casimir-Polder interaction that produce identical results. To be noted is that only the TM modes contribute.

## 14.7 Force on an Atom in a Spherical Gap

Let the outer radius be  $b$ , the inner radius  $a$  and the radial position of the atom be  $r$ . The medium surrounding the vacuum gap has the dielectric function  $\varepsilon(\omega)$ . This geometry involves four interfaces and in a straightforward approach the final matrix would be the product of four matrices. The matrix elements in this retarded treatment are rather bulky and difficult to put in print. We will use three matrices, where the middle one is that for the thin diluted gas shell, and take advantage of (14.49). To make the expressions even more compact we make use of the two types of  $2^l$  pole polarizabilities, introduced in Sect. 14.1. Thus, the matrix is  $\tilde{\mathbf{M}} = \tilde{\mathbf{M}}_0 \cdot \tilde{\mathbf{M}}_1 \cdot \tilde{\mathbf{M}}_2$  and

$$M_{11} + M_{12} = M_{11}^0 (M_{11}^2 + M_{12}^2) (1 \alpha_l^{(0(2))}) \cdot \tilde{\mathbf{M}}_1 \cdot \begin{pmatrix} 1 \\ -\alpha_l^2 \end{pmatrix}. \quad (14.89)$$

Now, let us introduce  $\delta\tilde{\mathbf{M}}_1$  so that

$$\tilde{\mathbf{M}}_1 = \begin{pmatrix} 1 & 0 \\ 0 & 1 \end{pmatrix} + \delta\tilde{\mathbf{M}}_1. \quad (14.90)$$

Then

$$\begin{aligned} \tilde{f}_{l,m} &= \frac{M_{11}^1 + \alpha_l^{(0(2))} M_{21}^1 - \alpha_l^2 (M_{12}^1 + \alpha_l^{(0(2))} M_{22}^1)}{(1 - \alpha_l^{(0(2))} \alpha_l^2) (M_{11}^1 + M_{12}^1)} \\ &\approx 1 - \frac{\delta M_{12}^1 [1 + \alpha_l^2 (1 - \alpha_l^{(0(2))})] - \alpha_l^{(0(2))} \delta M_{21}^1 + \alpha_l^{(0(2))} \alpha_l^2 (\delta M_{22}^1 - \delta M_{11}^1)}{(1 - \alpha_l^{(0(2))} \alpha_l^2)}, \end{aligned} \quad (14.91)$$

where we have kept terms up to linear order in the atom density. We have chosen as reference system a system with the spherical gap and the gas shell well separated from each other. Thus we have divided our mode condition function both with that for a free gas film and that for the spherical gap.

For TM modes we have

$$\begin{aligned} \delta\tilde{\mathbf{M}}_1^{\text{TM}} &= -(\delta N) 2\pi\alpha^{at} q_0 i \begin{pmatrix} \xi_l' \zeta_l' + \xi_l \zeta_l \frac{l(l+1)}{(q_0 r)^2} & [\xi_l']^2 + [\xi_l]^2 \frac{l(l+1)}{(q_0 r)^2} \\ -[\zeta_l']^2 - [\zeta_l]^2 \frac{l(l+1)}{(q_0 r)^2} & -\xi_l' \zeta_l' - \xi_l \zeta_l \frac{l(l+1)}{(q_0 r)^2} \end{pmatrix}; \\ \alpha_l^{2,\text{TM}} &= \frac{\zeta_l(q_0 a) \psi_l'(q_m a) - n \zeta_l'(q_0 a) \psi_l(q_m a)}{\xi_l(q_0 a) \psi_l'(q_m a) - n \xi_l'(q_0 a) \psi_l(q_m a)}, \\ \alpha_l^{0(2),\text{TM}} &= \frac{n \xi_l(q_m b) \xi_l'(q_0 b) - \xi_l'(q_m b) \xi_l(q_0 b)}{n \xi_l(q_m b) \zeta_l'(q_0 b) - \xi_l'(q_m b) \zeta_l(q_0 b)}, \end{aligned} \quad (14.92)$$

where  $q_0 = \omega/c$ ,  $q_m = n\omega/c$ , and  $n = \sqrt{\varepsilon}$ . All Ricatti-Bessel functions in the matrix have the argument  $(q_0 r)$ .

For TE modes the functions are

$$\begin{aligned} \delta \tilde{\mathbf{M}}_1^{\text{TE}} &= -(\delta N) 2\pi \alpha^{at} q_0 i \begin{pmatrix} \xi_l(q_0 r) \zeta_l(q_0 r) & [\xi_l(q_0 r)]^2 \\ -[\zeta_l(q_0 r)]^2 & -\xi_l(q_0 r) \zeta_l(q_0 r) \end{pmatrix}; \\ \alpha_l^{2,\text{TE}} &= \frac{\zeta_l'(q_0 a) \psi_l(q_m a) - n \zeta_l(q_0 a) \psi_l'(q_m a)}{\xi_l'(q_0 a) \psi_l(q_m a) - n \xi_l(q_0 a) \psi_l'(q_m a)}; \\ \alpha_l^{0(2),\text{TE}} &= \frac{n \xi_l'(q_m b) \xi_l(q_0 b) - \xi_l(q_m b) \xi_l'(q_0 b)}{n \xi_l'(q_m b) \zeta_l(q_0 b) - \xi_l(q_m b) \zeta_l'(q_0 b)}. \end{aligned} \tag{14.93}$$

Here one may take the opportunity to check the results. If we let  $\alpha_l^{0(2)} = 0$  we regain the results for an atom outside a solid sphere, in Sect. 14.4. If we instead let  $\alpha_l^2 = -1$  we regain the results for an atom in a spherical cavity, in Sect. 14.5.

Next we study the interaction between an atom and a thin spherical shell. We begin with placing the atom outside the shell.

### 14.8 Force on an Atom Outside a 2D Spherical Shell

We start from the geometry in Fig. 14.7. We use already from the outset the matrices for a gas layer at  $r = b = a + d$  and a spherical 2D film at  $r = a$ . These were given in (14.37), (14.38), (14.43), and (14.44). We find

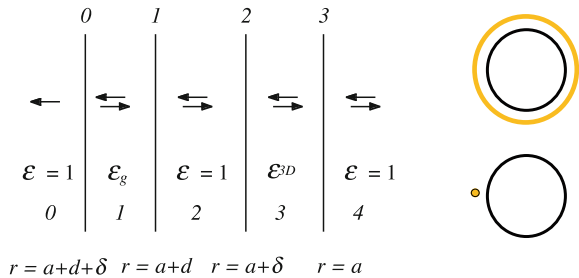
$$\begin{aligned} \tilde{f}_l^{\text{TM}} &= 1 - (\delta n) 4\pi \alpha^{at} q_0 i \left[ [\xi_l'(q_0 b)]^2 + [\xi_l(q_0 b)]^2 \frac{l(l+1)}{(q_0 b)^2} \right] \\ &\quad \times \frac{\delta \tilde{\varepsilon}^{3D} q_0 i [\psi_l'(q_0 a)]^2}{[1 - \delta \tilde{\varepsilon}^{3D} q_0 i \xi_l'(q_0 a) \psi_l'(q_0 a)]}, \end{aligned} \tag{14.94}$$

and

$$\tilde{f}_l^{\text{TE}} = 1 - (\delta n) 4\pi \alpha^{at} i q_0 [\xi_l(q_0 b)]^2 \frac{\delta \tilde{\varepsilon}^{3D} i q_0 [\psi_l(q_0 a)]^2}{1 - \delta \tilde{\varepsilon}^{3D} i q_0 [\xi_l(q_0 a) \psi_l(q_0 a)]}. \tag{14.95}$$

We have also derived these results in the alternative way followed in the preceding sections. The interaction energy per atom is

**Fig. 14.7** The geometry of a thin gas layer at distance  $d$  from a thin spherical or cylindrical shell of radius  $a$  in the fully retarded treatment. Adapted from [5]



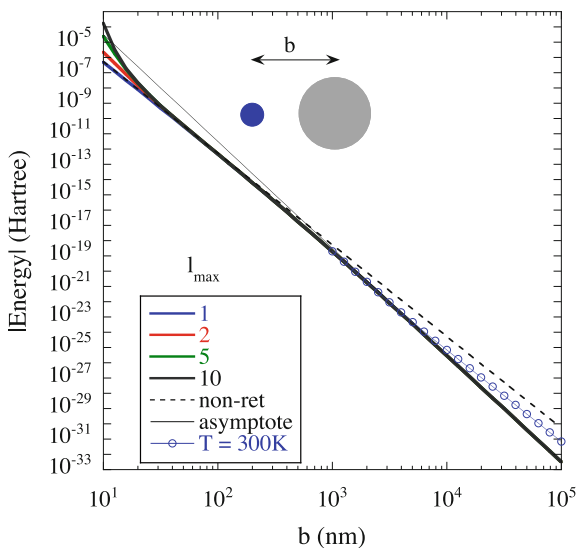
$$\begin{aligned}
 \frac{E(b)}{4\pi n b^2 \delta} &= \frac{\hbar}{4\pi n b^2 \delta} \int_0^\infty \frac{d\xi}{2\pi} \sum_{l=1}^\infty (2l+1) \ln \left[ \tilde{f}_l^{\text{TM}}(i\xi) \tilde{f}_l^{\text{TE}}(i\xi) \right] \\
 &= -\frac{\hbar}{b^2} \int_0^\infty \frac{d\xi}{2\pi} \sum_{l=1}^\infty (2l+1) \alpha^{at}(i\xi) \delta \tilde{\varepsilon}^{3D}(i\xi) \left(\frac{\xi}{c}\right)^2 \\
 &\quad \times \left\{ \frac{\left[ \xi_l' \left( i \frac{\xi b}{c} \right) \right]^2 - \left[ \xi_l \left( i \frac{\xi b}{c} \right) \right]^2 \frac{l(l+1)}{\left( \frac{\xi b}{c} \right)^2} \left[ \psi_l' \left( i \frac{\xi a}{c} \right) \right]^2}{\left[ 1 + \delta \tilde{\varepsilon}^{3D}(i\xi) \left( \frac{\xi}{c} \right) \xi_l' \left( i \frac{\xi a}{c} \right) \psi_l' \left( i \frac{\xi a}{c} \right) \right]} \right. \\
 &\quad \left. + \frac{\left[ \xi_l \left( i \frac{\xi b}{c} \right) \right]^2 \left[ \psi_l \left( i \frac{\xi a}{c} \right) \right]^2}{1 + \delta \tilde{\varepsilon}^{3D}(i\xi) \left( \frac{\xi}{c} \right) \left[ \xi_l \left( i \frac{\xi a}{c} \right) \psi_l \left( i \frac{\xi a}{c} \right) \right]} \right\}, \tag{14.96}
 \end{aligned}$$

where we have let  $\delta$ , the thickness of the gas layer, go to zero when passing from the first to the second line. The force on the atom is  $\mathbf{F}(b) = -\hat{\mathbf{r}}dE(b)/db$ . We apply this result to a lithium atom outside a graphene like sphere in next section.

### 14.8.1 Interaction Between a Li-Atom and a Graphene Sphere

As an example we give the results for a Li-atom outside a graphene sphere in Fig. (14.8). The results are from using (14.96). The polarizability for Li was obtained from the London approximation (8.60) with the parameters given in Fig. 8.2 and for the spherical shell the  $\delta \tilde{\varepsilon}^{3D}(i\xi)$  entering  $\alpha_l^{2D}(a; i\xi)$  was taken from (10.24). We have added the non-retarded result from Fig. 10.10 to illustrate the effect of retardation.

**Fig. 14.8** The interaction between a Li atom and a graphene sphere as a function of distance  $b$ . The radius,  $a$ , of the spherical shell is 10 nm. The results are from using (14.96) and each curve is for a different truncation of the summation over  $l$ . For comparison we have shown the non-retarded result, *dashed curve*, from Fig. 10.10. The *thin curve with circles* is the room temperature result. See the text for details



For large  $b$  values the fully retarded result approaches an asymptote that can be found from using (12.34), where one of the static polarizabilities is that of the lithium atom,  $\alpha_{\text{Li}}(0)$ , and one is the polarizability of the graphene sphere,  $\alpha_{\text{gra.sph.}}(0)$ . The polarizability for the graphene sphere we get from (10.25),

$$\alpha_l^{2D}(a; \omega) = \frac{\delta\tilde{\varepsilon}^{3D}(\omega) l(l+1) a^{2l+1}}{(2l+1)a + \delta\tilde{\varepsilon}^{3D}(\omega) l(l+1)}, \quad (14.97)$$

with  $l = 1$ , and  $\omega = 0$ . Since the static value of  $\delta\tilde{\varepsilon}^{3D}(\omega)$  diverges  $\alpha_{\text{gra.sph.}}(0) = a^3$ . Thus the large  $b$  asymptote is

$$E(b) = -\frac{23\hbar c \alpha_{\text{Li}}(0) \alpha_{\text{gra.sph.}}(0)}{4\pi b^7} = -\frac{23\hbar c (163.82a_0^3) (a^3)}{4\pi b^7}. \quad (14.98)$$

This asymptote is given as the thin straight line in Fig. 14.8. We have furthermore added the room temperature result ( $T = 300\text{K}$ ) at the large  $b$  end of the figure, the thin curve with circles. Next, we move the atom inside the spherical shell.

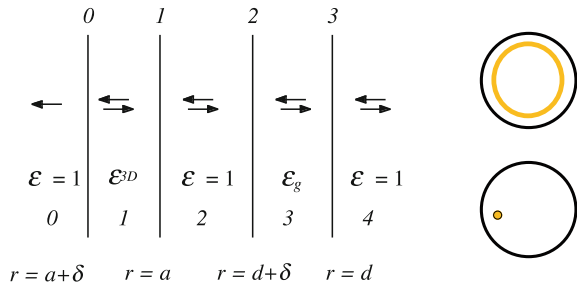
## 14.9 Force on an Atom Inside a 2D Spherical Shell

We start from the geometry in Fig. 14.9. We use already from the outset the matrices for a spherical 2D film at  $r = a$  and a gas layer at  $r = d$ . These were given in (14.37), (14.38), (14.43), and (14.44). We find

$$\begin{aligned} \tilde{f}_l^{\text{TM}} &= 1 + M_{12}^0 \frac{(\delta M_{21}^1 + \delta M_{22}^1) - (\delta M_{11}^1 + \delta M_{12}^1)}{M_{11}^0 + M_{12}^0} \\ &= 1 - iq_0 \delta\tilde{\varepsilon}^{3D} \frac{1}{2} \left[ \xi'(q_0 a) \right]^2 \frac{(\delta M_{21}^1 + \delta M_{22}^1) - (\delta M_{11}^1 + \delta M_{12}^1)}{1 - iq_0 \delta\tilde{\varepsilon}^{3D} \psi'(q_0 a) \xi_l'(q_0 a)} \\ &= 1 - \frac{iq_0 \delta\tilde{\varepsilon}^{3D} [\xi_l'(q_0 a)]^2 4\pi N \alpha^{at} \delta i q_0}{1 - iq_0 \delta\tilde{\varepsilon}^{3D} \psi'(q_0 a) \xi_l'(q_0 a)} \left\{ [\psi_l'(q_0 d)]^2 + \frac{l(l+1)}{(q_0 d)^2} [\psi_l(q_0 d)]^2 \right\}, \end{aligned} \quad (14.99)$$

and

**Fig. 14.9** The geometry of a thin gas layer at radius  $d$  inside a thin spherical or cylindrical shell of radius  $a$  in the fully retarded treatment. Adapted from [5]



$$\begin{aligned}
\tilde{f}_l^{\text{TE}} &= 1 + M_{12}^0 \frac{(\delta M_{21}^1 + \delta M_{22}^1) - (\delta M_{11}^1 + \delta M_{12}^1)}{M_{11}^0 + M_{12}^0} \\
&= 1 - iq_0 \delta \tilde{\varepsilon}^{3D} \frac{1}{2} [\xi_l(q_0 a)]^2 \frac{(\delta M_{21}^1 + \delta M_{22}^1) - (\delta M_{11}^1 + \delta M_{12}^1)}{1 - iq_0 \delta \tilde{\varepsilon}^{3D} \psi(q_0 a) \xi_l(q_0 a)} \\
&= 1 - \frac{iq_0 \delta \tilde{\varepsilon}^{3D} [\xi_l(q_0 a)]^2 4\pi N \alpha^{at} \delta iq_0 [\psi_l(q_0 d)]^2}{1 - iq_0 \delta \tilde{\varepsilon}^{3D} \psi(q_0 a) \xi_l(q_0 a)}.
\end{aligned} \tag{14.100}$$

The interaction energy per atom is

$$\begin{aligned}
\frac{E(d)}{4\pi N d^2 \delta} &= \frac{\hbar}{4\pi n d^2 \delta} \int_0^\infty \frac{d\xi}{2\pi} \sum_{l=1}^\infty (2l+1) \ln \left[ \tilde{f}_l^{\text{TM}}(i\xi) \tilde{f}_l^{\text{TE}}(i\xi) \right] \\
&= -\frac{\hbar}{d^2} \int_0^\infty \frac{d\xi}{2\pi} \sum_{l=1}^\infty (2l+1) \alpha^{at}(i\xi) \delta \tilde{\varepsilon}^{3D}(i\xi) \left(\frac{\xi}{c}\right)^2 \\
&\quad \times \left\{ \frac{\left[ \left[ \psi_l'(i\frac{\xi d}{c}) \right]^2 - \left[ \psi_l(i\frac{\xi d}{c}) \right]^2 \frac{1(l+1)}{\left(\frac{\xi d}{c}\right)^2} \right] \left[ \xi_l'(i\frac{\xi a}{c}) \right]^2}{\left[ 1 + \delta \tilde{\varepsilon}^{3D}(i\xi) \left(\frac{\xi}{c}\right) \xi_l'(i\frac{\xi a}{c}) \psi_l'(i\frac{\xi a}{c}) \right]} \right. \\
&\quad \left. + \frac{\left[ \xi_l(i\frac{\xi a}{c}) \right]^2 \left[ \psi_l(i\frac{\xi d}{c}) \right]^2}{1 + \delta \tilde{\varepsilon}^{3D}(i\xi) \left(\frac{\xi}{c}\right) \left[ \xi_l(i\frac{\xi a}{c}) \psi_l(i\frac{\xi a}{c}) \right]} \right\},
\end{aligned} \tag{14.101}$$

where we have let  $\delta$ , the thickness of the gas layer, go to zero when passing from the first to the second line. The force on the atom is  $\mathbf{F}(d) = -\hat{\mathbf{r}} dE(d)/dd$ .

We illustrate this result with a lithium atom inside a graphene-like sphere.

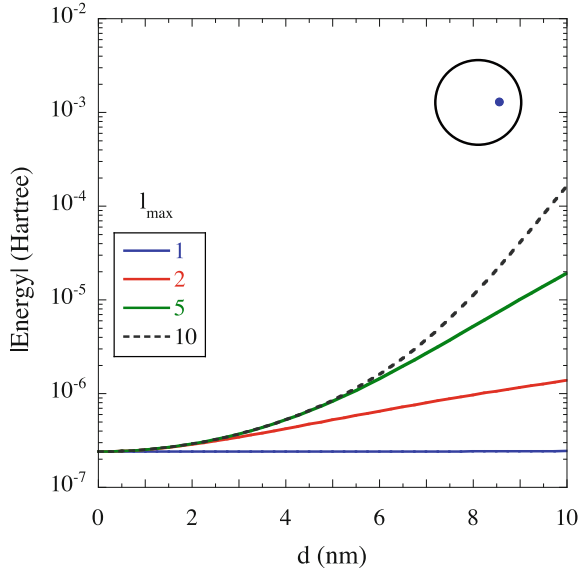
### 14.9.1 Force on a Li-Atom Inside a Graphene Sphere

As an example we give the results for a Li-atom inside a graphene sphere in Fig. 14.10. The results are from using (14.101). The polarizability for Li was obtained from the London approximation (8.60) with the parameters given in Fig. 8.2 and for the spherical shell the  $\delta \tilde{\varepsilon}^{3D}(i\xi)$  entering  $\alpha_l^{2D(2)}(a; i\xi)$  was taken from (10.24). From comparison with Fig. 10.12 we see that the retardation effects are negligible for this example. We can view this comparison as an extra test of the formalism and of our derivations. Next we turn to two concentric spherical shells.

## 14.10 Interaction Between Two 2D Spherical Shells

We consider two concentric thin spherical shells in vacuum. Since the films are in vacuum  $q_0 = \omega/c$ . The outer shell has radius  $b$  and the inner radius  $a$ . Here the matrix is  $\mathbf{M} = \mathbf{M}_0 \cdot \mathbf{M}_1$  where for TM modes

**Fig. 14.10** The interaction on a Li atom inside a graphene sphere as a function of distance  $d$  from the center. The radius,  $a$ , of the spherical shell is 10 nm. The results are from using (14.101) and each curve is for a different truncation of the summation over  $l$ . See the text for details



$$\begin{aligned} \tilde{\mathbf{M}}_0^{\text{TM}} &= \begin{pmatrix} 1 & 0 \\ 0 & 1 \end{pmatrix} - \frac{\delta\tilde{\epsilon}^{3\text{D}}q_0i}{2} \begin{pmatrix} \xi_l'(q_0b) \zeta_l'(q_0b) & [\xi_l'(q_0b)]^2 \\ -[\zeta_l'(q_0b)]^2 & -\xi_l'(q_0b) \zeta_l'(q_0b) \end{pmatrix}; \\ \tilde{\mathbf{M}}_1^{\text{TM}} &= \begin{pmatrix} 1 & 0 \\ 0 & 1 \end{pmatrix} - \frac{\delta\tilde{\epsilon}^{3\text{D}}q_0i}{2} \begin{pmatrix} \xi_l'(q_0a) \zeta_l'(q_0a) & [\xi_l'(q_0a)]^2 \\ -[\zeta_l'(q_0a)]^2 & -\xi_l'(q_0a) \zeta_l'(q_0a) \end{pmatrix}, \end{aligned} \quad (14.102)$$

and the condition for modes is

$$\begin{aligned} M_{11}^{\text{TM}} + M_{12}^{\text{TM}} &= 1 - \frac{\delta\tilde{\epsilon}^{3\text{D}}q_0i}{2} [\xi_l'(q_0b) \zeta_l'(q_0b) \\ &\quad + [\xi_l'(q_0b)]^2 + \xi_l'(q_0a) \zeta_l'(q_0a) + [\xi_l'(q_0a)]^2] \\ &\quad + \left(\frac{\delta\tilde{\epsilon}^{3\text{D}}q_0i}{2}\right)^2 [\xi_l'(q_0b) \zeta_l'(q_0b) \xi_l'(q_0a) \zeta_l'(q_0a) \\ &\quad - [\xi_l'(q_0b)]^2 [\zeta_l'(q_0a)]^2] = 0. \end{aligned} \quad (14.103)$$

For TE modes the two matrices are

$$\begin{aligned} \tilde{\mathbf{M}}_0^{\text{TE}} &= \begin{pmatrix} 1 & 0 \\ 0 & 1 \end{pmatrix} - \frac{\delta\tilde{\epsilon}^{3\text{D}}q_0i}{2} \begin{pmatrix} \xi_l(q_0b) \zeta_l(q_0b) & [\xi_l(q_0b)]^2 \\ -[\zeta_l(q_0b)]^2 & -\xi_l(q_0b) \zeta_l(q_0b) \end{pmatrix}; \\ \tilde{\mathbf{M}}_1^{\text{TE}} &= \begin{pmatrix} 1 & 0 \\ 0 & 1 \end{pmatrix} - \frac{\delta\tilde{\epsilon}^{3\text{D}}q_0i}{2} \begin{pmatrix} \xi_l(q_0a) \zeta_l(q_0a) & [\xi_l(q_0a)]^2 \\ -[\zeta_l(q_0a)]^2 & -\xi_l(q_0a) \zeta_l(q_0a) \end{pmatrix}, \end{aligned} \quad (14.104)$$

and the condition for modes becomes

$$\begin{aligned}
M_{11}^{\text{TE}} + M_{12}^{\text{TE}} &= 1 - \frac{\delta\tilde{\varepsilon}^{3\text{D}} q_0 i}{2} [\xi_l(q_0 b) \zeta_l(q_0 b) \\
&\quad + [\xi_l(q_0 b)]^2 + \xi_l(q_0 a) \zeta_l(q_0 a) + [\xi_l(q_0 a)]^2] \\
&\quad + \left(\frac{\delta\tilde{\varepsilon}^{3\text{D}} q_0 i}{2}\right)^2 [\xi_l(q_0 b) \zeta_l(q_0 b) \xi_l(q_0 a) \zeta_l(q_0 a) \\
&\quad \quad - [\xi_l(q_0 b)]^2 [\zeta_l(q_0 a)]^2] = 0.
\end{aligned} \tag{14.105}$$

The mode condition function for TM modes is

$$\tilde{f}_{l,m}^{\text{TM}}(i\xi) = 1 - \frac{[\delta\tilde{\varepsilon}^{3\text{D}} q_0 i]^2 [\psi_l'(q_0 a)]^2 [\xi_l'(q_0 b)]^2}{[1 - \delta\tilde{\varepsilon}^{3\text{D}} q_0 i [\xi_l'(q_0 b) \psi_l'(q_0 b)]] [1 - \delta\tilde{\varepsilon}^{3\text{D}} q_0 i [\xi_l'(q_0 a) \psi_l'(q_0 a)]]} \tag{14.106}$$

and for TE modes

$$\tilde{f}_{l,m}^{\text{TE}}(i\xi) = 1 - \frac{[\delta\tilde{\varepsilon}^{3\text{D}} q_0 i]^2 [\psi_l(q_0 a)]^2 [\xi_l(q_0 b)]^2}{[1 - \delta\tilde{\varepsilon}^{3\text{D}} q_0 i [\xi_l(q_0 b) \psi_l(q_0 b)]] [1 - \delta\tilde{\varepsilon}^{3\text{D}} q_0 i [\xi_l(q_0 a) \psi_l(q_0 a)]]} \tag{14.107}$$

Here, our notation may unfortunately cause some confusion. Note that  $\xi$  is the variable along the imaginary frequency axis and  $\xi_l$  is a Riccati-Bessel function. We have chosen to express the mode condition functions in terms of the functions  $\xi_l$  and  $\psi_l$  to simplify the transformation into real valued functions of real valued arguments according to (14.21).

We have chosen as reference system a system where the two shells are separated from each other and at infinite distance from each other. The interaction energy is what it takes to bring the shells together and putting the inner shell inside the outer shell. The interaction energy is

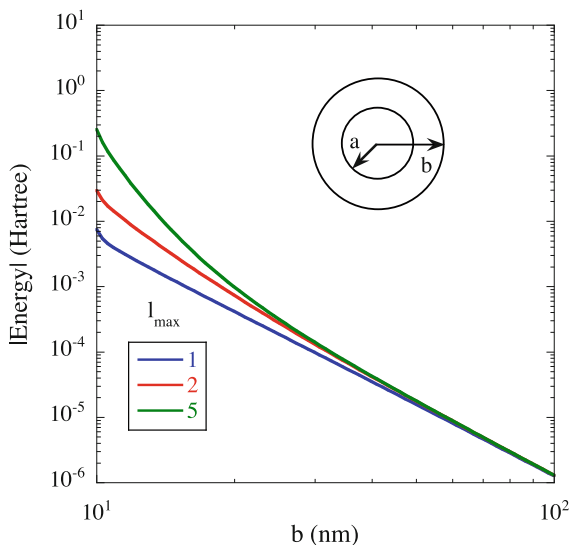
$$\begin{aligned}
E &= \hbar \int_0^\infty \frac{d\xi}{2\pi} \sum_{l=1}^\infty \sum_{m=-l}^l \ln \left( \tilde{f}_{l,m}^{\text{TM}}(i\xi) \tilde{f}_{l,m}^{\text{TE}}(i\xi) \right) \\
&= \hbar \int_0^\infty \frac{d\xi}{2\pi} \sum_{l=1}^\infty (2l+1) \left[ \ln \left( \tilde{f}_l^{\text{TM}}(i\xi) \right) + \ln \left( \tilde{f}_l^{\text{TE}}(i\xi) \right) \right]
\end{aligned} \tag{14.108}$$

where we have made use of the fact that the integrand is independent of  $m$ . The summation over  $m$  then just adds a factor of  $(2l+1)$ .

### 14.10.1 Interaction Between Two Concentric Graphene Spheres

As an example we give in Fig. 14.11 the interaction energy for two concentric graphene spheres. We let the radius,  $a$ , of the inner sphere be 10nm and let the radius,  $b$ , of outer sphere vary between 10nm and 100nm. We have treated the graphene spheres as strictly 2D spherical shells with the effective dielectric function given in (10.24). Each curve is for a different truncation of the summation over  $l$ . The

**Fig. 14.11** The interaction between two concentric graphene spheres as a function of the radius,  $b$ , of the outer sphere. The radius,  $a$ , of the inner sphere is 10 nm. The results are from using (14.108) with the mode condition functions from (14.106) and (14.107). Each curve is for a different truncation of the summation over  $l$ . See the text for details



smaller the value of  $b$  the more terms are needed in the summation. The reference system is one where the smaller inner sphere has been taken outside the larger outer sphere and the two are at infinite distance from each other. The energy in Fig. 14.11 is the energy gain when the smaller sphere is brought to and inserted into the larger sphere. The energy in (14.108) is negative.

## 14.11 Force on an Atom in Between Two 2D Spherical Films

Here we may reuse the results from Sect. 14.7. The only difference is the expressions for the  $2^l$  pole polarizabilities. The mode condition function is

$$\begin{aligned} \tilde{f}_{l,m} &= \frac{M_{11}^1 + \alpha_l^{2D0(2)} M_{21}^1 - \alpha_l^{2D2} (M_{12}^1 + \alpha_l^{2D0(2)} M_{22}^1)}{(1 - \alpha_l^{2D0(2)} \alpha_l^{2D2}) (M_{11}^1 + M_{12}^1)} \\ &\approx 1 - \frac{\delta M_{12}^1 [1 + \alpha_l^{2D2} (1 - \alpha_l^{2D0(2)})] - \alpha_l^{2D0(2)} \delta M_{21}^1 + \alpha_l^{2D0(2)} \alpha_l^{2D2} (\delta M_{22}^1 - \delta M_{11}^1)}{(1 - \alpha_l^{2D0(2)} \alpha_l^{2D2})}, \end{aligned} \quad (14.109)$$

where we have kept terms up to linear order in the atom density. We have chosen as reference system a system with the spherical films and the gas shell well separated from each other. Thus we have divided our mode condition function both with that for a free gas film and that for the thin spherical films.

For TM modes we have

$$\begin{aligned}
\delta\tilde{\mathbf{M}}_1^{\text{TM}} &= -(\delta N) 2\pi\alpha^{at} q_0 i \left( \begin{array}{cc} \xi_l' \zeta_l' + \xi_l \zeta_l \frac{l(l+1)}{(q_0 r)^2} & [\xi_l']^2 + [\xi_l]^2 \frac{l(l+1)}{(q_0 r)^2} \\ -[\zeta_l']^2 - [\zeta_l]^2 \frac{l(l+1)}{(q_0 r)^2} & -\xi_l' \zeta_l' - \xi_l \zeta_l \frac{l(l+1)}{(q_0 r)^2} \end{array} \right); \\
\alpha_l^{2\text{D2, TM}} &= -\frac{2+\delta\tilde{\varepsilon}^{3\text{D}} q_0 i [\zeta_l'(q_0 a)^2 + \xi_l'(q_0 a)\zeta_l'(q_0 a)]}{2-\delta\tilde{\varepsilon}^{3\text{D}} q_0 i [\xi_l'(q_0 a)^2 + \xi_l(q_0 a)\zeta_l'(q_0 a)]}; \\
\alpha_l^{2\text{D0(2), TM}} &= \frac{-\delta\tilde{\varepsilon}^{3\text{D}} q_0 i \xi_l'(q_0 b)^2}{2-\delta\tilde{\varepsilon}^{3\text{D}} q_0 i \xi_l'(q_0 b)\zeta_l'(q_0 b)},
\end{aligned} \tag{14.110}$$

where  $q_0 = \omega/c$ . All Ricatti-Bessel functions in the matrix have the argument  $(q_0 r)$ . For TE modes the functions are

$$\begin{aligned}
\delta\tilde{\mathbf{M}}_1^{\text{TE}} &= -(\delta N) 2\pi\alpha^{at} q_0 i \left( \begin{array}{cc} \xi_l(q_0 r)\zeta_l(q_0 r) & [\xi_l(q_0 r)]^2 \\ -[\zeta_l(q_0 r)]^2 & -\xi_l(q_0 r)\zeta_l(q_0 r) \end{array} \right); \\
\alpha_l^{2\text{D2, TE}} &= -\frac{2+\delta\tilde{\varepsilon}^{3\text{D}} q_0 i [\zeta_l(q_0 a)^2 + \xi_l(q_0 a)\zeta_l(q_0 a)]}{2-\delta\tilde{\varepsilon}^{3\text{D}} q_0 i [\xi_l(q_0 a)^2 + \xi_l(q_0 a)\zeta_l(q_0 a)]}; \\
\alpha_l^{2\text{D0(2), TE}} &= \frac{-\delta\tilde{\varepsilon}^{3\text{D}} q_0 i \xi_l(q_0 b)^2}{2-\delta\tilde{\varepsilon}^{3\text{D}} q_0 i \xi_l(q_0 b)\zeta_l(q_0 b)}.
\end{aligned} \tag{14.111}$$

Now we are done with the spherical geometries and end the chapter by calculating the Casimir interaction between two atoms.

## 14.12 Force Between Two Atoms from Summation of Pair Interactions

We derived the Casimir interaction between two atoms in Sect. 12.1. It is possible to find this result via a short-cut, viz. by using the result from the summation over pair interactions in Sect. 6.1. The procedure is the following: choose a geometry with two objects of different material; calculate the result using the summation over pair interactions; calculate the result using the full formalism and take the diluted limit; compare the two results and identify parameters.

We choose to apply this procedure on an atom of species 1 at the distance  $R$  from a ball of atomic species 2. We let the ball have the radius  $R_2$  and the atom density  $n^{3D}$ . We make the ansatz that the interaction between the atoms is given by the potential  $V = -Br^{-7}$  and we intend to identify the coefficient  $B$ . The result from summation over pair interactions (6.13) with this ansatz is

$$E(R) = -\frac{B}{R^7} \frac{4\pi R_2^3 n^{3D}}{3}. \tag{14.112}$$

We have assumed that there is vacuum in between the objects. The corresponding result in the full formalism (14.62) is

$$\begin{aligned}
E(R) &= -\frac{\hbar}{R^2} \int_0^\infty \frac{d\xi}{2\pi} \sum_{l=1}^\infty (2l+1) \alpha_1^{at}(\xi) \frac{i(\xi R/c)}{R} \\
&\times \left\{ \left[ \xi_l'(\xi R/c) \right]^2 + \frac{l(l+1)[\xi_l(\xi R/c)]^2}{(\xi R/c)^2} \right\} \frac{n_2 \psi_l'(\xi R_2/c) \psi_l(\xi n_2 R_2/c) - \psi_l(\xi R_2/c) \psi_l'(\xi n_2 R_2/c)}{n_2 \xi_l'(\xi R_2/c) \psi_l(\xi n_2 R_2/c) - \xi_l(\xi R_2/c) \psi_l'(\xi n_2 R_2/c)} \\
&+ \left[ \xi_l(\xi R/c) \right]^2 \frac{\psi_l'(\xi R_2/c) \psi_l(\xi n_2 R_2/c) - n_2 \psi_l(\xi R_2/c) \psi_l'(\xi n_2 R_2/c)}{\xi_l'(\xi R_2/c) \psi_l(\xi n_2 R_2/c) - n_2 \xi_l(\xi R_2/c) \psi_l'(\xi n_2 R_2/c)} \Big\}.
\end{aligned} \tag{14.113}$$

We may here make use of the derivation we performed in Sect. 14.6. We study (14.88). Since we now are interested in the interaction energy between the atom and the whole ball we do not divide with the number of atoms in the ball. We have

$$\begin{aligned}
\frac{E}{(N_2 4\pi b^2 \delta)} &= \frac{\hbar}{(N_2 4\pi b^2 \delta)} \int_0^\infty \frac{d\xi}{2\pi} 3A^{\text{TM}}(b) N_1 \left. \frac{\partial B^{\text{TM}}(a)}{\partial N_1} \right|_{N_1=0} \\
&= -\frac{3\hbar}{(N_2 4\pi b^2 \delta) 2\pi} \int_0^\infty d\xi \delta 4\pi N_2 \alpha_2^{at}(\xi) \frac{\xi}{c} \frac{1}{2} \frac{1}{(\xi b/c)^4} \\
&\times N_1 \frac{1}{2} 4\pi \alpha_1^{at}(\xi) \frac{8}{9} (\xi a/c)^3 e^{-2\xi b/c} \\
&\times [3 + 6(\xi b/c) + 5(\xi b/c)^2 + 2(\xi b/c)^3 + (\xi b/c)^4] \\
&= |\xi \rightarrow \xi/b| \\
&= -\frac{\hbar}{b^7 \pi} \frac{4\pi a^3 N_1}{3} \int_0^\infty d\xi \alpha_2^{at}(\xi/b) \alpha_1^{at}(\xi/b) e^{-2\xi/c} \\
&\times [3 + 6(\xi/c) + 5(\xi/c)^2 + 2(\xi/c)^3 + (\xi b/c)^4].
\end{aligned} \tag{14.114}$$

Now, letting the distance  $b$  go toward infinity we have

$$\begin{aligned}
E(R) &\approx -\frac{\hbar}{R^7 \pi} \frac{4\pi R_2^3 n^{3D}}{3} \int_0^\infty d\xi \alpha_2^{at}(0) \alpha_1^{at}(0) e^{-2\xi/c} \\
&\times [3 + 6(\xi/c) + 5(\xi/c)^2 + 2(\xi/c)^3 + (\xi/c)^4] \\
&= |\xi \rightarrow \xi c| = -\frac{\hbar c \alpha_2^{at}(0) \alpha_1^{at}(0)}{R^7 \pi} \frac{4\pi R_2^3 n^{3D}}{3} \\
&\times \underbrace{\int_0^\infty d\xi e^{-2\xi} [3 + 6(\xi) + 5(\xi)^2 + 2(\xi)^3 + (\xi)^4]}_{23/4} \\
&= -\frac{23\hbar c \alpha_2^{at}(0) \alpha_1^{at}(0)}{4\pi R^7} \frac{4\pi R_2^3 n^{3D}}{3},
\end{aligned} \tag{14.115}$$

where we have replaced  $b$  with  $R$  and  $a$  with  $R_2$  to be consistent with the notation we used in the summation over pair interactions. Equating this result with the result in (14.112) we find

$$B = \frac{23\hbar c \alpha_2^{at}(0) \alpha_1^{at}(0)}{4\pi}. \tag{14.116}$$

This agrees with what we found with the corresponding derivation in planar structures in (13.147).

The procedure we have just gone through is a short-cut for finding the van der Waals interaction between two atoms. It furthermore acts as a test of the consistency of our formalism.

## References

1. From (9.6.2) and (9.6.3) in *Handbook of Mathematical Functions*, ed. by M. Abramowitz, I.A. Stegun (U.S. Government Printing Office, 1964)
2. M. Kerker, *The Scattering of Light and Other Electromagnetic Radiation*, ed. by E.M. Loebel (Academic Press, New York, 1969), p. 41
3. P. Debye, *Ann. Phys.* **30**, 57 (1909)
4. M. Born, E. Wolf, *Principles of Optics* (Pergamon Press, Oxford, 1959)
5. Bo E. Sernelius, *Phys. Rev. B* **90**, 155457 (2014)
6. R. Ruppin, *Electromagnetic Surface Modes*, ed. A.D. Boardman (John Wiley, New York, 1982)
7. I. Brevik, J.B. Aarseth, J.S. Høye, *Phys. Rev. E* **66**, 026119 (2002)
8. Bo E. Sernelius, *Graphene* **1**, 21 (2012)
9. Bo E. Sernelius, *J. Phys. Condens. Matter* **27**, 214017 (2015)
10. See (6.38) of [12]
11. H.B.G. Casimir, D. Polder, *Phys. Rev.* **73**, 360 (1948)
12. Bo E. Sernelius, *Surface Modes in Physics* (Wiley-VCH, Berlin, 2001)

# Chapter 15

## Dispersion Interaction in Cylindrical Structures



**Abstract** After a section in which we adapt the general formalism presented in Chap. 7 to cylindrical structures we start by introducing the basic structure elements: a single cylindrical interface, a thin diluted cylindrical gas film, and a 2D cylindrical film. A general cylindrical structure can then be constructed by stacking these elements coaxially. The thin gas layer is special; it is used to find the interaction on an atom at a general position in the cylindrical structure. Then we go through some common structures and present a limited number of illustrating examples; the examples involve gold cylinders, cylindrical graphene shells, and lithium atoms. The derivations are much more cumbersome in the cylindrical structure compared to in the planar and spherical cases.

### 15.1 Adapting the General Method of Chap. 7 to Cylindrical Structures

To find the normal modes for a layered cylinder including retardation effects we need to solve the wave equation for the electric and magnetic fields in all layers and use the proper boundary conditions at the interfaces. To solve the vector wave equation the vector Helmholtz equation, (7.22), is not a trivial task. One can instead solve the problem by introducing Hertz-Debye potentials  $\pi_1$  and  $\pi_2$ . They are solutions to the scalar wave equation, (7.23). We let  $\pi_1$  be the potential that generates TM modes and  $\pi_2$  be the potential that generates TE modes. In a cylindrical system the TM mode has its magnetic field perpendicular to the cylinder axis and the TE mode has its electric field perpendicular to the cylinder axis. Separation of variables,  $\pi = R(r) \Theta(\theta) Z(z)$ , leads to one differential equation for each of the variables,

$$\begin{aligned} r \frac{d}{dr} \left[ r \frac{dR(r)}{dr} \right] + \left[ (q^2 - h^2) r^2 - m^2 \right] R(r) &= 0; \\ \frac{d^2 \Theta(\theta)}{d\theta^2} + m^2 \Theta(\theta) &= 0; \\ \frac{d^2 Z(z)}{dz^2} + h^2 Z(z) &= 0. \end{aligned} \quad (15.1)$$

The variable  $h$  is the projection of the incoming momentum  $h$  on the cylinder axis and  $q = [\tilde{n}(\omega) \omega / c]$ . The general solution for the potentials is expressed in terms of

$$\pi_{i,m} = \left[ R_m \left( \sqrt{q^2 - h^2} r \right) \right] \left[ e^{im\theta} \right] \left[ e^{ihz} \right] \left[ e^{-i\omega t} \right], \quad (15.2)$$

$$m = 0, \pm 1, \pm 2 \dots$$

The radial part  $R(r)$  is a solution to the Bessel equation,

$$z^2 \frac{d^2 \omega}{dz^2} + z \frac{d\omega}{dz} + (z^2 - v^2) \omega = 0. \quad (15.3)$$

The Bessel equation has many different solutions:

- Bessel functions of the first kind:  $J_{\pm v}(z)$ .
- Bessel functions of the second kind:  $Y_v(z)$  (Weber's function, Neumann's function).
- Bessel functions of the third kind:  $H_v^{(1)}(z)$ ,  $H_v^{(2)}(z)$  (Hankel functions).

Each is a regular function of  $z$  throughout the complex  $z$ -plane cut along the negative real axis. They are related to each other according to

$$\begin{aligned} Y_v(z) &= [J_v(z) \cos(v\pi) - J_{-v}(z)] / \sin(v\pi); \\ H_v^{(1)}(z) &= J_v(z) + iY_v(z); \\ H_v^{(2)}(z) &= J_v(z) - iY_v(z). \end{aligned} \quad (15.4)$$

Let us study a layered cylinder of radius  $r_0$  consisting of  $N$  layers and an inner cylindrical core. We have  $N + 2$  media and  $N + 1$  interfaces. Let the numbering be as follows. Medium 0 is the medium surrounding the cylinder, medium 1 is the outermost layer, medium  $N$  the innermost layer, and  $N + 1$  the innermost cylindrical core. Let  $r_n$  be the inner radius of layer  $n$ . This is completely in line with the system represented by Fig. 7.1.

We will use the two Hankel versions since they represent waves that go in either the positive or negative  $r$ -directions. We assume a time dependence of the form  $e^{-i\omega t}$ . With this choice the first Hankel function,  $H_v^{(1)}(kr) e^{-i\omega t} \propto e^{i(kr - \omega t)}$ , represents a wave moving in the positive radial direction (toward the left in Fig. 7.1) while the second,  $H_v^{(2)}(kr) e^{-i\omega t} \propto e^{-i(kr + \omega t)}$ , represents a wave moving in the negative radial direction (toward the right in Fig. 7.1). Thus the general solution for the potentials is

$$\begin{aligned} \pi &= \sum_{m=0}^{\infty} [a_m H_m^{(2)}(kr) + b_m H_m^{(1)}(kr)] e^{im\theta} e^{ihz} e^{-i\omega t}; \\ k &= \sqrt{q^2 - h^2}. \end{aligned} \quad (15.5)$$

Let us now use the boundary conditions that the tangential components of  $\mathbf{E}$  and  $\tilde{\mathbf{H}}$  are continuous at the interface between layer  $n$  and  $n + 1$ . We get [1]

$$\begin{aligned} [(\partial/\partial r) \pi_1^n + (imh/q_n r) \pi_2^n]_{r=r_n} &= [(\partial/\partial r) \pi_1^{n+1} + (imh/q_{n+1} r) \pi_2^{n+1}]_{r=r_n}; \\ [(q_n^2 - h^2) \pi_1^n]_{r=r_n} &= [(q_{n+1}^2 - h^2) \pi_1^{n+1}]_{r=r_n}; \\ [q_n (\partial/\partial r) \pi_2^n - (imh/r) \pi_1^n]_{r=r_n} &= [q_{n+1} (\partial/\partial r) \pi_2^{n+1} - (imh/r) \pi_1^{n+1}]_{r=r_n}; \\ [[(q_n^2 - h^2)/q_n] \pi_2^n]_{r=r_n} &= [[(q_{n+1}^2 - h^2)/q_{n+1}] \pi_2^{n+1}]_{r=r_n}, \end{aligned} \quad (15.6)$$

where  $q_n = \tilde{n}_n(\omega)(\omega/c)$ .

This gives

$$\begin{aligned}
& a_{1,m}^n k_n H_m^{(2)'}(k_n r_n) + b_{1,m}^n k_n H_m^{(1)'}(k_n r_n) \\
& + a_{2,m}^n \left(\frac{imh}{q_n r_n}\right) H_m^{(2)}(k_n r_n) + b_{2,m}^n \left(\frac{imh}{q_n r_n}\right) H_m^{(1)}(k_n r_n) \\
& = a_{1,m}^{n+1} k_{n+1} H_m^{(2)'}(k_{n+1} r_n) + b_{1,m}^{n+1} k_{n+1} H_m^{(1)'}(k_{n+1} r_n) \\
& + a_{2,m}^{n+1} \left(\frac{imh}{q_{n+1} r_n}\right) H_m^{(2)}(k_{n+1} r_n) + b_{2,m}^{n+1} \left(\frac{imh}{q_{n+1} r_n}\right) H_m^{(1)}(k_{n+1} r_n); \\
& a_{1,m}^n k_n^2 H_m^{(2)}(k_n r_n) + b_{1,m}^n k_n^2 H_m^{(1)}(k_n r_n) \\
& = a_{1,m}^{n+1} k_{n+1}^2 H_m^{(2)}(k_{n+1} r_n) + b_{1,m}^{n+1} k_{n+1}^2 H_m^{(1)}(k_{n+1} r_n); \\
& -a_{1,m}^n \left(\frac{imh}{r_n}\right) H_m^{(2)}(k_n r_n) - b_{1,m}^n \left(\frac{imh}{r_n}\right) H_m^{(1)}(k_n r_n) \\
& + a_{2,m}^n q_n k_n H_m^{(2)'}(k_n r_n) + b_{2,m}^n q_n k_n H_m^{(1)'}(k_n r_n) \\
& = -a_{1,m}^{n+1} \left(\frac{imh}{r_n}\right) H_m^{(2)}(k_{n+1} r_n) - b_{1,m}^{n+1} \left(\frac{imh}{r_n}\right) H_m^{(1)}(k_{n+1} r_n) \\
& + a_{2,m}^{n+1} q_{n+1} k_{n+1} H_m^{(2)'}(k_{n+1} r_n) + b_{2,m}^{n+1} q_{n+1} k_{n+1} H_m^{(1)'}(k_{n+1} r_n); \\
& a_{2,m}^n \left(\frac{k_n^2}{q_n}\right) H_m^{(2)}(k_n r_n) + b_{2,m}^n \left(\frac{k_n^2}{q_n}\right) H_m^{(1)}(k_n r_n) \\
& = a_{2,m}^{n+1} \left(\frac{k_{n+1}^2}{q_{n+1}}\right) H_m^{(2)}(k_{n+1} r_n) + b_{2,m}^{n+1} \left(\frac{k_{n+1}^2}{q_{n+1}}\right) H_m^{(1)}(k_{n+1} r_n).
\end{aligned} \tag{15.7}$$

This may be arranged as

$$\tilde{\mathbf{A}}_n \begin{pmatrix} a_{1,m}^n \\ b_{1,m}^n \\ a_{2,m}^n \\ b_{2,m}^n \end{pmatrix} = \tilde{\mathbf{A}}_{n+1} \begin{pmatrix} a_{1,m}^{n+1} \\ b_{1,m}^{n+1} \\ a_{2,m}^{n+1} \\ b_{2,m}^{n+1} \end{pmatrix}, \tag{15.8}$$

and we may now identify the matrix

$$\tilde{\mathbf{A}}_n = \begin{pmatrix} k_n H_m^{(2)'} & k_n H_m^{(1)'} & \frac{imh}{q_n r_n} H_m^{(2)} & \frac{imh}{q_n r_n} H_m^{(1)} \\ k_n^2 H_m^{(2)} & k_n^2 H_m^{(1)} & 0 & 0 \\ -\frac{imh}{r_n} H_m^{(2)} & -\frac{imh}{r_n} H_m^{(1)} & q_n k_n H_m^{(2)'} & q_n k_n H_m^{(1)'} \\ 0 & 0 & \frac{k_n^2}{q_n} H_m^{(2)} & \frac{k_n^2}{q_n} H_m^{(1)} \end{pmatrix}, \tag{15.9}$$

where we have omitted the argument  $(k_n r_n)$  in all Hankel functions and their derivatives.

For the special case when  $h = 0$  we see that the matrices are on block form:

$$\tilde{\mathbf{A}}_n = \begin{pmatrix} k_n H_m^{(2)'} & k_n H_m^{(1)'} & 0 & 0 \\ k_n^2 H_m^{(2)} & k_n^2 H_m^{(1)} & 0 & 0 \\ 0 & 0 & q_n k_n H_m^{(2)'} & q_n k_n H_m^{(1)'} \\ 0 & 0 & \frac{k_n^2}{q_n} H_m^{(2)} & \frac{k_n^2}{q_n} H_m^{(1)} \end{pmatrix}, \tag{15.10}$$

which means that the TM and TE modes decouple for  $h = 0$ .<sup>1</sup>

Now, the resulting matrix  $\tilde{\mathbf{M}}_n = \tilde{\mathbf{A}}_n^{-1} \cdot \tilde{\mathbf{A}}_{n+1}$  becomes too large to write down in matrix form. Instead, we list each element:

$$\begin{aligned}
M_{11} &= \frac{1}{Wk_n^3} \left[ k_n^2 H_m^{(1)} k_{n+1} H_m^{(2)+'} - k_n H_m^{(1)'} k_{n+1}^2 H_m^{(2)+} \right]; \\
M_{12} &= \frac{1}{Wk_n^3} \left[ k_n^2 H_m^{(1)} k_{n+1} H_m^{(1)+'} - k_n H_m^{(1)'} k_{n+1}^2 H_m^{(1)+} \right]; \\
M_{13} &= \frac{1}{Wk_n^3} H_m^{(1)} H_m^{(2)+} (imh/q_{n+1}r_n) \left[ k_n^2 - k_{n+1}^2 \right]; \\
M_{14} &= \frac{1}{Wk_n^3} H_m^{(1)} H_m^{(1)+} (imh/q_{n+1}r_n) \left[ k_n^2 - k_{n+1}^2 \right]; \\
M_{21} &= \frac{1}{Wk_n^3} \left[ -k_n^2 H_m^{(2)} k_{n+1} H_m^{(2)+'} + k_n H_m^{(2)'} k_{n+1}^2 H_m^{(2)+} \right]; \\
M_{22} &= \frac{1}{Wk_n^3} \left[ -k_n^2 H_m^{(2)} k_{n+1} H_m^{(1)+'} + k_n H_m^{(2)'} k_{n+1}^2 H_m^{(1)+} \right]; \\
M_{23} &= \frac{1}{Wk_n^3} H_m^{(2)} H_m^{(2)+} (imh/q_{n+1}r_n) \left[ k_{n+1}^2 - k_n^2 \right]; \\
M_{24} &= \frac{1}{Wk_n^3} H_m^{(1)+} H_m^{(2)} (imh/q_{n+1}r_n) \left[ k_{n+1}^2 - k_n^2 \right]; \\
M_{31} &= \frac{1}{Wk_n^3} H_m^{(1)} H_m^{(2)+} (imh/q_n r_n) \left[ k_{n+1}^2 - k_n^2 \right]; \\
M_{32} &= \frac{1}{Wk_n^3} H_m^{(1)} H_m^{(1)+} (imh/q_n r_n) \left[ k_{n+1}^2 - k_n^2 \right]; \\
M_{33} &= \frac{1}{Wk_n^3} \left[ (k_n^2/q_n) H_m^{(1)} q_{n+1} k_{n+1} H_m^{(2)+'} - q_n k_n H_m^{(1)'} (k_{n+1}^2/q_{n+1}) H_m^{(2)+} \right]; \\
M_{34} &= \frac{1}{Wk_n^3} \left[ (k_n^2/q_n) H_m^{(1)} q_{n+1} k_{n+1} H_m^{(1)+'} - q_n k_n H_m^{(1)'} (k_{n+1}^2/q_{n+1}) H_m^{(1)+} \right]; \\
M_{41} &= \frac{1}{Wk_n^3} H_m^{(2)} H_m^{(2)+} (imh/q_n r_n) \left[ k_n^2 - k_{n+1}^2 \right]; \\
M_{42} &= \frac{1}{Wk_n^3} H_m^{(1)+} H_m^{(2)} (imh/q_n r_n) \left[ k_n^2 - k_{n+1}^2 \right]; \\
M_{43} &= \frac{1}{Wk_n^3} \left[ - (k_n^2/q_n) H_m^{(2)} q_{n+1} k_{n+1} H_m^{(2)+'} + q_n k_n H_m^{(2)'} (k_{n+1}^2/q_{n+1}) H_m^{(2)+} \right]; \\
M_{44} &= \frac{1}{Wk_n^3} \left[ - (k_n^2/q_n) H_m^{(2)} q_{n+1} k_{n+1} H_m^{(1)+'} + q_n k_n H_m^{(2)'} (k_{n+1}^2/q_{n+1}) H_m^{(1)+} \right].
\end{aligned} \tag{15.11}$$

We have suppressed all arguments of the Hankel functions and their derivatives. All functions with a + added as a superscript have the argument  $(k_{n+1}r_n)$  and the ones without the superscript have the argument  $(k_n r_n)$ .  $W$  is short for the Wronskian,  $W [H_m^{(1)}(x), H_m^{(2)}(x)] = H_m^{(1)}(x) H_m^{(2)'}(x) - H_m^{(1)'}(x) H_m^{(2)}(x) = -4i/\pi x$ . Now, we have all we need to determine the fully retarded normal modes in a layered cylindrical structure. We give some examples in the following sections.

### Summary of key relations for the derivation of dispersion interactions in cylindrical structures:

In a cylindrical structure  $h$ , the wave number along the cylinder axis, and  $m$  are the proper quantum numbers that characterize a normal mode. The dispersion curve for a mode can have several branches,  $i$ ,  $\omega = \omega_{h,m}^i$ . They are solutions to the condition for modes,  $f_{h,m}(\omega) = 0$ , where  $f_{h,m}(\omega)$  is the mode condition function. When finding the interaction energy of the system one has to sum over both  $h$ ,  $m$  and  $i$ . Since we often let the system have unlimited extension along the cylinder axis it is appropriate to calculate the interaction energy per unit length. For zero temperature the interaction energy is

<sup>1</sup>This also happens for  $m = 0$ .

$$E = \frac{\hbar}{2} \frac{1}{L} \sum_h \sum_{m=-\infty}^{\infty} \int_{-\infty}^{\infty} \frac{d\xi}{2\pi} \ln f_{h,m}(i\xi) \rightarrow \frac{\hbar}{2} \int_{-\infty}^{\infty} \frac{dh}{2\pi} \sum_{m=-\infty}^{\infty} \int_{-\infty}^{\infty} \frac{d\xi}{2\pi} \ln f_{h,m}(i\xi), \quad (15.12)$$

and at finite temperature

$$\mathfrak{F} = \frac{1}{L} \sum_h \sum_{m=-\infty}^{\infty} \frac{1}{\beta} \sum_{n=0}^{\infty} \ln f_{h,m}(i\xi_n) \rightarrow \int_{-\infty}^{\infty} \frac{dh}{2\pi} \sum_{m=-\infty}^{\infty} \frac{1}{\beta} \sum_{n=0}^{\infty} \ln f_{h,m}(i\xi_n), \quad (15.13)$$

where  $L$  is the length of the system and  $\xi_n = 2\pi n/\hbar\beta$ . The arrows indicate what happens when we let  $L$  go toward infinity. In the fully retarded treatment

$$f_{h,m} \equiv \begin{vmatrix} (M_{11} + M_{12}) & (M_{13} + M_{14}) \\ (M_{31} + M_{32}) & (M_{33} + M_{34}) \end{vmatrix}, \quad (15.14)$$

where  $\tilde{\mathbf{M}}$  is the matrix for the whole structure. The matrix for interface  $n$  is a  $4 \times 4$  matrix where the elements contain the two Hankel functions and their derivatives. The matrix is too spacious to be written down here. The Wronskian for the two functions is

$$W[H_m^{(1)}(x), H_m^{(2)}(x)] = H_m^{(1)}(x) H_m^{(2)'}(x) - H_m^{(1)'}(x) H_m^{(2)}(x) = -4i/\pi x. \quad (15.15)$$

The relation between the Bessel function of the first kind,  $J_m$ , and the Hankel functions,  $H_m^{(n)}$ , is

$$2J_m(z) = H_m^{(1)}(z) + H_m^{(2)}(z) \quad (15.16)$$

## 15.2 Basic Structure Elements

A general cylindrical structure can be generated by stacking a number of basic structure elements coaxially around each other. The most basic element is a solid cylinder. Sometimes it is convenient to use layers as elements. A special layer is a 2D cylindrical film. Another is a thin cylindrical diluted gas layer which can be used in the derivation of the interaction between atoms and the cylindrical structure. We start with the solid cylinder.

### 15.2.1 Solid Cylinder

For a solid cylinder of radius  $a$  and dielectric function  $\tilde{\epsilon}_1(\omega)$  in an ambient of dielectric function  $\tilde{\epsilon}_0(\omega)$ , as illustrated in Fig. 14.1, we have  $\tilde{\mathbf{M}} = \tilde{\mathbf{M}}_0$ , and the type of combinations of matrix elements that appear in the mode condition are:

$$\begin{aligned}
 M_{11} + M_{12} &= \frac{2}{Wk_0^3} [k_0^2 H_m^{(1)} k_1 J_m' - k_0 H_m^{(1)'} k_1^2 J_m]; \\
 M_{13} + M_{14} &= \frac{2}{Wk_0^3} H_m^{(1)} J_m (imh/q_1 a) [k_0^2 - k_1^2]; \\
 M_{21} + M_{22} &= \frac{2}{Wk_0^3} [-k_0^2 H_m^{(2)} k_1 J_m' + k_0 H_m^{(2)'} k_1^2 J_m]; \\
 M_{23} + M_{24} &= \frac{2}{Wk_0^3} H_m^{(2)} J_m (imh/q_1 a) [k_1^2 - k_0^2]; \\
 M_{31} + M_{32} &= \frac{2}{Wk_0^3} H_m^{(1)} J_m (imh/q_0 a) [k_1^2 - k_0^2]; \\
 M_{33} + M_{34} &= \frac{2}{Wk_0^3} [(k_0^2/q_0) H_m^{(1)} q_1 k_1 J_m' - q_0 k_0 H_m^{(1)'} (k_1^2/q_1) J_m]; \\
 M_{41} + M_{42} &= \frac{2}{Wk_0^3} H_m^{(2)} J_m (imh/q_0 a) [k_0^2 - k_1^2]; \\
 M_{43} + M_{44} &= \frac{2}{Wk_0^3} [-(k_0^2/q_0) H_m^{(2)} q_1 k_1 J_m' + q_0 k_0 H_m^{(2)'} (k_1^2/q_1) J_m],
 \end{aligned} \tag{15.17}$$

where we have used the relation  $2J_m(z) = H_m^{(1)}(z) + H_m^{(2)}(z)$ . We have suppressed all arguments of the functions. The suppressed arguments are  $(k_0 a)$  for the  $H$ -functions and their derivatives and  $(k_1 a)$  for the  $J$ -functions and their derivatives.

The condition for modes is according to (7.15)  $(M_{11} + M_{12})(M_{33} + M_{34}) = (M_{13} + M_{14})(M_{31} + M_{32})$ , which leads to

$$\left( \frac{1}{k_1} \frac{J_m'(k_1 a)}{J_m(k_1 a)} - \frac{1}{k_0} \frac{H_m^{(1)'}(k_0 a)}{H_m^{(1)}(k_0 a)} \right) \left( \frac{q_1^2}{k_1} \frac{J_m'(k_1 a)}{J_m(k_1 a)} - \frac{q_0^2}{k_0} \frac{H_m^{(1)'}(k_0 a)}{H_m^{(1)}(k_0 a)} \right) = (mh/a)^2 \left( \frac{1}{k_1^2} - \frac{1}{k_0^2} \right)^2. \tag{15.18}$$

This is in complete agreement with Ruppin in (107) on page 389 in [2]. When either  $m$  or  $h$  or both are zero the TM and TE modes decouple. If they are decoupled letting the first factor on the left-hand side be equal to zero defines the TE modes and letting the second factor be equal to zero defines the TM modes.

Next we move on to a thin diluted gas film.

### 15.2.2 Thin Cylindrical Diluted Gas Film

Here we proceed in the same way as in Sect. 11.2.3 but the matrices are now much more involved. Here both  $\alpha$  and  $\delta$  appear in the arguments of the functions. In the non-retarded case only  $\delta$  did. We first expand the matrix for the gas layer in  $\alpha$  and keep terms up to linear in  $\alpha$ . We have

$$\begin{aligned}
 \tilde{\mathbf{M}}_{\text{gaslayer}} &= \tilde{\mathbf{M}}_0 \cdot \tilde{\mathbf{M}}_1; \\
 \tilde{\mathbf{M}}_0 &\approx \tilde{\mathbf{I}} + \alpha \tilde{\mathbf{M}}_0^1; \quad \tilde{\mathbf{M}}_1 \approx \tilde{\mathbf{I}} + \alpha \tilde{\mathbf{M}}_1^1; \\
 \tilde{\mathbf{M}}_{\text{gaslayer}} &\approx \tilde{\mathbf{I}} + \alpha \left( \tilde{\mathbf{M}}_0^1 + \tilde{\mathbf{M}}_1^1 \right).
 \end{aligned} \tag{15.19}$$

The elements of  $\tilde{\mathbf{M}}_0^1$  are in the first row

$$\begin{aligned}
 M_{11} &= \frac{i\pi k_0(b+\delta)}{8} \left(\frac{q_0}{k_0}\right)^2 \left[ H_m^{(1)} H_m^{(2)'} - 2H_m^{(1)'} H_m^{(2)} \right. \\
 &\quad \left. + k_0(b+\delta) (H_m^{(1)} H_m^{(2)''} - H_m^{(1)'} H_m^{(2)'}) \right]; \\
 M_{12} &= \frac{i\pi k_0(b+\delta)}{8} \left(\frac{q_0}{k_0}\right)^2 \left[ -H_m^{(1)'} H_m^{(1)} \right. \\
 &\quad \left. + k_0(b+\delta) (H_m^{(1)} H_m^{(1)''} - H_m^{(1)'} H_m^{(1)'}) \right]; \\
 M_{13} &= \frac{m\pi}{4} H_m^{(1)} H_m^{(2)} \frac{h}{k_0} \left(\frac{q_0}{k_0}\right); \\
 M_{14} &= \frac{m\pi}{4} H_m^{(1)} H_m^{(1)} \frac{h}{k_0} \left(\frac{q_0}{k_0}\right),
 \end{aligned} \tag{15.20}$$

in the second row

$$\begin{aligned}
 M_{21} &= \frac{i\pi k_0(b+\delta)}{8} \left(\frac{q_0}{k_0}\right)^2 \left[ H_m^{(2)'} H_m^{(2)} \right. \\
 &\quad \left. - k_0(b+\delta) (H_m^{(2)} H_m^{(2)''} - H_m^{(2)'} H_m^{(2)'}) \right]; \\
 M_{22} &= \frac{i\pi k_0(b+\delta)}{8} \left(\frac{q_0}{k_0}\right)^2 \left[ -H_m^{(2)} H_m^{(1)'} + 2H_m^{(2)'} H_m^{(1)} \right. \\
 &\quad \left. - k_0(b+\delta) (H_m^{(2)} H_m^{(1)''} - H_m^{(2)'} H_m^{(1)'}) \right]; \\
 M_{23} &= -\frac{m\pi}{4} H_m^{(2)} H_m^{(2)} \frac{h}{k_0} \left(\frac{q_0}{k_0}\right); \\
 M_{24} &= -\frac{m\pi}{4} H_m^{(1)} H_m^{(2)} \frac{h}{k_0} \left(\frac{q_0}{k_0}\right),
 \end{aligned} \tag{15.21}$$

in the third row

$$\begin{aligned}
 M_{31} &= -\frac{m\pi}{4} H_m^{(1)} H_m^{(2)} \frac{h}{k_0} \left(\frac{q_0}{k_0}\right); \\
 M_{32} &= -\frac{m\pi}{4} H_m^{(1)} H_m^{(1)} \frac{h}{k_0} \left(\frac{q_0}{k_0}\right); \\
 M_{33} &= \frac{i\pi k_0(b+\delta)}{8} \left\{ H_m^{(1)} H_m^{(2)'} + H_m^{(1)'} H_m^{(2)} \right. \\
 &\quad \left. + \left(\frac{q_0}{k_0}\right)^2 \left[ H_m^{(1)} H_m^{(2)'} - 2H_m^{(1)'} H_m^{(2)} \right. \right. \\
 &\quad \left. \left. + k_0(b+\delta) (H_m^{(1)} H_m^{(2)''} - H_m^{(1)'} H_m^{(2)'}) \right] \right\}; \\
 M_{34} &= \frac{i\pi k_0(b+\delta)}{8} \left[ 2H_m^{(1)} H_m^{(1)'} + \left(\frac{q_0}{k_0}\right)^2 \times \right. \\
 &\quad \left. (-H_m^{(1)} H_m^{(1)'} + k_0(b+\delta) (H_m^{(1)} H_m^{(1)''} - H_m^{(1)'} H_m^{(1)'}) \right],
 \end{aligned} \tag{15.22}$$

and in the fourth row

$$\begin{aligned}
 M_{41} &= \frac{m\pi}{4} H_m^{(2)} H_m^{(2)} \frac{h}{k_0} \left(\frac{q_0}{k_0}\right); \\
 M_{42} &= \frac{m\pi}{4} H_m^{(1)} H_m^{(2)} \frac{h}{k_0} \left(\frac{q_0}{k_0}\right); \\
 M_{43} &= -\frac{i\pi k_0(b+\delta)}{8} \left\{ 2H_m^{(2)} H_m^{(2)'} - (\omega/c k_0)^2 \times \right. \\
 &\quad \left. [H_m^{(2)} H_m^{(2)'} + k_0(b+\delta) (H_m^{(2)} H_m^{(2)''} - H_m^{(2)'} H_m^{(2)'})] \right\}; \\
 M_{44} &= -\frac{i\pi k_0(b+\delta)}{8} \left\{ H_m^{(2)} H_m^{(1)'} + H_m^{(2)'} H_m^{(1)} \right. \\
 &\quad \left. + \left(\frac{q_0}{k_0}\right)^2 \left[ H_m^{(2)} H_m^{(1)'} - 2H_m^{(2)'} H_m^{(1)} \right. \right. \\
 &\quad \left. \left. + k_0(b+\delta) (H_m^{(2)} H_m^{(1)''} - H_m^{(2)'} H_m^{(1)'}) \right] \right\}.
 \end{aligned} \tag{15.23}$$

The suppressed arguments are in all elements  $k_0(b + \delta)$ . The elements of  $\tilde{\mathbf{M}}_1^1$  are in the first row

$$\begin{aligned}
 M_{11} &= \frac{i\pi k_0 b}{8} \left(\frac{q_0}{k_0}\right)^2 \left[ H_m^{(1)'} H_m^{(2)} + (k_0 b) (H_m^{(1)'} H_m^{(2)'} - H_m^{(1)''} H_m^{(2)}) \right]; \\
 M_{12} &= \frac{i\pi k_0 b}{8} \left(\frac{q_0}{k_0}\right)^2 \left[ H_m^{(1)} H_m^{(1)'} + (k_0 b) (H_m^{(1)'} H_m^{(1)'} - H_m^{(1)} H_m^{(1)''}) \right]; \\
 M_{13} &= -\frac{m\pi}{4} H_m^{(1)} H_m^{(2)} \frac{h}{k_0} \left(\frac{q_0}{k_0}\right); \\
 M_{14} &= -\frac{m\pi}{4} H_m^{(1)} H_m^{(1)} \frac{h}{k_0} \left(\frac{q_0}{k_0}\right),
 \end{aligned} \tag{15.24}$$

in the second row

$$\begin{aligned}
 M_{21} &= -\frac{i\pi k_0 b}{8} \left(\frac{q_0}{k_0}\right)^2 \left[ H_m^{(2)} H_m^{(2)'} + (k_0 b) (H_m^{(2)'} H_m^{(2)'} - H_m^{(2)} H_m^{(2)''}) \right]; \\
 M_{22} &= -\frac{i\pi k_0 b}{8} \left(\frac{q_0}{k_0}\right)^2 \left[ H_m^{(1)} H_m^{(2)'} + (k_0 b) (H_m^{(1)'} H_m^{(2)'} - H_m^{(1)} H_m^{(2)''}) \right]; \\
 M_{23} &= \frac{m\pi}{4} H_m^{(2)} H_m^{(2)} \frac{h}{k_0} \left(\frac{q_0}{k_0}\right); \\
 M_{24} &= \frac{m\pi}{4} H_m^{(1)} H_m^{(2)} \frac{h}{k_0} \left(\frac{q_0}{k_0}\right),
 \end{aligned} \tag{15.25}$$

in the third row

$$\begin{aligned}
 M_{31} &= \frac{m\pi}{4} H_m^{(1)} H_m^{(2)} \frac{h}{k_0} \left(\frac{q_0}{k_0}\right); \\
 M_{32} &= \frac{m\pi}{4} H_m^{(1)} H_m^{(1)} \frac{h}{k_0} \left(\frac{q_0}{k_0}\right); \\
 M_{33} &= \frac{i\pi k_0 b}{8} \left\{ -H_m^{(1)} H_m^{(2)'} - H_m^{(1)'} H_m^{(2)} \right. \\
 &\quad \left. + \left(\frac{q_0}{k_0}\right)^2 \left[ H_m^{(1)'} H_m^{(2)} + (k_0 b) (H_m^{(1)'} H_m^{(2)'} - H_m^{(1)''} H_m^{(2)}) \right] \right\}; \\
 M_{34} &= \frac{i\pi k_0 b}{8} \left\{ -H_m^{(1)} H_m^{(1)'} - H_m^{(1)'} H_m^{(1)} \right. \\
 &\quad \left. + \left(\frac{q_0}{k_0}\right)^2 \left[ H_m^{(1)'} H_m^{(1)} + (k_0 b) (H_m^{(1)'} H_m^{(1)'} - H_m^{(1)''} H_m^{(1)}) \right] \right\},
 \end{aligned} \tag{15.26}$$

and in the fourth row

$$\begin{aligned}
 M_{41} &= -\frac{m\pi}{4} H_m^{(2)} H_m^{(2)} \frac{h}{k_0} \left(\frac{q_0}{k_0}\right); \\
 M_{42} &= -\frac{m\pi}{4} H_m^{(1)} H_m^{(2)} \frac{h}{k_0} \left(\frac{q_0}{k_0}\right); \\
 M_{43} &= \frac{i\pi k_0 b}{8} \left\{ H_m^{(1)} H_m^{(1)'} + H_m^{(1)'} H_m^{(1)} \right. \\
 &\quad \left. - \left(\frac{q_0}{k_0}\right)^2 \left[ H_m^{(2)'} H_m^{(2)} + (k_0 b) (H_m^{(2)'} H_m^{(2)'} - H_m^{(2)''} H_m^{(2)}) \right] \right\}; \\
 M_{44} &= \frac{i\pi k_0 b}{8} \left\{ H_m^{(1)'} H_m^{(2)} + H_m^{(1)} H_m^{(2)'} \right. \\
 &\quad \left. - \left(\frac{q_0}{k_0}\right)^2 \left[ H_m^{(1)} H_m^{(2)'} + (k_0 b) (H_m^{(1)'} H_m^{(2)'} - H_m^{(1)} H_m^{(2)''}) \right] \right\}.
 \end{aligned} \tag{15.27}$$

The suppressed arguments are in all elements  $(k_0 b)$ . Next we expand  $\tilde{\mathbf{M}}_{\text{gaslayer}}$  from (15.19) in  $\delta$  up to and including the linear term. We note that the zeroth order term of  $\tilde{\mathbf{M}}_0^1$  exactly cancels  $\tilde{\mathbf{M}}_1^1$ . Thus

$$\tilde{\mathbf{M}}_{\text{gaslayer}} \approx \tilde{\mathbf{I}} + \alpha \delta \left[ \frac{\partial \tilde{\mathbf{M}}_0^1}{\partial \delta} \right]_{\delta=0} = \tilde{\mathbf{I}} + \alpha \delta \tilde{\mathbf{B}}. \quad (15.28)$$

The elements of the introduced matrix  $\tilde{\mathbf{B}}$  are in the first row

$$\begin{aligned} B_{11} &= \frac{i\pi k_0}{8} \left( \frac{q_0}{k_0} \right)^2 \left\{ H_m^{(1)} H_m^{(2)'} - 2H_m^{(1)'} H_m^{(2)} \right. \\ &\quad \left. + (k_0 b) \left( 3H_m^{(1)} H_m^{(2)''} - 3H_m^{(1)'} H_m^{(2)'} - 2H_m^{(1)''} H_m^{(2)} \right) \right. \\ &\quad \left. + (k_0 b)^2 \left( -H_m^{(1)''} H_m^{(2)'} + H_m^{(1)} H_m^{(2)'''} \right) \right\}; \\ B_{12} &= \frac{i\pi k_0}{8} \left( \frac{q_0}{k_0} \right)^2 \left[ -H_m^{(1)'} H_m^{(1)} \right. \\ &\quad \left. + (k_0 b) \left( H_m^{(1)} H_m^{(1)''} - 3H_m^{(1)'} H_m^{(1)'} \right) \right. \\ &\quad \left. + (k_0 b)^2 \left( -H_m^{(1)'} H_m^{(1)''} + H_m^{(1)} H_m^{(1)'''} \right) \right]; \\ B_{13} &= \frac{m\pi k_0}{4} \left[ H_m^{(1)'} H_m^{(2)} + H_m^{(1)} H_m^{(2)'} \right] \frac{h}{k_0} \left( \frac{q_0}{k_0} \right); \end{aligned} \quad (15.29)$$

in the second row

$$\begin{aligned} B_{21} &= \frac{i\pi k_0}{8} \left( \frac{q_0}{k_0} \right)^2 \left[ H_m^{(2)} H_m^{(2)'} \right. \\ &\quad \left. - (k_0 b) \left( H_m^{(2)} H_m^{(2)''} - 3H_m^{(2)'} H_m^{(2)'} \right) \right. \\ &\quad \left. - (k_0 b)^2 \left( -H_m^{(2)'} H_m^{(2)''} + H_m^{(2)} H_m^{(2)'''} \right) \right]; \\ B_{22} &= -\frac{i\pi k_0}{8} \left( \frac{q_0}{k_0} \right)^2 \left\{ H_m^{(2)} H_m^{(1)'} - 2H_m^{(2)'} H_m^{(1)} \right. \\ &\quad \left. + (k_0 b) \left( 3H_m^{(2)} H_m^{(1)''} - 3H_m^{(2)'} H_m^{(1)'} - 2H_m^{(2)''} H_m^{(1)} \right) \right. \\ &\quad \left. + (k_0 b)^2 \left( -H_m^{(2)''} H_m^{(1)'} + H_m^{(2)} H_m^{(1)'''} \right) \right\}; \\ B_{23} &= -\frac{m\pi k_0}{4} \left[ 2H_m^{(2)} H_m^{(2)'} \right] \frac{h}{k_0} \left( \frac{q_0}{k_0} \right); \\ B_{24} &= -\frac{m\pi k_0}{4} \left[ H_m^{(1)'} H_m^{(2)} + H_m^{(1)} H_m^{(2)'} \right] \frac{h}{k_0} \left( \frac{q_0}{k_0} \right), \end{aligned} \quad (15.30)$$

in the third row

$$\begin{aligned} B_{31} &= -\frac{m\pi k_0}{4} \left[ H_m^{(1)'} H_m^{(2)} + H_m^{(1)} H_m^{(2)'} \right] \frac{h}{k_0} \left( \frac{q_0}{k_0} \right); \\ B_{32} &= -\frac{m\pi k_0}{4} \left[ 2H_m^{(1)} H_m^{(1)'} \right] \frac{h}{k_0} \left( \frac{q_0}{k_0} \right); \\ B_{33} &= \frac{i\pi k_0}{8} \left[ H_m^{(1)} H_m^{(2)'} + H_m^{(1)'} H_m^{(2)} \right. \\ &\quad \left. + (k_0 b) \left( H_m^{(1)} H_m^{(2)'} + 2H_m^{(1)'} H_m^{(2)'} + H_m^{(1)''} H_m^{(2)} \right) \right. \\ &\quad \left. + \frac{i\pi (k_0)}{8} \left( \frac{q_0}{k_0} \right)^2 \left[ H_m^{(1)} H_m^{(2)'} - 2H_m^{(1)'} H_m^{(2)} \right. \right. \\ &\quad \left. \left. + (k_0 b) \left( 3H_m^{(1)} H_m^{(2)''} - 2H_m^{(1)''} H_m^{(2)} - 3H_m^{(1)'} H_m^{(2)'} \right) \right. \right. \\ &\quad \left. \left. + (k_0 b)^2 \left( -H_m^{(1)''} H_m^{(2)'} + H_m^{(1)} H_m^{(2)'''} \right) \right] \right]; \\ B_{34} &= \frac{i\pi k_0}{8} \left[ 2H_m^{(1)} H_m^{(1)'} \right. \\ &\quad \left. + (k_0 b) \left( 2H_m^{(1)'} H_m^{(1)'} + 2H_m^{(1)} H_m^{(1)''} \right) \right. \\ &\quad \left. + \frac{i\pi (k_0)}{8} \left( \frac{q_0}{k_0} \right)^2 \left[ -H_m^{(1)} H_m^{(1)'} \right. \right. \\ &\quad \left. \left. + (k_0 b) \left( H_m^{(1)} H_m^{(1)''} - 3H_m^{(1)'} H_m^{(1)'} \right) \right. \right. \\ &\quad \left. \left. + (k_0 b)^2 \left( -H_m^{(1)'} H_m^{(1)''} + H_m^{(1)} H_m^{(1)'''} \right) \right] \right], \end{aligned} \quad (15.31)$$

and in the fourth row

$$\begin{aligned}
B_{41} &= \frac{m\pi k_0}{4} \left[ 2H_m^{(2)} H_m^{(2)'} \right] \frac{h}{k_0} \left( \frac{q_0}{k_0} \right); \\
B_{42} &= \frac{m\pi k_0}{4} \left[ H_m^{(1)'} H_m^{(2)} + H_m^{(1)} H_m^{(2)'} \right] \frac{h}{k_0} \left( \frac{q_0}{k_0} \right); \\
B_{43} &= \frac{-i\pi k_0}{8} \left[ 2H_m^{(2)} H_m^{(2)'} \right. \\
&\quad \left. + (k_0 b) \left( 2H_m^{(2)'} H_m^{(2)'} + 2H_m^{(2)} H_m^{(2)''} \right) \right. \\
&\quad \left. + \frac{-i\pi(k_0)}{8} \left( \frac{q_0}{k_0} \right)^2 \left[ -H_m^{(2)} H_m^{(2)'} \right. \right. \\
&\quad \left. \left. + (k_0 b) \left( H_m^{(2)} H_m^{(2)'} - 3H_m^{(2)'} H_m^{(2)'} \right) \right. \right. \\
&\quad \left. \left. + (k_0 b)^2 \left( -H_m^{(2)'} H_m^{(2)''} + H_m^{(2)} H_m^{(2)'''} \right) \right] \right]; \\
B_{44} &= -\frac{i\pi k_0}{8} \left[ H_m^{(2)} H_m^{(1)'} + H_m^{(2)'} H_m^{(1)} \right. \\
&\quad \left. + (k_0 b) \left( H_m^{(2)} H_m^{(1)''} + 2H_m^{(2)'} H_m^{(1)'} + H_m^{(2)''} H_m^{(1)} \right) \right. \\
&\quad \left. - \frac{i\pi(k_0)}{8} \left( \frac{q_0}{k_0} \right)^2 \left[ H_m^{(2)} H_m^{(1)'} - 2H_m^{(2)'} H_m^{(1)} \right. \right. \\
&\quad \left. \left. + (k_0 b) \left( 3H_m^{(2)} H_m^{(1)''} - 2H_m^{(2)''} H_m^{(1)} - 3H_m^{(2)'} H_m^{(1)'} \right) \right. \right. \\
&\quad \left. \left. + (k_0 b)^2 \left( -H_m^{(2)''} H_m^{(1)'} + H_m^{(2)} H_m^{(1)'''} \right) \right] \right].
\end{aligned} \tag{15.32}$$

The suppressed arguments are in all elements  $k_0 b = k_0(a + d)$ . Now we have derived the matrix for a thin diluted cylindrical gas shell. The next element is a 2D cylindrical film.

### 15.2.3 2D Cylindrical Film

In many situations one is dealing with very thin films. These may be considered 2D. Important examples are a graphene sheet and a 2D electron gas. In the derivation we let the film have finite thickness  $\delta$  and be characterized by a 3D dielectric function  $\tilde{\epsilon}^{3D}$ . We then let the thickness go toward zero. The 3D dielectric function depends on  $\delta$  as  $\tilde{\epsilon}^{3D} \sim 1/\delta$  for small  $\delta$ . In the planar structure we could, in the limit when  $\delta$  goes toward zero, obtain a momentum dependent 2D dielectric function. Here we only keep the long wave length limit of the 2D dielectric function [2, 3]. Here, the matrices are much more complicated than in Sect. 11.2.4 so we cannot give an as elegant derivation. We let the layer have radius  $r$  and thickness  $\delta$ , which we let go toward zero.

The matrix is  $\tilde{\mathbf{M}}^{2D} = \tilde{\mathbf{M}}_0 \cdot \tilde{\mathbf{M}}_1$ . We let  $\tilde{\mathbf{M}}_0$  be at  $r + \delta$  and  $\tilde{\mathbf{M}}_1$  be at  $r$ . We could equally well have let  $\tilde{\mathbf{M}}_0$  be at  $r$  and  $\tilde{\mathbf{M}}_1$  be at  $r - \delta$ . We expand the matrix in  $\delta$  and keep in mind that  $\tilde{\epsilon}^{3D}$  goes toward infinity when  $\delta$  goes toward zero in such a way that  $\delta \tilde{\epsilon}^{3D}$  stays finite. The derivation is rather tedious since  $\tilde{\epsilon}^{3D}$  appears in many places in both matrices. One further complication is that it appears also in the function arguments. After much work we arrive at the following matrix elements:

$$\begin{aligned}
M_{11} &= 1 - \frac{i\pi r}{4} q_0^2 \delta \tilde{\varepsilon}^{3D} H_m^{(1)'} [k_0 r] H_m^{(2)'} [k_0 r], \\
M_{12} &= -\frac{i\pi r}{4} q_0^2 \delta \tilde{\varepsilon}^{3D} H_m^{(1)'} [k_0 r] H_m^{(1)'} [k_0 r], \\
M_{13} &= \frac{\pi m h}{4} \frac{q_0}{k_0} \delta \tilde{\varepsilon}^{3D} H_m^{(1)'} [k_0 r] H_m^{(2)} [k_0 r], \\
M_{14} &= \frac{\pi m h}{4} \frac{q_0}{k_0} \delta \tilde{\varepsilon}^{3D} H_m^{(1)} [k_0 r] H_m^{(1)'} [k_0 r], \\
M_{21} &= \frac{i\pi r}{4} q_0^2 \delta \tilde{\varepsilon}^{3D} H_m^{(2)'} [k_0 r] H_m^{(2)'} [k_0 r], \\
M_{22} &= 1 + \frac{i\pi r}{4} q_0^2 \delta \tilde{\varepsilon}^{3D} H_m^{(1)'} [k_0 r] H_m^{(2)'} [k_0 r], \\
M_{23} &= -\frac{\pi m h}{4} \frac{q_0}{k_0} \delta \tilde{\varepsilon}^{3D} H_m^{(2)} [k_0 r] H_m^{(2)'} [k_0 r], \\
M_{24} &= -\frac{\pi m h}{4} \frac{q_0}{k_0} \delta \tilde{\varepsilon}^{3D} H_m^{(1)} [k_0 r] H_m^{(2)'} [k_0 r], \\
M_{31} &= -\frac{\pi m h}{4} \frac{q_0}{k_0} \delta \tilde{\varepsilon}^{3D} H_m^{(1)} [k_0 r] H_m^{(2)'} [k_0 r], \\
M_{32} &= -\frac{\pi m h}{4} \frac{q_0}{k_0} \delta \tilde{\varepsilon}^{3D} H_m^{(1)} [k_0 r] H_m^{(1)'} [k_0 r], \\
M_{33} &= 1 - i \left[ \frac{\pi (mh)^2}{4} \frac{1}{k_0^2 r} + \frac{\pi}{4} k_0^2 r \right] \delta \tilde{\varepsilon}^{3D} H_m^{(1)} [k_0 r] H_m^{(2)} [k_0 r], \\
M_{34} &= -i \left[ \frac{\pi (mh)^2}{4} \frac{1}{k_0^2 r} + \frac{\pi}{4} k_0^2 r \right] \delta \tilde{\varepsilon}^{3D} H_m^{(1)} [k_0 r] H_m^{(1)} [k_0 r], \\
M_{41} &= \frac{\pi m h}{4} \frac{q_0}{k_0} \delta \tilde{\varepsilon}^{3D} H_m^{(2)} [k_0 r] H_m^{(2)'} [k_0 r], \\
M_{42} &= \frac{\pi m h}{4} \frac{q_0}{k_0} \delta \tilde{\varepsilon}^{3D} H_m^{(1)'} [k_0 r] H_m^{(2)} [k_0 r], \\
M_{43} &= i \left[ \frac{\pi (mh)^2}{4} \frac{1}{k_0^2 r} + \frac{\pi}{4} k_0^2 r \right] \delta \tilde{\varepsilon}^{3D} H_m^{(2)} [k_0 r] H_m^{(2)} [k_0 r], \\
M_{44} &= 1 + i \left[ \frac{\pi (mh)^2}{4} \frac{1}{k_0^2 r} + \frac{\pi}{4} k_0^2 r \right] \delta \tilde{\varepsilon}^{3D} H_m^{(1)} [k_0 r] H_m^{(2)} [k_0 r].
\end{aligned} \tag{15.33}$$

To arrive at this result we have made use of (15.15) in all elements and (15.3) in some. We will need the following element pairs:

$$\begin{aligned}
M_{11} + M_{12} &= 1 - \frac{i\pi r}{2} q_0^2 \delta \tilde{\varepsilon}^{3D} H_m^{(1)'} [k_0 r] J_m' [k_0 r], \\
M_{13} + M_{14} &= \frac{\pi m h}{2} \frac{q_0}{k_0} \delta \tilde{\varepsilon}^{3D} H_m^{(1)'} [k_0 r] J_m [k_0 r], \\
M_{21} + M_{22} &= 1 + \frac{i\pi r}{2} q_0^2 \delta \tilde{\varepsilon}^{3D} H_m^{(2)'} [k_0 r] J_m' [k_0 r], \\
M_{23} + M_{24} &= -\frac{\pi m h}{2} \frac{q_0}{k_0} \delta \tilde{\varepsilon}^{3D} H_m^{(2)'} [k_0 r] J_m [k_0 r], \\
M_{31} + M_{32} &= -\frac{\pi m h}{2} \frac{q_0}{k_0} \delta \tilde{\varepsilon}^{3D} H_m^{(1)} [k_0 r] J_m' [k_0 r], \\
M_{33} + M_{34} &= 1 - i \frac{\pi}{2} \left[ (mh)^2 + k_0^2 r \right] \delta \tilde{\varepsilon}^{3D} H_m^{(1)} [k_0 r] J_m [k_0 r], \\
M_{41} + M_{42} &= \frac{\pi m h}{2} \frac{q_0}{k_0} \delta \tilde{\varepsilon}^{3D} H_m^{(2)} [k_0 r] J_m' [k_0 r], \\
M_{43} + M_{44} &= 1 + i \frac{\pi}{2} \left[ (mh)^2 \frac{1}{k_0^2 r} + k_0^2 r \right] \delta \tilde{\varepsilon}^{3D} H_m^{(2)} [k_0 r] J_m [k_0 r],
\end{aligned} \tag{15.34}$$

where we have made use of (15.16). Now we are done with the basic structure elements and turn to the list of common structures. We start with an atom outside a cylinder.

### 15.3 Force on an Atom Outside a Cylinder

The geometry of this problem is illustrated in Fig. 14.3. We have  $\tilde{\mathbf{M}} = \tilde{\mathbf{M}}_0 \cdot \tilde{\mathbf{M}}_1 \cdot \tilde{\mathbf{M}}_2 = \tilde{\mathbf{M}}_{\text{gaslayer}} \cdot \tilde{\mathbf{M}}_2$ . In (15.28) we found the matrix for  $\tilde{\mathbf{M}}_{\text{gaslayer}}$ . We introduce some short-hand notation. Let

$$\begin{aligned}\tilde{\mathbf{A}} &= \tilde{\mathbf{M}}_2; \\ \tilde{\mathbf{C}} &= \tilde{\mathbf{B}} \cdot \tilde{\mathbf{A}} = \left[ \frac{\partial \tilde{\mathbf{M}}_0}{\partial \delta} \right]_{\delta=0} \cdot \tilde{\mathbf{A}}; \\ \tilde{\mathbf{M}} &\approx \tilde{\mathbf{A}} + \delta \alpha \tilde{\mathbf{C}}.\end{aligned}\quad (15.35)$$

Expressed in terms of the elements of these matrices the condition for modes becomes

$$\begin{aligned}[(A_{11} + A_{12}) + \delta \alpha (C_{11} + C_{12})][(A_{33} + A_{34}) + \delta \alpha (C_{33} + C_{34})] \\ - [(A_{13} + A_{14}) + \delta \alpha (C_{13} + C_{14})][(A_{31} + A_{32}) + \delta \alpha (C_{31} + C_{32})] = 0,\end{aligned}\quad (15.36)$$

and to linear order in  $\delta$

$$\begin{aligned}(A_{11} + A_{12})(A_{33} + A_{34}) - (A_{13} + A_{14})(A_{31} + A_{32}) \\ + \delta \alpha [(A_{11} + A_{12})(C_{33} + C_{34}) - (A_{13} + A_{14})(C_{31} + C_{32}) \\ + (C_{11} + C_{12})(A_{33} + A_{34}) - (C_{13} + C_{14})(A_{31} + A_{32})] = 0.\end{aligned}\quad (15.37)$$

From this we find the mode condition function is

$$\begin{aligned}f = 1 + \delta \alpha [(A_{11} + A_{12})(C_{33} + C_{34}) \\ - (A_{13} + A_{14})(C_{31} + C_{32}) + (C_{11} + C_{12})(A_{33} + A_{34}) \\ - (C_{13} + C_{14})(A_{31} + A_{32})] / \\ [(A_{11} + A_{12})(A_{33} + A_{34}) - (A_{13} + A_{14})(A_{31} + A_{32})] \\ - \delta \alpha (B_{11} + B_{12} + B_{33} + B_{34}),\end{aligned}\quad (15.38)$$

or expressed in the  $\tilde{\mathbf{A}}$  and  $\tilde{\mathbf{B}}$  elements

$$\begin{aligned}f = 1 + \delta \alpha \{ B_{32} [(A_{11} + A_{12})(A_{23} + A_{24}) \\ - (A_{13} + A_{14})(A_{21} + A_{22})] \\ + B_{34} [(A_{11} + A_{12})(A_{43} + A_{44}) - (A_{13} + A_{14})(A_{41} + A_{42}) \\ - (A_{11} + A_{12})(A_{33} + A_{34}) + (A_{13} + A_{14})(A_{31} + A_{32})] \\ + B_{12} [(A_{33} + A_{34})(A_{21} + A_{22}) - (A_{31} + A_{32})(A_{23} + A_{24}) \\ - (A_{11} + A_{12})(A_{33} + A_{34}) + (A_{13} + A_{14})(A_{31} + A_{32})] \\ + B_{14} [(A_{33} + A_{34})(A_{41} + A_{42}) - (A_{31} + A_{32})(A_{43} + A_{44})] \} / \\ [(A_{11} + A_{12})(A_{33} + A_{34}) - (A_{13} + A_{14})(A_{31} + A_{32})].\end{aligned}\quad (15.39)$$

Note that we have chosen as reference system a system of two independent ones, one with the solid cylinder alone and the other with the thin cylinder alone. The calculated energy is then the interaction energy between the two objects.

Now, the retarded (Casimir) interaction energy between an atom and a cylinder is given by

$$\begin{aligned}
E &= \hbar \int_0^\infty \frac{d\xi}{2\pi} \sum_{m=-\infty}^\infty L \int_{-\infty}^\infty \frac{dh}{2\pi} \ln [f_m(h, i\xi)] \\
&\approx \hbar \int_0^\infty \frac{d\xi}{2\pi} \sum_{m=-\infty}^\infty L \int_{-\infty}^\infty \frac{dh}{2\pi} [f_m(h, i\xi) - 1] \\
&\approx \hbar \int_0^\infty \frac{d\xi}{2\pi} \sum_{m=-\infty}^\infty \int_{-\infty}^\infty \frac{dh}{2\pi} \frac{2\alpha^{at}}{b} \\
&\quad \times \{B_{32} [(A_{11} + A_{12})(A_{23} + A_{24}) - (A_{13} + A_{14})(A_{21} + A_{22})] \\
&\quad + B_{34} [(A_{11} + A_{12})(A_{43} + A_{44}) - (A_{13} + A_{14})(A_{41} + A_{42}) \\
&\quad - (A_{11} + A_{12})(A_{33} + A_{34}) + (A_{13} + A_{14})(A_{31} + A_{32})] \\
&\quad + B_{12} [(A_{33} + A_{34})(A_{21} + A_{22}) - (A_{31} + A_{32})(A_{23} + A_{24}) \\
&\quad - (A_{11} + A_{12})(A_{33} + A_{34}) + (A_{13} + A_{14})(A_{31} + A_{32})] \\
&\quad + B_{14} [(A_{33} + A_{34})(A_{41} + A_{42}) - (A_{31} + A_{32})(A_{43} + A_{44})] \} / \\
&\quad [(A_{11} + A_{12})(A_{33} + A_{34}) - (A_{13} + A_{14})(A_{31} + A_{32})], \tag{15.40}
\end{aligned}$$

where we have used that  $\alpha = 2\alpha^{at} / (bL\delta)$ . Remember that  $b = a + d$  is the distance to the atom from the cylinder axis and  $d$  is the closest distance from the atom to the cylinder. The radial coordinate in the  $A$  elements is  $a$  and in the  $B$  elements is  $b$ . The  $\tilde{A}$  elements are equal to the  $\tilde{M}$  elements in (15.17) and the  $\tilde{B}$  elements are given in (15.29)–(15.32). Next we give the actual expressions for all these combinations of matrix elements.

$$\begin{aligned}
&(A_{11} + A_{12})(A_{23} + A_{24}) - (A_{13} + A_{14})(A_{21} + A_{22}) \\
&= \left(\frac{2}{Wk_0^3}\right)^2 \frac{k_1^4 k_0^4}{q_1 q_0} \left[\frac{1}{k_0^2} - \frac{1}{k_1^2}\right] \frac{q_0}{k_0} iW (mh/a) J_m^2 \\
&= \left(\frac{2}{Wk_0^3}\right)^2 \frac{k_1^4 k_0^4}{q_1 q_0} [J_m(k_1 a)]^2 \frac{4q_0}{\pi k_0^2 a} (mh/a) \left[\frac{1}{k_0^2} - \frac{1}{k_1^2}\right], \tag{15.41}
\end{aligned}$$

$$\begin{aligned}
&(A_{11} + A_{12})(A_{43} + A_{44}) - (A_{13} + A_{14})(A_{41} + A_{42}) \\
&- (A_{11} + A_{12})(A_{33} + A_{34}) + (A_{13} + A_{14})(A_{31} + A_{32}) \\
&= -\left(\frac{2}{Wk_0^3}\right)^2 \frac{k_0^4 k_1^4}{q_0 q_1} [J_m(k_1 a)]^2 2H_m^{(1)}(k_0 a) J_m(k_0 a) \left\{ \left[ \frac{1}{k_1} \frac{J_m'(k_1 a)}{J_m(k_1 a)} - \frac{1}{k_0} \frac{H_m^{(1)'}(k_0 a)}{H_m^{(1)}(k_0 a)} \right] \right. \\
&\quad \times \left[ \frac{q_1^2}{k_1} \frac{J_m'(k_1 a)}{J_m(k_1 a)} - \frac{q_0^2}{k_0} \frac{J_m'(k_0 a)}{J_m(k_0 a)} \right] - (mh/a)^2 \left[ \frac{1}{k_0^2} - \frac{1}{k_1^2} \right]^2 \left. \right\}, \tag{15.42}
\end{aligned}$$

$$\begin{aligned}
&(A_{33} + A_{34})(A_{21} + A_{22}) - (A_{31} + A_{32})(A_{23} + A_{24}) \\
&- (A_{11} + A_{12})(A_{33} + A_{34}) + (A_{13} + A_{14})(A_{31} + A_{32}) \\
&= -\left(\frac{2}{Wk_0^3}\right)^2 \frac{k_0^4 k_1^4}{q_0 q_1} [J_m(k_1 a)]^2 2H_m^{(1)}(k_0 a) J_m(k_0 a) \left\{ \left[ \frac{q_1^2}{k_1} \frac{J_m'(k_1 a)}{J_m(k_1 a)} - \frac{q_0^2}{k_0} \frac{H_m^{(1)'}(k_0 a)}{H_m^{(1)}(k_0 a)} \right] \right. \\
&\quad \times \left[ \frac{1}{k_1} \frac{J_m'(k_1 a)}{J_m(k_1 a)} - \frac{1}{k_0} \frac{J_m'(k_0 a)}{J_m(k_0 a)} \right] - (mh/a)^2 \left[ \frac{1}{k_0^2} - \frac{1}{k_1^2} \right]^2 \left. \right\}, \tag{15.43}
\end{aligned}$$

$$\begin{aligned}
&(A_{33} + A_{34})(A_{41} + A_{42}) - (A_{31} + A_{32})(A_{43} + A_{44}) \\
&= -\left(\frac{2}{Wk_0^3}\right)^2 \frac{k_1^4 k_0^4}{q_1 q_0} [J_m(k_1 a)]^2 \frac{4q_0}{\pi k_0^2 a} (mh/a) \left[\frac{1}{k_0^2} - \frac{1}{k_1^2}\right], \tag{15.44}
\end{aligned}$$

and

$$\begin{aligned}
 & (A_{11} + A_{12})(A_{33} + A_{34}) - (A_{13} + A_{14})(A_{31} + A_{32}) \\
 &= \left(\frac{2}{Wk_0^3}\right)^2 \frac{k_0^4 k_1^4}{q_0 q_1} [J_m(k_1 a)]^2 [H_m^{(1)}(k_0 a)]^2 \left\{ \left[ \frac{1}{k_1} \frac{J_m'(k_1 a)}{J_m(k_1 a)} - \frac{1}{k_0} \frac{H_m^{(1)'}(k_0 a)}{H_m^{(1)}(k_0 a)} \right] \right. \\
 & \times \left. \left[ \frac{q_1^2}{k_1} \frac{J_m'(k_1 a)}{J_m(k_1 a)} - \frac{q_0^2}{k_0} \frac{H_m^{(1)'}(k_0 a)}{H_m^{(1)}(k_0 a)} \right] + (mh/a)^2 \left[ \frac{1}{k_0^2} - \frac{1}{k_1^2} \right]^2 \right\}. \quad (15.45)
 \end{aligned}$$

We have suppressed all arguments of the functions. The suppressed arguments are  $(k_0 a)$  for the  $H$ -functions and their derivatives and  $(k_1 a)$  for the  $J$ -functions and their derivatives. Note that the factor  $(2/Wk_0^3)^2$  in common of all three  $A$  expressions cancels out in the integrand of (15.40).

The  $B$  elements in (15.40) become

$$\begin{aligned}
 B_{12} &= -\frac{i\pi}{4b} \left(\frac{q_0}{k_0}\right)^2 \left\{ m^2 [H_m^{(1)}(k_0 b)]^2 + (k_0 b)^2 [H_m^{(1)'}(k_0 b)]^2 \right\}; \\
 B_{14} &= \frac{\pi}{4} 2m H_m^{(1)}(k_0 b) H_m^{(1)'}(k_0 b) h \left(\frac{q_0 b}{k_0 b}\right); \\
 B_{32} &= -\frac{\pi}{4} 2m H_m^{(1)}(k_0 b) H_m^{(1)'}(k_0 b) h \left(\frac{q_0 b}{k_0 b}\right); \\
 B_{34} &= \frac{i\pi}{4b} \left\{ [m^2 - (k_0 b)^2] [H_m^{(1)}(k_0 b)]^2 + (k_0 b) [H_m^{(1)'}(k_0 b)]^2 \right\} \\
 & - \frac{i\pi}{4b} \left(\frac{q_0 b}{k_0 b}\right)^2 \left\{ m^2 [H_m^{(1)}(k_0 b)]^2 + (k_0 b)^2 [H_m^{(1)'}(k_0 b)]^2 \right\}. \quad (15.46)
 \end{aligned}$$

To arrive at these expressions we have made use of the modified Bessel equation and its derivative to rid us of second and third order derivatives of the Hankel functions.

Now, the arguments of the functions are all imaginary on the imaginary axis. It may be favorable to have real-valued arguments,  $(\gamma_0 h a)$ ,  $(\gamma_1 h a)$ , and  $(\gamma_0 h b)$  instead of  $(k_0 a)$ ,  $(k_1 a)$ , and  $(k_0 b)$ , respectively, where  $\gamma_0(\omega) = \sqrt{1 - (\omega/ch)^2}$  and  $\gamma_1(\omega) = \sqrt{1 - [\tilde{n}(\omega)\omega/ch]^2}$ , respectively. On the imaginary frequency axis these become real valued,  $\gamma_0(i\xi) = \sqrt{1 + (\xi/ch)^2}$  and  $\gamma_1(i\xi) = \sqrt{1 + [\tilde{n}(i\xi)\xi/ch]^2}$ , respectively. To achieve real valued arguments we transform the functions to the modified Bessel functions  $I_m(z)$  and  $K_m(z)$ . The transformation rules are [3]:

$$\begin{aligned}
 H_m^{(1)}(ix) &= \frac{2}{\pi} \frac{1}{i^{m+1}} K_m(x); \\
 H_m^{(1)'}(ix) &= -\frac{2}{\pi} \frac{1}{i^m} K_m'(x); \\
 H_m^{(2)}(ix) &= 2i^m S_m(x); \\
 H_m^{(2)'}(ix) &= 2i^{m-1} S_m'(x); \\
 J_m(ix) &= i^m I_m(x); \\
 J_m'(ix) &= i^{m-1} I_m'(x); \\
 H_m^{(1)}(ix) J_m(ix) &= -\frac{2}{\pi} i K_m(x) I_m(x); \\
 H_m^{(2)}(ix) J_m(ix) &= 2(-1)^m S_m(x) I_m(x); \\
 H_m^{(1)}(ix) H_m^{(2)}(ix) &= -\frac{4}{\pi} i K_m(x) S_m(x), \quad (15.47)
 \end{aligned}$$

where we have introduced the complex valued function,  $S_m(x)$ ,

$$S_m(x) = \frac{1}{\pi} i(-1)^m K_m(x) + I_m(x). \quad (15.48)$$

The modified Bessel functions of real valued arguments are real valued. With these transformations and after the removal of a common factor,

$$\left(\frac{2}{Wk_0^3}\right)^2 \frac{k_0^4 k_1^4}{q_1 q_0} J_m^2, \quad (15.49)$$

that cancels out in (15.40) the factors containing  $A$  elements in (15.40) become

$$\begin{aligned} & (A_{11} + A_{12})(A_{23} + A_{24}) - (A_{13} + A_{14})(A_{21} + A_{22}) \\ &= i \frac{4}{\pi} \frac{(\xi a/c)}{(\gamma_0 ha)^2} (mha) \left[ \frac{1}{(\gamma_0 ha)^2} - \frac{1}{(\gamma_1 ha)^2} \right], \end{aligned} \quad (15.50)$$

$$\begin{aligned} & (A_{11} + A_{12})(A_{43} + A_{44}) - (A_{13} + A_{14})(A_{41} + A_{42}) \\ & - (A_{11} + A_{12})(A_{33} + A_{34}) + (A_{13} + A_{14})(A_{31} + A_{32}) \\ &= i \frac{4}{\pi} K_m(\gamma_0 ha) I_m(\gamma_0 ha) \left\{ \left[ \frac{-1}{(\gamma_1 ha)} \frac{I_m'(\gamma_1 ha)}{I_m(\gamma_1 ha)} + \frac{1}{(\gamma_0 ha)} \frac{K_m'(\gamma_0 ha)}{K_m(\gamma_0 ha)} \right] \right. \\ & \times \left. \left[ \frac{(\tilde{n}_1 \xi a/c)^2}{(\gamma_1 ha)} \frac{I_m'(\gamma_1 ha)}{I_m(\gamma_1 ha)} - \frac{(\xi a/c)^2}{(\gamma_0 ha)} \frac{I_m'(\gamma_0 ha)}{I_m(\gamma_0 ha)} \right] - (mha)^2 \left[ \frac{1}{(\gamma_0 ha)^2} - \frac{1}{(\gamma_1 ha)^2} \right]^2 \right\}, \end{aligned} \quad (15.51)$$

$$\begin{aligned} & (A_{33} + A_{34})(A_{21} + A_{22}) - (A_{31} + A_{32})(A_{23} + A_{24}) \\ & - (A_{11} + A_{12})(A_{33} + A_{34}) + (A_{13} + A_{14})(A_{31} + A_{32}) \\ &= i \frac{4}{\pi} K_m(\gamma_0 ha) I_m(\gamma_0 ha) \left\{ \left[ -\frac{(\tilde{n}_1 \xi a/c)^2}{(\gamma_1 ha)} \frac{I_m'(\gamma_1 ha)}{I_m(\gamma_1 ha)} + \frac{(\xi a/c)^2}{(\gamma_0 ha)} \frac{K_m'(\gamma_0 ha)}{K_m(\gamma_0 ha)} \right] \right. \\ & \times \left. \left[ \frac{1}{(\gamma_1 ha)} \frac{I_m'(\gamma_1 ha)}{I_m(\gamma_1 ha)} - \frac{1}{(\gamma_0 ha)} \frac{I_m'(\gamma_0 ha)}{I_m(\gamma_0 ha)} \right] - (mha)^2 \left[ \frac{1}{(\gamma_0 ha)^2} - \frac{1}{(\gamma_1 ha)^2} \right]^2 \right\}, \end{aligned} \quad (15.52)$$

$$\begin{aligned} & (A_{33} + A_{34})(A_{41} + A_{42}) - (A_{31} + A_{32})(A_{43} + A_{44}) \\ &= -i \frac{4}{\pi} \frac{(\xi a/c)}{(\gamma_0 ha)^2} (mha) \left[ \frac{1}{(\gamma_0 ha)^2} - \frac{1}{(\gamma_1 ha)^2} \right], \end{aligned} \quad (15.53)$$

and

$$\begin{aligned} & (A_{11} + A_{12})(A_{33} + A_{34}) - (A_{13} + A_{14})(A_{31} + A_{32}) \\ &= (-1)^m \frac{4}{\pi^2} \left[ K_m(\gamma_0 ha) \right]^2 \left\{ \left[ \frac{1}{(\gamma_1 ha)} \frac{I_m'(\gamma_1 ha)}{I_m(\gamma_1 ha)} - \frac{1}{(\gamma_0 ha)} \frac{K_m'(\gamma_0 ha)}{K_m(\gamma_0 ha)} \right] \right. \\ & \times \left. \left[ \frac{(\tilde{n}_1 \xi a/c)^2}{(\gamma_1 ha)} \frac{I_m'(\gamma_1 ha)}{I_m(\gamma_1 ha)} - \frac{(\xi a/c)^2}{(\gamma_0 ha)} \frac{K_m'(\gamma_0 ha)}{K_m(\gamma_0 ha)} \right] - (mha)^2 \left[ \frac{1}{(\gamma_0 ha)^2} - \frac{1}{(\gamma_1 ha)^2} \right]^2 \right\}. \end{aligned} \quad (15.54)$$

The  $B$  elements in (15.40) become

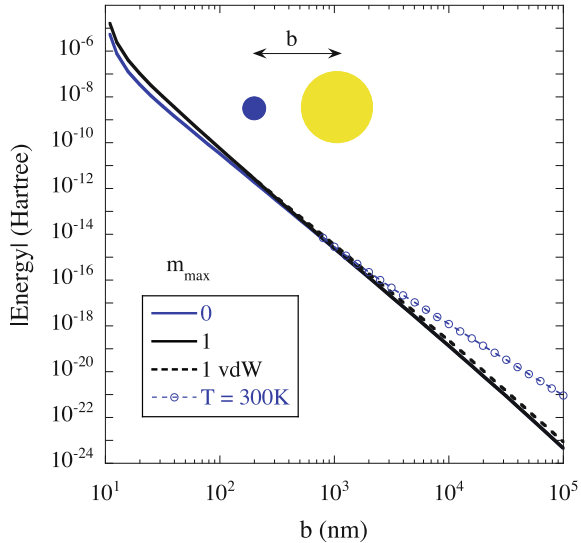
$$\begin{aligned}
 B_{12} &= i \frac{(-1)^m}{\pi b} \frac{(q_0 b)^2}{(h\gamma_0 b)^2} \left\{ m^2 [K_m(h\gamma_0 b)]^2 + (h\gamma_0 b)^2 K_m'(h\gamma_0 b)^2 \right\}, \\
 B_{14} &= i (-1)^m \frac{2mh}{\pi} \frac{(q_0 b)}{(h\gamma_0 b)} K_m(h\gamma_0 b) K_m'(h\gamma_0 b), \\
 B_{32} &= -i (-1)^m \frac{2mh}{\pi} \frac{(q_0 b)}{(h\gamma_0 b)} K_m(h\gamma_0 b) K_m'(h\gamma_0 b), \\
 B_{34} &= -i (-1)^m \frac{1}{\pi b} (h\gamma_0 b)^2 \left\{ [K_m(h\gamma_0 b)]^2 \left[ \frac{m^2}{(h\gamma_0 b)^2} + 1 \right] + [K_m'(h\gamma_0 b)]^2 \right\} \\
 &+ i (-1)^m \frac{1}{\pi b} (q_0 b)^2 \left\{ [K_m(h\gamma_0 b)]^2 \left[ \frac{m^2}{(h\gamma_0 b)^2} \right] + [K_m'(h\gamma_0 b)]^2 \right\}.
 \end{aligned}
 \tag{15.55}$$

To arrive at these expressions we have made use of the modified Bessel equation and its derivative to rid us of second and third order derivatives of the modified Bessel functions.

Since the derivations are rather involved one should make as many checks as possible. We have checked our results by taking the non-retarded limit of the resulting integrand in (15.40) and have reproduced the integrand of (11.38). In the following section we make a direct, numerical, check by calculating the interaction between a lithium atom and a gold cylinder. The results should agree with the non-retarded results in the small-separation limit.

The force on the atom is  $\mathbf{F}(b) = -\hat{\mathbf{r}}dE(b)/db$ .

**Fig. 15.1** The interaction energy for a Li atom next to a gold cylinder of radius  $a = 10$  nm. The distance between the atom and the cylinder axis is denoted by  $b$ . The retarded result, *solid curves*, was obtained from (15.40). The non-retarded result, *dashed curve*, is from Fig. 11.1. The *thin curve with circles* is the room temperature result. See the text for details



### 15.3.1 Force Between a Li-Atom and a Gold Cylinder

As an example of atom-cylinder interactions we show in Fig. 15.1a the interaction between a Li atom and a gold cylinder. The polarizability for Li was obtained from the London approximation (8.60) with the parameters given in Fig. 8.2. For gold we used the polarizability as shown in Fig. 9.3. The  $b$ -dependence does not follow a simple power law,  $E \sim b^{-6}$ , predicted by the summation over pair method (6.27). The retarded result has a slightly steeper slope than the non-retarded beyond a certain distance. Thus, both the non-retarded and retarded results for metal cylinders deviate from the behavior predicted by the summation of pair interactions as described in Sect. 6.1. We should also note that the negative slope does increase with less than one power unit when retardation sets in. We have furthermore added the room temperature result ( $T = 300$  K) at the large  $b$  end of the figure, the thin curve with circles.

## 15.4 Force on an Atom Outside a 2D Cylindrical Shell

In this section we derive the interaction between an atom and a 2D cylindrical shell. It could approximate the interaction between an atom and a nano tube. The geometry is illustrated in Fig. 14.5. The derivation proceeds along the lines in Sect. 15.3 and the matrix  $\tilde{\mathbf{A}}$  is replaced by  $\tilde{\mathbf{M}}^{2D}$  with the elements given in (15.33) and with  $r = a$ . The combinations of element we need are

$$(A_{11} + A_{12})(A_{23} + A_{24}) - (A_{13} + A_{14})(A_{21} + A_{22}) \\ = -\pi (mh) \left(\frac{q_0}{k_0}\right) \delta\tilde{\varepsilon}^{3D} J_m' J_m, \quad (15.56)$$

$$(A_{11} + A_{12})(A_{43} + A_{44}) - (A_{13} + A_{14})(A_{41} + A_{42}) \\ - (A_{11} + A_{12})(A_{33} + A_{34}) + (A_{13} + A_{14})(A_{31} + A_{32}) \\ = i\pi \left[ (mh)^2 \frac{1}{k_0^2 a} + k_0^2 a \right] \delta\tilde{\varepsilon}^{3D} J_m J_m + \frac{\pi^2}{2} q_0^2 k_0^2 a^2 (\delta\tilde{\varepsilon}^{3D})^2 H_m^{(1)'} J_m' J_m J_m, \quad (15.57)$$

$$(A_{33} + A_{34})(A_{21} + A_{22}) - (A_{31} + A_{32})(A_{23} + A_{24}) \\ - (A_{11} + A_{12})(A_{33} + A_{34}) + (A_{13} + A_{14})(A_{31} + A_{32}) \\ = i\pi a q_0^2 \delta\tilde{\varepsilon}^{3D} J_m' J_m' + \frac{\pi^2}{2} [k_0^2 a^2] (q_0)^2 (\delta\tilde{\varepsilon}^{3D})^2 H_m^{(1)} J_m J_m' J_m', \quad (15.58)$$

$$(A_{33} + A_{34})(A_{41} + A_{42}) - (A_{31} + A_{32})(A_{43} + A_{44}) \\ = \pi (mh) \left(\frac{q_0}{k_0}\right) \delta\tilde{\varepsilon}^{3D} J_m J_m', \quad (15.59)$$

and

$$(A_{11} + A_{12})(A_{33} + A_{34}) - (A_{13} + A_{14})(A_{31} + A_{32}) \\ = 1 - i\delta\tilde{\varepsilon}^{3D} \frac{\pi}{2} \left\{ q_0^2 a H_m^{(1)'} J_m' + \left[ (mh)^2 \frac{1}{k_0^2 a} + k_0^2 a \right] H_m^{(1)} J_m \right\} \\ - (\delta\tilde{\varepsilon}^{3D})^2 \left(\frac{\pi}{2}\right)^2 q_0^2 (k_0 a)^2 H_m^{(1)} J_m H_m^{(1)'} J_m'. \quad (15.60)$$

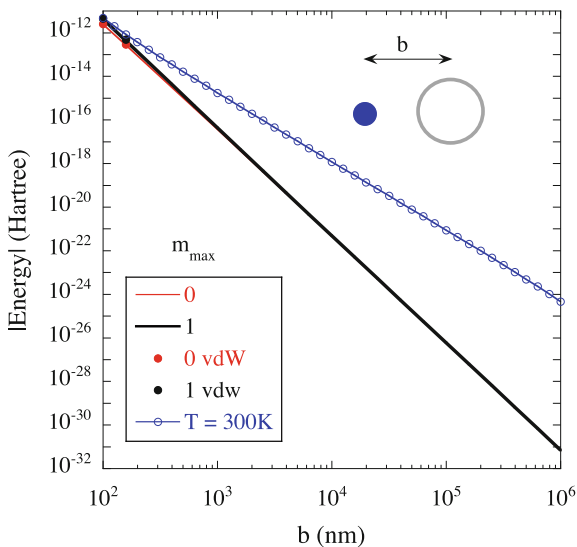


**Fig. 15.2** The interaction between a Li atom and a graphene cylinder as a function of distance  $b$ . The radius,  $a$ , of the cylindrical shell is 10 nm. The results are from using (15.40) and for two truncations,  $m = 0$  and  $m = 1$ , of the summation over  $m$ . We see that the  $m = 1$  contribution is negligible except for a very small region to the left in the figure. The *solid circles* are the results from the non-retarded treatment and we see that these results tie nicely on to the retarded results. The *thin curve with circles* is the room temperature result

The argument of all the above Bessel functions is  $(k_0 a)$ .

On the imaginary frequency axis these combinations of element become

$$\begin{aligned} & (A_{11} + A_{12})(A_{23} + A_{24}) - (A_{13} + A_{14})(A_{21} + A_{22}) \\ & = i\pi(-1)^m \frac{(mha)}{(\gamma_0 ha)} (\xi/c) \delta\tilde{\epsilon}^{3D} (i\xi) I_m'(\gamma_0 ha) I_m(\gamma_0 ha), \end{aligned} \quad (15.61)$$

$$\begin{aligned} & (A_{11} + A_{12})(A_{43} + A_{44}) - (A_{13} + A_{14})(A_{41} + A_{42}) \\ & - (A_{11} + A_{12})(A_{33} + A_{34}) + (A_{13} + A_{14})(A_{31} + A_{32}) \\ & = -i(-1)^m \pi \frac{1}{a} \left[ \frac{(mha)^2}{(\gamma_0 ha)^2} + (\gamma_0 ha)^2 \right] \delta\tilde{\epsilon}^{3D} I_m(\gamma_0 ha)^2 \\ & + i(-1)^m \pi (\xi/c)^2 (\gamma_0 ha)^2 [\delta\tilde{\epsilon}^{3D} (i\xi)]^2 K_m'(\gamma_0 ha) I_m'(\gamma_0 ha) I_m(\gamma_0 ha)^2, \end{aligned} \quad (15.62)$$

$$\begin{aligned} & (A_{33} + A_{34})(A_{21} + A_{22}) - (A_{31} + A_{32})(A_{23} + A_{24}) \\ & - (A_{11} + A_{12})(A_{33} + A_{34}) + (A_{13} + A_{14})(A_{31} + A_{32}) \\ & = i(-1)^m \pi a (\xi/c)^2 \delta\tilde{\epsilon}^{3D} (i\xi) I_m'(\gamma_0 ha)^2 \\ & + i(-1)^m \pi (\gamma_0 ha)^2 (\xi/c)^2 [\delta\tilde{\epsilon}^{3D} (i\xi)]^2 K_m(\gamma_0 ha) I_m(\gamma_0 ha) I_m'(\gamma_0 ha)^2, \end{aligned} \quad (15.63)$$

$$\begin{aligned} & (A_{33} + A_{34})(A_{41} + A_{42}) - (A_{31} + A_{32})(A_{43} + A_{44}) \\ & = -i(-1)^m \pi \left( \frac{mha}{\gamma_0 ha} \right) (\xi/c) \delta\tilde{\epsilon}^{3D} (i\xi) I_m(\gamma_0 ha) I_m'(\gamma_0 ha), \end{aligned} \quad (15.64)$$

and

$$\begin{aligned}
 & (A_{11} + A_{12})(A_{33} + A_{34}) - (A_{13} + A_{14})(A_{31} + A_{32}) \\
 & = 1 - \delta\tilde{\epsilon}^{3D}(i\xi) \left\{ (\xi/c)^2 a K_m'(\gamma_0 ha) I_m'(\gamma_0 ha) \right. \\
 & \quad \left. - \left[ \frac{(mha)^2}{(\gamma_0 ha)^2} + (\gamma_0 ha)^2 \right] \frac{1}{a} K_m(\gamma_0 ha) I_m(\gamma_0 ha) \right\} \\
 & - \left[ \delta\tilde{\epsilon}^{3D}(i\xi) \right]^2 (\xi/c)^2 (\gamma_0 ha)^2 K_m(\gamma_0 ha) I_m(\gamma_0 ha) K_m'(\gamma_0 ha) I_m'(\gamma_0 ha).
 \end{aligned} \tag{15.65}$$

To find the interaction energy between an atom and the thin cylindrical shell we use (15.40) with the factors containing  $A$  elements from (15.61)–(15.65) and the  $B$  elements from (15.55).

Two examples where the results apply are a cylinder made of a graphene like film and a thin metal film, respectively. Then the expressions for  $\delta\tilde{\epsilon}(i\xi)$  as given in (10.24) can be used [4, 5].

We have checked our results by taking the non-retarded limit of the resulting integrand in (15.40) and have reproduced the integrand of (11.44).

### 15.4.1 Interaction Between a Li-Atom and a Graphene Cylinder

As an example we give the results for a Li-atom outside a graphene like cylinder in Fig. 15.2. The results are from using (15.40) with the combination of  $A$  elements from (15.61)–(15.65) and the  $B$  elements from (15.55). The polarizability for Li was obtained from the London approximation (8.60) with the parameters given in Fig. 8.2 and for the cylindrical shell the  $\delta\tilde{\epsilon}^{3D}(i\xi)$  entering  $\alpha_l^{2D}(a; i\xi)$  was taken from (10.24). At large distances only the  $m = 0$  and  $m = \pm 1$  terms give important contributions and follow the power law  $\sim b^{-5}$ . We find that the retardation effects are negligible in this case. This is very interesting. We have found that retardation has negligible effect on the interaction between two planar, pristine graphene sheets, between one planar, pristine graphene sheet and a metal wall, and here between an atom and a cylindrical, pristine graphene shell. We found, however, that retardation affected the interaction between an atom and a spherical, pristine graphene shell. The room temperature result ( $T = 300$  K) is given as the thin curve with circles. Here it modifies the result at a relatively small  $b$  value.

## References

1. M. Kerker, in *The Scattering of Light and Other Electromagnetic Radiation*, ed. by E.M. Loebel (Academic Press, New York 1969), p. 259
2. R. Ruppin, in *Electromagnetic Surface Modes*, ed. by A.D. Boardman (Wiley, New York, 1982)
3. From (9.6.2) and (9.6.3) in *Handbook of Mathematical Functions*, ed. by M. Abramowitz, I.A. Stegun, (U.S. Government Printing Office, 1964)

4. Bo E. Sernelius, *Graphene* **1**, 21 (2012)
5. Bo E. Sernelius, *J. Phys. Condens. Matter* **27**, 214017 (2015)

# Chapter 16

## Summary and Outlook



We have presented a general formalism for determining the electromagnetic normal modes in layered structures. We have furthermore shown how to calculate the dispersion energy and forces for these structures, both at zero and finite temperature. For the convenience of the reader we have derived in detail what is needed to address the three most common geometrical classes viz. the planar, spherical and cylindrical. We have presented both non-retarded and fully retarded treatments. We have also given the resulting relations for a large number of illustrating examples.

Systems with a general number of layers can be handled and the thickness of each layer can have any value; even 2D layers are allowed which means that graphene, graphene-like, and 2D electron gases can be treated.

Within the formalism it is possible to obtain the force on an atom inside or outside the layered structures. We have given many examples of this in the text. We have even derived the van der Waals and Casimir-Polder interactions between two atoms using the formalism for spherical structures in Sects. 10.5 and 15.6, respectively.

Throughout this work we have been careful to define our system and used as boundary condition that outside the system there are only outgoing waves and no incoming waves toward the system. All normal modes included in the treatment are caused by time dependent charge- and current-densities within the system. Now, incoming waves are also solutions to Maxwell's equations but would be caused by objects outside our system. The energy of these could change when objects within our system are moved relative each other and hence affect the force between the objects. However, the influence of the external objects decreases with the distance between these objects and our system and can be neglected if the distance is big enough. As a *gedanken experiment* we could in the planar case put the whole system inside a cubic box of finite size and with totally reflecting walls. We now let the box be included in our system. Then there are incoming waves towards the original system

but not towards our new system. This approach is used in the standard derivation<sup>1</sup> of the Casimir effect. When we let the size of the box go to infinity the effect of the box vanishes. That we reproduced the Casimir classical result in (14.25) using our boundary conditions with no incoming waves supports the approach we have used throughout this book. The approach has also been thoroughly scrutinized and tested in many other places in the book.

We end by giving a handful of suggestions for further studies in the field of dispersion interactions.

We have here focused on the three most common geometries. As we mentioned in Chap. 7 our general method can be used in 13 geometries within the non-retarded formalism and in 11 within the retarded. Of interest could be, e.g., edges, wedges, and needle shaped objects. The ground is laid for further exploration.

We have not been dwelling on a controversy in the thermal Casimir effect in metallic systems; we only touched upon it briefly in Sect. 14.13. It has not been fully resolved yet and it is not clear if the problems lie in the experimental or theoretical part. Work still remains to be done.

We have not considered colloidal systems containing electrolytes like many biological systems. In those systems the interactions cause the materials to lose their homogeneity. This cannot be handled in a simple way within our formalism. The charged particles are there polarizable ions. We can handle polar and ionic crystals where the polar atoms or ions are just shifted slightly from their equilibrium positions but not allowed to move throughout the whole material. There are ways though, to approach these problems like invoking the Poisson-Boltzmann equation.

Another interesting topic is possible effects of electromagnetic fields on the interaction between biological cells and on other biological tissue. One possible negative result is effects from using cell phones. Other, positive effects could be the possibility to use light therapy of various sorts.

We have studied dispersion interactions based on electromagnetism. The corresponding induced interactions based on the other fundamental interactions should be investigated.

There is a struggle going on in finding geometries and material combinations that lead to repulsive forces. Repulsive forces are preferable in e.g. construction of nano machines since stiction is a common problem in nano technology.<sup>2</sup> Meta-materials of chiral type were a possible candidate for a while but the repulsive components were found to be too weak. The search continues.

---

<sup>1</sup>See Bo E. Sernelius, *Surface Modes in Physics* (Wiley-VCH, Berlin, 2001), Sect. 4.3.

<sup>2</sup>The dispersion forces are relatively strong on the nano scale. Small structures have a tendency to stick to surfaces and it is sometimes impossible to free them without breaking the structure. This is called stiction.

We have here only treated systems at thermodynamic equilibrium. Much work goes on for systems out of thermal equilibrium. One interesting possibility could be to manipulate the forces by finding alternative ways than thermal to populate the normal modes.

We believe that the future lies in interdisciplinary work involving medicine, biology and technology and hopefully this book can help, stimulate and inspire.

# Appendix A

## Interaction Power Laws Depending on Shape and Orientation

In this appendix we present comparisons between the asymptotic power laws found with the formalism in the book and with the method of pair interactions; the van der Waals limit in Table [A.1](#); the Casimir limit in Table [A.2](#).

**Table A.1** Asymptotic power laws in the van der Waals limit (law for the interaction energy)

Geometry	Power law	From pair interactions
Metal-half-space–metal-half-space	$d^{-2}$	$d^{-2}$ (half-space–half-space) <sup>a</sup>
Pristine graphene–metal-half-space	no	$d^{-3}$ (film–half-space) <sup>b</sup>
Doped graphene–metal-half-space	no	$d^{-3}$ (film–half-space) <sup>b</sup>
2D-metal-film–metal-half-space	$d^{-5/2}$	$d^{-3}$ (film–half-space) <sup>b</sup>
Pristine graphene–pristine graphene	$d^{-3}$	$d^{-4}$ (film–film) <sup>c</sup>
Doped graphene–doped graphene	no	$d^{-4}$ (film–film) <sup>c</sup>
2D-metal-film–2D-metal-film	$d^{-5/2}$	$d^{-4}$ (film–film) <sup>c</sup>
Atom–metal-halfspace	$d^{-3}$	$d^{-3}$ (atom–half-space) <sup>d</sup>
Atom–pristine graphene	$d^{-4}$	$d^{-4}$ (atom–film) <sup>e</sup>
Atom–doped graphene	no	$d^{-4}$ (atom–film) <sup>e</sup>
Atom–2D-metal-film	$d^{-7/2}$	$d^{-4}$ (atom–film) <sup>e</sup>
Atom–atom	$d^{-6}$	$d^{-6}$ (atom–atom) <sup>f</sup>
Atom–spherical shell	$d^{-6}$	$d^{-6}$ (atom–spherical shell) <sup>g</sup>
Atom–ball	$d^{-6}$	$d^{-6}$ (atom–ball) <sup>h</sup>
Ball–ball	$d^{-6}$	$d^{-6}$ (ball–ball) <sup>i</sup>
Atom–cylinder	$d^{-5}$	$d^{-5}$ (atom–cylinder) <sup>j</sup>
Cylinder–cylinder	$d^{-5}$	$d^{-5}$ (cylinder–cylinder) <sup>k</sup>

<sup>a</sup>(6.7) for  $\lambda = 6$ <sup>b</sup>(6.9) for  $\lambda = 6$ <sup>c</sup>(6.8) for  $\lambda = 6$ <sup>d</sup>(6.4) for  $\lambda = 6$ <sup>e</sup>(6.3) for  $\lambda = 6$ <sup>f</sup>(6.1) for  $\lambda = 6$ <sup>g</sup>(6.11) for  $\lambda = 6$ <sup>h</sup>(6.13) for  $\lambda = 6$ <sup>i</sup>(6.16) for  $\lambda = 6$ <sup>j</sup>(6.24) for  $\lambda = 6$ <sup>k</sup>(6.25) for  $\lambda = 6$

**Table A.2** Asymptotic power laws in the Casimir Limit (law for the interaction energy)

Geometry	Power law	From pair interactions
Metal-half-space–metal-half-space	$d^{-3}$	$d^{-3}$ (half-space–half-space) <sup>a</sup>
Pristine graphene–metal-half-space	$d^{-3}$	$d^{-4}$ (film–half-space) <sup>b</sup>
Doped graphene–metal-half-space	$d^{-3}$	$d^{-4}$ (film–half-space) <sup>b</sup>
2D-metal-film–metal-half-space	$d^{-3}$	$d^{-4}$ (film–half-space) <sup>b</sup>
Pristine graphene–pristine graphene	$d^{-3}$	$d^{-5}$ (film–film) <sup>c</sup>
Doped graphene–doped graphene	$d^{-3}$	$d^{-5}$ (film–film) <sup>c</sup>
2D-metal-film–2D-metal-film	$d^{-3}$	$d^{-5}$ (film–film) <sup>c</sup>
Atom–metal-halfspace	$d^{-4}$	$d^{-4}$ (atom–half-space) <sup>d</sup>
Atom–pristine graphene	$d^{-4}$	$d^{-5}$ (atom–film) <sup>e</sup>
Atom–doped graphene	$d^{-4}$	$d^{-5}$ (atom–film) <sup>e</sup>
Atom–2D-metal-film	$d^{-4}$	$d^{-5}$ (atom–film) <sup>e</sup>
Atom–atom	$d^{-7}$	$d^{-7}$ (atom–atom) <sup>f</sup>
Atom–spherical shell	$d^{-7}$	$d^{-7}$ (atom–spherical shell) <sup>g</sup>
Atom–ball	$d^{-7}$	$d^{-7}$ (atom–ball) <sup>h</sup>
Ball–ball	$d^{-7}$	$d^{-7}$ (ball–ball) <sup>i</sup>
Atom–cylinder	no	$d^{-6}$ (atom–cylinder) <sup>j</sup>
Cylinder–cylinder		$d^{-6}$ (cylinder–cylinder) <sup>k</sup>

<sup>a</sup>(6.7) for  $\lambda = 7$

<sup>b</sup>(6.9) for  $\lambda = 7$

<sup>c</sup>(6.8) for  $\lambda = 7$

<sup>d</sup>(6.4) for  $\lambda = 7$

<sup>e</sup>(6.3) for  $\lambda = 7$

<sup>f</sup>(6.1) for  $\lambda = 7$

<sup>g</sup>(6.11) for  $\lambda = 7$

<sup>h</sup>(6.13) for  $\lambda = 7$

<sup>i</sup>(6.14) for  $\lambda = 7$

<sup>j</sup>(6.27) for  $\lambda = 7$

<sup>k</sup>(6.28) for  $\lambda = 7$

## Appendix B

# Transforming Between Unit Systems

**Table B.1** If we have an expression in CGS units and want the corresponding expression in SI units we just replace all quantities in the middle column with the corresponding quantity in the rightmost column

Quantity	CGS	SI
Velocity of light	$c$	$\sqrt{1/\mu_0\epsilon_0}$
Electric field	$\mathbf{E}$	$\sqrt{4\pi\epsilon_0}\mathbf{E}$
Potential	$\Phi$	$\sqrt{4\pi\epsilon_0}\Phi$
Voltage	$V$	$\sqrt{4\pi\epsilon_0}V$
Displacement	$\mathbf{D}$	$\sqrt{4\pi/\epsilon_0}\mathbf{D}$
Charge density	$\rho$	$\sqrt{1/4\pi\epsilon_0}\rho$
Charge	$q$	$\sqrt{1/4\pi\epsilon_0}q$
Current density	$\mathbf{J}$	$\sqrt{1/4\pi\epsilon_0}\mathbf{J}$
Current	$\mathbf{I}$	$\sqrt{1/4\pi\epsilon_0}\mathbf{I}$
Polarization	$\mathbf{P}$	$\sqrt{1/4\pi\epsilon_0}\mathbf{P}$
Magnetic induction	$\mathbf{B}$	$\sqrt{4\pi/\mu_0}\mathbf{B}$
Magnetic field	$\mathbf{H}$	$\sqrt{4\pi\mu_0}\mathbf{H}$
Magnetization	$\mathbf{M}$	$\sqrt{\mu_0/4\pi}\mathbf{M}$
Conductivity	$\sigma$	$\sigma/4\pi\epsilon_0$
Capacitance	$C$	$C/4\pi\epsilon_0$
Dielectric function	$\epsilon$	$\epsilon/\epsilon_0 = \epsilon_r$
Magnetic permeability	$\mu$	$\mu/\mu_0 = \mu_r$
Resistance	$R$	$4\pi\epsilon_0R$
Impedance	$Z$	$4\pi\epsilon_0Z$
Inductance	$L$	$4\pi\epsilon_0L$

## Appendix C

# The Fourier Transform

The Fourier transform can be defined in different ways. We define the Fourier transforms with respect to position and time and their inverses in the following way:

$$\begin{aligned}
 f(\mathbf{q}) &= \int d^3r e^{-i\mathbf{q}\cdot\mathbf{r}} f(\mathbf{r}), \\
 f(\mathbf{r}) &= \frac{1}{\Omega} \sum_{\mathbf{q}} e^{i\mathbf{q}\cdot\mathbf{r}} f(\mathbf{q}) = \int \frac{d^3q}{(2\pi)^3} e^{i\mathbf{q}\cdot\mathbf{r}} f(\mathbf{q}), \\
 f(\omega) &= \int_{-\infty}^{\infty} dt e^{i\omega t} f(t), \\
 f(t) &= \int_{-\infty}^{\infty} \frac{d\omega}{2\pi} e^{-i\omega t} f(\omega), \\
 f(\mathbf{q}, \omega) &= \int d^3r \int_{-\infty}^{\infty} dt e^{-i(\mathbf{q}\cdot\mathbf{r} - \omega t)} f(\mathbf{r}, t), \\
 f(\mathbf{r}, t) &= \int \frac{d^3q}{(2\pi)^3} \int_{-\infty}^{\infty} \frac{d\omega}{2\pi} e^{i(\mathbf{q}\cdot\mathbf{r} - \omega t)} f(\mathbf{q}, \omega),
 \end{aligned} \tag{C.1}$$

where  $\Omega$  on the second line is the volume of the system, if finite. For an infinite system the summation over discrete wave vectors goes over into an integral over a continuous variable.

With these sign conventions, Fourier transforming differential equations has the following substitutional effects:

$$\begin{aligned}
 \frac{\partial}{\partial t} &\rightarrow -i\omega \\
 \nabla \cdot &\rightarrow i\mathbf{q} \cdot \\
 \nabla \times &\rightarrow i\mathbf{q} \times
 \end{aligned} \tag{C.2}$$

# Appendix D

## Dielectric Functions

The dielectric function in a 3D system is

$$\varepsilon(\mathbf{q}, \omega) = 1 + \alpha(\mathbf{q}, \omega) = 1 - v_q \chi(\mathbf{q}, \omega), \tag{D.1}$$

where  $\alpha(\mathbf{q}, \omega)$  is the polarizability. In 2D the corresponding relation is

$$\varepsilon(\mathbf{k}, \omega) = 1 + \alpha^{2D}(\mathbf{k}, \omega) = 1 - v_k^{2D} \chi^{2D}(\mathbf{k}, \omega). \tag{D.2}$$

In what follows we present different versions for the polarizability.

### D.1 Longitudinal Function for Electron Gas

The longitudinal polarizability for an electron gas in RPA is

$$\begin{aligned} \alpha_L(\mathbf{q}, z) &= -v_q \chi(\mathbf{q}, z) \\ &= \frac{v_q}{\hbar} 2 \int \frac{d^3k}{(2\pi)^3} n(\mathbf{k}) [1 - n(\mathbf{k} + \mathbf{q})] \left[ \frac{1}{z + \frac{1}{\hbar}(\varepsilon_{\mathbf{k}+\mathbf{q}} - \varepsilon_{\mathbf{k}})} - \frac{1}{z - \frac{1}{\hbar}(\varepsilon_{\mathbf{k}+\mathbf{q}} - \varepsilon_{\mathbf{k}})} \right], \end{aligned} \tag{D.3}$$

where the factor 2 in front of the integral comes from the summation over spin. This function is analytic everywhere off the real frequency axes and a straightforward calculation yields for  $T = 0$

$$\begin{aligned} \alpha_L(Q, Z) &= \frac{v}{2\pi} \frac{1}{Q^2} \left\{ 1 + \frac{Q^2 - (Z - Q^2)^2}{4Q^3} \ln \left[ \frac{Q - (Z - Q^2)}{-Q - (Z - Q^2)} \right] \right. \\ &\quad \left. - \frac{Q^2 - (Z + Q^2)^2}{4Q^3} \ln \left[ \frac{-Q + (Z + Q^2)}{Q + (Z + Q^2)} \right] \right\}, \end{aligned} \tag{D.4}$$

where

$$y = \frac{m\epsilon^2}{\hbar^2 k_F}; \quad Z = \frac{\hbar z}{4E_F}; \quad Q = \frac{k}{2k_F}; \quad E_F = \frac{\hbar^2 k_F^2}{2m}; \quad k_F = (3\pi^2 n)^{1/3}. \quad (\text{D.5})$$

The logarithm is taken from the branch for which  $|\arg \ln(z)| \leq \pi$ . From this function the different forms are for  $T = 0$  obtained according to

$$\begin{aligned} \alpha_L^R(Q, W) &= \alpha_L(Q, W + i\eta) \\ \alpha_L^A(Q, W) &= \alpha_L(Q, W - i\eta) \\ \alpha_L^T(Q, W) &= \alpha_L[Q, W + i\eta \text{sign}(W)], \end{aligned} \quad (\text{D.6})$$

where  $W$  now is a real quantity and  $\eta$  is infinitesimal. The time ordered function is even with respect to  $W$ . The real part of all three functions are even and equal. The following relations are valid:

$$\begin{aligned} \text{Re}\alpha_L^R(Q, W) &= \text{Re}\alpha_L^A(Q, W) = \text{Re}\alpha_L^T(Q, W) \\ &= \text{Re}\alpha_L^R(Q, -W) = \text{Re}\alpha_L^A(Q, -W) = \text{Re}\alpha_L^T(Q, -W) \\ \text{Im}\alpha_L^T(Q, W) &= \text{Im}\alpha_L^R(Q, -W) \\ \text{Im}\alpha_L^R(Q, W) &= -\text{Im}\alpha_L^R(Q, -W) = \text{sign}(W)\text{Im}\alpha_L^T(Q, W) \\ \text{Im}\alpha_L^A(Q, W) &= -\text{Im}\alpha_L^A(Q, -W) = -\text{sign}(W)\text{Im}\alpha_L^T(Q, W). \end{aligned} \quad (\text{D.7})$$

We stress that (D.6) and (D.7) are only valid for  $T = 0$ . We note that it suffices to study the time ordered or retarded function for  $W \geq 0$ .

$$\begin{aligned} \text{Re}\alpha_L^{R,T}(Q, W) &= \frac{y}{2\pi} \frac{1}{Q^2} \left\{ 1 + \frac{Q^2 - (W - Q^2)^2}{4Q^3} \ln \left| \frac{Q - (W - Q^2)}{Q + (W - Q^2)} \right| \right. \\ &\quad \left. - \frac{Q^2 - (W + Q^2)^2}{4Q^3} \ln \left| \frac{Q - (W + Q^2)}{Q + (W + Q^2)} \right| \right\}. \end{aligned} \quad (\text{D.8})$$

The imaginary part can be written in the following compact way

$$\begin{aligned} \text{Im}\alpha_L^{R,T}(Q, W) &= -\frac{y}{8Q^3} \left\{ -2W + \left| W + \frac{1}{2} [Q^2 + (W/Q)^2 - 1] \right| \right. \\ &\quad \left. - \left| W - \frac{1}{2} [Q^2 + (W/Q)^2 - 1] \right| \right\}. \end{aligned} \quad (\text{D.9})$$

All the different forms of the polarizability were obtained by calculating the function in (D.4) either just above or just below the real frequency axes. We will also in some calculations need the expression for this function on the imaginary axes. It is

$$\begin{aligned} \alpha_L(Q, i\mathcal{E}) &= \frac{y}{2\pi} \frac{1}{Q^2} \left\{ 1 + \frac{\mathcal{E}^2 + Q^2 - Q^4}{4Q^3} \ln \left[ \frac{\mathcal{E}^2 + Q^2(1+Q)^2}{\mathcal{E}^2 + Q^2(1-Q)^2} \right] \right. \\ &\quad \left. - \frac{\mathcal{E}}{Q} \left[ \tan^{-1} \frac{Q(1+Q)}{\mathcal{E}} + \tan^{-1} \frac{Q(1-Q)}{\mathcal{E}} \right] \right\}, \end{aligned} \quad (\text{D.10})$$

where

$$y = \frac{me^2}{\hbar^2 k_F}; \quad \mathcal{E} = \frac{\hbar\xi}{4E_F}; \quad Q = \frac{k}{2k_F}; \quad E_F = \frac{\hbar^2 k_F^2}{2m}. \quad (\text{D.11})$$

The function  $\tan^{-1}$  is taken from the branch where  $-\pi/2 < \tan^{-1} < \pi/2$ .

## D.2 Transverse Function for Electron Gas

The transverse polarizability for an electron gas in RPA is

$$\alpha_T(Q, i\mathcal{E}) = \frac{y}{8\pi} \frac{1}{Q^2 \mathcal{E}^2} \left\{ (Q^2 + Q^4 - 3\mathcal{E}^2) + \frac{(2\mathcal{E}Q^2)^2 - (\mathcal{E}^2 + Q^2 - Q^4)^2}{4Q^3} \ln \frac{(Q+Q^2)^2 + \mathcal{E}^2}{(Q-Q^2)^2 + \mathcal{E}^2} + 2\frac{\mathcal{E}}{Q} (\mathcal{E}^2 + Q^2 - Q^4) \left[ \tan^{-1} \left( \frac{Q+Q^2}{\mathcal{E}} \right) + \tan^{-1} \left( \frac{Q-Q^2}{\mathcal{E}} \right) \right] \right\}, \quad (\text{D.12})$$

where

$$y = \frac{me^2}{\hbar^2 k_F}; \quad \mathcal{E} = \frac{\hbar\xi}{4E_F}; \quad Q = \frac{k}{2k_F}; \quad E_F = \frac{\hbar^2 k_F^2}{2m}; \quad k_F = (3\pi^2 n)^{1/3}. \quad (\text{D.13})$$

The function  $\tan^{-1}$  is taken from the branch where  $-\pi/2 < \tan^{-1} < \pi/2$ .

## D.3 Longitudinal Function for 2D Electron Gas

The longitudinal polarizability for a 2D electron gas in RPA is

$$\alpha_L^{2D}(Q, i\mathcal{E}) = \frac{y}{Q} \left\{ 1 - \left[ \sqrt{(Q^4 - \mathcal{E}^2 - Q^2)^2 + (2\mathcal{E}Q^2)^2} + (Q^4 - \mathcal{E}^2 - Q^2)^2 \right]^{1/2} / Q^2 \right\}, \quad (\text{D.14})$$

where

$$y = \frac{me^2}{\hbar^2 k_F}; \quad \mathcal{E} = \frac{\hbar\xi}{4E_F}; \quad Q = \frac{k}{2k_F}; \quad E_F = \frac{\hbar^2 k_F^2}{2m}; \quad k_F = \sqrt{2\pi n^{2D}}. \quad (\text{D.15})$$

## D.4 Longitudinal Function for Graphene

The longitudinal susceptibility for graphene in RPA is

**Pristine graphene at  $T = 0$ :**

$$\chi_L^{2D}(\mathbf{k}, z) = -\frac{1}{4\hbar} \frac{k^2}{g(\mathbf{k}, z)}; \quad \chi_L^{2D}(\mathbf{k}, i\xi) = -\frac{1}{4\hbar} \frac{k^2}{g(\mathbf{k}, i\xi)}, \quad (\text{D.16})$$

where

$$\begin{aligned} g(\mathbf{k}, z) &= \sqrt{v^2 k^2 - z^2}, \\ g(\mathbf{k}, i\xi) &= \sqrt{v^2 k^2 + \xi^2}. \end{aligned} \quad (\text{D.17})$$

**Pristine graphene at  $T \neq 0$ :**

$$\begin{aligned} \chi_L^{2D}(\mathbf{k}, z) &= -\frac{k^2}{4\hbar} \left[ \frac{1}{g(\mathbf{k}, z)} + \frac{8}{\pi v^2 k^2} \int_0^1 dx p(\mathbf{k}, z, x) \right], \\ \chi_L^{2D}(\mathbf{k}, i\xi) &= -\frac{k^2}{4\hbar} \left[ \frac{1}{g(\mathbf{k}, i\xi)} + \frac{8}{\pi v^2 k^2} \int_0^1 dx p(\mathbf{k}, i\xi, x) \right], \end{aligned} \quad (\text{D.18})$$

where

$$\begin{aligned} p(\mathbf{k}, z, x) &= \frac{1}{\beta} \ln \left[ 1 + 2 \cosh(\hbar\beta z x) e^{-\theta_T(\mathbf{k}, z, x)} + e^{-2\theta_T(\mathbf{k}, z, x)} \right] \\ &\quad - \frac{\hbar z}{2} (1 - 2x) \frac{\sinh(\hbar\beta z x)}{\cosh \theta_T(\mathbf{k}, z, x) + \cosh(\hbar\beta z x)} \\ &\quad - \sqrt{x(1-x)} \frac{\hbar z^2}{g(\mathbf{k}, z)} \frac{\cosh(\hbar\beta z x) + e^{-\theta_T(\mathbf{k}, z, x)}}{\cosh \theta_T(\mathbf{k}, z, x) + \cosh(\hbar\beta z x)}, \\ p(\mathbf{k}, i\xi, x) &= \frac{1}{\beta} \ln \left[ 1 + 2 \cos(\hbar\beta \xi x) e^{-\theta_T(\mathbf{k}, i\xi, x)} + e^{-2\theta_T(\mathbf{k}, i\xi, x)} \right] \\ &\quad - \frac{\hbar \xi}{2} (1 - 2x) \frac{\sin(\hbar\beta \xi x)}{\cosh \theta_T(\mathbf{k}, i\xi, x) + \cos(\hbar\beta \xi x)} \\ &\quad + \sqrt{x(1-x)} \frac{\hbar \xi^2}{g(\mathbf{k}, i\xi)} \frac{\cos(\hbar\beta \xi x) + e^{-\theta_T(\mathbf{k}, i\xi, x)}}{\cosh \theta_T(\mathbf{k}, i\xi, x) + \cos(\hbar\beta \xi x)}, \end{aligned} \quad (\text{D.19})$$

and

$$\begin{aligned} \theta_T(\mathbf{k}, z, x) &= \hbar\beta g(\mathbf{k}, z) \sqrt{x(1-x)}, \\ \theta_T(\mathbf{k}, i\xi, x) &= \hbar\beta g(\mathbf{k}, i\xi) \sqrt{x(1-x)}, \end{aligned} \quad (\text{D.20})$$

where the functions  $g(\mathbf{k}, z)$  and  $g(\mathbf{k}, i\xi)$  are given in (D.17).

**Doped graphene:**

In the equations for doped graphene we use dimensionless variables:  $x = k/2k_F$ ,  $y = \hbar\xi/2E_F$  and  $\tilde{z} = \hbar z/2E_F$ , where  $k_F = \sqrt{\pi n}$  and  $E_F = \hbar v k_F$  are the fermi momentum and fermi energy, respectively.

In a general point in the complex  $z$ -plane we have

$$\begin{aligned}\chi_L^{2D}(\mathbf{k}, z) &= -D_0 \left\{ 1 + \frac{x^2}{4\sqrt{x^2 - \tilde{z}^2}} [\pi - f(x, \tilde{z})] \right\}; \\ f(x, \tilde{z}) &= \text{asin}\left(\frac{1-\tilde{z}}{x}\right) + \text{asin}\left(\frac{1+\tilde{z}}{x}\right) \\ &\quad - \frac{\tilde{z}-1}{x} \sqrt{1 - \left(\frac{\tilde{z}-1}{x}\right)^2} + \frac{\tilde{z}+1}{x} \sqrt{1 - \left(\frac{\tilde{z}+1}{x}\right)^2},\end{aligned}\tag{D.21}$$

and along the imaginary axis,

$$\begin{aligned}\chi_L^{2D}(\mathbf{k}, i\xi) &= -D_0 \left\{ 1 + \frac{x^2}{4\sqrt{y^2 + x^2}} [\pi - g(x, y)] \right\}; \\ g(x, y) &= \text{atan}[h(x, y)k(x, y)] + l(x, y); \\ h(x, y) &= \frac{2\left\{ [x^2(y^2-1) + (y^2+1)^2]^2 + (2yx^2)^2 \right\}^{1/4}}{\sqrt{(x^2+y^2-1)^2 + (2y)^2 - (y^2+1)}}, \\ k(x, y) &= \sin \left\{ \frac{1}{2} \text{atan} \left[ \frac{2yx^2}{x^2(y^2-1) + (y^2+1)^2} \right] \right\}, \\ l(x, y) &= \frac{\sqrt{-2x^2(y^2-1) - 2(y^4 - 6y^2 + 1) + 2(y^2+1)\sqrt{x^4 + 2x^2(y^2-1) + (y^2+1)^2}}}{x^2},\end{aligned}\tag{D.22}$$

where  $D_0 = \sqrt{4n/\pi \hbar^2 v^2}$ .

## D.5 Transverse Function for Graphene

The transverse susceptibility for graphene in RPA is

**Pristine graphene at  $\mathbf{T} = \mathbf{0}$ :**

$$\begin{aligned}\chi_T^{2D}(\mathbf{k}, z) &= \frac{k^2}{4\hbar z^2} g(\mathbf{k}, z), \\ \chi_T^{2D}(\mathbf{k}, i\xi) &= -\frac{k^2}{4\hbar \xi^2} g(\mathbf{k}, i\xi),\end{aligned}\tag{D.23}$$

where the functions  $g(\mathbf{k}, z)$  and  $g(\mathbf{k}, i\xi)$  are given in (D.17).

**Pristine graphene at  $\mathbf{T} \neq \mathbf{0}$ :**

$$\begin{aligned}\chi_T^{2D}(\mathbf{k}, z) &= \frac{k^2}{4\hbar z^2} \left[ g(\mathbf{k}, z) - \frac{8}{\pi v^2 k^2} \int_0^1 dx h(\mathbf{k}, z, x) \right], \\ \chi_T^{2D}(\mathbf{k}, i\xi) &= -\frac{k^2}{4\hbar \xi^2} \left[ g(\mathbf{k}, i\xi) - \frac{8}{\pi v^2 k^2} \int_0^1 dx h(\mathbf{k}, i\xi, x) \right],\end{aligned}\tag{D.24}$$

where

$$\begin{aligned}
h(\mathbf{k}, z, x) &= -\frac{z^2}{\hbar\beta} \ln \left[ 1 + 2 \cosh(\hbar\beta z x) e^{-\theta_T(\mathbf{k}, z, x)} + e^{-2\theta_T(\mathbf{k}, z, x)} \right] \\
&\quad - \left[ 2g^2(\mathbf{k}, z) + z^2 \right] \frac{\xi}{2} (1 - 2x) \frac{\sinh(\hbar\beta z x)}{\cosh \theta_T(\mathbf{k}, z, x) + \cosh(\hbar\beta z x)} \\
&\quad + \sqrt{x(1-x)} g^3(\mathbf{k}, z) \frac{\cosh(\hbar\beta z x) + e^{-\theta_T(\mathbf{k}, z, x)}}{\cosh \theta_T(\mathbf{k}, z, x) + \cosh(\hbar\beta z x)}, \\
h(\mathbf{k}, i\xi, x) &= \frac{\xi^2}{\hbar\beta} \ln \left[ 1 + 2 \cos(\hbar\beta \xi x) e^{-\theta_T(\mathbf{k}, i\xi, x)} + e^{-2\theta_T(\mathbf{k}, i\xi, x)} \right] \\
&\quad - \left[ 2g^2(\mathbf{k}, i\xi) - \xi^2 \right] \frac{\xi}{2} (1 - 2x) \frac{\sin(\hbar\beta \xi x)}{\cosh \theta_T(\mathbf{k}, i\xi, x) + \cos(\hbar\beta \xi x)} \\
&\quad + \sqrt{x(1-x)} g^3(\mathbf{k}, i\xi) \frac{\cos(\hbar\beta \xi x) + e^{-\theta_T(\mathbf{k}, i\xi, x)}}{\cosh \theta_T(\mathbf{k}, i\xi, x) + \cos(\hbar\beta \xi x)},
\end{aligned} \tag{D.25}$$

where the functions  $g(\mathbf{k}, z)$  and  $g(\mathbf{k}, i\xi)$  were given in (D.17) and the functions  $\theta_T(\mathbf{k}, z, x)$  and  $\theta_T(\mathbf{k}, i\xi, x)$  were given in (D.20).

# Index

## A

Aarseth, J. B., 336, 370  
ABC problem (Additional Boundary Conditions), 189  
Abraham-Minkowski controversy, 122  
Abramowitz, M., 370, 391  
Agronovich, V. M., 206  
Alexandrov, A. F., 206  
Alkali-metal dimers, 146–149, 263, 264, 267, 268  
Analytic functions, 3, 45–50, 82, 262, 405  
Arago, D. F., 206  
Argument principle, 3, 47, 50, 82, 87, 91, 150  
Asgari, R., 43  
Au, 169, 291

## B

Bakshi, P., 206  
Balian, R., 122  
Balian, R. B., 122  
Barlas, Y., 43  
Batsanov, S. S., 271  
Bessel equation, 374  
  modified, 234, 386, 388  
Bessel function  
  first kind, 374  
  modified, 234–236, 239, 240, 343, 386–388  
  second kind, 374  
  third kind, 374  
Bethe, H. A., 106  
Bimonte, G., 122  
Björk, P., 122, 206, 336

Bloch, C., 122  
Boardman, A. D., 370  
Bogdankevich, L. S., 206  
Bohr-van Leeuwen theorem, 122  
Bordag, M., 5, 122, 336  
Born, M., 370  
Boström, M., 5, 43, 206, 336  
Boundary conditions, 19, 22, 24–26, 33, 63, 78, 86, 94, 97, 126–128, 130, 153, 154, 178, 180, 182–184, 188, 189, 192, 199, 200, 204, 210, 234, 304, 306, 308, 310, 317, 321, 339, 341, 373, 374  
Branch cut, 47  
Branch point, 47  
Brevik, I., 5, 122, 336, 370  
Brown, L. S., 122  
Buhmann, S. Y., 5, 122  
Büscher, R., 122

## C

Capasso, F., 5, 122  
Casimir, H. B. G., 5, 106, 336, 370  
Causality, 13, 53  
Cavity  
  cylindrical, 243  
  spherical, 219, 354  
Chen, Wei, 206  
Chulkov, E. V., 206  
Churchill, Ruel V., 60  
Colloid, 1  
Commutation relation, 76  
Complex analysis, 45  
Constitutive relations, 13, 15, 19, 23, 43, 94

- Contour integration, 47  
 Convolution integrals, 13, 144, 259  
 Coordinates  
   bispherical, 125  
   cartesian, 125, 154, 273  
   confocal ellipsoidal, 125  
   confocal paraboloidal, 125  
   conical, 125  
   cylindrical, 125, 233, 373  
   elliptic cylindrical, 125  
   oblate spheroidal, 125  
   parabolic cylindrical, 125  
   paraboloidal, 125  
   prolate spheroidal, 125  
   spherical, 125, 209, 339  
   toroidal, 125  
 Correlation energy, 87, 90, 94, 118  
 Coupling constant, 88, 119, 120  
 Craig, R. A., 206  
 Cs, 149, 269  
 Cylinder, 114, 115, 117, 118, 233, 235, 373, 376  
 Cylindrical cavity, 219
- D**  
 Dalvit, D. A. R., 5, 336  
 Das Sarma, S., 43  
 Debye, P., 370  
 Decca, R. S., 336  
 2D electron gas, 40, 158, 166, 169, 287, 291, 349, 382  
 Derjaguin, B., 122  
 2D film, 32, 178, 181, 304, 308, 349, 362, 364, 365, 368, 382, 391  
 Diagrammatic perturbation theory, 57, 118, 120  
 Dipole moment, 143, 144, 146, 149, 259, 260  
   time-dependent, 42, 259  
 Dispersion, 74  
   curve, 73, 74, 86–88, 91, 155, 188, 195, 201, 202, 205, 211, 235  
   spatial, 4, 28, 30, 156, 158, 166, 187, 188, 191, 194, 195, 197, 198, 201–203, 205, 206, 287, 300, 306, 313, 318, 319, 323, 325, 326, 329, 332–336  
   temporal, 187  
 Distribution function  
   Boltzmann, 66, 270  
   bosons, 65  
   classical particles, 66, 270  
   fermions, 65  
   massless bosons, 66
- 2D metal film, 166, 287  
 Duplantier, B., 122  
 Dzyaloshinskii, I. E., 5
- E**  
 Echenique, P. M., 206  
 Eigenstates, 76  
 Eigenvalue, 76  
 Electron  
   rest-energy, 90  
   self-energy, 89, 93  
 Emig, T., 122  
 Englman, R., 206  
 Enthalpy, 64  
 Entire function, 46  
 Equation of continuity, 14, 16, 18, 34, 188, 189, 199, 314, 315  
 Equation of state  
   Casimir-Polder, 268  
   ideal gas, 135  
   non-ideal gas, 138  
   van der Waals, 139  
 Esquivel, R., 206, 336  
 Esquivel-Sirvent, R., 122  
 Exact differential, 62, 65  
 Exchange energy, 87, 90, 93, 94  
 Exponential function, 46
- F**  
 Farina, C., 43  
 Feibelman, P. J., 206  
 Feynman diagrams, 39, 57, 119  
 Feynman, R. P., 106  
 Fields, 10  
   auxiliary, 10  
   fundamental, 10  
 Fischbach, E., 336  
 Fischer, B., 206  
 Fluctuations, 1, 221  
 Force  
   Casimir, 1  
   Casimir-Polder, 2, 4, 9, 42, 259, 263, 265, 359, 360  
   dispersion, 1  
   electromagnetic, 9  
   fundamental, 9  
   gravitational, 9  
   inter-molecular, 1  
   nuclear  
     strong, 9  
     weak, 9  
   van der Waals, 1

- Fourier transform, 13  
 Fresnel equations, 23, 30  
 Fuchs, R., 336  
 Fujiwara, H., 43
- G**
- Gauge  
   Coulomb, 17, 18, 32, 55, 120, 189, 315  
   Lorentz, 19, 33, 53, 55, 189  
   transformations, 17  
 Gauss (divergence) theorem, 20  
 Geyer, G. L., 336  
 Gibbs-Duham relation, 65  
 Gibbs-Duham relation, 65  
 Gibbs (free) energy, 64, 136  
   2D version, 137  
 Gibbs (free) energy, 64, 136  
   2D version, 137  
 Gies, H., 122  
 Gold, 160–162, 164, 168, 169, 171, 172, 195,  
   202, 218, 220–222, 242, 243, 245,  
   247, 248, 283, 284, 289, 291, 293,  
   353, 354, 358, 359, 388, 389  
 Golestanian, R., 122  
 González, A. E., 122  
 González, A. E., 122  
 González, J., 43  
 González, J., 43  
 Graham, N., 122  
 Graphene, 40, 158, 165, 166, 168, 169, 175,  
   222, 223, 229, 230, 252, 253, 285,  
   299, 367, 368, 391  
 Greiner, W., 5  
 Guinea, F., 43
- H**
- Halevi, P., 206  
 Hamaker, H.C., 122  
 Hamiltonian, 74, 79, 120  
 Hanke, A., 122  
 Hankel function, 374  
 Harmonic oscillator, 74, 75  
 Heald, M. A., 43  
 Heckenberg, N. R., 122  
 Helmholtz' equation, 85, 125, 130, 273, 339,  
   373  
 Helmholtz' equation, 85, 125, 130, 273, 339,  
   373  
 Helmholtz (free) energy, 63, 64, 66, 67, 82,  
   85, 136, 150  
 Helmholtz (free) energy, 63, 64, 66, 67, 82,  
   85, 136, 150
- Hermite polynomials, 75  
 Hertz-Debye potentials, 130, 273, 339, 373  
 Hertz-Debye potentials, 130, 273, 339, 373  
 Hertz, H., 5  
 Hertz, H., 5  
 Høye, J. S., 336, 370  
 Hwang, E. H., 43  
 Hyperbolic cosine, 46  
 Hyperbolic cotangent, 46  
 Hyperbolic sine, 46
- I**
- Iannuzzi, D., 122  
 Ibanescu, M., 122  
 Ideal metal, 1, 86, 278, 279, 283, 285–287,  
   290, 299, 300, 313, 335  
 Impedance  
   surface, 332  
   wave, 23, 29  
 Ingold, G. L., 122  
 Interaction  
   Casimir, 1, 279  
   Casimir-Polder, 2, 9, 42, 259, 263, 265,  
   359, 361  
   dispersion, 1  
   electromagnetic, 9  
   fundamental, 9  
   gravitational, 9  
   nuclear  
     strong, 9  
     weak, 9  
   van der Waals, 1, 142, 146, 149, 221  
 Intercalation, 176, 253  
 Internal energy, 62–66, 84, 149, 150  
 Ishida, H., 206  
 Isolated singular point, 46  
 Israelachvili, J. N., 5
- J**
- Jackson, J. D., 206  
 Jaffe, R. L., 122  
 Joannopoulos, J. D., 122
- K**
- K, 148, 149, 263, 264, 269  
 Kardar, M., 122  
 Kempa, K., 206  
 Kenneth, O., 122  
 Kerker, M., 370, 391  
 Kim, W. J., 336  
 Klich, I., 122

- Kliewer, K. L., 336  
 Klimchitskaya, G. L., 5, 43, 122, 336  
 Klingmüller, K., 122  
 Kort-Kamp, W. J. M., 43  
 Kramers Kronig dispersion relations, 57, 60, 161
- L**
- Lagois, J., 206  
 Lambrecht, A., 122  
 Lamoreaux, S. K., 5, 335, 336  
 Langbein, D., 5, 122  
 Langfeld, K., 122  
 Laplace's equation, 85, 125, 130, 154, 209, 233  
 Laurent expansion, 47  
 Lebedev, P. N., 5  
 Li, 149, 171, 172, 175, 176, 218, 220, 242, 243, 245, 264, 269, 293, 299, 300, 353, 354, 358, 388, 389, 391  
 Liebsch, A., 206  
 Lifshitz, J. N., 5  
 Light dispersion curve, 74, 86–88, 91, 326, 332–334  
 Lindhard, J., 336  
 Loebel, E. M., 391  
 Logarithm, 47  
 London approximation, 145, 147–149, 151, 171, 187, 218, 221, 226, 228, 232, 242, 245, 249, 251, 263, 264, 293, 353, 359, 363, 365, 389, 391  
 London, F., 5, 151  
 Longitudinal part, 14, 18, 35  
 Lo Nostro, P., 5  
 López, D., 336  
 Lucas, A. A., 206
- M**
- MacDonald, A. H., 43  
 Maclay, G. J., 122  
 Magnetization, 14  
 Mahan, G. D., 106  
 Mahanty, J., 5  
 Many-body approach, 118, 120  
 Maradudin, A. A., 206  
 Marinescu, M., 151, 271  
 Marion, J. B., 43  
 Massless bosons, 66, 79, 80  
 Maxwell, James Clerk, 10, 43  
 Maxwell, James Clerk, 10, 43  
 Maxwell's equations, 9  
 Maxwell's equations, 9
- McCauley, A. P., 5  
 Mermin, N. D., 336  
 Metal film, 166, 167, 169, 176, 215, 287, 291, 299, 300  
 Mills, D. L., 206  
 Milonni, P. W., 5  
 Milton, K. A., 5, 122, 336  
 Mitchel, D. J., 122  
 Mochan, W. L., 206, 336
- Modes**
- bulk, 85, 87, 130, 154, 157, 333, 334
  - electric, 106, 154, 155, 185, 191, 192, 203, 206
  - longitudinal, 89
  - magnetic, 106, 154, 155, 185, 191, 195, 203, 206
  - spurious, 130
  - surface, 69, 85, 86, 93, 157, 170, 187, 195, 325
  - transverse, 90
  - transverse electric, 96, 131, 274
  - transverse magnetic, 95, 131, 274
  - vacuum, 85–87, 292
- Mode-summation method, 82, 145, 150  
 Mode-summation method, 82, 145, 150  
 Mohideen, U., 5, 336  
 Mostepanenko, V. M., 5, 43, 122, 336  
 Moyaerts, L., 122  
 Munday, J. N., 5  
 Müller, B., 5
- N**
- Na, 148, 149, 263, 264, 269  
 Nernst heat theorem, 336  
 Nernst, W., 336  
 Neto, P. A. M., 122  
 Neumann function, 374  
 Nieminen, T. A., 122  
 Nijboer, B. R. A., 106, 206  
 Ninham, B. W., 5, 106, 122  
 Noguez, C., 122  
 Normal incidence, 23  
 Normal modes, 69
  - electromagnetic, 69
- O**
- Oblique incidence, 25  
 Ohm's law, 15  
 Operator
  - annihilation, 121
  - creation, 75, 121
  - destruction, 75, 121

- lowering, 75
  - number, 79
  - raising, 75
  - Overbeek, J. T. G., 1
- P**
- Palik, E. D., 206
  - Parsegian, V. A., 5, 106
  - Particles
    - classical, 66
    - indistinguishable, 65
    - massive, 66
    - massless, 66, 79
  - Path-integral methods, 122
  - Pekar, S. I., 206
  - Pereg-Barnea, T., 43
  - Persson, C., 43
  - Pfeifer, R. N. C., 122
  - Phonon, 66, 74, 77, 78
  - Pitaevskii, P. P., 5
  - Plane of incidence, 25
  - Plasma frequency, 92, 187, 202
  - Plasmon, 87–89
    - 2D, 158
    - surface, 187, 194, 195, 202, 325, 326
  - Plummer, E. W., 206
  - Plunien, G., 5
  - Podgornik, R., 5
  - Poisson's equation, 18
  - Polariton, 187
  - Polarizability
    - atomic, 145, 147, 148, 151, 159, 187, 214, 232, 238, 259, 264, 280, 347
    - excess, 159, 214, 238, 280, 347
    - multipole, 210, 213, 215, 216, 218, 219, 221, 222, 225, 227, 235–237, 239, 240, 242, 244
  - Polarization, 14
  - Polarization bubble, 39, 118, 119
  - Polder, D., 5, 336, 370
  - Pole, 45, 47–51, 53, 56–58, 82–85, 89, 91, 194
  - Polini, M., 43
  - Potential
    - coupled induced, 181
    - scalar, 17–19, 32, 51, 53, 55, 62, 120, 121, 130, 154, 189, 209, 233
    - vector, 17–19, 33, 51, 52, 55, 120, 121, 190, 193, 196, 315, 322, 324
  - Power, E. A., 336
  - p-polarized, 26, 29, 121, 275, 278, 332
  - p-polarized, 26, 29, 121, 275, 278, 332
  - Proximity Force Approximation (PFA), 109, 115, 222, 247, 248
- Q**
- Quantization, 74
    - first, 74
    - second, 74
  - Quantum Electrodynamics (QED), 122
  - Quantum Field Theory (QFT), 122
- R**
- Rahi, S. J., 122
  - Random Phase Approximation (RPA), 120, 194, 195, 202, 319, 326, 405, 407–409
  - Rb, 149, 269
  - Residue, 47, 49, 50, 83
  - Retardation, 11, 18, 19, 32
  - Reynaud, S., 122
  - Ricatti-Bessel equation, 340, 342, 345
  - Ricatti-Bessel function, 340, 342, 343, 348, 361, 367, 369
    - first kind, 340
    - second kind, 340
    - third kind, 340
  - Richmond, P., 122
  - Rodriguez, A. W., 5, 122
  - Rodriguez-Lopez, P., 5
  - Román-Velázquez, C. E., 122
  - Rukhadze, A. A., 206
  - Ruppin, R., 206, 370
- S**
- Schaden, M., 122
  - Schaich, W. L., 206
  - Schmit, J., 206
  - Schram, K., 106, 206
  - Schubert, C., 122
  - Screening, 242
    - in a 2D system, 39
  - Sernelius, Bo E., 5, 43, 67, 106, 122, 131, 151, 206, 336, 370, 391
  - Shpunt, A., 122
  - Silkin, V. M., 206
  - Singularity, 46, 93
  - Singular point, 46–49
  - Slab, 158, 163
    - gold, 164, 284
  - Sols, F., 43
  - Sources
    - bound, 10

conduction, 10  
 coupled induced, 178, 182, 304, 308  
 external, 10  
 free, 10  
 total, 10  
 Sphere, 117, 118, 209, 211, 339, 343  
 Spherical harmonics, 210, 340  
 Spheroid, 116, 117, 122  
 s-polarized, 26, 28–30, 121, 275, 278, 332  
 s-polarized, 26, 28–30, 121, 275, 278, 332  
 Spruch, L., 122  
 Spurious modes, 130  
 Stauber, T., 43  
 Stegun, I. A., 370, 391  
 Stern, F., 122  
 Stiction, 394  
 Stokes (curl) theorem, 21  
 Stress Tensor, 122  
 Susceptibility, 13  
   electric, 13  
   magnetic, 13  
   multipole, 215  
 Sushkov, A. O., 336  
 Svetovoy, V. B., 206, 336  
  
**T**  
 Thermal wave length, 136  
 Thermodynamic potential, 64  
 Time inversion symmetry, 53  
 Tkatchenko, A., 5  
 Transverse part, 14, 17, 18, 35, 93, 315  
 Trunov, N. N., 5  
 Tsuei, K.-D., 206

**U**

Unitsystem  
   CGS, 11  
   SI, 11

**V**

Van der Waals, J. D., 5, 151  
 van der Waals, J. D., 5, 151  
 Van Kampen, N. G., 106, 206  
 van Kampen, N. G., 106, 206  
 Variable  
   extensive, 63, 135  
   intensive, 63, 135  
 Verwey, E. J. W., 1  
 Villarreal, C., 206, 336  
 Vozmediano, M. A. H., 43

**W**

Wagner, J., 122  
 Wave equation, 19, 53, 125, 130, 339, 373  
 Weber function, 374  
 Wolf, E., 370  
 Woods, L. M., 5  
 Wronskian, 234, 236, 240, 342, 344, 376,  
   377  
 Wunsch, B., 43

**Y**

You, L., 151, 271  
 Young, T., 5

**Z**

Zero-point energy, 81, 82, 84, 87, 178, 179